

CLEO: QELS-Fundamental Science

08:00–10:00

FM1A • Quantum Metrology and Measurement

Presider: Nicholas Peters; Oak Ridge National Lab, USA

FM1A.1 • 08:00 **Tutorial**

Quantum Measurement Techniques: Modern Approaches and Trends, Aephraim M. Steinberg^{1,2}; ¹Dept. of Physics & CQIQ, Univ. of Toronto, Canada; ²Canadian Inst. for Advanced Research, Canada. While quantum measurement has long been seen as a deep philosophical conundrum, technological progress and new potential applications such as quantum information processing have turned it into a respectable experimental discipline as well. I will introduce a modern perspective on real-world quantum measurement, including the new paradigm of “weak measurement” and its (controversial) potential for addressing fundamental issues as well as for improving the precision of practical measurement.



Aephraim Steinberg is a Professor of Experimental Quantum Optics at the Univ. of Toronto. Working with entangled photons and ultracold atoms, his lab has made numerous contributions to the science of quantum measurement, ranging from the observation of superluminal tunneling times to advances in quantum tomography to entanglement-assisted superresolution to “violating” the Heisenberg relation. He is a Fellow of the APS and The Optical Society, and his work has been twice selected as among the top 10 physics “Breakthroughs of the Year” by Physics World.

08:00–10:00

FM1B • Exciton Dynamics in 1D/2D Nanostructures

Presider: Kin Mak; Columbia Univ., USA

FM1B.1 • 08:00

Ultrafast Terahertz Probes of Interacting Dark Excitons in Chirality-specific Single-walled Carbon Nanotubes, Liang Luo^{1,2}, Ioannis Chatzakos^{1,2}, Aaron Patz^{1,2}, Jigang Wang^{1,2}; ¹Physics and Astronomy, Iowa State Univ., USA; ²Ames Lab-US DOE, USA. Ultrafast terahertz intra-excitonic transition ~6 meV reveals stable quasi-1D many-exciton states that evolve uniquely from a predominant dark exciton population to complex phase-space filling of both dark and bright pair states in (6,5) SWNTs

FM1B.2 • 08:15

Control of Coherent Intersubband Excitations by a Nonresonant THz Pulse, Michael Woerner¹, Carmine Somma¹, Drew Morrill¹, Giulia Folpini¹, Klaus Reimann¹, Thomas Elsaesser¹, Klaus Biermann²; ¹Max Born Inst., Germany; ²Paul Drude Inst., Germany. Using fully phase-resolved two-dimensional terahertz spectroscopy we study coherent intersubband Rabi oscillations in GaAs quantum wells. A strong terahertz field modifies particularly the phase of the nonlinearly emitted field during the Rabi oscillation.

FM1B.3 • 08:30

Measurement of Transversal Polarization Forces on Excitons in GaAs Quantum Wells, Eric Martin^{1,3}, Markus Borsch², Mackillo Kira², Steven Cundiff^{1,3}; ¹JILA, Univ. of Colorado & NIST, USA; ²Philipps-Univ. Marburg, Germany; ³Univ. of Colorado, USA. We observe resonant optical tweezing of quantum-well excitons created by an excitation pulse. The ultrafast dynamics of a small excitation spot show that the tweezing is due to the first-order polarization induced by the pump.

08:00–10:00

FM1C • Nonlinear Metamaterials

Presider: Vinod Menon; City College of New York, USA

FM1C.1 • 08:00 **Tutorial**

Recent Progress in Optical Metamaterials, Xiang Zhang¹; ¹Univ. of California Berkeley, USA. I will discuss progress in metamaterials including symmetry breaking related phenomena. I will also discuss non-Hermitian optics and parity-time symmetry and PT lasers of single mode.



Xiang Zhang is the Ernest S. Kuh Chaired Professor at the Univ. of California Berkeley and Director of Materials Science Division at Lawrence Berkeley National Laboratory. He is also the Director of the NSF Nano-scale Science and Engineering Center. He is a member of the US National Academy of Engineering, Academia Sinica and fellow of APS, OSA, AAAS and SPIE. His group's research in optical metamaterials was selected by Times Magazine as Top 10 Scientific Discoveries in 2008. In 2014, he was awarded Fitzroy Medal for pioneering contributions in metamaterials and superlens. He received his BS/MS in physics in Nanjing Univ., China, and Ph.D from UC Berkeley.

08:00–10:00

FM1D • Accelerating Beams & Beamshaping Application

Presider: Demetrios Christodoulides; Univ. of Central Florida, USA

FM1D.1 • 08:00

Laser Guided Curved Electric Discharges, Matteo Clerici^{1,2}, Yi Hu², Carles Milián³, Arnaud Couairon³, Demetrios N. Christodoulides⁴, Zhigang Chen⁵, Luca Razzari², François Vidal², François Légaré², Daniele Faccio¹, Roberto Morandotti²; ¹Heriot-Watt Univ., UK; ²INRS-EMT, Canada; ³Centre de Physique Théorique, Ecole Polytechnique, France; ⁴College of Optics, Univ. of Central Florida, USA; ⁵Dept. of Physics and Astronomy, San Francisco State Univ., USA. We report laser-guided electric discharges along curved trajectories, and hence around obstacles in line of sight between electrodes. Furthermore, beam self-healing enables direct discharge on target even when the laser beam directly hits the obstacle.

FM1D.2 • 08:15

Improving Electron Microscopy by Shaping the Electron Beam Wavefunction, Maor Mutzafi¹, Ido Kaminer^{2,1}, Gal Harari¹, Mordechai Segev¹; ¹Physics, Technion Israel Inst. of Technology, Israel; ²Physics, MIT, USA. We show a novel technique to enhance resolution and SNR in electron microscopes - by shaping the quantum wavefunction of electrons. Our technique overcomes fundamental limits that currently set the resolution and SNR in electron microscopy.

FM1D.3 • 08:30

Prolonging the Lifetime of Relativistic Particles by Self-Accelerating Dirac Wavepackets, Ido Kaminer^{2,1}, Mikael Rechtsman¹, Rivka Bekenstein¹, Jonathan Nemirovsky¹, Mordechai Segev¹; ¹Technion Israel Inst. of Technology, Israel; ²Dept. of Physics, MIT, USA. We show that shaping the wavepackets of Dirac particles can alter fundamental relativistic effects such as length contraction and time dilation. For example, shaping decaying particles as self-accelerating Dirac wavepackets extends their lifetime.

There is still time to register for a Short Course!

Visit Registration to learn about the courses still available.

Monday, 11 May

SC270 • High Power Fiber Lasers and Amplifiers
SC271 • Quantum Information-Technologies and Applications
SC301 • Quantum Cascade Lasers: Science, Technology, Applications and Markets
SC376 • Plasmonics

Tuesday, 12 May

SC352 • Introduction to Ultrafast Pulse Shaping—Principles and Applications
SC362 • Cavity Optomechanics: Fundamentals and Applications of Controlling and Measuring Nanoand Micro-mechanical Oscillators with Laser Light
SC410 • Finite Element Modelling Methods for Photonics and Optics

Visit page 16 for complete Short Course Information.

CLEO: QELS-
Fundamental Science

08:00–10:00

FM1E • Symposium on Single-photon Nonlinear Optics I

Presider: Jacob Taylor; NIST, USA

FM1E.1 • 08:00 **Invited**

Demonstration of Deterministic Photon-Photon Interactions with a Single Atom, Serge Rosenblum¹, Itay Shomroni¹, Yulia Lovsky¹, Orel Bechler¹, Gabriel Guendelman¹, Barak Dayan¹; ¹Weizmann Inst. of Science, Israel. We demonstrate all-optical deterministic photon-atom and photon-photon interactions with a single Rb atom coupled to high-Q fiber-coupled microresonator. This scheme enables all-optical photon routing, passive quantum memory and quantum gates activated solely by single photons.

FM1E.2 • 08:30

Observation of the Nonlinear Phase Shift Due to Single Post-Selected Photons, Amir Feizpour¹, Matin Hallaji¹, Greg Dmochowski¹, Aephraim M. Steinberg¹; ¹Physics, Univ. of Toronto, Canada. We implement a strong optical nonlinearity using electromagnetically-induced transparency in cold atoms, and measure the resulting nonlinear phase shift for postselected photons. We believe that this represents the first direct measurement of the cross-phase shift due to individual photons.

CLEO: Science & Innovations

08:00–10:00

SM1F • Semiconductor Laser Physics

Presider: Sven Hofling; Univ. of St. Andrews., UK

SM1F.1 • 08:00 **Invited**

Quantum Coherent Interactions in Room Temperature InAs/InP Quantum Dot Amplifiers, Gadi Eisenstein¹; ¹Technion Israel Inst. of Technology, Israel. We survey the latest advances in initiation and observation of quantum coherent interactions in room temperature quantum dot amplifiers operating at 1550 nm. Single and double pulse FROG measurements accompanied by detailed modeling are described.

SM1F.2 • 08:30

Crossed Exciton States in Complex Semiconductor Nanostructures, Nina Owschmikow¹, Mirco Kolarczik¹, Yuecel Kaptan¹, Nicolai B. Grosse¹, Ulrike K. Woggon¹; ¹Technische Universität Berlin, Germany. Based on gain excitation spectra derived from two-color pump-probe experiments, we identify crossed exciton states formed in semiconductor nanostructures of mixed dimensionality and investigate their influence on the carrier dynamics.

08:00–10:00

SM1G • Nanostructures

Presider: Ofer Levi; Univ. of Toronto, Canada

SM1G.1 • 08:00

Germanium Nanowires as Spectrally-selective Photodetectors in the Visible-to-Infrared, Amit Solanki¹, Kenneth B. Crozier^{2,3}; ¹Harvard Univ., USA; ²School of Physics, Univ. of Melbourne, Australia; ³Dept. of Electrical and Electronic Engineering, Univ. of Melbourne, Australia. We experimentally demonstrate arrays of vertical Ge nanowires as spectrally-selective photodetectors at visible to infrared wavelengths. Measurements reveal that the external quantum efficiency spectra of fabricated devices vary with the radius of the constituent nanowires.

SM1G.2 • 08:15

Ultrafine ferroelectric nanostructure in layered Mg:LiNbO₃ thin film, Taichi Okada^{1,2}, Masaki Shimizu^{1,2}, Satoshi Horikawa^{1,2}, Takuya Utsugida^{1,2}, Kazufumi Fujii¹, Sunao Kurimura^{1,2}, Hirochika Nakajima²; ¹National Inst. for Materials Science, Japan; ²Waseda Univ., Japan. We reported a fabrication of ultrafine ferroelectric domain structure with 540 nm period into layered Mg-doped/insulator/non-doped LiNbO₃.

SM1G.3 • 08:30 **Invited**

Tunable Coloration with Flexible High-Contrast Metastructures, Li Zhu¹, Jonas Kapraun¹, James Ferrara¹, Connie J. Chang-Hansnain¹; ¹Univ. of California Berkeley, USA. Actively controlling the perceived color of objects is highly desirable for a variety of applications. We report a new flexible high contrast metastructure (HCM) with color being varied by stretching the elastomeric membrane.

08:00–10:00

SM1H • THz Quantum Cascade Lasers

Presider: David Burghoff; MIT, USA

SM1H.1 • 08:00

Selection of Longitudinal Modes in a Terahertz Quantum Cascade Laser via Narrow-band Injection Seeding, Hanond Nong¹, Shovon Pal¹, Sergej Markmann¹, Negar Hekmat¹, Paul Dean², Reshma A. Mohandas², Li Lianhe², Edmund Linfield², Giles Davies², Andreas D. Wieck¹, Nathan Jukam¹; ¹Ruhr-Universität Bochum, Germany; ²Univ. of Leeds, UK. A terahertz quantum cascade laser is injection seeded with narrowband seed pulses generated from a periodically poled lithium niobate crystal. The spectral emission of the quantum cascade laser is controlled by the seed spectra.

SM1H.2 • 08:15

kW-Peak-Power Terahertz-Wave Parametric Generation and 70 dB-Dynamic-Range Detection Based on Efficient Surface-Coupling Configuration, Yuma Takida¹, Takashi Notake¹, Kouji Nawata¹, Yu Tokizane¹, Shin'ichiro Hayashi¹, Hiroaki Minamide¹; ¹RIKEN, Japan. We have demonstrated kW-peak-power terahertz (THz)-wave parametric generation and 70 dB-dynamic-range detection by using efficient surface-coupling configuration. The system is capable of producing and detecting monochromatic THz-wave pulses in the wide frequency range from 0.8 to 2.8 THz.

SM1H.3 • 08:30

Broadly-Tunable Room-Temperature Monolithic Terahertz Quantum Cascade Laser Sources, Aiting Jiang¹, Seungyong Jung¹, Yifan Jiang¹, Karun Vijayraghavan¹, Jaehyun Kim¹, Mikhail A. Belkin¹; ¹Univ. of Texas at Austin, USA. We report a monolithic terahertz source made of an array of 10 electrically-tunable mid-infrared quantum cascade lasers with intra-cavity terahertz difference-frequency generation. Continuous tunability between 2 and 4 THz is demonstrated at room temperature.

Technical Digest and Postdeadline Papers
Available Online

- Visit www.cleoconference.org
- Select Access Digest Paper link
- Use your registration email address and password

Access is provided only to full technical attendees.

Meeting Room
211 B/D

CLEO: Science & Innovations

08:00–10:00

SM11 • Silicon Photonics

President: Bahram Jalali; Univ. of California Los Angeles, USA

SM11.1 • 08:00

Plasmonic-organic hybrid (POH) modulators for OOK and BPSK signaling at 40 Gbit/s, Argishti Melikyan¹, Kira Köhne¹, Matthias Lauer¹, Robert Palmer¹, Sebastian R. Koeber¹, Sascha Muehlbrandt¹, Philipp Schindler¹, Delwin Elder², Stefan Wolf¹, Wolfgang Heni³, Christian Haffner³, Yuri Fedoryshyn³, David Hillerkuss³, Martin Sommer¹, Larry Dalton², Dries VanThourhout⁴, Wolfgang Freude¹, Manfred Kohl¹, Juerg Leuthold³, Christian Koos³; ¹Karlsruher Institut für Technologie, Germany; ²Dept. of Chemistry, Univ. of Washington, USA; ³ETH Zürich, Switzerland; ⁴Ghent Univ. - IMEC, Belgium. We report on plasmonic-organic hybrid(POH) phase modulator generating error free (BER<10⁻¹⁰) BPSK signals at 40Gbit/s. In addition, generation and direct detection of 40Gbit/s OOK signals are discussed using POH Mach-Zehnder modulators on the transmitter side.

SM11.2 • 08:15

Ultra-Compact Hybrid Silicon-VO₂ Electroabsorption Optical Switch, Arash Joushaghani¹, Junho Jeong¹, Suzanne Paradis², David Alain², J. Stewart Aitchison¹, Joyce K. Poon¹; ¹Electrical and Computer Engineering, Univ. of Toronto, Canada; ²Defence Research and Development Canada - Valcartier, Canada. A 1 μm-long hybrid Si-VO₂ electroabsorption switch with integrated electrical contacts is demonstrated. A record extinction ratio of ~12 dB/μm is achieved over a bandwidth of ~100 nm with a power dissipation of 2.55 mW.

SM11.3 • 08:30

Hybrid Silicon Ring Laser with Unidirectional Emission, Wesley D. Sacher¹, Michael Davenport², Martijn J. Heck², Jared Mikelsen¹, Joyce K. Poon¹, John Bowers²; ¹Dept. of Electrical and Computer Engineering, Univ. of Toronto, Canada; ²Dept. of Electrical and Computer Engineering, Univ. of California at Santa Barbara, USA. A hybrid silicon ring laser in which the counter-clockwise circulating power is coupled into the clockwise mode is demonstrated. Unidirectional clockwise laser output is achieved with a suppression ratio of 19 dB over the counter-clockwise mode.

Meeting Room
212 A/C

CLEO: Applications & Technology

08:00–10:00

AM1J • Light Sources and Devices for Biomedical Imaging I

President: Ilya Bezel; KLA-Tencor Corp., USA

AM1J.1 • 08:00 **Invited**

The Cell Laser, Seok-Hyun A. Yun^{1,2}; ¹Harvard Medical School, USA; ²Massachusetts General Hospital, USA. The first demonstration of a cell laser in 2011 opened new avenues for generating coherent light from living matters. Here we show progress in this new class of light sources and demonstrate their applications for sensing.

AM1J.2 • 08:30

Analysis of Optical Properties of Cell Lasers and Their Use as Biological Sensors, Matjaz Humar^{2,1}, Seok-Hyun A. Yun²; ¹Condensed Matter Dept., J. Stefan Inst., Slovenia; ²Wellman Center for Photomedicine, Dept. of Dermatology, Harvard Medical School and Massachusetts General Hospital, USA. We analyzed single-cell lasers made from different cell types and fluorescent dyes. Two mirrors enclose the cells forming a laser cavity. The different transversal cell laser modes are dependent on cell shape, refractive index and gain distribution enabling single cell characterization and sensing.

Meeting Room
212 B/D

08:00–10:00

AM1K • Microprocessing Ultra-Fast Processing of Dielectrics

President: Yves Bellouard; Ecole Polytechnique Federale de Lausanne, Switzerland

AM1K.1 • 08:00 **Invited**

Ultrashort Pulse Lasers for Precise Processing: Results of a Recent German Research Initiative, Stefan Nolte¹; ¹Friedrich-Schiller-Universität Jena, Germany. We review results of 10 joint research projects on ultrashort pulse technology. Topics include novel laser sources, reliable components and specialized applications from eye surgery to processing of semiconductors, carbon fiber reinforced plastics and metals.

AM1K.2 • 08:30

High Density Data Storage in Transparent Plastics Using Femtosecond Laser Microstructuring, Deepak L. Kallepalli¹; ¹Physics Dept., Univ. of Ottawa, Canada. We report high data storage ~ 66 GB/cm³ in Poly (methylmethacrylate) by utilizing locally confined fluorescent data bits fabricated by a femtosecond (fs) laser.

Marriott
Salon I & II

CLEO: Science & Innovations

08:00–10:00

SM1L • Fiber Sensing and Measurement

President: Axel Schulzgen; Univ. of Central Florida, USA

SM1L.1 • 08:00 **Invited**

Novel Technologies for High Precision Characterization of Fibers, Andrew D. Yablon¹; ¹Interfiber Analysis, LLC, USA. Optical fiber gain profiling, spectrogram modal analysis, and interferometric refractive index and residual stress measurement are reviewed. These novel characterization technologies are important for designing, assembling and optimizing fiber-based lasers and amplifiers.

SM1L.2 • 08:30

Design and Fabrication of Side-channel Photonic Crystal Fiber for Surface Enhanced Raman Scattering Applications, Nan Zhang^{1,2}, Georges Humbert³, Tianxun Gong^{1,4}, Ping Shum^{1,2}, Jean-Louis Auguste³, Zhifang Wu^{1,2}, Malini Olivo^{4,5}, Quyen X. Dinh^{2,6}, Lei Wei¹; ¹School of Electrical and Electronic Engineering, Nanyang Technological Univ., Singapore; ²CINTRA CNRS/NTU/THALES, Singapore; ³Univ. of Limoges/CNRS, France; ⁴Bio-Optical Imaging Group, Singapore Bioimaging Consortium (SBIC), A*STAR, Singapore; ⁵School of Physics, National Univ. of Ireland, Ireland; ⁶R&T Dept., Thales Solutions Asia Pte Ltd, Singapore. We demonstrate a side-channel photonic crystal fiber for surface enhanced Raman scattering applications. A low detection concentration of 5 pM 4-aminothiophenol solution and an accumulative effect of Raman signal along the fiber length are achieved.



CLEO: Science & Innovations

08:00–09:45

SM1M • Parametric Processing*Presider: Francesca Parmigiani; Univ. of Southampton, UK*SM1M.1 • 08:00 **Tutorial**

Optical and Hybrid Signal Processing, Stojan Radic¹; ¹Univ. of California, San Diego, USA. Physics and implementation of optical signal processing in communication and sensing links is introduced. Hybrid processing schemes capable of interfacing with high-rate network traffic and electronic backplane are described and illustrated using application examples.



Stojan Radic graduated from the Inst. of Optics, Univ. of Rochester, in 1995 and has subsequently served at Corning and Bell Laboratories. After leaving Bell Laboratories, he was a Nortel Chair at Duke Univ.. Currently he is a professor and a Director of the Photonics System Laboratory at Qualcomm Inst. at the Univ. of California San Diego. Radic is a Fellow of The Optical Society and serves as an editor with IEEE Photonics Technology Letters and Optics Express Journals. Radic's laboratory currently pursues national projects in coherent communications, advanced signal processing and unconventional medical imaging.

08:00–09:45

SM1N • Symposium on Remote Atmospheric Lasing I*Presider: Pavel Polynkin; Univ. of Arizona, USA*SM1N.1 • 08:00 **Invited**

Remote Backward-Propagating Lasing of Nitrogen and Oxygen in Air, Arthur Dogariu¹, Richard Miles¹; ¹Princeton Univ., USA. We present the latest developments in remote atmospheric air lasing. Stimulated emission induced by two-photon atomic excitation following molecular dissociation creates robust coherent emission in the backwards direction.

08:00–10:00

SM1O • Advanced Spectroscopic Techniques*Presider: Scott Howard; Univ. of Notre Dame, USA*

SM1O.1 • 08:00

Analysis of Trace Gas Mixtures Using an External Cavity Quantum Cascade Laser Sensor, Mark C. Phillips¹, Matthew S. Taubman¹, Brian Brumfield¹, Jason Kriesel²; ¹Pacific Northwest National Lab, USA; ²Opto-Knowledge Systems Inc., USA. We measure and analyze mixtures of trace gases at ppb-ppm levels using an external cavity quantum cascade laser sensor with a 1-second response time. Accurate spectral fits are obtained in the presence of overlapping spectra.

SM1O.2 • 08:15

Fundamental Limits in Chirped Laser Dispersion Spectroscopy, Genevieve Plant¹, Andreas Hangauer¹, Gerard Wysocki¹; ¹Princeton Univ., USA. We present performance analysis of chirped laser dispersion spectroscopy (CLaDS) under shot noise limited conditions. A comparison to direct laser absorption spectroscopy (DLAS) is also provided.

SM1O.3 • 08:30 **Invited**

Mid-IR Quantum Cascade Lasers as an Enabling Technology for Analytical Chemistry, Christian Kristament¹, Markus Brandstetter¹, Andreas Schwaighofer¹, Mirta Alcaraz¹, Bernhard Lendl¹; ¹Chemical Technologies and Analytics, Vienna Univ. of Technology, Austria. An overview on the state of the art on the analysis of liquids by QCLs is given with special focus on the determination of secondary structure elements in aqueous protein solutions using an EC-QCL system.

08:00–10:00

SM1P • Few-cycle Infrared Sources*Presider: Nobuhisa Ishii; Institute for Solid State Physics, Japan*

SM1P.1 • 08:00

A Compact Single Cycle Driver for Strong Field Applications based on a Self-compression in a Kagome Fiber, Guangyu Fan¹, Tadas Balciunas¹, Stefan Hässler¹, Coralie Fourcade Dutin², Tobias Witting³, Aleksandr Voronin⁴, Aleksei Zheltikov^{4,5}, Frédéric Gérôme⁶, Gerhard Paulus⁶, Andrius Baltuska¹, Fetah Benabid²; ¹Vienna Univ. of Technology, Photonics Inst., Austria; ²Univ. de Limoges, GPPMM group, Xlim Research Inst., France; ³Imperial College London, Blackett Lab, UK; ⁴M.V. Lomonosov Moscow State Univ., Physics Dept., International Laser Center, Russia; ⁵Texas A & M Univ., College Station Texas, Dept. of Physics and Astronomy, USA; ⁶Universität Jena, Institut fuer Optik und Quantenelektronik, Germany. We report on Kagome fiber based self-compression of 100 μ J IR pulses to single cycle duration and demonstrate HHG in an integrated scheme which allows a compact isolated attosecond XUV source implementation above 50 eV.

SM1P.2 • 08:15

Mid-IR 0.4TW Pulses Achieved Through Hollow-Core Fiber Compression, Vincent Cardin¹, Nicolas Thiré¹, Vincent Wanie¹, Samuel Beaulieu¹, François Légaré¹, Bruno E. Schmidt¹; ¹INRS-EMT, Canada. By employing hollow-core fiber compression using a stretched flexible fiber, we achieved 2-cycles pulses centered on 1.8 μ m with more than 5mJ energy per pulse.

SM1P.3 • 08:30

Broadband ZGP OPA Pumped by Femtosecond Ho:YAG Chirped Pulse Amplifier, Pavel Malevich², Tsuneto Kanai², Gregory Gitzinger¹, Raman Maksimenka¹, Nicolas Forget¹, Andrius Baltuska^{2,3}, Audrius Pugzlys^{2,3}; ¹Fastlite, France; ²Vienna Univ. of Technology, Austria; ³Center for Physical Sciences & Technology, Lithuania. We demonstrate a broadband parametric amplifier at 6 μ m driven by a femtosecond 2.1 μ m Ho:YAG chirped-pulse amplifier. The scheme offers an all-in-one solution for seeding, pumping and phase stabilization of few-cycle pulses in ZnGeP₂ and similar mid-IR crystals.



CLEO: QELS-Fundamental Science

FM1A • Quantum Metrology
and Measurement—Continued

FM1A.2 • 09:00

Experimentally Quantifying the Advantages of Weak-Values-Based Metrology, Gerardo Viza^{1,2}, Julian Martinez^{1,2}, Gabriel Alves³, Andrew N. Jordan^{1,2}, John Howell^{1,2}; ¹Dept. of Physics and Astronomy, Univ. of Rochester, USA; ²The Center for Coherence and Quantum Optics, Univ. of Rochester, USA; ³Instituto de Física, Universidade Federal do Rio de Janeiro, Brazil. We measure optical beam deflections both using a weak-values technique and by focusing. By introducing controlled modulations, the WVT outperforms focusing. Post-selecting on 1% of the photons, we obtain 99% of the available Fisher information.

FM1A.3 • 09:15

Particle vs. Mode Entanglement in Optical Quantum Metrology, Nicolas Quesada¹, Jaspreet Sahota¹; ¹Univ. of Toronto, Canada. We present a constructive proof of the fact that mode entanglement is not necessary for optical quantum enhanced metrology (QEM) but particle entanglement is. We provide a particle entanglement witness that detects all path symmetric states useful for QEM in a Mach-Zender interferometer.

FM1B • Exciton Dynamics
in 1D/2D Nanostructures—
Continued

FM1B.4 • 08:45

Ultrafast Modulation of Strong Light-Matter Coupling, Christoph Lange¹, Emiliano Cancellieri², Lee A. Rozema³, Rockson Chang³, Shreyas Potnis³, Aephraim M. Steinberg³, Mark Steger⁴, David W. Snoke⁴, Loren N. Pfeiffer⁵, Kenneth W. West⁵, Alex Hayat⁶; ¹Universität Regensburg, Germany; ²Univ. of Sheffield, UK; ³Dept. of Physics, Centre for Quantum Information and Quantum Control, and Inst. for Optical Sciences, Univ. of Toronto, Canada; ⁴Dept. of Physics and Astronomy, Univ. of Pittsburgh, USA; ⁵Dept. of Electrical Engineering, Princeton Univ., USA; ⁶Dept. of Electrical Engineering, Technion, Israel. We modulate strong coupling in a GaAs/AlGaAs microcavity by transiently decoupling exciton and cavity through the optical Stark effect induced by intense, red-detuned laser pulses. Pulses longer (1500 fs) and shorter (225 fs) than the Rabi cycle time of 500 fs yield distinctly different line shapes.

FM1B.5 • 09:00

Coherent Control of Correlation Transport between Semiconductor Quantum Wells, Osmo Vänskä^{1,2}, Ilkka Tittonen², Stephan W. Koch¹, Mackillo Kira¹; ¹Philipps-Universität Marburg, Germany; ²Aalto Univ., Finland. Terahertz control of semiconductor excitations is analyzed theoretically in a double-quantum-well by theoretical modeling. The results demonstrate that selective transport of electrons, excitons and even pure correlations is realizable in present-day experiments.

FM1B.6 • 09:15

Quantum Optics with Dropletions, Martin Mootz¹, Mackillo Kira¹, Stephan W. Koch¹, Andrew E. Almand-Hunter^{2,3}, Kai Wang², Steven Cundiff^{2,3}; ¹Dept. of Physics, Philipps-Universität Marburg, Germany; ²JILA, Univ. of Colorado and National Inst. of Standards and Technology, USA; ³Dept. of Physics, Univ. of Colorado, USA. Dropletions are highly correlated quasiparticles, recently found in GaAs quantum wells. We demonstrate that they can be controlled by adjusting light source's quantum fluctuations and that their size grows with increasing temperature.

FM1C • Nonlinear
Metamaterials—Continued

FM1C.2 • 09:00

Third-Harmonic Generation from Silicon Oligomers and Metasurfaces, Maxim R. Shcherbakov³, Dragomir N. Neshev¹, Ben Hopkins¹, Alexander S. Shorokhov³, Isabelle Staudé¹, Elizaveta V. Melik-Gaykazyan³, Andrey Miroshnichenko¹, Igal Brener², Andrey A. Fedyanin³, Yuri S. Kivshar¹; ¹Nonlinear Physics Centre, Research School of Physics and Engineering, The Australian National Univ., Australia; ²Center for Integrated Nanotechnologies, Sandia National Lab, USA; ³Faculty of Physics, Lomonosov Moscow State Univ., Russia. Third-harmonic generation spectroscopy of silicon oligomers and metasurfaces reveals the nonlinear spectra reshaping with electric and magnetic dipolar Mie-type resonances and up-conversion increase by two orders of magnitude as compared to the bulk silicon.

FM1C.3 • 09:15

Multipolar analysis of linear and nonlinear unidirectional response from plasmonic dimers, Ekaterina Poutrina^{2,1}, Augustine Urbas²; ¹UES, Inc., USA; ²Air Force Research Lab, USA. We develop the retrieval procedure for linear and nonlinear polarizabilities of plasmonic nanodimers and present examples of unidirectional scattering and nonlinear unidirectional generation from such geometries. Related effective parameters of periodic dimer arrangements are discussed.

FM1D • Accelerating Beams
& Beamshaping Application—
Continued

FM1D.4 • 08:45

Accelerating Self-Imaging: the Airy-Talbot Effect, Yaakov Lumer¹, Lee Drori¹, Yaov Hazan¹, Mordechai Segev¹; ¹Physics Dept., Technion Israel Inst. of Technology, Israel. We present self-imaging of optical waves along curved trajectories, theoretically and experimentally. Unlike the Talbot effect, the field wave need not be periodic. Paraxially, self-imaging persists indefinitely, while non-paraxially is limited by overall bending angle.

FM1D.5 • 09:00

Optical Wavepackets Overcoming Gravitational Effects, Rivka Bekenstein¹, Ran Schley¹, Maor Mutzafi¹, Carmel Rotschild¹, Mordechai Segev¹; ¹Technion Israel Inst. of Technology, Israel. We find specific wavepackets that overcome analogue gravitational phenomena due to the complex interplay between interference effects and various optical gravitational effects, and demonstrate them in experiments with nonlocal nonlinear interactions.

FM1D.6 • 09:15

Three-Dimensional Abruptly Autofocusing Optical Wave Packet, Qian Cao^{2,3}, Chenchen Wan^{2,1}, Xin Huang², Andy Chong^{2,4}; ¹DESY, Germany; ²Electro-Optics Program, Univ. of Dayton, USA; ³FS-CFEL-2, Center of Free-Electron Laser Science, Germany; ⁴Physics, Univ. of Dayton, USA. We generate a three-dimensional (3D) autofocusing wave packet by combining counter-propagating Airy pulses and an Airy ring beam. A 3D profile measurement reveals unique 3D autofocusing of such wave packet in a linear medium.

CLEO: QELS-
Fundamental ScienceFM1E • Symposium on Single-
photon Nonlinear Optics I—
Continued

FM1E.3 • 08:45

How a Single Photon Can Act Like Many Photons, Matin Hallaji¹, Amir Feizpour¹, Greg Dmochowski¹, Josiah Sinclair¹, Aephraim M. Steinberg¹; ¹Physics, Univ. of Toronto, Canada. The weak nonlinear effect of a single photon on a probe beam is amplified by postselecting on a rare final state (“WVA” effect). The resulting cross-phase shift is up to five times greater than the usual single-photon phase shift.

FM1E.4 • 09:00 **Invited**

Few-photon Nonlinear Optics Using Interacting Rydberg Atoms, Sebastian Hofferberth¹; ¹Harvard Univ., USA. Mapping the interaction between Rydberg excitations onto photons enables the realization of optical nonlinearities on the single-photon level. We present a single-photon transistor, where one gate photon controls the transmission of many source photons.

SM1F • Semiconductor Laser
Physics—Continued

SM1F.3 • 08:45

High-Speed Electrical Modulation of Polariton Lasers, Md Zunaid Baten¹, Thomas Frost¹, Saniya Deshpande¹, Pallab K. Bhat-tacharya¹; ¹Univ. of Michigan, USA. Room temperature electrical modulation response of a bulk GaN-based electrically injected polariton laser is reported. The frequency response is derived from the measured time-resolved electroluminescence and a maximum -3dB bandwidth of 0.65 GHz is obtained.

SM1F.4 • 09:00

Lasers With Distributed Loss Have Sub-linear Power Output, Tobias Mansuripur², Guy-Mael de Naurois¹, Alexey Belyanin², Federico Capasso¹; ¹School of Engineering and Applied Sciences, Harvard Univ., USA; ²Dept. of Physics, Texas A&M Univ., USA; ³Dept. of Physics, Harvard Univ., USA. We provide a simple explanation for why laser media with distributed loss should have a sublinear output power characteristic. This understanding clarifies the role of long-range spatial hole burning in reducing the efficiency of semiconductor lasers, and is essential for optimizing power output.

SM1F.5 • 09:15

Measuring a Radiative Recombination Current in an Optically Pumped Gain Medium, Robert Thomas¹, Peter M. Smowton¹, Peter Blood¹; ¹Cardiff Univ., UK. An analytical technique for determining the radiative current in optically pumped gain media is presented. A means of separately identifying the effects of gain compression and pump non-uniformities in amplified spontaneous emission spectra is introduced.

CLEO: Science & Innovations

SM1G • Nanostructures—
Continued

SM1G.4 • 09:00

Hybrid Diamond-Silicon Carbide Structures Incorporating Silicon-Vacancies in Diamond as Quantum Emitters, Jingyuan Linda Zhang¹, Hitoshi Ishiwata¹, Marina Radulaski¹, Thomas M. Babinec¹, Kai Muller¹, Konstantinos G. Lagoudakis¹, Robert Edginton¹, Kassem Alassaad², Gabriel Ferro², Nicholas Melosh¹, Zhi-Xun Shen¹, Jelena Vuckovic¹; ¹Stanford Univ., USA; ²Universite de Lyon, France. We demonstrate a novel technique for generating several hybrid solid state nano- and micro-photon devices. Our approach combines the growth of nano-diamonds on silicon carbide substrate from molecular diamond with the use of these particles as hard mask for pattern transfer into the substrate.

SM1G.5 • 09:15

Experimental Demonstration of CMOS-Compatible Long-Range Dielectric-Loaded Surface Plasmon-Polariton Waveguides (LR-DLSPWs), Roy T. Zektzer¹, Boris Desiatov¹, Noa Mazurski¹, Sergey bozhevolnyi², Uriel Levy¹; ¹The Hebrew Univ. of Jerusalem, Israel; ²Technology and Innovation, Univ. of Southern Denmark, Denmark. We demonstrate the design, fabrication and experimental characterization of longrange dielectric-loaded SPP waveguides (LR-DLSPWs) that are compatible with CMOS technology. The demonstrated waveguides feature good mode confinement together with long propagation at telecom wavelengths.

SM1H • THz Quantum Cascade
Lasers—Continued

SM1H.4 • 08:45

QCL-based Metrological-grade THz Spectroscopy Tools, Luigi Consolino¹, Mario Siciliani de Cumis¹, Davide Mazzotti¹, Annamaria Campa¹, Marco Ravaro¹, Miriam S. Vitiello², Saverio Bartalini¹, Pablo Cancio Pastor¹, Paolo De Natale¹; ¹CNR - INO, Italy; ²CNR-NEST, Italy. We present the latest results on high-resolution QCL-based THz spectroscopy: the possibility to perform saturated absorption or cavity-enhanced spectroscopy on THz molecular transitions, strengthened by the realization of a new generation THz FCS.

SM1H.5 • 09:00 **Invited**

Coherent absorption control in polaritonic systems, Alessandro Tredicucci¹; ¹NEST, Istituto Nanoscienze-CNR, Italy; ²Dipartimento di Fisica “E. Fermi”, Università di Pisa, Italy. Coherent Perfect Absorption is discussed in the context of strongly-coupled polariton systems. It occurs when the cavity loss rate matches the material one, as demonstrated for intersubband transitions in a photonic crystal resonator.

CLEO: Science & Innovations

SM11 • Silicon Photonics—Continued

SM11.4 • 08:45

Integrated on-chip C-band optical spectrum analyzer using dual-ring resonators, Ying Li¹, Qi Li¹, Yang Liu², Tom Baehr-Jones², Michael Hochberg², Keren Bergman¹; ¹Columbia Univ., USA; ²Coriant Advanced Technology Group, USA. We demonstrate an on-chip optical spectrum analyzer (OSA) using two cascade optical ring resonators. The OSA's span is wider than 50nm and resolution is ~0.1nm. A germanium photodetector and a p-i-n modulator are integrated on the chip and used for detection.

SM11.5 • 09:00

Effective Carrier Sweepout In A Silicon Waveguide by a Metal-Semiconductor-Metal Structure, Yunhong Ding¹, Hao Hu¹, Haiyan Ou¹, Leif K. Oxenløwe¹, Kresten Yvind¹; ¹DTU Fotonik, Dept. of Photonics Engineering, Technical Univ. of Denmark, Denmark. We demonstrate effective carrier depletion by metal-semiconductor-metal junctions for a silicon waveguide. Photo-generated carriers are efficiently swept out by applying bias voltages, and a shortest carrier lifetime of only 55 ps is demonstrated.

SM11.6 • 09:15

Apodized Focusing Fully Etched Sub-wavelength Grating Couplers With Ultra-low Reflections, Yun Wang¹, Han Yun¹, Zeqin Lu¹, Richard Bojko², Fan Zhang¹, Michael Caverley¹, Nicolas A. Jaeger¹, Lukas Chrostowski¹; ¹Univ. of British Columbia, Canada; ²Univ. of Washington, USA. We experimentally demonstrated apodized focusing fully etched sub-wavelength grating couplers for the transverse electric (TE) mode. An insertion loss of 4.2 dB, 1-dB bandwidth of 36 nm, and back reflection of -24 dB have been obtained.

CLEO: Applications & Technology

AM1J • Light Sources and Devices for Biomedical Imaging I—Continued

AM1J.3 • 08:45

Sensitive and Selective Detection of Prostate Specific Antigen beyond ELISA Using Photonic Crystal Nanolaser, Shoji Hachuda¹, Takumi Watanabe¹, Daichi Takahashi¹, Toshihiko Baba¹; ¹Electrical and computer engineering, Yokohama National Univ., Japan. We sensitively detected prostate specific antigen (PSA) using photonic crystal nanolaser sensors. In pure water and impure sample including 1 μ M BSA, we detected <100 fM PSA, which is lower than the limit of ELISA.

AM1J.4 • 09:00

4.4 nJ, 114 fs Nd-doped Fiber Laser Pulses at 920nm for in Vivo Two-photon Microscopic Imaging, Bingying Chen¹, Tongxiao Jiang¹, Weijian Zong^{1,2}, Fuzeng Niu¹, Liangyi Chen¹, Zhigang Zhang¹, Yanrong Song³, Aimin wang¹; ¹Peking Univ., USA; ²China Dept. of Cognitive Sciences, Inst. of Basic Medical Sciences, China; ³Beijing Univ. of Technology, School of Applied Science, China. We optimized pre-chirp in an Nd-doped fiber amplifier to achieve high-quality femtosecond 920 nm pulses. The *in vivo* zebrafish imaging proves the laser amplifier an ideal source in two-photon microscopic imaging.

AM1J.5 • 09:15

Highly Compact, Low-Noise All-Solid-State Laser System for Stimulated Raman Scattering Microscopy, Tobias Steine¹, Vikas Kumar², Andy Steinmann¹, Marco Marangoni², Giulio Cerullo², Harald W. Giessen¹; ¹4th Physics Inst., Univ. of Stuttgart, Germany; ²IFN-CNR, Dipartimento di Fisica, Politecnico di Milano, Italy. We present a simple, compact and very robust laser source for low-noise stimulated Raman scattering microscopy using a single-stage optical parametric amplifier seeded with tunable cw radiation from an external-cavity diode laser.

AM1K • Microprocessing Ultra-Fast Processing of Dielectrics—Continued

AM1K.3 • 08:45

Femtosecond laser cutting of glass by controlled fracture propagation, Clemens Hoenninger¹, Konstantin Mishchik², Clémentine Javaux³, Ophélie Dematteo-Caulier², Stefan Skupin², Benoit Chimier², Guillaume Duchateau², Antoine Bourgeade⁴, Rainer Kling³, Amélie Letan¹, Eric Mottay¹, John Lopez²; ¹Amplitude Systemes, France; ²Université Bordeaux, CNRS, CEA, CELIA UMR5107, France; ³Alphanov, France; ⁴CEA, France. We present the use of a compact femtosecond laser with 300-fs pulse duration and pulse energy on the order of 10s of μ J for the cutting of glass by controlled fracture propagation.

AM1K.4 • 09:00 **Invited**

Microfabrication of Ion Trap Platforms with Integrated Optics and Three-dimensional Electrodes, Mark Dugan¹, Chris Schenck¹, Ali Said¹, Philippe Bado¹; ¹Translume Inc., USA. We discuss a laser-based process to fabricate three-dimensional electromagnetic microtraps on silica platforms. Design flexibility for extended electrode geometries with a high degree of optical access and component intergration is supported by this fabrication process.

CLEO: Science & Innovations

SM1L • Fiber Sensing and Measurement—Continued

SM1L.3 • 08:45

Distributed Temperature and Strain Discrimination Using a Few-Mode Fiber, An Li¹, Yifei Wang^{1,2}, Jian Fang¹, William Shieh¹; ¹Univ. of Melbourne, Australia; ²National ICT Australia, Australia. We propose a novel method for distributed measurement of temperature and strain using a few-mode fiber (FMF). High discrimination accuracies of 0.115 °C and 0.283 μ m are achieved, under a spatial resolution of 2.5 m.

SM1L.4 • 09:00

Simultaneous Measurement of Strain and Temperature using High Sensitivity Multicore Fiber Sensors, Amy Van Newkirk¹, Enrique Antonio-Lopez¹, Guillermo Salceda-Delgado^{1,2}, Mohammad Umar Piracha³, Rodrigo Amezcu-Correa¹, Axel Schulzgen¹; ¹Univ. of Central Florida, USA; ²CIO, Centro de Investigaciones en Optica, Mexico; ³FAZ Technology Inc., USA. We demonstrate strain sensors consisting of multicore fiber spliced between two single mode fibers, with increased sensitivity to a factor of 12x a standard FBG. Simultaneous decoupling of strain and temperature measurements are also demonstrated.

SM1L.5 • 09:15

Fiber Optic Sensors Based on Orbital Angular Momentum, Robert Niederritter¹, Mark E. Siemens², Juliet Gopinath³; ¹Dept. of Physics, Univ. of Colorado, USA; ²Dept. of Physics and Astronomy, Univ. of Denver, USA; ³Dept. of Electrical, Computer, and Energy Engineering, Univ. of Colorado, USA. Fiber optic sensors based on orbital angular momentum (OAM) have unexplored potential. We propose a design for an OAM-based fiber sensor and analyze its ability to measure changes in strain and temperature.

CLEO Mobile App

Use the conference app to plan your schedule; view program updates; receive special events reminders and access Technical Papers (*separate log-in required*).

- Go to www.cleoconference.org/app.
- Select the Apple App Store or Google Play link.
- Download the app.
- Log in to use app features such as contacting fellow conference attendees—using your registration I.D. and email address.

CLEO: Science & Innovations

SM1M • Parametric
Processing—Continued

SM1M.2 • 09:00

Optical phase lock loop circuit for Non-degenerate optical parametric phase sensitive amplifiers with wide signal-idler optical frequency spacing, Yasuhiro Okamura¹, Koryo Higashiyama¹, Masafumi Koga², Atsushi Takada¹; ¹The Univ. of Tokushima, Japan; ²Oita Univ., Japan. Optical phase lock loop circuit for non-degenerate parametric phase sensitive amplifiers with wide signal-idler light frequency spacing is proposed. The proof-of-principle experiment is successfully demonstrated for 40-GHz spaced signal-idler lights using 5-GHz beat signals.

SM1M.3 • 09:15

Multichannel Wavelength Multicasting for QAM Signals Free of Pump-Phase-Noise using Flexible Coherent Multi-Carrier Pumping, Guo-Wei Lu^{2,1}, Takahide Sakamoto¹, Tetsuya Kawanishi¹; ¹Natl. Inst. of Info. & Comm. Tech., Japan; ²Tokai Univ., Japan. We propose and demonstrate pump-phase-noise-free 2-to-7 multichannel wavelength multicasting for QAM signals using flexible coherent multi-carrier pump. <0.4dB penalty is obtained after multicasting with the proposed scheme even using 3-MHz-linewidth DFB laser as pump source.

SM1N • Symposium on
Remote Atmospheric Lasing I—
ContinuedSM1N.3 • 09:00 **Invited**

How Do Basic Nonlinear Optical Processes Lead to Atmospheric Lasing?, Robert W. Boyd^{1,2}; ¹Dept. of Physics, Univ. of Ottawa, Canada; ²Inst. of Optics, Univ. of Rochester, USA. We review some of the experimental observations of atmospheric lasing and describe how basic nonlinear optical processes such as self-focusing, beam filamentation, amplified spontaneous emission and super-radiance could lead to some of this behavior.

SM1O • Advanced
Spectroscopic Techniques—
Continued

SM1O.4 • 09:00

Background-Free Heterodyne Photoexpansion Infrared Nanospectroscopy, Feng Lu¹, Mingzhou Jin¹, Mikhail A. Belkin¹; ¹Univ. of Texas at Austin, USA. The unwanted photoacoustic pressure force in photoexpansion spectroscopy, which comes from light absorption of the sample not below the AFM tip, was suppressed at the heterodyne frequency of laser pulses and piezo-driven cantilever oscillation.

SM1O.5 • 09:15

Large Amplitude Wavelength Modulation Spectroscopy for Sensitive Measurements of Broad Absorbers, Torrey Hayden¹, Paul Schroeder¹, Gregory B. Rieker¹; ¹Univ. of Colorado at Boulder, USA. We demonstrate wavelength modulation spectroscopy of CO₂ at >30 atm using a fast-scanning MEMS laser. The technique shows promise for sensitive measurements of species with broadband absorption features, such as high-pressure gases and large molecules.

SM1P • Few-cycle Infrared
Sources—Continued

SM1P.4 • 08:45

Millijoule 1-ps Pulses from a kHz Ho:YAG Regenerative Amplifier Seeded with a Tm,Ho-Fiber Laser, Pavel Malevich¹, Tsuneto Kanai¹, Heinar Hoogland^{3,4}, Ronald Holzwarth^{3,5}, Andrius Baltuska^{1,2}, Audrius Pugzlys^{1,2}; ¹Vienna Univ. of Technology, Austria; ²Center for Physical Sciences & Technology, Lithuania; ³Menlo Systems GmbH, Germany; ⁴Dept. of Physics, Univ. of Erlangen-Nuremberg, Germany; ⁵Max-Planck-Inst. of Quantum Optics, Germany. We demonstrate a 2090-nm 1-ps MOPA based on a Tm,Ho-fiber laser seeder and a Ho:YAG regenerative amplifier delivering 1.25-mJ pulses at a repetition rate of 1-kHz as a prospective driver laser for mid-IR frequency conversion.

SM1P.5 • 09:00

Ultrastable and High-Power Yb: Fiber Amplifier for Nonlinear Frequency Conversion at High Repetition Rate, Patrick Storz¹, Marcel Wunram¹, Daniele Brida¹, Alfred Leitenstorfer¹; ¹Dept. of Physics, Univ. of Konstanz, Germany. We demonstrate an ultrastable Yb: fiber amplifier delivering 145 fs pulses with 6 μ J energy at 10 MHz repetition rate. The Er: fiber seed laser provides inherently synchronized broadband continua whose power is boosted via optical parametric amplification.

SM1P.6 • 09:15

Coherent Mid-IR Supercontinuum Generation in a Hydrogenated Amorphous Silicon Waveguide, Hongcheng Sun¹, Ke-Yao Wang¹, Reza Salem², Peter Fendel², Amy C. Foster¹; ¹Johns Hopkins Univ., USA; ²Thorlabs Inc., USA. A 790-nm wide Mid-IR supercontinuum generation, spanning from 1.63 μ m to 2.42 μ m, is demonstrated in a hydrogenated amorphous silicon waveguide. The pump source is a 160-fs Thulium doped fiber laser centered at 1910 nm.

CLEO: QELS-Fundamental Science

FM1A • Quantum Metrology
and Measurement—Continued

FM1A.4 • 09:30

Quantum Refractometer, Anna Paterova¹, Dmitry Kalashnikov¹, Sergei Kulik², Leonid A. Krivitsky¹; ¹Data Storage Inst., Singapore; ²Dept. of Physics, Lomonosov Moscow State Univ., Russia. We exploit interference of two Parametric Down Conversion (PDC) sources to observe infrared resonances of CO₂. Frequency correlations of PDC enable determination of the refractive index at IR wavelengths with visible range optics and photodetectors.

FM1A.5 • 09:45

Experimental Demonstration of Quantum Sensing in the Presence of Quantum Decoherence, Zheshen Zhang¹, Sara Mouradian¹, Franco N. Wong¹, Jeffrey Shapiro¹; ¹MIT, USA. We report the first experimental demonstration of an entanglement-enhanced sensing system that is resilient to environmental loss and noise.

FM1B • Exciton Dynamics
in 1D/2D Nanostructures—
Continued

FM1B.7 • 09:30

Terahertz Magneto-spectroscopy of Quantum Wells: Stability of High-Density Excitons in High Magnetic Fields, Qi Zhang¹, Weilu Gao¹, John Watson², Michael Manfra², Junichiro Kono¹; ¹Rice Univ., USA; ²Purdue Univ., USA. We study the dynamics of excitons in GaAs quantum wells via optical-pump/terahertz-probe spectroscopy in magnetic fields. We found that the 1s-2p intra-excitonic transition is robust at high magnetic fields even under high excitation fluences, indicating magnetically enhanced stability of excitons.

FM1B.8 • 09:45

Terahertz magneto-optical spectroscopy of two-dimensional hole and electron systems, Kamaraju Natarajan¹, Wei Pan², Ulf Ekenberg², Dejan M. Gvozdić⁴, stephane Boubanga-Tombet^{6,5}, Prashanth C. Upadhyaya^{1,6}, John Reno³, Antoinette J. Taylor¹, Rohit P. Prasankumar¹; ¹Center for Integrated nanotechnologies, Los Alamos National Laboratory, USA; ²Semiconsultants, Sweden; ³Sandia National Lab, USA; ⁴School of Electrical Engineering, Univ. of Belgrade, Serbia; ⁵Research Inst. of Electrical Communication, Tohoku Univ., Japan; ⁶Lab for Electro-Optics Systems Indian Space Research Organization, India. Terahertz magneto-optical spectroscopy on a two-dimensional hole gas reveal a nonlinear dependence on the applied magnetic field. This is due to its complex non-parabolic valence band structure, as verified by multiband Landau level theoretical calculations.

FM1C • Nonlinear
Metamaterials—Continued

FM1C.4 • 09:30

Enhanced Magnetic Second-Harmonic Generation from Resonant Metasurfaces, Sergey S. Kruk¹, Martin Weismann^{2,3}, Anton Bykov⁴, Evgeniy Mamonov⁴, Irina Kolmychek⁴, Tatiana Murzina⁴, Nicolae Panoiu², Dragomir N. Neshev¹, Yuri S. Kivshar¹; ¹Australian National Univ., Australia; ²Univ. College London, UK; ³Photon Design Ltd, UK; ⁴Moscow State Univ., Russia. We demonstrate enhancement of second-harmonic generation efficiency in resonant nanostructures supporting optically induced magnetic response. This is achieved through simultaneous excitation of electric and magnetic multipoles at the second-harmonic wavelength and their constructive interference.

FM1C.5 • 09:45

A new type of optical activity in a toroidal metamaterial, Tim Raybould¹, Vassili Fedotov¹, Nikitas Papsimakis¹, Ian Youngs², Wei Ting Chen³, Din Ping Tsai³, Nikolay Zheludev¹; ¹Univ. of Southampton, UK; ²DSTL, UK; ³National Taiwan Univ., Taiwan. We demonstrate experimentally and numerically the first ever observation of optical activity in a chiral metamaterial that is underpinned by the exotic resonant combination of an electric quadrupole and the elusive toroidal dipole.

FM1D • Accelerating Beams
& Beamshaping Application—
Continued

FM1D.7 • 09:30

Beam Shaping and Production of Vortex Beams in Coherent Raman Generation, Miaochan Zhi², Kai Wang³, Hua Xia¹, Alexandra Zhdanova¹, Maria Shutova¹, Alexei Sokolov¹; ¹Texas A&M Univ., USA; ²Biosystems and Biomaterials Division, National Inst. of Standards and Technology, USA; ³Dept. of Physics and JILA, Univ. of Colorado, USA. We explore the role of spatial shaping in nonlinear interactions of ultrafast laser beams. We investigate the coherent transfer of orbital angular momentum in PbWO₄ crystal by using two time-delayed linearly chirped infrared pulses.

FM1D.8 • 09:45

Visualizing Fast Molecular Dynamics by Coherent Feedback in an Optical Oscillator, Avi Pe'er¹, Igal Aharonovich¹; ¹Bar-Ilan Univ., Israel. We exploit the inherent mode competition in a laser resonator to solve in real time the major coherent control problem - how to shape a pulse that will dump a general wavepacket into a single target state.

10:00–10:30 Coffee Break, Concourse Level

NOTES

CLEO: QELS-
Fundamental ScienceFM1E • Symposium on Single-
photon Nonlinear Optics I—
Continued

FM1E.5 • 09:30 **Invited**
The Birth, Care, and Feeding of Cat States in Circuit QED: Quantum Jumps of Photon Parity, Robert Schoelkopf¹; ¹Yale Univ., USA. I will describe recent experiments where we store quantum information in Schrodinger cat states of a microwave cavity, and perform the first continuous observation of a quantum error syndrome, based on the photon number parity.

SM1F • Semiconductor Laser
Physics—Continued

SM1F.6 • 09:30
Suppressed Relaxation-Oscillation Dynamics in a DFB laser Monolithically Integrated with Weak Optical Feedback, Daan Lenstra¹, Domenico D'Agostino¹, Huib Ambrosius¹, Meint Smit¹; ¹Electrical Engineering, Eindhoven Univ. of Technology, Netherlands. We experimentally demonstrate a laser which operates under weak optical feedback, showing two broad regions of operation without relaxation-oscillation induced instabilities and where high side-mode suppression above 40 dB is maintained, irrespective of the feedback phase.

SM1F.7 • 09:45
Electrically pumped random lasing based on Au-ZnO nanowire Schottky junction, Fan Gao², Muhammad Morshed³, Sunayna Bashar³, Youdou Zheng², Shi Yi², Jianlin Liu¹; ¹Electrical and Computer Engineering, Univ. of California, USA; ²Nanjing Univ., China; ³Univ. of California, USA. Electrically pumped random lasing based on Au-ZnO nanowire Schottky junction diode is demonstrated. Good lasing behavior is achieved and excitonic recombination is responsible for lasing generation. It provides an alternative approach towards semiconductor random lasers.

CLEO: Science & Innovations

SM1G • Nanostructures—
Continued

SM1G.6 • 09:30
Flat metallic surface with sub-10-nm gaps using modified atomic-layer lithography, Dengxin Ji¹, Borui Chen¹, Xie Zeng¹, Tania Moein¹, Haomin Song¹, Qiaoqiang Gan¹, Alexander Cartwright¹; ¹State Univ. of New York at Buffalo, USA. We developed a novel atomic layer lithography procedure to fabricate large area flat metallic surfaces with sub-10-nm features, which is particularly useful for fabrication of nanostructures with strongly localized field enhancement.

SM1G.7 • 09:45
Investigation of the reflection and transmission of nano-scale gold films, Haoliang Qian¹, Yuzhe Xiao¹, Dominic Lepage¹, Zhao-wei Liu^{1,2}; ¹Dept. of Electrical and Computer Engineering, UC San Diego, USA; ²Materials Science and Engineering, UC San Diego, USA. The reflection and transmission of thin gold films with thickness varying from 2.5 nm to 30 nm are experimentally investigated. A theory is proposed and explains all experimental data.

SM1H • THz Quantum Cascade
Lasers—Continued

SM1H.6 • 09:30
Amplification of broadband terahertz pulses in a quantum cascade heterostructure, Juraj Darmo¹, Dominic Bachmann¹, Markus Roesch², Norbert Leder¹, Giacomo Scalari², Mattias Beck², Holger Arthaber¹, Jerome Faist², Karl Unterrainer¹; ¹Technische Universität Wien, Austria; ²ETH Zürich, Switzerland. We demonstrate an amplification of broadband terahertz pulses in the bandwidth of 500 GHz centered at 2.5 THz. The amplification is based on gain switched quantum cascade structure with the heterogeneous active region.

SM1H.7 • 09:45
A Hybrid Plasmonic Waveguide Terahertz Quantum Cascade Laser, Riccardo Degl'Innocenti¹, Yash Shah¹, Robert Wallis¹, Adam Klimont¹, Yuan Ren¹, David Jessop¹, Harvey Beere¹, David Ritchie¹; ¹Univ. of Cambridge, UK. We present a quantum cascade laser emitting around 2.9 THz, based on a new hybrid plasmonic waveguide design. The resultant optical mode provides a performance commensurate with a metal-metal waveguide, while improving the far-field pattern.

10:00–10:30 Coffee Break, Concourse Level



For Conference News & Insights
Visit blog.cleoconference.org

Meeting Room
211 B/D

CLEO: Science & Innovations

SM11 • Silicon Photonics—Continued

SM11.7 • 09:30

Sinusoidal Anti-coupling SOI Strip Waveguides, Fan Zhang¹, Han Yun¹, Valentina Donzella¹, Zeqin Lu¹, Yun Wang¹, Zhitian Chen¹, Lukas Chrostowski¹, Nicolas A. Jaeger¹; ¹Univ. of British Columbia, Canada. We experimentally demonstrate sinusoidal anti-coupling silicon-on-insulator strip waveguides, separated by 200 nm, that have a minimum inter-waveguide crosstalk suppression of 26.8 dB within the C-band for the fundamental transverse electric mode.

SM11.8 • 09:45

Asymmetric-waveguide-assisted 3-dB Broadband Directional Coupler, Zeqin Lu¹, Han Yun¹, Yun Wang¹, Zhitian Chen¹, Fan Zhang¹, Nicolas A. Jaeger¹, Lukas Chrostowski¹; ¹Univ. of British Columbia, Canada. We demonstrate 3-dB broadband directional couplers that use asymmetric-waveguide-based phase compensation. Average coupling ratios of 46.57% and 48.28% were obtained from 1500 nm to 1600 nm for transverse electric and transverse magnetic modes, respectively.

Meeting Room
212 A/C

CLEO: Applications & Technology

AM11J • Light Sources and Devices for Biomedical Imaging I—Continued

AM11J.6 • 09:30

High Power 780 nm Femtosecond Fiber Laser, Zuosheng Liu¹, Weijian Zong^{2,3}, Yizhou Liu¹, Lijun Zuo¹, Cai Wen¹, Tongxiao Jiang¹, Jian Zhang¹, Yuxuan Ma¹, Zhigang Zhang¹, Liangyi Chen¹, Aimin wang¹; ¹Peking Univ., China; ²The State Key Lab of Biomembrane and Membrane Biotechnology, Inst. of Molecular Medicine, China; ³China Dept. of Cognitive Sciences, Inst. of Basic Medical Sciences, China. We demonstrate an 880 mW 780 nm femtosecond laser based on a high-order dispersion compensated Er-doped fiber laser and frequency doubling. It has been used on a two-photon three-axis digital scanned light-sheet microscopy.

AM11J.7 • 09:45

A Six-Color Four Laser Mobile Platform for Multi-Spectral Fluorescence Imaging Endoscopy, John F. Black¹, Tyler Tate², Molly Keenan³, Elizabeth Swan², Urs Utzinger³, Jennifer Barton³; ¹Glannaventa, Inc., USA; ²College of Optical Sciences, Univ. of Arizona, USA; ³Biomedical Engineering, Univ. of Arizona, USA. A Q-switched alexandrite laser is frequency doubled and tripled to the ultraviolet, combined with 3 visible wavelengths, and fiber coupled to form the illumination source for a micro-endoscope designed for minimally invasive ovarian cancer screening.

Meeting Room
212 B/D

AM1K • Microprocessing Ultra-Fast Processing of Dielectrics—Continued

AM1K.5 • 09:30 **Invited**

Laser Processing of Optofluidic Devices for Lab-on-a-chip and Lab-in-fiber, Peter R. Herman¹; ¹Univ. of Toronto, Canada. Ultrafast laser 3D structuring enables fiber cladding circuits and optofluidic microsystems to form and integrate seamlessly inside optical fiber. Efficient coupling with the fiber core waveguide opens prospects for ubiquitous sensing networks and smart catheters.

Marriott
Salon I & II

CLEO: Science & Innovations

SM1L • Fiber Sensing and Measurement—Continued

SM1L.6 • 09:30

Optical manipulation of microparticles using graded-index fiber taper and its microfluidic sensing application, Yuan Gong¹, Chenlin Zhang¹, Yunjiang Rao¹; ¹Univ of Electronic Science & Tech China, China. Contactless optical manipulation of microparticles is demonstrated based on graded-index multimode fiber taper, which is further applied for microfluidic flow rate sensing. The manipulation length can be as long as 177.0 μm.

SM1L.7 • 09:45

Elongated abruptly tapered micro fiber interferometer for nanoparticles attraction and analyses, Nan-Kuang Chen¹, Zhao-Ying Chen¹, Kuan-Yu Lou¹, Wood-Hi Cheng², Chin-Lon Lin³; ¹National United Univ., Taiwan; ²National Chung Hsing Univ., Taiwan; ³Bell Labs and Bellcore, USA. The nanoparticle analyses based on elongated-abruptly-tapered microfiber interferometer. The charged nanoparticles generating from incomplete combustion of carbon-containing compounds are stringently attached onto micro interferometer at equal distance separation to analyze nanoparticle sizes.

10:00–10:30 Coffee Break, Concourse Level



Join the conversation. Use #CLEO15.
Follow us @cleoconf on Twitter.

CLEO: Science & Innovations

SM1M • Parametric Processing—Continued

SM1M.4 • 09:30
Broadband Counter-Phase Dithering of Multi-Terabit/s DP-QPSK Signals for Low Noise FWM with a Single CW Pump, Mark D. Pelusi¹, Karen Solis-Trapala², Hung Nguyen Tan², Takashi Inoue², Shu Namiki²; ¹School of Physics, Univ. of Sydney, Australia; ²National Inst. of Advanced Industrial Science and Technology (AIST), Japan. Counter-phase modulation of WDM 24x100Gb/s DP-QPSK channels in a polarization-insensitive fiber-loop is demonstrated for low noise degenerate four-wave mixing with a CW pump. The OSNR is boosted by »9dB enabling an average »4dB Q²-factor improvement.

SM1N • Symposium on Remote Atmospheric Lasing I—Continued

SM1N.4 • 09:30
Low-threshold bidirectional air lasing, Alexandre Laurain¹, Maik Scheller¹, Pavel G. Polynkin¹; ¹Univ. Of Arizona, USA. We demonstrate directional forward and backward emission from atmospheric oxygen and nitrogen pumped by a tunable deep-UV laser source. Significant emission enhancement is achieved, in both cases, through pre-dissociation by an additional IR laser pulse.

SM1O • Advanced Spectroscopic Techniques—Continued

SM1O.6 • 09:30
Fourier-Transform-Based Noise-Immune Cavity-Enhanced Optical Frequency Comb Spectroscopy, Amir Khodabakhsh¹, Alexandra C. Johansson¹, Lucile Rutkowski¹, Aleksandra Foltynowicz-Matyba¹; ¹Dept. of Physics, Umeå Univ., Sweden. We achieve absorption sensitivity of $6.4 \times 10^{-11} \text{ cm}^{-1} \text{ Hz}^{-1/2}$ per spectral element with near-infrared Fourier-transform-based noise-immune cavity-enhanced optical frequency comb spectroscopy (NICE-OFCS), which allows detection of CO₂ at ppb concentration levels.

SM1O.7 • 09:45
Photo-thermal Effects in Gases as a Method For Concentration Measurements, Karol Krzempek¹, Michal P. Nikodem², Krzysztof M. Abramski¹; ¹Laser&Fiber Electronics Group Wroclaw Univ. of Technology, Poland; ²Wroclaw Research Center EIT+, Poland. We present preliminary results on using photo-thermal effects for gas composition analysis. Proof-of-concept experiments will be discussed and several unique detection schemes will be presented.

SM1P • Few-cycle Infrared Sources—Continued

SM1P.7 • 09:30
220-fs 110-mJ Yb:CaF₂ Cryogenic Multi-pass Amplifier, Giedrius Andriukaitis¹, Edgar Kaksis¹, Gyula Polonyi³, József Fülöp⁴, Andrius Baltuska^{1,2}, Audrius Pugzlys^{1,2}; ¹Vienna Univ. of Technology, Austria; ²Center for Physical Sciences & Technology, Lithuania; ³MTA-PTE High-Field Terahertz Research Group, Hungary; ⁴Univ. of Pécs, Hungary. We report on the design and performance of a Yb:CaF₂ booster with a pass-by-pass compensated spatial gain narrowing. A 5-concave-mirror design affords a flexible number of passes as well as 4f-image relay and progressive beam magnification onto the laser crystal.

SM1P.8 • 09:45
An Approach for Intense Subcycle Pulse Generation in Air, Yuichiro Kida¹, Totaro Imasaka¹; ¹Kyushu Univ., Japan. Four-wave mixing in air is employed for the generation of energetic multicolor femtosecond pulses. After the subsequent propagation in air, the multicolor emissions are phase locked to each other to form intense subcycle laser pulses.

10:00–10:30 Coffee Break, Concourse Level

NOTES

CLEO: QELS-Fundamental Science

10:30–12:30

FM2A • Single Photon Sources

Presider: Aephraim Steinberg;
Univ. of Toronto, Canada

FM2A.1 • 10:30

Ultra-pure single-mode photon generation in high-Q silicon microdisks, Xiyuan Lu¹, Wei Jiang¹, Jidong Zhang¹, Qiang Lin¹; ¹Univ. of Rochester, USA. We report ultra-pure single-mode photon generation through four-wave mixing in high-Q silicon microdisks. The cross correlation of photon pairs peaks over 25,000 and the self-correlations of both photon modes peak around 1.8.

FM2A.2 • 10:45

Efficient Single Photon Generation using a Fiber-integrated Diamond Micro-Waveguide, Rishi Patel^{1,2}, Tim Schroder², Noel Wan², Luozhou Li², Sara Mouradian², Edward Chen², Dirk R. Englund²; ¹Stanford, USA; ²MIT, USA. We demonstrate the efficient coupling of a diamond micro-waveguide containing a single nitrogen-vacancy center to a single mode optical fiber. Strong photon anti-bunching is observed with a raw single-photon count rate exceeding 712,000 Hz.

FM2A.3 • 11:00

Enhancing the heralded single photon rate from a silicon photonic chip by pump pulse interleaving, Jiakun He¹, Xiang Zhang¹, Iman Jizan¹, Alex Clark¹, Duk-Yong Choi², Chang Joon Chae³, Benjamin J. Eggleton¹, Chunle Xiong¹; ¹School of Physics, Univ. of Sydney, Australia; ²Laser Physics Centre, Australian National Univ., Australia; ³Advanced Photonics Research Inst., Gwangju Inst. of Science and Technology, Korea. We demonstrate heralded single photon source on a silicon photonic chip by a pump interleaving technique. We have achieved 90±5% enhancement to single photon rate with only 14±2% reduction in quantum signal to noise ratio.

FM2A.4 • 11:15

Pure Heralded Single photons, Annamaria Dosseva², Lukasz Cincio¹, Agata Branczyk¹; ¹Perimeter Inst. for Theoretical Physics, Canada; ²Univ. of Waterloo, Canada. We show an order-of-magnitude increase in the spectral purity of heralded single photons by engineering the joint spectrum of downconverted photon-pairs. We do this by customizing the crystal poling configuration using simulated annealing.

10:30–12:30

FM2B • Ultrafast Dynamics in Quantum Dots and Organic Materials

Presider: Kamaraju Natarajan; Los Alamos National Lab, USA

FM2B.1 • 10:30

Femtosecond coherent nano-spectroscopy of coupled molecular dynamics, Joanna M. Atkin¹, Paul Sass¹, Honghua Yang¹, Paul Teichen², Joel Eaves², Markus B. Raschke^{1,2}; ¹Physics, Univ. of Colorado, USA; ²Chemistry, Univ. of Colorado, USA. We isolate the vibrational free-induction decay of a homogeneous molecular sub-ensemble using ultrafast infrared scattering-scanning near-field microscopy. The observed long lifetimes, intramolecular coherence transfer, and spatial variations in vibrational modes indicate non-ergodic behavior.

FM2B.2 • 10:45

Nanoscale Transport of Excitons at the Interface Between ZnO and a Molecular Monolayer, sebastian friede¹, Sergei Kuehn¹, Sergey Sadofev², Sylke Blumstengel², Fritz Henneberger², Thomas Elsaesser¹; ¹Max-Born-Inst., Germany; ²Institut für Physik, Humboldt-Universität zu Berlin, Germany. Time-resolved near-field optical microscopy maps exciton transport in a hybrid system. Within the 100 ps photoluminescence lifetime, an equilibrium distribution of surface and bound excitons displays lateral diffusion on a 50 nm length scale.

FM2B.3 • 11:00

Single Molecular Vibrational Relaxation Dynamics and Adsorbate Fluctuation, Kyoung-Duck Park¹, Vasily Kravtsov¹, Paul Sass¹, Joanna M. Atkin¹, Eric A. Muller¹, Markus B. Raschke¹; ¹Univ. of Colorado Boulder, USA. Tip-enhanced Raman spectroscopy at cryogenic temperatures probes the intrinsic linewidths of vibrational modes. Temperature dependence in small ensembles reveals ultrafast vibrational relaxation dynamics, conformational heterogeneity, and single molecule fluctuation on the seconds time scale.

FM2B.4 • 11:15

Probing Coherent Ultrafast Exciton Dissociation in a Polymer:Fullerene Photovoltaic Absorber, Antonietta De Sio¹, Ephraim Sommer¹, Margherita Maiuri², Julien Rehault², Carlo Andrea Rozzi³, Elisa Molinari³, Giulio Cerullo², Christoph Lienau¹; ¹Institut für Physik, Universität Oldenburg, Germany; ²Politecnico di Milano, Italy; ³CNR Centro S3, Italy. Combining high-time resolution optical spectroscopy and time-dependent density functional theory calculations, we provide strong evidence for the role of vibronic coupling in driving the initial steps of the current photogeneration in an organic photovoltaic system.

10:30–12:30

FM2C • Hyperbolic Metamaterials

Presider: Viktor Podolskiy; Univ. of Massachusetts Lowell, USA

FM2C.1 • 10:30

Mid-infrared Hyperbolic Metamaterial Based on Graphene-dielectric Multilayers, You-Chia Chang¹, Chang-Hua Liu¹, Che-Hung Liu¹, Zhaohui Zhong¹, Theodore B. Norris¹; ¹Univ. of Michigan, USA. We have designed and fabricated a mid-infrared hyperbolic metamaterial composed of alternating Al₂O₃ and chemical-vapor-deposited graphene. Infrared ellipsometry shows a topological transition from elliptical to hyperbolic dispersion at the wavelength of 7.4 μm.

FM2C.2 • 10:45

Thermal Radiation of Hyperbolic Metamaterials and Metallic Surfaces, Mikhail A. Noginov¹, Ahmad Mozafari¹, Thejaswi Tumkur¹, John Kitur¹, Evgenii Narimanov²; ¹Norfolk State Univ., USA; ²Purdue Univ., USA. We have studied angular distribution and spectra of thermal radiation of lamellar metal/dielectric metamaterials with hyperbolic dispersion and have found them to be reasonably close to the corresponding properties of simple metallic films.

FM2C.3 • 11:00

Optical Imaging with Photonic Hypercrystals, Zun Huang^{1,2}, Evgenii Narimanov^{1,2}; ¹School of Electrical and Computer Engineering, Purdue Univ., USA; ²Birck Nanotechnology Center, Purdue Univ., USA. We present an optical imaging system based on photonic hypercrystal, an artificial optical medium combining the properties of hyperbolic materials and photonic crystals. This system functions as a negative refraction lens with substantially reduced image aberrations.

FM2C.4 • 11:15

Light Emission in Nonlocal Plasmonic Nanowire Metamaterials, Brian Wells¹, Pavel Ginzburg², Anatoly V. Zayats², Viktor A. Podolskiy¹; ¹Univ Massachusetts Lowell, USA; ²Physics, King's College, UK. We analyze, analytically and computationally, light emission in nonlocal plasmonic nanowire metamaterials and analyze the contribution of longitudinal wave to the density of optical states in the system.

10:30–12:30

FM2D • Novel Optical Phenomena

Presider: Roberto Morandotti; INRS-Energie Mat & Tele Site Varennes, Canada

FM2D.1 • 10:30

Nonlinear Transmission of Light Through Biological Suspensions, Anna Bezyradina¹, Graham Siggins¹, Andrew Kalmbach², Edward Carpenter², Zhigang Chen^{1,3}; ¹Physics and Astronomy, San Francisco State Univ., USA; ²Romberg Tiburon Center for Environmental Studies, San Francisco State Univ., USA; ³TEDA Applied Physics Inst. and School of Physics, Nankai Univ., China. We study nonlinear light propagation through suspensions of *Synechococcus* cells. Such cyanobacteria in aqueous solution enable self-focusing or -defocusing of a light beam, leading to controlled transmission despite extremely low absorption and weak polarizability.

FM2D.2 • 10:45

Rapid Manipulation of the Spatial Coherence, Ronen Chriki¹, Micha Nixon¹, Vishwa Pal¹, Chene Tradonsky¹, Gilad Barach¹, Asher A. Friesem¹, Nir Davidson¹; ¹Physics of Complex Systems, Weizmann Inst. of Science, Israel. Efficient method for manipulating the spatial coherence of a laser is presented. Different mutual intensity coherence functions, such as cosine or Bessel functions, are obtained, and number of modes is controlled in 1D and 2D.

FM2D.3 • 11:00

Total Internal Reflection in Gain Media, Hanan Herzog Sheinfux¹, Bo Zhen^{1,2}, Ido Kamirer^{1,2}, Mordechai Segev¹; ¹Technion Israel Inst. of Technology, Israel; ²MIT, USA. We resolve the controversy around total internal reflection from gain media, propose new effects of (extremely) amplified reflection from a single interface, and show sensitivity to subwavelength features.

FM2D.4 • 11:15

CW Laser Light Condensation, Michael Zhuravov¹, Alexander Bekker¹, Boris Levit¹, Rafi Weill¹, Baruch Fischer¹; ¹Technion Israel Inst. of Technology, Israel. We present a first experimental demonstration of classical CW laser condensation in the frequency (mode) domain. It also sheds light on the general question of photon-BEC (Bose-Einstein condensation) in laser cavities.

CLEO: QELS-
Fundamental Science

10:30–12:30

FM2E • Symposium on Single-photon Nonlinear Optics II

Presider: Sergey Polyakov; NIST, USA

FM2E.1 • 10:30 **Invited**

Nonlinear Optics via Hybrid Quantum Systems, Xunnong Xu², Haitan Xu², Michael Gullans^{1,2}, Corey Stambaugh¹, Utku Kemiktarak², John Lawall¹, Jacob Taylor^{1,2}; ¹NIST, USA; ²Joint Quantum Inst., USA. Realization of a quantum optical nonlinearity at the single-photon level remains an outstanding challenge. Here we consider optomechanical and microwave-domain approaches for such nonlinearities, and develop applications in quantum sensing and simulation.

FM2E.2 • 11:00

Fluorescent Nanodiamonds from Molecular Diamond Seed, Hitoshi Ishiwata¹, Jingyuan Linda Zhang¹, Robert Edgington¹, Thomas M. Babinec¹, Kai Muller¹, Konstantinos G. Lagoudakis¹, Nicholas Melosh¹, Zhi-Xun Shen¹, Jelena Vuckovic¹; ¹Stanford Univ., USA. We present a new materials growth technique using diamondoid molecular diamonds as a seed for chemical vapor deposition growth. We show that both nanoscopic high quality diamond crystals with silicon vacancy color centers can be grown from self-assembled monolayers of pentamantane (C₂₆H₃₂).

FM2E.3 • 11:15

On-Chip generation of photon-triplet states in integrated waveguide structures, Stephan Krapick¹, Benjamin Brecht¹, Viktor Quiring¹, Raimund Ricken¹, Harald Herrmann¹, Christine Silberhorn¹; ¹Physics Dept., Univ. of Paderborn, Germany. We present a miniaturized integrated waveguide source providing 11.3±0.7 photon-triplet states per hour, measured with off-the-shelf components. By double-stage heralding and integration times of 83 hours, we achieve statistical significance of more than 27 σ .

10:30–12:30

SM2F • Novel Materials for Semiconductors Lasers

Presider: Peter Smowton; Cardiff Univ., UK

SM2F.1 • 10:30 **Invited**

Room-temperature lasing in GaAs nanowires embedding multi-stacked InGaAs/GaAs quantum dots, Jun Tatebayashi², Satoshi Kako², Jinfa Ho², Yasutomo Ota², Satoshi Iwamoto^{2,1}, Yasuhiko Arakawa^{2,1}; ¹IIS, the Univ. of Tokyo, Japan; ²NanoQUINE, the Univ. of Tokyo, Japan. We report the demonstration of room-temperature lasing in a single GaAs nanowire embedding 50-stacked In_{0.22}Ga_{0.78}As/GaAs quantum dots at a lasing emission energy of 1.37 eV with a threshold pump pulse fluence of 138 $\mu\text{J}/\text{cm}^2$.

SM2F.2 • 11:00

Nonpolar InGaN/GaN multi-quantum-well core-shell nanowire lasers, Changyi Li¹, Jeremy B. Wright², Sheng Liu^{2,3}, ping lu², Jeffrey Figiel², Benjamin Leung², Ting S. Luk^{2,3}, Igal Brener^{2,3}, Daniel Feezell¹, Steven Brueck¹, George Wang²; ¹Center for High Technology Materials, Univ. of New Mexico, USA; ²Sandia National Labs, USA; ³Center for Integrated Nanotechnology, Sandia National Labs, USA. Lasing is demonstrated from nonpolar III-nitride core-shell multi-quantum-well nanowires. The nanowire lasers were fabricated by coupling a top-down and bottom-up methodology and achieved lasing at wavelengths below the GaN bandedge.

SM2F.3 • 11:15

A novel, highly-strained structure with an integrated optical cavity for a low threshold germanium laser, Shashank Gupta¹, Donguk Nam¹, Jan Petykiewicz¹, David Sukhdeo¹, Jelena Vuckovic¹, Krishna Saraswati¹; ¹Stanford Univ., USA. We propose a novel low threshold, CMOS-compatible laser structure with a strained germanium gain medium and a photonic crystal cavity. We demonstrate 1.70% uniaxial tensile strain through experiments and design a high quality factor (>11,000) optical cavity around the gain medium.

CLEO: Science & Innovations

10:30–12:30

SM2G • Characterization Techniques

Presider: Avi Zadok; Bar-Ilan Univ., Israel

SM2G.1 • 10:30

Improvement for characterizing micro-ring resonator by low coherence interferometry measurement, Wei Kang Liu¹, Chun Yen Chen¹, Chia Chien Wei¹, Yung-Jui Chen¹; ¹National Sun-Yat-sen Univ., Taiwan. We demonstrate an effective technique which allows one to characterize a small radius micro-ring resonator via low coherence interferometric measurement beyond light source bandwidth limitation. The experimental results show significant improvements in the extracted parameters.

SM2G.2 • 10:45

Efficient Coefficient Extraction from Doublet Resonances in Microphotonic Resonator Transmission Functions, Adam Jones^{1,2}, Anthony L. Lentine¹, Christopher T. DeRose¹, Starbuck L. Andrew¹, Pomerene Andrew¹, Robert Norwood²; ¹Sandia National Labs, USA; ²Optical Sciences, Univ. of Arizona, USA. We develop a computationally efficient and robust algorithm to automatically extract the coefficients of doublet resonances and apply this technique to 418 resonances in ring resonator transmission data with a mean RMS deviation of 7.28×10^{-4} .

SM2G.3 • 11:00

Verdet Constant and Magnetic Permeability in Microstructured FePt Nanoparticles in PS-P2VP Copolymer Composite Films, Alex Miles¹, Palash Gangopadhyay¹, Yue Gai², Xinyu wang², James Watkins², Robert Norwood¹; ¹Univ. of Arizona, USA; ²Dept. of Polymer Science and Engineering, Univ. of Massachusetts Amherst, USA. Complex Faraday effect and magnetic permeability measurements on iron-platinum (FePt) nanoparticles embedded in a polystyrene-poly(2-vinyl)pyridine (PS-P2VP) copolymer matrix are reported. Possible applications include high performance biomagnetic field sensors and optical isolators.

SM2G.4 • 11:15

Diffusion Characterization Using Electron Beam Induced Current and Time-Resolved Photoluminescence of InAs/InAsSb Type-II Superlattices, Daniel Zuo¹, Runyu Liu¹, Dan Wasserman¹, James Mabon², Zhaoyu He³, Shi Liu³, Yong-Hang Zhang³, Emil A. Kadlec⁴, Benjamin V. Olson⁴, Eric A. Shaner⁴; ¹Dept. of Electrical and Computer Engineering, Univ. of Illinois at Urbana-Champaign, USA; ²Fredrick Seitz Materials Research Lab, Univ. of Illinois at Urbana-Champaign, USA; ³Center for Photonics Innovation and School of Electrical, Computer, and Energy Engineering, Arizona State Univ., USA; ⁴Sandia National Labs, USA. We present the characterization of minority carrier diffusion length and surface recombination velocity, as well as vertical diffusivity and mobility by performing an electron beam induced current measurement in addition to an optical lifetime measurement.

10:30–12:30

SM2H • Strong-Field THz Science and Technology

Presider: Koichiro Tanaka; Kyoto Univ., Japan

SM2H.1 • 10:30 **Tutorial**

Nonlinear THz Optics and Control in Complex Solids, Andrea Cavalleri^{1,2}, Matthias Hoffmann³; ¹Max Planck Inst. for the Structure and Dynamics of Matter, Germany; ²Dept. of Physics, Univ. of Oxford, UK; ³Stanford Linear Accelerator Laboratory, USA. I will discuss nonlinear interaction between THz light and matter. Especially, I will discuss the nonlinear response of infrared active phonons and superconducting plasmons in High T_c cuprates.



Matthias Hoffmann received his Diplom (2001) and PhD (2006) in physics at the University of Freiburg, Germany. As a postdoc at the Massachusetts Institute of Technology he developed intense THz sources for nonlinear spectroscopy. He then moved to the newly founded Max Planck Institute for Structure and Dynamics of Matter in Hamburg, Germany where his research was focused on interactions of strong THz fields with correlated electron systems such as high temperature superconductors. Since 2011 he is a staff scientist at the Stanford Linear Accelerator Laboratory where he explores non-equilibrium states of matter with femto-second x-ray pulses.

Meeting Room
211 B/D

CLEO: Science &
Innovations

10:30–12:30

SM21 • Silicon Photonic Systems

President: Chin-Hui (Janet) Chen;
Hewlett Packard Company, USA

SM21.1 • 10:30 **Invited**

Integrated Hardware-Software Implementation of Silicon Photonic Interconnected Computing System, Keren Bergman¹; ¹Columbia Univ., USA. Silicon photonics interconnect technology can potentially deliver computing systems energy efficient data movement with extreme bandwidth densities. We discuss the first complete experimental silicon photonic interconnected hardware-software implementation that demonstrates the system-level performance benefits.

SM21.2 • 11:00

Active Resonance Wavelength Stabilization for Silicon Microring Resonators Using Slope-Detection with an In-resonator Defect-state-absorption-based Photodetector, Yu Li¹, Andrew W. Poon¹; ¹Photonic Device Lab, Dept. of Electronic and Computer Engineering, The Hong Kong Univ. of Science and Technology, China. We demonstrate active resonance wavelength stabilization for silicon microrings with an in-resonator BF_2 -implanted photodetector using a slope-detection method. Our experiment reveals active resonance wavelength stabilization with ~1dB transmission intensity variations upon a 7°C 10MHz modulation.

SM21.3 • 11:15

Photoresistive Microring Heater with Resonance Control Loop, Christopher V. Poulton¹, Po Dong¹, Young-Kai Chen¹; ¹Bell Labs, Alcatel-Lucent, USA. We demonstrate a germanium photoresistive microring heater that acts as a single device to sense and tune the resonant wavelength of the ring. A control loop to lock the resonance to a laser is shown.

Meeting Room
212 A/C

CLEO: Applications
& Technology

10:30–12:30

AM2J • Light Sources and
Devices for Biomedical
Imaging II

President: Seok-Hyun Yun; Harvard
Medical School, USA

AM2J.1 • 10:30

A Full-Field Tomographic Imaging Camera Based on a Linearly Swept Frequency DFB at 1064 nm, Mark Harfouche¹, Naresh Satyan², George Rakuljic², Amnon Yariv³; ¹Electrical Engineering, California Inst. of Technology, USA; ²Telaris Inc., USA; ³Applied Physics and Materials Science, California Inst. of Technology, USA. High resolution, full-field tomograms are acquired in four exposures of a CCD camera using a swept laser. The imaged depth is selected by modulating the swept laser output power enabling volumetric imaging with no moving parts.

AM2J.2 • 10:45

A Joint Richardson-Lucy Deconvolution Algorithm for the Reconstruction of Multifocal Structured Illumination Microscopy Data, Florian Stroehl¹, Clemens F. Kaminski¹; ¹Univ. of Cambridge, UK. We demonstrate the reconstruction of multifocal structured illumination microscopy images using a joint Richardson-Lucy deconvolution algorithm, which is based on an underlying widefield image-formation model and particularly well suited for noise corrupted data.

AM2J.3 • 11:00

Electron-injection Detectors for Swept Source Optical Coherence Tomography, Vala Fathipour¹, Hooman Mohseni¹; ¹Northwestern Univ., USA. Electron-injection detectors are used in an OCT system for the first time. Compared to a commercial p-i-n detector, electron-injection detectors show ~20 dB higher SNR. This could lead to OCT systems without the need for balanced-detection.

AM2J.4 • 11:15

Concentric Si Annular Photodiode Arrays for Spatially Resolved Diffuse Reflectance Spectroscopy, Ozlem Senlik¹, Nan M. Jokerst¹; ¹Electrical and Computer Engineering, Duke Univ., USA. This paper describes the design, fabrication, and test of a custom concentric PD array for spatially resolved diffuse reflectance (SRDR) measurements. To the best of our knowledge, this is the first reported compact, densely packed semiconductor SRDR probe.

Meeting Room
212 B/D

CLEO: Science &
Innovations

10:30–12:30

AM2K • Microprocessing Laser
Processing of Silicon and Other
Materials

President: Peter Herman; Univ. of
Toronto, Canada

AM2K.1 • 10:30 **Invited**

Industrial Processing of Various Materials using Ultrashort Pulsed Laser Sources, Dimitrij Walter¹; ¹MANZ, Germany. Micro machining using ultra short laser pulses renders high ablation quality along with superb precision. Due to a very short interaction time in combination with high power densities various applications such as cutting, patterning, marking etc. may be carried out on a wide range of materials from brittle to ductile. Implementing suitable laser sources along and its periphery in high-throughput industrial machinery is a key for efficient production facilities.

AM2K.2 • 11:00

Nonlinear Laser Lithography for Enhanced Tribological Properties, Iaroslav Gnilitzkiy¹; ¹UNIMORE, Italy. This paper investigates a new field for application of femtosecond laser-induced periodic surface structures (LIPSS). We designed an innovative solution to reduce coefficient of friction of mechanical parts by using the nonlinear laser lithography technique (NLL).

AM2K.3 • 11:15

Radially Polarized Optical Vortex Micro-Converters Imprinted by Femtosecond Laser Nanostructuring in Amorphous Silicon, Rokas Drevinskas¹, Martynas Beresna¹, Mindaugas Gecevicius¹, andrey G. kazanski², oleg I. konkov³, Yuri P. Svirko⁴, Peter Kazansky¹; ¹Univ. of Southampton, UK; ²M.V. Lomonosov Moscow State Univ., Russia; ³A.F. Ioffe Physico-technical Inst., Russia; ⁴Univ. of Eastern Finland, Finland. We demonstrate space variant polarization and phase converters imprinted by femtosecond laser nanostructuring in hydrogenated amorphous silicon thin film. Giant birefringence of imprinted structures allows fabrication of microoptical element arrays.

Marriott
Salon I & II

CLEO: Science &
Innovations

10:30–12:30

SM2L • Modes in Fiber

President: Ayman Abouraddy;
Univ. of Central Florida, CREOL,
USA

SM2L.1 • 10:30

Multiple-Cladding-Resonance All-Solid Photonic Bandgap Fibers with Large Mode Area, Guancheng Gu¹, Fanting Kong¹, Thomas W. Hawkins¹, Maxwell Jones¹, Liang Dong¹; ¹Clemson Univ., USA. We demonstrated both theoretically and experimentally robust single-mode operation in all-solid photonic bandgap fibers with record effective mode areas of ~2650 μm^2 by introducing multiple strongly coupled smaller cores in the cladding.

SM2L.2 • 10:45

Scaling the mode area of Rare-Earth doped step index fiber under current state of the art MCVD technology, Deepak Jain¹, Yongmin Jung¹, Pranabesh Barua¹, Shaiful Alam¹, Jayanta Sahu¹; ¹Univ. of Southampton, UK. We demonstrate an ultra-low-NA (~0.038) Yb-doped step-index-fiber fabricated using conventional MCVD and solution-doping process. The fiber ensures ~700 μm^2 A_{eff} for effective-single-mode operation and 81% laser efficiency with $M^2 \sim 1.1$ at a bend diameter of 32cm.

SM2L.3 • 11:00

Experimental Observation of Non-Linear Mode Conversion in Few-Mode Fiber, Jing Xu¹, George S. Gordon², Timothy Wilkinson², Christophe Peucheret³; ¹Huazhong Univ. of Sci. and Tech., China; ²Engineering Dept., Electrical Engineering Division, UK; ³CNRS UMR 6082, Foton Lab, France. We show for the first time directly experimentally observed nonlinear spatial mode coupling in a 10 km long graded-index few-mode fiber.

SM2L.4 • 11:15

Reconstructing Core-to-Core Variations of Propagation Constant in Coupled Multicore Fiber for Quantum Walks, Peter J. Mosley¹, Itandehui Gris-Sanchez¹, James Stone¹, Robert Francis-Jones¹, Rowan A. Hoggarth¹, Douglas J. Ashton², Tim A. Birks¹; ¹Centre for Photonics and Photonic Materials, Univ. of Bath, UK; ²Dept. of Physics, Univ. of Bath, UK. We present a novel method of determining differences in propagation constant between coupled cores in multicore fiber by a Markov chain Monte Carlo reconstruction and discuss its implications for quantum walks of photons.

CLEO: Science & Innovations

10:30–12:00

SM2M • Nonlinear Signal Processing

Presider: Michael Vasilyev; Univ. of Texas at Arlington, USA

SM2M.1 • 10:30

Investigation into the Role of Pump to Signal Power Ratio in FWM-based Phase Preserving Amplitude Regeneration, Kyle Bottrill¹, Graham Hesketh¹, Francesca Parmigiani¹, David Richardson¹, P Petropoulos¹; ¹Univ. of Southampton, UK. We carry out a detailed experimental characterization of a four-wave mixing based amplitude limiter in highly nonlinear fiber based on the Bessel-like power transfer characteristics and highlight trade-offs for phase preserving capabilities.

SM2M.2 • 10:45

Investigation of 3-Channel All-Optical Regeneration in a Group-Delay-Managed Nonlinear Medium, Lu Li¹, Michael Vasilyev¹, Taras I. Lakoba²; ¹Electrical Engineering, Univ. of Texas at Arlington, USA; ²Dept. of Mathematics and Statistics, Univ. of Vermont, USA. We investigate three-channel performance of a stand-alone Mamyshev 2R regenerator based on Raman-assisted group-delay-managed medium. Our results indicate, for the first time to our knowledge, the feasibility of simultaneous regeneration of 100-GHz-spaced WDM channels.

SM2M.3 • 11:00

Spectrally Efficient Comb Source with Coupled Microresonators, Yoshitomo Okawachi¹, Steven Miller², Sven Ramelow¹, Kevin Luke², Alessandro Farsi¹, Michal Lipson^{2,3}, Alexander L. Gaeta^{1,3}; ¹School of Applied and Engineering Physics, Cornell Univ., USA; ²School of Electrical and Computer Engineering, Cornell Univ., USA; ³Kavli Inst. at Cornell for Nanoscale Science, USA. We demonstrate a spectrally efficient parametric comb source for WDM applications using a Si₃N₄ dual-coupled microring resonator. This geometry allows for operating wavelength flexibility and avoidance of mode crossings for stable comb generation.

SM2M.4 • 11:15

Broadband Uniform Wavelength Conversion and Time Compression of WDM Channels, Mohammad Amin Shoaie¹, Armand Vedadi¹, Camille-Sophie Brès¹; ¹École polytechnique fédérale de Lausanne, Switzerland. A scheme based on 2-pump OPA is proposed for uniform wavelength conversion and optimized compression. We show 4.7-fold compression over 32 nm range resulting in Gaussian pulses from sinusoidal modulation and enabling simultaneous compression of WDM channels for granularity adaptation.

10:30–12:30

SM2N • Symposium on Remote Atmospheric Lasing II

Presider: Ya Cheng; Shanghai Inst of Optics and Fine Mech, China

SM2N.1 • 10:30 **Invited**

From Single Photon Superradiance to Coherence-Brightened Lasers in the Sky, Marlan O. Scully^{1,2}; ¹TEXAS A&M UNIV., USA; ²BAYLOR UNIV., USA. A single photon stored in a large cloud of atoms provides new insights into the radiation physics of single-photon superradiance. In further work, we have developed a detailed theoretical study of a recent experiment [PNAS, 109, 15185 (2012)] in which a laser-like source is created in air by pumping with a nanosecond pulse. Our analysis indicates that the emission is largely governed by quantum coherence via cooperation between atoms of an ensemble.

SM2N.2 • 11:00 **Invited**

Lasing from Plasma Filaments in Air, Yi Liu¹, Sergey Mityukovskiy¹, Pengji Ding¹, Aurelien Houard¹, Andre Mysyrowicz¹; ¹Laboratoire d'Optique Appliquée, France. The stimulated emission obtained from the filamentation of a femtosecond laser pulse is discussed. The crucial role of pump laser polarization is emphasized.

10:30–12:30

SM2O • Fiber-based Sensing

Presider: Dirk Richter; Univ. of Colorado, USA

SM2O.1 • 10:30

Gas Sensing Fiber Network with Simultaneous Multi-node Detection using Range-resolved Chirped Laser Dispersion Spectroscopy, Genevieve Plant¹, Andreas Hangauer¹, Ming-Fang Huang², Ting Wang², Gerard Wysocki¹; ¹Princeton Univ., USA; ²NEC Labs America, USA. We present a laser-spectroscopic method for continuous and simultaneous interrogation of multiple passive gas sensor nodes in a fiber based sensor network. Enabled by chirped laser dispersion spectroscopy, methane leak detection is demonstrated as an example application.

SM2O.2 • 10:45

Fiberoptic Evanescent Wave Spectroscopy in Water at ppm Sensitivity with a tunable Quantum Cascade Laser, Guy-Maël De Naurois¹, Ilan Gaby¹, Federico Capasso¹, Abraham Katzir²; ¹Harvard Univ., USA; ²School of Physics and Astronomy, Sackler Faculty of Exact Sciences, Tel Aviv Univ., Israel. We present in water chemical spectroscopy by the use of a AgClBr fiber and a tunable mid-IR Quantum Cascade Laser source (QCL). We show detection of ppm concentration of ethanol in water.

SM2O.3 • 11:00

Characterization of Temperature and Strain Sensitivity of Low Cost Few-mode Fiber Based Interferometer Sensor, Yifei Wang^{2,1}, An Li¹, Xi Chen¹, William Shieh¹; ¹The Univ. of Melbourne, Australia; ²Victoria research Lab, NICTA Ltd., Australia. We experimentally characterize a two-mode fiber (TMF) based intermodal interferometer sensor for temperature and strain. A wavelength-temperature coefficient of - 43 pm/°C and wavelength-strain coefficient of - 2.3 pm/με have been characterized.

SM2O.4 • 11:15

Near-Infrared Absorption Gas Sensors using Metal-Organic Framework-Coated Optical Fibers, Alan X. Wang¹; ¹Oregon State Univ., USA. We report a near-infrared fiber-optic CO₂ sensor with only 8-centimeter sensing length coated with nanoporous metal-organic framework materials. We achieved 500ppm detection limit with an overall response time of 40 seconds in a gas cell.

10:30–12:30

SM2P • Novel Ultrafast Techniques

Presider: Robert Levis, Temple Univ., USA

SM2P.1 • 10:30

Coherent Pulse Stacking Amplification using Cascaded and Multiplexed Gires-Tournois Interferometers, Tong Zhou¹, John Ruppe¹, Cheng Zhu¹, I-Ning Hu¹, John Nees¹, Russell Wilcox², Wim Leemans², Almantas Galvanauskas¹; ¹Univ. of Michigan, USA; ²Lawrence Berkeley National Lab, USA. We show stacking of multiple equal-amplitude pulses into a single pulse using properly configured sequences of Gires-Tournois interferometers, which in conjunction of chirped pulse amplification in fibers can enable large increase in extractable pulse energies.

SM2P.2 • 10:45

Stabilizing the relative carrier-envelope phase of hybridly synchronized ultrafast Yb and Er fiber laser systems by the feed-forward scheme, Wei-Wei Hsiang¹, Bo-Jyun Fong¹, Wei-Ting Lin¹, Shang-Ying Wu², Jin-Long Peng³, Yinchieh Lai^{2,4}; ¹Dep. of Physics, Fu Jen Catholic Univ., Taiwan; ²Dept. of Photonics & Inst. of Electro-Optical Engineering, National Chiao-Tung Univ., Taiwan; ³Center for Measurement Standards, Industrial Technology Research Inst., Taiwan; ⁴Research Center for Applied Sciences, Academia Sinica, Taiwan. Stabilization of the relative carrier-envelope (CE) phase for hybridly synchronized two-color fs Yb and Er fiber laser systems is demonstrated for the first time by utilizing the feed-forward scheme based on an acousto-optic frequency shifter.

SM2P.3 • 11:00

Passive coherent combining of CEP-stable few-cycles pulses from a temporally divided hollow fiber compressor, Hermance Jacquemin^{4,1}, Aurelie Jullien⁴, Brigitte Mercier⁴, Marc Hanna², Frederic Druon², Dimitrios Papadopoulos³, Rodrigo Lopez-Martens⁴; ¹Thales Optronique SA, France; ²Institut d'Optique, France; ³LULL, France; ⁴Laboratoire d'Optique Appliquée, France. We demonstrate a robust passive coherent combining technique for post-compression of mJ energy CEP-stable laser pulses down to few-cycle duration in a gas-filled hollow fiber. High combining efficiency is achieved using carefully oriented calcite plates.

SM2P.4 • 11:15

Arbitrary-Detuning Asynchronous Optical Sampling with Amplified Laser Systems, Laura Antonucci¹, Adeline Bonalet¹, Xavier Solinas¹, Louis Danialt¹, Manuel Joffre¹; ¹Ecole Polytechnique, France. We demonstrate a new method for pump-probe spectroscopy by applying arbitrary detuning asynchronous optical sampling (AD-ASOPS) to two independent amplified laser systems. The resulting time dynamics ranges from 40 fs up to 1 ms.

CLEO: QELS-Fundamental Science

FM2A • Single Photon Sources—Continued

FM2A.5 • 11:30

Temporal Multiplexing toward Periodic and Deterministic Single-Photon Sources, Fumihiro Kaneda¹, Bradley Christensen¹, Jia Jun Wong¹, Heesu Park², Kevin McCusker^{1,3}, Paul Kwiat¹; ¹Univ. of Illinois at Urbana-Champaign, USA; ²Korea Research Inst. of Standards and Science, Korea; ³Northwestern Univ., USA. Utilizing time multiplexing of a heralded single-photon source based on spontaneous parametric downconversion pumped by periodic laser pulses, we observed large enhancements in the single-photon probability.

FM2A.6 • 11:45

Thermal light cannot be represented as a statistical mixture of pulses, Aurelia Chenu², Agata Branczyk¹, John E. Sipe²; ¹Perimeter Inst. for Theoretical Physics, Canada; ²Univ. of Toronto, Canada. Can thermal light be represented by a mixture of single pulses? It cannot; only a modified mixture can yield the correct first-order correlation function at equal space-points. Still, this fails to reproduce higher orders.

FM2A.7 • 12:00

Monolithic Source of Tunable Narrowband Photons for Future Quantum Networks, Sven Ramelow^{1,2}, Alessandro Farsi¹, Stephane Clemmen¹, Kevin Luke³, Michal Lipson^{3,4}, Alexander L. Gaeta^{1,4}; ¹School of Applied and Engineering Physics, Cornell Univ., USA; ²Faculty of Physics, Univ. of Vienna, Austria; ³School of Electrical and Computer Engineering, Cornell Univ., USA; ⁴Kavli Inst. at Cornell for Nanoscale Science, Cornell Univ., USA. Using high-Q Si₃N₄ microresonators, we generate the narrowest bandwidth (40 MHz) photon pairs, yet achieved for a chip-based source. Its high intrinsic stability and broad tunability are highly promising for interfacing to quantum memory networks.

FM2B • Ultrafast Dynamics in Quantum Dots and Organic Materials—Continued

FM2B.5 • 11:30

Decoupling Bulk and Surface Contributions in Water-Splitting Photocatalysts by In Situ Ultrafast Spectroscopy, Kannatassen Appavoo¹; ¹Center for Functional Nanomaterials, Brookhaven National Lab, USA. By performing ultrafast emission spectroscopy in an operating, bias-controlled photoelectrochemical cell, we distinguish between bulk and surface recombination processes in a nanostructured photocatalyst and correlate its electronic properties directly with its incident-photon-to-current efficiency.

FM2B.6 • 11:45

Fast High-Fidelity Hole Spin Initialisation in a Single Quantum Dot at Zero Magnetic Field, Alistair Brash¹, Luis M. Martins¹, Feng Liu¹, John H. Quilter^{1,2}, Maurice S. Skolnick¹, A. Mark Fox¹; ¹Dept. of Physics and Astronomy, Univ. of Sheffield, UK; ²Dept. of Physics, Royal Holloway, UK. Fast (~50 ps) initialisation of a long-lived hole spin qubit in a single InGaAs quantum dot is achieved by exciton ionisation. A QD exhibiting no fine structure yields fidelities exceeding 98% at zero external field thus forming a key building block for high fidelity quantum information processing.

FM2B.7 • 12:00

Femtosecond Hole Relaxation and Biexcitonic Transient Absorption in Single CdSe/ZnSe Quantum Dots, Christopher Hinz¹, Christian Trau¹, Johannes Haase¹, Benjamin Bauer¹, Alfred Leitnerstorfer¹, Denis Seletskiy¹; ¹Physics, Univ. of Konstanz, Germany. Femtosecond few-fermion dynamics in single CdSe/ZnSe quantum dots is studied by two-color pump-probe measurements. We observe sub-picosecond hole relaxation and induced absorption into biexciton states when pumping p-p and d-s transitions.

FM2C • Hyperbolic Metamaterials—Continued

FM2C.5 • 11:30

Simultaneous enhancement of decay rate and light extraction from active hyperbolic metamaterial, Tal Galfsky^{1,2}, Harish Krishnamoorthy^{1,2}, Ward Newman³, Evgenii Narimanov⁴, Zubin Jacob³, Vinod M. Menon^{1,2}; ¹Physics, Graduate Center of the City Univ. of New York, USA; ²Physics, City College of the City Univ. of New York, USA; ³Dept. of Electrical and Computer Engineering, Univ. of Alberta, Canada; ⁴Birck Nanotechnology Center, School of Computer and Electrical Engineering, Purdue Univ., USA. We demonstrate simultaneous enhancement in spontaneous emission rate and light extraction from hyperbolic metamaterials embedded with quantum dots using a high contrast grating. Enhancements of twenty-fold in extraction and thirteen-fold in emission rate are observed.

FM2C.6 • 11:45

Non-Resonant Hyperlens in the Visible Range, Jingbo Sun¹, Mikhail Shalaev¹, Natalia M. Litchinitser¹; ¹State Univ. of New York at Buffalo, USA. A non-resonant hyperlens operating in the visible wavelength range is demonstrated experimentally. Non-resonant indefinite properties, enabling low-loss, broadband sub-wavelength imaging, were realized using a fan-like structure made using a combination of top-down and bottom-up techniques.

FM2C.7 • 12:00

Multilayer Cladding with Hyperbolic Dispersion for Plasmonic Waveguides, Viktoriia Babicheva^{1,2}, Mikhail Y. Shalaginov², Satoshi Ishii^{2,3}, Alexandra Boltasseva^{2,4}, Alexander V. Kildishev²; ¹ITMO Univ., Russia; ²Purdue Univ., USA; ³International Center for Materials Nanoarchitectonics (MANA), National Inst. for Materials Science (NIMS), Japan; ⁴DTU Fotonik, Technical Univ. of Denmark, Denmark. We study the properties of plasmonic waveguides with a dielectric core and multilayer metal-dielectric claddings that possess hyperbolic dispersion. The waveguides hyperbolic multilayer claddings show better performance in comparison to conventional plasmonic waveguides.

FM2D • Novel Optical Phenomena—Continued

FM2D.5 • 11:30

Resonant Phase Matching of Josephson Junction Traveling Wave Parametric Amplifiers, Kevin O'Brien¹, Chris Macklin², Irfan Siddiqi², Xiang Zhang¹; ¹Univ. of California at Berkeley, USA; ²QNL, Univ. of California at Berkeley, USA. We propose a technique to phase-match Josephson-junction traveling wave parametric amplifiers to achieve high gain over a broad bandwidth for applications such as the multiplexed readout of quantum coherent circuits.

FM2D.6 • 11:45

Photoluminescence Upconversion Study of GaN Nanowires: Potential for Optical Refrigeration, Ruolin Chen¹, Guan Sun¹, Yujie J. Ding¹, Hieu Nguyen², Zetian Mi²; ¹Electrical and Computer Engineering, Lehigh Univ., USA; ²Electrical and Computer Engineering, McGill Univ., Canada. Up-converted photoluminescence of GaN nanowires is observed at the temperature above 375 K. At 475 K, the mechanism of the photoluminescence was identified as phonon-assisted bandtail emission. Such a phenomenon contributes to optical refrigeration.

FM2D.7 • 12:00

Guide-wave Photonic Pulling Force Using One-way Photonic Chiral Edge States, Danlu Wang¹, Chengwei Qiu³, Peter T. Rakich², Zheng Wang⁴; ¹Dept. of Physics, The Univ. Of Texas at Austin, USA; ²Dept. of Applied Physics, Yale Univ., USA; ³Dept. of Electrical and Computer Engineering, National Univ. of Singapore, Singapore; ⁴Dept. of Electrical and Computer Engineering, The Univ. Of Texas at Austin, USA. We provide a new scheme of photonic pulling force in one-way waveguides. Objects of arbitrary shape and dielectric properties can be pulled all the way to the light source, regardless of waveguide geometry.

CLEO: QELS-
Fundamental ScienceFM2E • Symposium on Single-
photon Nonlinear Optics II—
Continued

FM2E.4 • 11:30 **Invited**
Nonlinear Interactions in Optical Lattice Systems, Demetrios N. Christodoulides¹; ¹Univ. of Central Florida, USA. Photonic lattices provide a versatile classical platform for observing a host of nonlinear processes. In this talk we provide an overview of recent activities in such arrangements with a special emphasis on quantum-inspired systems.

FM2E.5 • 12:00
Complete Conversion of One to Two Photons in Dispersion-Engineered Nonlinear Waveguides, Alexander S. Solntsev¹, Andrey A. Sukhorukov¹; ¹Nonlinear Physics Centre, Research School of Physics and Engineering, Australian National Univ., Australia. We predict that complete deterministic conversion of one to two photons can be achieved at a finite propagation distance in specially engineered nonlinear waveguides, by designing quantum frequency mixing across a broad range of frequencies.

SM2F • Novel Materials for
Semiconductors Lasers—
Continued

SM2F.4 • 11:30
Long Wave, Room Temperature, II-VI - Based Quantum Cascade Emitters, Arvind Pawan Ravikumar¹, Thor A. Garcia², Joel De Jesus², Maria C. Tamargo², Claire F. Gmachl¹; ¹Princeton Univ., USA; ²The Graduate Center and The City College of New York of CUNY, USA. We demonstrate the first long-wave, room temperature II-VI materials based Quantum Cascade emitter around 7.2 μm . At 80 K, a device differential resistance of 2.6 Ω and a narrow electroluminescent width of 16% was obtained.

SM2F.5 • 11:45
Fe:ZnSe Channel Waveguide Laser Operating at 4122 nm, Adam Lancaster¹, Gary Cook², Sean McDaniel³, Jonathan Evans², Patrick Berry², Jonathan Shephard¹, Ajay Kar¹; ¹Heriot-Watt Univ., UK; ²Sensors Directorate, Air Force Research Lab, USA; ³Leidos Inc, USA. The first demonstration of a waveguide laser in Fe:ZnSe is presented. The waveguide laser produces 49 mW of output power at 4122 nm with a spectral bandwidth of 6 nm FWHM.

SM2F.6 • 12:00
Optically Pumped Distributed Feedback Laser from Organo-Lead Iodide Perovskite Thin Films, Songtao Chen¹, Wee Kiang Chong^{2,3}, Joonhee Lee¹, Kwangdong Roh¹, Emre Sari¹, Nripan Mathews⁴, Tze Chien Sum², Arto Nurmikko¹; ¹School of Engineering and Dept. of Physics, Brown Univ., USA; ²School of Physics & Mathematical Sciences, Nanyang Technological Univ., Singapore; ³Energy Research Inst. Nanyang Technological Univ., Singapore; ⁴School of Materials Science and Engineering, Nanyang Technological Univ., Singapore. Perovskite ($\text{CH}_3\text{NH}_3\text{PbI}_3$) films possessing optical quality were prepared by solution-based spin-casting at room temperature. We report near infrared lasing with well-defined spatially coherent output from second-order surface-emitting distributed feedback grating structure with perovskite active media.

CLEO: Science & Innovations

SM2G • Characterization
Techniques—Continued

SM2G.5 • 11:30
Broadband (3.9 - 9.6 μm) Photocurrent in Quantum Cascade Detector with Diagonal Transitions, Germano Maioli Penello¹, Benjamin Merke^{1,2}, Claire F. Gmachl¹, Deborah L. Sivco¹; ¹Princeton Univ., USA; ²Dept. of Physics, Univ. of Duisburg-Essen, Germany. By carefully designing diagonal transitions in the active region, we present a broadband mid-infrared quantum cascade detector with photocurrent ranging from 3.9 to 9.6 μm , more than 2 times broader than stacked designs.

SM2G.6 • 11:45
Spectral Dependence of Third-Order Nonlinear Optical Properties in InN, Hye-young Ahn¹, Min-Tse Lee¹; ¹National Chiao Tung Univ., Taiwan. Spectral dependence of nonlinear optical absorption cross-section (s) near and below the bandgap (E_g) is measured for InN by using Z-scan technique. A drastic increase of s near E_g can be understood by the band-filling model.

SM2G.7 • 12:00
Characterization of Graphene Photothermoelectric Detector via Two-wave Mixing Technique, Mohammad Mehdi Jadidi¹, Ryan J. Suess¹, Xinghan Cai², Andrei B. Sushkov², Martin Mittendorff¹, Michael S. Fuhrer², H. Dennis Drew², Thomas E. Murphy¹; ¹Inst. for Research in Electronics and Applied Physics, Univ. of Maryland, USA; ²Center for Nanophysics and Advanced Materials, Univ. of Maryland, USA. We study the response of a graphene photothermoelectric-based detector illuminated by two continuous-wave optical beams. The power and frequency dependence of the photoresponse are used to probe the graphene hot-electron cooling rates and mechanisms.

SM2H • Strong-Field THz
Science and Technology—
Continued

SM2H.2 • 11:30
Generation of mJ THz pulses in organic crystal pumped by a Cr:Mg₂SiO₄ laser, Carlo Vicario¹, Andrey Ovchinnikov², Sergey Ashitkov², S. I. Agratn², Vladimir E. Fortov², Christoph P. Hauri^{1,3}; ¹Paul Scherrer Inst., Switzerland; ²Joint Inst. for High Temperatures of RAS, Russia; ³Ecole Polytechnique Federale de Lausanne, Switzerland. We demonstrated 0.9 mJ terahertz pulses by optical rectification of a high-energy Cr:Mg₂SiO₄ laser in large organic crystal. The emitted spectrum covers 0.1-5 THz and the peak fields exceed 42 MV/cm and 14 Tesla.

SM2H.3 • 11:45
On Extracting the Maximum Terahertz Conversion Efficiency from Optical Rectification in Lithium Niobate, Sergio Carbajo^{2,3}, Paula Alcorta², Anne-Laure Calendron^{2,3}, Huseyin Cankaya², Xiaojun Wu², Koustuban Ravi¹, Frederike Ahr^{2,3}, Wenqian Ronny Huang¹, Franz X. Kaertner^{1,2}; ¹MIT, USA; ²Center for Free Electron Laser Science, Germany; ³Physics Dept., Univ. of Hamburg, Germany. We report on a record 2% extracted optical-to-terahertz conversion efficiency in the mm-wavelength range through optical rectification in cryogenically-cooled lithium niobate by exploiting spatial and temporal shaping of the optical pump beam.

SM2H.4 • 12:00
Generation of Elliptically Polarized Half-Cycle Terahertz Pulses Generated by 6H-SiC Large Aperture Photoconductive Antenna, xavier ropagnon¹, marcel bouvier², Christian-Yves Côté², Matt Reid³, Marc-André Gauthier¹, Tsuneyuki Ozaki¹; ¹INRS-EMT, Canada; ²Axis photonique INC, Canada; ³UNBC, Canada. We demonstrated the generation of elliptically half-cycle terahertz pulses with 167 nJ energy generated by a 6H-SiC large aperture photoconductive antenna covered by a phase mask. By optimizing the design of the antenna and the mask, we could generate circularly polarized half-cycle THz pulses.

CLEO: Science & Innovations

SM2I • Silicon Photonic Systems—Continued

SM2I.4 • 11:30

Demonstration of Reconfigurable Electro-Optical Directed-Logic Circuit by Carrier Depletion Micro-ring Resonators, Ciyuan Qiu^{2,1}, Weilu Gao², Richard Soref³, Jacob Robinson², Qianfan Xu²; ¹Shanghai Jiao Tong Univ., China; ²Rice Univ., USA; ³Univ. of Massachusetts, USA. Here we demonstrate a reconfigurable electro-optical directed-logic circuit based on a 4-fold array of switches. We showed that this circuit can be reconfigured to perform arbitrary two-input logic functions with speed up to 3 Gb/s.

SM2I.5 • 11:45

Integrated Mode-Locked Lasers in a CMOS-Compatible Silicon Photonic Platform, Cheryl M. Sorace-Agaskar¹, Patrick T. Callahan¹, Katia Shtyrkova¹, Anna Baldycheva^{1,2}, Michele Moresco¹, Jonathan Bradley¹, Michael Y. Peng¹, Nanxi Li¹, E. Salih Magden¹, Purnawirman Purnawirman¹, Michelle Y. Sander^{1,3}, Gerald Leake⁵, Douglas D. Coolbaugh⁵, Michael R. Watts¹, Franz X. Kaertner^{1,4}; ¹MIT, USA; ²Univ. of Exeter, UK; ³Boston Univ., USA; ⁴Univ. of Hamburg, Germany; ⁵College of Nanoscale Science and Engineering - Univ. of Albany, USA. Integrated components necessary for a mode-locked laser are demonstrated on a platform that allows for monolithic integration with active silicon photonics and CMOS circuitry. CW lasing and Q-switched mode-locking are observed in the full structures.

SM2I.6 • 12:00

Noise and fluctuations in silicon photonics caused by free carrier and two-photon absorption, Dimitris Dimitropoulos¹, Bahram Jalali²; ¹-, Greece; ²Electrical Engineering, UCLA, USA. Non-linear optical losses result from convergence of wafer scale economics and information theory in silicon nanophotonics. We discuss new sources of noise and fluctuations that arise from two-photon and free carrier plasma effects.

CLEO: Applications & Technology

AM2J • Light Sources and Devices for Biomedical Imaging II—Continued

AM2J.5 • 11:30

Two-photon excited ReaChR by a three-stage femtosecond optical parametric amplifier, Chia-lun Tsai¹, Po-Yen Hsiao¹, Ming-Chang Chen¹, Shang-Da Yang¹, Yen-Yin Lin¹, Ann-Shyn Chiang^{1,2}; ¹Natl Tsing Hua Univ, Taiwan; ²Academia Sinica, Taiwan. A three-stage optical parametric amplifier is built to produce 1 kHz, 31 fs, ~200 μ J signal pulses with tunable wavelengths. Red-activatable channelrhodopsin in fruit fly is optimally two-photon excited to copulation behavior at 1250 nm.

AM2J.6 • 11:45

End-Fire Silicon Waveguide Array as a Platform for High Power Beam Shaping and Steering, Michael Kossey¹, Charbel Rizk^{1,2}, Amy C. Foster¹; ¹Johns Hopkins Univ., USA; ²Johns Hopkins Applied Physics Lab, USA. We demonstrate a scalable array of end-firing silicon waveguides as a platform for high-speed, high-power operation beam-steering applications. We fabricate devices, culminating in 16x1 arrays with a measured central lobe FWHM of 7 \pm 0.6 $^\circ$.

AM2J.7 • 12:00

Tunable Dual Color Source For Multiphoton Imaging, Kriti Charan¹, Dylan Heberle¹, Chris Xu¹; ¹Cornell Univ., USA. We present a tunable-wavelength, multi-color source for imaging several fluorophores simultaneously. The source is based on amplitude modulation of the seed in a chirped-pulse amplification system, followed by soliton self-frequency shift in a large-mode-area fiber.

AM2K • Microprocessing Laser Processing of Silicon and Other Materials—Continued

AM2K.4 • 11:30 **Invited**

Excimer Laser Annealing for LTPS on Large Substrates, Rainer Paetzl¹; ¹Coherent GmbH, Germany. Low-Temperature Polycrystalline Silicon (LTPS) is the enabling backplane technology for AMOLED displays and small to medium sized high-resolution AMLCDs. Progress on Excimer Laser Annealing towards large-scale production of LTPS is described.

AM2K.5 • 12:00

Random Surface Texturing of mc-Silicon for Solar Cells with Picosecond Lasers; a Comparison between 1064 nm, 532 nm and 355 nm Laser Emission Wavelengths, sergio pellegrino⁴, luca longoni⁴, davide scorticati⁴, simona binetti¹, Alessia Le Donne¹, Andrea Rolfi¹, Emanuele Grilli¹, Chiara Busto², Beat Neuwenschwander³, Beat Jaeggi³; ¹Università Milano Bicocca, Italy; ²ENI, Italy; ³Bern Univ. of Applied Sciences, Switzerland; ⁴Laserpoint, Italy. Multicrystalline Silicon was textured with picosecond laser. Different laser wavelengths ($\lambda = 1064, 532, 355$ nm) where compared regarding laser-induced damage. We found that $\lambda = 355$ nm picosecond radiation resulted in shallower defect-reach region.

CLEO: Science & Innovations

SM2L • Modes in Fiber—Continued

SM2L.5 • 11:30

Comparing Inter-Core Skew Fluctuations in Multi-Core and Single-Core Fibers, Ruben S. Luis¹, Benjamin Puttnam¹, Jose M. Mendinueta¹, Werner Klaus¹, Yoshinari Awaji¹, Naoya Wada¹; ¹National Inst Information & Comm Tech, Japan. We measure the dynamic skew fluctuations between cores in a multicore fiber and show that they are more than one order of magnitude smaller than those of parallel single-core fibers over a 24 hour period.

SM2L.6 • 11:45

Spatiotemporal Nonlinear Optics in Multimode Fibers, Logan Wright¹, Demetrios N. Christodoulides², Frank W. Wise¹; ¹Cornell Univ., USA; ²College of Optics and Photonics, CREOL, Univ. of Central Florida, USA. We study nonlinear pulse propagation of high-energy ultrashort pulses in graded-index multimode fibers. By adjusting initial conditions, we observe and control a wide range of nonlinear effects including spatiotemporal effects resembling self-focusing and multiple filamentation.

SM2L.7 • 12:00

Complete Spatiotemporal Measurement of Ultrashort Pulses Emerging from Multimode Optical Fiber, Zhe Guang¹, Rick Trebino¹; ¹Georgia Inst. of Technology, USA. Using a newly developed technique, we measure the complete spatiotemporal field of ultrashort pulses emerging from dual-mode optical fibers, finding spatiotemporal complexity, introduced by the different spatial modes, having different group velocities and modal dispersions.

Technical Digest and Postdeadline Papers Available Online

- Visit www.cleoconference.org
- Select Access Digest Paper link
- Use your registration email address and password

Access is provided only to full technical attendees.

CLEO: Science & Innovations

SM2M • Nonlinear Signal
Processing—Continued

SM2M.5 • 11:30

Nonlinear Compensation with Modified Adaptive Digital Backpropagation in Flexigrid Networks, Edson Porto da Silva¹, Rameez Asif¹, Knud J. Larsen¹, Darko Zibar¹; ¹DTU Fotonik, Technical Univ. of Denmark, Denmark. We present a modified version of adaptive digital backpropagation based on EVM metric, and numerically access its performance in a flexigrid WDM scenario.

SM2M.6 • 11:45

Low Complexity and Adaptive Nonlinearity Compensation, Zhiyu Chen¹, Lianshan Yan¹, Anlin Yi¹, Lin Jiang¹, Yan Pan¹, Wei Pan¹, Bin Luo¹; ¹Ctr Info Photonics & Communications, China. A low complexity adaptive nonlinearity compensation algorithm is experimentally demonstrated based on variance of intensity noise and low-pass filter. Digital-back propagation efficiency is improved about four times in 40-Gb/s DP-QPSK transmission over 720-km SMF.

SM2N • Symposium on Remote
Atmospheric Lasing II—
Continued

SM2N.3 • 11:30 **Invited**
Standoff Sources of Coherent Radiation Initiated by Femtosecond Filaments, Daniil Kartashov¹, Skirmantas Alisauskas², Giedrius Andriukaitis², Audrius Puglys², Stefan Haessler², Andrius Baltuska², Mikhail Shneider³, Bjorn Landgraf¹, Andreas Hoffmann¹, Christian Spielmann¹, Pavel G. Polynkin⁴, Alexander Mitrofanov^{5,6}, Dmitri Sidorov-Biryukov^{5,6}, Aleksei Zheltikov^{5,7}, Jens Möhring⁸, Dmitri Starukhin⁸, Marcus Motzkus⁸, Misha Ivanov⁹, Maria Richter⁹, Felipe Morales⁹; ¹Inst. for Optics and Quantum Electronics, Friedrich-Schiller-Univ. Jena, Germany; ²Photonics Inst., Vienna Univ. of Technology, Austria; ³Dept. of Mechanical and Aerospace Engineering, Princeton Univ., USA; ⁴Univ. of Arizona, USA; ⁵International Laser Center, Lomonosov Moscow State Univ., Russia; ⁶Russian Quantum Center, Russia; ⁷Dept. of Physics and Astronomy, Texas A&M Univ., USA; ⁸Physikalisch-Chemisches Institut, Heidelberg Univ., Germany; ⁹Max-Born Inst., Germany. We present the results of experimental and theoretical investigations for remote initiation of lasing in nitrogen and air by femtosecond filaments generated by laser pulses with different wavelengths, polarization and applying adaptive control methods.

SM2N.4 • 12:00

Lasing Actions in a Flame Filament, Huailiang Xu¹, Ya Cheng²; ¹Jilin Univ., China; ²SIOM, China. We demonstrate lasing in a femtosecond filament with the combustion intermediate of CN as the gain target by femtosecond laser excitation. The lasing action is ascribed to amplified spontaneous emission.

SM2O • Fiber-based Sensing—
Continued

SM2O.5 • 11:30

Distributed Temperature and Strain Sensing using Spontaneous Brillouin Scattering in Optical Few-Mode Fibers, Yi Weng^{1,2}, Ezra Ip¹, Zhongqi Pan², Ting Wang¹; ¹NEC Labs America, Inc., USA; ²Dept. of Electrical & Computer Engineering, Univ. of Louisiana at Lafayette, USA. A novel approach to achieve simultaneous distributed temperature and strain sensing based on spontaneous Brillouin scattering in few-mode optical fibers is proposed and experimentally investigated, with high sensitivity using heterodyne detection and optical time-domain reflectometry.

SM2O.6 • 11:45

Simultaneous Measurement of Temperature and Refractive Index Using a Photonic Crystal Cavity on a Fiber Tip, Martijn Boerkamp², Yingying Lu², Jan Mink², Zarko Zobenica¹, Rob W. van der Heijden¹; ¹Applied Physics, Eindhoven Univ. of Technology, Netherlands; ²VTEC Lasers & Sensors, Netherlands. The operation of a luminescent semiconductor photonic crystal cavity on an optical fiber tip is demonstrated for simultaneous measurement of temperature and refractive index by measuring the wavelength-shifts of two different cavity modes.

SM2O.7 • 12:00

Distance Measurement Using Second Harmonic Signal Component of Two-Photon Absorption Photocurrent from Si-APD, Yosuke Tanaka¹, Yoshiki Yamada¹, Takashi Kurokawa¹; ¹Tokyo Univ. of Agriculture and Technology, Japan. We propose a laser distance measurement using second harmonic signal component of two-photon absorption photocurrent from a Si-APD. The proof-of-concept experiment demonstrates the accurate measurement with short data acquisition time of several tens of seconds.

SM2P • Novel Ultrafast
Techniques—Continued

SM2P.5 • 11:30

Optimized Ancillae Generation for Ultra-Broadband Two-Dimensional Spectral Shearing Interferometry, Cristian Manzoni¹, Rocio Borrego Varillas¹, Giulio Cerullo¹, Aurelio Oriana¹, Federico Branchi¹; ¹Politecnico di Milano, IFN-CNR, Italy. We introduce a scheme to overcome the challenges of ancillae preparation in traditional spectrally-sheared interferometry techniques for pulse characterization. The approach, applied to two-dimensional spectral shearing interferometry, reliably characterizes few-optical-cycle pulses from UV to IR.

SM2P.6 • 11:45

Generation of Parabolic Pulses with Optimized Duration & Energy by Use of Dispersive Frequency-to-time Mapping, Jeonghyun Huh¹, David Duchesne¹, José Azaña²; ¹Institut National de la Recherche Scientifique—Énergie, Matériaux et Télécommunications, Canada. Parabolic pulses with durations ranging from the picosecond to the sub-nanosecond range (100-ps reported here) were generated through frequency-to-time mapping. A virtual time-lens was applied in the spectral shaping stage in order to relax the constraints imposed by the far-field condition.

SM2P.7 • 12:00

Multiwavelength Ultrafast LiNbO₃ Raman Laser With Cascaded Terahertz-wave Generation, Aravindan M. Warriar¹, Jipeng Lin¹, Helen M. Pask¹, Andrew J. Lee¹, David J. Spence¹; ¹Macquarie Univ., Australia. We demonstrate an ultrafast Raman laser to extend the wavelength versatility of mode-locked lasers. Polariton scattering in LiNbO₃ is used to make a tunable ultrafast laser with potential for terahertz generation.

CLEO: QELS-Fundamental Science

FM2A • Single Photon Sources—Continued

FM2A.8 • 12:15

Ultra-fast heralded single photon source based on telecom technology and non-linear optics, Lufti Arif Ngah¹, Olivier Alibert¹, Laurent Labonté¹, Virginia D'Auria¹, Sebastien Tanzilli¹; ¹Lab.de Physique de la Matière Condensée, France. We realize an ultra-fast source of telecom single photons heralded at MHz-rates by combining a 10-GHz repetition-rate laser with off-the-shelf fiber components and waveguide non-linear stages. Measured 2nd-order autocorrelation functions are the lowest reported to date.

FM2B • Ultrafast Dynamics in Quantum Dots and Organic Materials—Continued

FM2B.8 • 12:15

Charged Exciton Linewidth Narrowing via Nuclear Spin Screening in an InAs QD Ensemble, Galan Moody¹, Mingming Feng¹, Corey McDonald¹, Richard P. Mirin¹, Kevin Silverman¹; ¹National Inst. of Standards and Technology, USA. Differential transmission spectroscopy of InAs QDs reveals that the positively charged exciton homogeneous linewidth is broadened by the electron hyperfine interaction. Application of a Faraday magnetic field screens the interaction, narrowing the linewidth by 25%.

FM2C • Hyperbolic Metamaterials—Continued

FM2C.8 • 12:15

Effect of a Hyperbolic Metamaterial on Radiation Patterns of a Single-Photon Source, Mikhail Y. Shalaginov¹, Alexei Lagutchev¹, Vladimir M. Shalaev¹, Alexander V. Kildishev¹; ¹Purdue Univ., USA. We explore the effect of a planar hyperbolic metamaterial (a superlattice of TiN and Al_{0.7}Sc_{0.3}N on MgO substrate) on the far-field radiation patterns of a single-photon source (a nitrogen-vacancy center in a nanodiamond).

FM2D • Novel Optical Phenomena—Continued

FM2D.8 • 12:15

Experimental Detection of Forces in an Optical Analog of Aharonov-Bohm Effect, Sergey Sukhov¹, Veerachart Kajorndejnukul¹, John Broky¹, Aristide Dogariu¹; ¹Univ. of Central Florida, CREOL, USA. Wavefront dislocations in scattering create an Aharonov-Bohm setting where nonconservative reaction forces can be detected experimentally. Observing the dynamics of microscopic particles clarifies the role the finite wave-packets on the transfer of wave's canonical momentum.

12:00–16:00 SC270 • High Power Fiber Lasers and Amplifiers
SC301 • Quantum Cascade Lasers: Science, Technology, Applications and Markets

12:30–13:30 Lunch Break (on your own)

13:00–16:00 SC271 • Quantum Information—Technologies and Applications
SC376 • Plasmonics

NOTES

**CLEO: QELS-
Fundamental Science**

CLEO: Science & Innovations

FM2E • Symposium on Single-photon Nonlinear Optics II—Continued

FM2E.6 • 12:15
Phase-Noise Limitations on Nonlinear-Optical Quantum Computing, Justin Dove¹, Christopher Chudzicki¹, Jeffrey H. Shapiro¹; ¹ *Research Laboratory of Electronics, MIT, USA*. We establish a framework for evaluating CPHASE gates that use single-photon Kerr nonlinearities in which one pulse overtakes another. We show that causality-induced phase noise precludes the possibility of high-fidelity π -radian conditional phase shifts.

SM2F • Novel Materials for Semiconductors Lasers—Continued

SM2F.7 • 12:15
Monolayer Tungsten Disulfide Laser, Yu Ye¹, Zi Jing Wong¹, Xiufang Lu², Hanyu Zhu¹, Yuan Wang¹, Xianhui Chen², Xiang Zhang^{1,3}; ¹*UC Berkeley, USA*; ²*Hefei National Lab for Physics Science at Microscale and Dept. of Physics, Univ. of Science and Technology of China, China*; ³*Lawrence Berkeley National Lab, Materials Sciences Division, USA*. We demonstrate the first realization of monolayer tungsten disulfide laser embedded in a microdisk resonator.

SM2G • Characterization Techniques—Continued

SM2G.8 • 12:15
Tricycloquinazoline-Based Organometallic Compounds for Optical Switching, William Shensky¹, Jianmin Shi¹, Michael J. Ferry¹, Timothy Pritchett¹; ¹*US Army Research Lab, USA*. The nonlinear absorption was studied for compounds linking tricycloquinazoline to a number of iridium groups. It was determined that the excited-state cross section was highest for the compound with a single iridium group.

SM2H • Strong-Field THz Science and Technology—Continued

SM2H.5 • 12:15
Extreme Terahertz brightness by focusing to a lambda-cubic volume, Christoph P. Hauri^{1,2}, Mostafa Shalaby¹; ¹*Paul Scherrer Institut, Switzerland*; ²*Ecole Polytechnique Federale de Lausanne, Switzerland*. We demonstrate bright low-frequency terahertz (<5 THz) radiation confined to a diffraction-limited spot size by wavefront manipulation. Focusing to a lambda-cubic volume provides bright THz radiation at the PW/m² level.

12:00–16:00 SC270 • High Power Fiber Lasers and Amplifiers
SC301 • Quantum Cascade Lasers: Science, Technology, Applications and Markets

12:30–13:30 Lunch Break (on your own)

13:00–16:00 SC271 • Quantum Information—Technologies and Applications
SC376 • Plasmonics

NOTES

Meeting Room
211 B/D

CLEO: Science & Innovations

SM2I • Silicon Photonic Systems—Continued

SM2I.7 • 12:15

High contrast and power-efficient thermally-controlled optical switch on Silicon-on-Insulator, Zheng Han², Gregory Moille¹, Xavier Checoury², Jérôme Bourderionnet¹, Gaëlle Lehoucq¹, Philippe Boucaud², Alfredo De Rossi¹, Sylvain Combrié¹; ¹Thales Research & Technology, France; ²Univ. Paris-Sud, CNRS UMR 8622, Institut d'Electronique Fondamentale, France. A low-loss and fast optical switch is demonstrated on Silicon-on-Insulator. Low insertion losses (6dB), a large dynamic contrast (30dB) and a wide tuning range (6nm) are achieved with an operating electric power consumption in the milliwatt range.

Meeting Room
212 A/C

CLEO: Applications & Technology

AM2J • Light Sources and Devices for Biomedical Imaging II—Continued

AM2J.8 • 12:15

Tether-less Implantable Upconverting Microscale Light Bulbs for Deep Brain Neural Stimulation and Imaging, Maysamreza Chamanzar¹, David Garfield², Jillian Iafrati³, Vikaas Sohal³, Bruce Cohen², P. James Schuck², Michel Maharbiz¹; ¹Univ. of California Berkeley, USA; ²Lawrence Berkeley National Lab, USA; ³UCSF, USA. We demonstrate the design and fabrication of implantable micro-scale light "bulbs" comprising of parylene-encapsulated upconverting lanthanide-doped nanocrystals (absorbing near-infrared and emitting blue light) for non-invasive targeted optogenetic stimulation of local neuronal ensembles.

Meeting Room
212 B/D

AM2K • Microprocessing Laser Processing of Silicon and Other Materials—Continued

AM2K.6 • 12:15

Elucidating the Mechanism of Nanocone and Nanohole Formation on Si by Optical Trap Assisted Nanopatterning, Ting Hsuan Chen¹, Yu-Cheng Tsai¹, Romain Fardel¹, Craig B. Arnold¹; ¹Princeton Univ., USA. Using optical trap-assisted nanopatterning (OTAN), we are able to control the formation of nanocones and nanoholes in Silicon. The effects are described by integrating FDTD and heat transfer modeling to account for the nanoscale features.

Marriott
Salon I & II

CLEO: Science & Innovations

SM2L • Modes in Fiber—Continued

SM2L.8 • 12:15

Transmission of Focused Picosecond Light Pulse through a Multimode Fiber, Yin Cen^{2,1}, Ying-Chih Chen^{2,1}; ¹Dept. of Physics, City Univ. of New York Graduate Center, USA; ²Dept. of Physics and Astronomy, Hunter College, USA. We report the experimental demonstration and numerical simulation for delivery of spatially focused temporally compressed picosecond laser pulse through a 10-meter-long step-index multimode fiber by shaping the wavefront of incident light using a deformable mirror.

12:00–16:00 SC270 • High Power Fiber Lasers and Amplifiers
SC301 • Quantum Cascade Lasers: Science, Technology, Applications and Markets

12:30–13:30 Lunch Break (on your own)

13:00–16:00 SC271 • Quantum Information—Technologies and Applications
SC376 • Plasmonics

NOTES

Monday, 11 May

CLEO: Science & Innovations

SM2N • Symposium on Remote Atmospheric Lasing II—Continued

SM2N.5 • 12:15
Characterization of Forward ASE Pulses Generated in Nitrogen with a Circularly Polarized Femtosecond Laser, Ya Cheng¹, Bin Zeng¹, Ziting Li¹, Jinping Yao¹, Hongqiang Xie¹, Guihua Li¹, Wei Chu¹, Chenrui Jing¹, Jielei Ni¹; ¹Shanghai Inst of Optics and Fine Mech, China. We report on generation of forward amplified spontaneous emission (ASE) pulses in nitrogen with a circularly polarized femtosecond pump laser as well as characterization of polarization and temporal properties of the ASE pulses.

SM2O • Fiber-based Sensing—Continued

SM2O.8 • 12:15
Multipoint Hollow Core Photonic Crystal Fiber Sensor Network Based on Intracavity Absorption Spectroscopy, Haiwei Zhang^{1,2}, Ying Lu^{1,2}, Wei Shi^{1,2}, Liangcheng Duan^{1,2}, Zhiqiang Zhao^{1,2}, Jianquan Yao^{1,2}; ¹School of Precision Instrument and Opto-electronics Engineering, Inst. of Laser and Opto-electronics, Tianjin Univ., China; ²Key Lab of Opto-electronics Information Technology (Tianjin Univ.), Ministry of Education, China. We firstly demonstrate an automatic intracavity absorption multipoint acetylene sensor network via dense wavelength division multiplexing filters by applying voltage gradient to the F-P tunable filter. The sensitivity is up to 100ppmV at 1536.71nm.

SM2P • Novel Ultrafast Techniques—Continued

SM2P.8 • 12:15
Injection-Locked VCSEL Arrays for Line-by-Line Pulse-Shaping with Update Times of Less Than 1 ns, Sharad Bhooplapur¹, Anthony Klee¹, Peter J. Delfyett¹; ¹Univ. of Central Florida, USA. Dynamic and static optical pulse shaping with line-by-line control is shown, using a 12-channel injection-locked VCSEL linear array. With channel modulation frequencies up to 3.125 GHz, pulse shape changes within 1 ns are conclusively demonstrated.

12:00–16:00 SC270 • High Power Fiber Lasers and Amplifiers
SC301 • Quantum Cascade Lasers: Science, Technology, Applications and Markets

12:30–13:30 Lunch Break (on your own)

13:00–16:00 SC271 • Quantum Information—Technologies and Applications
SC376 • Plasmonics

NOTES

CLEO: QELS-Fundamental Science

13:30–15:30

FM3A • Frequency Conversion*Presider: Xiao Li; Joint Quantum Inst., USA***FM3A.1 • 13:30**

Demonstration of background-free, phase-preserving parametric up-conversion at the single-photon level, Yu-Hsiang Cheng^{2,1}, Tim O. Thomay^{2,1}, Glenn S. Solomon^{2,1}, Alan L. Migdall^{2,1}, Sergey V. Polyakov¹; ¹National Inst. of Standards and Technology, USA; ²Joint Quantum Inst., National Inst. of Standards and Technology, Univ. of Maryland, USA. We demonstrate single-photon-level phase preservation in an up-converting interferometer. The up-conversion process is background-free to within experimental uncertainty, allowing high fringe contrast even at low photon levels. This enables faithful up-conversion of entangled photon pairs.

FM3A.2 • 13:45

Ultrafast Time-to-Frequency Demultiplexing of Polarization-Entangled Photons, John M. Donohue¹, Jonathan Lavoie^{1,2}, Kevin J. Resch¹; ¹Inst. for Quantum Computing and Dept. of Physics & Astronomy, Univ. of Waterloo, Canada; ²Group of Applied Physics, Univ. of Geneva, Switzerland. Using shaped pulses and nonlinear optics, we have experimentally demonstrated the demultiplexing of a train of polarization-encoded single photons through time-to-frequency conversion. We have shown this technique to preserve polarization entanglement with a partner photon.

FM3A.3 • 14:00

Low noise single photon frequency up-conversion using Ti-indiffused periodically-poled lithium niobate waveguides with efficient narrowband filtering, Zhenda Xie^{2,1}, Kai-hong Luo³, Harald Herrmann³, Christine Silberhorn³, Chee Wei Wong^{2,1}; ¹Columbia Univ., USA; ²Univ. of California, Los Angeles, USA; ³Paderborn Univ., Germany. We demonstrate single-photon frequency-upconversion using a titanium-infused periodically-poled lithium niobate waveguide by L-band erbium-doped fiber amplifier pump. Internal efficiencies up to 84.4% and dark-count rate of 44kHz are achieved with narrowband filtering down to 3.5GHz.

13:30–15:15

FM3B • Light-matter Interactions in 2D Nanostructures*Presider: Rohit Prasankumar; Los Alamos National Lab, USA***FM3B.1 • 13:30**

Ultrafast Coulomb Intervalley Interaction in Monolayer WS₂, Robert Schmidt¹, Gunnar Berghäuser², Ermin Malic², Andreas Knorr², Robert Schneider¹, Philipp Tonndorf, Steffen Michaelis de Vasconcellos¹, Rudolf Bratschkh¹; ¹Inst. of Physics and Center for Nanotechnology, Univ. of Münster, Germany; ²Dept. for Theoretical Physics, Technical Univ. Berlin, Germany. We reveal the ultrafast intervalley dynamics in monolayer WS₂ with a spectrally-resolved ultrafast pump-probe experiment and a microscopic theory. We find strong intervalley Coulomb coupling in the atomically thin semiconductor.

FM3B.2 • 13:45

Ultrafast mid-infrared intraexcitonic spectroscopy of monolayer MoS₂, Soonyoung Cha¹, Ji Ho Sung², Jooyoung Kim¹, Sangwan Sim¹, Moon-Ho Jo², Hyunyoung Choi¹; ¹School of Electrical and Electronic Engineering, Yonsei Univ., Korea; ²Center for Artificial Low Dimensional Electronic Systems, Inst. for Basic Science, Division of Advanced Materials Science, Pohang Univ. of Science and Technology (POSTECH), Korea. We report the first ultrafast mid-infrared (IR) spectroscopy in monolayer MoS₂. The observed mid-IR dynamics show multiple, yet broadened absorption, indicating the predominant intraexcitonic transition from the ground to the higher-lying excitonic states.

FM3B.3 • 14:00 Invited

Manipulating the Valley Pseudospin in MoS₂ Transistors, Kin F. Mak^{2,1}; ¹Columbia Univ., USA; ²Penn State Univ., USA. Monolayer MoS₂ possess a new valley-pseudospin degree of freedom besides electronic charge and spin. In this talk I will talk about our recent results on optical generation of valley polarization, based on which a novel Hall effect associated with the new degree of freedom is demonstrated. The mechanisms responsible for driving the new valley Hall effect will be discussed.

13:30–15:30

FM3C • Hyperbolic Metamaterial Waveguides*Presider: Ekaterina Poutrina; AFRL, USA***FM3C.1 • 13:30**

Super-Coulombic Energy Transfer: Engineering Dipole-Dipole Interactions with Metamaterials, Ward D. Newman¹, Cristian L. Cortes¹, David Purschke³, Amir Afshar², Zhijiang Chen¹, Glenda De los Reyes³, Frank Hegmann³, Kenneth Cadien², Robert Fedosejevs¹, Zubin Jacob¹; ¹Electrical and Computer Engineering, Univ. of Alberta, Canada; ²Dept. of Chemical and Materials Engineering, Univ. of Alberta, Canada; ³Dept. of Physics, Univ. of Alberta, Canada. We demonstrate experimentally that hyperbolic metamaterials fundamentally alter dipole-dipole interactions conventionally limited to the near-field. The effect is captured in long-range energy transfer and lifetime reduction of donor emitters due to acceptors placed 100 nm away.

FM3C.2 • 13:45

On-chip Super-robust All-dielectric Zero-Index Material, Shota Kita¹, Yang Li¹, Philip Muñoz¹, Orad Reshef¹, Daryl Vulis¹, Bobby Day¹, Eric Mazur¹, Charles Lieber¹, Marko Loncar¹; ¹Harvard Univ., USA. The robustness of the modal degeneracy for photonic Dirac cone can be engineered by designing all-dielectric pillar arrays giving on-chip platform of zero index material for any wavelength regime. We demonstrate this concept for telecom regime.

FM3C.3 • 14:00

Transparent subdiffraction optics: nanoscale light confinement without metal, Saman Jahani¹, Zubin Jacob¹; ¹Univ. of Alberta, Canada. We introduce a paradigm shift in light confinement strategy and show that light can be confined below the diffraction limit using completely transparent artificial media (metamaterials with $\epsilon_r > 1$ and $\mu_r = 1$).

13:30–15:30

FM3D • Frequency Conversion and its Application*Presider: Ryan Behunin; Yale Univ., USA***FM3D.1 • 13:30**

Nonlinear Frequency Mixing in a Surface Nanoscale Axial Photonics Resonator, Michael Kues², Christian Reimer², Tabassom Hamidfar¹, Roberto Morandotti², Pablo Bianucci¹; ¹Dept. of Physics, Concordia Univ., Canada; ²INRS-EMT, Canada. We report on four-wave mixing in a simple-to-fabricate surface nanoscale axial photonics resonator (SNAPR) obtained by pumping with two spectral modes while exploiting a self-locked pump scheme.

FM3D.2 • 13:45

Second-harmonic Generation in a Phase-Matched Nonlinear 2D Crystal, Mervin Zhao¹, Ziliang Ye¹, Yu Ye¹, Hanyu Zhu¹, Yuan Wang¹, Yoshihiro Iwasa², Xiang Zhang¹; ¹Univ. of California, USA; ²Applied Physics, Univ. of Tokyo, Japan. We studied the phase-matched SHG from thin crystals of 3R-MoS₂. Due to the noncentrosymmetric nature of the crystal, the typically observed intensity oscillation in 2H-MoS₂ is replaced with constructive interference of the second harmonic light.

FM3D.3 • 14:00

Efficient Generation of Twin Photons at Telecom Wavelengths with 10 GHz Repetition-Rate-Tunable Comb Laser, Rui-Bo Jin¹, Ryosuke Shimizu², Isao Morohashi¹, Kentaro Wakui¹, Masahiro Takeoka¹, Shuro Izumi^{1,3}, Takahide Sakamoto¹, Mikio Fujiwara¹, Taro Yamashita¹, Shigehito Miki¹, Hiroataka Terai¹, Zhen Wang¹, Masahide Sasaki¹; ¹NICT, Japan; ²Univ. of Electro-Communications, Japan; ³Sophia Univ., Japan. We demonstrate a down-conversion-based twin photon source pumped by a 10 GHz repetition-rate-tunable comb laser at 1553 nm wavelength. We show high Hong-Ou-Mandel interference visibilities, which are free from the pump-power induced degradation.

CLEO: QELS-
Fundamental Science

13:30–15:30

FM3E • Nonlinear Plasmonics

President: Roderick Davidson;
Vanderbilt Univ., USA

FM3E.1 • 13:30

Giant nonlinear response of polaritonic metasurfaces coupled to intersubband transition, JONGWON LEE¹, Nishant Nookala¹, Mykhailo Tymchenko¹, Juan Sebastian Gomez-Diaz¹, Frederic Demmerle², Gerhard Boehm², Markus-Christian Amann², Andrea Alu¹, Mikhail A. Belkin¹; ¹Electrical and Computer Engineering, Univ. of Texas at Austin, USA; ²Walter Schottky Institut, Technische Universität München, Germany. We report highly-nonlinear metasurfaces based on combining electromagnetically-engineered plasmonic nanoresonators with quantum-engineered intersubband nonlinearities. Experimentally, effective nonlinear susceptibility over 480 nm/V was measured for second-harmonic generation at normal incidence.

FM3E.2 • 13:45

Highly efficient SHG in NLO polymer-coated Au nanoparticles by doubly resonant excitations, Atsushi Sugita¹, Takuma Hirabayashi¹, Shunsuke Nihashi¹, Atsushi Ono¹, Yoshimasa Kawata¹; ¹Shizuoka Univ., Japan. We present localized SP-assisted SHG in NLO polymer-coated Au nanoparticles. More than threefold enhancement in the SHG conversion efficiencies was recorded by tuning the transition frequency of the NLO polymers to the excitation light frequency.

FM3E.3 • 14:00

Tip-enhanced Upconversion of Er³⁺/Yb³⁺:NaYF₄ Nanoparticles, Gengxu Chen¹, E Wu¹, Chengjie Ding¹, Botao Wu¹, Xueting Ci¹, Yan Liu¹, Youying Rong¹, Yingxian Xue¹, Heping Zeng¹; ¹State Key Lab of Precision Spectroscopy, East China Normal Univ., China. We demonstrated tip-enhanced upconversion luminescence from a single Er³⁺/Yb³⁺:NaYF₄ nanoparticle due to plasmonic effect. The gold-coated tip enabled improved reception and transmission of incident electromagnetic fields, which increased both absorption and emission processes.

13:30–15:30

SM3F • Ultrafast, High Speed
and High Power Semiconductor
Lasers

President: Leif Johansson;
Freedom Photonics, LLC, USA

SM3F.1 • 13:30

Intracavity Loss and Dispersion Managed Mode-Locked Diode Laser, Jan C. Balzer¹, Benjamin Döpke¹, Rouven H. Pilny¹, Carsten Brenner¹, Andreas Klehr², Götz Erbert², Günther Tränkle², Martin R. Hofmann¹; ¹Ruhr Universität Bochum, Germany; ²Ferdinand-Braun-Institut, Leibniz Institut für Höchstfrequenztechnik im Forschungsverbund Berlin e.V., Germany. We present a self-optimizing diode laser, which generates 216 fs Fourier-limited pulses after external pulse compression. This is achieved by a closed-loop learning concept that optimizes the intracavity spectral phase and amplitude.

SM3F.2 • 13:45

Sub-300-femtosecond Semiconductor Disk Lasers, Dominik Waldburger¹, Mario Mangold¹, Sandro M. Link¹, Matthias Golling¹, Emilio Gini², Bauke W. Tilma¹, Ursula Keller¹; ¹ETH Zurich, Switzerland; ²FIRST Center for Micro- and Nanoscience, Switzerland. We present the first sub-150-fs SESAM-modelocked vertical external-cavity surface-emitting laser (VECSEL) in the 100-mW average output power regime and the first sub-300-fs modelocked integrated external-cavity surface-emitting laser (MIXSEL) with 180 mW of average output power.

SM3F.3 • 14:00

Synthesis of coherent optical pulses using a field-programmable gate array (FPGA)-based gradient descent phase-locking algorithm with three semiconductor lasers, Kenneth J. Underwood¹, Andrew M. Jones¹, Juliet Gopinath¹; ¹Univ. of Colorado at Boulder, USA. We demonstrate optical pulse synthesis through coherent combination of AOM-separated light by phase-locking feedback from an FPGA. An order of magnitude improvement in phase stability is shown, limited by the noise of the AOM driver.

CLEO: Science & Innovations

13:30–15:30

SM3G • Group IV Photonics

President: Michael Menard; McGill
Univ., Canada

SM3G.1 • 13:30 **Invited**

Optical Interconnects based on Ge/SiGe Multiple Quantum Well Structures, Delphine Marris-Morini¹, Papichaya Chaisakul^{1,2}, Jacopo Frigerio³, Daniel Chrastina³, Vladyslav Vakarin¹, Stefano Cecchi³, Giovanni Isella³, Laurent Vivien¹; ¹Institut d'Electronique Fondamentale, Université Paris Sud, France; ²Dept. of Materials Engineering, The Univ. of Tokyo, Japan; ³Politecnico Di Milano, L-NESS, Italy; ⁴CNRS, Institut d'Electronique Fondamentale, France. Silicon photonics devices based on Ge/SiGe structures are promising. However their integration with silicon on insulator waveguides is a challenging point. We present an innovative approach to monolithically integrate low-voltage, broadband photonic interconnection on silicon.

SM3G.2 • 14:00

Relaxation Dynamics of Optically Generated Carriers in Graphene-on-Silicon Nitride Waveguide Devices, Jiaqi Wang¹, Zhenzhou Cheng¹, Qijie Xie¹, Chester Shu¹, Hon Ki Tsang¹; ¹The Chinese Univ. of Hong Kong, Hong Kong. We studied the carrier relaxation dynamics in graphene-on-silicon nitride waveguides. Optically generated carriers from a quasi-continuous wave pump laser show a microsecond response time while those generated from mode-locked laser pulses exhibit accelerated relaxation dynamics.

13:30–15:15

SM3H • THz Materials Science

President: David Cooke; McGill
Univ., Canada

SM3H.1 • 13:30

Extended-Drude Response of Photocarriers in InSb Revealed with Ultrabroadband Infrared Time-Domain Spectroscopy, Eiichi Matsubara^{1,2}, Tomohide Morimoto², Masaya Nagai², Masaaki Ashida²; ¹Dept. of Physics, Osaka Dental Univ., Japan; ²Graduate School of Engineering Science, Osaka Univ., Japan. We visualized the extension of Drude response of photoexcited carriers by energy-dependent scattering time and effective mass of electrons in InSb, making full use of the advantage of air plasma based ultrabroadband infrared time-resolved spectroscopy.

SM3H.2 • 13:45

Photovoltaic Polymer-Fullerene Blends: Terahertz Carrier Dynamics and Device Performance, Zuanming Jin¹, Dominik Gehrig¹, Clare Dyer-Smith¹, Edwin J. Heilweil², Frédéric Laquai¹, Mischa Bonn¹, Dmitry Turchinovich¹; ¹MPI for Polymer Research, Germany; ²National Inst. of Standards and Technology, USA. Ultrafast THz spectroscopy of photovoltaic polymer-fullerene blends PTB7:PC₇₀BM and P3HT:PC₇₀BM reveals differences in conductivity lifetimes and quantum yields, well correlated with different power conversion efficiencies of photovoltaic devices utilizing these compounds.

SM3H.3 • 14:00 **Invited**

Probing Superconducting Gap Dynamics with THz Pulses, Matthias Beck², Maximilian Klammer², Ian Rousseau², Gregory Gol'tsman³, Itay Diamant⁴, Yoram Dagan⁴, Jure Demsar^{1,2}; ¹Johannes Gutenberg Universität Mainz, Germany; ²Physics Dept., Univ. of Konstanz, Germany; ³Moscow State Pedagogical Univ., Russia; ⁴Raymond and Beverly Sackler School of Physics and Astronomy, Tel Aviv Univ., Israel. We studied superconducting gap dynamics in a BCS superconductor NbN and electron doped cuprate superconductor PCCO following excitation with near-infrared (NIR) and narrow band THz pulses. Systematic studies on PCCO imply very selective electron-phonon coupling.

Meeting Room
211 B/D

CLEO: Science &
Innovations

13:30–15:30
SM3I • WDMs and Filters
Presider: Jessie Rosenberg; International Business Machines Corp, USA

SM3I.1 • 13:30
Design of a Polarization-Insensitive WDM Demultiplexing Lattice Filter in SOI, Antoine Bois¹, Alexandre D. Simard¹, Wei Shi¹, Sophie LaRochelle¹; ¹Université Laval, Canada. We propose a novel design method for polarization-insensitive optical lattice filters. The technique takes advantage of the spectral periodicity of the Mach-Zehnder building blocks and optimizes the coupler and interferometer lengths to minimize cost functions.

SM3I.2 • 13:45
Inverse Design and Implementation of a Wavelength Demultiplexing Grating Coupler, Alexander Y. Piggott¹, Jesse Lu¹, Thomas M. Babinec¹, Konstantinos Lagoudakis¹, Jan Petykiewicz¹, Jelena Vuckovic¹; ¹Stanford Univ., USA. We have developed a general inverse design algorithm for designing micro- and nano-photonics devices, where the user only specifies the desired device performance. We experimentally demonstrate a vertical-incidence wavelength demultiplexing grating designed by this algorithm.

SM3I.3 • 14:00
All-Optically Controlled Fabry-Perot Cavity-Assisted Add-Drop Microring Resonator on a Silicon Chip, Weifeng Zhang¹, Jianping Yao¹; ¹Univ. of Ottawa, Canada. An all-optically controlled Fabry-Perot cavity-assisted add-drop microring resonator (MRR) on a silicon chip, in which one bus waveguide is replaced by a sidewall Bragg grating Fabry-Perot cavity, is proposed and experimentally demonstrated.

Meeting Room
212 A/C

CLEO: Applications
& Technology

14:00–15:30
AM3J • Neurophotonics and Optogenetics
Presider: Robert Campbell; Univ. of Alberta, Canada

AM3J.1 • 13:30 **Invited**
Withdrawn

AM3J.2 • 14:00 **Invited**
Visualizing Mammalian Brain Area Interactions by Dual-axis Two-photon Calcium Imaging, Mark Schnitzer¹; ¹Dept. of Biology and Applied Physics, Stanford Univ., USA. Fluorescence Ca²⁺ imaging enables large-scale recordings of neural activity, but collective dynamics across mammalian brain regions are generally inaccessible within single fields of view. Here we introduce a two-photon microscope possessing two articulated arms that can simultaneously image two brain areas (~0.38 mm² each), either nearby or distal, using microendoscopes, in awake behaving rodents.

Meeting Room
212 B/D

13:30–15:30
AM3K • Components and Enabling Technologies
Presider: Wilhelm Kaenders; Topptica Photonics AG, Germany

AM3K.1 • 13:30
High Speed Surface Micromachined MEMS Tunable VCSEL for Telecom Wavelengths, Sujoy Paul¹, Christian Gierl¹, Julijan Cesar¹, Quang Trung Le¹, Mohammadreza Malekizandi¹, Franko Kueppers¹, Benjamin Koegel², Juergen Roskopf², Christoph Gréus², Markus Göblich², Yan Xu², Christian Neumeier², Markus Ortsiefer²; ¹TU Darmstadt, Germany; ²Vertilas GmbH, Germany. We report direct modulation of a widely tunable surface micromachined MEMS VCSEL. The MEMS is electro-thermally actuated for tuning the emission wavelength over 60 nm with a center wavelength of 1554 nm. Error-free transmission is achieved at 10 Gbit/s for 47 nm tuning range.

AM3K.2 • 13:45
New Generation of VBGs for Efficient Spectral Beam Combination of Semiconductor Lasers, Vadim I. Smirnov¹; ¹OptiGrate Corp, USA. Novel types of volume Bragg gratings with enhanced parameters were recorded in PTR glass. They were used for efficient spectral beam combination of high power multimode semiconductor lasers with high spectral density of 1 nm/channel.

AM3K.3 • 14:00
Efficient Chirped Bragg Gratings for Stretching and Compression of High Energy Ultrashort Laser Pulses at 800 nm Spectral Region, Vadim I. Smirnov¹; ¹OptiGrate Corp, USA. This paper reports on new generation of recorded in PTR glass chirped gratings with enhanced beam quality and efficiency for stretching and compression of ultrashort laser pulses in 800 nm spectral region.

Marriott
Salon I & II

CLEO: Science &
Innovations

13:30–15:30
SM3L • Novel Fiber Materials
Presider: Shinji Yamashita; Univ. of Tokyo, Japan

SM3L.1 • 13:30
Glass-clad Ti:sapphire crystal fiber laser, Shih-Chang Wang¹, Chun-Yang Hsu¹, Dong-Yo Jheng¹, Tuan-Shu Ho¹, Teng-I Yang¹, Yaqin Xu¹, Sheng-Lung Huang¹; ¹National Taiwan Univ., Taiwan. Glass-clad Ti:sapphire crystal fibers were grown using the co-drawing laser-heated pedestal growth method. A laser threshold of less than 100 mW was achieved at room temperature with an a-cut-core diameter as small as 18 μm.

SM3L.2 • 13:45
Grating Effect in Lanthanum Aluminum Silicate Glass Fiber, Zhifang Wu^{1,2}, Xuguang Shao¹, Ping Shum^{1,2}, Hailiang Zhang^{1,2}, Tianye Huang^{1,2}, Nan Zhang^{1,2}, Georges Humbert³, Jean-Louis Auguste³, Stéphanie Leparmentier³, Kay Schuster⁴, Doris Litzkendorf⁴; ¹School of Electrical and Electronics Engineering, Nanyang Technological Univ., Singapore; ²CNRS-International-NTU-Thales Research Alliance (CINTRA), Singapore; ³XLIM Research Inst., UMR 7252 CNRS/Univ. of Limoges, France; ⁴Leibnitz Inst. of Photonic Technology (IPHT), Germany. We experimentally demonstrate a Type I grating effect in a lanthanum-aluminum silicate fiber for the first time, to the best of our knowledge. This grating shows a temperature sensitivity ~8.71 pm/^oC, which is lower than that of FBG in standard single-mode fiber.

SM3L.3 • 14:00
Mid-infrared Raman sources with highly GeO₂ doped silica optical fibers, Xinyong Dong^{3,2}, Lulu Wang^{1,4}, Xiaohui Li⁴, Ping Shum^{4,2}, Haibin Su^{3,2}, Qijie Wang⁴; ¹China Jiliang Univ., China; ²CINTRA, Research Techno Plaza, 50 Nanyang Drive, Singapore; ³Nanyang Technological Univ., School of Materials Science and Engineering, Singapore; ⁴Nanyang Technological Univ., School of Electrical & Electronic Engineering, Singapore. Mid-infrared Raman sources based on highly GeO-doped silica-fibers pumped at ~2.0 μm pulsed/cw lasers are studied. Supercontinuum generation up to 3.0 μm and cascaded Raman scattering up to 2.53 μm are achieved, respectively.

CLEO: Science & Innovations

13:30–15:30

SM3M • High Energy, High Power Systems & Enabling Technology*Presider: Jay Doster; Northrop Grumman Cutting Edge Optronics, USA*SM3M.1 • 13:30 **Tutorial**

High Power Diode Lasers for Pumping High Energy Solid State Lasers, Paul Crump¹, Carlo Frevert¹, Götz Erbert¹, Günther Tränkle¹; ¹Ferdinand-Braun Institut, Germany. The optical energy used in high-energy-class solid state laser facilities is generated by high power diode lasers. This tutorial reviews and summarizes progress in ongoing efforts world-wide to improve the performance of these critical components.



Paul Crump completed his Ph.D. in physics from Nottingham Univ. (UK) in 1996. After 6 years with Agilent Technologies and 6 years with nLight Photonics (USA), he joined the FBH (Berlin, Germany). Crump is currently group leader responsible for high-power broad area diode lasers and bars.

13:30–15:15

SM3N • Ultrafast High-field Phenomena and Laser Filamentation*Presider: Pavel Polynkin; Univ. of Arizona, USA*SM3N.1 • 13:30 **Invited**

Filament-Based Impulsive Raman Excitation of Vibrational and Rotational Modes of Polyatomic Molecules, Robert J. Levis¹; ¹Temple Univ., USA. Femtosecond laser filamentation serves as a source well-suited for detection using impulsive excitation of vibrational and rotational modes of molecules. The resulting coherent motion serves a route to remote detection through single shot Raman scattering.

SM3N.2 • 14:00

Picosecond Ionization Dynamics in Femtosecond Filaments at High Pressures, Xiaohui Gao¹, Gauri Patwardhan¹, Samuel Schrauth¹, Daiwei Zhu¹, Alexander L. Gaeta¹; ¹School of Applied and Engineering Physics, Cornell Univ., USA. We observe a 3-fold increase in the electron density within 30 picoseconds after the filamentary propagation of femtosecond pulses in 60-bar argon gases. This suggests that electron-impact ionization dominates on this time scale.

13:30–15:30

SM3O • Nano and Micro-Optical Sensors*Presider: Gerard Wysocki; Princeton Univ., USA*SM3O.1 • 13:30 **Invited**

Single Nucleic Acid Interactions Monitored with Optical Microcavity Biosensors, Frank Vollmer¹; ¹Max-Planck-Inst Physik des Lichts, Germany. We have developed a label-free biosensing platform that is capable of monitoring single DNA molecules and their interaction kinetics, hence achieving an unprecedented sensitivity in the optical domain.

SM3O.2 • 14:00

Differentiating surface and bulk interactions in nanoplasmonic interferometric sensor arrays, Beibei Zeng¹, Filbert Bartoli¹; ¹Lehigh Univ., USA. We present a nanoplasmonic interferometric sensor platform that can differentiate the adsorption of a thin protein layer on the sensor surface from bulk refractive index changes, exploiting the different penetration depths of multiple SPPs.

13:30–15:30

SM3P • Mode Locked Lasers*Presider: Omer Ilday; Bilkent Univ., Turkey*

SM3P.1 • 13:30

50.5 nJ, 750 fs all-fiber all polarization-maintaining fiber laser, Jiaqi Zhou¹, Xijia Gu¹; ¹ECE, Ryerson Univ., Canada. We report on our recent experiments of a 50.5 nJ, 750 fs ultra-stable dissipative soliton fiber laser in the presence of Raman scattering in a long ring cavity. We demonstrated that a transition from noise-like soliton to stable dissipate soliton took place at sufficiently high pulse energy.

SM3P.2 • 13:45

A Harmonically Mode-locked Femtosecond Fiber Laser using Bulk-structured Bi₂Te₃ Topological Insulator, Junsu Lee¹, Joonhoi Koo¹, Cheolhwan Chi¹, Ju Han Lee¹; ¹Univ. of Seoul, Korea. We experimentally demonstrate femtosecond harmonic mode-locking of a fiber laser using a bulk-structured Bi₂Te₃ topological insulator (TI)-deposited side-polished fiber.

SM3P.3 • 14:00

Tm/Ho Co-doped Mode-locked Fiber Laser based on Graphene Transferred on Side-polished Fiber, Xiaohui Li¹, Xuechao Yu¹, Zhiyu Yan¹, Qijie Wang², Xia Yu³, Ying Zhang³; ¹Nanyang Technological Univ., Singapore; ²Centre for Disruptive Photonic Technologies, Nanyang Technological Univ., Singapore; ³Singapore Inst. of Manufacturing Technology, Singapore. All-fiber Tm/Ho co-doped mode-locked fiber laser based on a side polished fiber with atom-layered graphene manufactured by chemical-vapor-deposition (CVD) method as platform has been investigated, which can operate from fundamental to thirteenth harmonic mode locking.

CLEO: QELS-Fundamental Science

FM3A • Frequency
Conversion—Continued

FM3A.4 • 14:15

Low-Noise Quantum Frequency Translation of Single Photons, Alessandro Farsi¹, Stephane Clemmen¹, Sven Ramelow¹, Alexander L. Gaeta¹; ¹Cornell Univ., USA. We demonstrate quantum frequency translation of single photons via four-wave-mixing Bragg scattering using a liquid nitrogen cooled dispersion-shifted fiber. We achieve 80% photon conversion efficiency with less than 0.001 noise photons per 5ns gate.

FM3A.5 • 14:30

Background-free Quantum Frequency Downconversion for Two-photon Interference of Heterogeneous Photon Sources, Leo Yu¹, Chandra M. Natarajan^{2,1}, Tomoyuki Horikiri^{3,1}, carsten langrock¹, Jason Pelc⁴, Mike G. Tanner⁵, Eisuke Abe³, Sebastian Maier⁶, Sven Höfling^{7,6}, Christian Schneider⁶, Martin Kamp⁶, Robert H. Hadfield², Martin M. Fejer¹, Yoshihisa Yamamoto^{1,3}; ¹Stanford Univ., USA; ²Univ. of Glasgow, UK; ³National Inst. of Informatics, Japan; ⁴Hewlett-Packard Labs, USA; ⁵Heriot-Watt Univ., UK; ⁶Univ. of Wurzburg, Germany; ⁷Univ. of St Andrews, UK. We report background-free, near-infrared-to-telecom quantum frequency downconversion, mediating two-photon interference with a mean wavepacket overlap larger than 0.89, regardless of the original separation between photon sources in wavelength (900- and 911-nm), wavepacket, and distance (2 km).

FM3A.6 • 14:45

Ramsey Interferometry for Manipulation of Single Photons, Alessandro Farsi¹, Stephane Clemmen¹, Sven Ramelow¹, Alexander L. Gaeta¹; ¹Cornell Univ., USA. We demonstrate a Ramsey interferometer for single photons via consecutive quantum frequency conversions where the phase depends on the propagation between the two interaction regions. Such an interferometer offers control over frequency encoded quantum states.

FM3B • Light-matter
Interactions in 2D
Nanostructures—Continued

FM3B.4 • 14:30

Single Photon Emission from Localized Excitons in Monolayer WSe₂, Philipp Tonndorf¹, Robert Schmidt¹, Johannes Kern¹, Michele Buscema², Gary Steele², Andres Castellanos-Gomez², Herre van der Zant², Steffen Michaelis de Vasconcellos¹, Rudolf Bratschitsch¹; ¹Inst. of Physics and Center for Nanotechnology, Univ. of Münster, Germany; ²Kavli Inst. of Nanoscience, Delft Univ. of Technology, Netherlands. We observe stable and narrowband single photon emission from localized quantum emitters in a WSe₂ monolayer. Photoluminescence excitation spectroscopy reveals that the emission originates from single excitons trapped in a local potential well.

FM3B.5 • 14:45

Emergent photophenomena in three dimensional van der Waals heterostructures, Bala Murali Krishna Mariserla¹, Michael K L Man¹, Soumya Vinod², Catherine Chin¹, Takaaki Harada¹, Jaime Taha-Tijerina², Chandra Sekhar Tiwary³, Patrick Nguyen², Patricia Chang⁴, Tharangattu N Narayanan⁵, Angel Rubio^{6,7}, Pulickel M Ajayan², Saikat Talapatra^{1,8}, Keshav M. Dani¹; ¹Femtosecond Spectroscopy Unit, Okinawa Int. of Sci. & Tech. Grad. Univ., Japan; ²Dept. of Materials Science and Nanoengineering, Rice Univ., USA; ³Materials Engineering, Indian Inst. of Science, India; ⁴Dept. of Chemistry, Rice Univ., USA; ⁵TIFR Center for Interdisciplinary Sciences (TCIS), Tata Inst. of Fundamental Research, India; ⁶: Max Planck Inst. for the Structure and Dynamics of Matter, Germany; ⁷Nano-Bio Spectroscopy Group and European Theoretical Spectroscopy Facility (ETSF), Universidad del Pais Vasco CFM CSIC-UPV/EHU-MPC & DIPC, Spain; ⁸Dept. of Physics, Southern Illinois Univ., USA. We report on the fabrication and observation of emergent opto-electronic phenomena in three dimensional, micron-sized van der Waals heterostructures self-assembled from atomic layers of graphene and hexagonal boron nitride in varying ratios.

FM3C • Hyperbolic
Metamaterial Waveguides—
Continued

FM3C.4 • 14:15

Light Guiding by Gauge Field for Photons, Qian Lin¹, Shanhui Fan¹; ¹Stanford Univ., USA. We propose a waveguiding mechanism based on the effective gauge field for photons, where the core and cladding are subject to different gauge potentials. This can be realized in a modulated resonator lattice, and provides a dynamically reconfigurable mechanism for generating a one-way waveguide.

FM3C.5 • 14:30

General Conditions for Lossless Propagation in Near-Infrared Hyperbolic Metamaterial Waveguides, Joseph S. Smalley¹, Felipe Vallini¹, Boubacar Kante¹, Yeshaiah Fainman¹; ¹Univ. of California at San Diego, USA. We present general conditions for lossless propagation in near-infrared hyperbolic metamaterial (HMM) waveguides with lateral confinement. We conclude that HMMs based on noble metals, rather than transparent conducting oxides, offer greatest promise for low-loss propagation.

FM3C.6 • 14:45

Dispersion Control of High-k Waves in Tapered Hyperbolic Waveguides, Nathaniel Kinsey², Paul West², Marcello Ferrera^{2,1}, Alexander V. Kildishev², Vladimir M. Shalaev², Alexandra Boltasseva²; ¹Engineering and Physical Sciences, Heriot-Watt, UK; ²Electrical and Computer Engineering, Purdue Univ., USA. The fundamental problem of efficiently outcoupling high-k waves from hyperbolic metamaterials is approached with an in-plane configuration, and enhanced with adiabatic tapering. This strategy may allow for better efficiency of Purcell enhanced quantum sources.

FM3D • Frequency Conversion
and its Application—Continued

FM3D.4 • 14:15

Significant Enhancement of Third- and Fifth-Harmonic Generation in Air via Two-Color, Time-Resolved Methods, Darshana Weerawarne¹, Ross Grynkol¹, Henry J. Meyer¹, Bonggu Shim¹; ¹SUNY Binghamton, USA. We report two orders of magnitude enhancement of third- and fifth-harmonic generation in air via time-resolved methods using two-color, femtosecond beams. We attribute the significant enhancement to cross-phase modulation and/or plasma assisted phase matching effects.

FM3D.5 • 14:30 **Invited**

Single-Pulse Two-dimensional Raman Spectroscopy, Hadas Frostig¹, Tim Bayer¹, Nirit Dudovich¹, Yonina C. Eldar², Yaron Silberberg¹; ¹Weizmann Inst., Israel; ²Technion, Israel. We present a single-pulse two-dimensional Raman spectroscopy scheme. Our scheme offers not only a major simplification of the conventional setup but also an inherent favoring of the direct fifth-order signal over the cascaded signal, the latter being a signal that carries no coupling information.

CLEO: QELS-
Fundamental ScienceFM3E • Nonlinear Plasmonics—
Continued

FM3E.4 • 14:15

Large and Ultrafast Nonlinear Absorption of an Air/Gold Plasmonic Waveguide, Alexandre Baron¹, Thang B. Hoang¹, Chao Fang¹, Maiken H. Mikkelsen¹, David R. Smith¹; ¹Duke Univ., USA. We investigate theoretically and experimentally the nonlinear propagation of surface plasmons on an air/gold interface which reveals large and ultrafast (≈ 100 fs) self-induced absorption. The experiment enables a direct measurement of the third-order nonlinear susceptibility.

FM3E.5 • 14:30

Tailoring the Shape of Metallic Nanocavities for Enhanced Four-Wave Mixing, Euclides C. Almeida¹, Yehiam Prior¹; ¹Weizmann Inst. of Science, Israel. Efficient four-wave mixing, with nonlinear response equivalent to BBO of the same thickness, is demonstrated for arrays of nanocavities milled in a free-standing gold film when their shape is properly designed.

FM3E.6 • 14:45

All-Optical Electric-Field-Induced Second-Harmonic Generation, Roderick Davidson^{1,2}, Anna Yanchenko³, Jed Ziegler¹, Sergey Avanesyan¹, Richard F. Haglund¹; ¹Physics, Vanderbilt Univ., USA; ²Quantum Information Sciences, Oak Ridge National Lab, USA; ³Physics, Univ. of Virginia, USA. Interferometric pump-probe spectroscopy is used to demonstrate all-optical second-harmonic generation from a polymer dielectric in a serrated nanogap structure. Strong optical frequency electric-fields from surface plasmons create ultrafast controllable nonlinear light pulses.

SM3F • Ultrafast, High Speed
and High Power Semiconductor
Lasers—Continued

SM3F.4 • 14:15

A High Power and Ultrahigh Frequency Mode-Locked Laser Monolithically Integrated with an SOA, Lianping Hou¹, John H. Marsh¹; ¹School of Engineering, Univ. of Glasgow, UK. We report 628 GHz and 1.20 THz pulse repetition frequencies with 142 mW peak powers from a passively mode-locked side-wall SGDBR laser integrated with an SOA, demonstrating high reproducibility, controllability and a wide operation range.

SM3F.5 • 14:30

Tracking the Ultrafast Light-Matter Interaction in Population-Inverted Quantum Dots via Quantum State Tomography, Nicolai B. Grosse¹, Nina Owschmikow¹, Alexej Koltchanov¹, Mirco Kolarczik¹, Ulrike K. Woggon¹, Roland Aust², Benjamin Lingnau², Kathy Lüdge²; ¹IOAP, Technische Universität Berlin, Germany; ²ITP, Technische Universität Berlin, Germany. Based on the full characterization of a pulse transmitted through a semiconductor optical amplifier by quantum state tomography, we determine the degree of population inversion and the momentary signal-to-noise ratio at sub-picosecond times and RT.

SM3F.6 • 14:45

Application of Strong Slow-Light Feedback to Boost the Modulation Bandwidth of VCSELs Beyond 70 GHz, Moustafa Ahmed^{1,2}, Ahmed Bakry¹, Hamed Dalir³, Fumio Koyama^{3,1}; ¹King Abdulaziz Univ., Saudi Arabia; ²Physics, Minia Univ., Egypt; ³Tokyo Inst. of Technology, Japan. We present modeling of strong slow-light feedback in VCSEL coupled with a transverse cavity. We show boosting of the modulation bandwidth to frequencies reaching 70 GHz as well as resonance modulation around 90 GHz.

CLEO: Science & Innovations

SM3G • Group IV Photonics—
Continued

SM3G.3 • 14:15

A Black Phosphorus FET Integrated on a Silicon Waveguide for High Speed, Low Dark Current Photodetection, Nathan Youngblood¹, Che Chen¹, Steven J. Koester¹, Mo Li¹; ¹UMN, USA. A waveguide-integrated black phosphorus photodetector with high responsivity and low dark current is demonstrated for telecom wavelengths with an RC-limited bandwidth of 3 GHz. Electrostatic doping and frequency dependent photo-response are used to identify photocurrent generation mechanisms.

SM3G.4 • 14:30

Germanium Photonic Crystal Nanobeam Cavity with $Q > 1,300$, Michihiro Kuroki¹, Satoshi Kako¹, Satomi Ishida¹, Katsuya Oda², Tatemu Ido², Satoshi Iwamoto¹, Yasuhiko Arakawa¹; ¹Inst. of Industrial Science and Inst. for Nano Quantum Information Electronics, Univ. of Tokyo, Japan; ²Hitachi Ltd., Japan. We fabricate germanium-based photonic crystal nanobeam cavities and observe a large enhancement (≈ 170 times) of room-temperature photoluminescence signal at a cavity resonance of $\approx 1,700$ nm. A cavity quality factor as high as 1,350 is achieved.

SM3G.5 • 14:45

A Direct Band Gap GeSn Laser on Si, Richard Geiger^{1,2}, Stephan Wirths³, Nils von den Driesch³, Zoran Ikonc⁴, Jean-Michel Hartmann⁵, Jerome Faist², Siegfried Mantl³, Detlev Grützmacher³, Dan Buca³, Hans Sigg¹; ¹Lab for Micro- and Nanotechnology, Paul Scherrer Inst., Switzerland; ²Inst. for Quantum Electronics, ETH Zürich, Switzerland; ³Peter Grünberg Inst. 9, Forschungszentrum Jülich, Germany; ⁴Inst. of Microwaves and Photonics, Univ. of Leeds, UK; ⁵CEA, LETI, France. Temperature-dependent photoluminescence spectroscopy reveals that partially strain-relaxed $\text{Ge}_{0.8}\text{Sn}_{0.13}$ exhibits a fundamental direct band gap. For such an alloy, we show lasing at ≈ 2.3 μm emission wavelength under optical pumping up to 90 K.

SM3H • THz Materials Science—
Continued

SM3H.4 • 14:30

Enhancement of THz emission from GaN surface by Ga vacancy-related defects, Yuji Sakai¹, Iwao Kawayama¹, Hidetoshi nakanishi², Masayoshi Tonouchi¹; ¹Osaka Univ., Japan; ²SCREEN Holdings Co., Ltd., Japan. The enhancement of terahertz emission from a GaN wafer induced by Ga vacancy-related defects was observed. This phenomena can be explained by the change of the band bending at these defects.

SM3H.5 • 14:45

Ultrabroadband, Lightweight, Flexible, and Polarization Sensitive Photodetector Based on Carbon Nanotube Fibers, Ahmed Zubair¹, Dmitri Tsentelovich², Colin C. Young², Naoki Fujimura³, Xuan Wang¹, Xiaowei He¹, Weilu Gao¹, Yukio Kawano³, Matteo Pasquali^{2,4}, Junichiro Kono^{1,5}; ¹Electrical and Computer Engineering, Rice Univ., USA; ²Chemical and Biomolecular Engineering, Rice Univ., USA; ³Physical Electronics, Tokyo Inst. of Technology, USA; ⁴Chemistry, Rice Univ., USA; ⁵Physics and Astronomy, Rice Univ., USA. We present a flexible ultrabroadband (visible to terahertz), polarization-sensitive carbon nanotube fiber photodetector. This photothermoelectric-effect-based room-temperature photodetector fabricated using a unique technique has high responsivities, up to 2.2 mA/W in the terahertz regime.

Meeting Room
211 B/D

CLEO: Science &
Innovations

SM3I • WDMs and Filters—
Continued

SM3I.4 • 14:15

Multichannel Optical Filters in Nanoscale Silicon Waveguides, Matthew W. Puckett¹, Felipe Vallini¹, Andrew Grieco¹, Shaya Fainman¹; ¹Univ. of California, San Diego, USA. We design and characterize asymmetric Bragg gratings in waveguides which possess multiple reflected wavelengths. We experimentally demonstrate devices with two independent stopbands, then use finite-difference time domain software to characterize more complex grating designs.

SM3I.5 • 14:30

Narrowband Waveguide Bragg Gratings with Fully-etched Side Corrugations and Large Fabrication Tolerance, Keng-Hsien Lin¹, Yung-Jr Hung¹, Chong-Jia Wu¹, Cheng-Yu Wang¹, Yung-Jui Chen¹; ¹National Sun Yat-sen Univ., Taiwan. Fully-etched cladding-modulated grating allows not only flexible control of the reflection response but also large fabrication tolerance. A reflection bandwidth of < 0.6 nm and a Bragg wavelength variation of within 1 nm is experimentally demonstrated.

SM3I.6 • 14:45

High-Quality Bragg Gratings Operating in Reflection without Circulators in SOI, Alexandre D. Simard¹, Sophie LaRochelle¹; ¹Universite Laval, Canada. We demonstrate that apodized Bragg gratings placed in the two arms of a Mach-Zehnder structure in SOI can provide high-quality filtering functions overcoming phase noise distortions. As examples, we present narrowband, phase-shifted and dispersion-less filters.

Meeting Room
212 A/C

CLEO: Applications
& Technology

AM3J • Neurophotonics and
Optogenetics—Continued

AM3J.3 • 14:30

Engineering the Next Generation of Optogenetic Reporters to Illuminate Neuronal Activity, Robert E. Campbell¹; ¹Univ. of Alberta, Canada. The Campbell group uses protein engineering to develop fluorescent protein-based reporters for cell imaging. I will describe our most recent efforts to engineer an improved generation of reporters for calcium ion, membrane potential, and neurotransmitters.

Invited

AM3K • Components and
Enabling Technologies—
Continued

AM3K.4 • 14:15

Beam Shaping Concepts with Aspheric Surfaces, Ulrike Fuchs¹, Sabrina Matthias²; ¹Asphericon GmbH, Germany; ²asphericon Inc, USA. The potpourri of aspheric surfaces offers many possibilities in optical design, even the chance for flexible beam shaping setups. Since these are refractive optical elements the beam shaping is robust with respect to wavelength changes.

AM3K.5 • 14:30

Generation of continuous-wave and pulsed vortex beams in an a-cut Nd:YVO₄ laser with annular end-pumping, Ajian Hu¹, Peifeng Chen¹, Ying Wang¹, Shumo Li¹; ¹Huazhong Univ of Science & Technology, China. We directly produced continuous-wave (CW) and pulsed first order Laguerre-Gaussian vortex beams from an annular end-pumped Nd:YVO₄ laser with a general fiber coupled LD source (core diameter, 800 μm).

AM3K.6 • 14:45

Development of YCOB Crystals for Large Aperture SHG, THG and OPA Applications, Yanqing Zheng¹; ¹Shanghai Inst. of Ceramics, CAS, USA. Large clear aperture elements bigger than 30 mm x 30 mm are difficult to growth and are of high cost for BBO, LBO crystals. YCOB grown by Czochralski method was shown a good choice of large aperture applications.

Marriott
Salon I & II

CLEO: Science &
Innovations

SM3L • Novel Fiber Materials—
Continued

SM3L.4 • 14:15

Low-Loss Tellurite Fibers With Embedded Nanodiamonds, Heike Ebendorff-Heidepriem¹, Yinlan Ruan¹, Hong Ji¹, Brett Johnson², Takeshi Ohshima⁴, Andrew Green-tree³, Brant C. Gibson³, Tanya Monro¹; ¹Univ. of Adelaide, Australia; ²Univ. of Melbourne, Australia; ³RMIT, Australia; ⁴Japan Atomic Energy Agency, Japan. We report the development of nanodiamond-doped tellurite fibers with both preserved single photon emission properties of the nanodiamonds embedded in the glass and fiber loss reduced to levels suitable for practical applications.

SM3L.5 • 14:30

Graphene-deposited Microfiber for Ultrafast Optical Modulation, Shaoliang Yu¹, Limin Tong¹; ¹State Key Lab of Modern Optical Instrumentation, Dept. of Optical Engineering, Zhejiang Univ., China. With a convenient and controllable evanescent-field-induced transfer method, graphene flakes were deposited on the surface of a 1-μm-diameter microfiber, which can be used for ultrafast optical modulation based on its distinct saturable absorption.

SM3L.6 • 14:45

Multiwavelength Thulium-doped Fiber Laser Based on Four-wave Mixing in Highly Germanium-doped Fiber, Tianye Huang¹, Xiaohui Li¹, Ping Shum¹, Qijie Wang¹, Xuguang Shao¹, Lulu Wang¹, Huizi Li¹, Zhifang Wu¹, Xinyong Dong¹; ¹Nanyang Technological Univ., Singapore. An all-fiber multiwavelength Tm-doped laser based on four-wave mixing in highly-germanium-doped-highly-nonlinear-fiber (HG-HNLF) has been demonstrated. By using 50-m HG-HNLF to provide intensity-dependent gain, 36 lasing lines with wavelength spacing of 0.86 nm within 30-dB bandwidth is obtained.

CLEO: Science & Innovations

SM3M • High Energy, High Power Systems & Enabling Technology—Continued

SM3M.2 • 14:30

A Solid State 100 mJ Diode Pumped Temporally and Spatially Shaped Front End System for Seeding a 10 Hz 100 J Laser System, Waseem Shaikh¹, Thomas Butcher¹, Saumyabrata Banerjee¹, Paul Mason¹, Klaus Ertel¹, Johnathan Phillips¹, Jodie Smith¹, Martin Divoky², Mariastefania De Vido¹, Oleg Cheklov¹, Justin Greenhalgh¹, Stephanie Tomlinson¹, Ian Musgrave¹, Cristina Hernandez-Gomez¹, John L. Collier¹; ¹CLF, STFC, UK; ²Laser, HiLase Project, Czech Republic. We describe a 100 mJ three component ytterbium based laser system operating at 1030 nm. Capabilities of both temporal pulse shaping and efficient active/passive spatial shaping for amplification in a 100 J system are incorporated.

SM3M.3 • 14:45

High energy pump laser for Multi-Petawatt laser, Olivier Casagrande¹, Christophe Derycke¹, Alexandre Soujaeff¹, Philippe Ramos¹, Laurent Boudjemaa¹, Christophe Simon-Boisson¹, Sebastien Laux¹, Francois Lureau¹; ¹Laser Solutions Unit, Thales Optronique, France. ATLAS 100, a compact high energy laser delivering more than 100 joules at the repetition rate of 1 shot per minute has been developed for the two 10 PetaWatt beamlines of ELI NP infrastructure.

SM3N • Ultrafast High-field Phenomena and Laser Filamentation—Continued

SM3N.3 • 14:15

On the Role of Freeman Resonances in Pump-Probe Measurements of the Non-linear Refractive Index, Michael Hofmann¹, Carsten Bree¹; ¹Weierstrass-Inst., Germany. We demonstrate the dramatic impact of Freeman resonances on the cross-induced transient refractive index. Its nonperturbative character must be carefully considered in pump-probe based measurements of the all-optical Kerr effect.

SM3N.4 • 14:30

Group-velocity mismatch effect in high-order harmonic generation, Carlos Hernandez-Garcia^{1,2}, Tenio Popmintchev¹, Margaret M. Murnane¹, Henry C. Kapteyn¹, Luis Plaja², Agnieszka Jaron-Becker¹, Andreas Becker¹; ¹JILA, Univ. of Colorado, USA; ²Universidad de Salamanca, Spain. We theoretically investigate the role of group velocity matching in high-order harmonic generation. We introduce the associated walk-off length, and present its scaling with wavelength and pulse duration.

SM3N.5 • 14:45 **Invited**

Laser Acceleration of Non-relativistic Electrons at Dielectric Structures: Status and Outlook, Joshua McNeur¹, Ang Li¹, Norbert Schönerberger¹, Alexander Tafel¹, Peter Hommelhoff^{1,2}; ¹Dept. of Physics, Univ. of Erlangen-Nuremberg, Germany; ²Max Planck Inst. for Quantum Optics, Germany. Dielectric laser acceleration of electrons is the optical counterpart of phase-synchronous RF-acceleration of electrons in classical accelerators, demonstrated by us and at Stanford/SLAC recently. We discuss concept, experiments and detail highlights of this high-gradient scheme.

SM3O • Nano and Micro-Optical Sensors—Continued

SM3O.3 • 14:15

Universal Enhancement of Raman Scattering Sensing by Plasmonic Nanotubes Coupled with Photonic Crystal Slab, Zheng Wang^{1,2}, Chao Liu^{1,3}, Swapnaji Chakravarty¹, D.L. Fan^{1,3}, Alan X. Wang⁵, Ray T. Chen^{1,2}; ¹Materials Science and Engineering Program, Texas Materials Inst., The Univ. of Texas at Austin, USA; ²Dept. of Electrical and Computer Engineering, The Univ. of Texas at Austin, USA; ³Dept. of Mechanical Engineering, The Univ. of Texas at Austin, USA; ⁴Omega Optics, Inc., USA; ⁵School of Electrical Engineering and Computer Science, Oregon State Univ., USA. We experimentally demonstrate 2-D photonic crystal slab-coupled plasmonic nanocapsules for surface enhanced Raman spectroscopy (SERS). A strong Raman signal enhancement can be unambiguously detected even with a low concentration 10 nM dye molecules.

SM3O.4 • 14:30

Low-Loss Titanium Dioxide Waveguides for Integrated Evanescent Raman Spectroscopy, Christopher C. Evans¹, Chengyu Liu¹, Jin Suntiwich¹; ¹Cornell Univ., USA. We propose an integrated-optical device consisting of a channel waveguide, capable of exciting and collecting Raman-scattered light of surrounding chemicals via the evanescent field, as a new chemical sensing platform.

SM3O.5 • 14:45

Monolithic Absorption Sensor Based on Bi-functional Quantum Cascade Structures, Daniela Ristanic¹, Benedikt Schwarz¹, Peter Reininger¹, Hermann Detz¹, Aaron M. Andrews¹, Werner Schrenk¹, Donald C. MacFarland¹, Tobias Zederbauer¹, Gottfried Strasser¹; ¹Technische Universität Wien, Austria. An integrated mid-infrared sensor consisting of an array of DFB lasers and detectors built from a bi-functional quantum cascade structure is demonstrated. The different frequencies enable the identification of the chemicals in a liquid mixture.

SM3P • Mode Locked Lasers—Continued

SM3P.4 • 14:15

Mid-infrared Two-color Optical Parametric Oscillator across a 30 THz Spectral Range, Yuwei Jin¹, Simona M. Cristescu¹, Frans J. Harren¹, Julien Mandon¹; ¹Dept. of Molecular and Laser Physics, Radboud Universiteit Nijmegen, Netherlands. We present a broadband tunable two-color optical parametric oscillator. The single cavity is capable of generating two idlers that are separated up to 30 THz. Fourier transform spectroscopy with this source has been demonstrated for multi-gas detection.

SM3P.5 • 14:30

Few-Femtosecond Synchronization Between a Few-MHz Ti:Sapphire Laser and a Multi-GHz Microwave Signal, Jungwon Kim¹, Matthew Walbran^{2,3}, Alexander Glierin^{2,3}, Kwangyun Jung¹, Peter Baum^{2,3}; ¹Korea Advanced Inst of Science & Tech, Korea; ²Ludwig-Maximilians Univ., Germany; ³Max-Planck Inst. for Quantum Optics, Germany. We show 3.7-fs (rms) synchronization between a 5-MHz, 0.5- μ J Ti:sapphire laser and a 6.2-GHz microwave signal [integration bandwidth: 1 Hz - 2.5 MHz]. This result may help advancing pump-probe imaging in free-electron lasers or ultrafast electron diffraction.

SM3P.6 • 14:45

Low Phase Noise Hybrid Silicon Mode Locked Laser Using On-Chip Coherent Photon Seeding, sudharsanan srinivasan¹, Erik Norberg², Tin Komljenovic¹, Michael Davenport¹, Greg Fish², John Bowers¹; ¹UCSB, USA; ²Aurion Inc., USA. We demonstrate 6dB improvement in phase noise of a mode-locked semiconductor laser using coherent photon seeding, achieving a record linewidth of 29kHz. The complete photonic-circuit including the feedback cavity is integrated on a single chip.

CLEO: QELS-Fundamental Science

FM3A • Frequency
Conversion—Continued

FM3A.7 • 15:00

Upconversion of Microwave to Optical Photons using Erbium Impurities in a Solid, Xavier Fernandez-Gonzalvo¹, Lewis A. Williamson¹, Yu-Hui Chen¹, Chunming Yin², Sven Rogge², Jevon J. Longdell¹; ¹Univ. of Otago, New Zealand; ²Physics, Univ. of New South Wales, Australia. We present a proposal for the efficient, quiet conversion of quantum states encoded as microwave photons into telecommunications photons using erbium dopants in solids. We also present initial results showing low efficiency conversion.

FM3A.8 • 15:15

Progress towards quantum state transfer between microwave and optical light using an electro-optomechanical resonator, Robert Peterson¹, Peter S. Burns¹, Reed Andrews¹, Thomas P. Purdy¹, Katarina Cicak², Raymond W. Simmonds², Cindy A. Regal¹, Konrad W. Lehnert^{1,2}; ¹JILA, USA; ²NIST, USA. We have constructed a bidirectional and efficient converter between microwave and optical light using a mechanically compliant membrane coupled via the optomechanical interaction. Ongoing work towards quantum state transfer is discussed.

FM3B • Light-matter
Interactions in 2D
Nanostructures—Continued

FM3B.6 • 15:00

Topologically tunable Fano resonance in $(\text{Bi}_{1-x}\text{In}_x)_2\text{Se}_3$, Sim Sangwan¹, Nimesh Koirala², Matthew Brahlek², Jun Park¹, Soonyoung Cha¹, Seongshik Oh², Hyunyoung Choi¹; ¹Yonsei Univ., Korea; ²Rutgers Univ., USA. We report new tunable Fano interference phenomena depending on topological phase in $(\text{Bi}_{1-x}\text{In}_x)_2\text{Se}_3$. The controlled spatial overlap of topological surface wavefunction with bulk phonon is responsible for the ultrafast tunability of the Fano resonance.

FM3B.7 • 15:15

Quantum Interference Control of Photocurrents in Topological Insulator Films, Derek A. Bas¹, Kevin Vargas-Valez¹, Sercan Babakiray¹, Trent A. Johnson¹, David Lederman¹, Tudor Stanescu¹, Alan D. Bristow¹; ¹West Virginia Univ., USA. Charge currents in thin films of Bi_2Se_3 are controlled using a two-color scheme that exploits quantum interference of single- and two-photon absorption pathways. Injection and shift currents are observed and linked to surface state excitations.

FM3C • Hyperbolic
Metamaterial Waveguides—
Continued

FM3C.7 • 15:00

Singular Evanescent Wave Resonances, Yu Guo¹, Zubin Jacob¹; ¹Univ. of Alberta, Canada. We report on the discovery of a unique resonance in moving media, impossible in a stationary system. It leads to giant non-contact fluctuational drag force between moving bodies (giant quantum friction).

FM3C.8 • 15:15

Mode selection filter using THz metamaterials surfaced on LiNbO_3 sub-wavelength slab waveguide, Bin Zhang¹, Chongpei Pan¹, Yusong Pan¹, Shibiao Wang¹, Qiang Wu¹, Jingjun Xu¹; ¹Nankai Univ., China. We implemented periodic bar arrays metamaterials to separate waveguide modes of terahertz waves propagating in a LiNbO_3 sub-wavelength waveguide. The spatial and temporal electric field profiles were recorded using a time-resolved phase contrast imaging system.

FM3D • Frequency Conversion
and its Application—Continued

FM3D.6 • 15:00

Raman oscillation, frequency upconversion, and Raman amplification at phonon-polariton resonance, Yujie J. Ding¹; ¹Lehigh Univ., USA. We have shown that Raman oscillation, frequency upconversion, and Raman amplification can be achieved in a second-order nonlinear medium at the phonon-polariton resonance.

FM3D.7 • 15:15

Enhanced stimulated Brillouin scattering via saturable phonon losses, Ryan Behunin¹, William H. Renninger¹, Heedeuk Shin¹, Prashanta Kharel¹, Eric Kittlaus¹, Faustin Carter¹, Peter T. Rakich¹; ¹Yale Univ., USA. Using stimulated Brillouin spectroscopy we demonstrate that nonlinear phonon dynamics emerging at cryogenic temperatures can be effectively harnessed to enhance Brillouin gain and extend phonon lifetimes in fiber.

15:30–16:00 Coffee Break, Concourse Level

16:00–18:00 JM4A • Plenary Session I, Grand Ballroom

18:30-19:30 OSA Technical Group Poster Sessions, Technical Session Corridor near 210 A-D

* Nanophotonics Technical Group

* Optoelectronics Technical Group

* Optical Fabrication and Testing Technical Group

18:30-19:30 Optical Material Studies Technical Group Networking Event, Meeting Room 211 B/D

18:30–20:30 OSA Student Member Happy Hour (RSVP Required)

CLEO: QELS-
Fundamental ScienceFM3E • Nonlinear Plasmonics—
Continued

FM3E.7 • 15:00

Scaling of the Nonlinear Response of Metal/Dielectric Plasmonic Waveguides, Alexandre Baron¹, Stéphane Larouche¹, Daniel J. Gauthier¹, David R. Smith¹; ¹Duke Univ., USA. The scaling of the nonlinear response of a single-interface plasmonic waveguide is studied, where both the metal and dielectric display nonlinearity. We introduce a figure-of-merit that guides metal/dielectric nanophotonic device design for specific applications.

FM3E.8 • 15:15

Suppression and Subsistence of Fano EIT Transmission Windows in Plasmonic-Vapor System, Liron Stern¹, Meir Y. Grajower¹, Uriel Levy¹; ¹Applied Physics, Hebrew Univ. of Jerusalem, Israel. We report on the sub Doppler transmission characteristics of a pump-probe V-type surface plasmon and atomic system. Suppression and subsistence of EIT windows is demonstrated due to the unique character of the plasmonic-atomic hybrid system.

SM3F • Ultrafast, High Speed
and High Power Semiconductor
Lasers—Continued

SM3F.7 • 15:00

DBR-free Semiconductor Disk Lasers, Zhou Yang¹, Alexander R. Albrecht¹, Jeffrey G. Cederberg², Mansoor Sheik-Bahae¹; ¹Univ. of New Mexico, USA; ²Sandia National Labs, USA. We demonstrate a novel DBR-free semiconductor disk laser, where multiple quantum well active region is fusion bonded directly onto a diamond heat spreader. CW output powers of 2.5 W have been demonstrated at 1150 nm.

SM3F.8 • 15:15

Low-temperature Optimized 940 nm Diode Laser Bars with 1.98 kW Peak Power at 203 K, Carlo Frevert¹, Paul Crump¹, Frank Bugge¹, Steffen Knigge¹, Arnim Ginolas¹, Götz Erbert¹; ¹Ferdinand-Braun-Institut, Leibniz-Institut fuer Hoechsthfrequenztechnik, Germany. Passively cooled 1-cm wide QCW diode laser bars with low-temperature optimized vertical designs reach output powers of 1.98 kW at 203 K, with conversion efficiency of 64% at 1 kW and 57% at 1.9 kW.

CLEO: Science & Innovations

SM3G • Group IV Photonics—
ContinuedSM3G.6 • 15:00 **Invited**

Monolithically Grown Superluminescent Diodes on Germanium and Silicon substrates, Qi Jiang¹, Siming Chen¹, Mingchu Tang¹, Jiang Wu¹, Alywn Seeds¹, Huiyun Liu¹; ¹UCL, UK. We demonstrate the first InAs/GaAs quantum-dot (QD) superluminescent diode (SLD) monolithically grown on both Ge and Si substrates by molecular beam epitaxy.

SM3H • THz Materials Science—
Continued

SM3H.6 • 15:00

Ultrafast Carrier Transport in Silicon Nanocrystal Superlattices, Hynek Nemeček¹, Petr Kuzel¹, Petr Maly², Sebastian Gutsch³, Daniel Hiller³, Margit Zacharias³; ¹Inst. of Physics AS CR, v.v.i, Czech Republic; ²Chares Univ., Czech Republic; ³Albert-Ludwigs-Universität of Freiburg, Germany. Time-resolved terahertz spectroscopy is employed to study silicon nanocrystals prepared by thermal decomposition of silicon-rich SiO_x layers. We observe that higher silicon content favors formation of larger silicon clusters with short-range percolation.

15:30–16:00 Coffee Break, Concourse Level

16:00–18:00 JM4A • Plenary Session I, Grand Ballroom

18:30-19:30 OSA Technical Group Poster Sessions, Technical Session Corridor near 210 A-D

* Nanophotonics Technical Group

* Optoelectronics Technical Group

* Optical Fabrication and Testing Technical Group

18:30-19:30 Optical Material Studies Technical Group Networking Event, Meeting Room 211 B/D

18:30–20:30 OSA Student Member Happy Hour (RSVP Required)

Meeting Room
211 B/D

CLEO: Science & Innovations

SM3I • WDMs and Filters—Continued

SM3I.7 • 15:00

Bragg Grating Spiral Strip Waveguide Filters for TM Modes, Zhitian Chen¹, Jonas Flueckiger¹, Xu Wang¹, Han Yun¹, Yun Wang¹, Zeqin Lu¹, Fan Zhang¹, Nicolas A. Jaeger¹, Lukas Chrostowski¹; ¹Univ. of British Columbia, USA. We demonstrate a 1 cm long Bragg grating filter, on a compact spiral SOI waveguide, for the fundamental transverse magnetic mode, that has a 0.5 nm bandwidth, 40 dB extinction ratio, and 1 dB/cm loss.

SM3I.8 • 15:15

Plasmonic Fano Nanoantenna for On-chip Wavelength Demultiplexing, Rui Guo¹, Manuel Decker¹, Frank Setzpfandt¹, Isabelle Staudel¹, Dragomir N. Neshev¹, Yuri S. Kivshar¹; ¹Australian National Univ., Australia. We demonstrate a single-element Fano nanoantenna allowing for strong directional coupling of light to a silicon waveguide depending on the operational wavelength. This antenna can spatially separate wavelength-encoded optical signals, realizing an ultra-compact plasmonic demultiplexer.

Meeting Room
212 A/C

CLEO: Applications & Technology

AM3J • Neurophotonics and Optogenetics—Continued

AM3J.4 • 15:00

Label-Free Imaging of Single Neuron Activities by Stimulated Raman Scattering, Delong Zhang¹, Hyeon Jeong Lee¹, Pei-Yu Shih¹, Ryan Drenan¹, Ji-Xin Cheng¹; ¹Purdue Univ., USA. We report the observation of single neuron activities by spectral focusing stimulated Raman scattering (SRS) microscopy. Changes in SRS signal intensity in live neurons correlate to action potentials indicated by fluorescent calcium indicator.

AM3J.5 • 15:15

Multifunctional Transparent Optoelectrode Array for *in-vivo* Optogenetic Studies, Joonhee Lee¹, Ilker Ozden¹, Yoon-Kyu Song^{2,3}, Arto Nurmikko¹; ¹Brown Univ., USA; ²Seoul National Univ., Korea; ³Advanced Inst.s of Convergence Technology, Korea. We developed fully transparent 2-dimensional intracortical neural probe microarrays based on ZnO single crystal. The unique material and device design enabled efficient multifunctional, multi-site patterned optical stimulation and simultaneous electrical recording in rodents.

Meeting Room
212 B/D

AM3K • Components and Enabling Technologies—Continued

AM3K.7 • 15:00

Development, Fabrication, and Real-World Applications of Polymeric Nanolayer Gradient Index Optical Components, Howard Fein¹, Michael Ponting¹; ¹PolymerPlus LLC, USA. Specially formulated Gradient-Index polymeric optical materials offer capabilities not possible in present GRIN optics. A novel technology that enables large scale processing of nanolayered polymer films into real, performance-enhancing lenses for military Night-Vision-Goggle eyepieces is discussed.

AM3K.8 • 15:15

Fabrication of dielectric Bragg reflectors composed of CaF₂ and ZnS for delicate laser materials, Alex Palatnik¹, Merav Muallem¹, Gilbert D. Nessim¹, Yaakov Tischler¹; ¹Chemistry, Bar Ilan Univ., Israel. We describe the fabrication and characterization of highly reflecting distributed Bragg reflectors (DBR) composed of thermally evaporated thin films of CaF₂ and ZnS without substrate heating. Proposed technique enables DBR deposition on delicate laser materials.

Marriott
Salon I & II

CLEO: Science & Innovations

SM3L • Novel Fiber Materials—Continued

SM3L.7 • 15:00

Thermo-optic Degradation of Single-Modedness in Active LMA fibers and Simple Compensation Mechanisms, V R Supradeepa¹, John M. Fini²; ¹Indian Inst. of Science, India; ²OFS Labs, USA. We demonstrate significant thermo-optic degradation of single-modedness in active large mode area fibers due to heat generation in the fiber. We propose and demonstrate through simulations, simple compensation mechanisms using custom length dependent fiber coiling.

SM3L.8 • 15:15

Influence of Al/Ge ratio on radiation-induced attenuation in nanostructured erbium-doped fibers preforms, Monica Leon-Pichel¹, Matthieu Lancry¹, Nadège Ollier², Laurent Bigot³, Hicham El Hamzaoui³, Inna Savelli³, Alain Pastouret⁴, Ekaterina Burov⁴, Bertrand Poumellec¹, Mohamed Bouazaoui³; ¹Universite de Paris Sud, France; ²IRAMIS/DSM/CNRS/Ecole Polytechnique, France; ³PhLAM/IRCICA, France; ⁴Draka Comteq France, France. We studied the radiation resistance of Er³⁺-doped fiber preforms manufactured with different technologies: Si and Al nanoparticles and sol-gel fibers. They have been irradiated with gamma rays and then studied using absorption and EPR spectroscopies.

15:30–16:00 Coffee Break, Concourse Level

16:00–18:00 JM4A • Plenary Session I, Grand Ballroom

18:30-19:30 OSA Technical Group Poster Sessions, Technical Session Corridor near 210 A-D

- * Nanophotonics Technical Group
- * Optoelectronics Technical Group
- * Optical Fabrication and Testing Technical Group

18:30-19:30 Optical Material Studies Technical Group Networking Event, Meeting Room 211 B/D

18:30–20:30 OSA Student Member Happy Hour (RSVP Required)

CLEO: Science & Innovations

SM3M • High Energy, High Power Systems & Enabling Technology—Continued**SM3M.4 • 15:00**

Recent Advances on the J-KAREN laser upgrad, Hiromitsu Kiriya¹, Michiaki Mori¹, Alexander Pirozhkov¹, Koichi Ogura¹, Mamiko Nishiuchi¹, Masaki Kando¹, Hironao Sakaki¹, Akira Kon¹, Masato Kanasaki¹, Hirotaka Tanaka³, Yuji Fukuda¹, James Koga¹, Akito Sagisaka¹, Timur Esirkepov¹, Yukio Hayashi¹, Hideyuki Kotaki¹, Sergei Bulanov¹, Kiminori Kondo¹, Paul Bolton¹, Yuji Mashiba², Makoto Asakawa², Ondrej Slezak⁴, Magda Sawicka-Chyla⁴, Venkatesan Jambunathan⁴, Antonio Lucianetti⁴, Tomas Mocek⁴; ¹Japan Atomic Energy Agency, Japan; ²Faculty of Science and Engineering, Kansai Univ., Japan; ³Interdisciplinary Graduate School of Engineering Sciences, Kyushu Univ., Japan; ⁴HILASE, Czech Republic. We report recent progress on the J-KAREN laser upgrade to realize 10^{22} W/cm² intensity at 0.1 Hz. Our current high-spatiotemporal-quality broadband pulses of over 20 J will be further amplified in the final amplifier.

SM3M.5 • 15:15

Apparatus and Techniques for Measuring Laser Damage Resistance of Large-Area, Multilayer Dielectric Mirrors for Use with High Energy, Picosecond Lasers, Raluca A. Negres¹, Isaac Bass¹, Ken A. Stanion¹, Gabe Guss¹, David A. Cross¹, David A. Alessi¹, Chris Stolz¹, Christopher W. Carr¹; ¹Lawrence Livermore National Lab, USA. We present techniques for measuring the damage performance of a variety of optical components with ps laser pulses, introduce a novel beam diagnostic technique, and explore the sensitivity of damage resistance to laser spot size for the case of high-reflectivity, multilayer dielectric (MLD) mirrors.

SM3N • Ultrafast High-field Phenomena and Laser Filamentation—Continued**SM3O • Nano and Micro-Optical Sensors—Continued****SM3O.6 • 15:00**

Frequency locked cascaded micro ring resonators enabling real time and highly precise long and short time sensing, Liron Stern¹, Gal Keinan¹, Alex Naiman¹, Noa Mazurski¹, Uriel Levy¹; ¹Applied Physics, Hebrew Univ. of Jerusalem, Israel. We demonstrate an ultrasensitive differential sensing apparatus, based on a frequency locked cascaded micro-resonator scheme. By measuring the lasers beat frequency a highly sensitive sensor both in short (seconds) and long (hours) times is demonstrated.

SM3O.7 • 15:15

Whispering gallery mode-based magnetometer, Trung D. Vo¹, Eric Magi², Benjamin J. Eggleton², Brian Ferguson¹; ¹Dept. of Defence, Defence Science & Technology Organisation, Australia; ²CUDOS, the Univ. of Sydney, Australia. We demonstrate a compact all-optical magnetic sensor based on whispering gallery modes in a photonic crystal fiber infiltrated with ferrofluid. We achieve a sensitivity of ~ 0.18 pm/ μ T and a resolution of ~ 222 nT.

SM3P • Mode Locked Lasers—Continued**SM3P.7 • 15:00**

Broadband, Low Noise Modelocked Semiconductor Laser with Intracavity Programmable Dispersion Control, Anthony Klee¹, Kristina Bagnell¹, Peter J. Delfyett¹; ¹Univ. of Central Florida, CREOL, USA. An intracavity pulseshaper is used to broaden the spectrum of a 10 GHz semiconductor frequency comb to greater than 28 nm. Timing jitter is measured to be 15.4 fs integrated from 1 kHz to 100 MHz offset.

SM3P.8 • 15:15

All-optical Q-switching limiter for a 5-GHz SESAM-modelocked laser with record-high peak power, Alexander Klenner¹, Ursula Keller¹; ¹Eidgenössische Tech Hochschule Zurich, Switzerland. We use a Kerr-lens induced all-optical limiter to reduce Q-switching instabilities in a high-power diode-pumped 5GHz SESAM-modelocked Yb:CALGO laser. This supports cw modelocking with 4.1W average output power and 96fs pulses, leading 7.5kW peak power.

15:30–16:00 Coffee Break, Concourse Level

16:00–18:00 JM4A • Plenary Session I, Grand Ballroom

18:30-19:30 OSA Technical Group Poster Sessions, Technical Session Corridor near 210 A-D

* Nanophotonics Technical Group

* Optoelectronics Technical Group

* Optical Fabrication and Testing Technical Group

18:30-19:30 Optical Material Studies Technical Group Networking Event, Meeting Room 211 B/D

18:30–20:30 OSA Student Member Happy Hour (RSVP Required)

CLEO: QELS-Fundamental Science

JOINT

08:00–10:00

FTu1A • Quantum Entanglement I

Presider: James Dailey; Applied Communication Sciences, USA

FTu1A.1 • 08:00

Generation of Hybrid Entanglement of Light Between Wave-like and Particle-like Qubits, Hanna LE JEANNIC¹, Olivier Morin¹, Kun Huang^{1,2}, Jianli Liu¹, Claude Fabre¹, Josselin Ruaudel¹, Youn-Chang Jeong¹, Julien Laurat¹; ¹Laboratoire Kastler Brossel, UPMC-Sorbonne Universites, CNRS, ENS-PSL Research Univ., College de France, France; ²State Key Lab of Precision Spectroscopy, East China Normal Univ., China. The wave-particle duality of light has led to two different encodings for optical quantum information processing. We report here the remote generation of entanglement between particle-like discrete-variable qubits and wave-like continuous-variable qubits.

FTu1A.2 • 08:15

Witness of Macroscopic Entanglement in Classical Statistical Optical Fields, Xiaofeng Qian¹, bethany little¹, John Howell¹, Joseph H. Eberly¹; ¹Univ. of Rochester, USA. We examine correlations between polarization and amplitude degrees of freedom for classical statistical optical fields with Bell-analysis experiments. Strong violations of the Clauser-Horne-Shimony-Holt inequality are observed. These constitute a new witness of classical macroscopic entanglement.

FTu1A.3 • 08:30

Generation of multipartite spin entanglement from multimode squeezed states, Niranjana Sridhar¹, Olivier Pfister¹; ¹Univ. of Virginia, USA. We investigate the use of the Schwinger representation for casting multimode squeezed states into multipartite spin entangled states. While the generalization is not straightforward, we can still find highly entangled multipartite states.

08:00–09:45

FTu1B • Ultrafast Dynamics in Strongly Correlated Materials

Presider: Robert Kaindl; Lawrence Berkeley National Lab, USA

FTu1B.1 • 08:00

Mott behavior in $K_xFe_{2-y}Se_2$ superconductors revealed by pump-probe spectroscopy, Chunfeng Zhang¹, Wei Li¹, Min Xiao²; ¹Nanjing Univ., China; ²Dept. of Physics, Univ. of Arkansas, USA. Pump-probe spectroscopic data on $K_xFe_{2-y}Se_2$ superconductors exhibit signatures of orbital-selective Mott transition with a significant enhancement of a slow decay component alongside a decrease in oscillatory coherent-phonon signals upon raising temperature to 160 K.

FTu1B.2 • 08:15

Critical Speeding-Up of Non-Equilibrium Electronic Relaxation Near Ising-Nematic Transition in Unstrained $Ba(Fe_{1-x}Co_x)_2As_2$, Aaron Patz^{1,2}, Tianqi Li^{1,2}, Sheng Ran^{1,2}, Sergey Bud'ko^{1,2}, Paul Canfield^{1,2}, Jigang Wang^{1,2}; ¹Physics, Iowa State Univ., USA; ²Ames Lab -USDOE, USA. We observe a critical speeding up in the electronic relaxation time that implies that nematic fluctuations govern the electronic thermalization/cooling dynamics and that magnetic fluctuations dominate the nonlinear signals that arise from the Ising-nematicity.

FTu1B.3 • 08:30

Ultrafast dissection of excitonic and structural orders in a persisting charge density wave, Michael Porer¹, Ursula Leierseder¹, Jean-Michel Ménard¹, Hatem Dachraoui², Leonidas Mouchliadis³, Ilias E. Perakis³, Ulrich Heinzmann², Jure Demsar⁴, Kai Rossnagel⁵, Rupert Huber¹; ¹Dept. of Physics, Univ. of Regensburg, Germany; ²Molecular and Surface Physics, Univ. of Bielefeld, Germany; ³Dept. of Physics, Univ. of Crete & FORTH/IESL, Greece; ⁴Inst. of Physics, Ilmenau Univ. of Technology, Germany; ⁵Inst. of Experimental and Applied Physics, Univ. of Kiel, Germany. We monitor the terahertz fingerprints of electronic and structural orders of the charge density wave in 1T-TiSe₂ on the femtosecond scale. NIR photoexcitation selectively melts electronic ordering while the structural distortion persists in a coherently excited state.

08:00–10:00

FTu1C • Optics of Metasurfaces

Presider: Viktor Podolskiy; Univ. of Massachusetts Lowell, USA

FTu1C.1 • 08:00

Ohmic Loss Produces Chiral Dichroism in Plasmonic Metasurfaces: First Experimental Demonstration, Gennady Shvets¹, Nihal Arju¹, Mikhail A. Belkin¹, Rainer Hillenbrand², Feng Lu¹, Martin Schnell², Jongwon Lee¹, Alexander B. Khanikaev³; ¹Univ. of Texas at Austin, USA; ²CIC nanoGUNE Consolider, Spain; ³Physics, Queens College, USA. A combination of experimental techniques is used to demonstrate that optical field concentration and Ohmic losses in planar chiral plasmonic metasurfaces depends on the handedness of circularly polarized light. Chiral dichroism in transmission is demonstrated.

FTu1C.2 • 08:15

Liquid Crystal Tuning of All-dielectric Metasurfaces, Juergen Sautter¹, Isabelle Staude¹, Manuel Decker¹, Evgenia Rusak¹, Igal Brener², Dragomir N. Neshev¹, Yuri S. Kivshar¹; ¹Australian National Univ., Australia; ²Sandia Natl Labs, USA. We experimentally realize active tuning of electric and magnetic resonances of all-dielectric optical metasurfaces based on the temperature-dependent refractive-index change of liquid crystals. We achieve 40nm spectral tuning and modulation contrast of 500%.

FTu1C.3 • 08:30

Dynamic Beam Steering in Micro-fluidic-meta-surface, Libin Yan¹, Pin Chieh Wu¹, Qinghua Song¹, Weiming Zhu¹, Zhang Wu¹, Din Ping Tsai², Federico Capasso³, Ai-Qun Liu¹; ¹School of Electrical and Electronic Engineering, Nanyang Technological Univ., Singapore; ²Dept. of Physics, National Taiwan Univ., Taiwan; ³Harvard Univ., USA. We present a widely tunable metasurface composed of microfluidic antennas with subwavelength thickness for dynamic beam steering. By controlling actively the length of supercell, the reflection can be tuned to arbitrary direction under normal illumination.

08:00–10:00

JTu1D • Symposium on Advanced Optical Microscopy for Brain Imaging I

Presider: Na Ji; Howard Hughes Medical Inst., USA

JTu1D.1 • 08:00 **Invited**

Multi-photon Microscopy to Image Neuronal and Vascular Function in the Mammalian Brain, David Kleinfeld¹; ¹Univ. of California, San Diego, USA. I will review the application of two-photon laser scanning microscopy to problems in neuroscience as well as discuss current needs and challenges for the analysis of neuronal circuits and signaling in neocortical and other forebrain structures in mouse.

JTu1D.2 • 08:30 **Invited**

Reconstructing Nervous System Development and Function with Light-Sheet Microscopy, Philipp Keller¹; ¹Howard Hughes Medical Inst., USA. I will present our integrated, imaging-based technology framework for reconstructing development and function of the early nervous system *in vivo*, which combines high-speed multi-view light-sheet microscopy with automated approaches to large-scale image analysis.

CLEO: QELS-
Fundamental Science

08:00–10:00
FTu1E • 2D Materials
for Nanoplasmonics and
Nanophotonics
President: To be Determined

FTu1E.1 • 08:00 **Invited**
Nano-photonic Phenomena in van der Waals heterostructures, Dmitri N. Basov¹; ¹Univ. of California, San Diego, USA. In van der Waals heterostructures assembled from atomically thin layers of graphene, hexagonal boron nitride and other related materials electronic, plasmonic and phonon polaritonic phenomena are all intertwined. We explored these effects via infrared nano-imaging.

FTu1E.2 • 08:30
Generation of Graphene Surface Plasmons and Their Applications in Beam Steering, Mohamed Farhat¹, Pai-Yen Chen², Sebastien Guenneau³, Hakan Bagci¹; ¹King Abdulah Univ of Science & Tech, Saudi Arabia; ²Wayne State Univ., USA; ³Aix-Marseille Univ., France. We propose a novel concept that uses mechanical and electronic properties of graphene to efficiently couple light to surface plasmon polaritons. A graphene-based infrared beam-former based on the concept of surface leaky-wave is also discussed.

08:00–10:00
STu1F • Optical Integration on
Chip
President: Weidong Zhou; Univ. of
Texas at Arlington, USA

STu1F.1 • 08:00
Multicast 4x20 Silicon Photonic MEMS Switches, Sangyoon Han¹, Tae Joon Seok¹, Chang Kyu Kim¹, Richard S. Muller¹, Ming C. Wu¹; ¹Univ. of California Berkeley, USA. We report on monolithic 4x20 silicon photonic MEMS switches capable of multicast functions. The switch has small footprint (1.2x4.5mm²), low optical insertion loss (<4.0dB), fast switching (9.6µs). 1x2 and 1x4 multicasts were successfully demonstrated.

STu1F.2 • 08:15
All-optical programmable integrated signal processor, Hongchen Yu¹, Minghua Chen¹, Hongwei Chen¹, Sigang Yang¹, Shizhong Xie¹; ¹Tsinghua Univ., China. An all-optical programmable signal processor has been proposed and experimentally demonstrated. The record resolution is measured to be 145 MHz and the processing range can be enlarged by a channelized filter to > 100 GHz.

STu1F.3 • 08:30 **Invited**
Nonlinear Integrated Optoelectronics, Shayan Mookherjee¹; ¹Univ. of California, San Diego, USA. Compared to traditional crystal-based nonlinear optical devices, photonic integrated circuits on a silicon platform may enable advanced and parallelized functionality in chip-scale energy-efficient nonlinear optics, such as combinations of mixers, filters and photodetectors.

CLEO: Science & Innovations

08:00–10:00
STu1G • Cascade Lasers I
President: Sanjay Krishna; Univ. of
New Mexico, USA

STu1G.1 • 08:00
Evaluating the temporal profile of quantum cascade laser frequency combs, David P. Burghoff¹, Yang Yang¹, Darren Hayton², J.R. Gao^{2,3}, John Reno⁴, Qing Hu¹; ¹MIT, USA; ²SRON, Netherlands; ³TU Delft, Netherlands; ⁴Sandia, USA. The temporal profile of frequency combs based on quantum cascade lasers has been unclear for some time. We show how the SWIFTS technique directly measures such properties, obtaining combs' intensities and frequencies versus time.

STu1G.2 • 08:15
Injection Seeding and Modelocking of Metal-metal Terahertz Quantum Cascade Lasers, Feihu WANG¹, anthony Brewer^{2,1}, Joshua Freeman^{1,3}, Jean Maysonnave¹, Souad Moumdji⁴, Raffaele Colombelli⁴, Iman Kundu³, Li Lianhe³, Edmund Linfield³, Giles Davies³, Harvey Beere², David Ritchie², Sukhdeep Dhillon¹, Jérôme Tignon¹; ¹Laboratoire Pierre Aigrain, Ecole Normale Supérieure-PSL Research Univ., CNRS, Université Pierre et Marie Curie-Sorbonne Universités, Université Paris Diderot-Sorbonne Paris Cité, France; ²Semiconductor Physics Group, Univ. of Cambridge, UK; ³School of Electronic and Electrical Engineering Univ. of Leeds, UK; ⁴Institut d'Electronique Fondamentale, Université Paris Sud, France. Injection seeding of terahertz quantum-cascade-lasers with metal-metal waveguides is demonstrated at liquid nitrogen temperatures through injection of phase-locked terahertz pulses. Coherent detection and modelocking of the QCL are demonstrated with the generation of 11ps pulse.

STu1G.3 • 08:30
Investigation of Time-resolved Gain Dynamics in an Injection Seeded Terahertz Quantum Cascade Laser, Sergej Markmann¹, Hanond Nong¹, Shovon Pal¹, Negar Hekmat¹, Paul Dean², Reshma A. Mohandas², Li H. Lianhe², Edmund Linfield², Giles Davies², Andreas D. Wieck¹, Nathan Jukam¹; ¹Ruhr-Universität Bochum, Germany; ²Univ. of Leeds, UK. The evolution of the gain of terahertz quantum cascade laser during injection seeding is probed as a function of time. Oscillations of the gain are commensurate with the variations of the field envelope.

08:00–10:00
STu1H • Terahertz Photonics
President: Marco Rahm; Technische
Universität Kaiserslautern,
Germany

STu1H.1 • 08:00
Investigation of Extraordinary Optical Transmission Inside a Terahertz Parallel-Plate Waveguide, Kimberly S. Reichel¹, Peter Y. Lu², Rajind Mendis¹, Daniel Mittleman¹; ¹Dept. of Electrical and Computer Engineering, Rice Univ., USA; ²Dept. of Physics, Harvard Univ., USA. We study extraordinary optical transmission by placing a metal screen with a 1-D array of holes inside a parallel-plate waveguide at terahertz frequencies. We find excitation with TE₁ or TEM mode strongly affects output transmission characteristics.

STu1H.2 • 08:15
Dynamic light-induced THz resonators in a waveguide, Lauren Gingras¹, Marcel Georgin¹, David G. Cooke¹; ¹McGill Univ., Canada. We demonstrate all-optical photoinjection of a one-dimensional resonator inside a terahertz parallel-plate waveguide. The pulsed pump enables us to study dynamic effects where the structure is written on timescales faster than the terahertz transit time.

STu1H.3 • 08:30
THz Artificial Dielectric Lens, Rajind Mendis¹, Masaya Nagai², Yiqiu Wang¹, Nicholas Karl¹, Daniel Mittleman¹; ¹Rice Univ., USA; ²Osaka Univ., Japan. We demonstrate a THz lens designed using an artificial-dielectric medium fabricated from a stack of stainless-steel plates. The lens is capable of focusing a 20 mm diameter beam to a spot size of 4 mm.

Meeting Room
211 B/D

CLEO: Science & Innovations

08:00–10:00

STu11 • Nonlinear Optics

Presider: Qiang Lin; Univ. of Rochester, USA

STu11.1 • 08:00

Miniaturized Optical Frequency References in the Telecom Regime, Liron Stern¹, Ehiran Talker¹, Noa Mazurski¹, Boris Desiatov¹, Marissa Shefer², Aharon Segal², Uriel Levy¹; ¹Applied Physics, Hebrew Univ. of Jerusalem, Israel; ²Micro System and Smart Technologies, Rafael, Israel. We present two platforms for miniaturized telecom optical frequency references, based on TPA in rubidium vapor. Record efficiency of light vapor interaction in a serpentine atomic cladding wave guide, and micro-machined mm-scale cells are demonstrated.

STu11.2 • 08:15

Non-reciprocal light storage in a silica microsphere, Chunhua Dong¹, Zhen Shen¹, Changling Zou¹, Yanlei Zhang¹, Wei Fu¹, Guang-Can Guo¹; ¹Univ of Science and Technology of China, China. We report an experimental study of Brillouin-scattering-induced transparency (BSIT) in a silica microsphere. Because of the phase-matching requirement, the non-reciprocal light storage based on the BSIT is observed in our experiment.

STu11.3 • 08:30

Highly Efficient Four-Wave Mixing in an AlGaAs-On-Insulator (AlGaAsOI) Nano-Waveguide, Minhao Pu¹, Luisa Ottaviano¹, Elizaveta Semenova¹, Kresten Yvind¹; ¹Danmarks Tekniske Universitet, Denmark. We propose an AlGaAs-on-insulator platform for nonlinear integrated photonics. We demonstrate highly efficient four-wave mixing in a 3-mm long AlGaAs-on-insulator nano-waveguide. A conversion efficiency of -21.1 dB is obtained with only a 45-mW pump.

Meeting Room
212 A/C

CLEO: Applications & Technology

08:00–10:00

ATu1J • Applications for Energy and Environment

Presider: David Bomse; Mesa Photonics, USA

ATu1J.1 • 08:00

A Bistatic, Open-Path, Quantum Cascade Laser Array-Based Sensor for Methane and Nitrous Oxide Measurements, Anna P. Michel¹, Jason Kapit³, Mark F. Witinski^{1,2}, Roman Blanchard², Aysun Gokoglu²; ¹School of Engineering and Applied Sciences, Harvard Univ., USA; ²Eos Photonics, USA; ³Applied Ocean Physics and Engineering, Woods Hole Oceanographic Institution, USA. A next-generation bistatic, open-path sensor is currently in development that utilizes a Quantum Cascade cascade Laser laser array for the source in order to achieve methane and nitrous oxide detection over path lengths exceeding 100 m.

ATu1J.2 • 08:15

UAV-based laser spectrometer to quantify methane from agricultural and petrochemical activities, Lei Tao¹, Da Pan¹, Levi Golston¹, Kang Sun¹, Suman Saripalli², Mark A. Zondlo¹; ¹Dept. of Civil and Environmental Engineering, Princeton Univ., USA; ²KalScott Engineering, USA. A lightweight (1.8 kg) UAV-based methane sensor using a 3.27 mm GaSb DFB laser has been developed. Small UAVs can quantify very localized methane emissions but severely constrain sensor mass/volume while still requiring high-sensitivity detection.

ATu1J.3 • 08:30

Modeling the dependence of fork geometry on the performance of quartz enhanced photoacoustic spectroscopic sensors, Samara Firebaugh¹, Angelo Sampaolo², Pietro Patimisco², Vincenzo Spagnolo², Frank K. Tittel³; ¹Electrical and Computer Engineering, USA Naval Academy, USA; ²Dipartimento Interateneo di Fisica, Universita e Politecnico di Bari, Italy; ³Dept. of Electrical and Computer Engineering, Rice Univ., USA. A finite element model for Quartz Enhanced Photoacoustic Spectroscopy (QEPAS) was developed and applied to study the dependence of performance on sensor dimensions. This model can be a design tool for optimizing tuning fork dimensions.

Meeting Room
212 B/D

CLEO: Science & Innovations

08:00–10:00

STu1K • Integrated Optofluidics: Sensing, Guiding and Tailored Fabrication

Presider: Timo Mappes; Carl Zeiss AG, Germany

STu1K.1 • 08:00

Field-portable optofluidic plasmonic biosensor for wide-field and label-free monitoring of molecular interactions, Ahmet F. Coskun^{1,5}, Arif Cetin^{2,3}, Betty Galarreta^{2,4}, Daniel A. Alvarez², Hatice Altug^{3,2}, Aydogan Ozcan^{5,6}; ¹Division of Chemistry and Chemical Engineering, California Inst. of Technology, USA; ²Dept. of Electrical and Computer Engineering, Boston Univ., USA; ³Bioengineering Dept., EPFL, Switzerland; ⁴Departamento de Ciencias-Quimica, Pontificia Universidad Catolica del Peru, Peru; ⁵Dept.s of Electrical Engineering and Bioengineering, UCLA, USA; ⁶California NanoSystems Inst., UCLA, USA. We demonstrate a field-portable optofluidic plasmonic sensing device, weighing 40 g and 7.5 cm in height, which merges plasmonic microarrays with dual-wavelength lensfree on-chip imaging for real-time monitoring of protein binding kinetics.

STu1K.2 • 08:15

Spectrally Reconfigurable Multi-Spot Trap on Optofluidic ARROW Chip, Kaelyn D. Leake², Michael Olson¹, Damla Ozcelik², Aaron Hawkins¹, Holger Schmidt²; ¹Electrical and Computer Engineering, Brigham Young Univ., USA; ²School of Engineering, Univ. of California, Santa Cruz, USA. We demonstrate an on-chip spectrally reconfigurable multi-spot trap using an integrated multimode interference waveguide. This device is able to trap multiple particles simultaneously as well as transport particles along a channel in controlled manner.

STu1K.3 • 08:30

Physical insight into optical coupling between photoreceptor cell nuclei, Hoang T. Xuan¹; ¹Singapore-MIT Alliance, Singapore. We study optical coupling and light transport among photoreceptor cell nuclei of mammals' retina. This study also sheds light on light focusing and transport phenomena along microsphere-chain waveguides. The resonance's role is discussed in details.

Marriott
Salon I & II

08:00–10:00

STu1L • Symposium on Breaking Limits with Unconventional Optical Fields I

Presider: Qiwen Zhan; Univ. of Dayton, USA

STu1L.1 • 08:00 **Invited**

Tailoring Light at the Source: Structured Light from Laser Resonators, Andrew Forbes^{1,2}; ¹CSIR National Laser Centre, South Africa; ²Physics, Univ. of the Witwatersrand, South Africa. We outline various approaches to creating structured light directly from a laser cavity. By exploiting intra-cavity dynamic and geometric phase control, as well as complex amplitude modulation, custom modes may be generated on-demand.

STu1L.2 • 08:30

High-Topological Charge Vortex Tweezers with Continuous Control of Orbital Angular Momentum by Ultrafast Laser Machining, Rokas Drevinskas¹, Mindaugas Gecevičius¹, Martynas Beresna¹, Peter Kazansky¹; ¹Univ. of Southampton, UK. We demonstrate a single beam generated optical vortices of topological charge up to 100 with tunable orbital angular momentum. The continuous control of torque without altering the intensity distribution was implemented in optical trapping.

Tuesday, 12 May

There is still time to register for a Short Course!

Visit Registration to learn about the courses still available.

Tuesday, 12 May

SC352 • Introduction to Ultrafast Pulse Shaping—Principles and Applications

SC362 • Cavity Optomechanics: Fundamentals and Applications of Controlling and Measuring Nanoand Micro-mechanical Oscillators with Laser Light

SC410 • Finite Element Modelling Methods for Photonics and Optics

View page 16 for complete Short Course Information.

**CLEO: Applications
& Technology**

08:00–10:00

**ATu1M • Process Control and
Metrology Applications**

*Presider: Jana Jägerová; UiT
Norges Arktiske Universitet,
Norway*

ATu1M.1 • 08:00 **Invited**

Advanced optical distance measurements using femtosecond laser pulses, Seung-Woo Kim¹, Young-Jin Kim¹, Byung Jae Chun¹, Keun-woo Lee¹, Seongheum Han¹, Yoon-Soo Jang¹, HuynJay Kang¹; ¹*Korea Advanced Inst of Science & Tech, Korea*. Femtosecond lasers began to draw attention as a new light source for high-precision absolute distance measurements (ADMs) allowing for advanced principles such as synthetic wavelength generation, Fourier-transform-based dispersive analysis and multi-wavelength interferometry. In this talk, we present the state-of-the-art measurement principles and performance demonstrated by exploiting the unique temporal and spectral characteristics of femtosecond laser pulses for ADM applications.

ATu1M.2 • 08:30

High speed two-dimensional temporal compressive sampling microscopic camera, Qiang Guo¹, Hongwei Chen¹, Minghua Chen¹, Zhiliang Weng¹, Yunhua Liang¹, Fangjian Xing¹, Shizhong Xie¹; ¹*Tsinghua Univ., China*. A two-dimensional temporal compressive sampling microscopic camera with a frame rate of 500 kHz is demonstrated in this paper, achieving higher frame rate and lower sampling bandwidth than the conventional compressive sampling cameras.

CLEO: Science & Innovations

08:00–10:00

**STu1N • Fiber Components &
Devices**

*Presider: Juliet Gopinath; Univ. of
Colorado at Boulder, USA*

STu1N.1 • 08:00

Splicing Tapered Inhibited-coupling Hypocycloid-core Kagome Fiber to SMF Fibers, Zheng Ximeng¹, Benoît Debord¹, Meshaal Alharbi¹, Luca Vincetti², Frédéric Gérôme¹, Fetah Benabid¹; ¹*Xlim Research Inst., UMR CNRS 7252, Univ. of Limoges, France, France*; ²*Dept. of Engineering, Univ. of Modena and Reggio Emilia, Italy*. We report on tapered inhibited coupling Kagome-fiber with a down-ratio as large as 2.4 while maintaining the hypocycloid-core shape. The insertion-loss of SMF spliced to tapered Kagomefiber was measured with minimum of 0.48dB at 1550nm.

STu1N.2 • 08:15

High Power Effects in Long Period Optical Fiber Gratings, Tristan Kremp¹, Jeffrey W. Nicholson¹, John M. Fini², Paul S. Westbrook¹; ¹*OFS Fitel LLC, USA*; ²*JDS Uniphase, USA*. We investigate nonlinear effects in long period gratings in a large mode area fiber. Simulations indicate that self-focusing effects can be significant at the power levels where self and cross phase modulation impair the mode conversion.

STu1N.3 • 08:30

High Power WDM with Narrow Wavelength Separations, Bhabana Pati¹, wenyen Tian¹, Amy Van Newkirk², Axel Schulzgen²; ¹*Q-Peak, Inc., USA*; ²*College of optics and photonics, CREOL, USA*. We designed and manufactured a high power WDM to enable a high power Raman lasers. We used a custom designed glass processing machine to fuse the WDM. We tested the WDM at 100 W of power with 0.05 dB loss.

08:00–10:00

**STu1O • Advanced Ultrafast
Sources**

*Presider: Hiromitsu Kiriya;
Japan Atomic Energy Agency,
Japan*

STu1O.1 • 08:00 **Invited**

Laser Technologies and Challenges for XFEL Beamlines, Alan Fry^{1,2}; ¹*SLAC National Accelerator Lab, USA*; ²*PULSE Inst., Stanford Univ., USA*. X-ray FEL facilities place challenging demands on the stability and configuration of ultrafast optical lasers for user experiments; future facilities will push the frontiers for high peak and average power ultrafast lasers.

STu1O.2 • 08:30

Sub-300 fs, 0.5 mJ Pulse at 1kHz from Ho:YLF Amplifier and Kagome Pulse Compression, Krishna murari^{1,2}, Huseyin Canakaya^{1,2}, Benoît Debord³, Peng Li¹, Giovanni Cirmi¹, Shaobo Fang¹, Giulio M. Rossi¹, Oliver D. Muecke¹, Peter Kroetz², Gregory J. Stein⁴, Axel Ruehl¹, Ingmar Hartl¹, Frédéric Gérôme³, Fetah Benabid³, Franz Kaertner^{1,4}; ¹*Deutsche Electron Synchrotron, Germany*; ²*Centre For Free Electron Laser Science, Germany*; ³*GPPMM Group, Xlim Research Inst., France*; ⁴*MIT, USA*. We demonstrate a compact 290 fs, 0.5 mJ laser source at 2-mm wavelength generated from mJ-level 3.4-ps pulses from a fiber laser seeded Ho:YLF regenerative amplifier system via pulse compression in a gas-filled Kagome type HC-PCF.

CLEO: QELS-Fundamental Science

JOINT

FTu1A • Quantum
Entanglement I—Continued

FTu1A.4 • 08:45

Measurement of Quantum Two-Mode Squeezing Inspired by Classical Radio-Frequency Analogies, Yaakov Shaked¹, Tzahi Geller¹, Avi Pe'er¹; ¹Bar-Ilan Univ., Israel. From analogy to RF theory and applications, we devise general measurement schemes for two-mode squeezing using nonlinear optical mixing as the physical detector. We provide complete quantum and classical theory, with RF and optical demonstrations.

FTu1A.5 • 09:00

Varying the Entanglement of 1.55 μm Photon Pairs Generated by a Silicon Nanophotonic Chip, Ranjeet Kumar¹, Marc Savanier¹, Jun Rong Ong¹, Shayam Mookherjee¹; ¹Univ. of California San Diego, USA. We characterize the strength of entanglement corresponding to different Joint Spectral Intensities of telecommunications-wavelength photon pairs generated using spontaneous four-wave mixing in a diode-pumped compact CMOS-compatible silicon chip.

FTu1A.6 • 09:15

Twin Photon Pairs in a High-Q Silicon Microresonator, Steven Rogers¹, Xiyuan Lu¹, Wei Jiang², Qiang Lin^{3,2}; ¹Dept. of Physics and Astronomy, Univ. of Rochester, USA; ²Inst. of Optics, Univ. of Rochester, USA; ³Dept. of Electrical and Computer Engineering, Univ. of Rochester, USA. We report the generation of twin photon pairs in a high-Q silicon microdisk resonator. The device is able to produce pairs at a flux of 5.31×10^5 pairs/s within a bandwidth of 0.73 GHz, and a coincidence-to-accidental ratio as large as 155, the highest value reported to date for twin photon pairs.

FTu1B • Ultrafast Dynamics in
Strongly Correlated Materials—
Continued

FTu1B.4 • 08:45

Probing Short- and Long-range Stripe Correlations in a Nickelate via Multi-THz Spectroscopy, Giacomo Coslovich¹, Wei-Sheng Lee², Hans Bechtel², Michael M. Martin², Takao Sasagawa¹, Zhi-Xun Shen³, Robert A. Kaindl¹; ¹Materials Sciences Division, Lawrence Berkeley National Lab, USA; ²Advanced Light Source, Lawrence Berkeley National Lab, USA; ³SIMES, SLAC National Accelerator Lab and Stanford Univ., USA; ⁴Materials and Structures Lab, Tokyo Inst. of Technology, Japan. We report optical-pump THzprobe reflectivity studies around the resonance frequency (≈ 11 THz) of the in-plane bending mode of a stripe-ordered nickelate. The experiments reveal signatures of both short and long-range nanoscale charge order dynamics.

FTu1B.5 • 09:00

Ultrafast Dynamics of Multiferroic $h\text{-LuFeO}_3$, John Bowlan¹, Xiaoshan Xu², Kishan Sinha², Stuart Trugman¹, Antoinette J. Taylor¹, Rohit P. Prasankumar¹, Dmitry Yarotski¹; ¹Los Alamos National Lab, USA; ²Physics and Astronomy, Univ. of Nebraska, Lincoln, USA. Hexagonal LuFeO_3 is a multiferroic showing ferroelectricity and antiferromagnetism at room temperature. Below $T_g=130$ K, it becomes ferrimagnetic. Ultrafast optical pump-probe measurements reveal that the dynamics are correlated with the structural changes responsible for ferrimagnetism.

FTu1B.6 • 09:15

Transient Exchange Interaction in a Helical Antiferromagnet, Matt Langner¹, Sujoy Roy¹, A. F. Kemper¹, Y.-D. Chuang¹, S. Mishra¹, R. B. Versteeg¹, Yi Zhu¹, M. P. Hertlein¹, T. E. Glover¹, K. Dumesnil², R. W. Schoenlein¹; ¹Lawrence Berkeley National Lab, USA; ²Institut Jean Lamour, France. We measure dynamics of the helical ordering in the Lanthanide metal Dy resulting from transient changes in the conduction electron Fermi surface and subsequent scattering events that transfer the excitation to the core spin.

FTu1C • Optics of
Metasurfaces—Continued

FTu1C.4 • 08:45

Diffraction Interface Theory: A nonlocal approach to metasurfaces, Christopher Roberts¹, Sandeep Inampudi¹, Viktor A. Podolskiy¹; ¹Univ. of Massachusetts Lowell, USA. We present a novel formalism to describe diffractive optics of metasurfaces, diffractive interface theory (DIT).

FTu1C.5 • 09:00

Surface plasmon polariton control with Metasurfaces, Patrice Genevet¹, Daniel Wintz², Antonio Ambrosio², Alan She², Federico Capasso¹; ¹A*star, SIMTech, Singapore; ²Harvard, USA. Acting as subwavelength converters with controllable responses, metasurfaces can now engineer surface plasmon for applications in integrated optics and flat photonics. Plasmon focusing, wavelength demultiplexing, and generation and control of plasmons will be discussed.

FTu1C.6 • 09:15

Broadband High-Efficiency Half-Wave Plate Using Plasmonic Metasurface, Fei Ding^{1,2}, Zhuoxian Wang¹, Vladimir M. Shalaev¹, Alexander V. Kildishev¹; ¹Birck Nanotechnology Center, School of Electrical & Computer Engineering, Purdue Univ., USA; ²Centre for Optical and Electromagnetic Research, Zhejiang Univ., China. We demonstrate an ultrathin, broadband half-wave plate in the near-infrared range using a plasmonic metasurface. Simulated and experimental results indicate that such a broadband and high-efficiency performance is sustained over a wide range of incident angles.

JTU1D • Symposium on
Advanced Optical Microscopy
for Brain Imaging I—Continued

JTU1D.3 • 09:00

Invited

Integrated Neurophotonics: Toward Massively-Parallel Mapping of Brain Activity, Michael L. Roukes¹; ¹California Inst. of Technology, USA. I describe a new paradigm for functional imaging that surmounts limitations of free-space optics - based on integrated nanophotonics, to distribute an ultraminaturized imager within the brain; and optogenetics, to transduce neural signals into the optical domain.



For Conference News & Insights
Visit blog.cleoconference.org

CLEO: QELS-
Fundamental ScienceFTu1E • 2D Materials
for Nanoplasmonics and
Nanophotonics—Continued

FTu1E.3 • 08:45

Plasmon Resonance in Single- and Double-layer CVD Graphene Nanoribbons, Di Wang^{1,2}, Naresh K. Emani^{1,2}, Ting-Fung Chung³, Ludmila Prokopeva^{1,2}, Alexander V. Kildishev^{1,2}, Vladimir M. Shalav^{1,2}, Yong P. Chen^{3,1}, Alexandra Boltasseva^{1,2}; ¹Electrical & Computer Engineering, Purdue Univ., USA; ²Birk Nanotechnology Center, USA; ³Physics, Purdue Univ., USA. Dynamic tunability of the plasmonic resonance in graphene nanoribbons is desirable in the near-infrared. We demonstrated a constant blue shift of plasmonic resonances in double-layer graphene nanoribbons with respect to single-layer graphene nanoribbons.

FTu1E.4 • 09:00

Nanoantenna-enhanced light-matter interaction in atomically thin WS₂, Johannes Kern¹, Andreas Trügler², Iris Niehaus¹, Johannes Ewering¹, Robert Schmidt¹, Robert Schneider¹, Sina Najmaei³, Antony George³, Jing Zhang³, Jun Lou³, Ulrich Hohenester², Steffen Michaelis de Vasconcellos¹, Rudolf Bratschkis¹; ¹Inst. of Physics and Center for Nanotechnology, Univ. of Münster, Germany; ²Inst. of Physics, Univ. of Graz, Austria; ³Dept. of Mechanical Engineering and Material Science, Rice Univ., USA. We present a hybrid system consisting of an atomically-thin semiconductor and a plasmonic nanoantenna. The intense optical near-fields provided by the antenna increase the photoluminescence intensity of WS₂ by more than one order of magnitude.

FTu1E.5 • 09:15

Enhanced Spontaneous Emission from an Optical Antenna Coupled WSe₂ Monolayer, Michael Eggleston¹, Sujay Desai¹, Kevin Messer¹, Surabhi Madhvarathy¹, Jun Xiao¹, Xiang Zhang¹, Eli Yablonovitch¹, Ali Javey¹, Ming C. Wu¹; ¹Univ. of California Berkeley, USA. A self-aligned process is developed to couple monolayer WSe₂ (30nm x 300nm) to a silver cavity-backed slot-antenna. Optical emission measurements show 340x enhancement in spontaneous emission. Carrier lifetimes of <1ps are measured by streak camera.

CLEO: Science & Innovations

STu1F • Optical Integration on
Chip—Continued

STu1F.4 • 09:00

Unidirectional Coupling with Two Matched Dielectric and Metal Long-Period Gratings along a Polymer Waveguide, Kin S. Chiang¹, Bing Zou¹; ¹City Univ. of Hong Kong, Hong Kong. We propose a grating structure for the achievement of unidirectional coupling, which consists of two matched dielectric and metal long-period gratings. We verify our idea theoretically and experimentally with gratings formed along a polymer waveguide.

STu1F.5 • 09:15

An Opto-Electro-Mechanical Phase Shifter, Marcel W. Pruessner¹, Doewon Park¹, Todd H. Stievater¹, Dmitry A. Kozak^{2,1}, William S. Rabinovich¹; ¹US Naval Research Lab, USA; ²NRC Postdoc, USA. We demonstrate an opto-electro-mechanical phase shifter. A suspended microbridge is electrostatically actuated to strongly-interact with a weakly-confined waveguide mode. The resulting effective index tuning substantially exceeds that achievable with thermo-optic and electro-optic approaches.

STu1G • Cascade Lasers I—
Continued

STu1G.4 • 08:45

Scanning Voltage Microscopy Study of Lasing and Non-lasing Terahertz Quantum Cascade Lasers, Rudra Dhar¹, Ghasem Razavipour¹, Emmanuel Dupont², Zbig Wasilewski¹, Dayan Ban¹; ¹Univ. of Waterloo, Canada; ²National Research Council, Canada. Scanning voltage microscopy results clearly show that the formation of electric field domains is responsible for the missing of lasing operation in a resonant-phonon based terahertz quantum cascade laser with a highly diagonal transition.

STu1G.5 • 09:00

Two-Dimensional Pump Frequency Study of THz Generation in Mid-Infrared Quantum Cascade Lasers, Yifan Jiang¹, Karun Vijayraghavan¹, Frederic Demmerle², Gerhard Boehm², Markus-Christian Amann², Mikhail A. Belkin¹; ¹The Univ. of Texas at Austin, USA; ²Technische Universität München, Germany. The dependence of THz difference-frequency generation in mid-infrared quantum cascade lasers on the position of mid-infrared pump frequencies is investigated. Experiments are performed at room-temperature using dual-diffraction-grating modified Littrow-type external cavity setup.

STu1G.6 • 09:15

Laterally-Coupled Dual-Grating Distributed Feedback Lasers for Generating Mode-Beat Terahertz Signals, Lianping Hou¹, Mohsin Haji², Iain Eddie³, Hongliang Zhu⁴, John H. Marsh¹; ¹School of Engineering, Univ. of Glasgow, UK; ²National Physical Lab, UK; ³3CST Global Ltd, UK; ⁴Inst. of Semiconductors, China. We present a laterally-coupled AlGaInAs/InP DFB laser emitting two longitudinal modes simultaneously within the same cavity and integrated with EAM. A stable 0.82 THz beating signal was observed over a wide range of bias parameters.

STu1H • Terahertz Photonics—
Continued

STu1H.4 • 08:45

Efficient Terahertz Phase Modulation Using Vanadium Dioxide Meta-Surfaces, Mohammed Reza Hashemi¹, Shang-Hua Yang^{1,2}, Tongyu Wang³, Nelson Sepúlveda³, Mona Jarrahi^{1,2}; ¹Univ. of California, Los Angeles, USA; ²Univ. of Michigan, USA; ³Michigan State Univ., USA. Voltage-controlled THz phase modulation using vanadium dioxide reconfigurable meta-surfaces is presented and a proof-of-concept phase modulator for sub-THz frequencies is fabricated. We demonstrate the highest reported phase modulation of 600 at 85 GHz through a fully-integrated device platform.

STu1H.5 • 09:00

Ultrathin Flexible and Optically Tunable Terahertz Bandpass Filter with Embedded Silicon, Michael A. Hoeh¹, Jens Neu¹, Klemens M. Schmitt¹, Marco Rahm¹; ¹Technische Universität Kaiserslautern, Germany. A new fabrication technique for ultra-thin, flexible and optically tunable metamaterials with embedded silicon is presented. We demonstrated a 25- μ m-thick optically tunable terahertz bandpass filter with a maximal amplitude transmission of 80 % and an amplitude modulation depth of 94 % at 0.65 THz.

STu1H.6 • 09:15

Terahertz Surface Wave Modulation in a Dielectric Slab Metasurface, Nicholas Karl¹, Hou-Tong Chen², Antoinette J. Taylor², Igal Brener³, Alexander Benz³, John Reno³, Rajind Mendis¹, Daniel Mittleman¹; ¹Dept. of Electrical and Computer Engineering, Rice Univ., USA; ²Center for Integrated Nanotechnologies, Los Alamos National Lab, USA; ³Center for Integrated Nanotechnologies, Sandia National Labs, USA. We experimentally and numerically investigate a switchable dielectric-slab-waveguide metasurface device. We use an active metasurface to manipulate the interaction with a propagating THz surface wave, giving us dynamic control of the wave at 0.3 THz.

Meeting Room
211 B/D

CLEO: Science & Innovations

STu11 • Nonlinear Optics—Continued

STu11.4 • 08:45

Low-power on-chip all-optical Kerr switch with silica microcavity, Wataru Yoshiki¹, Takasumi Tanabe¹; ¹Keio Univ., Japan. We achieved on-chip optical Kerr switching with an input power of 2 mW using a silica toroid microcavity. This is the lowest power for any demonstrated on-chip optical Kerr switch.

STu11.5 • 09:00

Broadband low-phase-noise 18 GHz Kerr frequency microcomb, Shu-Wei Huang¹, Jinghui Yang¹, Heng Zhou², Mingbin Yu³, Dim-Lee Kwong³, Chee Wei Wong¹; ¹UCLA, USA; ²Univ. of Electronic Science and Technology of China, China; ³Inst. of Microelectronics, Singapore. We report a half-octave-spanning Kerr frequency comb which has the record-low phase noise floor with -130 dBc/Hz at 1 MHz offset for 18 GHz carrier frequency, and long-term Allan deviation of $7 \cdot 10^{-11}/\tau^{0.84}$ with active stabilization.

STu11.6 • 09:15

High-Q Silicon Nitride Microresonator for Low Power Frequency Comb Initiation at Normal Dispersion Regime, Yi Xuan¹, Yang Liu¹, Xiaoxiao Xue¹, Pei-Hsun Wang¹, Jian Wang¹, Ben Niu¹, Kyunghun Han¹, Min TENG¹, Daniel E. Leaird¹, Andrew M. Weiner¹, Minghao Qi¹; ¹Purdue Univ., USA. SiN microresonators with a cross section of $3 \times 0.6 \mu\text{m}^2$ and an FSR of 25 GHz were demonstrated with intrinsic Qs up to 17 million, showing frequency comb onset power as low as 5.6 mW.

Meeting Room
212 A/C

CLEO: Applications & Technology

ATu1J • Applications for Energy and Environment—Continued

ATu1J.4 • 08:45

Ultralow-Noise Infrared Spectroscopy at Single-Photon Level Based on Frequency Upconversion System, Wenjie Wu¹, Ruikai Tang¹, Xiongjie Li¹, Haifeng Pan¹, EWu¹, Heping Zeng¹; ¹East China Normal Univ., China. We realized an efficient infrared spectrometer with high detection sensitivity at single photon level by using the wavelength tunable frequency upconversion detection technique with synchronized laser source. This kind of spectrometers also can be used in remote spectrum analysis.

ATu1J.5 • 09:00

Thermal Emission of GaAs Nanowire Solar Cells, Shao-Hua Wu¹, Michelle Povinelli¹; ¹Electrical Engineering, Univ. of Southern California, USA. Despite concentrated light absorption and low thermal conductivities, GaAs nanowire solar cells can still have larger thermal emission cooling power than planar ones, resulting in a nearly 10 K lowering in operating temperature.

ATu1J.6 • 09:15

Temperature-dependent Characterization of $G_{0.94}Sn_{0.06}$ Light-Emitting Diode Grown on Si via CVD, Seyed Amir Ghetmiri², Wei Du¹, Yiyin Zhou¹, Joe Margetis³, Thach Pham², Aboozar Mosleh¹, Benjamin Conley¹, Amjad Nazzal⁴, Gregory Sun⁵, Richard Soref⁶, John Tolle³, Hameed Naseem², Baohua Li⁶, Shui-Qing Yu²; ¹Univ. of Arkansas, USA; ²Electrical engineering, Univ. of Arkansas, USA; ³ASM, USA; ⁴Electrical Engineering and Physics, Wilkes Univ., USA; ⁵Dept. of Engineering, Univ. of Massachusetts Boston, USA; ⁶Arctonic LLC, USA. Temperature-dependent electroluminescence from a double heterostructure n-Ge/i-Ge_{0.94}Sn_{0.06}/p-Ge LED was studied. The peak position of EL spectra showed a blue-shift as the temperature decreased. A maximum emission power of 7 mW was obtained under the current density of 800 A/cm².

Meeting Room
212 B/D

CLEO: Science & Innovations

STu1K • Integrated Optofluidics: Sensing, Guiding and Tailored Fabrication—Continued

STu1K.4 • 08:45

Optofluidic Polarization Beam Splitter, Yang Liu¹, Lei Shi¹, Xudong Fan², Xinliang Zhang¹; ¹Huazhong Univ of Science and Technology, China; ²Biomedical Engineering, Univ. of Michigan, USA. An efficient polarization beam splitter (PBS) based on a silica microcapillary is proposed and experimentally demonstrated. This PBS relies on the inherent-geometry-induced birefringence. A maximum extinction ratio of up to 25 dB is achieved.

STu1K.5 • 09:00

Optical Waveguides from a Lithographically-Defined Wetting of a High-Index Liquid, Christopher C. Evans¹, Emily Hsu¹, Michelle Ji¹, Chengyu Liu¹, Jin Suntivich¹; ¹Cornell Univ., USA. We present a new approach to realize liquid-core optical waveguides via selective wetting on lithographically patterned oleophobic and oleophilic patches for sensing and adaptable optics applications.

STu1K.6 • 09:15

Density Assisted Optofluidic Fabrication of 3D Shaped Particles, Kevin Paulsen¹, Aram Chung¹; ¹RPI, USA. We present a novel method of creating complex 3D particles by flow deformation and UV light polymerization. An infinite number of particle shapes can be obtained by manipulating flow and light conditions.

Marriott
Salon I & II

STu1L • Symposium on Breaking Limits with Unconventional Optical Fields I—Continued

STu1L.3 • 08:45

Optical Coherency Matrix Tomography of Unconventional Beams, Kumel Kagalwala¹, H. Esat Kondacki¹, Ayman F. Abouraddy¹, Bahaa E. Saleh¹; ¹Univ. of Central Florida, CREOL, USA. We present the first experimental measurement of the coherency matrix **G** associated with an electromagnetic beam with two binary degrees of freedom. We consider beams with polarization and a spatially varying amplitude or phase: spatial parity modes and orbital angular momentum modes, respectively.

STu1L.4 • 09:00

Study of Turbulence Induced Orbital Angular Momentum Channel Crosstalk in a 1.6 km Free-Space Optical Link, Martin P. Lavery¹, Bettina Heim², Christian Peuntinger², Ebrahim Karimi⁴, Omar S. Magaña-Loaiza³, Thomas Bauer², Christoph Marquardt², Alan Willner⁵, Robert W. Boyd^{3,4}, Miles Padgett¹, Gerd Leuchs²; ¹Univ. of Glasgow, UK; ²Max Planck Inst. for the Science of Light and Inst. of Optics, Information and Photonics, Friedrich-Alexander-Universität Erlangen-Nürnberg, Germany; ³Inst. of Optics, Univ. of Rochester, USA; ⁴Dept. of Physics, Univ. of Ottawa, Canada; ⁵Electrical Engineering, Univ. of Southern California, USA. We experimentally study the turbulence induced crosstalk between orbital angular momentum channels transmitted over a 1.6 km optical link. Our presented results indicate that turbulence mitigation techniques will be required for links of this length.

STu1L.5 • 09:15

Single-aperture STED illumination using a q-plate and fiber, Lu Yan¹, Ebrahim Karimi², Patrick Gregg¹, Robert W. Boyd^{2,3}, Siddharth Ramachandran¹; ¹Dept. of Electrical and Computer Engineering, Boston Univ., USA; ²Dept. of Physics, Univ. of Ottawa, Canada; ³Inst. of Optics, Univ. of Rochester, USA. We demonstrate single-aperture STED nanoscopy illumination with vortex-fiber modes excited by a dispersive q=1/2 plate at visible wavelengths. The vortex-fiber-compatible bias-voltage-tunable mode conversion of q-plates enables easy switching between multiple STED-wavelength pairs.

CLEO: Applications
& TechnologyATu1M • Process Control and
Metrology Applications—
Continued

ATu1M.3 • 08:45

Design Challenges of a High Speed Tunable Laser Interrogator for Future Spacecraft Health Monitoring, Selwan K. Ibrahim¹, John O'Dowd¹, Raymond McCue¹, Arthur Honniball¹, Martin Farnan¹; ¹FAZ Technology Ltd., Ireland. We report the performance results achieved for a high speed, high resolution optical FBG interrogator with a repeatability <5fm@80Hz BW and precision <200fm (p-p), designed for space applications on a launcher or atmospheric re-entry vehicle.

ATu1M.4 • 09:00

Safety Monitoring of Long Distance Power Transmission Cables and Oil Pipelines with OTDR Technology, Huijuan Wu¹, Ya Qian¹, Hanyu Li¹, Shunkun Xiao¹, Zhizhong Fu¹, Yunjiang Rao¹; ¹Univ of Electronic Sci & Tech of China, China. This paper presents two typical applications of polarization- and phase-sensitive OTDRs, which are representative Distributed Optical Fiber Sensors (DOFSs), for on-line safety monitoring of long-distance power transmission cables and oil pipelines in the energy industry.

ATu1M.5 • 09:15

Curvature Sensor Based on Long-Period Grating in Dual Concentric Core Fiber, Zhifang Wu^{1,2}, Nan Zhang^{1,2}, Ping Shum^{1,2}, Xuguang Shao¹, Hailiang Zhang^{1,2}, Tianye Huang^{1,2}, Georges Humbert³, Jean-Louis Auguste³, Frédéric Gérôme³, Jean-Marc Blondy³, Quyen X. Dinh²; ¹School of Electrical and Electronics Engineering, Nanyang Technological Univ., Singapore; ²CNRS-International-NTU-Thales Research Alliance (CINTRA), Singapore; ³XLIM Research Inst., UMR 7252 CNRS/Univ. of Limoges, France. We report on a curvature sensor based on a long-period grating in a dual-concentric-core fiber. By measuring the relative shifting of two adjacent resonant dips, the curvature sensitivity reaches 7.635 nm/m⁻¹.

CLEO: Science & Innovations

STu1N • Fiber Components &
Devices—Continued

STu1N.4 • 08:45

Towards a Plasma-Core PCF for Tunable UV-DUV Radiation, Benoît Debord¹, Frédéric Gérôme¹, Damien Passerieux¹, Philippe Coche², Luis Lemos Alves², Fetah Benabid¹; ¹Xlim Research Inst., UMR CNRS 7252, Univ. of Limoges, France; ²Instituto de Plasmas e Fusão Nuclear, Instituto Superior Técnico, Universidade de Lisboa, Portugal. We report on recent results toward development of tunable and miniaturized UV-DUV radiation using microwave-driven plasma-core photonic crystal fiber. Gas-mixture optimized UV-DUV emission and highly efficient microwave ring resonators couplers are demonstrated.

STu1N.5 • 09:00

Hollow Core Silicon-Silica Bragg Fiber, Subhasis Chaudhuri¹, Justin Sparks¹, Rongrui He¹, John Badding¹; ¹Pennsylvania State Univ., USA. A hollow core four layered Bragg fiber has been fabricated using silicon and silica as alternating layers via high-pressure chemical vapor deposition, which can be used for the guidance of near infrared light.

STu1N.6 • 09:15

Inspection of Defect-Induced Mode Coupling in Hollow-Core Photonic Bandgap Fibers Using Time-of-Flight, Nicholas H. Wong¹, Syed Reza Sandoghchi¹, Yongmin Jung¹, Tom Bradley¹, Natalie V. Wheeler¹, Naveen Baddela¹, John R. Hayes¹, Francesco Poletti¹, Marco Petrovich¹, Shaiful Alam¹, P. Petropoulos¹, david Richardson¹; ¹Univ. of Southampton, UK. We analyze defect-induced mode coupling in a hollow-core photonic bandgap fiber using time-of-flight, and show its utility in complementing optical time-domain reflectometry.

STu1O • Advanced Ultrafast
Sources—Continued

STu1O.3 • 08:45

Ultrafast Diode-Pumped Ti:Sapphire Laser Generating 200-mW Average Power in 68-fs Pulses, Kutun Gurel¹, Martin Hoffmann¹, Clara J. Saraceno^{1,2}, Valentin J. Wittwer¹, Sargis Hakobyan¹, Bojan Resan³, Andreas Rohrbacher³, Kurt Weingarten³, Stéphane Schilt¹, Thomas Sudmeyer¹; ¹Laboratoire Temps-Fréquence, Université de Neuchâtel, Switzerland; ²Inst. for Quantum Electronics, ETH Zurich, Switzerland; ³JDSU Ultrafast Lasers AG, Switzerland. We present the highest average power from a diode-pumped Ti:Sapphire laser. Using self-starting SESAM-modelocking we obtain 200 mW in 68-fs pulses at 378 MHz. The laser is pumped by two air-cooled 520 nm AlInGaN laser diodes.

STu1O.4 • 09:00

CPA-free ultrafast fiber laser source based on pre-chirp managed nonlinear amplification, Damian N. Schimpf^{1,2}, Wei Liu¹, Tino Eidam^{3,4}, Jens Limpert^{3,4}, Andreas Tünnermann^{3,4}, Franz Kaertner^{1,2}, Guoqing Chang^{1,2}; ¹Center for Free-Electron Laser Science, DESY, Germany; ²The Hamburg Centre for Ultrafast Imaging, Germany; ³Inst. of Applied Physics, Abbe Center of Photonics, Friedrich-Schiller-Universität Jena, Germany; ⁴Helmholtz Institut Jena, Germany. Pre-chirp managed nonlinear amplification delivering high quality 60 fs pulses is compared to conventionally employed CPA. We present a compact rod-type system that outputs >100 W at 75 MHz.

STu1O.5 • 09:15

Optimized SESAMs for Kilowatt Ultrafast Lasers, Andreas Diebold¹, Thomas Zengerle¹, Mario Mangold¹, Cinia Schriber¹, Florian Emaury¹, Martin Hoffmann², Clara J. Saraceno^{1,2}, Matthias Golling¹, David Follman³, Garrett Cole^{3,4}, Markus Aspelmeyer⁵, Thomas Sudmeyer², Ursula Keller¹; ¹Dept. of Physics, ETH Zurich, Switzerland; ²Laboratoire Temps-Fréquence, Université de Neuchâtel, Switzerland; ³Crystaline Mirror Solutions LLC, USA; ⁴Crystalline Mirror Solutions GmbH, Austria; ⁵Vienna Center for Quantum Science and Technology, Austria. We present SESAMs with different substrate-removal techniques, optimized for kW power operation. These SESAMs show significant improvements in terms of surface quality without affecting their nonlinear parameters.

CLEO: QELS-Fundamental Science

JOINT

FTu1A • Quantum
Entanglement I—Continued

FTu1A.7 • 09:30

Falsifying Local Realism, Lynden Shalm¹, Yanbao Zhang¹, Kevin Coakley¹, Scott Glancy¹, Sae Woo Nam¹, Emanuel Knill¹; ¹NIST, USA. Standard methods of analyzing Bell's inequalities are fundamentally flawed when it comes to ruling out local realism. Here we present a powerful analysis technique that can falsify local realism in a certifiable manner.

FTu1A.8 • 09:45

Quantum Entanglement Distillation Using an Optical Metamaterial, Muriel Béchu¹, Motoki Asano², Mark Tame^{3,4}, Sahin K. Ozdemir⁵, Rikizou Ikuta⁶, Takashi Yamamoto², Durdu Guney⁶, Lan Yang⁷, Martin Wegener^{1,7}, Nobuyuki Imoto²; ¹Inst. of Applied Physics, Karlsruhe Inst. of Technology, Germany; ²Dept. of Material Engineering Science, Osaka Univ., Japan; ³School of Chemistry and Physics, Univ. of KwaZulu Natal, South Africa; ⁴National Inst. for Theoretical Physics, Univ. of KwaZulu Natal, South Africa; ⁵Dept. of Electrical and Systems Engineering, Washington Univ., USA; ⁶Dept. of Electrical and Computer Engineering, Michigan Technological Univ., USA; ⁷Inst. of Nanotechnology, Karlsruhe Inst. of Technology, Germany. We perform an entanglement distillation protocol on pure and mixed states using optical metamaterials composed of gold nano-antennas and measure the density matrices by quantum-state tomography. The fidelity is improved from 0.85 to 0.97.

FTu1B • Ultrafast Dynamics in
Strongly Correlated Materials—
Continued

FTu1B.7 • 09:30

Direct Observation of Magnon Dynamics in Multiferroic HoMnO₃, Pamela R. Bowlan¹, Dmitry Yarotski¹, Namjung Hur², Antoinette J. Taylor¹, Rohit P. Prasankumar¹; ¹Center for Integrated Nanotechnologies, Los Alamos National Lab, USA; ²Dept. of Physics, Inha Univ., Korea (the Democratic People's Republic of). We directly resolve energy transfer pathways from electrons to magnons in multiferroic HoMnO₃ using ultrafast optical/terahertz spectroscopy. This reveals that energy is initially transferred from electrons to phonons and subsequently to magnons through spin-lattice relaxation.

FTu1C • Optics of
Metasurfaces—Continued

FTu1C.7 • 09:30

Plasmonic Metasurface for Color Hologram, Yao-Wei Huang¹, Wei Ting Chen¹, Wei-Yi Tsai¹, Pin Chieh Wu¹, Chih-Ming Wang³, Gregory Sun², Din Ping Tsai^{1,4}; ¹Dept. of Physics, National Taiwan Univ., Taiwan; ²Dept. of Engineering, Univ. of Massachusetts Boston, USA; ³Inst. of Opto-electronic Engineering, National Dong Hwa Univ., Taiwan; ⁴Research Center for Applied Sciences, Academia Sinica, Taiwan. We report a full-color meta-hologram based on a reflective metasurface. The reconstructed image of the meta-hologram is polarization-dependent with three primary colors, arranged in a plasmonic array in visible light region.

FTu1C.8 • 09:45

Achromatic metasurfaces enable multi-wavelength flat optical components: demonstration of a dispersion-less beam deflector, Francesco Aieta¹, Mikhail Kats¹, Patrice Genevet¹, Reza Khorasaninejad¹, Federico Capasso¹; ¹SEAS, Harvard Univ., USA. Achromatic metasurfaces are introduced for multiwavelength light control. A wavelength-dependent phase response preserves the functionality within a certain bandwidth. Scattering properties of dielectric resonators are explored to demonstrate a dispersion-free beam deflector and an achromatic lens.

JTu1D • Symposium - Advanced
Optical Microscopy for Brain
Imaging I—Continued

JTu1D.4 • 09:30

Invited

Photoacoustic Tomography: Ultrasonically Beating Optical Diffusion and Diffraction, Lihong V. Wang¹; ¹Washington Univ. in St. Louis, USA. Photoacoustic tomography provides *in vivo* multiscale functional, metabolic, molecular, and histologic imaging across the scales of organelles, cells, tissues, and organs with consistent contrast. Penetration and resolution have reached 7 cm and 90 nm, respectively.

09:00–12:00 SC352 • Introduction to Ultrafast Pulse Shaping—Principles and Applications

SC362 • Cavity Optomechanics: Fundamentals and Applications of Controlling and Measuring Nano- and Micro-mechanical Oscillators with Laser Light

SC410 • Finite Element Modelling Methods for Photonics and Optics

10:00–10:30 Coffee Break, Concourse Level



CLEO: QELS-
Fundamental ScienceFTu1E • 2D Materials
for Nanoplasmonics and
Nanophotonics—Continued

FTu1E.6 • 09:30

Ultrafast Nonlinear Absorption and Nonlinear Refraction of 2D Layered Molybdenum Dichalcogenide Semiconductors, Kangpeng Wang¹, Jung Wang², Long Zhang², Werner Blau¹; ¹Trinity College Dublin, Ireland; ²Shanghai Inst. of Optics and Fine Mechanics, China. The nonlinear optical properties of a series of layered transition metal dichalcogenides prepared by liquid-phase exfoliation technique, i.e., MoX₂ (X=S, Se and Te), were investigated by open- and closed- aperture z-scan from visible to near-infrared.

FTu1E.7 • 09:45

Pseudospin Selective Microcavity Polariton Emission From Two-dimensional Atomic Crystal, Zheng Sun¹, Xiaoze Liu¹, Hsuan-Hao Huang², Yu-Wen Tseng², Yi-Hsien Lee², Stéphane Kéna Cohen³, Vinod M. Menon¹; ¹Physics, City Univ. of New York, USA; ²National Tsing Hua Univ., Taiwan; ³École Polytechnique de Montréal, Canada. We demonstrate helicity-dependent microcavity polariton emission from 2D atomic crystal at room temperature via non-resonance pump. The observed effect is in contrast to conventional spin polariton emission above the condensation threshold.

CLEO: Science & Innovations

STu1F • Optical Integration on
Chip—Continued

STu1F.6 • 09:30

Optofluidic Double-layer Fano Resonance Photonic Crystal Slab Liquid Sensors, Shuling Wang¹, Yonghao Liu¹, Deyin Zhao¹, Yichen Shuai¹, Hongjun Yang¹, Weidong Zhou¹, Yuze A. Sun¹; ¹Univ. of Texas at Arlington, USA. We report refractive index sensing with ultra-compact surface-normal double-layer stacked Fano resonance photonic crystal slabs. A quality factor of 6,757 and a limit of detection of 5.6x10⁻⁵ RIU were experimentally demonstrated, respectively.

STu1F.7 • 09:45

All-Fiber Polarization-Maintaining Electrooptic Pulse-Picker, Mikael Malmström^{2,1}, Simon Boivinet^{3,4}, Oleksandr Tarasenko⁵, Jean-Bernard Lecourt³, Yves Hernandez³, Walter Margulis^{5,1}, Fredrik Laurell¹; ¹Dept. of Applied Physics, Laser Physics, Kungliga Tekniska Hogskolan, Sweden; ²Dept. of Engineering Sciences, Applied Materials Science, Uppsala Univ., Sweden; ³Applied Photonics Dept., Multitel, Belgium; ⁴Electromagnetism and Telecommunication Dept., Univ. of Mons, Belgium; ⁵Dept. of Fiber Optics, Acreo AB, Sweden. An alignment free all-fiber pulse-picker running at variable repetition rate for selecting pulses from an 86 MHz mode-locked Yb-fiber laser at 0-0.6 MHz with better than 35 dB extinction ratio is presented.

STu1G • Cascade Lasers I—
Continued

STu1G.7 • 09:30

Optical Sideband Generation up to Room Temperature with Mid-Infrared Quantum Cascade Lasers, Sarah Houver¹, Armand Lebreton¹, Pierrick Cavalié¹, Margaux Renaudat Saint-Jean², Maria Amanti², Carlo Sirtori², Li Lianhe³, Edmund Linfield³, Giles Davies³, Teldo Pereira⁴, Jérôme Tignon¹, Sukhdeep Dhillon¹; ¹Laboratoire Pierre Aigrain, USA; ²Laboratoire Matériaux et Phénomènes Quantiques, France; ³Univ. of Leeds, UK; ⁴Universidade Federal de Mato Grosso, Brazil. Room temperature sideband generation on an optical carrier is demonstrated using mid-infrared quantum cascade lasers. This is achieved via an enhancement of the nonlinear susceptibility via resonant interband and intersubband excitations, compensating the large phase-mismatch.

STu1G.8 • 09:45

Long-infrared InAs-based quantum cascade lasers, Daniel Chastanet¹, Adel Bousseksou¹, Raffaele Colombelli¹, Guillaume Lollia², Michael Bahriz², Alexei Baranov², Roland Teissier²; ¹IEF, CNRS-Université Paris Sud, France; ²IES, Université Montpellier 2 and CNRS, France. We report recent developments on InAs/AlSb based quantum cascade laser operating at of 17-19 μm , with improved design and metal-metal ridge resonators. The maximum operating temperature is 333 K at $\lambda=17.9 \mu\text{m}$. We also report distributed feedback lasers featuring spectrally single mode operation.

STu1H • Terahertz Photonics—
Continued

STu1H.7 • 09:30

Terahertz Radiation Enhancement in Large-Area Photoconductive Sources by Using Plasmonic Nanoantennas, Nezhim Yardimci¹, Shang-Hua Yang^{2,1}, Christopher Berry², Mona Jarrahi^{1,2}; ¹Univ. of California - Los Angeles, USA; ²Univ. of Michigan, USA. We demonstrate that incorporating plasmonic nanoantennas in large-area photoconductive sources enables record-high terahertz radiation powers as high as 3.8 mW over 0.1-5 THz and an order-of-magnitude higher optical-to-terahertz conversion efficiencies compared to conventional designs.

STu1H.8 • 09:45

Mechanically tunable bi-layer terahertz metamaterials, Liming Liu^{2,3}, Wen-chen Chen¹, David A. Powell³, Willie J. Padilla¹, Fouad Karouta⁴, Haroldo T. Hattori², Dragomir N. Neshev³, Ilya Shadrivov³; ¹Dept. of Physics, Boston College, USA; ²School of Engineering and Information Technology, UNSW, Australia; ³Nonlinear Physics Centre, Australian National Univ., Australia; ⁴Dept. of Electronic Materials Engineering, Australian National Univ., Australia. We propose a post-processing approach for tuning terahertz metamaterials by modifying the coupling between two metamaterial layers. We demonstrate that this method allows the metamaterial resonance to be shifted by 31% of the central frequency.

09:00–12:00 SC352 • Introduction to Ultrafast Pulse Shaping—Principles and Applications
SC362 • Cavity Optomechanics: Fundamentals and Applications of Controlling and Measuring Nano- and Micro-mechanical Oscillators with Laser Light
SC410 • Finite Element Modelling Methods for Photonics and Optics

10:00–10:30 Coffee Break, Concourse Level

Meeting Room
211 B/D

CLEO: Science & Innovations

STu11 • Nonlinear Optics—Continued

STu11.7 • 09:30

Octave-Spanning Supercontinuum Generation in a Silicon Nitride Waveguide Pumped by a Femtosecond Fiber Laser at 1.9 μm , Reza Salem^{2,1}, Yoshitomo Okawachi³, Mengjie Yu³, Michael Lamont³, Kevin Luke⁴, Peter Fendel², Michal Lipson⁴, Alexander L. Gaeta³; ¹PicoLuz, LLC, USA; ²Thorlabs, Inc., USA; ³Applied and Engineering Physics, Cornell Univ., USA; ⁴Electrical and Computer Engineering, Cornell Univ., USA. We report supercontinuum generation from 1250 - 2600 nm using a 2-cm-long silicon nitride waveguide pumped with an all-fiber femtosecond laser source at 1920 nm.

STu11.8 • 09:45

Low-Noise Stimulated Brillouin Lasing in a Microrod Resonator, William Loh¹, Joe Becker¹, Frederick N. Baynes¹, Adam Green¹, Daniel C. Cole¹, Franklyn Quinlan¹, Hansuek Lee², Kerry Vahala², Scott B. Papp¹, Scott Diddams¹; ¹NIST, USA; ²California Inst. of Technology, USA. We demonstrate a Brillouin microcavity laser based on a microrod resonator exhibiting a frequency noise of 140 Hz/ $\sqrt{\text{Hz}}$ at 10 Hz offset. The corresponding laser linewidth is measured to be below 400 Hz.

Meeting Room
212 A/C

CLEO: Applications & Technology

ATu1J • Applications for Energy and Environment—Continued

ATu1J.7 • 09:30

Advanced Laser Lift Off in the Manufacturing of LEDs, Marco Mendes¹, Cristian Porneala¹, Xiangyang Song¹, Mathew Hannon¹, Rouzbeh Sarrafi¹, Joshua Schoenly¹, Dana Sercel¹, Sean Dennigan¹, Roy VanGemert¹, Heath Chaplin¹, John Bickley¹, Jeff Sercel¹; ¹IPG Photonics - Microsystems Division, USA. Advanced laser lift off (LLO) techniques leading to high quality and high throughput fabrication of vertical and flip chip GaN and AlN based LEDs are discussed.

ATu1J.8 • 09:45

Enhancement of Quantum Dot Luminescence by using Plasmonic Resonance Scheme of Stacking Asymmetric Split-Ring Metamaterials, Tien Lin Shen¹, Tsung-Sheng Kao¹, Hao-Chung Kuo¹; ¹National Chiao Tung Univ., Taiwan. Coupling of nanostructured metal with quantum dots have been widely used in various technologies. We have designed a stacking split-ring metamaterial with tunable resonance and enhanced the quantum dots fluorescence by a factor over 4.5.

Meeting Room
212 B/D

CLEO: Science & Innovations

STu1K • Integrated Optofluidics: Sensing, Guiding and Tailored Fabrication—Continued

STu1K.7 • 09:30

Tailoring Light Flow in Microfluidics, Haitao Zhao¹, Lip Ket Chin¹, Weiming Zhu¹, Eric Peng Huat Yap², Wee Ser¹, Ai-Qun LIU¹; ¹School of Electrical and Electronic Engineering, Nanyang Technological Univ., Singapore; ²Lee Kong Chian School of Medicine, Nanyang Technological Univ., Singapore. This paper proposes an approach to tailor the light flow by using the liquid diffusion-generated gradient. A microfluidic network is designed to generate the required linear and parabolic profiles. Maxwell's fisheye lens and optical bend are realized on a single microfluidic chip.

STu1K.8 • 09:45

Ultra-broadband SERS substrates for "all" excitation wavelengths, Nan Zhang¹, Kai Liu¹, Haomin Song¹, Xie Zeng¹, Dengxin Ji¹, Qiaoqiang Gan¹; ¹State Univ. of New York at Buffalo, USA. We developed an ultra-broadband super-absorbing metasurface substrate for SERS sensing. In contrast to conventional substrates working for limited excitation wavelengths, this structure can work for almost "all" available laser lines from 450-nm to 1000-nm.

Marriott
Salon I & II

STu1L • Symposium on Breaking Limits with Unconventional Optical Fields I—Continued

STu1L.6 • 09:30

Increasing the Quantum Number, Dimensionality and Complexity of Entanglement, Robert Fickler^{1,2}, Mario Krenn^{1,2}, Radek Lapkiewicz^{1,2}, Marcus Huber^{3,4}, William N. Plick^{1,5}, Sven Ramelow^{1,6}, Anton Zeilinger^{1,2}; ¹Vienna Center for Quantum Science and Technology, Faculty of Physics, Univ. of Vienna, Austria; ²Austrian Academy of Sciences, Inst. for Quantum Optics and Quantum Information, Austria; ³Fisica Teorica: Informacio i Fenomens Quanticas, Departament de Fisica, Universitat Autònoma de Barcelona, Spain; ⁴ICFO-Institut de Ciències Fotoniques, Spain; ⁵CNRS - Telecom ParisTech, France; ⁶Cornell Univ., USA. We use transverse spatial modes of photons to demonstrate quantum entanglement of angular momentum up to 300 quanta and verify (100x100)-dimensional entanglement. Additionally, we investigate entanglement of complex polarization patterns and find interesting entanglement structures.

Invited

09:00–12:00 SC352 • Introduction to Ultrafast Pulse Shaping—Principles and Applications
SC362 • Cavity Optomechanics: Fundamentals and Applications of Controlling and Measuring Nano- and Micro-mechanical Oscillators with Laser Light
SC410 • Finite Element Modelling Methods for Photonics and Optics

10:00–10:30 Coffee Break, Concourse Level

CLEO Mobile App

Use the conference app to plan your schedule; view program updates; receive special events reminders and access Technical Papers (*separate log-in required*).

- Go to www.cleoconference.org/app.
- Select the Apple App Store or Google Play link.
- Download the app.
- Log in to use app features such as contacting fellow conference attendees—using your registration I.D. and email address.

**CLEO: Applications
& Technology****ATu1M • Process Control and
Metrology Applications—
Continued****ATu1M.6 • 09:30**

Highly Sensitive Liquid Level Sensor using a Polymer Optical Bragg Grating for Industrial Applications, Carlos Marques¹, Gang-Ding Peng², David J. Webb¹; ¹Aston Inst. of Photonic Technologies, Aston Univ. B4 7ET Birmingham, UK, UK; ²Univ. of New South Wales, School of Electrical Engineering and Telecommunications, Australia. A novel and highly sensitive liquid level sensor based on a polymer optical fiber Bragg grating (POFBG) is reported for the first time. The sensitivity of the sensor is found to be 57 pm/cm of liquid, enhanced by more than a factor of 5 when compared to an equivalent sensor based on silica fiber.

ATu1M.7 • 09:45

Integrated Fabry-Perot/Fiber Bragg Grating Sensor for Simultaneous Measurement, Peixiang Lu¹, Fahad M. Abdulhussein²; ¹Huazhong Univ of Science and Technology, China; ²Inst. of laser for postgraduate studies, Baghdad Univ., Iraq. An all-fiber sensor for simultaneous measurements is demonstrated. Fiber Bragg grating (FBG) inside the core of all solid photonic band gap fiber (ASPBGF) was connected to FPI micro cavity for simultaneously measure load and temperature with sensitivities 4.07nm/N and 13.7pm/°C respectively.

CLEO: Science & Innovations**STu1N • Fiber Components &
Devices—Continued****STu1N.7 • 09:30**

Kagome-type HC-PCF pulse compression: high average power (>100 W), high efficiency and very low noise performance, Florian Emaury¹, Andreas Diebold¹, Benoît Debord², Frédéric Gérôme², Clara J. Saraceno^{1,3}, Thomas Sudmeyer³, Fetah Benabid², Ursula Keller¹; ¹ETH Zurich, Switzerland; ²XLIM, France; ³Univ. of Neuchatel, Switzerland. We present sub-100-fs external pulse compression and noise characterization from ultrafast multi-100-W thin disk lasers using gas-filled-Kagome-type HC-PCFs. We demonstrate high compression efficiency and excellent phase and amplitude low-noise properties.

STu1N.8 • 09:45

Scaling Laws in Tube Lattice Fibers, Masruri Masruri², Annamaria Cucinotta², Luca Vincetti¹; ¹Dept. of Engineering "Enzo Ferrari", Univ. of Modena and Reggio Emilia, Italy; ²Dept. of Information Engineering, Univ. of Parma, Italy. Scaling laws of confinement loss and dielectric overlap in circularly arranged tube lattice fibers are numerically analyzed. Confinement loss scales as the 4.5 power of wavelength-core size ratio whereas dielectric overlap dependence is weaker.

**STu1O • Advanced Ultrafast
Sources—Continued****STu1O.6 • 09:30**

Multi-Terawatt CO₂ Laser with Chirped-Pulse Amplification, Mikhail N. Polyanskiy¹, Marcus Babzien¹, Igor Pogorelsky¹; ¹Brookhaven National Lab, USA. A chirped-pulse amplification technique is implemented for the first time in a picosecond CO₂ laser. A considerable increase in peak power is achieved, mainly as a result of eliminating nonlinear effects in the optical elements.

STu1O.7 • 09:45

Generation of 33-fs laser pulses from a Kerr-lens mode-locked Yb:CaYAlO₄ laser, Ziyi Gao¹, Jiangfeng Zhu¹, Junli Wang¹, Zhiyi Wei², Lihe Zheng³, Liangbi Su³, Jun Xu³; ¹Xidian Univ., China; ²Beijing National Lab for Condensed Matter Physics, Inst. of Physics, Chinese Academy of Sciences, China; ³Key Lab of Transparent and Opto-functional Inorganic Materials, Shanghai Inst. of Ceramics Chinese Academy of Sciences, China. We experimentally demonstrated a diode-pumped Kerr-lens mode-locked femtosecond laser based on a Yb:CaYAlO₄ crystal. Pulses with a duration as short as 33 fs at the center wavelength of 1059 nm were obtained.

09:00–12:00 SC352 • Introduction to Ultrafast Pulse Shaping—Principles and Applications
SC362 • Cavity Optomechanics: Fundamentals and Applications of Controlling and Measuring Nano- and Micro-mechanical Oscillators with Laser Light
SC410 • Finite Element Modelling Methods for Photonics and Optics

10:00–10:30 Coffee Break, Concourse Level

**Technical Digest and Postdeadline Papers
Available Online**

- Visit www.cleoconference.org
- Select Access Digest Paper link
- Use your registration email address and password

Access is provided only to full technical attendees.

CLEO: QELS-Fundamental Science

JOINT

10:30–12:30

FTu2A • Quantum Entanglement II

Presider: Todd Pittman; Univ. of Maryland Baltimore County, USA

FTu2A.1 • 10:30

Chip-to-chip quantum entanglement distribution, Jianwei Wang¹, Matteo Villa¹, Damien Bonneau¹, Raffaele Santagati¹, Joshua W. Silverstone¹, Chris Erven¹, Shigehito Miki², Taro Yamashita², Mikio Fujiwara², Masahide Sasaki², Hirotsuka Terai², Michael G. Tanner³, Robert H. Hadfield³, Jeremy O'Brien¹, Mark G. Thompson¹; ¹Centre for Quantum Photonics, H. H. Wills Physics Lab & Dept. of Electrical and Electronic Engineering, Univ. of Bristol, UK; ²National Inst. of Information and Communications Technology (NICT), Japan; ³School of Engineering, Univ. of Glasgow, UK. We present the first experimental demonstration of quantum entanglement distribution between silicon integrated photonic chips, linked by a single mode optical fiber. Entanglement states generation, transmission, manipulation and measurement are implemented intra/inter chips.

FTu2A.2 • 10:45

Realization of Sub-picosecond Clock Synchronization based on Second-Order Quantum Coherence, Runai Qian¹, Ruifang Dong¹, Yiwei Zhai¹, Mengmeng Wang¹, Shaofeng Wang¹, Feiyan Hou¹, Tao Liu¹, Shougang Zhang¹; ¹Key Lab of Time and Frequency Primary Standards, National Time Service Center, CAS, China. Based on the second-order quantum interference between entangled photons generated by parametric down conversion, we have demonstrated a proof-of-principle experiment of synchronizing two clocks separated by 4-km fiber link. A sub-picosecond accuracy is achieved.

FTu2A.3 • 11:00

Controlling frequency distinguishability of photons using cross phase modulation, Nobuyuki Matsuda¹; ¹NTT Basic Research Labs, Japan. The frequency distinguishability of photon pairs was controlled using spectral reshaping via cross phase modulation. A non-classical dip in a Hong-Ou-Mandel quantum interference experiment was observed for the photons with diminished spectral distinguishability.

10:30–12:15

FTu2B • Quantum Optics in Semiconductor Microcavities

Presider: Keshav Dani; Okinawa Inst of Science & Technology, Japan

FTu2B.1 • 10:30 **Tutorial**

Manipulating Quantum Fluids of Light in Microstructured Semiconductor Cavities, Jacqueline Bloch¹; ¹LPN, CNRS, France. Semiconductor microcavities provide a new platform for quantum fluids of light manipulation, quantum simulation, and non-linear optical device development. Recent experimental achievements will be discussed with particular emphasis on polaritonic circuits and polaritons in lattices.



Jacqueline Bloch is Director of Research at CNRS. The group she leads has pioneered several avenues in the exploration of polariton condensate physics. Bloch has authored 140 publications and given more than 85 invited talks and seminars. She is a member of the National Committee for Scientific Research (CoNRS).

10:30–12:15

FTu2C • Topological Photonics I

Presider: Marta Autore; Dip. di Fisica, Italy

FTu2C.1 • 10:30

Optical Access to Topological-Insulator Surface States with Plasmonic Rotating Fields, Grisha Spektor¹, Asaf David¹, Guy Bartal¹, Meir Orenstein¹, Alex Hayat¹; ¹Technion, Israel Inst. of Technology, Israel. We implemented a square plasmonic cavity supporting an array of counter rotating field elements. The controlled, highly confined angular momenta array is a means for coupling to the spin helical surface states of topological insulators.

FTu2C.2 • 10:45

Reflections-Free Wave Propagation at the Interface of Photonic Topological Insulators: Theory and Experiment, Tzuhsuan Ma¹, Kueifu Lai¹, Gennady Shvets¹; ¹Physics, Univ. of Texas at Austin, USA. A comprehensive library of photonic topological insulators (gyromagnetic, bianisotropic, and 2D-asymmetric) is established. An interface between any two of them supports reflectionless surface waves, as is experimental demonstrated for wave propagation along a zigzag interface.

FTu2C.3 • 11:00

Large Chern number one-way waveguides, Scott Skirlo¹, Yuichi Igarashi¹, Ling Lu¹, Marin Soljacic¹; ¹MIT, USA. We predict quantum anomalous Hall phases in photonic crystals with large Chern numbers of 2, 3 and 4, and demonstrate their applications. Finally, we present experimental evidence for multimode unidirectional waveguides at microwave frequencies.

10:30–12:30

JTU2D • Symposium on Advanced Optical Microscopy for Brain Imaging II

Presider: Chris Xu; Cornell Univ., USA

JTU2D.1 • 10:30 **Invited**

Adaptive Optics to Study the Structure and Function of the Human Visual System, Austin J. Roorda¹; ¹Univ. of California Berkeley, USA. Adaptive optics (AO) corrects the blur caused by the eye's optical imperfections, enabling optical access to single human retinal cells. An AO scanning laser ophthalmoscope is described for cellular level retinal imaging and vision testing.

JTU2D.2 • 11:00 **Invited**

Wave Front Shaping and Optogenetics, Valentina Emiliani¹; ¹Neurophotonic Laboratory, CNRS and Univ. Paris Descartes, France. A series of optical methods (temporal focusing, computer generated holography and generalized phase contrast) for patterned optogenetic with cellular resolution will be presented with exemplary experiments in vitro and in vivo.

**CLEO: QELS-
Fundamental Science**

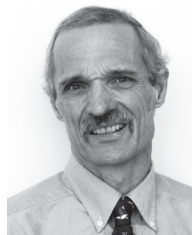
10:30–12:30

**Ftu2E • Plasmonic
Nanoantennas and Nanocavities**
*Presider: Rashid Zia; Brown Univ.,
USA***Ftu2E.1 • 10:30****Filter Design Method for Construction of
3D Plasmonic Directional Light Sensors**,
Matthew Davis^{1,2}, Jay K. Lee¹, Amit Agrawal²,
Henri J. Lezec²; ¹Electrical Engineering and
Computer Science, Syracuse Univ., USA;
²Center for Nanoscale Science and Technol-
ogy, National Inst. of Standards and Technol-
ogy, USA. We propose an analytic method for
plasmonic filter design, freeing the design
process from time-consuming FDTD
simulations. We demonstrate the utility of the
design model by constructing a prototype 3D
plasmonic directional light sensor.**Ftu2E.2 • 10:45****Hybrid Metal-Dielectric Nanoantennas for
Directional Emission Enhancement**, Evgenia
Rusak¹, Rui Guo¹, Isabelle Staudé¹, Manuel
Decker¹, Juergen Sautter¹, Andrey Mirosh-
nichenko¹, David A. Powell¹, Dragomir N.
Neshev¹, Yuri S. Kivshar¹; ¹Australian National
Univ., Australia. We suggest a novel hybrid
nanoantenna, consisting of a gold nanorod
and a silicon nanodisk, which provides giant
enhancement of directional emission
together with high radiation efficiency. We
demonstrate its fabrication by two-step
electron-beam lithography.**Ftu2E.3 • 11:00****Slanted 3D Plasmonic Antenna Arrays**,
Pierfrancesco Zilio¹, Mario Malerba¹, Andrea
Toma¹, Francesco De Angelis¹; ¹Istituto
Italiano di Tecnologia, Italy. We report ex-
perimental and Finite Elements simulation
results of slanted silver nanoantenna dimers
arrays on silver baseplate. Strong field
enhancements and diffractive couplings are
correlated to the peculiar near-field prop-
erties of these structures.**CLEO: Science & Innovations**

10:30–12:30

**Stu2F • Optical Interconnect
on Chip**
*Presider: Weidong Zhou; Univ. of
Texas at Arlington, USA***Stu2F.1 • 10:30****Hybrid 3D Photonic Integrated Circuit for
Optical Phased Array Beam Steering**, Bin-
bin Guan¹, Chuan Qin¹, Ryan P. Scott¹, Burcu
Ercan¹, Nicolas K. Fontaine², Tiehui Su¹, S.J.B.
Yoo¹; ¹Dept. of Electrical and Computer Engi-
neering, Univ. of California, Davis, USA; ²Bell
Labs, Alcatel-Lucent, USA. We demonstrate a
hybrid integrated optical phased array (OPA)
based on a 2D photonic integrated circuit
and 3D waveguides. The 4×4 OPA supports
4.93° horizontal and vertical beam steering
near 1550 nm with 7.1-dB loss.**Stu2F.2 • 10:45****Multi-Chip Integration of Lasers and Sili-
con Photonics by Photonic Wire Bonding**,
Muhammad Rodlin Billah¹, Tobias Hoose¹,
Temitiope Onanuga¹, Nicole Lindenmann¹,
Philipp Dietrich¹, Tobias Wingert¹, Maria
Laura Goedecke¹, Andreas Hofmann¹, Ute
Troppenz², Ariane Sigmund², Martin Möhrle²,
Wolfgang Freude³, Christian Koos¹; ¹Karl-
lsruhe Inst. of Technology, Germany; ²Heinrich
Hertz Inst., Fraunhofer Institut für Telecom-
munications, Germany; ³Inst. of Photonics
and Quantum Electronics, Karlsruhe Inst. of
Technology, Germany. We demonstrate cou-
pling of a horizontal-cavity surface-emitting
laser (HCSEL) to a silicon photonic chip using
photonic wire bonding. The technique does
not require high-precision alignment of the
chips. Measured coupling losses amount to
approximately 4.1 dB.**Stu2F.3 • 11:00** **Invited****High-Speed and Stable Operation of Highly
Unidirectional III-V/Silicon Microring Lasers
for On-chip Optical Interconnects**, Kazuya
Ohira¹, Hirotaka Uemira¹, Norio Iizuka¹, Ha-
rühiko Yoshida¹, Hiroshi Uemura¹, Yoichiro
Kurita¹, Hideto Furuyama¹, Mizunori Ezaki¹;
¹Photonics Electronics Technology Research
Association, Japan. We demonstrated high-
speed, stable and unidirectional microring
III-V laser diodes with in-cavity feedback
silicon waveguide, and the integration with
III-V photodetector on a silicon-on-insulator
platform to achieve on-chip data transmission
with a data rate of 12.5 Gb/s.

10:30–12:30

Stu2G • Cascade Lasers II
*Presider: Raffaele Colombelli;
Universite Paris Sud and CNRS,
France***Stu2G.1 • 10:30** **Tutorial****High-Brightness Interband Cascade Lasers**,
Jerry R. Meyer¹, Chadwick L. Canedy¹, Chul
S. Kim¹, Mijin Kim², William W. Bewley¹,
Charles Merritt¹, Igor Vurgatman¹; ¹US Naval
Research Lab, USA; ²Sotera Defense Solu-
tions, Inc., USA. Mid-IR interband cascade
lasers will be reviewed. Advantages include
3-6 mm spectral coverage, wallplug efficiency
up to 18% when operated in cw mode at
ambient temperature, and ultra-low threshold
drive power.

Jerry R. Meyer completed his Ph.D. in Phys-
ics at Brown Univ. in 1977. Since then he has
carried out basic and applied research at the
Naval Research Laboratory in Washington
DC, where he is the Navy Senior Scientist
for Quantum Electronics (ST) and Acting
Head of the Quantum Optoelectronics Sec-
tion. He is a Fellow of OSA, APS, IEEE, IOP,
SPIE. In 2012, he was recipient of NRL's 2012
E. O. Hulbert Annual Science Award, and
co-recipient of the IEEE Photonics Society
Engineering Achievement Award. He has co-
authored over 360 refereed journal articles,
30 patents (7 licensed), and over 150 invited
conference presentations.

10:30–12:15

**Stu2H • THz Spectroscopy
of Graphene and Magnetic
Materials**
*Presider: Dmitry Turchinovich;
Max Planck Inst. for Polymer
Research, Germany***Stu2H.1 • 10:30** **Invited****Terahertz Nonlinear Magnetic Response in
Antiferromagnets**, Koichiro Tanaka^{1,2}, Y
Mukai^{1,3}, H Hirori^{2,3}, T Yamamoto⁴, H Kageya-
ma^{2,4}; ¹Dept. of Physics, Kyoto Univ., Japan;
²Inst. for Integrated Cell-Material Sciences
(WPI-iCeMS), Kyoto Univ., Japan; ³CREST,
Japan Science and Technology Agency,
Japan; ⁴Dept. of Energy and Hydrocarbon
Chemistry, Kyoto Univ., Japan. We report on
the nonlinear magnetization dynamics of a
HoFeO₃ crystal induced by a strong terahertz
magnetic field resonantly enhanced with a
split ring resonator. The terahertz magnetic
field induces a large magnetization change of
40% of the spontaneous magnetization. The
frequency of the antiferromagnetic resonance
decreases in proportion to the square of the
magnetization change.**Stu2H.2 • 11:00****Nonlinear THz Transmission of Gated
Graphene**, Sayyed Hadi Razavipour¹, Wayne
Yang¹, Francois Blanchard¹, Abdeladim Guer-
moune¹, Michael Hilke¹, David G. Cooke¹;
¹McGill, Canada. THz field-induced transpar-
ency has been measured and characterized
for gel-gated multilayer graphene. It is shown
that upon changing the Fermi level by ionic
electrostatic gating, the transmission bleach-
ing decreases as the Fermi level approaches
the Dirac point.

Meeting Room
211 B/D

CLEO: Science & Innovations

10:30–12:30
STu2I • Nonlinear Optics in Microresonators and Nanostructures
President: Paulina Kuo; NIST, USA

STu2I.1 • 10:30 **Invited**
Nonlinear and Quantum Optics with Whispering Gallery Resonators, Dmitry V. Strekalov¹; ¹Jet Propulsion Lab, USA. Whispering Gallery Mode resonators made from optically nonlinear crystals have small mode volume and extremely high quality factor which makes them ideal for various nonlinear conversion process at low power, ultimately at single photon level.

STu2I.2 • 11:00
Surface-normal Coupled Four-wave Mixing in a High Contrast Grating Resonator, Tianbo Sun¹, Connie J. Chang-Hansnain¹; ¹EECS, Univ. of California, Berkeley, USA. We demonstrate four-wave mixing using a Si-based high contrast gratings (HCG) resonator directly coupled in surface-normal direction. Quality-factor of the resonator is ~7000 and peak conversion efficiency is -19.5dB at low pump power levels.

Meeting Room
212 A/C

CLEO: Applications & Technology

10:30–12:30
ATu2J • Solar Optics and Cells
President: Homan Yuen; Solar Junction, USA

ATu2J.1 • 10:30 **Invited**
Self-Tracking Concentrator for Photovoltaics, Peter Kozodoy¹, Christopher Gladden¹, Michael Pavilonis¹, Christopher Rhodes¹, Tobias Wheeler¹, Chadwick Casper¹; ¹Glint Photonics, Inc., USA. We present a novel solar concentrator architecture in which integrated microscale liquid optics provide passive solar tracking, eliminating the need for high-precision mechanical tracking. Optical efficiency as high as 72% and effective acceptance angle of 50° are demonstrated. The design can reduce the cost of concentrator photovoltaics and broaden its applicability.

ATu2J.2 • 11:00
Microphotonic spectrum-splitting & concentration for high-efficiency photovoltaic, Nabil Mohammed¹, Peng Wang¹, Daniel Friedman², Kannan Ramanathan², Lorelle Mansfield², Rajesh Menon¹; ¹Univ. of Utah, USA; ²NREL, USA. We present a diffractive microphotonic element that can split solar spectrum into 2 or more spectral bands, and concentrate these bands onto optimal absorbers. We experimentally demonstrated an increase in output power of 35% with a 3-band configuration.

Meeting Room
212 B/D

CLEO: Science & Innovations

10:30–12:30
STu2K • Computational Bioimaging
President: Kevin Tsia; Univ. of Hong Kong, Hong Kong

STu2K.1 • 10:30
Low-Light Reflective Correlation Imaging, Milad Akhlaghi Bouzan¹, Thomas Kohlgraf-Owens¹, Aristide Dogariu¹; ¹CREOL, College of Optics and Photonics, Univ. of Central Florida, USA. Numerical and experimental evaluation of a reflective microscopy technique based on sequential random pattern illumination and integrated detection is conducted to demonstrate imaging at the low-light levels of interest for live-cell imaging.

STu2K.2 • 10:45
Differential Interference Imaging via Radio-frequency Sideband Encoding, Ali M. Fard^{1,2}, Ata Mahjoubfar², Bahram Jalali²; ¹Harvard Medical School, USA; ²Univ. of California Los Angeles, USA. We introduce and demonstrate an imaging modality that performs differential interference imaging via frequency-to-space mapping and radio-frequency (RF) heterodyne detection.

STu2K.3 • 11:00
High-resolution On-chip Imaging using Synthetic Aperture, Wei Luo¹, Alon Greenbaum¹, Yibo Zhang¹, Aydogan Ozcan¹; ¹Univ. of California Los Angeles, USA. We report a synthetic-aperture-based on-chip lensfree microscope. Having a wide field-of-view of ~20.5 mm², this technique sets the largest numerical aperture (1.4) for on-chip microscopy.

Marriott
Salon I & II

10:30–12:30
STu2L • Symposium on Breaking Limits with Unconventional Optical Fields II
President: Uriel Levy; The Hebrew Univ. of Jerusalem, Israel

STu2L.1 • 10:30 **Invited**
Relativistic Few-cycle Cylindrical Vector Beams for Novel Table-top Particle Accelerators, Sergio Carbajo^{1,2}, Emilio A. Nanni¹, Liang Jie Wong¹, R.J. Dwayne Miller^{2,3}, Franz X. Kaertner^{1,2}; ¹MIT, USA; ²Center for Free Electron Laser Science, Germany; ³Univ. of Toronto, Canada. Few-cycle highly-intense radially polarized lasers unfold a novel compact accelerator uniquely capable of direct laser-to-particle energy transfer. We present the technology that proves this concept yielding highly-directional multi-GeV/m non-relativistic electron accelerating gradients.

STu2L.2 • 11:00
Topological Nature of Optical Bound States in the Continuum and its Application in Generating High-order Vector beams, Bo Zhen¹, Chia Wei Hsu¹, Ling Lu¹, A. Doug Stone², Marin Soljacic¹; ¹MIT, USA; ²Yale Univ., USA. We demonstrate all robust bound states in the continuum in photonic crystal slabs are vortex centers in the polarization directions of far-field radiation. They are robust because they carry conserved and quantized topological charges under PT symmetry. They also generate high-order vector beams.



Join the conversation. Use #CLEO15.
Follow us @cleoconf on Twitter.

Marriott
Salon III

CLEO: Applications
& Technology

10:30–12:30
ATu2M • Process Controls,
Monitoring & Novel Sources
Presider: Oliver Heckl; Univ. of
Colorado at Boulder JILA, USA

ATu2M.1 • 10:30 **Invited**
MIR Spectroscopy beyond Trace Levels -
Environmental and Industrial Applications,
Lukas Emmenegger¹; ¹EMPA, Switzerland.
MIR spectroscopy using QCL allows sensitive,
selective and fast gas detection. This is illus-
trated by many environmental and industrial
applications. Recent developments show
significant advances towards portable, high-
sensitivity sensors for multiple components.

ATu2M.2 • 11:00
Application of a widely tunable Sampled
Grating Distributed Bragg Quantum
Cascade laser for multi-species spectroscopy,
Abdou Diba¹, Feng Xie², Barry Gross¹,
Chung-en Zah², Fred Moshary¹; ¹Electrical
Engineering, City College of New York, USA;
²Science and Technology, Corning Incorporate,
USA. We demonstrate the feasibility of
multicomponent trace gas sensing using a
tunable sampled-grating distributed Bragg
reflector QCL. We have achieved continuous
fine tuning over 10 cm⁻¹ to retrieve N₂O,
H₂O and CO.

Marriott
Salon V & VI

CLEO: Science &
Innovations

10:30–12:30
STu2N • Control & Diagnostics
Presider: Heng Li; Stanford Univ.,
USA

STu2N.1 • 10:30
Optical differentiation wavefront sensor
based on binary pixelated transmission fil-
ters, Jie Qiao^{1,2}, Anton Travinsky¹, Christophe
Dorrier²; ¹Rochester Inst. of Technology, USA;
²Aktiwave LLC, USA. An optical differentiation
wavefront sensor based on measurements of
wavefront slopes in two orthogonal directions
obtained by far-field spatial modulation with
a binary pixelated filter inducing a linear
amplitude transmission is demonstrated.

STu2N.2 • 10:45
Design and performance of an integrated
phase and amplitude diversity sensor,
Nicolas Védrenne¹, Frédéric Cassaing¹,
Laurent M. Mugnier¹, Vincent Michau¹,
Gregory Iaquaniello³, Leonardo Blanco³,
Gilles Chériaux^{2,3}; ¹Theoretical and Applied
Optics Dept., Onera, The French Aerospace
Lab, France; ²Laboratoire pour l'Utilisation
des Lasers Intenses, Ecole Polytechnique,
France; ³Laboratoire d'Optique Appliquée,
LOA-UMR7639, France. The practical imple-
mentation of a phase diversity sensor for high
resolution measurement of disturbed laser
beams is detailed here. Numerical simula-
tions show that, with simple material, a 60x60
map of complex amplitude with lambda/100
accuracy can be obtained.

STu2N.3 • 11:00
High-Contrast, Closed-Loop Control of Laser
Beam Profiles, Leva E. McIntire^{1,3}, Martin
Divoky², Wayne H. Knox¹, Seung-Whan Bahk³,
Jonathan D. Zuegel³; ¹The Inst. of Optics,
Univ. of Rochester, USA; ²HILASE, Inst. of
Physics ASCR, Czech Republic; ³Lab for Laser
Energetics, Univ. of Rochester, USA. A 1053-
nm laser beam profile was controlled using
the diffractive mode of a spatial light modula-
tor in closed loop for the first time, producing
high-contrast spatial intensity shaping, as well
as independent wavefront control.

Visit CLEO:EXPO

Open, Tuesday at 14:30 in Exhibit Hall 1&2

- * See the Newest Industry Products from more than 200 Companies on the Exhibit Floor!
- * Tech Playground – Hands-On Innovation & Solutions

Check the Buyer's Guide for more information.

CLEO: QELS-Fundamental Science

JOINT

FTu2A • Quantum
Entanglement II—Continued

FTu2A.4 • 11:15

Bell State Free Dense Coding with Linear Optics, Pavel Lougovski¹, Dmitry B. Uskov²; ¹*Oak Ridge National Lab, USA*; ²*Dept. of Mathematics and Natural Sciences, Brescia Univ., USA*. We explore the possibility of implementing dense coding with linear optics and coincidence photodetection without Bell state discrimination. We discover that such implementations exist for two-photon in N-mode (N=4,6,8) scenarios and provide examples.

FTu2A.5 • 11:30

Experimental Reconstruction of Time-Bin-Entangled Qutrit States using Polarization Projective Measurements, Samantha Nowierski^{1,2}, Neal N. Oza², Prem Kumar², Gregory S. Kanter²; ¹*Applied Physics, Northwestern Univ., USA*; ²*Electrical Engineering and Computer Science, Northwestern Univ., USA*. We generate and reconstruct two-photon, 100-ps-separated time-bin-entangled qutrit states. By pairwise mapping time bins onto orthogonal polarizations, we perform a tomography and demonstrate high fidelity to maximally entangled qutrit states

FTu2A.6 • 11:45

Distributing Energy-Time Entangled Photon Pairs in Demultiplexed Channels over 110 km, Djeylan Aktas¹, Bruno Fedrici¹, Florian Kaiser¹, Laurent Labonté¹, Sebastien Tanzilli¹; ¹*Université de Nice Sophia Antipolis, Laboratoire de Physique de la Matière Condensée, CNRS UMR7336, France*. We propose a novel approach to quantum cryptography using the latest demultiplexing technology to distribute photonic entanglement over a fully fibred network. We achieve unprecedented bit-rates, beyond the state of the art for similar approaches.

FTu2B • Quantum Optics in
Semiconductor Microcavities—
Continued

FTu2B.2 • 11:30

Quantum Optics for Studying Ultrafast Processes in Condensed Matter, Martina Esposito¹, Francesco Randi¹, Francesca Giusti¹, Davide Boschetto², Fulvio Parmigiani^{1,3}, Daniele Fausti^{1,3}; ¹*Univ. of Trieste, Italy*; ²*ENSTA ParisTech, France*; ³*Elettra Sincrotrone Trieste S.C.p.A., Italy*. Quantum state reconstruction techniques are used to address non equilibrium matter states. Proof of principle experiments reveal that few photons coherent pulses can be squeezed by the interaction with impulsively excited coherent phonons in quartz.

FTu2B.3 • 11:45

A Spin-controlled Microcavity Laser, Feng-kuo Hsu¹, Wei Xie¹, Yi-Shan Lee², Sheng-Di Lin², Chih-Wei Lai¹; ¹*Michigan State Univ., USA*; ²*National Chiao Tung Univ., Taiwan*. We demonstrate highly circularly polarized lasing under non-resonant elliptically polarized optical pumping in a semiconductor microcavity at room temperature.

FTu2C • Topological
Photonics I—Continued

FTu2C.4 • 11:15

Topological Control of Bloch Oscillations of Edge Modes in Photonic Lattices, Yonatan Plotnik¹, Miguel A. Bandres¹, Yaakov Lumer¹, Mikael Rechtsman¹, Mordechai Segev¹; ¹*Technion Israel Inst. of Technology, Israel*. We demonstrate a novel method for controlling the modal trajectories of Bloch oscillations initiated on the edge of a honeycomb lattice, via the topology of its band structure.

FTu2C.5 • 11:30

Single-Sided Diffraction by PT-Symmetric Metasurfaces, Nicholas S. Nye¹, Mohammad-Ali Miri¹, Demetrios N. Christodoulides¹; ¹*Univ. of Central Florida, CREOL, USA*. We explore light diffraction by parity-time-symmetric metasurfaces. Such structures can lead to one-sided diffraction when operating close to their exceptional points. In this regime, the negative diffraction orders are eliminated while the positive are enhanced.

FTu2C.6 • 11:45

PT-symmetric cavities with simultaneous unidirectional lasing and reflectionless modes, Hamidreza Ramezani¹, Hao-kun Li¹, Yuan Wang¹, Xiang Zhang¹; ¹*Univ. of California Berkeley, USA*. Using parity-time (PT) symmetric cavities, we introduce a new family of spectral singularities with highly directional response. At these singularities the PT-symmetric cavity support a simultaneous lasing mode from one side and zero reflection mode from the opposite side.

JTu2D • Symposium on
Advanced Optical Microscopy
for Brain Imaging II—Continued

JTu2D.3 • 11:30

Invited

Rapid Adaptive Optical Recovery of Diffraction-Limited Resolution Over Large Multicellular Volumes, Eric Betzig¹; ¹*Howard Hughes Medical Inst., USA*. The heterogeneity of biological tissue essential to life induces aberrations that wreak havoc on image quality. I will describe our work with adaptive optical microscopy to recover optimal performance under such challenging conditions.



CLEO: QELS-
Fundamental ScienceFTu2E • Plasmonic
Nanoantennas and
Nanocavities—Continued

FTu2E.4 • 11:15

Parity-time symmetry breaking and amplifier-absorber transitions in plasmonic nanoparticles, Nasim Mohammadi Estakhri¹, Andrea Alu¹; ¹*Electrical and Computer Engineering, The Univ. of Texas at Austin, USA*. Abrupt transitions in the scattering response of parity-time (PT)-symmetric nanoparticles is discussed. Based on the closed-form analytical solution of a complex scattering problem, we show that material imbalance can generate strong absorbing or amplifying scattering states above PT threshold.

FTu2E.5 • 11:30

Coil-type Fano Resonances: a Plasmonic Approach to Magnetic Sub-diffraction Confinement, Simone Panaro¹, Adnan Nazir¹, Remo Proietti Zaccaria¹, Carlo Liberale¹, Francesco De Angelis¹, Andrea Toma¹; ¹*Italian Inst. of Technology, Italy*. Matrices of nanodisk trimers are introduced as plasmonic platforms for the generation of localized magnetic hot-spots. In Fano resonance condition, the optical magnetic fields can be squeezed in sub-wavelength regions, opening promising scenarios for spintronics.

FTu2E.6 • 11:45

Coupling Nano-Antennas to Microcavities: Radiative Interactions Cause Strong and Tunable Frequency Shifts, Freerk Ruesink¹, Hugo M. Doleman¹, Ruud Hendrikx¹, Femius Koenderink¹, Ewold Verhagen¹; ¹*FOM Inst. AMOLF, Netherlands*. We develop coupled cavity-antenna systems in which the frequency and linewidth of the eigenmodes can be strongly tuned. Interference of cavity and antenna radiation provides the dominating contribution to changes of dispersion and dissipation.

STu2F • Optical Interconnect on
Chip—Continued

STu2F.4 • 11:30

Heterogeneous Microring and Mach-Zehnder Lithium Niobate Electro-Optical Modulators on Silicon, Ashutosh Rao¹, Aniket Patil², Jeff Chiles¹, Marcin Malinowski¹, Spencer Novak^{1,3}, Kathleen Richardson^{1,3}, Payam Rabiei², Sasan Fathpour^{1,4}; ¹*CREOL, The College of Optics and Photonics, Univ. of Central Florida, USA*; ²*Partow Technologies LLC, USA*; ³*School of Materials Science and Engineering, COMSET, Clemson Univ., USA*; ⁴*Dept. of Electrical and Computer Engineering, Univ. of Central Florida, USA*. Heterogeneous integration of submicron films of lithium niobate on silicon substrates, rib-loaded with chalcogenide glass, is used to demonstrate lithium niobate microring modulators with Q of 1.2×10^5 and Mach-Zehnder modulators with V_{π} of 3.8 V/cm.

STu2F.5 • 11:45

Hybrid Silicon and Lithium Niobate Racetrack Modulator with Large Spurious Free Dynamic Range, Li Chen¹, Jiahong Chen¹, Jonathan T. Nagy¹, Ronald M. Reano¹; ¹*Ohio State Univ., USA*. We present a hybrid silicon and LiNbO₃ racetrack modulator with spurious free dynamic range of 98.1 dB Hz^{2/3} at 1 GHz, which is comparable to a packaged LiNbO₃ Mach-Zehnder modulator biased at quadrature.

STu2G • Cascade Lasers II—
Continued

STu2G.2 • 11:30

Double-Ridge Interband Cascade Lasers for High-Power Spectroscopy in the Mid-Infrared, Carl Borgentun¹, Siamak Forouhar¹, Clifford Frez¹, Ryan Briggs¹, Mahmood Bagheri¹, Mathieu Fradet¹; ¹*Jet propulsion Lab, USA*. Lasers employing a new double-ridge waveguide design emit 18 mW at 3.57 μ m and 20 mW at 3.37 μ m. The top ridge confines the optical mode while the bottom ridge limits lateral current spreading.

STu2G.3 • 11:45

Type-I Interband Cascade Lasers Near 3.2 μ m, James Gupta¹, Geof Aers¹, Emmanuel Dupont¹, Jean-Marc Baribeau¹, Xiaohua Wu¹, Yuchao Jiang², Lu Li², Rui Yang², Matthew Johnson³; ¹*National Research Council of Canada, Canada*; ²*School of Electrical and Computer Engineering, Univ. of Oklahoma, USA*; ³*Homer L. Dodge Dept. of Physics and Astronomy, Univ. of Oklahoma, USA*. Interband cascade lasers with type-I InGaAsSb/AlAsSb quantum well active regions were demonstrated. Ridge-waveguide devices exhibit room-temperature continuous-wave emission at 3.2 μ m, providing a potential alternative to quantum cascade and diode lasers in this wavelength range.

CLEO: Science & Innovations

STu2H • THz Spectroscopy
of Graphene and Magnetic
Materials—Continued

STu2H.3 • 11:15

Terahertz Emission in Double-Graphene-Layer Structure, Deepika Yadav¹, Boubanga T. Stephane¹, Takayuki Watanabe¹, Victor Ryzhii^{1,2}, Taiichi Otsuji¹; ¹*Research Inst. of Electrical Communication, Tohoku Univ., Japan*; ²*Inst. of Ultra-High-Frequency Semiconductor Electronics, Russia*. Terahertz emission by the photon-assisted resonant radiative transitions between graphene layers (GLs) in double-GL structures is theoretically and experimentally demonstrated. Devices such as terahertz/infrared lasers based on this technology are very promising for terahertz optoelectronics.

STu2H.4 • 11:30

Intense Terahertz Field-induced Carrier Dynamics in Gated Monolayer Graphene, Hassan Hafez Eid¹, P. Lévesque², Ibraheem Al-Naib³, Marc M. Dignam³, Xin Chai¹, D Ferachou¹, R Martel², Tsuneyuki Ozaki¹; ¹*INRS-EMT, Canada*; ²*Université de Montréal, Canada*; ³*Queen's Univ., Canada*. Using optical-pump/THz-probe spectroscopy on gated, undoped graphene, we find that as the amplitude of the THz probe is increased, we observe a cross-over from optically-induced transmission decrease to increase.

STu2H.5 • 11:45

Graphene on Nanoscale Gratings for Terahertz Smith-Purcell Radiation, Khwanchai Tantiwanichapan¹, Xuanye Wang¹, Anna Swan¹, Roberto Paiella¹; ¹*Electrical and Computer Engineering, Boston Univ., USA*. Generation of THz radiation based on the Smith-Purcell effect in graphene deposited on a periodic hole array is investigated numerically. Technologically significant output power levels at geometrically tunable THz frequencies are computed.

Meeting Room
211 B/D

CLEO: Science & Innovations

STu2I • Nonlinear Optics in Microresonators and Nanostructures—Continued

STu2I.3 • 11:15

Cascaded Four-Wave Mixing in Silicon-on-Sapphire Microresonators at $\lambda=4.5$ μm , Stefan Kalchmair¹, Raji Shankar², Shota Kita¹, Christopher Mittag¹, Irfan Bulu², Marko Loncar¹; ¹Harvard Univ., USA; ²Schlumberger-Doll Research Lab, USA. We report cascaded four-wave mixing in a silicon micro-ring resonator operating at 4.5 μm wavelength. Our results present an important milestone for extending optical frequency combs further into the mid-infrared range.

STu2I.4 • 11:30

Second Harmonic Generation In a GaN Photonic Crystal Cavity on Silicon, Philippe Boucaud¹, Yijia Zeng¹, Iannis Roland¹, Xavier Checoury¹, Zheng Han¹, Moustafa El Kurdi¹, Sébastien Sauvage¹, Bruno Gayral², Christelle Brimont³, Thierry Guillet³, Meletios Mexis⁴, Fabrice Semond⁴; ¹IEF-CNRS-Univ Paris Sud, France; ²Univ. Grenoble Alpes, INAC-SP2M, CEA-CNRS, France; ³L2C-Université Montpellier 2, France; ⁴CRHEA-CNRS, France. We report on near-infrared second harmonic generation in a free-standing gallium nitride photonic crystal cavity fabricated on a silicon substrate. High-resolution spatial imaging allows us to correlate harmonic emission pattern and second-order polarization P_x .

STu2I.5 • 11:45

Resonant Wavelength Conversion in Gallium Phosphide Nanostructures, David Lake^{1,2}, Matthew Mitchell^{1,2}, Aaron Hryciw², Harishankar Jayakumar¹, Paul E. Barclay^{1,2}; ¹Physics, Univ. of Calgary, Canada; ²NRC-National Inst. for Nanotechnology, Canada. Second Harmonic Generation in gallium phosphide microdisks is demonstrated.

Meeting Room
212 A/C

CLEO: Applications & Technology

ATu2J • Solar Optics and Cells—Continued

ATu2J.3 • 11:15 **Invited**

High Concentration Solar Photovoltaic Systems using Glass Dish Collectors, Roger P. Angel^{2,1}; ¹Univ. of Arizona, USA; ²REhnu, Inc, USA. Glass solar reflectors, similar to those widely used to concentrate sunlight in solar thermal plants, form the basis for REhnu's HCPV generators. Multijunction cells are housed in small, upgradeable units at each mirror focus.

ATu2J.4 • 11:45

Microcavity-Integrated Colored Perovskite Solar Cells, Kyu-Tae Lee¹, Masanori Fukuda¹, Chengang Ji¹, L. Jay Guo¹; ¹EECS, Univ. of Michigan, USA. We demonstrate optical cavity-embedded perovskite solar cells capable of creating transmissive colors that can be easily tuned by altering the spacer layer thickness in the cavity and simultaneously generating ~4% of power conversion efficiency.

Meeting Room
212 B/D

CLEO: Science & Innovations

STu2K • Computational Bioimaging—Continued

STu2K.4 • 11:15

Compressive 39.6-gigapixel/s continuous imaging using spectrally-structured ultrafast laser pulses, Bryan T. Bosworth¹, Jasper Stroud¹, Dung Tran¹, Trac Tran¹, Sang Chin¹, Mark A. Foster¹; ¹Johns Hopkins Univ., USA. We demonstrate ultrahigh-speed spectral shaping of broadband laser pulses to create structured illumination of a high-speed flow for compressive microscopy. We achieve up to 39.6 gigapixel/s continuous imaging rates using a 720-MHz ADC sampling rate.

STu2K.5 • 11:30

Compressive Optical Imaging Using Wavelength Dependent Scattering, Jaewook Shin¹, Mark A. Foster¹; ¹Johns Hopkins Univ., USA. We demonstrate 2D compressive image reconstruction from wavelength-defined illumination patterns generated by wavelength-dependent scattering from a single-mode fiber with a TiO₂-tip.

STu2K.6 • 11:45

Field-Portable Nanoparticle and Virus Sizing Enabled by On-Chip Microscopy and Vapor-Condensed Nanolenses, Euan McLeod¹, T. U. Dincer¹, Muhammed Veli¹, Yavuz N. Ertas¹, Chau Nguyen¹, Wei Luo¹, Alon Greenbaum^{1,2}, Alborz Feizi¹, Aydogan Ozcan¹; ¹Univ. of California Los Angeles, USA; ²California Inst. of Technology, USA. Vapor-condensed nanolenses make label-free lensfree holographic microscopy sensitive to individual particles 40 nm and larger. Detected signals correlate with particle size with accuracy ± 11 nm. Automated image processing measures $>10^5$ particles within a single field-of-view.

Marriott
Salon I & II

STu2L • Symposium on Breaking Limits with Unconventional Optical Fields II—Continued

STu2L.3 • 11:15

Multiple Wavefront Shaping by a Single Gradient Metasurface, Nir Shitrit¹, Dekel Veksler¹, Elhanan Maguid¹, Dror Ozeri¹, Vladimir Kleiner¹, Erez Hasman¹; ¹Technion-Israel Inst. of Technology, Israel. We report on a generic concept to control multiple wavefronts by disordered gradient metasurfaces (DGMs) with a custom-tailored geometric phase. DGMs offer all-optical manipulation by multitask wavefront shaping via a single ultrathin photonic nanodevice.

STu2L.4 • 11:30 **Invited**

Cylindrical Vector Beams for Spectroscopic Imaging of Single Molecules and Nanoparticles and Localization with Nanometer Precision in Tunable Microresonators, Alfred J. Meixner¹; ¹Eberhard-Karls-Univ, Germany. Due to their unique polarization properties cylindrical vector beams are ideal for imaging and spectroscopy single nanoparticles or quantum systems in confocal optical microscopy with a high numerical aperture objective lens or a parabolic mirror.

Technical Digest and Postdeadline Papers Available Online

- Visit www.cleoconference.org
- Select Access Digest Paper link
- Use your registration email address and password

Access is provided only to full technical attendees.

Marriott
Salon III

CLEO: Applications
& Technology

ATu2M • Process Controls,
Monitoring & Novel Sources—
Continued

ATu2M.3 • 11:15

Direct Calorimetric Measurement of Powder Absorptivity, Alexander M. Rubenchik¹, Sheldon S. Wu¹, Mary M. LeBlanc¹, Scott C. Mitchell¹, Noel L. Peterson¹, Ilya V. Golosker¹; ¹Lawrence Livermore National Lab, USA. We present a method for direct calorimetric measurement of powder absorptivity using a thin laser illuminated disc. Powder porosity is measured independently and a scheme eliminating the effect of convective and radiative losses is implemented.

ATu2M.4 • 11:30

Withdrawn

ATu2M.5 • 11:45

Robust Non-Reciprocal Optical DC Phase Shift Measurement with Differential Modulation Phase Detection, Xun Gu¹, Sergio V. Marchese¹, Klaus Bohnert¹; ¹Corporate Research, ABB Switzerland Ltd, Switzerland. We propose and experimentally demonstrate a novel differential modulation phase detection scheme, which unleashes the powerful modulation phase detection technique for use in sensors with a bulk-optic sensing element, such as an electro-optic voltage sensor.

Marriott
Salon V & VI

CLEO: Science &
Innovations

STu2N • Control &
Diagnostics—Continued

STu2N.4 • 11:15

Adaptive Laser Beam Shaping with a Linearized Transport-of-Intensity Equation, Leonardo Blanco¹, Nicolas Védrenne², Vincent Michau², Laurent M. Mugnier², Gilles Cheriaux^{1,3}; ¹Laboratoire d'Optique Appliquée - ENSTA, France; ²DOTA, ONERA - The French Aerospace Lab, France; ³LULI, Ecole Polytechnique, France. We present a novel method to control the phase and amplitude of a femtosecond laser beam using a linearized version of the transport-of-intensity equation. Simulations show a peak power improvement better than 30%.

STu2N.5 • 11:30

High-throughput Lensfree Ion-Track Analysis for Laser-Driven Accelerators, Wei Luo¹, Faizan Shabbir¹, Chao Gong¹, Cagatay Gulec¹, Jeremy Pigeon¹, Jessica Shaw¹, Alon Greenbaum¹, Ting-wei Su¹, Ahmet F. Coskun¹, Sergei Tochitsky¹, Chandrashekhar Joshi¹, Aydogan Ozcan¹; ¹Univ. of California Los Angeles, USA. We report a lensfree imaging based high-throughput ion-track analysis platform for laser driven accelerators. This computational on-chip imaging platform, owing to its large field-of-view of 18cm², provides >20-fold improved imaging speed than lens-based analysis systems

STu2N.6 • 11:45

A Time-Multiplexed Pulse-Shaping System for Generating Multiple High-Bandwidth, Low-Jitter Optical Waveforms, Christophe Dorrer¹, Wade Bittle¹, Robert Cuffney¹, Elizabeth Hill¹, John Kelly¹, Tanya Kosci¹, Jonathan D. Zuegel¹; ¹Univ. of Rochester, USA. A time-multiplexed fiber-based system that can deliver eight low-jitter optical waveforms to eight distinct laser systems using a single Mach-Zehnder pulse-shaper driven by an arbitrary waveform generator and a low-loss, high-extinction demultiplexer is described.

CLEO: QELS-Fundamental Science

JOINT

FTu2A • Quantum
Entanglement II—Continued

FTu2A.7 • 12:00

Multi-photon Generation and Interference in an Interferometric Optical Fiber Gyroscope, Tianzhu Niu¹, Shuai Dong¹, Wei Zhang¹, Junjie Wu², Weijun Zhang², Lixing You², Yidong Huang¹, Zhen Wang²; ¹Tsinghua Univ., China; ²Shanghai Inst. of Microsystem and Information Technology, China. Two-photon and four-photon interference are realized in an interferometric fiber optical gyroscope, respectively. The visibility of four-photon interference fringe is 29.4% with a high coincidence count rate of 1000 per minute.

FTu2A.8 • 12:15

Experimental Tests of Nonlocality with Entangled Photons, Bradley Christensen¹, Nicolas Gisin², Nicolas Brunner^{3,4}, Yeong-Cherng Liang⁵, Paul Kwiat¹; ¹Univ. of Illinois, USA; ²Group of Applied Physics, Université de Genève, Switzerland; ³Département de Physique Théorique, Université de Genève, Switzerland; ⁴H. H. Wills Physics Lab, Univ. of Bristol, UK; ⁵Inst. for Theoretical Physics, ETH Zurich, Switzerland. We report on a variety of Bell tests performed with a high-quality photonic entanglement source. These tests begin to quantify nonlocal resources available in quantum mechanics, as well as place bounds on beyond-quantum theories.

FTu2B • Quantum Optics in
Semiconductor Microcavities—
Continued

FTu2B.4 • 12:00

Polariton Condensates in Complex Potential Landscapes, Christian Schneider¹, Karol Winkler¹, Anne Schade¹, Robert Dall², Matthias Amthor¹, Elena Ostrovskaya², Martin Kamp¹, Sven Hoeffling^{1,3}; ¹University of Würzburg, Germany; ²Australian National Univ., Australia; ³Univ. of St. Andrews, UK. We establish a technology which allows for deep and tunable polariton trapping. Pronounced band structures with full gaps and condensation at high symmetry points is observed in square lattice arrangements of evanescently coupled potential traps.

FTu2B.5 • 12:15

Withdrawn

FTu2C • Topological
Photonics I—Continued

FTu2C.7 • 12:00

Parity-time (PT) symmetric topological interface states, Steffen Weimann², Mikael Rechtsman^{3,4}, Yonatan Plotnik³, Yaakov Lumer³, Konstantinos Makris^{5,1}, Mordechai Segev³, Alexander Szameit²; ¹Princeton Univ., USA; ²Inst. of Applied Physics, Abbe Center of Photonics, Friedrich-Schiller-Universität Jena, Germany; ³Physics Dept. and Solid State Inst., Technion-Israel Inst. of Technology, Israel; ⁴Physics Dept., The Pennsylvania State Univ., USA; ⁵Inst. for Theoretical Physics, Vienna Univ. of Technology, Austria. We demonstrate theoretically and experimentally topological interface states in a passive effective PT-symmetric dimerized waveguide array. The PT-symmetric system has unbroken PT symmetry: all eigenvalues in the spectrum are real, despite the system's non-Hermiticity.

JTu2D • Symposium on
Advanced Optical Microscopy
for Brain Imaging II—Continued

JTu2D.4 • 12:00

Invited Ultrafast Fluorescent Probes for Brain Activity Imaging, Michael Lin¹; ¹Depts. of Pediatrics and Bioengineering, Stanford Univ., USA. Methods for visualizing electrical activity in neurons would be useful for understanding circuit function. We describe the ASAP family of voltage indicators featuring cofactor independence, bright fluorescence, large responses, efficient membrane localization, and fast kinetics.

12:30–13:30 Lunch (on your own)

13:30–14:30 JTu3A • Plenary Session II, Grand Ballroom

14:30–20:00 Exhibition Open, Exhibit Halls 1 & 2

14:30–16:00 Coffee Break (14:30–15:00) and Unopposed Exhibit Only Time, Exhibit Hall

15:00–17:00 Market Focus: Spectroscopy and Gas Sensing, Exhibit Hall Theater

CLEO: QELS-
Fundamental ScienceFTu2E • Plasmonic
Nanoantennas and
Nanocavities—Continued

FTu2E.7 • 12:00

Localized Surface Phonon Polariton Resonators in GaN, Kaijun Feng¹, William Streier², S.M. Islam¹, Jai Verma¹, Debdeep Jena¹, Dan Wasserman², Anthony Hoffman¹; ¹Univ. of Notre Dame, USA; ²Univ. of Illinois Urbana Champaign, USA. GaN micro-disk resonator arrays were fabricated and measured within the Restrahlen band of GaN. Far-IR spectroscopy shows evidence for localized surface phonon polariton resonances, results which are confirmed by finite-element models of the fabricated structures.

FTu2E.8 • 12:15

Plasmonic whispering-gallery modes in a semiconductor-insulator-metal hybrid structure, Chien-Ju Lee¹, Han Yeh¹, Yen-Chun Chen², Chun-Yuan Wang², Shangir Gwo², Jer-Shing Huang³, Wen-Hao Chang¹; ¹Dept. of Electrophysics, National Chiao Tung Univ., Taiwan; ²Dept. of Physics, National Tsing Hua Univ., Taiwan; ³Dept. of Chemistry, National Tsing Hua Univ., Taiwan. We demonstrate a plasmonic cavity based on a hybrid semiconductor-insulator-metal structure, which can support plasmonic whispering-gallery modes (WGMs). By optimizing the insulator gap thickness, coupled modes consisting of photonic and plasmonic WGM with efficient cavity feedback can be formed.

CLEO: Science & Innovations

STu2F • Optical Interconnect on
Chip—Continued

STu2F.6 • 12:00

Si₃N₄ Multilayer Platform for Photonic Integrated Circuits, Kuanping Shang¹, Shish-nath Pathak¹, Binbin Guan¹, Guangyao Liu¹, Chuan Qin¹, Ryan P. Scott¹, S.J.B. Yoo¹; ¹Univ. of California, Davis, USA. We design, fabricate, and demonstrate an optimized silicon nitride multilayer platform including ultra-low interlayer vertical coupling loss of 0.05 dB, multilayer crossing loss of 0.265 dB at 90° crossing angle, and 50 μm bending radius.

STu2F.7 • 12:15

Crystalline Silicon on Silicon Nitride Hybrid Platform for Integrated Photonic Applications, Amir Hossein Hosseinnia¹, Amir H. Atabaki¹, Qing Li¹, Hesam Moradinejad¹, Majid Sodagar¹, Farshid Ghasemi¹, Ali Eftekhari¹, Ali Adibi¹; ¹Georgia Inst. of Technology, USA. We demonstrate a hybrid material platform, in which a layer of crystalline silicon is placed on top of a silicon nitride on a silicon dioxide die. We also report an efficient interlayer coupling structure with 0.02 dB insertion loss. Using this hybrid platform, high-Q resonators are demonstrated.

STu2G • Cascade Lasers II—
Continued

STu2G.4 • 12:00

Ultra-Broadband (3.3-12.5 μm) Single Stack Quantum Cascade Gain Medium, Loan Le¹, Xiaojun Wang², Jen-Yu Fan², Mariano Troccoli², Deborah L. Sivco¹, Claire F. Gmachl¹; ¹Princeton Univ., USA; ²AdTech Optics Inc., USA. Electroluminescence spanning 3.3 μm to 12.5 μm and with a full width half maximum of 4 μm is achieved using a single stack quantum cascade gain medium. The free-running laser emits from 7.4 μm to 12.1 μm.

STu2G.5 • 12:15

High Power Spiral Cavity Quantum Cascade Superluminescent Emitter, Mei Chai Zheng¹, Nyan L. Aung¹, Abanti Basak¹, Peter Q. Liu², Xiaojun Wang³, Jen-Yu Fan³, Mariano Troccoli³, Claire F. Gmachl¹; ¹Princeton Univ., USA; ²Inst. of Quantum Electronics, ETH Zürich, Switzerland; ³AdTech Optics Inc., USA. Quantum cascade devices have been shaped into compact, yet long spiral cavities to increase mid-infrared superluminescence power. A peak power of ~57 mW at 250 K is obtained with a coherence length of ~107 μm.

STu2H • THz Spectroscopy
of Graphene and Magnetic
Materials—Continued

STu2H.6 • 12:00

Polarization-Dependent Terahertz Spectroscopy of Macroscopically Aligned Carbon Nanotubes, Weilu Gao¹, Ahmed Zubair¹, John Robinson¹, Xiaowei He¹, Colin C. Young², Dmitri Tsentelovich², Noe Alvarez², Robert Hauge⁴, Matteo Pasquali^{2,4}, Junichiro Kono^{1,5}; ¹Dept. of Electrical and Computer Engineering, Rice Univ., USA; ²Dept. of Chemical and Biomolecular Engineering, Rice Univ., USA; ³Dept. of Mechanical, Industrial and Nuclear Engineering, Univ. of Cincinnati, USA; ⁴Dept. of Chemistry, Rice Univ., USA; ⁵Dept. of Physics and Astronomy, Rice Univ., USA. We have examined the anisotropic terahertz response of highly aligned single-wall, double-wall, and multiwall carbon nanotubes and quantitatively characterized their performance as low-cost terahertz polarizers.

12:30–13:30 Lunch (on your own)

13:30–14:30 JTU3A • Plenary Session II, Grand Ballroom

14:30–20:00 Exhibition Open, Exhibit Halls 1 & 2

14:30–16:00 Coffee Break (14:30–15:00) and Unopposed Exhibit Only Time, Exhibit Hall

15:00–17:00 Market Focus: Spectroscopy and Gas Sensing, Exhibit Hall Theater

Meeting Room
211 B/D

CLEO: Science & Innovations

STu2I • Nonlinear Optics in Microresonators and Nanostructures—Continued

STu2I.6 • 12:00

Coherent Second Harmonic Generation in a Quantum Well-Metasurface Coupled System, omri wolf¹, Salvatore Campione¹, Alexander Benz¹, Arvind P. Ravikumar², Sheng Liu¹, Emil A. Kadlec¹, Eric Shaner¹, John F. Klem¹, Michael B. Sinclair¹, Igal Brener¹; ¹Sandia National Lab, USA; ²Princeton Univ., USA. Strongly coupling metallic nanoresonators with specially designed intersubband-transitions in quantum-wells results in efficient, saturation-limited second-harmonic (SH) generation. This method also grants full control over the polarization and phase-front of the emitted SH radiation.

STu2I.7 • 12:15

Low-Power Parametric Wavelength Conversion in 45nm Microelectronics CMOS Silicon-On-Insulator Technology, Cale M. Gentry¹, Mark T. Wade¹, Xiaoge Zeng¹, Fabio Pavanello¹, Milos Popovic¹; ¹Univ. of Colorado at Boulder, USA. We demonstrate seeded four-wave mixing in a photonic circuit fabricated within an unmodified commercial microelectronics CMOS SOI platform, using a minimally dispersive microcavity design.

Meeting Room
212 A/C

CLEO: Applications & Technology

ATu2J • Solar Optics and Cells—Continued

ATu2J.5 • 12:00 **Invited**

Wide-angle Nonimaging Optics for Concentration and Illumination; Principles and Applications, Roland Winston¹; ¹Univ. of California Merced, USA. Nonimaging designs allow non-tracking wide angle solar concentrators to attain high temperature operation. Of special interest to the optics community is the deep connection between the "Hottel strings" and the flow-line algorithm of nonimaging optics design.

Meeting Room
212 B/D

CLEO: Science & Innovations

STu2K • Computational Bioimaging—Continued

STu2K.7 • 12:00

A cannula-based computational fluorescence microscope for neuronal imaging, Ganghun Kim¹, Naveen Nagarajan¹, Amihai Meiri¹, Sean Merrill¹, Mario Capecchi¹, Erik Jorgensen¹, Rajesh Menon¹; ¹Univ. of Utah, USA. We applied nonlinear optimization to convert a cannula into a high-resolution computational-fluorescence microscope. The microscope was used to image fluorescent microspheres, genetically-encoded mouse-brain slices, genetically-encoded and fluorescent-stained *C. elegans* nematodes.

STu2K.8 • 12:15

Adaptive Optics in Three-Photon Fluorescence Microscopy, David Sinefeld¹, Hari P. Paudel², Dimitre G. Ouzounov¹, Thomas G. Bifano², Chris Xu¹; ¹Applied and engineering physics, Cornell Univ., USA; ²Photonics Center, Boston Univ., USA. We demonstrate three-photon fluorescence adaptive-optics system based on 1660-nm femtosecond pulses and MEMS spatial light modulator. We use the higher nonlinearity of the signal resulting in $\times 700$ improvement in fluorescence beads signal after aberrations correction.

Marriott
Salon I & II

STu2L • Symposium on Breaking Limits with Unconventional Optical Fields II—Continued

STu2L.5 • 12:00 **Invited**

Smaller Spot Formation by Vector Beam for Higher Resolution Microscopy, Shunichi Sato¹, Yuichi Kozawa¹; ¹Tohoku Univ., Japan. Smaller focal spot formation by using vector beams is demonstrated for achieving higher lateral resolution, which is beyond conventional diffraction limit, in confocal microscopy, two-photon microscopy and subtraction microscopy.

Tuesday, 12 May

12:30–13:30 Lunch (on your own)

13:30–14:30 JTu3A • Plenary Session II, Grand Ballroom

14:30–20:00 Exhibition Open, Exhibit Halls 1 & 2

14:30–16:00 Coffee Break (14:30–15:00) and Unopposed Exhibit Only Time, Exhibit Hall

15:00–17:00 Market Focus: Spectroscopy and Gas Sensing, Exhibit Hall Theater

Marriott
Salon III

CLEO: Applications
& Technology

ATu2M • Process Controls,
Monitoring & Novel Sources—
Continued

ATu2M.6 • 12:00

Demonstration of Soliton Self Shifting Employing Er³⁺ Doped VLMA- and HOM-Fiber Amplifiers, Armin Zach¹, Wilhelm Kaenders¹, Jeffrey W. Nicholson², John M. Fini², Anthony DeSantolo²; ¹TOPTICA Photonics AG, Germany; ²OFS Labs, USA. We demonstrate soliton self-frequency shifted Very-Large-Mode-Area and Higher-Order-Mode fiber amplifiers. The output wavelength is shifted more than 50 nm with a soliton pulse energy of up to 186 nJ. Subsequent, high-efficiency, frequency doubling is demonstrated.

ATu2M.7 • 12:15

Difference-frequency Generation of Spectrally Bright, ~1 W Average-power Mid-IR Radiation Using a ns-pulse Fiber Laser, Paul Belden¹, DaWun Chen¹, Fabio Di Teodoro¹; ¹The Aerospace Corporation, USA. We obtained average power/pulse energy of ~1W/5mJ at ~3520nm wavelength via difference-frequency generation in periodically poled lithium niobate using an all-fiber, few-ns pulsed laser source operating at 1064nm and a 10mW continuous-wave 1525 nm single-frequency diode laser.

Marriott
Salon V & VI

CLEO: Science & Innovations

STu2N • Control &
Diagnostics—Continued

STu2N.7 • 12:00

Sub-Femtosecond Free-Electron Laser Pulses, Wolfram Helml¹, Andreas R. Maier², Wolfgang Schweinberger³, Ivanka Grguras², Paul Radcliffe⁴, Gilles Doumy⁵, Chris Roedig⁶, Justin Gagnon³, Marc Messerschmidt⁷, Sebastian Schorb⁷, Christoph Bostedt⁷, Florian Grüner², Louis F. DiMauro⁶, Denis Cubaynes⁸, John D. Bozek⁷, Thomas Tschentscher⁴, John T. Costello⁹, Michael Meyer⁴, Ryan Coffee⁷, Stefan Düsterer¹⁰, Adrian L. Cavalieri², Reinhard Kienberger¹; ¹Physik-Dept., Technische Universität München, Germany; ²CFEL, Germany; ³Max-Planck-Institut für Quantenoptik, Germany; ⁴European XFEL, Germany; ⁵Argonne National Lab, USA; ⁶Ohio State Univ., USA; ⁷LCLS, USA; ⁸Institut des Sciences Moléculaires d'Orsay, France; ⁹School of Physical Sciences and National Center for Plasma Science and Technology, Ireland; ¹⁰DESY, Germany. Deploying the so-called 'Streaking Spectroscopy' technique at LCLS, we demonstrate a non-invasive scheme for temporal characterization of X-ray pulses with sub-femtosecond resolution. Analyzing the substructure indicates pulse durations on the order of hundreds of attoseconds.

STu2N.8 • 12:15

Remote two-color optical-to-optical synchronization between two passively mode-locked lasers, Heng Li^{1,2}, Li-Jin Chen³, Haynes Pak Hay Cheng³, Justin E. May², Steve Smith², Kerstin Muehlig², Akshaya Utamadoss^{2,4}, Josef C. Frisch², Alan Fry², Franz Kaernter^{5,6}, Philip H. Bucksbaum^{1,2}; ¹Stanford Univ., USA; ²SLAC National Accelerator Lab, USA; ³Idesta Quantum Electronics, LLC., USA; ⁴Dept. of Electrical Engineering, Princeton Univ., USA; ⁵Dept. of Electrical Engineering and Computer Science, and Research Lab of Electronics, MIT, USA; ⁶Center for Free-Electron Laser Science, and Physics Dept., DESY, and Univ. of Hamburg, Germany. We present remote two-color optical-to-optical synchronization between a Ti:sapphire and Er-doped fiber laser through 360 m single-mode fiber with 3.3 fs rms jitter over 24 hours.

12:30–13:30 Lunch (on your own)

13:30–14:30 JTu3A • Plenary Session II, Grand Ballroom

14:30–20:00 Exhibition Open, Exhibit Halls 1 & 2

14:30–16:00 Coffee Break (14:30–15:00) and
Unopposed Exhibit Only Time, Exhibit Hall

15:00–17:00 Market Focus: Spectroscopy and Gas Sensing,
Exhibit Hall Theater

CLEO: QELS-Fundamental Science

16:00–18:00

FTu4A • Fundamental Quantum Optics

Presider: William Munro; NTT Basic Research Labs, Japan

FTu4A.1 • 16:00

Direct measurement of the Wigner function by photon-number-resolving detection, Niranjana Sridhar¹, Reihaneh Shahrokhsahi¹, Aaron Miller², Thomas Gerrits³, Adriana Lita³, Sae Woo Nam³, Olivier Pfister¹; ¹Univ. of Virginia, USA; ²Albion College, USA; ³National Inst. of Standards and Technology, USA. We extended the seminal experiment of Banaszek et al. of quantum tomography by photon counting without Radon transform postprocessing to the more general case of photon fluxes with more than one photon per detection time.

FTu4A.2 • 16:15

Direct measurement of the quantum density matrix in the basis of azimuthal angle, Mohammad Mirhosseini¹, Omar S. Magaña-Loaiza¹, Seyed Mohammad Hashemi Rafsanjani¹, Changchen Chen¹, Ebrahim Karimi², Robert W. Boyd^{2,1}; ¹Inst. of Optics, Univ. of Rochester, USA; ²Dept. of Physics, Univ. of Ottawa, Canada. We theoretically propose and experimentally demonstrate a method for directly measuring the density matrix of an unknown quantum system in the basis of azimuthal angle. We apply our method for characterizing 7-dimensional pure and mixed superpositions of orbital-angular-momentum modes.

FTu4A.3 • 16:30

Quantum Process Estimation with Unknown Measurements, Brian J. Smith¹, Merlin Cooper¹, Michal Karpinski¹; ¹Univ. of Oxford, UK. Quantum process estimation without assumptions about measurements used is presented. The detector response is characterized with a finite set of probe states. Numerical simulations for quantum optical processes demonstrate the technique for complex systems.

16:00–18:00

FTu4B • Light-matter Interaction in Graphene/Other Carbon-based Materials

Presider: Keshav Dani; OIST, Japan

FTu4B.1 • 16:00

Ultrafast electron diffraction can visualize strong-field phenomena in graphene, Vladislav S. Yakovlev^{1,3}, Ferenc Krausz^{2,3}, Mark Stockman¹, Peter Baum^{2,3}; ¹Center for Nano-Optics (CeNO), Dept. of Physics and Astronomy, Georgia State Univ., USA; ²Fakultät für Physik, Ludwig-Maximilians-Universität München, Germany; ³Attosekundenphysik, Max-Planck-Institut für Quantenoptik, Germany. We show with simulations that ultrafast electron diffraction can provide snapshots of charge-density evolution in condensed matter with few-femtosecond and sub-atomic resolutions. Using graphene as an example, we discuss real-space aspects of light-matter interaction.

FTu4B.2 • 16:15

Ultrafast Pseudospin Dynamics in Graphene, Alexander Grupp¹, Maxim Trushin¹, Giancarlo Soavi^{1,2}, Arne Budweg¹, Domenico De Fazio³, Antonio Lombardo³, Andrea C. Ferrari³, Wolfgang Belzig¹, Alfred Leitenstorfer¹, Daniele Brida¹; ¹University of Konstanz, Germany; ²Dipartimento di Fisica, Politecnico di Milano, Italy; ³Cambridge Graphene Centre, Cambridge Univ., UK. We investigate pseudospin-selective ultrafast optical excitation in monolayer graphene. We track the evolution of anisotropy in momentum space as a function of excited carrier density. Results are well described by an analytical model.

FTu4B.3 • 16:30

Lateral Photo-Dember Effect in Graphene, Chang-Hua Liu¹, You-Chia Chang¹, Seung-hyun Lee¹, Yaozhong Zhang², Yafei Zhang², Theodore B. Norris¹, Zhaohui Zhong¹; ¹Univ. of Michigan, USA; ²Shanghai Jiao Tong Univ., China. The photocurrent at graphene/metal junctions under femtosecond laser excitation is found to have its polarity fully determined by asymmetry in the electron-hole mobility; this suggests the existence of unexpected lateral photo-Dember effect in graphene.

16:00–18:00

FTu4C • Topological Photonics II

Presider: Natalia Litchinitser; State Univ. of New York at Buffalo, USA

FTu4C.1 • 16:00

Optical Topological Transitions in Photonic Hypercrystals, Evgenii E. Narimanov¹; ¹Purdue Univ., USA. We demonstrate that Dirac dispersion cones in photonic hypercrystals originate from an optical topological transition. The resulting singularity in the photonic density of states has a strong effect on the emissivity of the hypercrystal.

FTu4C.2 • 16:15

Observing Light Dynamics in Micro-sized Schwarzschild Metric, Rivka Bekenstein¹, Yossef kabessa², Or Tal¹, Miguel A. Bandres¹, Aharon J. Agranat², Mordechai Segev¹; ¹Physics Dept. and Solid State Inst., Technion Israel Inst. of Technology, Israel; ²Dept. of Applied Physics and the Brojde Center for Innovative Engineering and Computer Science, Hebrew Univ. of Jerusalem, Israel. We study the dynamics of light in the Schwarzschild metric using a specifically fabricated micro-sized curved waveguide analogous to the black hole and the wormhole metrics, demonstrating complex dynamics and tunneling through the horizon.

FTu4C.3 • 16:30 **Invited**

Dirac Plasmons in Topological Insulators, Stefano Lupi¹; ¹INFN and Dip. di Fisica, Italy. Topological Insulators, characterized by 2D Dirac fermions on their surface, sustain Dirac plasmons. In this talk, I will discuss the terahertz response of these plasmons vs. a strong magnetic field, and their sub-ps dynamics.

16:00–18:00

FTu4D • Optical Filamentation and Compression

Presider: Steven Cundiff; Univ. of Colorado at Boulder JILA, USA

FTu4D.1 • 16:00

250-GW Sub-Three-Cycle Multi-Millijoule Mid-IR Pulses Self-Compressed in a YAG Plate, Valentina Shumakova¹, Pavel Mal'evich¹, Skirmantas Alisauskas¹, Aleksander Voronin³, Aleksei Zheltikov^{3,4}, Daniele Faccio⁵, Daniil Kartashov⁶, Raman Maksimenka⁷, Gregory Gitzinger⁷, Nicolas Forget⁷, Andrius Baltuska^{1,2}, Audrius Pugzlys^{1,2}; ¹Vienna Univ. of Technology, Austria; ²Center for Physical Sciences & Technology, Lithuania; ³Physics Dept., International Laser Center, M.V. Lomonosov Moscow State Univ., Russia; ⁴Dept. of Physics and Astronomy, Texas A&M Univ., USA; ⁵Inst. of Photonics and Quantum Sciences, Heriot-Watt Univ., UK; ⁶Friedrich-Schiller Univ. Jena, Germany; ⁷FASTLITE, France. Virtually lossless self-compression of 10-mJ 3.9- μ m sub-100 fs pulses in bulk YAG resulting in 9-mJ 33-fs pulses is reported. Generated peak power exceeds 250 GW which is suitable for filamentation in ambient air.

FTu4D.2 • 16:15

Mid-IR Filamentation in Dielectrics: 3-octave-spanning Supercontinuum Generation and Sub-2-cycle Self-compression, Hou Kun Liang¹, Peter R. Kroger¹, Ross Grynko², Ondrej Novak¹, Chun-Lin L. Chang¹, Gregory J. Stein¹, Darshana Weerawarne², Bonggu Shim², Franz Kaerntner^{1,3}, Kyung-Han Hong¹; ¹MIT, USA; ²Binghamton Univ., State Univ. of New York, USA; ³Univ. of Hamburg, Germany. We report on 3-octave supercontinuum generation from ZnS in the normal dispersion regime and self-compression of mid-IR pulses to sub-2-cycle in CaF₂ in the anomalous dispersion regime. Temporal characterization shows good agreement with 3D simulations.

FTu4D.3 • 16:30

White-light Generation Pumped by Sub-ps Pulse, Anne-Laure Calendron^{1,2}, Huseyin Cankaya^{1,2}, Giovanni Cirmi^{1,2}, Giulio M. Rossi^{1,2}, Franz Kaerntner^{1,3}; ¹Deutsches Elektronen Synchrotron, Germany; ²Universität Hamburg, The Hamburg Centre for Ultrafast Imaging, Germany; ³Dept. of Electrical Engineering and Computer Science, MIT-RLE, USA. The phase and stability characterization of white-light supercontinuum generated by sub-picosecond pulses at 1 μ m in YAG and sapphire for different pump focusing and duration shows compressible pulses, suitable for applications like waveform synthesis.

**CLEO: QELS-
Fundamental Science**

16:00–18:00

**FTu4E • Plasmonic Nanoantennas
for Sensing and Focusing***Presider: Arian Kriesch; University
of Erlangen, Germany*

FTu4E.1 • 16:00

Infrared Vibrational Molecular Hybridization with a Single Optical Antenna, Eric A. Muller¹, Benjamin Pollard¹, Hans Bechtel², Ronen Adato³, Hatice Altug⁴, Honghua Yang¹, Michael M. Martin², Markus B. Raschke¹; ¹Univ. of Colorado Boulder, USA; ²Advanced Light Source Division, Lawrence Berkeley National Lab, USA; ³Boston Univ., USA; ⁴Ecole Polytechnique Federale de Lausanne (EPFL), Switzerland. We observe impedance matched coupling between molecular vibrations and infrared optical antennas. Broadband synchrotron near-field spectroscopy reveals antenna-vibration hybridization, mode splitting, and tip excitation of coupled dark plasmon modes.

FTu4E.2 • 16:15

High-Brilliance Mid-Infrared Femtosecond Light Source for Surface-Enhanced Infrared Spectroscopy, Frank Neubrech¹, Tobias Steinfeld¹, Andy Steinmann¹, Xinghui Yin¹, Harald W. Giessen¹; ¹Univ. of Stuttgart, Germany. We combine surface-enhanced infrared absorption and a high brilliance optical parametric light source to enable ultra-sensitive and fast Fourier-transform infrared spectroscopy of only 10 000 molecules; inaccessible with conventional thermal light sources or synchrotron radiation.

FTu4E.3 • 16:30

Plasmonic Nanoantennas on Nanopedestals for Ultra-Sensitive Vibrational IR-Spectroscopy, Dordaneh Etezadi¹, Arif Cetin¹, Hatice Altug¹; ¹EPFL, Switzerland. We experimentally demonstrate that elevating polarization-insensitive nanoring antennas on nanopedestals enables high surface enhanced infrared absorption (SEIRA) signals. This is due to larger and accessible nearfields offering better overlap with biomolecules.

CLEO: Science & Innovations

16:00–18:00

**STu4F • Components and
Optical Interconnects***Presider: Leif Johansson;
Freedom Photonics, LLC, USA*

STu4F.1 • 16:00

A Comb Laser-Driven DWDM Silicon Photonic Transmitter with Microring Modulator for Optical Interconnect, Chin-Hui (Janet) Chen¹, Tsung-Ching Huang¹, Daniil Livshitz², Alexey Gubenko², Sergey Mikhlin², Vladimir Mikhlin², Marco Fiorentino¹, Raymond Beausoleil¹; ¹Hewlett Packard Company, USA; ²Innolume GmbH, Germany. A five-channel microring modulator-based DWDM silicon photonic transmitter driven by a quantum dot comb laser is demonstrated for the first time. 10Gbps eye diagrams are shown at both 25°C and 40°C.

STu4F.2 • 16:15

5 x 20 Gb/s III-V on Silicon Electroabsorption Modulator Array Heterogeneously Integrated with a 1.6nm Channel-Spacing Silicon AWG, Xin Fu^{1,2}, Qiangsheng Huang^{1,2}, Yingtao Hu², Martijn Tassaert², Jochem Verbist³, Jianxin Cheng⁴, Keqi Ma¹, Jianhao Zhang¹, Kaixuan Chen⁴, Chenzhao Zhang⁴, Yaocheng Shi¹, Johan Bauwelinck³, Gunther Roelkens², Sailing He^{1,4}; ¹Zhejiang Univ., China; ²Photonics Research Group, Belgium; ³INTEC_design, Belgium; ⁴South China Normal Univ., China. We demonstrate a five-channel wavelength division multiplexed modulator module that heterogeneously integrates a 1.6nm channel-spacing arrayed-waveguide grating and a 20Gbps electroabsorption modulator array, showing the potential for 100 Gbps capacity on a 1.5x0.5 mm² footprint.

STu4F.3 • 16:30 **Invited**

Demonstration of Error Free Operation Up To 32 Gb/s From a CMOS Integrated Monolithic Nano-Photonic Transmitter, Douglas M. Gill¹, Chi Xiong¹, Jonathan Proessel¹, Jessie Rosenberg¹, John Ellis-Monaghan², Jason Orcutt¹, Marwan Khater¹, Doris Viens³, Yuri A. Vlasov¹, Wilfried Haensch¹, William Green¹; ¹IBM T.J. Watson Research Center, USA; ²Systems & Technology Group, Microelectronics Division, IBM, USA; ³Systems & Technology Group, Microelectronics Division, IBM, Canada. We present a monolithic CMOS Integrated Nano Photonic transmitter with a link sensitivity comparable to a 25 Gb/s commercial reference transmitter, exhibiting a 5.2 dB extinction ratio, 4.9 dB insertion loss, and error free operation up to 32 Gb/s.

16:00–18:00

STu4G • Cascade Lasers III*Presider: Jerry Meyer; US Naval
Research Lab, USA*

STu4G.1 • 16:00

Sampled Grating Quantum Cascade Lasers with High Tuning Stability, Stefan Kalchmair¹, Romain Blanchard², Tobias Mansuripur¹, Guy-Mael de Naurois¹, Laurent Diehl², Christian Pflügl², Mark F. Witinski², Federico Capasso¹, Marko Loncar¹; ¹Harvard Univ., USA; ²Eos Photonics, Inc., USA. We report a sampled grating quantum cascade laser with excellent tuning stability over the full tuning range (106 cm⁻¹). Spatial hole burning and facet reflections can cause unpredictable mode jumping. We present a stabilization method.

STu4G.2 • 16:15

Surface emitting, single-mode quantum cascade laser array, Christopher Bonzon¹, Pierre Jouy¹, Johanna Wolf¹, Martin Suess¹, Mattias Beck¹, Jerome Faist¹; ¹ETHZ, Switzerland. We present the first realization of a single-mode surface-emitting quantum cascade laser array. The ten lasers operate over a bandwidth of 175 cm⁻¹ from 8-10 um and show similar pumping characteristics. The device is suitable for spectroscopic applications due to its continuous wave operation.

STu4G.3 • 16:30

Coherent Beam-Combining of Quantum Cascade Amplifier Arrays, Brian G. Saar¹, Kevin Creedon¹, Leo Missaggia¹, Christine A. Wang¹, Michael K. Connors¹, Joseph Donnelly¹, George W. Turner¹, Antonio Sanchez-Rubio¹, William Herzog¹; ¹MIT Lincoln Lab, USA. We present design, packaging and coherent beam combining of quantum cascade amplifier (QCA) arrays, measurements of QCA phase noise, the drive-current-to-optical-phase transfer function, and the small signal gain for QCAs

16:00–18:00

**STu4H • THz Spectroscopic
Techniques***Presider: Philip Taday; TeraView
Ltd, UK*

STu4H.1 • 16:00

Self-referenced Transient THz Spectroscopy with ABCD Detection, Francesco D'Angelo¹, Sapun Parekh¹, Mischa Bonn¹, Dmitry Turchinovich¹; ¹Max Planck Inst. f. Polymer Research, Germany. A new scheme for simultaneous acquisition of reference and sample THz signals in transient THz spectroscopy with ABCD detection is demonstrated, with demodulation at pump beam chopping and ABCD voltage switching frequencies.

STu4H.2 • 16:15

Electron Dynamics in a Gold Thin Film Accelerated via an Intense Terahertz Field, Yasuo Minami¹, Thang D. Dao², Tadaaki Nagao², Jun Takeda¹, Masahiro Kitajima³, Ikufumi Katayama¹; ¹Yokohama National Univ., Japan; ²National Inst. for Materials Science, Japan; ³LxRay Co. Ltd, Japan. Nonlinear electron dynamics in gold thin films was observed via intense terahertz spectroscopy. Under the intense terahertz wave illumination, the damping constant of electrons becomes smaller due to the suppression of the grain-boundary effect on electrons induced by the intense terahertz field.

STu4H.3 • 16:30

Time-resolved THz Laser spectra using a Fibre-interfaced Optical Heterodyne system, Thomas Folland¹, Antonio ramospellido¹, Owen Marshall¹, Harvey Beere², David Ritchie², Subhasish Chakraborty¹; ¹Univ. of Manchester, UK; ²Univ. of Cambridge, UK. We report the first fully fibre-interfaced heterodyne system for time-resolved spectral characterization of THz quantum cascade lasers. By exploiting the bias probe rise time we study the current dependant mode tuning with 50ns temporal resolution.

Meeting Room
211 B/D

CLEO: Science & Innovations

16:00–18:00
STu4I • Mid-IR Photonics
President: Bernhard Lendl;
Technische Universität Wien, USA

STu4I.1 • 16:00
Nano-Silicon-Photonic Fourier Transform Infrared (FTIR) Spectrometer-on-a-Chip, Bin Dong^{1,2}, Hong Cai², Yuandong Gu², Zhenchuan Yang³, Yufeng Jin³, Yilong Hao³, Dimlee Kwong², Ai-Qun LIU¹; ¹Nanyang Technological Univ., Singapore; ²Inst. of Microelectronics, Singapore; ³Peking Univ., China. This paper reports a nano-silicon-photonic Fourier transform infrared (FTIR) spectrometer-on-a-chip, which is integrated with fiber-waveguide coupler and photo detector on a waveguide based silicon photonic chip.

STu4I.2 • 16:15
Monolithically Integrated Quantum Cascade Lasers, Detectors and Dielectric Waveguides at 9.5 μ m for Far-Infrared Lab-on-Chip Chemical Sensing, Yi Zou¹, Karun Vijayraghavan¹, Parker Wray¹, Swapnajat Chakravarty², Mikhail A. Belkin¹, Ray T. Chen^{1,2}; ¹Univ. of Texas at Austin, USA; ²Omega Optics Inc., USA. We provide the first experimental demonstration of room temperature far-infrared lab-on-chip chemical sensing via monolithic integration of quantum cascade laser, quantum cascade detector and dielectric waveguides at the long infrared wavelength of 9.5 μ m.

STu4I.3 • 16:30
Experimental Demonstration of Mid-Infrared Hole and Slotted Photonic Crystal Waveguides in Silicon on Sapphire, Yi Zou¹, Parker Wray¹, Swapnajat Chakravarty², Ray T. Chen^{1,2}; ¹Univ. of Texas at Austin, USA; ²Omega Optics Inc., USA. We provide the first experimental demonstration of propagation characteristics of hole and slotted two dimensional photonic crystal waveguides in silicon-on-sapphire at mid-infrared wavelength of 3.43 μ m.

Meeting Room
212 A/C

CLEO: Applications & Technology

16:00–18:00
ATu4J • Environmental Sensing
President: Mark Phillips; Pacific Northwest National Lab, USA

ATu4J.1 • 16:00 **Invited**
Nitrogen oxide radicals and organic nitrate photochemistry in Earth's atmosphere, Ronald Cohen¹; ¹Univ. of California Berkeley, USA. Textbook descriptions of atmospheric nitrogen oxide photochemistry focus on the role of NO_x as a control over OH and on limiting behavior at high and low NO_x. In this talk I will explore the intermediate NO_x regime, focusing on the role of organic nitrates as a control over atmospheric NO_x and HO_x free radicals.

ATu4J.2 • 16:30
Transportable Dual-Modulation Faraday Rotation Spectrometer for Time-Multiplexed Nitric Oxide Isotope Ratiometry, Eric J. Zhang¹, Stacey Huang¹, Michael Silvernagel², Gerard Wysocki¹; ¹Electrical Engineering, Princeton Univ., USA; ²Electrical Engineering, Univ. of Notre Dame, USA. We present a transportable dual-modulation Faraday rotation spectrometer with minor isotope (15NO) detection sensitivity of 0.35 ppbv-Hz-1/2, corresponding to 1.4x the shot-noise limit. NO isotope line-switching is implemented for quasi-simultaneous time-multiplexed isotope measurements.

Meeting Room
212 B/D

CLEO: Science & Innovations

16:00–18:00
STu4K • Biosensing
President: Ralph Jimenez; Univ. of Colorado at Boulder, USA

STu4K.1 • 16:00 **Invited**
Micro-Cavity based Force Sensors - A Novel and Simple Interferometric Tool for Cell-Mechanical Investigations, Nils M. Kronenberg¹, Philipp Liehm¹, Anja Steude¹, Malte C. Gather¹; ¹Univ. of St Andrews, UK. We have developed a completely new approach to measure vertical and horizontal forces of biological cells cultured on 2D substrata by interferometrically detecting deformations of a soft micro-resonator with an elastic filling.

STu4K.2 • 16:30
Wide Dynamic Range Specific Detection of Therapeutic Drugs by Photonic Crystal Microcavity Arrays, Hai Yan¹, Chun-Ju Yang¹, Yi Zou¹, Naimei Tang^{1,2}, Swapnajat Chakravarty², Ray T. Chen^{1,2}; ¹The Univ. of Texas at Austin, USA; ²Omega Optics Inc., USA. Six orders of magnitude wide dynamic range (0.1 ng/ml to over 100 μ g/ml), label-free detection of gentamicin small molecules with silicon photonic crystal microcavity biosensors multiplexed by multimode interference power splitters was experimentally demonstrated. Detection specificity was confirmed.

Marriott
Salon I & II

16:00–18:00
STu4L • Higher-Order Modes & Mode Coupling in Fiber
President: Poul Kristensen; OFS Fitel Denmark I/S, Denmark

STu4L.1 • 16:00 **Invited**
Astrophotonics: The Future of Astronomical Instrumentation, Joss Bland-Hawthorn¹; ¹Univ. of Sydney, Australia. Astrophotonics has already made important contributions to astronomical and space instrumentation. The early developments built on technologies arising out of telecommunications but the field has begun to "give back" to traditional photonic fields.

STu4L.2 • 16:30
Input and Output Coupling in Higher Order Mode Fibers, Jeffrey Demas¹, Lars Rishoej¹, Siddharth Ramachandran¹; ¹Boston Univ., USA. We convert higher order fiber modes into Gaussian beams using binary phase plates, and characterize the resulting M² and coupling efficiency to single-mode fiber (~64%). Reciprocally, the system is used to excite modes in multi-mode fiber with purity >13dB.

**CLEO: Applications
& Technology**

16:00–18:00

**ATu4M • Novel Sources for
Industrial Applications**

Presider: Richard Solarz; KLA-Tencor Corp, USA

ATu4M.1 • 16:00 **Invited**

Lasers in the 2 μ m SWIR spectral regime and their Applications, Tony Hoult¹; ¹IPG Photonics Corp, USA. For a particular laser type to be widely adopted for industrial materials processing, a minimum laser power is required. The development of supra 100 watt thulium fiber lasers means that another laser type has now been added to that relatively short list.

ATu4M.2 • 16:30 **Invited**

High Power Laser-Sustained Plasma Lightsources for KLA-Tencor Broadband Inspection Tools, Ilya Bezel¹, Gil Delgado¹, Matthew Derstine¹, Ken Gross¹, Richard Solarz¹, Anatoly Schemelinin¹, David Shortt¹; ¹KLA-Tencor Corp, USA. For the last 8 years, the brightness of UV lightsources in KT Broadband inspection tools increased by orders of magnitude due to advances in LSP technology. Challenges of LSP in high-power regime are discussed here.

CLEO: Science & Innovations

16:00–18:00

STu4N • Ultrafast Imaging and Spectroscopy

Presider: Cristian Manzoni; IFN-CNR, Italy

STu4N.1 • 16:00

Motion Picture Femtophotography with Sequentially Timed All-optical Mapping Photography, keiichi nakagawa¹, Atsushi Iwasaki¹, Yu Oishi², Ryoichi Horisaki³, Akira Tsukamoto⁴, Aoi Nakamura⁵, Kenichi Hiroswawa⁵, Hongen Liao¹, Takashi Ushida¹, Keisuke Goda^{1,6}, Fumihiko Kannari⁵, Ichiro Sakuma¹; ¹Univ. of Tokyo, USA; ²RIKEN, Japan; ³Osaka Univ., Japan; ⁴National Defense Academy, Japan; ⁵Keio Univ., Japan; ⁶Univ. of California, Los Angeles, Armenia. We present a method for motion-picture femtophotography that performs continuous, single-shot, burst image acquisition without the need for repetitive measurements. We capture the dynamics of laser ablation and phonon propagation with the imaging method.

STu4N.2 • 16:15

Ultrafast Imaging using Simultaneous Spatially and Temporally Resolved Wavelength-Multiplexed Photography (SSTWP), Takakazu Suzuki¹, Fumihiko Isa¹, Leo Fujii¹, Kenichi Hiroswawa¹, Fumihiko Kannari¹; ¹Keio Univ., Japan. We propose and experimentally demonstrate the simultaneous spatially and temporally resolved wavelength-multiplexed photography device (SSTWP) with a diffractive optical element and a band-pass filter. Using frequency chirped pulses, we realize ultrafast imaging.

STu4N.3 • 16:30

Imaging through permuted optical probes, Barmak Heshmat¹, IK Hyun Lee¹, Hisham Bedri¹, Ramesh Raskar¹; ¹MIT, USA. Using time of flight we have enabled an optical brush to calibrate itself and image with its randomly positioned fibers, this offers a flexible field of view and is intrinsically multi-spectral. Therefore, it has potential application for endoscopy, imaging in turbid media and near-field probing.

16:00–18:00

STu4O • OPCPA Systems & Pump Lasers

Presider: Constantin Haefner; Lawrence Livermore National Lab, USA

STu4O.1 • 16:00 **Invited**

Scaling High Peak Powers to High Average Powers - Opportunities in Innovation and Technology, John L. Collier¹; ¹STFC Rutherford Appleton Lab, UK. This talk will describe our programmes to scale diode pumped PW and parametric systems to high average power as a new basis for applications based on compact, efficient and reliable secondary sources.

STu4O.2 • 16:30 **Invited**

220mJ Ultrafast Thin-Disk Regenerative Amplifier, Sandro Klingebiel¹, Marcel Schultze¹, Catherine Y. Teisset¹, Robert Bessing¹, Matthias Haefner¹, Stephan Prinz¹, Martin Gorjan^{2,3}, Dirk H. Sutter⁴, Knut Michel¹, Helena G. Barros², zsuzsanna Major^{2,3}, Ferenc Krausz^{2,3}, Thomas Metzger¹; ¹TRUMPF Scientific Lasers GmbH + Co. KG, Germany; ²Dept. für Physik, Ludwig-Maximilians-Universität München, Germany; ³Max-Planck-Institut für Quantenoptik, Germany; ⁴Trumpf Laser GmbH, Germany. We report on a chirped-pulse regenerative thin-disk amplifier generating 220 mJ pulse energy at 1 kHz repetition rate with a pulse duration of 1.9 ps for pumping few-cycle optical parametric amplifiers (OPA).



Join the conversation. Use #CLEO15.
Follow us @cleoconf on Twitter.

CLEO: QELS-Fundamental Science

FTu4A • Fundamental Quantum Optics—Continued

FTu4A.4 • 16:45

Reducing the Free-Space Group Velocity of Single Photons by Transverse Structuring, Daniel Giovannini¹, Jacqueline Romero¹, Václav Potoček¹, Gergely Ferenczi¹, Fiona Speirits¹, Stephen Barnett¹, Daniele Faccio², Miles Padgett¹; ¹School of Physics and Astronomy, Univ. of Glasgow, UK; ²School of Engineering and Physical Sciences, Heriot-Watt Univ., UK. The group velocity of light in free space is decreased by controlling the transverse spatial structure of the beam. We present experimental results in the single-photon regime, supported by a simple geometric argument and a full theoretical treatment.

FTu4A.5 • 17:00

Hong-Ou-Mandel Interference between Transverse Spatial Waveguide Modes, Aseema Mohanty¹, Mian Zhang¹, Sven Ramelow², Paulo Nussenzveig³, Michal Lipson^{1,4}; ¹School of Electrical and Computer Engineering, Cornell Univ., USA; ²School of Applied and Engineering Physics, Cornell Univ., USA; ³Instituto de Física, Universidade de São Paulo, Brazil; ⁴Kavli Inst. at Cornell for Nanoscale Science, Cornell Univ., USA. We demonstrate Hong-Ou-Mandel interference between different transverse spatial modes in a silicon nitride multimode waveguide. We show over 90% visibility between modes, providing a promising route for scalable on-chip quantum information processing.

FTu4A.6 • 17:15

Quantum Walk Coherences on a Dynamical Percolation Graph, Fabian Elster¹, Sonja Barkhofen¹, Thomas Nitsche¹, Jaroslav Novotný², Aurél Gábris^{2,3}, Igor Jex², Christine Silberhorn¹; ¹Applied Physics, Univ. of Paderborn, Germany; ²Dept. of Physics, Faculty of Nuclear Sciences and Physical Engineering, Czech Technical Univ. in Prague, Czech Republic; ³Dept. of Theoretical Physics, Univ. of Szeged, Hungary. We implement a quantum walk on a percolation graph leveraging a time-multiplexed quantum walk architecture to create broken links between the graph nodes. We test our system by verifying non-Markovian signatures resulting from induced open system dynamics.

FTu4B • Light-matter Interaction in Graphene/Other Carbon-based Materials—Continued

FTu4B.4 • 16:45

Terahertz Generation by Dynamical Photon Drag Effect in Graphene, Juliette Mangeney¹, Jean Maysonnave¹, Simon Huppert¹, Feihu Wang¹, Simon Maero¹, Claire Berger^{2,4}, Walt A. de Heer², Theodore B. Norris³, Louis-Anne de Vaulchier¹, Sukhdeep Dhillon¹, Robson Ferreira¹, Jérôme Tignon¹; ¹Laboratoire Pierre Aigrain, Ecole Normale Supérieure-PSL Research Univ., CNRS, Université Pierre et Marie Curie-Sorbonne Universités, Université Paris Diderot-Sorbonne Paris Cité, France; ²School of Physics, Georgia Inst. of Technology, USA; ³Univ. of Michigan, USA; ⁴Université Grenoble Alpes/CNRS, Institut Néel, France. Room temperature terahertz generation is demonstrated in graphene under femtosecond optical excitation. This is induced by dynamical photon drag, which relies on the transfer of light momentum to the carriers by ponderomotive and magnetic forces.

FTu4B.5 • 17:00

Microscopic Origins of the Terahertz Carrier Relaxation and Cooling Dynamics in Graphene, Momchil T. Mihnev^{1,2}, Charles J. Divin^{1,2}, Faris Kadi³, Torben Winzer⁴, Seunghyun Lee¹, Che-Hung Liu¹, Zhaohui Zhong¹, Xiaohan Wang⁴, Rodney S. Ruoff⁴, Claire Berger⁵, Walt A. de Heer⁵, Ermin Malic³, Andreas Knorr³, Theodore B. Norris^{1,2}; ¹Dept. of Electrical Engineering and Computer Science, Univ. of Michigan, USA; ²Center for Ultrafast Optical Science, Univ. of Michigan, USA; ³Institut für Theoretische Physik, Nichtlineare Optik und Quantenelektronik, Technische Universität Berlin, Germany; ⁴Dept. of Mechanical Engineering and the Materials Science and Engineering Program, The Univ. of Texas at Austin, USA; ⁵School of Physics, Georgia Inst. of Technology, USA. We combine ultrafast time-resolved THz spectroscopy and microscopic modeling to study the hot-carrier relaxation and cooling dynamics in graphene; we demonstrate that the dynamics are the result of the intricate interplay between carrier-carrier and carrier-phonon interactions.

FTu4B.6 • 17:15

Ultrabroadband THz Conductivity of Non-equilibrium Dirac Fermions in Graphene, Giacomo Coslovich¹, Ryan P. Smith¹, Sufei Shi^{1,2}, Jan H. Buss¹, Jeremy T. Robinson³, Feng Wang^{1,2}, Robert A. Kaindl¹; ¹Lawrence Berkeley National Lab, USA; ²Dept. of Physics, Univ. of California at Berkeley, USA; ³Naval Research Lab, USA. We employ ultrabroadband THz pulses to expose the high-frequency transport of non-equilibrium Dirac fermions in graphene. Tuning the Fermi level reveals a transient response characteristic of high-energy photo-excited carriers with strongly enhanced interactions.

FTu4C • Topological Photonics II—Continued

FTu4C.4 • 17:00

One-Way Topological Transitions in Magnetoplasmonic Hyperbolic Metamaterials, Binyamin Stein¹, Alex Leviyev¹, Tal Galfsky^{3,2}, Harish Krishnamoorthy^{1,2}, Igor L. Kuskovsky^{1,2}, Vinod M. Menon^{3,2}, Alexander B. Khanikaev^{1,2}; ¹Physics, Queens College of the City Univ. of New York, USA; ²Physics, Graduate Center of the City Univ. of New York, USA; ³Physics, The City College of New York, USA. It is shown that hyperbolic metamaterials with reduced spatial symmetry and the time-reversal symmetry broken by magnetization exhibit multiple nonreciprocal hyperbolic regimes. Magnetization induced one-way topological phase transitions between elliptical and hyperbolic regimes are demonstrated.

FTu4C.5 • 17:15

Integrated impedance-matched photonic Dirac-cone metamaterials, Yang Li¹, Shota Kita¹, Philip Muñoz¹, Orad Reshef¹, Daryl Vulis¹, Marko Loncar¹, Eric Mazur¹; ¹Harvard Univ., USA. We design and fabricate an on-chip Dirac-cone metamaterial with impedance-matched zero index at 1550 nm. This design can serve as an on-chip platform to implement applications of Dirac-cone metamaterials in integrated photonics, such as supercoupling.

FTu4D • Optical Filamentation and Compression—Continued

FTu4D.4 • 16:45

Transition between linear and nonlinear focusing regimes during filamentation, Khan Lim¹, Magali Durand¹, Matthieu Baudelet¹, Martin Richardson¹; ¹Univ. of Central Florida, CREOL, USA. The transition between linear and nonlinear regimes of focusing for laser filamentation is described and shows the balance between plasma physics and nonlinear propagation for the stability of the laser filament and its properties.

FTu4D.5 • 17:00

Superfilamentation in water with tight focusing laser beams, Fedor V. Potemkin¹, Evgeniy I. Mareev¹, Alexey Podshivalov¹, Vyacheslav M. Gordienko¹; ¹M. V. Lomonosov Moscow State Univ., Russia. We report whole life cycle of superfilament excited in tight focusing beams in water. Extreme energy delivery achieved under superfilamentation is reflected in strong post-effects (cavitation bubbles and shock waves), which can completely characterize superfilament.

FTu4D.6 • 17:15

Generation and Enhancement of XUV Pulse from UV Filament Interaction in Argon, Di Wang¹, Wenxue Li¹, Liangen Ding¹, Heping Zeng¹; ¹East China Normal Univ., China. We demonstrated the generation and enhancement of XUV pulse at 89 nm by non-collinear interaction between UV filaments in argon. The experimental result agrees well with the simulated data.

CLEO: QELS-
Fundamental ScienceFTu4E • Plasmonic Nanoantennas
for Sensing and Focusing—
Continued

FTu4E.4 • 16:45

3D Plasmonic nanostar structures for recyclable SERS applications, Manohar Chirumamilla^{2,1}, Anisha Gopalakrishnan², Andrea Toma², Remo Proietti Zaccaria², Francesco De Angelis², Roman Krahn²; ¹Dept. Of Physics and Nanotechnology, Aalborg Univ., Denmark; ²Nanostructures, Istituto Italiano di Tecnologia, Italy. Nanofabrication of metallic nanostructures/nanoparticles enables the detection of analyte molecules at ultra-low concentrations with the aid of plasmon induced hot-spots. Here we present a cost effective approach to recycle the SERS substrates for label free bio-sensing applications.

FTu4E.5 • 17:00

Plasmonics of Ultranarrow Gaps Shunted by Organic Conductive Junctions, Christos Tserkezis¹, Felix Benz², Lars O. Herrmann², Bart de Nijs², Alan Sanders², Daniel O. Sigle², Jeremy Baumberg², Javier Aizpurua²; ¹Donostia International Physics Center and Centro de Fisica de Materiales CSIC-UPV/EHU, Spain; ²Nanophotonics Centre, Cavendish Lab, Dept. of Physics, Univ. of Cambridge, UK. The optical response of plasmonic cavities formed by metallic nanoparticles deposited on a metallic substrate separated by self-assembled monolayers of conductive organic molecules can be precisely controlled by the exact chemical composition of the monolayers.

FTu4E.6 • 17:15

Subwavelength Sensing Elements from Film-Coupled Silver Nanocubes, Alex Powell¹, Andrew Watt¹, Hazel Assender¹, Jason M. Smith¹; ¹Univ. of Oxford, UK. By placing a moisture-sensitive polymer spacer between a silver nanocube and an Ag film, the extreme sensitivity of the plasmon resonance excited between them to spacer thickness is exploited to create a novel sub-wavelength sensing element.

STu4F • Components and
Optical Interconnects—
Continued

Efficient III-V/Si Hybrid SOAs for Optical Interconnects, Stanley Cheung¹, Kuanping Shang¹, Yasumasa Kawakita¹; ¹Univ. of California Davis, USA. We present 1.55 μm hybrid III-V/Si SOA designs and experimentally determine wall-plug-efficiency (WPE) values for 2 mW and 0.1 mW input power amplification. Flared SOAs yield WPE = 12.1% for output power > 10 mW and straight SOAs achieve WPE = 7.2%.

STu4F.5 • 17:15

56 Gb/s PAM-4 Data Transmission Over a 1 m Long Multimode Polymer Interconnect, Nikos Bamiedakis¹, Jinlong Wei¹, Jian Chen¹, Petter Westbergh², Anders Larsson², Richard V. Penty¹, Ian H. White¹; ¹Univ. of Cambridge, UK; ²Chalmers Univ. of Technology, Sweden. Advanced modulation formats can enable >40 Gb/s data rates in waveguide-based optical interconnects without the need for high-specification optoelectronic components. Record 56Gb/s PAM-4 data transmission is demonstrated over a 1 m-long multimode polymer waveguide.

CLEO: Science & Innovations

STu4G • Cascade Lasers III—
Continued

STu4G.4 • 16:45

Room Temperature Operation of a Photonic Crystal Quantum Cascade Laser, Romain Peretti¹, Valeria Liverini¹, Johanna Wolf¹, Christopher Bonzon¹, Sebastian Lourduos², Wondwosen Metaferia², Mattias Beck¹, Jerome Faist¹; ¹ETH Zurich, Switzerland; ²Lab of Semiconductor Materials, School of ICT, KTH-Royal Inst. of Technology, Sweden. We report on design, fabrication and investigation of a buried heterostructure photonic crystal quantum cascade laser operating in the mid-IR (8.5 μm) at room temperature, leading to single mode emission on a 600 μm by 600 μm mesa.

STu4G.5 • 17:00 **Invited**

Perspectives for intersubband polariton lasers and Bose-Einstein condensation of intersubband polaritons, Raffaele Colombelli¹, Jean-Michel Manceau¹; ¹Univ. Paris Sud and CNRS, France. Intersubband polaritons are mixed states, partially micro-cavity photon and partially intersubband excitation, which behave as bosons below a certain density. We discuss the perspectives toward the development of mid-IR and THz intersubband polariton bosonic lasers.

STu4H • THz Spectroscopic
Techniques—Continued

STu4H.4 • 16:45

Terahertz Response of Long-lived Photoexcited Electrons in Silicon Observed Using Single-shot Terahertz Spectroscopy, Ikufumi Katayama¹, Kaisei Masuda¹, Kohei Horiuchi¹, Yasuo Minami¹, Jun Takeda¹; ¹Yokohama National Univ., Japan. We observed photoexcited carriers in silicon by using single-shot terahertz spectroscopy. This technique can significantly reduce the measurement time and repetition rate of pump pulses, enabling us to observe the dynamics of long-lived photoexcited carriers without a pileup effect.

STu4H.5 • 17:00

Real-Time Absolute Frequency Measurement of CW-THz Wave Based on a Free-Running THz Comb, Takashi Ogura¹, Kenta Hayashi¹, Hajime Inaba^{4,2}, Kaoru Minoshima^{3,2}, Takeshi Yasui^{1,2}; ¹Tokushima Univ., Japan; ²ERATO Intelligent Optical Synthesizer Project, Japan; ³The Univ. of Electro-Communications, Japan; ⁴National Inst. of Advanced Industrial Science and Technology, Japan. We demonstrated a real-time frequency measurement of CW-THz wave using a single free-running THz comb. The absolute frequency of the CW-THz wave is measured with an accuracy of 8.7×10^{-12} at a rate of 10 Hz.

STu4H.6 • 17:15

Generation and Stabilization of THz-waves with Extraordinary Low Line Width and Phase Noise, Stefan Preussler¹, Thomas Schneider¹, Hassanain Al-Taij¹; ¹Institut für Hochfrequenztechnik, Technische Universität Braunschweig, Germany. The generation and stabilization of high quality mm- and THz-waves via extraction of two lines from a fs-laser, with frequencies up to 3 THz, line width below 1 Hz and phase noise of -134 dBc/Hz is presented.

CLEO: Science & Innovations

STu4I • Mid-IR Photonics—Continued

STu4I.4 • 16:45

Near Field Optical Measurements of Silicon Waveguide in Mid-IR Regime Using Scanning Thermal Microscopy, Meir Y. Grajower¹, Yoel Sebbag¹, Alex Naiman¹, Boris Desiatov¹, Uriel Levy¹; ¹Hebrew Univ. of Jerusalem, Israel. We observe for the first time the near field optical intensity distribution of silicon nanophotonic devices operating in the mid-IR spectrum using our scanning thermal microscopy and demonstrate its advantages over conventional NSOM technique.

STu4I.5 • 17:00

On-Chip Modulation in the Mid-Infrared with Silicon-on-Lithium-Niobate Photonics, Jeff Chiles¹, Sasan Fathpour¹; ¹CREOL, Univ. of Central Florida, USA. Mid-infrared (3.39 μm) optical modulators are demonstrated for the first time on the silicon-on-lithium-niobate platform, with a $V_{\pi/2}$ of 26 V-cm, extinction ratio of 8 dB, and on-chip insertion losses of 3.3 dB.

STu4I.6 • 17:15

Microscopic Analysis of Quantum-Confined Stark Effect of Group IV Quantum Wells for Mid-Infrared Si-Based Electroabsorption Modulators, Takeshi Fujisawa¹, Kunimasa Saitoh¹; ¹Graduate school of information science and technology, Hokkaido Univ., Japan. Quantum-confined Stark effect of Ge(Sn)/SiGe(Sn) quantum wells (QWs) is analyzed by many-body theory. Calculated absorption spectra of Ge/SiGe-QWs are in good agreement with the experiment. Also, the effect of Sn-incorporation is investigated for mid-infrared applications.

CLEO: Applications & Technology

ATu4J • Environmental Sensing—Continued

ATu4J.3 • 16:45

Quantifying Primary Reactive Nitrogen Emissions Using Open-Path, Quantum Cascade Laser-Based Sensors, Kang Sun¹, Lei Tao¹, Da Pan¹, Levi Golston¹, Yue Tian², Ming-Fang Huang², Junqiang Hu², Ting Wang², Mark A. Zondlo¹; ¹Princeton Univ., USA; ²NEC Labs America, USA. A compact QCL-based open-path NO sensor is developed at 5.26 μm for high sensitivity and fast response. Combined with existing NH_3 and N_2O sensors, this system measures primary emissions of reactive nitrogen to the atmosphere.

ATu4J.4 • 17:00

Airborne Multi-Gas Sensor, David Bomsel¹, Marwood N. Ediger¹, Andrei B. Vakhtin¹; ¹Mesa Photonics, USA. Carbon dioxide and methane are detected simultaneously using two-tone frequency modulation spectroscopy. Detection limits are 1.5 ppm $\text{Hz}^{-1/2}$ and 3.5 ppb $\text{Hz}^{-1/2}$, respectively, over 0.1 to 100 s. External phase modulators apply the two tones.

ATu4J.5 • 17:15

CAMS - Compact Atmospheric Multi-Species Spectrometer, Dirk Richter¹, Petter Weibring¹, James Walega¹, Alan Fried¹, Scott M. Spuler², Matthew Taubman³; ¹Univ. of Colorado, USA; ²Earth Observing Lab, National Center for Atmospheric Research, USA; ³Pacific Northwest National Lab, USA. We present the design, development, and field performance of an airborne mid-IR spectrometer configured for the simultaneous sensitive detection of CH_2O (~40 pptv, 1 Hz) and C_2H_6 (~15 pptv, 1 Hz).

CLEO: Science & Innovations

STu4K • Biosensing—Continued

STu4K.3 • 16:45

Silicon Nitride Coupled-Resonator Optical-Waveguide-based Biosensors using Visible-Light-Scattering Pattern Recognition, Jiawei Wang¹, Andrew W. Poon¹; ¹Photonic Device Lab, Dept. of Electronics and Computer Engineering, Hong Kong Univ. of Science and Technology, China. We demonstrate silicon nitride coupled-resonator optical-waveguide-based biosensors using visible-light-scattering pattern recognition with pixelized mode-field-intensity distributions. Our 16-microring sensor reveals 14 eigenstates. Our algorithm suggests an average sensitivity of ~372 RIU⁻¹.

STu4K.4 • 17:00

Phospholipid-functionalized microgoblet lasers for biomolecular detection, Uwe R. Bog¹, Falko Brinkmann¹, Sentayehu Fetene Wondimu¹, Tobias Wienhold¹, Sarah Kraemer¹, Christian Koos¹, Heinz Kalt¹, Sebastian Koerber¹, Timo Mappes³, Michael Hirtz¹, Harald Fuchs²; ¹Karlsruher Institut für Technologie, Germany; ²Westfälische-Wilhelms-Universität, Germany; ³Carl Zeiss AG, Germany. We present our latest results on microgoblet lasers as biosensors. Surface functionalization is performed with high resolution and throughput by aligned microcontact stamping. We show simultaneous device readout, the resulting cross-referencing capabilities and functionalization reconfiguration.

STu4K.5 • 17:15

193nm Lithography Fabricated High Sensitivity Photonic Crystal Microcavity Biosensors for Plasma Protein Detection in Patients with Pancreatic Cancer, Chun-Ju Yang¹, Naimei Tang^{1,2}, Hai Yan¹, Swapnajt Chakravarty², Donghui Li³, Ray T. Chen^{1,2}; ¹The Univ. of Texas at Austin, USA; ²Omega Optics Inc., USA; ³UT MD Anderson Cancer Center, USA. High sensitivity L13-type two-dimensional photonic crystal microcavities with nanoholes were fabricated by 193nm photolithography. 0.03 picomolar concentration pancreatic cancer biomarker in patient serum samples was experimentally detected to 10 \times lower dilution than ELISA.

STu4L • Higher-Order Modes & Mode Coupling in Fiber—Continued

STu4L.3 • 16:45

Large Mode Area Guidance in a Simple Fiber Structure, Lars Rishoej¹, Maxwell Jones², Jeffrey Demas¹, Gautam Prabhakar¹, Lu Yan¹, Thomas W. Hawkins², John Ballato², Siddharth Ramachandran¹; ¹Boston Univ., USA; ²COMSET, Clemson Univ., USA. We demonstrate higher-order-mode ($A_{\text{eff}} \sim 1800 \mu\text{m}^2$) propagation in a 100- μm -OD pure-silica fiber with a low-index polymer jacket commonly used for fiber-laser pump-guidance. This simple structure obviates the need for complex designs deemed necessary for realizing large-mode-area fibers.

STu4L.4 • 17:00

High Energy Pulse Amplification in a Higher-Order Mode Fiber Amplifier with Axicon for Output Mode Conversion, Jeffrey W. Nicholson¹, John M. Fini¹, A. DeSantolo¹, Paul S. Westbrook¹, Robert Windeler¹, Tristan Kremp¹, Clifford Headley¹, David DiGiovanni¹; ¹OFS Labs, USA. High energy, 700 μJ , one nanosecond pulses and 490 femtosecond, 50 μJ pulses are demonstrated in an Er-doped, higher-order-mode fiber amplifier. An axicon at the output enables efficient, nonlinearity-free reconversion to a low M^2 beam.

STu4L.5 • 17:15

Microstructured suspended core fiber for cylindrical vector beams propagation, Hong Ji¹, Yinlan Ruan¹, Heike Ebendorff-Heidepriem¹, Wen Qi Zhang¹, Shahraam Afshar¹, Tanya Monro¹; ¹the Univ. of Adelaide, Australia. A suspended core fiber based on lead silicate glass has been fabricated to generate doughnut beams. Preliminary results demonstrated a potential to be a good candidate for fiber based cylindrical vector beams generation and propagation.

CLEO: Applications
& Technology

CLEO: Science & Innovations

ATu4M • Novel Sources for Industrial Applications—Continued

STu4N • Ultrafast Imaging and Spectroscopy—Continued

STu4O • OPCPA Systems & Pump Lasers—Continued

ATu4M.3 • 17:00

High-energy, 34 fs, fiber source via nonlinear compression in hypocycloid-core Kagome fiber, Achut Giree^{3,4}, Florent Guichard^{1,2}, Yoann Zaouter², Marc Hanna¹, Guillaume Machinet², Benoît Debord³, Frédéric Gérôme^{5,6}, Pascal Dupriez⁷, Clemens Hoeningner², Eric Mottay², Fetah Benabid^{5,6}, Patrick Georges¹; ¹Lab Charles Fabry de l'Inst d'Optique, France; ²Amplitude Systemes, France; ³MBI, Germany; ⁴Amplitude Technologies, France; ⁵XLIM Inst., France; ⁶GLO photonics, France; ⁷Alphanov, France. We report on the nonlinear compression of 330 fs and 70 μJ pulses from a high energy fiber amplifier system down to 34 fs and 50 μJ pulses using an air-filled 40 μm hypocycloid-core Kagome fiber.

ATu4M.4 • 17:15

1.75 kW CW Narrow Linewidth Yb-doped all-fiber Amplifiers for Beam Combining Application, YunFeng Qi¹, ming lei¹, chi liu¹, bing he¹, jun zhou¹; ¹Shanghai Inst of Optics and Fine Mech, USA. We reported on a Yb-doped all-fiber amplifier when seeded with a 20 GHz line-width master oscillator. By using mode controlling technology, an output power of 1.75 kW with near-diffraction limited beam quality (M2=1.77) was observed.

STu4N.4 • 16:45

Coherent Diffraction Imaging with Absorption Contrast using Broadband Tabletop Soft X-ray Sources, Guido Cadenazzi², Brian K. McFarland¹, Nina R. Weisse-Bernstein¹, Matthew C. Tyson¹, George Rodriguez¹, Richard L. Sandberg¹; ¹Los Alamos National Lab, USA; ²La Trobe Univ., Australia. We demonstrate nanometer scale resolution with absorption contrast without the need for scanning wavelength as is typically done. This is accomplished by applying polychromatic coherent diffraction imaging with a tabletop, ultrafast, broadband high harmonic source.

STu4N.5 • 17:00

Probing Ultrafast Magnetization Dynamics using Bright Circularly Polarized High Harmonics, Dmitry Zusin¹, Ronny Knut^{1,3}, Patrik Grychtol¹, Ofer Kfir², Christian Gentry¹, Hans Nembach³, Justin Shaw³, Tom Silva³, Avner Fleischer^{2,4}, Oren Cohen², Henry C. Kapteyn¹, Margaret M. Murnane¹; ¹Dept. of Physics and JILA, Univ. of Colorado and NIST, USA; ²Solid State Inst. and Physics Dept., Technion, Israel; ³Electromagnetics Division, National Inst. of Standards and Technology, USA; ⁴Dept. of Physics and Optical Engineering, Ort Braude College, Israel. We generate bright circularly polarized high harmonics and use this new table-top light source to capture ultrafast magnetization dynamics for the first time by measuring laser-driven ultrafast demagnetization in a FeCr alloy.

STu4N.6 • 17:15

Attenuated total reflectance infrared spectroscopy with chirped-pulse upconversion, Takao Fuji¹, Hideto Shirai¹, Constance Duchesne^{1,2}, Yuji Furutani¹; ¹National Inst.s of Natural Sciences, Japan; ²Chimie ParisTech, France. Chirped-pulse upconversion technique has been applied to attenuated total reflectance infrared spectroscopy. The system was applied to observe the dynamics of exchanging process of buffers for biological tissues.

STu4O.3 • 17:00

Picosecond, 115 mJ Energy, 200 Hz Repetition Rate Cryogenic Yb:YAG Bulk-amplifier, Michaël Hemmer¹, Fabian Reichert¹, Kelly Zapata¹, Martin Smrz^{2,1}, Anne-Laure Calendron^{1,3}, Huseyin Cankaya^{1,3}, Kyung-Han Hong⁴, Franz Kaerntner^{1,3}, Luis E. Zapata¹; ¹Center for Free-Electron Laser Science (CFEL), Germany; ²Hilase Center, Inst. of Physics AS CR, Czech Republic; ³The Hamburg Center for Ultrafast Imaging and Dept. of Physics, Germany; ⁴MIT, USA. We report on a compact, high-energy, cryogenically-cooled Yb:YAG bulk-amplifier delivering energies > 100 mJ at 200 Hz repetition rate with excellent beam quality and spectrum supporting 5-ps pulses.

STu4O.4 • 17:15

100 mJ thin disk regenerative amplifier at 1 kHz as a pump for picosecond OPCPA, Jakub Novák^{1,2}, Pavel Bakule¹, Jonathan T. Green¹, Zbynek Hubka^{1,2}, Bedrich Rus¹; ¹ELI-Beamlines, Inst. of Physics ASCR, v. v. i. (FZU), Czech Republic; ²Faculty of Nuclear Sciences and Physical Engineering, Czech Technical Univ., Czech Republic. Stable operation with energy >100mJ of the Yb:YAG thin disk regenerative amplifier at 1kHz has been achieved. The amplifier is being developed as a pump for the picosecond OPCPA of the L1 beamline at ELI-Beamlines.



**Conference Reception
and Poster Session**

 Join us for this exciting event on
 Tuesday from 18:00–20:00
 in the CLEO:Expo.

CLEO: QELS-Fundamental Science

FTu4A • Fundamental Quantum Optics—Continued

FTu4A.7 • 17:30

Efficient Boson Sampling Schemes using Dispersion and Pulse Shaping, Mihir Pant¹, Dirk R. Englund¹; ¹MIT, USA. We present Boson Sampling schemes in the time-frequency basis that allow for more modes, fewer sources and detectors and are more tolerant to temporal mismatch than Boson Sampling schemes using photons in many spatial modes.

FTu4A.8 • 17:45

Repeat-Until-Success Cubic Phase Gate, Kevin A. Marshall¹, Raphael Pooser^{2,3}, George Siopes³, Christian Weedbrook⁴; ¹Univ. of Toronto, Canada; ²Quantum Information Science Group, Oak Ridge National Lab, USA; ³Dept. of Physics and Astronomy, The Univ. of Tennessee, USA; ⁴QKD Corp., Canada. Here we introduce an experimentally viable 'repeat-until-success' implementation of the cubic phase gate, required for universal quantum computation, using sequential photon subtractions. Our scheme offers benefits in the expected time until success, although we require a primitive quantum memory.

FTu4B • Light-matter Interaction in Graphene/Other Carbon-based Materials—Continued

FTu4B.7 • 17:30

Ultrafast Photo-Excitation Dynamics of Nitrogen-Vacancy Defects in Diamond, Ronald Ulbricht^{1,2}, Shuo Dong², Julian Schwartz², Hyeon-Deuk Kim⁴, Yoshitaka Tanimura⁴, Bala Murali Krishna Mariserla⁵, Keshav M. Dani⁵, Zhi-Heng Loh²; ¹Dept. of Physics, Univ. of Colorado, USA; ²Division of Chemistry and Biological Chemistry, Nanyang Technological Univ., Singapore; ³Accelerator and Fusion Research Division, Lawrence Berkeley National Lab, USA; ⁴Dept. of Chemistry, Kyoto Univ., Japan; ⁵Femtosecond Spectroscopy Unit, Okinawa Inst. of Science and Technology, Japan. We probe the ultrafast dynamics of the electronic excited state of nitrogen-vacancy defects in diamond for temperatures 10K-300K, observing vibrational relaxation times of 40fs and temperature-dependent bi-exponential anisotropy dynamics related to electron motion in Jahn-Teller-distorted orbitals.

FTu4B.8 • 17:45

Controlling Carbon Nanotube Mechanics with Optical Microcavities, Mian Zhang¹, Arthur Barnard¹, Paul McEuen¹, Michal Lipson¹; ¹Cornell Univ., USA. We demonstrate optomechanically induced amplification of carbon nanotube (CNT) mechanical modes using optical microcavities. We also show direct imaging of the spatial profile of CNT mechanical modes using optical readout.

FTu4C • Topological Photonics II—Continued

FTu4C.6 • 17:30

Probing the Ultrathin Limit of Hyperbolic Meta-material: Nonlocality Induced Topological Transitions, Long Chen^{1,2}, Cheng Zhang², Jing Zhou², L. Jay Guo^{1,2}; ¹Applied Physics, Univ. of Michigan, USA; ²Dept. of Electrical Engineering and Computer Science, Univ. of Michigan, USA. Hyperbolic meta-materials based on ultrathin metal-dielectric multilayers have been studied by considering the nonlocal response of electrons in metal. We show that nonlocality will induce topological transitions of the iso-frequency surfaces and limit light-matter interactions.

FTu4C.7 • 17:45

Photonic Topological Edge Modes without an Edge, Yaniv Tenenbaum Katan¹, Yaakov Lumer¹, Yonatan Plotnik¹, Mikael Rechtsman¹, Mordechai Segev¹; ¹Technion, Israel. We present photonic topological modes without a topological edge: topologically protected states which reside at a non-topological interface in the bulk of a photonic topological insulator (a honeycomb lattice of helical waveguides).

FTu4D • Optical Filamentation and Compression—Continued

FTu4D.7 • 17:30

Plasma density measurement along femtosecond laser filament via enhanced THz spectroscopy, Tie-Jun Wang¹; ¹SIOM, Chinese Academy of Sciences, China. We report on a longitudinally resolved measurement of plasma density along femtosecond laser filament in air via needlelike high-voltage DC electric field enhanced THz spectroscopy. Longitudinal distribution of plasma density of $\sim 10^{15}$ cm⁻³ along laser filament has been successfully recorded.

FTu4D.8 • 17:45

Spatial Dependence of the Interaction between a Single Aerosol and a Laser Filament on its Reformation, Cheonha Jeon¹, Danielle Harper¹, Khan Lim¹, Magali Durand¹, Michael Chini¹, Matthieu Baudelet¹, Martin Richardson¹; ¹Univ. of Central Florida, CREOL, USA. The analysis of the filament destruction and reformation as a single aerosol is positioned along the radial and longitudinal axes of the filament provides more understanding of the propagation of filaments in aerosol-containing media.

16:30–18:00 IEEE Journal of Quantum Electronics Celebrates 50 Years, Willow Glen, Marriott

NOTES

**CLEO: QELS-
Fundamental Science**

**FTu4E • Plasmonic Nanoantennas
for Sensing and Focusing—
Continued**

FTu4E.7 • 17:30

Efficient Integration of Sub-5-nm-gap Plasmonic Crystal Cavities with Plasmonic Waveguides, Myung-Ki Kim¹, Yong-Hee Lee¹; ¹KAIST, Korea. We propose a three-dimensionally tapered 2-nm-gap plasmonic crystal cavity which can efficiently couple to an integrated waveguide with over 90% efficiency. Along with the theoretical study, we successfully fabricated the 3D-tapered plasmonic crystal cavity integrated with a plasmonic waveguide.

FTu4E.8 • 17:45

Hybridisation of antenna and cavity modes in nanoparticle-on-mirror plasmonic nanocavities, Christos Tserkezis¹, Ruben Esteban¹, Daniel O. Sigle², Jan Mertens², Lars O. Herrmann², Jeremy Baumberg², Javier Aizpurua¹; ¹Donostia International Physics Center and Centro de Fisica de Materiales CSIC-UPV/EHU, Spain; ²Nanophotonics Centre, Cavendish Lab, Dept. of Physics, Univ. of Cambridge, UK. Longitudinal antenna and transverse cavity modes can be excited when bringing a faceted plasmonic nanoparticle close to a metallic substrate. Their interaction leads to a rich optical response, understandable in terms of the modal symmetry.

CLEO: Science & Innovations

**STu4F • Components and
Optical Interconnects—
Continued**

STu4F.6 • 17:30

56 Gb/s, PAM-4 Transmission Over 25 km, Using IQ Modulator and Unequally Spaced Levels, Cristian Prodanuic^{1,2}, Nebojsa Stojanovic¹, Fotini Karinou¹, Gernot Goegerl¹, Zhang Qiang¹, Roberto Llorente Saez²; ¹Optical Technologies, Huawei Technologies Düsseldorf GmbH, Germany; ²Nanophotonics Technology Centre, Universidad Politécnica de Valencia, Spain. We propose a PAM-4 modulation scheme with unequally spaced levels in order to mitigate chirp effects caused by IQ modulators. Experimental results of 56 Gb/s transmission over 25 km link demonstrate the robustness of this modulation concept.

STu4F.7 • 17:45

6.25 Gb/s POF Link Using GaN μ LED Arrays and Optically Generated Pulse Amplitude Modulation, Xin Li¹, Nikos Bamiedakis¹, Jinlong Wei¹, Jonathan Mckendry², Enyuan Xie², Ricardo Ferreira², Erdan Gu², Martin Dawson², Richard V. Penty¹, Ian H. White¹; ¹Univ. of Cambridge, UK; ²Dept. of Physics, Univ. of Strathclyde, UK. Optically-generated PAM schemes using μ LED arrays are implemented for high-speed POF links for the first time. 6.25Gb/s PAM-16 transmission is demonstrated using 4 μ LEDs, exhibiting 3.8dB greater power-margin than a link with a single μ LED.

**STu4G • Cascade Lasers III—
Continued**

STu4G.6 • 17:30

Continuous Wave Room Temperature External Ring Cavity Quantum Cascade Laser, Michael Hemingway¹, Deivis Vaitiekus¹, John Cockburn¹, Nils Hempler², Gareth Maker², Graeme Malcolm², Dmitry G. Revlin¹; ¹Univ. of Sheffield, UK; ²M Squared Lasers, UK. Mid infrared, tunable quantum cascade laser operating in free-space external ring cavity in continuous wave regime at room temperature is demonstrated for the first time. Out-coupled optical power up to 17 mW has been achieved.

STu4G.7 • 17:45

Monolithic Integration of Quantum Cascade Lasers and Passive Components, Juan Montoya¹, Christine A. Wang¹, Kevin Creedon¹, Anish Goyal¹, Jeffrey Daulton¹, Joseph Donnelly¹, Leo Missaggia¹, Antonio Sanchez-Rubio¹, William Herzog¹; ¹Massachusetts Inst of Tech Lincoln Lab, USA. We present a method to integrate quantum cascade lasers with passive components using proton implantation. Proton implantation reduces the intersubband and free-carrier absorption optical loss. We have measured a loss $\alpha=0.33$ cm⁻¹ in proton implanted waveguides.

**STu4H • THz Spectroscopic
Techniques—Continued**

STu4H.7 • 17:30

Transition from Plasmon Coupling to Plasmon-Microcavity Hybridization, Qinghua Song^{1,2}, Pin Chieh Wu², Weiming Zhu², wu zhang², Zhongxiang shen², Qing Xuan Liang³, Zhen Chuan Yang⁴, Yu Feng Jin⁴, Yilong Hao⁴, Tarik Bourouina⁵, Yamin Leprince-Wang¹, Ai-Qun Liu²; ¹UPEM, Université Paris-Est, France; ²Nanyang Technological Univ., Singapore; ³School of Mechanical Engineering, Xi'an Jiaotong Univ., China; ⁴National Key Lab of Science and Technology on Micro/Nano Fabrication, Inst. of Microelectronics, Peking Univ., China; ⁵ESYCOM, ESIEE, Université Paris-Est, France. We report a coupling mode transition from pure plasmon coupling to plasmon-microcavity hybridization in THz using liquid metal whose shape can be tuned, not only from disk to droplet, but also from 2D to 3D.

STu4H.8 • 17:45

Single Nanowire Terahertz Detectors, Kun Peng¹, Patrick Parkinson², Lan Fu¹, Qiang Gao¹, Nian Jiang¹, Ya-Nan Guo¹, Fan Wang¹, Hannah Joyce^{2,3}, Jessica Boland², Michael Johnston², Hark Tan¹, Chennupati Jagadish¹; ¹The Australian National Univ., Australia; ²Univ. of Oxford, UK; ³Univ. of Cambridge, UK. Photoconductive terahertz detectors based on single GaAs/AlGaAs nanowire were designed, fabricated and incorporated into the pulsed time-domain technique, showing a promise for nanowires in terahertz applications such as near-field terahertz sensors or on-chip terahertz micro-spectrometers.

16:30–18:00 IEEE Journal of Quantum Electronics Celebrates 50 Years, Willow Glen, Marriott

NOTES

Blank area for notes.

CLEO: Science & Innovations

CLEO: Applications & Technology

CLEO: Science & Innovations

STu4I • Mid-IR Photonics—Continued

STu4I.7 • 17:30

All-optical Modulation in Germanium-on-silicon Waveguides in the Mid-infrared, Li Shen¹, Noel Healy¹, Collin Mitchell¹, Jordi Penades¹, Milos Nedeljkovic¹, Goran Mashanovich¹, Anna C. Peacock¹; ¹Optoelectronics Research Centre, Univ. of Southampton, UK. All-optical modulation is demonstrated in low loss germanium-on-silicon waveguides at mid-infrared wavelengths. The results indicate the suitability of this platform for optical signal processing in this long wavelength regime.

STu4I.8 • 17:45

Broadband Mid-Infrared Frequency Comb Generation in a Si₃N₄ Microresonator, Kevin Luke¹, Yoshitomo Okawachi¹, Michael Lamont¹, Alexander L. Gaeta¹, Michal Lipson¹; ¹Cornell Univ., USA. We demonstrate broadband frequency comb generation in the mid-infrared from 2.3 to 3.5 μm in a Si₃N₄ microresonator with Q=850,000 fabricated using an optimized process for decreasing intrinsic losses and overcoming stress limitations.

ATu4J • Environmental Sensing—Continued

ATu4J.6 • 17:30

Advancing a Deep Sea Near-Infrared Laser Spectrometer for Dual Isotope Measurements, Anna P. Michel¹, Scott Wankel¹, Jason Kapit¹, Peter Girguis², Manish Gupta³; ¹Woods Hole Oceanographic Institution, USA; ²Harvard Univ., USA; ³Los Gatos Research, USA. A deep-sea near-infrared laser-based sensor, utilizing off-axis integrated cavity output spectroscopy, was enhanced to achieve in situ sensing dual isotope sensing (δ¹³CO₂, δ¹³CH₄) of both fluid and bubble samples.

ATu4J.7 • 17:45

Advances in Diode Laser Based Lidar for Profiling Atmospheric Water Vapor, Scott M. Spuler¹, Kevin Repasky², Bruce Morley¹, Drew Moen², Tammy Weckwerth¹, Matthew Hayman¹, Amin Nehrir²; ¹National Center for Atmospheric Research, USA; ²Electrical and Computer Engineering, Montana State University, USA; ³NASA Langley Research Center, USA. The design of an advanced diode laser based differential absorption lidar (DIAL) is discussed which is capable of operation over a wide range atmospheric conditions. The instrument was field tested for 50 days and the results were compared to collocated instrumentation.

STu4K • Biosensing—Continued

STu4K.6 • 17:30

High Contrast Grating Resonator for Label-Free Biosensor, Tianbo Sun¹, Shu Kan², Gerard Marriott², Connie J. Chang-Hansnain¹; ¹EECS, Univ. of California, Berkeley, USA; ²Bioengineering, Univ. of California, Berkeley, USA. We present a novel label-free biosensor using Si-based high-contrast grating resonator with Q ~3000. The biosensor is coupled using a single-mode fiber and realizes high sensitivity in the specific detection of target proteins at 100pg/ml.

STu4K.7 • 17:45

On-chip Integrated Differential Optical Microring Biosensing Platform Based on a Dual Lamina Flow Scheme, Dongwan Kim¹, Paula Popescu¹; ¹Applied Physics, Caltech, USA. We propose an on-chip integrated differential optical silicon nitride microring biosensing platform which uses a dual lamina flow scheme. This platform reduces the fabrication complexity involved in the fabrication of the reference resonator.

STu4L • Higher-Order Modes & Mode Coupling in Fiber—Continued

STu4L.6 • 17:30

Fano Resonance in Inhibited Coupling Kagome Fiber, Abhilash Amsanpally¹, Benoît Debord¹, Meshaal Alharbi¹, Ekaterina Ilinova¹, Luca Vincetti², Frédéric Gérôme¹, Fetha Benabid¹; ¹Xlim Research Inst., UMR CNRS 7252, Univ. of Limoges, France; ²Dept. of Engineering, Univ. of Modena and Reggio Emilia, Italy. We report on the first experimental observation of Fano resonances in inhibited-coupling guiding Kagome fiber. A high-spectral resolution fiber-transmission showed the typical Fano asymmetric feature and a high dynamic-range near-field imaging resolved the core-cladding coupling.

STu4L.7 • 17:45

Triple-cup Hypocycloid-Core Inhibited-Coupling Kagome Hollow-Core Photonic Crystal Fiber, Luca Vincetti^{1,2}, Benoît Debord¹, Meshaal Alharbi¹, Frédéric Gérôme¹, Fetha Benabid¹; ¹GPPMM Xlim Research Inst., UMR CNRS 7252, Univ. of Limoges, France; ²Dept. of Engineering, Univ. of Modena and Reggio Emilia, Italy. We report on design and fabrication of a new hypocycloid core-contour Kagome HC-PCF based on a triangular-like shaped core exhibiting smaller effective area and comparable confinement loss than previous hypocycloid core-contour Kagome fibers.

16:30–18:00 IEEE Journal of Quantum Electronics Celebrates 50 Years, Willow Glen, Marriott

NOTES

18:00–20:00

JTU5A • Poster Session I and Conference Reception

JTU5A.1

Enhanced optical limiting effects in multi-photon absorbers using cylindrical vector beams, Gu Bing¹, Jia-Lu Wu¹, Ning Sheng¹, Dahui Liu¹, Yiping Cui¹; ¹*Southeast Univ., China*. Optical limiting effects can be enhanced by designing nonlinear optical materials and by exploiting various limiting mechanisms. Here, we present the enhancement of optical limiting effects by manipulating the polarization distribution of the light field.

JTU5A.2

Multi-nonlinear Effects in a Two-crystal Optical Parametric Oscillator, Yuwei Jin¹, Simona M. Cristescu¹, Frans J. Harren¹, Julien Mandon¹; ¹*Dept. of Molecular and Laser Physics, Radboud Univ. Nijmegen, Netherlands*. We present the observation of several nonlinear effects in a two-crystal femtosecond optical parametric oscillator. Unusual parametric processes are observed when the total cavity length is detuned up to 7.3-mm within this synchronously pumped optical parametric oscillator.

JTU5A.3

Observing the effects of Time Ordering in Single Photon Frequency Conversion, Nicolas Quesada¹, John E. Sipe¹; ¹*Univ. of Toronto, Canada*. We show how time ordering effects in single photon frequency conversion (FC) can be revealed by using the fact that the joint conversion amplitude in FC is a nonlinear function of the pump electric field.

JTU5A.4

The Effect of Orbital Angular Momentum on Nondiffracting Optical Pulses, Marco Orignotti¹, Claudio Conti^{2,3}, Alexander Szameit¹; ¹*Friedrich-Schiller Univ IAP, Germany*; ²*Inst. of Complex Systems ISC-CNR, Italy*; ³*Dept. of Physics, Univ. Sapienza, Italy*. We study the effects of orbital angular momentum on a nondiffracting optical pulse, and show that there exist a limit on the amount of OAM that a pulse can carry without modifying its temporal properties.

JTU5A.5

Femtosecond dynamics of a spaser and unidirectional emission from a perfectly spherical nanoparticle, Juan Sebastian Totoro Gongora¹, Andrey Miroshnichenko², Yuri S. Kivshar², Andrea Fratallocchi¹; ¹*PRIMALIGHT, King Abdullah Univ. of Science and Technology (KAUST), Saudi Arabia*; ²*Nonlinear Physics Centre, Research School of Physics and Engineering, Australian National Univ., Australia*. We investigate the femtosecond dynamics of the spaser emission by combining ab-initio simulations and thermodynamic analysis. Interestingly, the emission is characterized by rotational evolution, opening to the generation of unidirectional emission from perfectly spherical nanoparticles.

JTU5A.6

Frequency Comb Generation on a Silicon Chip, Andrei Rogov¹, Evgenii Narimanov¹; ¹*Purdue Univ., USA*. We present a new approach to achieving frequency comb generation on a silicon chip by means of optical switching in microring resonators.

JTU5A.7

A simple method for the measurement of the optical pulse width on-site the mass spectrometer, Tomoko Imasaka¹, Akifumi Hamachi¹, Tomoya Okuno¹, Totaro Imasaka¹; ¹*Kyushu Univ., Japan*. The laser pulse width was measured on-site the mass spectrometer by scanning a dispersion in the pulse compressor. A pulse width of 49 fs measured was close to 35 fs calculated from the spectrum.

JTU5A.8

Radiation Pressure Induced Nonlinear Optofluidics in Liquid Whispering Gallery Mode Resonator, Aram Lee¹, Peng Zhang², Sunghwan Jung², Yong Xu¹; ¹*Electrical and Computer Engineering, Virginia Tech, USA*; ²*Biomedical Engineering and Mechanics, Virginia Tech, USA*. We analyze a nonlinear optofluidic process produced by radiation pressure of a high quality factor whispering gallery mode in a liquid droplet. Using liquid properties that are experimentally attainable, we find that such a process may lead to photon-photon interaction at single photon energy level.

JTU5A.9

Correlated Study of Terahertz Pulse Generation and Plasma Density During Two-Color Filamentation in Air, Jiayu Zhao¹, Yizhu Zhang², Tao Zeng¹, Jing Yang¹, Weiwei Liu¹; ¹*Nankai Univ., China*; ²*Shanghai Advanced Research Inst., China*. The variation of plasma density, which is sensitive to the BBO crystal rotation angle, is systematically investigated in this work. According to our results, the well-known photocurrent model could not reproduce the characteristics of the THz pulse generated in both polarization directions.

JTU5A.10

Internal Conical Diffraction of a Top-hat Beam, Ronan T. Darcy¹, James G. Lunney¹, John Donegan¹; ¹*Trinity College Dublin, Ireland*. The evolution of a beam undergoing internal conical diffraction exhibits a sensitive dependence on the spatial profile of the incident beam. We investigate the case of a top-hat incident beam undergoing conical diffraction.

JTU5A.11

Generation of Versatile Vortex Linear Light Bullet, Xin Huang¹, Qian Cao^{2,3}, Han Li¹, Peiyun Li¹, Andy Chong^{1,2}; ¹*Univ. of Dayton, USA*; ²*Deutsches-Elektronen Synchrotron, Germany*; ³*Dept. of Physics, Univ. of Hamburg, Germany*. We demonstrate a versatile vortex linear light bullet as a vortex Airy-Bessel wave packet for the first time. Its non-varying three-dimensional (3D) vortex field in linear propagation is verified by 3D measurements.

JTU5A.12

Photon pair generation in leaky coupled-resonator optical waveguides via spontaneous four-wave mixing, Mohsen Kamandar¹, Marc M. Dignam¹; ¹*Queen's Univ. at Kingston, Canada*. A fully quantum mechanical formalism is developed to calculate photon pair detection probabilities in leaky coupled-resonator optical waveguide. Using our formalism we have studied the effect of loss on pair evolution as well as higher order pair generations in the system.

JTU5A.13

Surface enhanced nonlinear optics using lithography-free metasurfaces, Kai Liu¹, Tianmu Zhang¹, Dengxin Ji¹, Joseph Murphy¹, Haomin Song¹, Tim Thomay¹, Kebin Shi², Qiaoqiang Gan¹, Alexander Cartwright¹; ¹*State Univ. of New York at Buffalo, USA*; ²*Peking Univ., China*. We demonstrate a strong enhancement of second harmonic generation based on a three-layered super absorbing metasurface consisting of an ultrathin spacer layer sandwiched by an array of random metallic nanoparticles and a metal ground plane.

JTU5A.14

Measuring Orbital Angular Momentum of Light With a Single, Stationary Lens, Samuel N. Alperin¹, Mark E. Siemens¹, Robert D. Niederriter², Juliet Gopinath³; ¹*Dept. of Physics and Astronomy, Univ. of Denver, USA*; ²*Dept. of Physics, Univ. of Colorado, Boulder, USA*; ³*Dept. of Electrical, Computer, and Energy Engineering, Univ. of Colorado, Boulder, USA*. We demonstrate that average orbital angular momentum (OAM) can be measured with a simplified twist parameter measurement technique. This technique uses a stationary apparatus composed of only a cylindrical lens and a CCD.

JTU5A.15

Coherent Artifact Study of Multiphoton Intrapulse Interference Phase Scan, Michelle Rhodes¹, Rick Trebino¹; ¹*Georgia Inst. of Technology, USA*. We study intensity-and-phase measurements of unstable trains of pulses using multiphoton intrapulse interference phase scan (MIIPS). MIIPS retrieves only a coherent artifact and so can under-estimate pulse lengths, but wider measured traces can indicate instability.

JTU5A.16

Parity-Time Anti-Symmetric Parametric Amplifier, Diana A. Antonosyan¹, Alexander S. Solntsev¹, Andrey A. Sukhorukov¹; ¹*Nonlinear Physics Centre, Research School of Physics and Engineering, Australian National Univ., Australia*. We predict that directional coupler of quadratically nonlinear and lossy waveguides can perform ultrafast signal switching and parametric amplification, using the pump-controlled breaking of the parity-time anti-symmetry associated with nonlinear wave mixing.

JTU5A.17

Spectral analysis of the optical pulses produced by the interaction of optical and THz pulses in a ZnTe crystal, Marion Cornet¹, Jérôme Degert¹, Emmanuel Abraham¹, Eric Freysz^{1,2}; ¹*Université de Bordeaux, France*; ²*LOMA, Université de Bordeaux, UMR 5798, CNRS, France*. The spectra of the optical pulses generated during the interaction of THz and optical pulses in a ZnTe crystal indicate that, besides sum and difference frequency mixing, spectral components associated to cross-phase modulation are produced.

JTU5A.18

Waves of constant intensity and their instabilities in non-Hermitian photonic structures, Konstantinos Makris^{2,1}, Ziad Musslimani³, Demetrios N. Christodoulides⁴, Stefan Rotter²; ¹*Princeton Univ., USA*; ²*Inst. for Theoretical Physics, Vienna Univ. of Technology, Austria*; ³*Mathematics, Florida State Univ., USA*; ⁴*College of Optics-CREOL, Univ. of Central Florida, USA*. We study, for the first time, the modulation instability of a new class of constant intensity solutions (valid also for linear non-hermitian media) of nonlinear Schrödinger equation in the presence of a complex optical potential.

JTU5A.19

Composite multi-vortex diffraction-free beams and van Hove singularities in honeycomb lattices, Vassilis Paltoglou¹, Zhigang Chen², Nikolaos K. Efremidis¹; ¹*Dept. of Mathematics and Applied Mathematics, Univ. of Crete, Greece*; ²*Dept. of Physics and Astronomy, San Francisco State Univ., USA*. We find that honeycomb lattices support diffraction-free multi-vortices above the van-Hove singularity. Exact solutions for the spinor components are obtained in the Dirac limit. Right at the singularity the solutions become infinite extend stripes.

JTU5A.20

Hybrid Chalcogenide Microstructured Optical Fiber for Mid-infrared Soliton Self-frequency Shift, Tonglei Cheng¹, Yasuhiro Kanou¹, Xiaojie Xue¹, Dinghuan Deng¹, Lei Zhang¹, Lai Liu¹, Morio Matsumoto², Hiroshige Tezuka², Takenobu Suzuki¹, Yasutake Ohishi¹; ¹*ofmlab, Japan*; ²*Furukawa Denshi Co., Ltd., Japan*. A hybrid AsSe₂-As₂S₃ microstructured optical fiber is fabricated by the rod-in-tube drawing technique. Soliton self-frequency shift with a soliton center wavelength from ~2.986 to 3.419 nm is observed at the pump wavelength of ~2.8 nm.

JTU5A.21

Tunable Pulse Compression by Nonlinear Cross-Phase Modulation using Cascaded Electro-Optic Effects, Guangzhen Li¹, Haowei Jiang¹, Xianfeng Chen¹, Yuping Chen¹; ¹*Shanghai Jiaotong Univ., China*. We demonstrate the first pulse compression induced by cross-phase modulation through cascading Pockels effects. It provides first practically useful solutions for enhanced effective third-order nonlinearity independent of light intensity.

JTU5A.22

Second Harmonics of Phase Locked Laser Arrays, Chene Tradonsky¹, Nir Davidson¹, Vishwa Pal¹, Asher A. Friesem¹, Micha Nixon¹, Eitan Ronen¹, Ronen Chrikri¹; ¹*Weizmann Inst. of Science, Israel*. Second harmonic generation in coupled laser arrays is exploited to convert out-of-phase lasers into in-phase lasers and reveal hitherto unknown properties of some laser array geometries.

18:00–20:00

JTU5A • Poster Session I and Conference Reception

JTU5A.23

Tapered Seven-core Photonic Crystal Fiber for Flat Supercontinuum Generation, Xing Luo¹, Jinggang Peng¹, Lan Chen¹, Luyun Yang¹, Nengli Dai¹, Haiqing Li¹, Jinyan Li¹; ¹Wuhan National Lab for Optoelectronics, China. We report the broadband supercontinuum (SC) generation in a tapered seven-core photonic crystal fiber (PCF). The introducing of a section of taper waist dramatically alters the group velocity and making the SC flatter.

JTU5A.24

Mechanism of THz Generation from Graphite, Yan Yin^{3,1}, Tong Ye³, Yiwen E³, Yuping Yang², Sheng Meng³, Li Wang^{3,1}; ¹Cooperative Innovation Centre of Terahertz Science, China; ²Central Univ. for Nationalities, China; ³Inst. of Physics, CAS, China. We employ an electric gating method to modulate the surface field of graphite and study the THz generation. The result reveals the mechanism, the similarities and differences to semiconductors, and the effective mass difference of electrons and holes.

JTU5A.25

Quantum Nanoantennas for Making Nonlinear and Self-Modulatable Metasurface, Mohamed Farhat¹, Pai-Yen Chen²; ¹King Abdullah Univ of Science & Tech, Saudi Arabia; ²Wayne State Univ., USA. We investigate the plasmonic nanodipole antenna with sub-microscopic nanogap. Relevant quantum conductivities, including linear and nonlinear components, are observed due to the photon-assisted quantum tunneling, realizing optical nano-radiators with enhanced amplitude and frequency modulations.

JTU5A.26

All Periodically-poled Crystals Based Source of Tunable, Continuous-wave, Single-frequency, Ultraviolet Radiation, Aadhi A^{1,2}, Apurv Chaitanya N^{1,2}, Ravindra pratap singh¹, Goutam Kumar Samanta¹; ¹Physical Research Lab, India; ²Indian Inst. of Technology-Gandhinagar, India. We report on all periodically-poled crystals based singly-resonant optical parametric oscillator (SRO) generating continuous-wave, single-frequency, tunable UV radiation with maximum output power of 336mW in 18.5 MHz line-width at 399.2nm. It has tunability of 18nm.

JTU5A.27

A Novel Graphene-Silicon Hybrid Waveguide for Nonlinearity Enhancement in Near-Infrared Band, Qiang Jin¹, Jiamei Lu¹, Qiang Yan¹, Xibin Li¹, Qianyu Gao¹, Shiming Gao¹; ¹Zhejiang Univ., China. A novel graphene-silicon hybrid waveguide is proposed to enhance the nonlinearity in near-infrared band using a MoO₃ overlayer for light confinement. A four-wave mixing efficiency of -27.3 dB is numerically obtained in a 25- μ m-long waveguide.

JTU5A.28

Chemical Vapor Deposition (CVD) of Graphene for Four-Wave-Mixing (FWM) Based QPSK Wavelength Conversion, Xiao Hu¹, Andong Wang¹, Mengqi Zeng², Chengcheng Gui¹, Lei Fu², Jing Wang¹; ¹Wuhan National Lab for Optoelectronics, Huazhong Univ. of Science & Technology, China; ²College of Chemistry and Molecular Science, Wuhan Univ., China. We experimentally demonstrate FWM based wavelength conversion of a 10 Gbaud/s QPSK signal with graphene grown by CVD method. The observed OSNR penalty is around 1 dB for QPSK wavelength conversion.

JTU5A.29

Nonlinear Optical Properties Of A Graphene-Polyvinyl Alcohol Composite From 1550 nm To 2400 nm, Giorgos Demetriou¹, Fabio Biancalana¹, Henry T. Bookey^{2,1}, Ajay Kar¹; ¹Inst. of Photonics and Quantum Sciences, Heriot Watt Univ., UK; ²Fraunhofer CAP, UK. The nonlinear optical properties of a graphene-Polyvinyl alcohol (G-PVA) composite are studied in the femtosecond temporal regime by employing the Z-scan technique. The nonlinear coefficients β_{eff} , n_{eff} and n_2 are calculated via numerical fitting.

JTU5A.30

1.2 W-average-power, Yb-fiber-pumped, Picosecond Ultraviolet Source at 355 nm Based on BiB₂O₆, Suddapalli Chaitanya Kumar¹, Enrique sanchez Bautista¹, Majid Ebrahim-Zadeh^{1,2}; ¹ICFO - The Inst. of Photonic Science, Spain; ²Instituto Catalana de Recerca i Estudis Avancats (ICREA), Pas-seig Lluís Companys 23, Spain. We report a compact, stable, 79.5-MHz, Yb-fiber-based, picosecond UV source generating 1.2-W of power at 355 nm with a stability better than 0.4% rms over 3 hours, and pointing stability <45 μ rad in good spatial-beam-quality.

JTU5A.31

Kerr nonlinearity of Thulium-doped fiber near 2 μ m, Svyatoslav Kharitonov¹, Adrien Billat¹, Ludovic Zulliger¹, Steevy Cordette¹, Armand Vedadi¹, Camille-Sophie Brès¹; ¹STI-IEL, Photonic Systems Lab (PHOSL), EPFL, Switzerland. The nonlinear coefficient and group velocity dispersion of a thulium-doped fiber near 2 μ m are evaluated via four-wave mixing. Nonlinearity of thulium-doped fiber can be used for the design of doped-fiber lasers in this spectral region.

JTU5A.32

Impact of Higher-Order Dispersion on the Performance of a Kerr Frequency Comb as Affected by the Generated Dispersive Wave, Changjing Bao¹, Lin Zhang², Yan Yan¹, Andrey Matsko³, Guodong Xie¹, Long Li¹, Lionel Kimerling², Jurgen Michel², Lute Maleki³, alan willner¹; ¹Dept. of Electrical Engineering, Univ. of Southern California, USA; ²Dept. of Materials Science and Engineering, MIT, USA; ³OEwaves Inc., USA. The dispersive wave generated from the higher-order dispersion perturbation is found to limit the Kerr comb performance in microring resonators. A negative fourth-order dispersion can potentially reduce the effect of dispersive wave.

JTU5A.33

1 MW peak power at 266 nm in nonlinear YAl₃(BO₃)₄ (YAB) single crystal, Lihe Zheng¹, jinlei ren², Pascal Loiseau², Gerard Aka², Takunori Taira¹, Daniel Rytz²; ¹Inst. for Molecular Science, Japan; ²PSL Research Univ., Inst. de Recherche de Chimie Paris IRCP, Chimie ParisTech, France; ³FEE GmbH, Germany. YAl₃(BO₃)₄ crystal enables the highest UV power of 1.8 MW and shortest pulse of 118 ps with power conversion efficiency of 37 % at 266 nm by using LBO crystal and Nd:YAG/Cr:YAG microchip laser.

JTU5A.34

Phase-matching properties of GaS_{0.4}Se_{0.6} for difference-frequency generation in the 100.4-1030.6 μ m range, Kiyoshi Kato¹, Valentin Petrov², Nobuhiro Umemura¹; ¹Chitose Inst of Science and Technology, Japan; ²Nonlinear optics and ultrafast spectroscopy, Max-Born Inst., Germany. This paper reports the phase-matching properties of GaS_{0.4}Se_{0.6} for DFG between a Nd:YAG laser and a Nd:YAG laser-pumped BBO/OPO in the 100.4-1030.6 μ m range and refines the Sellmeier equations for GaS_xSe_{1-x} (x=0, 0.4, and 1.0).

JTU5A.35

Real-time detection of formaldehyde using PPLN-based mid-infrared laser for study of sick house syndrome, Masaki Asobe¹, Yutaro Takemiya¹, Shoutsu Rin¹, Yuhei Matsuya¹, Teruyo Aoki¹, Akira Katoh¹, Ryuta Someya¹, Akira Tokura², Hirokazu Takenouchi², Shigeru Yamaguchi¹; ¹Tokai Univ., Japan; ²NTT Device Technology Labs, Japan. We studied the detection of formaldehyde using a compact 3-mm DFG light source based on a PPLN waveguide. Single-pass DFG of laser diodes enables wavelength modulation spectroscopy and real-time detection.

JTU5A.36

2D Quadratic Nonlinear Photonic Crystal for Pulsed Orange Generation in a Dual-Wavelength Nd:YVO₄ Laser, Yen-Hung Chen¹, Wei-Kun Chang¹, Hung-Ping Chung¹, Pin-Yu Chou¹; ¹National Central Univ., Taiwan. A novel LiNbO₃ 2D aperiodic nonlinear photonic crystal was constructed to work simultaneously as a dual-wavelength Q-switch and a sum frequency generator in a Nd:YVO₄ laser. ~531-W peak-power orange light was obtained with this laser.

JTU5A.37

Dynamic Instabilities of Self-Excited Oscillation in Optical Ring Resonator, Jianguo Huang^{1,2}, Bin Dong², Hong Cai³, Yuandong Gu³, Jiuhui Wu¹, Tianing Chen¹, Ai-Qun Liu²; ¹Xian Jiaotong Univ., China; ²Nanyang Technological Univ., Singapore; ³Inst. of Microelectronics, A*STAR, Singapore. We demonstrated the nonlinear dynamic instabilities in the self-excited oscillations in the silicon ring resonators. A hysteresis loop is observed both in forward and backward tuning of the input wavelength and the input power.

JTU5A.38

Low-threshold collinear parametric Raman comb generation in calcite, Michal Jelinek¹, Vaclav Kubecek¹, Helena Jelinkova¹, Sergej Smetanin²; ¹Czech Technical Univ. in Prague, Czech Republic; ²Prokhorov General Physics Inst. of Russian Academy of Sciences, Russia. The optimal conditions of low-threshold collinear parametric Raman-comb generation in calcite from the 477-nm second anti-Stokes to 692-nm fourth Stokes component under 20-ps laser excitation at 532-nm are demonstrated in good agreement with theoretical model.

JTU5A.39

High-power silica-based Raman fiber amplifier at 2147 nm, Jiang Liu¹, Fangzhou Tan¹, Hongxing Shi¹, Pu Wang¹; ¹Beijing Univ. of Technology, China. We demonstrated a silica-based Raman all-fiber amplifier delivering as much as 14.3W of output power at a wavelength of 2147nm. The conversion efficiency for the Raman fiber amplifier was 38.5% from 1963nm to 2147nm.

JTU5A.40

Raman scattering and Kerr shock induced breather soliton in Kerr frequency comb generation, Chengying Bao¹, Changxi Yang¹, Lin Zhang², Lionel Kimerling², Jurgen Michel²; ¹Tsinghua Univ, USA; ²MIT, USA. We found Raman scattering and Kerr shock tend to induce breather soliton in Kerr frequency comb generation. They will also degrade the coherence property of the excited breather soliton.

JTU5A.41

Spatial and Spectral Ellipsometry of Light Filaments, Ladan Arissian¹, Shermineh Rostami¹, Jean-Claude Diels¹; ¹Univ. of New Mexico, USA. Measuring the continuum polarization against pulse ellipticity of a laser filament is introduced as a new paradigm for quantifying nonlinearities in filamentation such as ionization paths, molecular alignment, nonlinear index and field intensity.

JTU5A.42

Broadband Phase-Matched Second-Harmonic Generation via Dielectric-Loaded Surface Plasmon Polariton Waveguide, Sangsik Kim¹, Minghao Qi¹; ¹School of Electrical and Computer Engineering and Birk Nanotechnology Center, Purdue Univ., USA. We present the concept of broadband phase-matching for second-harmonic generation with a dielectric-loaded surface plasmon polariton waveguide. Nonlinear coupled mode analysis is conducted to evaluate the broadband response and the conversion efficiency of second-harmonic generation.

JTU5A.43

Chip-based frequency conversion by four-wave-mixing Bragg scattering in Si₃N₄ microrings, Qing Li^{2,1}, Marcelo I. Davanco², Kartik Srinivasan²; ¹Maryland NanoCenter, Univ. of Maryland, USA; ²National Inst. of Standards and Technology, USA. We demonstrate frequency conversion via four-wave-mixing Bragg scattering in Si₃N₄ microrings. The intra-chip conversion efficiency in 40- μ m-radius microrings is -17 dB, a >40 dB increase compared to 1.2-cm-long Si₃N₄ waveguides under equal pumping conditions.

18:00–20:00

JTU5A • Poster Session I and Conference Reception

JTU5A.44

Full (3+1)D Split-Step Technique for Spatial Mode Analysis of White Light Generation in Bulk Kerr-Media, Haider Zia¹, Aradhana Choudhuri¹, Ingmar Hartl², R.J. Dwayne Miller^{1,3}, Axel Ruehl²; ¹Max Planck Inst. for the Structure and Dynamics of Matter, Germany; ²Deutsches Elektronen-Synchrotron (DESY), Germany; ³Dept.s of Chemistry and Physics, Univ. of Toronto, Canada. We present a novel full (3+1)D split-step numerical model for white-light generation including all major physical effects. We present a detailed spatial mode analysis and derive imaging systems to re-shape the spatial distribution.

JTU5A.45

Silicon Waveguide based Two-Input Simultaneous Quaternary Hybrid Doubling/Subtraction (2A-B, 2B-A) Using Degenerate FWM and QPSK, Chengcheng Gui¹, Jian Wang¹; ¹Wuhan National Lab for Optoelectr, China. By exploiting two degenerate four-wave mixing in a silicon waveguide and quadrature phase-shift keying (QPSK) signals, we experimentally demonstrate two-input (A, B) simultaneous optical quaternary hybrid doubling/subtraction (2A-B, 2B-A).

JTU5A.46

Efficient and ultra-compact computational metamaterials for integrated photonics and free-space applications, Bing Shen¹, Peng Wang¹, Randy C. Polson¹, Rajesh Menon¹; ¹Univ. of Utah, USA. We applied nonlinear optimization to design metamaterials as free-space polarizers, integrated fiber couplers, polarization splitter/rotators, etc. Such devices exhibit at least comparable or better performance than their conventional counterparts, but occupy a much smaller size.

JTU5A.47

Photodetector based on lateral graphene p-n junction created by electron-beam irradiation, Xuechao Yu¹, Qi Jie Wang^{1,2}; ¹School of Electrical and Electronic Engineering, OPTIMUS, Photonics Centre of Excellence, Singapore; ²Centre for Disruptive Photonic Technologies, Nanyang Technological Univ., Singapore. Graphene p-n junctions fabricated by electron irradiation method that induces n-type doping in the intrinsic p-type graphene are demonstrated. Photoresponse was obtained because the photoexcited electron-hole pairs can be separated in the graphene p-n junction by the built-in potential.

JTU5A.48

Light Confinement in Hyperuniform Photonic Slabs: High-Q Cavities and Low-Loss Waveguides, Timothy Amoah¹, Marian Florescu¹; ¹Univ. of Surrey, UK. Using FDTD and band structure simulations, we demonstrate efficient confinement of TE radiation in high-Q optical-cavities and low-loss waveguides in planar hyperuniform-disordered architectures based on a design strategy that has potential to be a general purpose platform for optical microcircuits.

JTU5A.49

Tunable Spectral Engineering of Coupled Silicon Microcavities, Mario C. Souza¹, Luis A. Barea¹, Gustavo Wiederhecker¹, Antonio A. von Zuben¹, Newton C. Frateschi¹; ¹Universidade Estadual de Campinas, Brazil. We demonstrate the generation and control of optical resonance mode-splitting arising from a single-notch resonances using coupled silicon microring resonators with electrically controlled counter-propagating mode excitation.

JTU5A.50

Efficiency Improvement of Crystalline-Si Solar Cell Using the Combination of Europium Doped Silicate Phosphors Down Shifting and SiO₂ Antireflective Coating, Guo-Chang Yang¹, Wen-Jeng Ho¹, Chien-Wu Yeh¹, Rwei-Siang Sue¹, Yu-Tang She¹, Chia-Hua Hu¹, Yu-Jie Deng¹; ¹National Taipei Univ. of Technology, Taiwan. Impressive efficiency enhancement of 15.38% of crystalline-silicon solar-cell with Eu-doped silicate-phosphors and SiO₂-layer using spin-on technique is demonstrated. Reflectance, external quantum efficiency, and photovoltaic I-V characteristics are used to examine the down-shifting effectiveness.

JTU5A.51

High-index-contrast Grating Mirrors Implemented on the Polysilicon Gates of a Standard Bulk CMOS Process, Yung-Jr Hung¹, Ming-Chun Hsieh¹; ¹National Sun Yat-sen Univ., Taiwan. High-index-contrast grating implemented in bulk CMOS can provide 95% surface reflectivity with 50 nm bandwidth for TE polarization. Higher reflectivity is achievable by creating air cavities beneath HCGs to avoid the optical leakage to the substrate.

JTU5A.52

A Compact Polarization Beam Splitter Based on Augmented Low Index Guiding Structure, Xiao Sun¹, Muhammad Z. Alam¹, J. Stewart Aitchison¹, Mo Mojahedil¹; ¹Univ. of Toronto, Canada. A compact broadband polarization beam splitter based on the augmented low index guiding scheme is proposed. TM and TE modes are separated in two layers with the TM mode confined in the lower index layer.

JTU5A.53

Highly Compact Polarization Insensitive Strip-Slot Waveguide Mode Converter, Qingzhong Deng¹, Qiaojing Yan¹, Lu Liu¹, Xinbai Li¹, Zhiping Zhou¹; ¹State Key Lab of Advanced Optical Communication Systems and Networks, School of Electronics Engineering and Computer Science, Peking Univ., China. A polarization insensitive strip-slot waveguide mode converter with large fabrication tolerance is proposed based on symmetric multimode interference (MMI). This converter can achieve efficient strip-slot waveguide coupling (TE:94.9%, TM:94.6%) while the dimensions are only 1.18μm×3μm.

JTU5A.54

Triple Metal-Film Subwavelength Gratings on Both Sides of a Silicon Substrate for Mid-Infrared Polarizers, Kazuo Shiraishi¹, Shogo Higuchi¹, Hiroshi Kakinuma¹, Jun Shimizu¹, Hidehiko Yoda¹, Hiroshi Ohno¹; ¹Utsunomiya Univ., Japan. Triple metal-film subwavelength gratings on both sides of a thin silicon substrate are fabricated for polarizers in the mid-infrared. An extinction ratio of higher than 30dB together with insertion loss of 2 dB is obtained.

JTU5A.55

Nanobump Microresonators at the Fiber Surface, Leonid A. Kochkurov¹, Misha Sumetsky¹; ¹Aston Univ., UK. It is shown that an asymmetric nanometer-high bump at the fiber surface causes strong localization of whispering gallery modes. Our theory explains and describes the experimentally observed nanobump microresonators in Surface Nanoscale Axial Photonics.

JTU5A.56

Surface Mode in Photonic Crystal Fishbone Nanocavity for Highly Efficient Optical Sensing and Trapping, Tsan-Wen Lu¹, Po-Tsung Lee¹; ¹National Chiao Tung Univ., Taiwan. A novel one-dimensional photonic crystal fishbone (FB) with surface wave is proposed. Via designing high quality FB nanocavity, high sensitivity for optical sensing and strong optical force for optical trapping in fluidics can be obtained.

JTU5A.57

Design of On-Chip Dielectric Elliptical Meta-Reflectarray for Bessel Beams Generation and N-Fold Orbital Angular Momentum (OAM) Multicasting, Jing Du¹, Zhidan Xu¹, Long Zhu¹, Shuhui Li¹, Jian Wang¹; ¹Huazhong Univ. of Sci. and Tech., China. We design dielectric meta-reflectarrays to realize Bessel beams generation and OAM multicasting. The purities of generated Bessel beams are higher than 0.93 and the crosstalks between the multicasted OAM channels and their neighboring ones are less than -14 dB.

JTU5A.58

Microring resonator design with improved quality factors using quarter Bezier curves, Hamed Pishvai Bazargani¹, José Azaña¹, Lukas Chrostowski², Jonas Flueckiger²; ¹INRS, Canada; ²UBC, Canada. A new design concept to improve the quality factor of ring resonators using quarter Bezier curves has been investigated. Quality factor improvements by 3 times have been achieved for a 3-μm radius ring resonator.

JTU5A.59

Optimized emission in nanorod arrays through quasi-aperiodic inverse design, Patrick Anderson¹, Michelle Povinelli¹; ¹Univ. of Southern California, EE, USA. We investigate a new class of quasi-aperiodic nanorod structures for emission enhancement. Using inverse design we identify one optimized structure which produces a 1.48X enhancement in extracted power relative to a periodic array.

JTU5A.60

Lasing in optimized two dimensional iron-nail-shape nanorod photonic crystals, Soon-Yong Kwon¹, Seul-Ki Moon¹, Jae-Hyuck Choi², Se-Hwan Jang², Kwang-Yong Jeong², Hong-Gyu Park², Jin-Kyu Yang¹; ¹Kongju National Univ., Korea; ²Korea Univ., Korea. We demonstrated lasing at the band edges in optimized two-dimensional iron-nail-shape nanorod photonic crystals by optical pumping at room temperature. The size of the nanorod gradually increased toward the edge of the pattern in order to reduce the optical loss in horizontal direction.

JTU5A.61

Optomechanical Crystal Cavity with Ultra-small Effective Motion Mass based on Split-nanobeam Structure, Yeping Zhang¹, Kaiyu Cui¹, Zhilei Huang¹, Xue Feng¹, Yidong Huang¹, Fang Liu¹, Wei Zhang¹; ¹Tsinghua Univ., China. A split-nanobeam optomechanical crystal cavity is proposed. By adjusting the split width, an ultra-small effective motion mass as small as 5.2fg is realized with a high mechanical frequency of 7.55GHz.

JTU5A.62

Mode Conversion Based on Dielectric Metamaterial in Silicon, David Ohana¹, Boris Desiatov¹, Noa Mazurski¹, Uriel Levy¹; ¹The Hebrew Univ. of Jerusalem, Israel. We design, analyze and experimentally demonstrate a novel mode converter in silicon waveguide based on a graded index co-directional grating coupler. Numerical simulations results and microscope images of modes' far field are presented and discussed.

JTU5A.63

Design of Integrated Circularly Polarized Orbital Angular Momentum (OAM) Beam Emitter Using Microring with Interleaved Tailored Angular Gratings, Jingwen Ma¹, Jing Du¹, Xiao Hu¹, Jian Wang¹; ¹Wuhan National Lab for Optoelectr, China. By exploiting microring with interleaved tailored angular gratings, we present a simple design of integrated circularly polarized orbital angular momentum (OAM) beam emitter. The Stokes parameter S₃ is above 0.97 with high OAM purity of 99.84%.

JTU5A.64

Multifunctional, tunable and wideband all-filter based on θ shaped microfiber resonator, Zhilin Xu¹, Qizhen Sun^{1,2}, Borui Li¹, Yiyang Luo¹, Wengao Lu¹, Haipeng Luo¹, Deming Liu¹, Lin Zhang²; ¹Huazhong Univ. of Science and Technology, China; ²Aston Univ., UK. A compact θ shaped microfiber resonator for multifunctional, tunable and wideband filter is proposed. The filtering performance of reflection and transmission spectra depending on coupling coefficients and cavity length is theoretically investigated and experimentally demonstrated.

JTU5A.65

Photocurrent Density Enhancement of a III-V Inverse Quantum Dot Intermediate Band Gap Photovoltaic Device, Jeongdong Kim¹, Xiaogang Chen¹, Xiuling Li¹, James Coleman¹; ¹Univ. of Illinois, USA. We measured the photocurrent density of quantum well (QW) and inverse quantum dot (IQD) photovoltaic devices. The photocurrent per unit area of IQD was enhanced as the carrier confinement became stronger with increasing diameter.

18:00–20:00

JTU5A • Poster Session I and Conference Reception

JTU5A.66

Plasmonic Mode-Evolution-based Polarization Rotator and Coupler, Sangsik Kim¹, Minghao Qi¹; ¹*School of Electrical and Computer Engineering and Birk Nanotechnology Center, Purdue Univ., USA*. A plasmonic mode-evolution-based device rotates the TE mode in silicon waveguide and couples it to the hybrid plasmonic mode with a 92% peak coupling factor and 3-3 dB bandwidth of over 500 nm at near infrared.

JTU5A.67

Aluminum Micro-Patch Arrays for Highly-Sensitive Vibration Spectroscopy, Duk-Yong Choi¹, Barry Luther-Davies¹, Vivek R. Shrestha², Sang-Shin Lee²; ¹*The Australian National Univ., Australia*; ²*Kwangwoon Univ., Korea*. We demonstrate collective plasmonic resonance from aluminum micro-patch arrays patterned on slide glass. This cost-efficient device can be applied in extremely sensitive vibration spectroscopy.

JTU5A.68

High Sensitivity Dark Mode Plasmonic Resonance of Gold Nanoantennas Arrays in Evanescent Waves, Kuo-Ping Chen¹, Yi-Hsun Chen¹, Yu-Lun Kuo¹, Zhen-hong Yang¹, Che-Yuan Chang¹; ¹*National Chiao-Tung Univ., Taiwan*. Plasmonic dark modes of gold nanoantennas are observed in evanescent waves. Dark mode not only has a higher extinction coefficient but also achieves higher sensitivity to the surrounding environment. The sensitivity of the dark mode is 4.84 times that of the bright mode in figure of merit.

JTU5A.69

Optionally focusing with plasmonic vortex lens, Hailong Zhou¹, Jianji Dong¹, Yifeng Zhou¹, Xinliang Zhang¹; ¹*Wuhan National Lab for Optoelectronics, China*. We present a specific plasmonic vortex lens (PVL) structure to focus the surface plasmon polariton wave on an arbitrary spatial position.

JTU5A.70

Ultrathin High Efficiency Photodetectors Based on Near Field Enhanced Optical Absorption, Moshe Zohar¹, Mark Auslender¹, Shlomo Hava¹; ¹*Ben Gurion Univ. of the Negev, Israel*. Ultrathin photodetectors, comprising a thin film optical absorber between two transparent layers near a quarter-wave high refractive index one and subwavelength grating, are designed to attain ~100% peak spectral absorbance. Near-field enhancement mechanism of the absorption is demonstrated.

JTU5A.71

High visibility on-chip quantum interference of single surface plasmons, Yong-Jing Cai¹, Ming Li¹, Xifeng Ren¹, Chang-Ling Zou¹, Xiao Xiong¹, Hua-Lin Lei¹, Bi-Heng Liu¹, Guo-Ping Guo¹, Guang-Can Guo¹; ¹*Univ of science and technology of China, China*. In this work, the on-chip quantum interference of two single surface plasmons was achieved and the high visibility (greater than 90%) proves the bosonic nature of single plasmons. The effect of intrinsic losses in plasmonic waveguides is also discussed.

JTU5A.72

Nanophotonic Modulator with Bismuth Ferrite as Low-loss Switchable Material, Viktoriia Babicheva^{2,1}, Sergei Zhukovsky^{2,1}, Andrei Lavrinenko²; ¹*ITMO Univ., Russia*; ²*DTU Fotonik, Technical Univ. of Denmark, Denmark*. We propose a nanophotonic waveguide modulator with bismuth ferrite as a tunable material. Due to near-zero losses in bismuth ferrite, modulation with up to 20 dB/μm extinction ratio and 12 μm propagation length is achieved.

JTU5A.73

Optical Modulation of Graphene-Cladded Silicon Photonic Crystal Cavity, Lin Gan¹, Zhe Shi¹, Tinghui Xiao¹, Honglian Guo¹, Zhiyuan Li¹; ¹*CAS Inst. of Physics, China*. We demonstrate all-optical tuning of a graphene-cladded silicon photonic crystal cavity. A continuous-wave laser is focused on the cavity and a large resonant shift is observed. Several physical reasons causing the shift are discussed in details.

JTU5A.74

Plasmonic Enhancement of Eu:Y₂O₃ Luminescence By Al Percolated Layer, Nora Abdellaoui¹, Antonio Pereira¹, Alice Berthelot¹, Bernard Moine¹, Nicholas Blanchard¹, Anne Pillonnet¹; ¹*Institut Lumière Matière, France*. We propose the design of plasmonic nanostructure for Eu³⁺ luminescence enhancement. We control our crystalline structure with a nanosized precision thanks to Eu³⁺ crystalline probe and we show luminescence enhancement thanks to Al Plasmon in UV.

JTU5A.75

Second Harmonic Generation from Symmetric and Asymmetric Gold Nanoantennas, Wei-Liang Chen¹, Fan-Cheng Lin², Jer-Shing Huang², Yu-Ming Chang¹; ¹*Center for Condensed Matter Sciences, National Taiwan Univ., Taiwan*; ²*Dept. of Chemistry, National Tsing Hua Univ., Taiwan*. We measure second harmonic generation (SHG) from symmetric and asymmetric gold nanoantennas and find that asymmetric antennas in fundamental bonding resonance with excitation can lead to four time SHG enhancement than that of symmetric nanoantennas.

JTU5A.76

Phase change dispersion of plasmonic nano-objects, Xie Zeng¹, Haifeng Hu¹, Yongkang Gao², Dengxin Ji¹, Nan Zhang¹, Haomin Song¹, Kai Liu¹, Qiaoqiang Gan¹; ¹*State Univ. of New York at Buffalo, USA*; ²*Alcatel-Lucent Bell Labs, USA*. The phase change dispersion during the surface plasmon wave coupling process was extracted experimentally using a slit-groove interferometer and validated through numerical simulation, enriching the fundamental understanding of plasmonic subwavelength optics on a chip.

JTU5A.77

Near Field Measurements of the Scattering Phase Function with Evanescent Field Excitation, Roxana Rezvani Naraghi^{1,2}, Sergey Sukhov¹, Aristide Dogariu¹; ¹*CREOL, The College of Optics and Photonics, Univ. of Central Florida, USA*; ²*Dept. of Physics, Univ. of Central Florida, USA*. Scattering phase functions of spherical particles excited with evanescent waves are measured using near-field optical scanning microscopy. Polarization dependent cross-sections and asymmetry parameters are determined to improve the predictive capabilities of light transport models.

JTU5A.78

Ruby-Nanocrystal-Enhanced Random Dye Lasers, wan zakhia wan ismail¹, Wan Aizuddin Wan Razali¹, andrei zyagin¹, David Coustts¹, Ewa Goldys¹, Judith Dawes¹; ¹*Macquarie Univ., Australia*. Rhodamine 6G random dye lasers are more efficient with ruby nanocrystal scatterers than with alumina, exhibiting reduced threshold despite the increased absorption of ruby nanocrystals.

JTU5A.79

Topological Darkness Revisited: a Four-dimensional Picture, Haomin Song¹, Xie Zeng¹, Dengxin Ji¹, Nan Zhang¹, Kai Liu¹, Qiaoqiang Gan¹; ¹*The State Univ of New York at Buffalo, USA*. We present a complete description of "topological darkness" in a four-dimensional space regarding optical constants (i.e. n and k) of effective media, wavelengths and incident angles, which is essential for enhanced light-matter interaction in thin-films.

JTU5A.80

Plasmon Optical Trapping in Silicon Nitride Trench Waveguide, Qiancheng Zhao¹, Caner Guclu¹, Yuewang Huang¹, Filippo Capolino¹, Ozdal Boyraz¹; ¹*Univ. of California, Irvine, USA*. Optical trapping by using bowtie antennas deposited on top of a microfluidic SiN trench waveguide is investigated. We show that the presence of plasmonic field enhancement boosts the vertical trapping force by 3 orders of magnitude.

JTU5A.81

Near Total Resonant Light Absorption in a Graphene Monolayer at Multiple Tunable Wavelengths with Aperiodic Multilayer Structures, Iman Zand¹, Ali Haddadpour¹, Christopher Granier¹, Jonathan Dowling¹, Georgios Veronis¹; ¹*Louisiana State Univ., USA*. We investigate a one-dimensional system consisting of a graphene monolayer sandwiched between two aperiodic multilayer structures. We show that such a system can achieve near total resonant light absorption in graphene at multiple tunable wavelengths.

JTU5A.82

Visible Excitation of Surface Plasmon Polariton and Strengthened Nonlinearity in ITO coated Fe:LiNbO₃, Hua Zhao¹, liang li¹, Hao Wang¹, Jingwen Zhang^{1,2}; ¹*Harbin Inst. of Technology, China*; ²*Boston Applied Technologies, Inc., USA*. Anisotropic 2D diffraction orders were observed in ITO coated 1.0-mm thick iron-doped lithium niobate slabs, which can be satisfactorily by excitation of SPPs near ITO/LN interface modified by pyroelectric and bulk photovoltaic effects.

JTU5A.83

Enhancement of Single Quantum Emitters Using Ultra-Widely Tunable Nanofiber Bragg Cavities, Andreas W. Schell^{1,2}, Hideaki Takashima^{3,2}, Shunja Kamioka⁴, Yasuko Oe^{4,2}, Shiro Fujita², Masazumi Fujiwara⁴, Oliver Benson¹, Shigeki Takeuchi^{2,3}; ¹*Humboldt-Universität zu Berlin, Japan*; ²*Dept. of Electronic Science and Engineering, Kyoto Univ., Japan*; ³*Research Inst. for Electronic Science, Hokkaido Univ., Japan*; ⁴*The Inst. of Scientific and Industrial Research, Osaka Univ., Japan*. We introduce nanofiber Bragg cavities fulfilling three important requirements: small mode-volume, wide tuning-range, and efficient fiber-coupling. In a first application, we show enhancement of single quantum emitters such as quantum dots and nitrogen vacancy centers.

JTU5A.84

Surface Plasmonic Array Sensors (SPIAS): From Color Sensing to Surface Enhanced Raman Spectroscopy, Jaspreet Walia¹, Iman Khodadad¹, reza Khorasaninejad¹, Simarjeet Saini¹; ¹*Univ. of Waterloo, Canada*. A periodic arrangement of gold crescents is shown to have very high Raman scattering enhancement factors, ~10⁶, as well as structural color generation properties. This opens up the possibility for a two-level sensing platform which could be tailored for a wide variety of applications.

JTU5A.85

High Temperature Plasmonics: Optical Effects on Different Nanostructures, Alessandro Alabastri¹, Andrea Toma¹, Mario Malerba¹, Francesco De Angelis¹, Remo Proietti Zaccaria¹; ¹*Istituto Italiano di Tecnologia, Italy*. We show the effect of high temperature on the plasmonic properties of metallic nanospheres and nano-rods. It is found that the damping modifications due to temperature change, modify both the near and far field optical response.

JTU5A.86

Greatly Enhanced Kerr Nonlinearity Induced by Subwavelength-Confining Anisotropic Purcell Factors in Plasmonic Nanocavity, hongyi chen¹; ¹*Peking Univ., China*. Combining the coherent effects in quantum optics and anisotropic Purcell factors given by surface plasmons, we theoretically investigate the greatly enhanced Kerr nonlinearity of double lambda atomic system with two vertical dipole moments.

JTU5A.87

A Photonic Crystal Explanation For a Butterfly Wing Color, Alessandro Alabastri¹, Hai Wang¹, Andrea Toma¹, Remo Proietti Zaccaria¹; ¹*Istituto Italiano di Tecnologia, Italy*. We have theoretically explained the origin of the green/yellow colour emitted by the wings of the Teinopalpus Imperialis butterfly. The results well explain why the wings of this kind of butterfly reflect light in the green/yellow region of the optical spectrum.

18:00–20:00

JTU5A • Poster Session I and Conference Reception

JTU5A.88

Control of entanglement of two-level atoms using graphene, ANDREI NEMILENTSAU¹, Seyyed A. Hassani¹, George Hanson¹, Stephen Hughes²; ¹Univ. of Wisconsin Milwaukee, USA; ²Queen's Univ., Canada. Dynamics of two-level atoms (TLAs) above lossy graphene are studied using a master equation model, and improvement of entanglement compared to the vacuum case is demonstrated. Entanglement can be controlled by graphene biasing.

JTU5A.89

Color Hologram Generation Using a Pancharatnam-Berry Phase Manipulating Metasurface, Sajid Choudhury¹, Amr Shaltout¹, Vladimir M. Shalaev¹, Alexandra Boltasheva¹, Alexander V. Kildishev¹; ¹Purdue Univ., USA. We propose a new scheme to generate polychromatic holograms by manipulating the Pancharatnam-Berry phase. Using anisotropic transmission characteristics and tuning the resonant wavelengths of nanoslits, multicolor holograms can be produced for arbitrary RGB images.

JTU5A.90

Femtosecond Nanoplasmonic Dephasing of Individual Silver Nanoparticles, Rachel Glenn¹, Richa Mittal¹, Ilyas Saytashiev¹, Vadim Lozovoy¹, Marcos Dantus^{1,2}; ¹Dept. of Chemistry, Michigan State Univ., USA; ²Dept. of Physics and Astronomy, Michigan State Univ., USA. We detect the coherence of localized surface plasmon resonances in individual silver nanoparticles via accurately delayed femtosecond laser pulses. The Fourier transform of the time-resolved spectra reveals nanoplasmonic coherence components and their corresponding dephasing rates.

JTU5A.91

Fourier Plane Imaging Microscopy, Luis Grave de Peralta¹, Ayrton A. Bernussi¹; ¹Texas Tech Univ., USA. Super-resolution images were obtained using a simple microscope formed by an ultrathin condenser and an objective lens. This was because the Fourier plane images carried more information about the object than real plane images do.

JTU5A.92

Room temperature lasing characteristics in metal-cavity GaN shallow grating and spiral structures, Liao Shu-Wei^{1,2}; ¹National Chiao Tung Univ., Taiwan; ²Dept. of Photonics & Inst. of Electro-Optical Engineering, Taiwan. We demonstrated a metal-cavity GaN spiral structure lasing at room temperature with the threshold power density about 17 W/cm² under circularly polarized pumping condition. The emission wavelength is approximately 363 nm.

JTU5A.93

Tuning metacavity modes by the symmetry breaking of metasurface, hui liu¹; ¹nanjing Univ., China. A metacavity composed from metasurface is designed and experimentally demonstrated. Due to the symmetry breaking of the metasurface, the degeneracy of the different polarized cavity states is lifted. It shifts the resonating frequencies of two polarized cavity modes.

JTU5A.94

Phase control by Graphene metasurface, Zu-Bin Li¹; ¹Nankai Univ., China. We numerically design and study graphene metasurface to modulate the phase of reflective light. And the phase shift from $-\pi$ to π is achieved. By using graphene metasurface, we realize negative reflection and nano focusing.

JTU5A.95

Accurately Simulating Focusing Beams using Monte Carlo Techniques, Brett H. Hokr^{1,2}, Joel Bixler^{1,3}, Gabe Elpers⁴, Byron Zollars⁴, Robert Thomas³, Vladislav Yakovlev¹, Marlan O. Scully^{1,5}; ¹Texas A&M Univ., USA; ²TASC Inc., USA; ³Bioeffects Division, Optical Radiation Branch, 711th Human Performance Wing, Human Effectiveness Directorate, USA; ⁴Nanohmcs, Inc., USA; ⁵Baylor Univ., USA. A simple method for accurately simulating focusing beams, which obey Gaussian optics, in the context of traditional Monte Carlo simulations is presented. This technique will allow rapid implementation into existing Monte Carlo codes.

JTU5A.96

Breaking Malus' Law: Enhancing Asymmetric Light Transmission with Metasurfaces, Cheng Zhang¹, Carl Pfeiffer¹, Taehee Jang¹, Vishva Ray¹, Anthony Grbic¹, L. Jay Guo¹; ¹Univ. of Michigan, USA. A structure providing broadband asymmetric light transmission at 1.5 μm with a suppression ratio of 24:1 is achieved with a metasurface consisting of three cascaded layers of gold nano-wires, with a total thickness of $N/5$.

JTU5A.97

Making Structured Metals Ultrabroadband Transparency by Surface Plasmons, Ruwen Peng¹, Ren-Hao Fan¹, Xian-Rong Huang², Mu Wang¹; ¹Nanjing Univ., China; ²Argonne National Lab, USA. We present theoretically and experimentally that one-dimensional and two-dimensional metallic gratings can become transparent and completely antireflective for extremely broadband electromagnetic waves by relying on surface plasmons or spoof surface plasmons.

JTU5A.98

Spacer-dependent coupled and decoupled super absorbing metasurfaces, Kai Liu¹, Nan Zhang¹, Dengxin Ji¹, Haomin Song¹, Xie Zeng¹, Qiaoqiang Gan¹; ¹State Univ. of New York at Buffalo, USA. We differentiate the spacer-dependent peak shift in coupled and decoupled super absorbing metasurfaces based on magnetic resonance and interference mechanism, respectively, which was experimentally validated by low-cost structures fabricated by lithography-free processes.

JTU5A.99

Stadium Mushroom Metasurface for Electro-Optical Ignition of Gas Plasma, Ebrahim Forati¹, Shiva Piltan¹, Dan Sievenpiper¹; ¹Univ. of California San Diego, USA. A metasurface is proposed to combine DC and laser induced discharges in micro scales. The structure is intended to be used as a platform for a new class of microplasma devices with electro-optical activation.

JTU5A.100

Dual-Band Metasurface Based Nano-Cavities, Amr Shaltout¹, Vladimir M. Shalaev¹, Alexander V. Kildishev¹; ¹Electrical and Computer Engineering, Purdue Univ., USA. Fabry-Pérot nano-cavities with metasurface mirrors are developed to obtain multi-band resonances at the wavelengths that exceed the diffraction limit. Independently tuned resonance bands are thus not limited to the integer multiples of a fundamental tone.

JTU5A.101

Theoretical Demonstration of Weyl Points in 3D srs Photonic Crystals, Elena Goi^{1,2}, Benjamin P. Cumming^{1,2}, Min Gu^{1,2}; ¹Centre for Micro-Photonics and CUDOS, Australia; ²Faculty of Science, Engineering and Technology, Swinburne Univ. of Technology, Australia. We present the theoretical study of achiral 2-srs-networks and we show that these structures possess the frequency-isolated linear point degeneracies in their three-dimensional dispersion relations that define the Weyl points.

JTU5A.102

Ultra-broad Flat Band Light Absorber Based on Multi-sized Slow-wave Hyperbolic Metamaterial Thin-films, Fei Ding¹, Lei Mo¹; ¹Centre for Optical and Electromagnetic Research, Zhejiang Univ., China. We realize a broadband absorber by using a hyperbolic metamaterial composed of alternating aluminum-alumina thin films based on superposition of multiple slow-wave modes. Our super absorber ensures broadband and polarization-insensitive light absorption in the visible and near-infrared regime.

JTU5A.103

Light Energy Trapping and Localization in RE³⁺ Doped PLZT Ceramics, Jingwen Zhang¹, Caixia Xu¹, Long Xu¹, Hua Zhao¹; ¹Harbin Inst. of Technology, China. Single-pass gain over theoretical value and pulsation in amplified seeding light were observed in RE³⁺ doped PLZT ceramic plates. Theoretical consideration based on light energy trapping and localization was given to elucidate the findings.

JTU5A.104

Withdrawn

JTU5A.105

Tunable VO₂/Au hyperbolic metamaterial, Srujana Prayakrao¹, Brock Mendoza², Andrew Devine², Chan Kyaw³, Robert Van Dover², Mikhail A. Noginov¹; ¹Norfolk State Univ., USA; ²Cornell Univ., USA; ³Morehouse College, USA. We have fabricated and studied thin films of VO₂ and lamellar VO₂/Au metamaterials. Optical properties of the VO₂/Au metamaterials are consistent with the transition between the hyperbolic and metallic phases occurring at elevated temperatures.

JTU5A.106

Miniaturization Resonators in Mimicking Electromagnetically Induced Transparency, Dejia Meng¹; ¹Hust, China. Electromagnetically induced transparency is mimicked by nested split ring resonators. The nested resonator offers a miniaturization with polarization-insensitive properties, high quality-factors and absorptions which may have essential applications in wireless communications and phased arrays

JTU5A.107

Negative-index Polarization-independent Metamaterial, Morteza Karami¹, Christopher Rosenbury¹, Steven Kitchin¹, Michael A. Fiddy¹; ¹Univ of North Carolina at Charlotte, USA. We introduce a polarization-independent left-handed metamaterial. Mirrored S-shaped resonators are shown to exhibit negative refractive index; and a crossed design based on these resonators is demonstrated as a polarization insensitive metamaterial with negative index.

CLEO: QELS-Fundamental Science

08:00–10:00

FW1A • Symposium on Cavity Quantum Electrodynamics I*Presider: Glenn Solomon; Joint Quantum Inst., USA*FW1A.1 • 08:00 **Invited**

James P. Gordon Memorial Speakership: Quantum State Control with Atoms and Cavities, Jean-Michel Raimond^{1,2}, Theo Rybarczyk², Bruno Peaudecerf², Mariane Penasa², Stefan Gerlich², Sebastien Gleyzes², Michel Brune², Serge Haroche², Igor Dot-senko²; ¹Universite Pierre-et-Marie-Curie, France; ²LKB, Collège de France, UPMC, CNRS, France. We measure the photon number in a microwave cavity probed by circular Rydberg atoms using the Past Quantum State approach. It leads to a considerable noise reduction and allows us to access normally hidden information.

FW1A.2 • 08:30

Cavity-Modified Collective Rayleigh Scattering of Exactly Two Atoms, Rene Reimann¹, Wolfgang Alt¹, Tobias Kampschulte¹, Tobias Macha¹, Lothar Ratschbacher¹, Natalie Thau¹, Seokchan Yoon¹, Dieter Meschede¹; ¹Physics, Bonn Univ. - IAP, Germany. We report on observing cooperative radiation of exactly two neutral atoms strongly coupled to an optical cavity. The roles of cavity backaction and of the relative atom-field coupling phases are discussed. Our results are important for the realization of phase-sensitive cavity QED protocols.

08:00–10:00

FW1B • Novel Sources for Attoscience*Presider: Oliver Muecke; Deutsches Elektronen Synchrotron, Germany*FW1B.1 • 08:00 **Invited**

Bright High Harmonics with Tunable Polarization, Oren Cohen¹; ¹Technion Israel Inst. of Technology, Israel. Generation and application of bright phase-matched high-order harmonic with fully tunable polarization - from linear through elliptic to circular - is presented.

FW1B.2 • 08:30

Carbon K-edge NEXFAS spectroscopy from a table-top soft x-ray high harmonics source driven by sub-2-cycle, CEP stable, 1.85- μm 1-kHz laser pulses, Seth L. Cousin¹, Francisco Silva¹, Stephan Teichmann¹, Michael Hemmer¹, Barbara Buades¹, Jens Biegert^{1,2}; ¹ICFO -The Inst. of Photonic Sciences, Spain; ²ICREA - Institució Catalana de Recerca i Estudis Avançats, Spain. A high-flux table-top coherent soft x-ray high harmonic generation source, driven by sub-2-cycle, 1.85 μm , 1 kHz laser pulses, is applied to a condensed phase sample revealing the carbon binding orbitals of polyimide.

08:00–10:00

FW1C • Optics of Complex Media I*Presider: Alexey Yamilov; Missouri Univ of Science & Technology, USA*

FW1C.1 • 08:00

Retrieving time-dependent Green's functions in optics with low-coherence interferometry, Amaury Badon¹, Geoffroy Lerosey¹, Claude Boccara¹, Mathias Fink¹, Alexandre Aubry¹; ¹Institut Langevin, France. We report on the passive measurement of time-dependent Green's functions with low-coherence interferometry. We show how the mutual coherence function of an incoherent wavefield can directly yield the Green's functions between scatterers of a complex medium.

FW1C.2 • 08:15

Preferential emission into epsilon-near-zero metamaterial, Tal Galfsky^{1,2}, Zheng Sun^{1,2}, Zubin Jacob³, Vinod M. Menon^{1,2}; ¹Physics, Graduate Center of the City Univ. of New York, USA; ²Physics, City College of the City Univ. of New York, USA; ³Dept. of Electrical and Computer Engineering, Univ. of Alberta, Canada. We report preferential emission from ZnO nanoparticles into an epsilon near zero metamaterial. The structure is designed to have the parallel component of its dielectric constant approach zero at the maximum emission wavelength of ZnO.

FW1C.3 • 08:30

Topological Defect Lasers, Sebastian Knitter¹, Seng Fatt Liew¹, Wen Xiong¹, Mikhael I. Guy^{2,4}, Glenn S. Solomon^{3,4}, Hui Cao¹; ¹Dept. of Applied Physics, Yale Univ., USA; ²Science & Research Software Core, Yale Univ., USA; ³Joint Quantum Inst., Univ. of Maryland, USA; ⁴National Inst. of Standards and Technology, USA. We demonstrate topological defect lasers in a GaAs membrane with embedded InAs quantum dots. By introducing a disclination to a square-lattice of elliptical air holes, we obtain spatially confined lasing modes that support powerflow vortices.

08:00–10:00

FW1D • Integrated Nonlinear Devices*Presider: Luca Razzari; INRS-Energie Materiaux et Telecom, Canada*FW1D.1 • 08:00 **Invited**

Integrated Lithium Niobate Nonlinear Optical Devices, Cheng Wang¹, Michael J. Burek¹, zin lin¹, Haig A. Atikian¹, Vivek Venkataraman¹, I-chun Huang¹, Peter Stark¹, Marko Loncar¹; ¹Harvard Univ., USA. We demonstrate robust and scalable fabrication of lithium niobate nanophotonic devices including microdisk and microring resonators. Our devices feature optical quality factors over 10^5 and are promising for nonlinear optical applications.

FW1D.2 • 08:30

A Nonlinear Polymer Waveguide Implemented Using an Augmented Low Index Guide, Muhammad Z. Alam¹, Xiao Sun¹, Mo Mojahedi¹, J. Stewart Aitchison¹; ¹Univ. of Toronto, Canada. We propose a new scheme which is easy to implement and can be used to integrate low index nonlinear materials with silicon photonics to achieve high non-linearly without suffering nonlinear losses.

CLEO: QELS-
Fundamental Science

08:00–10:00

FW1E • Quantum Emission and Plasmonics

Presider: Nanfang Yu; Columbia Univ., USA

FW1E.1 • 08:00

Propagation of quantum signal in plasmonic waveguides, Xifeng Ren^{1,2}, Yong-Jing Cai^{1,2}, Ming Li^{1,2}, Chang-Ling Zou^{1,2}, Xiao Xiong^{1,2}, Hua-Lin Lei^{1,2}, Bi-Heng Liu^{1,2}, Guo-Ping Guo^{1,2}, Guang-Can Guo^{1,2}; ¹Key Lab of quantum information, Univ. of science and technology of China, China; ²Synergetic Innovation Center of Quantum Information and Quantum Physics, Univ. of Science and Technology of China, China. Here we introduce two works on quantum plasmonics: high-visibility on-chip quantum interference of single surface plasmons and transmission of quantum polarization entanglement in a nanoscale hybrid plasmonic waveguide. Our works can bridge nanophotonics and quantum optics.

FW1E.2 • 08:15

Plasmonic Nanopatch Antennas for Large Purcell Enhancement, Gleb M. Akselrod^{1,2}, Christos Argyropoulos^{1,2}, Thang B. Hoang^{1,4}, Cristian Ciraci^{1,5}, Chao Fang², Jiani Huang^{1,4}, David R. Smith^{1,2}, Maiken H. Mikkelsen^{1,2}; ¹Center for Metamaterials and Integrated Plasmonics, Duke Univ., USA; ²Electrical and Computer Engineering, Duke Univ., USA; ³Dept. of Electrical and Computer Engineering, Univ. of Nebraska-Lincoln, USA; ⁴Dept. of Physics, Duke Univ., USA; ⁵Center for Biomolecular Nanotechnologies, Istituto Italiano di Tecnologia, Italy. We demonstrate Purcell enhancements of ~1000 from fluorescent molecules embedded in a plasmonic antenna with sub-10 nm gap between metals. Simulations and experiments reveal the high radiative efficiency and directionality of the antenna.

FW1E.3 • 08:30

Enhanced Single Photon Emission from Quantum Dots Coupled to Localized Surface Plasmons, Brandon Demory¹, Tyler Hill², chu-hsiang teng¹, Lei Zhang², Hui Deng², Pei-Cheng Ku¹; ¹Electrical Engineering and Computer Science, Univ. of Michigan, USA; ²Physics, Univ. of Michigan, USA. The coupling between excitons and localized surface plasmons in two-level systems can lead to enhanced spontaneous emission and was studied using site-controlled InGaN quantum dots. The dynamics and the Purcell effect were measured and analyzed.

CLEO: Science & Innovations

08:00–10:00

SW1F • Surface Emitting Semiconductors Lasers

Presider: Weidong Zhou; Univ. of Texas at Arlington, USA

SW1F.1 • 08:00

Position-modulated Photonic-crystal Lasers and Control of Beam Direction and Polarization, Tsuyoshi Okino¹, Kyoko Kitamura¹, Daiki Yasuda¹, Yong Liang¹, Susumu Noda¹; ¹Kyoto Univ., Japan. We propose and demonstrate position-modulated photonic-crystal lasers which can control the output-beam directions two-dimensionally and have various polarizations. The results promise to greatly enhance the range of possible laser-scanning applications.

SW1F.2 • 08:15

Compact Vortex Beam Emitter Laterally Integrated with VCSEL Array, Kenji Tanabe¹, Xiaodong GU¹, Akihiro Matsutani¹, Fumio Koyama¹; ¹Tokyo Inst. of Technology, Japan. We demonstrate the integration of VCSEL array and vortex-beam-emitters, composed of double-ring-shaped Bragg-reflector waveguides functioning as diffraction element. A possibility of compact VCSEL-based emitters, creating and multiplexing vortex beams with different orbital momentums is suggested.

SW1F.3 • 08:30

Resonance Tuning and Coherent Operation in Anti-Guided Vertical-Cavity Laser Arrays, Stewart Fryslie¹, Meng P. Tan², Matthew Johnson³, Kent D. Choquette¹; ¹Univ. of Illinois Urbana-Champaign, USA; ²Intel Corp., USA; ³U.S. Air Force, USA. We demonstrate that photonic crystal anti-guided VCSEL arrays can be tuned to coherent operation by control of the cavity resonance by independent control of the bias currents.

08:00–10:00

SW1G • Optical Frequency Comb Spectroscopy

Presider: Mark Phillips; Pacific Northwest National Lab, USA

SW1G.1 • 08:00

Mid-Infrared frequency comb for rapid detection of CH₄ and H₂O in open air, Lora Nugent-Glandorf¹, Fabrizio R. Giorgetta¹, Scott A. Diddams¹; ¹NIST, USA. We present open-air trace-gas spectroscopy utilizing a mid-infrared frequency comb. The MIR beam spanning 300 nm propagates through 26 m of atmosphere and absorption spectra are collected in 2 ms with a Virtual-Image Phased-Array spectrometer.

SW1G.2 • 08:15

Dual-Frequency Comb Measurements of Atmospheric Absorption: Comparison with HITRAN Database Parameters, Gregory B. Rieker^{1,2}, Fabrizio R. Giorgetta², William C. Swann², Laura C. Sinclair², Christopher L. Cromer², Esther Baumann², Ian R. Coddington², Nathan R. Newbury²; ¹Univ. of Colorado at Boulder, USA; ²National Inst. of Standards & Technology, USA. Near-infrared frequency-comb spectroscopy is used to measure CO₂ absorption over a 2-km outdoor path under well-mixed atmospheric conditions. We compare integrated area, linecenter, and Lorentz widths extracted from Voigt fits to the data with HITRAN.

SW1G.3 • 08:30

Dual-Comb Spectroscopy based on Quantum Cascade Laser Frequency Combs, Gustavo Villares¹, Francesco Cappelli^{1,2}, Andreas Hugi^{1,3}, Stéphane Blaser⁴, Jerome Faist¹; ¹IQE, Physics Dept., ETH Zurich, Switzerland; ²CNR-INO and LENS, Italy; ³IRsweep GmbH, Switzerland; ⁴Alpes Lasers SA, Switzerland. Mid-infrared dual-comb spectroscopy by means of quantum cascade laser frequency combs is demonstrated. Broadband high resolution molecular spectroscopy is performed, showing the potential of quantum cascade laser combs as a compact, all solid-state, chemical sensor.

08:00–10:00

SW1H • Ultrashort Pulse Characterization

Presider: Takao Fuji; National Inst. of Natural Sciences, Japan

SW1H.1 • 08:00 **Invited**

Solid State Light Field Sampling and Light Phase Detection, Tim Paasch-Colberg¹; ¹Max-Planck-Institut für Quantenoptik, Germany. The conductivity of a solid state device is reversibly increased by several orders of magnitude on a femtosecond timescale using the instantaneous electric field of an intense few-cycle laser pulse to create ultrafast detectable currents.

Meeting Room
211 B/D

CLEO: Science & Innovations

08:00–10:00
SW11 • Micro & Nanophotonics
President: To be Determined

SW11.1 • 08:00 **Invited**
Integrated Photonic Devices with Single Quantum Dots, A. Mark Fox¹, Edmund Clarke², Rikki Coles¹, James Dixon¹, Isaac J. Luxmoore¹, Maxime Hugues², Maxim Makhonin¹, John O'Hara¹, Nikola Prtljaga¹, Andrew Ramsay¹, Ben Royall¹, Nicholas Wasley¹, Maurice S. Skolnick¹; ¹Physics & Astronomy, Univ. of Sheffield, UK; ²EPSRC National Centre for III-V Technologies, Univ. of Sheffield, UK. The integration of InAs quantum dots as on-chip single-photon sources in GaAs photonic circuits is reviewed. A Hanbury Brown-Twiss effect is demonstrated using a monolithic directional coupler, together with coherent emission under resonant excitation.

SW11.2 • 08:30
Observation of Einstein's Rings and Optical Gravitational Collimation, Chong Sheng², Rivka Bekenstein¹, hui liu², Shining Zhu², Mordechai Segev¹; ¹Technion Israel Inst. of Technology, Israel; ²National Lab of solid State Microstructures & Dept. and Physics, Collaborative Innovation Center of Advanced Microstructures, Nanjing Univ., China. We experimentally observe Einstein's Rings caused by gravitational lensing by designing a refractive index profile analogous to the curvature of a star. We employ the experiment to produce collimated optical beams in homogenous media.

Meeting Room
212 A/C

CLEO: Applications & Technology

08:00–10:00
AW1J • Biomedical Imaging and Sensing I
President: Xuan Liu; New Jersey Inst. of Technology, USA

AW1J.1 • 08:00 **Invited**
Multipurpose Information Encoding using interleaved Optical Coherence Tomography, Audrey Ellerbee¹; ¹Stanford Univ., USA. We present interleaved OCT as a unique strategy to exploit long coherence lengths for novel spectral multiplexing schemes that permit multi-purpose information encoding and streamlined image acquisition.

AW1J.2 • 08:30 **Invited**
Quantitative Imaging of Tissue Polarization Property by Jones Matrix Optical Coherence Tomography, Yoshiaki Yasuno¹; ¹Univ. of Tsukuba, Japan. A quantitative polarization sensitive optical coherence tomography which measures tissue Jones matrix is presented. Jones matrix based signal processing is applied to obtain quantitative birefringence. Its clinical utility is examined by measuring in vivo human eyes.

Meeting Room
212 B/D

CLEO: Science & Innovations

08:00–10:00
SW1K • Laser-Induced Structuring in Bulk Material
President: Richard Haglund; Vanderbilt Univ., USA

SW1K.1 • 08:00
Fabrication of complex three-dimensional metallic microstructures based on femtosecond laser micromachining, Feng Chen¹, Qing Yang¹, Chao Shan¹; ¹Xi'an Jiaotong Univ., China. The fabrication of complex metallic microstructures based on femtosecond laser micromachining and metal microsolidify process is demonstrated. This method is beneficial for building complex embedded 3D metal microstructures, electronic components, and hybrid electronic-microfluidic devices.

SW1K.2 • 08:15
Fs-laser Induced Optical Changes in Zinc Aluminum Phosphate Glasses, Javier Hernandez Rueda¹, Charmayne E. Smith², Richard K. Brow², Denise M. Kroll¹; ¹Univ. of California Davis, USA; ²Missouri Univ. of Science and Technology, USA. The fs-laser induced refractive index change in zinc aluminum phosphate glasses and its underneath structural modifications have been investigated both at the surface and in bulk.

SW1K.3 • 08:30 **Invited**
Optical Aspect of Ultrafast Laser Ablation on Transparent Dielectrics: Ciliary White Light, Yi Liu¹, Yohann Brelet¹, Zhanbing He², Linwei Yu³, Yue Zhong⁴, Zhinan Zeng⁴, Ruxin Li⁴, Aurelien Houard¹, Arnaud Couairon⁵, Andre Mysyrowicz¹; ¹Laboratoire d'Optique Appliquée, ENSTA/CNRS/Ecole Polytechnique, France; ²Electron Microscopy for Materials Research (EMAT), Univ. of Antwerp, Belgium; ³Laboratoire de Physique des Interfaces et des Couches Minces, Ecole Polytechnique, France; ⁴Shanghai Inst. of Optics and Fine Mechanics, China; ⁵Centre de Physique Théorique, Ecole Polytechnique, France. We report on a new nonlinear optical phenomenon during laser ablation on transparent dielectrics, coined as ciliary white light. It is universally observed on 14 different dielectrics with femtosecond pulses at 800 nm and 1.8 μm.

Marriott
Salon I & II

08:00–10:00
SW1L • Mid-IR & Supercontinuum Fiber Sources
President: Fetah Benabid; Xlim Research Insitute, France

SW1L.1 • 08:00 **Invited**
Multimaterial Chalcogenide Fibers and Devices for the Mid-IR, Ayman F. Abou-raddy¹; ¹Univ. of Central Florida, CREOL, USA. Chalcogenide glass fibers offer a fruitful playground for mid-infrared nonlinear optics but are hampered by mechanical fragility and high chromatic dispersion. I review recent efforts on novel of chalcogenide fibers that address these perennial issues.

SW1L.2 • 08:30
Tunable Single Longitudinal Mode Tm-doped Fiber Ring Laser, Jae-Keun Yoo^{1,2}, Sun Do Lim^{1,2}, Seung Kwan Kim¹; ¹Physical Metrology, Korea Research Inst. of Standards and Science, Korea; ²Measurement Science, Korea Univ. of Science and Technology, Korea. We present a tunable single longitudinal mode Tm-doped fiber ring laser incorporating a self-constructed saturable absorption grating and a blazed grating with wavelength tunability of over 100 nm. The spectral and temporal characteristics of the laser output are described.



CLEO: Science & Innovations

08:00–10:00

SW1M • Coherent Communications

Presider: Takashi Sugihara; Mitsubishi Electric Corporation, Japan

SW1M.1 • 08:00

Phase Diversity Method for Optical Coherent Receiver, Thang M. Hoang¹, Mohamed Osman¹, Mathieu Chagnon¹, Qunbi Zhuge¹, David Patel¹, David Plant¹; ¹McGill Univ., Canada. We present the first phase-diversity coherent receiver for an arbitrary hybrid. Colorless experiment of 10x132-Gb/s PDM-QPSK is demonstrated with reduced components and with less than 0.5 dB in OSNR penalty compared to traditional coherent receivers.

SW1M.2 • 08:15

Multi-Gigabit Coherent Communications Using Low-Rate FEC to Approach the Shannon Capacity Limit, David J. Geisler¹, Venkat Chandar^{1,2}, Timothy M. Yarnall¹, Mark L. Stevens¹, Scott A. Hamilton¹; ¹Massachusetts Inst of Tech Lincoln Lab, USA; ²D. E. Shaw and Co., USA. Combining a rate-1/4 forward error-correcting code, a coherent receiver, and an optical phase-locked loop yields near error-free performance with 2-dB photon-per-bit sensitivity, which is <3-dB from the Shannon limit for a rate-1/4, pre-amplified, coherent receiver.

SW1M.3 • 08:30

Phase Noise-Robust LLR Calculation with Linear/Bilinear Transform for LDPC-Coded Coherent Communications, Toshiaki Koike-Akino¹, David S. Millar¹, Keisuke Kojima¹, Kieran Parsons¹; ¹Mitsubishi Electric Research Labs, USA. We propose a modified log-likelihood ratio (LLR) calculation for an LDPC decoder to be robust against residual phase noise at the demodulator. The proposed scheme is based on a linear/bilinear transform offers 1 to 2dB gain in the presence of large phase noise.

08:00–10:00

SW1N • Applications of Optical Resonators

Presider: Lin Zhu; Clemson Univ., USA

SW1N.1 • 08:00

Single ring resonator QPSK modulator, Binhuang Song¹, Leimeng Zhuang¹, Chen Zhu¹, Bill Corcoran^{1,2}, Arthur Lowery^{1,2}; ¹Monash Univ., Australia; ²Centre for Ultrahigh-bandwidth Devices for Optical Systems (CUDOS), Australia. We propose a new implementation of a QPSK modulator using a simple single ring resonator. That requires only $\pi/10$ phase shift. Signal generated have a better dispersion tolerance than from a single phase modulator.

SW1N.2 • 08:15

Automated Calibration of High-Order Microring Filters, Jason Mak¹, Wesley Sacher¹, Jared Mikkelsen¹, Tianyuan Xue¹, Zheng Yong¹, Joyce Poon¹; ¹Edward S. Rogers Sr. Dept. of Electrical & Computer Engineering, Univ. of Toronto, Canada. We demonstrate the automated calibration of a 5th-order silicon microring filter using an optimization algorithm. The procedure only requires a single input wavelength and was implemented on a microcontroller with simple ADC and DAC circuitry.

SW1N.3 • 08:30 **Tutorial**

Selected Applications of Ultra-high Q Whispering Gallery Mode Resonators, Lute Maleki¹; ¹OEwaves Inc, USA. Emerging applications aided by advances in physics and technology of Whispering Gallery Mode microresonators will be discussed.



Lute Maleki is a Founder and President & CEO of OEwaves, Inc. Previously at the Jet Propulsion Lab he created and led the Quantum Sciences and Technologies Group. Dr. Maleki's research includes study and development of ultra-stable photonic oscillators; whispering gallery mode optical microresonators; atomic clocks based on ion traps and laser cooled atoms; quantum sensors. He has over 50 U.S. Patents, authored 150 refereed publications, serves on technical program committees, is a Fellow of the IEEE, American Physical Society and The Optical Society. He received the IEEE Rabi Award, NASA's Exceptional Engineering Achievement Medal and IEEE UFFC Sawyer Award.

08:00–10:00

SW1O • Ultrafast Technologies Based on Aperiodical Quasi-Phase Matching

Presider: Yen-Hung Chen; National Central Univ., Taiwan

SW1O.1 • 08:00 **Tutorial**

Tailoring Nonlinear Interactions with Aperiodic Quasi-Phase Matching, Martin M. Fejer¹; ¹Stanford Univ., USA. The evolution of three-wave mixing processes can be controlled with aperiodic QPM structures. We describe underlying concepts, engineering of spectral amplitude and phase, and adiabatic processes, illustrated with examples including few-cycle OPCPA, octave spanning frequency combs, and quantum frequency conversion.



Martin Fejer is Professor of Applied Physics, and was Senior Associate Dean of Humanities and Sciences and Chair of the Applied Physics department at Stanford Univ. He received his B.A. in Physics from Cornell Univ., and his M.S. and Ph.D. in Applied Physics from Stanford Univ.. His current research interests are in nonlinear optical materials and devices, guided wave optics, microstructured ferroelectrics and semiconductors, ultrafast optics, classical and quantum optical signal processing, and materials with low dissipation. He has published over 400 papers in these areas, and holds over 30 patents. Fejer is a fellow of IEEE and The Optical Society (OSA). He was awarded OSA's R. W. Wood Prize and has been a member of the OSA Board of Directors and the Board of Governors of IEEE-LEOS.

CLEO: QELS-Fundamental Science

FW1A • Symposium on Cavity
Quantum Electrodynamics I—
Continued

FW1A.3 • 08:45 **Invited**
Photonic Quantum-Information Processing with Quantum Dots in Photonic Crystals, Peter Lodahl¹; ¹*Univ. of Copenhagen, Denmark*. Quantum dots in photonic crystals have proven to be a very suitable platform for quantum-information processing. We review current progress on the ability to deterministically interface single photons and single quantum dots in photonic crystal waveguides and the chiral spin-photon interfaces.

FW1A.4 • 09:15
An ultrasmall mode volume cantilever-based Fabry-Pérot microcavity, Hrishikesh Kelkar¹, Daqing Wang^{1,2}, Björn Hoffmann¹, Silke Christiansen^{3,1}, Stephan Götzinger^{2,1}, Vahid Sandoghdar^{1,2}; ¹*Max Planck Inst. for the Science of, Germany*; ²*Friedrich Alexander Univ. Erlangen-Nuremberg, Germany*; ³*Helmholtz Centre Berlin for Materials and Energy, Germany*. A tunable Fabry-Pérot microcavity consisting of a 2.6 μm curvature mirror and 0.4 numerical aperture is fabricated. We study the effect of a nanoparticle on the cavity modes and discuss the coupling of single molecules to it.

FW1B • Novel Sources for
Attoscience—Continued

FW1B.3 • 08:45
Suppression of Resonant-induced Harmonics of Tin with Tunable Laser Wavelengths, Muhammad Ashiq Fareed¹, Sudipta Mondal¹, Nicolas Thiré¹, Maxime Boudreau¹, Yoann Pertot¹, Bruno E. Schmidt¹, François Légaré¹, Tsuneyuki Ozaki¹; ¹*INRS-EMT, Canada*. We investigate the behavior of resonant-induced harmonics from tin using driving lasers with tunable wavelengths. The intensity of the resonant harmonic is suppressed by the tuning laser wavelength around 1.8 μm to understand the interaction dynamics of continuum electron with the autoionizing state.

FW1B.4 • 09:00
Control of attosecond pulse and XUV high-order harmonic generation with spatially-chirped laser pulses, Carlos Hernandez-Garcia^{1,2}, Agnieszka Jaron-Becker¹, Andreas Becker¹, Charles G. Durfee³; ¹*JILA, Univ. of Colorado, USA*; ²*Universidad de Salamanca, Spain*; ³*Physics, Colorado School of Mines, USA*. We present a technique to drive high-order harmonics with angularly spatially chirped pulses. Our calculations show that each harmonic is emitted with angular chirp, leading to dramatically improved control of spectral and temporal spatial resolution.

FW1B.5 • 09:15
Relativistic High Harmonics Driven by Two-Color Incident Fields, Matthew Edwards¹, Julia Mikhailova¹; ¹*Princeton Univ., USA*. Particle-in-cell simulations suggest that relativistic high-harmonic generation using overdense plasmas will be substantially enhanced by adding second harmonic to the incident laser field. This mechanism also offers a new diagnostic of the laser-plasma interaction.

FW1C • Optics of Complex
Media I—Continued

FW1C.4 • 08:45
Localization of Light at Vanishingly Small Disorder-Levels with Heavy Photons, Alexandre Baron¹, Rémi Faggiani², Xiaorun Zang², Loïc Lalouat³, Sebastian A. Schulz⁴, Kévin Vynck², Bryan O'Regan⁵, Benoit Cluzel³, Frédérique de Fornel³, Thomas Krauss⁵, Philippe Lalanne²; ¹*Duke Univ., USA*; ²*Université de Bordeaux, France*; ³*Université de Bourgogne, France*; ⁴*Univ. of Ottawa, Canada*; ⁵*Univ. of York, UK*. We investigate the formation of localized modes in randomly-perturbed photonic-crystal waveguides near the photonic band-edge. We show that the key parameter driving the formation process is the effective photon mass rather than the group index.

FW1C.5 • 09:00 **Invited**
Coherent Perfect Absorbers and Coherent Enhancement of Absorption, A. Douglas Stone¹, Hui Cao¹, Yidong Chong², Li Ge³, Sebastien Popoff⁴, Arthur Goetschy⁵; ¹*Yale Univ., USA*; ²*Nanyang Technical Univ., Singapore*; ³*CUNY Staten Island, USA*; ⁴*CNRS-LTCl, France*; ⁵*Institut Langevin, France*. Coherent illumination and wave-front shaping can be used to make a weakly absorbing cavity perfectly absorbing and to enhance strongly the absorption of a multiple scattering medium.

FW1D • Integrated Nonlinear
Devices—Continued

FW1D.3 • 08:45
Pump-Degenerate Phase-Sensitive Amplification in Amorphous Si Waveguides, Hongcheng Sun¹, Ke-Yao Wang¹, Amy C. Foster¹; ¹*Johns Hopkins Univ., USA*. We demonstrate phase-sensitive amplification in hydrogenated amorphous silicon waveguides based on pump-degenerate four-wave mixing at 90 MHz and 10 GHz. An 11.7 dB (6.6 dB) phase-sensitive extinction ratio is achieved at 90 MHz (10 GHz).

FW1D.4 • 09:00
Nonlinear Silicon Photonics and the Moment Method, Simon Lefrancois¹, Chad A. Husko¹, Andrea Blanco-Redondo^{1,2}, Benjamin J. Eggleton¹; ¹*Univ. of Sydney, Australia*; ²*Tecnalia, Spain*. We develop a moment method theory for nonlinear propagation in silicon waveguides. Expressions for pulse parameters, free-carrier blueshift and acceleration are derived. We apply this to propagation in silicon photonic crystal waveguides and nanowires.

FW1D.5 • 09:15
Low Power All-Optical Switching in a Gallium Arsenide Photonic Molecule, Ranjoy Bose¹, Jason Pelc¹, Charles Santori¹, Raymond Beausoleil¹; ¹*Hewlett Packard Labs, USA*. We demonstrate low power all-optical switching in a gallium arsenide (GaAs) photonic molecule with resonances near the material band edge. The enhanced nonlinear effects in this spectral region result in a low estimated switching energy of a few femtojoules with 45% transmission contrast.

CLEO: QELS-
Fundamental ScienceFW1E • Quantum Emission and
Plasmonics—Continued

FW1E.4 • 08:45

Plasmonic Giant Semiconductor Nanocrystals with Enhanced Light Output and Suppressed Blinking for Biomedical Applications, sid sampat¹, Niladri karan², Aaron Keller², Andrei Piryatinski³, Oleksiy Roslyak⁴, Christina Hanson², Yagnaseni Ghosh², han htoon², jennifer hollingsworth², anton malko¹; ¹U Texas at Dallas, USA; ²Material Physics and Applications Division, CINT, Los Alamos National Lab, USA; ³Theoretical Division: Physics of Condensed Matter and Complex Systems, Los Alamos National Lab, USA; ⁴Physics, Fordham Univ., USA. We study single particle PL emission signatures of giant semiconductor nanocrystals overcoated with silica shells and ultrathin gold layers. We observe complex metal/semiconductor coupling and plasmonic interactions leading to either emission quenching or photobrightening.

FW1E.5 • 09:00

Quantum Model of Plasmon-Quantum Emitter Interaction in the Strong-Coupling Regime, Roderick Davidson^{1,2}, Pavel Lougovski², Benjamin Lawrie²; ¹Physics, Vanderbilt Univ., USA; ²Quantum Information Sciences, Oak Ridge National Lab, USA. A full quantum model incorporating realizable materials properties is developed for interactions between a plasmonic resonator and a single two-level quantum emitter, enabling fabrication of plasmonic nanostructures for the strong coupling regime of cavity-quantum-electrodynamics.

FW1E.6 • 09:15

Efficient Fiber Collection of Nitrogen-Vacancy Center Emission from Diamond Nano Beams, Harishankar Jayakumar¹, Behzad Khanaliloo^{1,2}, Paul E. Barclay^{1,2}; ¹Univ. of Calgary, Canada; ²National Research Center-National Inst. for Nanotechnology, Canada. We present tapered diamond nano beams, which allows efficient collection of diamond nitrogen vacancy emission through phase-matched coupling to a tapered optical fiber.

SW1F • Surface Emitting
Semiconductors Lasers—
Continued

SW1F.4 • 08:45

Effect of In-plane Mirror Dispersion on Vertical Cavities Based on High-Contrast Grating Mirrors, Alireza Taghizadeh¹, Jesper Mork¹, Il-Sug Chung¹; ¹Technical Univ. of Denmark, Denmark. We report how the in-plane dispersion of a high-index-contrast grating reflector influences the transverse mode properties such as shorter wavelengths for lower-order transverse modes and different transverse-mode wavelength spacings for modes with the same size.

SW1F.5 • 09:00

Smooth lasing transition in high β buried multiple-quantum-well 2D photonic crystal lasers, Masato Takiguchi^{1,2}, Hideaki Taniyama^{1,2}, Hisashi Sumikura^{1,2}, Danang M. Birowosuto^{1,2}, Eiichi Kuramochi^{1,2}, Akihiko Shinya^{1,2}, Tomonari Sato^{1,3}, Koji T. Takeda^{1,3}, Shinji Matsuo^{1,3}, Masaya Notomi^{1,2}; ¹NTT Nanophotonics Center, NTT Corporation, Japan; ²NTT Basic Research Labs, NTT Corporation, Japan; ³NTT Device Technology Labs, NTT Corporation, Japan. By adopting high β buried-multiple-quantum-well photonic crystal nanocavities, we have demonstrated smooth lasing operation, which indicates thresholdless-like lasing theoretically predicted, by mean of light-in vs light-out curve analysis, linewidth analysis, and photon correlation measurements.

SW1F.6 • 09:15

Broadband Self-Swept High Contrast Grating VCSEL, Stephen Gerke¹, Weijian Yang¹, Kar Wei Ng¹, Christopher Chase², Yi Rao², Connie J. Chang-Hansnain¹; ¹Univ. of California Berkeley, USA; ²Bandwidth10 Inc., USA. We demonstrate a 1550 nm broadband self-swept VCSEL with 23-nm wavelength range at 131 kHz sweep rate. The mechanical oscillation of the ultra-lightweight HCG top mirror is excited optomechanically by photons inside the lasing cavity.

CLEO: Science & Innovations

SW1G • Optical Frequency
Comb Spectroscopy—
Continued

SW1G.4 • 08:45

Noise properties in multi-heterodyne spectrometers based on quantum- and interband-cascade lasers, Andreas Hangauer¹, Jonas Westberg¹, Michael Soskind^{2,1}, Eric J. Zhang¹, Gerard Wysocki¹; ¹Princeton Univ., USA; ²Rutgers, USA. The noise properties of two multi-heterodyne spectrometers based on multi-mode semiconductor lasers (QCLs and ICLs) are investigated to determine their performance limitations. Both technologies provide well-defined multi-heterodyne beat-note structures suitable for spectroscopic measurements.

SW1G.5 • 09:00

Multiheterodyne Spectroscopy with Electro-Optic Frequency Combs, David Long¹, Adam J. Fleisher¹, Joseph T. Hodges¹, David F. Plusquellic¹; ¹NIST, USA. Waveguide-based, electro-optic modulators were used to generate pitch-agile, optical frequency combs from a single continuous-wave laser. These combs are then detected via a multi-heterodyne approach where the absorption information is down-converted into the radiofrequency domain.

SW1G.6 • 09:15

Broadband, Comb-resolved, High-Finesse Enhancement Cavity Spectrometer with Graphene Modulator, Kevin F. Lee¹, Grzegorz Kowzan^{1,2}, Chien-Chung Lee³, C. Mohr¹, Jie Jiang¹, Thomas R. Schibli³, Piotr Maslowski², M. E. Fermand¹; ¹IMRA America, Inc., USA; ²Nicolaus Copernicus Univ., Poland; ³Univ. of Colorado, USA. We transmit a frequency comb through an enhancement cavity by PDH locking with a graphene modulator. We comb-resolve the 1940 to 2115 nm spectrum with stable repetition rate and offset frequency via Fourier transform spectrometry.

SW1H • Ultrashort Pulse
Characterization—Continued

SW1H.3 • 08:45

Cross-Correlation Frequency-Resolved Optical Gating for Characterization of A Train of Monocycle Optical Pulses, Yuta Nakano¹, Yuichiro Kida¹, Kazuya Motoyoshi¹, Tataro Imasaka^{1,2}; ¹Dept. of Applied Chemistry, Kyushu Univ., Graduate School of Engineering, Japan; ²Division of Optoelectronics and Photonics, Kyushu Univ., Center for Future Chemistry, Japan. A cross-correlation frequency-resolved optical gating is developed for the characterization of an optical pulse train consisting of monocycle pulses. An optical beat is employed for resolving the ultrafast temporal intensity variation in the train.

SW1H.4 • 09:00

A Spectrally Resolved Lateral-Shearing Interferometer for Measurement of Relative Group Delay Using a Periodic Entrance Slit in a Spectrometer, Seung-Wan Bahk¹, Christophe Dorrer¹, Rick Roides¹, Jake Bromage¹; ¹Univ. of Rochester, USA. A concept for a spectrally resolved lateral-shearing interferometer is proposed to measure pulse front and radial group delay. A periodic slit in a spectrometer enables a simpler spatial interference scheme than a Mach-Zehnder interferometer.

SW1H.5 • 09:15

Pulse Characterization in Ultrafast Microscopy: a Comparison of FROG, MIIPS and G-MIIPS, Alberto Comin¹, Michelle Rhodes², Richard Ciesielski¹, Rick Trebino², Achim Hartschuh¹; ¹Dept. Chemie, Ludwig-Maximilians-Universitaet Muenchen, Germany; ²Georgia Inst. of Technology, USA. MIIPS is a popular method for compressing femtosecond pulses. It is not ideal for complex pulses, like those produced by self-phase modulation. We show that several limitations are fixed by an improvement called G-MIIPS.

Technical Digest and Postdeadline Papers
Available Online

- Visit www.cleoconference.org
- Select Access Digest Paper link
- Use your registration email address and password

Access is provided only to full technical attendees.

Meeting Room
211 B/D

CLEO: Science & Innovations

SW11 • Micro & Nanophotonics—Continued

SW11.3 • 08:45

Theory and Practice of Resonant Antireflection, Ken Xingze Wang¹, Shanhui Fan¹; ¹Stanford Univ., USA. Antireflection can be achieved using optical resonances. We show theoretically that complete resonant antireflection is possible if the resonances radiate in a balanced manner and the periodicity of the structure is subwavelength for normal incidence.

SW11.4 • 09:00

Silicon Super-Resolution in the Visible, Asaf David¹, Bergin Gjonaj¹, Guy Bartal¹; ¹Technion Israel Inst. of Technology, Israel. Planar Silicon waveguides provide up to 4 times wavelength compression, yielding sub-100nm focusing for visible light. Our near-field measurements for red light (671nm) show both wavelength compression (280nm) and super-focusing (80nm, bright and dark spots).

SW11.5 • 09:15

Design Rule of 2D High Contrast Gratings and Engineering of Orbital Angular Momentum of Light, Pengfei Qiao^{1,2}, Li Zhu², Connie J. Chang-Hansnain²; ¹Univ of Illinois at Urbana-Champaign, USA; ²Univ. California at Berkeley, USA. A design rule to obtain broadband high reflection and transmission in 2D high contrast gratings is proposed. Our design method is convenient for engineering the orbital angular momentum of light using 2D grating array.

Meeting Room
212 A/C

CLEO: Applications & Technology

AW1J • Biomedical Imaging and Sensing I—Continued

AW1J.3 • 09:00

Invited

The Ultimate Road to Real Time 3D Optical Coherence Tomography Imaging, Tiancheng Huo¹, Xiao Zhang¹, Chengming Wang¹, Tianyuan Chen¹, Wenchao Liao¹, Wenxin Zhang¹, Shengnan Ai¹, Jui-Cheng Hsieh¹, Ping Xue¹; ¹State Key Lab of Low-dimensional Quantum Physics and Dept. of Physics, Tsinghua Univ. and Collaborative Innovation Center of Quantum Matter, China. We have presented linear-in-wavenumber swept laser and all-optical 40MHz swept-source as the optical source, and compressed sensing and time serial optical computing to process the massive imaging data for real time 3D optical coherence tomography imaging.

Meeting Room
212 B/D

CLEO: Science & Innovations

SW1K • Laser-Induced Structuring in Bulk Material—Continued

SW1K.4 • 09:00

Formation of nanogratings in porous glass initiated by excitation of plasma waves at interfaces, Yang Liao¹, Jielei Ni¹, Lingling Qiao¹, Min Huang², Ya Cheng¹; ¹Shanghai Inst of Optics and Fine Mech, China; ²Sun Yat-sen Univ., China. The evolution of nanogratings in a porous glass was directly observed, revealing that the nanogratings origin from the standing plasma waves at the interfaces excited by femtosecond laser pulses.

SW1K.5 • 09:15

Board-Level Optical Interconnect Using Glass, sheng huang¹, Kevin P. Chen¹, Ming-Jun Li²; ¹Univ. of Pittsburgh, USA; ²Corning Inc., USA. This paper reports ultrafast laser fabrication of waveguide circuits and 45° vertical coupling micromirrors in fused silica for board-level optical interconnect applications. Excellent micromirror surface quality was obtained and 0.24-dB per reflection at $\lambda=632\text{nm}$ was demonstrated.

Marriott
Salon I & II

SW1L • Mid-IR & Supercontinuum Fiber Sources—Continued

SW1L.3 • 08:45

Resonantly Pumped Amplification in a Thulium-doped Large Mode Area Photonic Crystal Fiber, Alex Sincore¹, Lawrence Shah¹, Martin Richardson¹; ¹Univ. of Central Florida, USA. We demonstrate resonantly pumped amplification in a thulium-doped photonic crystal fiber. This enables greatly increased efficiencies compared to 795nm or 1550nm pumping and is attractive for pulsed amplification.

SW1L.4 • 09:00

Tunable Single-Frequency DFB Fiber Laser at 2.8 μm , Vincent Michaud-Belleau¹, Martin Bernier¹, Vincent Fortin¹, Jerome Genest¹, R  al Vall  e¹; ¹Centre d'optique, photonique et laser, Universit   Laval, Canada. We report a tunable single-frequency laser emission near 2.8 μm from an all-fiber distributed feedback laser. A 20 kHz linewidth is measured with a tunability of $\sim 1\text{ nm}$ at a step resolution of 3 pm.

SW1L.5 • 09:15

Wavelength Tunable Mid-infrared Er³⁺:ZBLAN Fiber Laser at 3.5 μm using Dual Wavelength Pumping, Ori Henderson-Sapir¹, Jesper Munch¹, David J. Ottaway¹; ¹Univ. of Adelaide, Australia. An Er³⁺:ZBLAN glass fiber laser which lases at 3.5 μm and produces 370 mW when operated at room temperature is reported. Good efficiency is obtained using a dual wavelength pumping scheme. Over 200 nm of wavelength tuning is demonstrated using a three mirror resonator configuration.

CLEO Mobile App

Use the conference app to plan your schedule; view program updates; receive special events reminders and access Technical Papers (*separate log-in required*).

- Go to www.cleoconference.org/app.
- Select the Apple App Store or Google Play link.
- Download the app.
- Log in to use app features such as contacting fellow conference attendees—using your registration I.D. and email address.

CLEO: Science & Innovations

SW1M • Coherent
Communications—Continued

SW1M.4 • 08:45

FPGA-based Non-binary QC-LDPC Coding for High-Speed Coherent Optical Transmission, Ding Zou¹, Ivan B. Djordjevic¹, ¹Univ. of Arizona, USA. We present a large-girth-non-binary QC-LDPC code suitable for beyond 100 Gb/s optical transmission and describe its implementation in FPGA. Great performance with Q-limit of 5.0 dB at BER of 10⁻¹⁰ has been found, which corresponds to NCG of 11.95 dB at 10-15.

SW1M.5 • 09:00

Experimental Demonstration of Simultaneous Phase Noise Suppression and Automatically Locked Tunable Homodyne Reception for a 20-Gbaud QPSK Signal, Amirhossein Mohajerin Ariaei¹, Morteza Ziyadi¹, ahmed almainan¹, yinwen cao¹, Mohammad-Reza Chitgarha¹, Youichi akasaka², Jeng-Yuan Yang², motoyoshi sekiya², joseph touch³, Moshe Tur⁵, carsten langrock⁴, Martin M. Fejer⁴, alan willner¹; ¹Univ. of Southern California (USC), USA; ²Fujitsu Labs of America, USA; ³Information Sciences Inst., USA; ⁴Stanford Univ-Edward L. Ginzton Lab, USA; ⁵Tel Aviv Univ., Israel. We experimentally demonstrate simultaneous phase-noise suppression and automatically locked homodyne reception for 20-Gbaud QPSK signal. The phase noise deviation can be reduced by a factor ~3. Open I/Q eyes are obtained after the noise mitigation.

SW1M.6 • 09:15

Enhanced Spectral Efficiency of 2.36 bits/s/Hz using Multiple Layer Overlay Modulation for QPSK over a 14-km Single Mode Fiber Link, Guodong Xie¹, Long Li¹, Yongxiong Ren¹, Hao Huang¹, Zhe Zhao¹, peicheng liao¹, ahmed almainan¹, yinwen cao¹, Yan Yan¹, Changjing Bao¹, Nisar Ahmed¹, Zhe Wang¹, Nima Ashrafi^{2,3}, Solyman Ashrafi², moshe tur⁴, alan willner¹; ¹U. of Southern California, USA; ²NxGen Partners, USA; ³Univ. of Texas at Dallas, USA; ⁴Tel Aviv Univ., Israel. A multiple-layer-overlay (MLO) modulation format is employed for a 14-km optical fiber link and an enhanced spectral efficiency of 2.36 bits/s/Hz is achieved by multiplexing 3-layer signals with each layer carrying a 2-Gbit/s QPSK signal.

SW1N • Applications of Optical
Resonators—Continued

(see page 137 for SW1N.4)

SW1O • Ultrafast Technologies
Based on Aperiodical Quasi-
Phase Matching—Continued

SW1O.2 • 09:00

Chirped Quasi-Phase-Matching Grating Design for Broad-Bandwidth, Engineerable-Phase Adiabatic Second-Harmonic Generation, Yu-Wei Lin¹, Chris Phillips², Martin M. Fejer¹; ¹Stanford Univ., USA; ²ETH Zurich, Switzerland. The use of adiabatic conversion for broadband, efficient, and robust second-harmonic generation with engineerable spectral phase is analyzed theoretically and numerically, and verified by experiment. The advantages compared with conventional methods are also discussed.

SW1O.3 • 09:15

Toward Multi-Octave Pulse Shaping by Adiabatic Frequency Conversion, Peter Krogen¹, Haim Suchowski², Houkun Liang¹, Franz X. Kaertner^{1,3}, Jeffrey Moses^{4,1}; ¹Dept. of Electrical Engineering and Computer Science and Research Lab of Electronics, MIT, USA; ²Raymond and Beverly Sackler School of Physics and Astronomy, Tel Aviv Univ., Israel; ³Center for Free-Electron Laser Science, DESY and Physics Dept., Univ. of Hamburg, Germany; ⁴School of Applied and Engineering Physics, Cornell Univ., USA. We demonstrate complex mid-IR spectral phase and amplitude shaping spanning 2.5-5 μ m, based on down-conversion of a shaped near-IR source, using chirped-pulse adiabatic difference frequency generation. The technique can be extended to multi-octave bandwidths.

CLEO: QELS-Fundamental Science

FW1A • Symposium on Cavity
Quantum Electrodynamics I—
Continued

FW1A.5 • 09:30 **Invited**
Towards Scalable Quantum Networks of Spin Qubits in Photonics Integrated Circuits, Dirk R. Englund¹, Luozhou Li¹, Tim Schroder¹, Edward Chen¹, Michael Walsh¹, Igal Bayn¹, Sara L. Mouradian¹, Matthew E. Trusheim¹, Ming Lu², Mircea Cotlet³, Matthew Markham², Daniel Twitchen², Michal Lipson⁴, Karl K. Berggren¹; ¹MIT, USA; ²Element 6, USA; ³Center for Functional Nanomaterials, Brookhaven National Lab, USA; ⁴School of Electrical and Computer Engineering, Cornell Univ., USA. We discuss progress towards the development of on-chip quantum networks of multiple spin qubits in nitrogen vacancy (NV) centers in diamond. We report NV-nanocavity systems in the strong Purcell regime; implantation of NVs with nanometer-scale apertures, including into cavity field maxima; hybrid on-chip networks for integration of multiple functional NV-cavity systems; and scalable integration of superconducting nanowire single photon detectors on-chip.

FW1B • Novel Sources for
Attoscience—Continued

FW1B.6 • 09:30
All-Optical, Three-Dimensional Electron Pulse Compression, Liang Jie Wong^{2,1}, Byron Freelon¹, Timm Rohwer¹, Nuh Gedik¹, Steven Johnson¹; ¹MIT, USA; ²Singapore Inst. of Manufacturing Technology, Singapore. We propose a method of compressing and focusing electron pulses to attosecond durations and sub-micrometer-dimensions using the optical ponderomotive force. Applications include ultrafast electron diffraction, flat electron beam creation, and free-electron-based coherent terahertz emission schemes.

FW1B.7 • 09:45
Femtosecond Stark-Chirped Rapid Adiabatic Passage by Single Spectrally Shaped Pulse, Hangyeol Lee¹, Hyosub Kim¹, Hanlae Jo¹, Jaewook Ahn¹; ¹KAIST, Korea. Complete population inversion of two-level atoms in a magneto-optical trap is demonstrated by off-resonant two laser pulses shaped from a single ultrafast laser pulse. The observed phenomenon is explained in the context of femto-second laser version of Stark-chirped rapid adiabatic passage.

FW1C • Optics of Complex
Media I—Continued

FW1C.6 • 09:30
Efficient Thermal-Light and Light-Thermal Conversion by a Selective Emitter/Absorber, Jing Zhou¹, Xi Chen¹, L. Jay Guo¹; ¹Univ. of Michigan, USA. We use a diluted refractory metal as a selective emitter/absorber to enhance the efficiencies of thermal-light and light-thermal conversions. The absorptivity (emissivity) was measured at high temperatures up to 750°C.

FW1C.7 • 09:45
Microcavity Laser Linewidth Theory, Adi Pick¹, Alex Cerjan², David Liu², Alejandro Rodriguez⁴, Yidong Chong⁵, A. Douglas Stone³, Steven Johnson²; ¹Physics, Harvard Univ., USA; ²MIT, USA; ³Yale Univ., USA; ⁴Princeton Univ., USA; ⁵Nanyang Technological Univ., Singapore. We present a multimode laser-linewidth formula that generalizes previous theories, including corrections for cavity losses, nonlinear gain and dispersion, but is derived in a more general setting and is therefore applicable to complex wavelength-scale lasers.

FW1D • Integrated Nonlinear
Devices—Continued

FW1D.6 • 09:30
Single Mode Broad Area PT-Symmetric Microring Lasers, William Hayenga¹, Mohammad-Ali Miri¹, Hossein Hodaei¹, Absar Ullahsan¹, Mathias Heinrich¹, Demetrios N. Christodoulides¹, Mercedeh Khajavikhan¹; ¹Univ. of Central Florida, CREOL, USA. Single-transverse and longitudinal mode lasing is demonstrated in a PT-symmetric semiconductor microring arrangement. The proposed scheme is versatile, robust to fabrication errors, and allows for high brightness operation while maintaining spectral purity.

FW1D.7 • 09:45
Spontaneous mirror-symmetry breaking in two coupled nanolasers, Philippe Hamel¹, Samir Haddadi¹, Fabrice Raineri¹, Paul Monnier¹, Grégoire Beaudoin¹, Isabelle Sagnes¹, Ariel Levenson¹, Alejandro M. Giacomotti¹; ¹CNRS/LPN, France. We experimentally show spontaneous breaking of mirror-symmetry in two evanescently coupled photonic crystal nanocavity-lasers. A transition from a delocalized mode, to two spatially localized states is observed. Coexistence of these states is demonstrated.

10:00–18:30 Exhibition Open, Exhibit Halls 1 & 2

10:00–10:30 Coffee Break, Exhibit Hall



For Conference News & Insights
Visit blog.cleoconference.org

CLEO: QELS-
Fundamental ScienceFW1E • Quantum Emission and
Plasmonics—Continued

FW1E.7 • 09:30

Carrier Multiplication in a Single Semiconductor Nanocrystal, Fengrui Hu¹, Bihu Lv¹, Chunfeng Zhang¹, Xiaoyong Wang¹, Min Xiao¹; ¹Nanjing Univ. The UV-excited photoluminescence was measured for single CdSe nanocrystals and an average carrier multiplication efficiency of ~13.1% was obtained when the excitation photon energy was set at ~2.46 times of the nanocrystal energy gap.

FW1E.8 • 09:45

Spin Control in Charged Quantum Dots by Twisted Light, Guillermo Quinteiro¹, Tilmann Kuhn²; ¹Universidad de Buenos Aires, Argentina; ²Universitat Muenster, Germany. Strongly focused twisted light may have strong field components in the propagation direction. By manipulating light-hole excitons in a charged quantum dot with such beams the spin of an excess electron can be efficiently controlled.

CLEO: Science & Innovations

SW1F • Surface Emitting
Semiconductors Lasers—
Continued

SW1F.7 • 09:30

Printed Photonic Crystal Bandedge Surface-emitting Lasers on Silicon, Shihchia Liu¹, Deyin Zhao¹, Hongjun Yang¹, Zhenqiang Ma², Carl Reuterskiöld-Hedlund³, Mattias Hammar³, Weidong Zhou¹; ¹Univ. of Texas at Arlington, USA; ²Electrical and Computer Engineering, Univ. of Wisconsin-Madison, USA; ³School of Information and Communication Technology, KTH-Royal Inst. of Technology, Sweden. We report experimental demonstration of a hybrid III-V/Si photonic crystal surface-emitting laser (PCSEL) based on membrane transfer printing technique. Single mode operation was observed with linewidth of 5 Å and side-mode suppression ratio (SMSR) greater than 20 dB.

SW1F.8 • 09:45

Electrically Tunable Organic Vertical Cavity Surface Emitting Laser, Wendi Chang¹, Apoorva Murarka¹, Annie Wang¹, Vladimir Bulovic¹, Jeffrey H. Lang¹; ¹Electrical Engineering and Computer Science, MIT, USA. Using solvent-free composite membrane transfer, we demonstrate an electrically tunable organic visible light-emitting laser with reversible tuning range of 10nm under 6V actuation. Large-area scalability of utilized fabrication methods suggests potential use in all-optical pressure-sensing surfaces.

SW1G • Optical Frequency
Comb Spectroscopy—
Continued

SW1G.7 • 09:30

Optical Frequency Combs of Multi-GHz Line-spacing for Real-time Multi-heterodyne Spectroscopy, Atsushi Ishizawa¹, Tadashi Nishikawa^{2,3}, Ming Yan^{3,4}, Guy Millot⁵, Hideki Gotoh¹, Theodor Hänsch^{3,4}, Nathalie Picqué^{3,4}; ¹NTT Basic Research Labs, Japan; ²Tokyo Denki Univ., Japan; ³Max-Planck-Institut für Quantenoptik, Germany; ⁴Ludwig-Maximilians-Universität München, Germany; ⁵Laboratoire Interdisciplinaire Carnot de Bourgogne, France. Dual-comb spectroscopy using electro-optic-modulator-based frequency combs broadened in a highly nonlinear fiber opens up new opportunities for analytical spectroscopy. One hundred thousand spectra per second are measurable with a 10-THz span and a 157-GHz resolution.

SW1G.8 • 09:45

Mid-Infrared Optical Frequency Combs based on Difference Frequency Generation for Dual-Comb Spectroscopy, Flavio C. Cruz^{2,1}, Daniel L. Maser², Todd Johnson², Gabriel Ycas², Andrew Klose², Laura C. Sinclair², Ian Coddington², Nathan R. Newbury², Scott Diddams²; ¹Universidade Estadual de Campinas, Brazil; ²Time & Frequency Division, National Inst. of Standards and Technology, USA. Dual optical frequency combs at 2.8-3.4 μm with powers >210 mW were produced with femtosecond fiber-lasers and difference frequency generation. Interferograms between the combs have been demonstrated as a step towards mid-infrared dual-comb spectroscopy.

SW1H • Ultrashort Pulse
Characterization—Continued

SW1H.6 • 09:30

Ultrafast Graphene Photodetector for On-chip Broadband Auto-correlator, Ren-Jye Shiue¹, Yuanda Gao², James Hone², Dirk R. Englund¹; ¹MIT, USA; ²Mechanical Engineering, Columbia Univ., USA. We report an integrated graphene photodetector on top of a silicon waveguide with a maximum responsivity of 0.36 A/W and a 3dB high-speed cut-off frequency of 42 GHz. Furthermore, nonlinear photocurrent in graphene under pulse excitation enables direct on-chip characterization of ultrafast pulses.

SW1H.7 • 09:45

Quantitative Characterization of Polarization States of Axisymmetrically Polarized Pulses Generated by Coherent Beam Combining, Masato Suzuki¹, Keisaku Yamane^{1,2}, Kazuhiko Oka¹, Yasunori Toda^{1,2}, Ryuji Morita^{1,2}; ¹Hokkaido Univ., Japan; ²JST, CREST, Japan. By using the extended Stokes parameters and the degree of polarization defined for the spatial distribution (DOP-SD), we fully quantitatively characterize the polarization states of arbitrary (DOP-SD>0.96) axisymmetrically-polarized femtosecond pulses generated by coherent beam combining.

10:00–18:30 Exhibition Open, Exhibit Halls 1 & 2

10:00–10:30 Coffee Break, Exhibit Hall



Join the conversation. Use #CLEO15.
Follow us @cleoconf on Twitter.

Meeting Room
211 B/D

CLEO: Science & Innovations

SW11 • Micro & Nanophotonics—Continued

SW11.6 • 09:30

Cloaking of Metal Contacts on Solar Cells, Martin F. Schumann^{1,2}, Samuel Wiesendanger³, Jan-Christoph Goldschmidt⁴, Karsten Bittkau⁵, Ulrich W. Paetzold⁵, Alexander Sprafke⁶, Ralf B. Wehrspohn⁶, Carsten Rockstuhl^{2,7}, Martin Wegener^{1,2}; ¹*Inst. of Applied Physics, Karlsruhe Inst. of Technology, Germany*; ²*Inst. of Nanotechnology, Karlsruhe Inst. of Technology, Germany*; ³*Inst. of Condensed Matter Theory and Solid State Optics, Friedrich-Schiller-Universität Jena, Germany*; ⁴*Fraunhofer Inst. for Solar Energy Systems ISE, Germany*; ⁵*Institut für Energie- und Klimaforschung (IEK-5), Forschungszentrum Jülich GmbH, Germany*; ⁶*Inst. of Physics, Martin Luther Univ. Halle-Wittenberg, Germany*; ⁷*Inst. of Theoretical Solid-State Physics, Karlsruhe Inst. of Technology, Germany*. We design by transformation optics, fabricate by three-dimensional direct laser writing, and characterize experimentally polymer-based cloaks for 20 μm wide gold-wire contacts on a silicon wafer. The contact shadowing effect is reduced by 90%.

SW11.7 • 09:45

Photovoltaic performance Improvement of Si HIT Solar Cell by Incorporating Flower-Like light trapping Structures, Sheng-Han Tsai¹, Ming-Lun Lee², Vin-Cent Su², Chien-Hsiung Hsu², Yao-Hong You^{2,3}, Po-Hsun Chen^{2,3}, Yen-Pu Chen², Zheng-Hung Hung¹, Chieh-Hsiung Kuan^{1,2}; ¹*Graduate Inst. of Photonics and Optoelectronics, National Taiwan Univ., Taiwan*; ²*Graduate Inst. of Electronics Engineering, National Taiwan Univ., Taiwan*; ³*R&D Division, Kingwave Corporation, Taiwan*. We implemented the flower-like light trapping structures on the surface of HIT solar cell to achieve a great reflectance reduction and effectively improve the J_{SC} from 34.32 mA/cm² to 39.4 mA/cm² compared to the reference.

Meeting Room
212 A/C

CLEO: Applications & Technology

AW1J • Biomedical Imaging and Sensing I—Continued

AW1J.4 • 09:30

Differential Mueller-matrix formalism for polarization sensitive optical coherence tomography, Martin Villiger^{1,2}, Norman Lippok^{1,2}, Brett Bouma^{1,2}; ¹*Wellman Center for Photomedicine, USA*; ²*Harvard Medical School, USA*. The differential Mueller matrix offers useful insight into the polarization properties of biological tissue imaged with polarization sensitive optical coherence tomography. We present the theory and experimentally demonstrate local depolarization in addition to local retardation.

AW1J.5 • 09:45

Effects of Wavelength and Side Lobes on Airy Beam for Optical Coherence Tomography, Miao Zhang¹, Ping Yu¹, Zhijun Ren²; ¹*Univ. of Missouri-Columbia, USA*; ²*Zhejiang Normal Univ., China*. Optical coherence tomography system using a broad wavelength band Airy beam generated by a transmissive cubic phase mask. We experimentally show that the detrimental effects from the side lobes and wavelength dependent curvature are negligible.

Meeting Room
212 B/D

CLEO: Science & Innovations

SW1K • Laser-Induced Structuring in Bulk Material—Continued

SW1K.6 • 09:30

Direct Laser Writing of 3D Gratings and Diffraction Optics, Michael Moebius¹, Kevin Vora¹, SeungYeon Kang¹, Phil Muñoz¹, Guoliang Deng¹, Eric Mazur¹; ¹*Harvard Univ., USA*. We fabricate 3D gratings and diffraction optics using direct laser writing. Diffraction patterns of gratings agree with Laue theory. We demonstrate zone plates for visible wavelengths. Direct laser writing is promising for integrated diffraction optics.

SW1K.7 • 09:45

Harnessing Polarization Spatio-Temporal Coupling: A New Degree of Freedom in Ultrafast Laser Material Processing, Aabid Patel¹, Martynas Beresna¹, Peter Kazansky¹; ¹*Univ. of Southampton, UK*. Polarization spatio-temporal coupling reveals new degree of freedom in ultrafast laser material processing. Control of modification in fused silica is demonstrated with the use of prism compressors and polarization azimuth of ultrashort pulse laser beam.

Marriott
Salon I & II

SW1L • Mid-IR & Supercontinuum Fiber Sources—Continued

SW1L.6 • 09:30

Power Scaling of 2.94 μm Fiber Lasers, Vincent Fortin¹, Martin Bernier¹, Réal Vallée¹; ¹*Centre d'optique, photonique et laser, Université Laval, Canada*. Recent advances in high power erbium-doped fluoride fiber lasers near 2.94 μm are reviewed. Based on an all-fiber architecture, a 20 W record output power was achieved at this wavelength of interest for medical applications.

SW1L.7 • 09:45

Two-Octave Mid-Infrared Supercontinuum Generation in As-Se Suspended Core Fibers, Uffe Møller¹, Christian R. Petersen¹, Irnis Kubat¹, Yi Yu², Xin Gai², Laurent Brilland³, David Méchin³, Celine Caillaud⁴, Johann Troles⁴, Barry Luther-Davies², Ole Bang^{1,5}; ¹*DTU Fotonik, Dept. of Photonics Engineering, Technical Univ. of Denmark, Denmark*; ²*Centre for Ultrahigh bandwidth Devices for Optical Systems, Laser Physics Centre, Australian National Univ., Australia*; ³*R&D Platform of Photonics Bretagne, Perfos, France*; ⁴*Institut des Sciences Chimiques de Rennes, Université de Rennes 1, France*; ⁵*NKT Photonics, Denmark*. A more than two-octave mid-infrared supercontinuum with an average output power of 15.6 mW covering 1.7-7.5 μm (1333-5900 cm⁻¹) is generated in a low-loss As₃₈Se₆₂ suspended core fiber with core diameter of 4.5 μm.

10:00-18:30 Exhibition Open, Exhibit Halls 1 & 2

10:00-10:30 Coffee Break, Exhibit Hall

CLEO: Science & Innovations

SW1M • Coherent
Communications—Continued

SW1M.7 • 09:30 **Invited**
DSP-complexity Reduction of QAM-based Coherent Optical Networks Enabled by Seed Lightwave Distribution, Jun Sakaguchi¹, Motohiro Kumagai¹, Ying Li¹, Tetsuya Ido¹, Yoshinari Awaji¹, Naoya Wada¹; ¹NICT, Japan. A new network scheme employing stable seed lightwave distribution is investigated for reducing QAM demodulation complexity. We perform 150 km seed distribution before 100 km WDM-PDM-64QAM transmission and achieve simple demodulation without phase estimation.

SW1N • Applications of Optical
Resonators—Continued

SW1N.4 • 09:30
Silicon Photonic Filters for Compact High Extinction Ratio Power Efficient (CHERPe) Transmitters, Steven Spector¹, Jeffrey M. Knecht¹, Robert T. Schulein¹, David O. Caplan¹; ¹Massachusetts Inst of Tech Lincoln Lab, USA. We experimentally investigate integrated photonic microring resonator filters as frequency windows in CHERPe transmitters. The impact of filter-order on optical loss, power handling, modulation extinction ratio enhancement, and waveform distortion is assessed.

SW1N.5 • 09:45
28 Gb/s BPSK Modulation in a Coupling-tuned Silicon Microring Resonator, Rui Yang¹, Linjie Zhou¹, haike zhu¹, Jianping Chen¹; ¹Shanghai Jiao Tong Univ., China. We demonstrate 28 Gb/s binary phase-shift keying modulation in a silicon microring integrated with a Mach-Zehnder coupler. The BPSK signal has a Q-factor of 6.3 dB and an EVM of 23.3% with 3 V drive voltage.

SW1O • Ultrafast Technologies
Based on Aperiodical Quasi-
Phase Matching—Continued

SW1O.4 • 09:30
Soliton Modelocking With Normal Dispersion via Adiabatic Excitation of $\nu^{(2)}$ Solitons in Apodized Fanout PPLN Devices, Christopher R. Phillips¹, Aline Sophie Mayer¹, Alexander Klenner¹, Ursula Keller¹; ¹ETH Zurich, Switzerland. We demonstrate soliton modelocking of a Yb:CALGO laser via cascaded second-order nonlinearities whereby the second-harmonic is adiabatically excited/de-excited in an apodized-fanout-PPLN crystal. We obtain 100-fs pulses at 540 MHz with 760 mW average power.

SW1O.5 • 09:45
Fast Tunable Picosecond Optical Parametric Oscillator Based on Chirped Quasi-Phase Matching, Delphine Descloux¹, Jean-Baptiste Dherbecourt¹, Jean-Michel Melkonian¹, Myriam Raybaut¹, Cyril Drag², Antoine Godard¹; ¹Onera, France; ²Laboratoire Aimé Cotton, France. We report on a picosecond OPO combining an aperiodically poled nonlinear crystal and a rapidly tunable intracavity spectral filter. Fast tuning over 80 nm around 3.84 μm is carried out in less than few milliseconds.

10:00–18:30 Exhibition Open, Exhibit Halls 1 & 2

10:00–10:30 Coffee Break, Exhibit Hall

10:00–12:00 JW2A • Poster Session II

JW2A.1 Withdrawn

JW2A.2
Entanglement Diversity in Monolithic Waveguides, Dongpeng Kang¹, Minseok Kim¹, Haoyu He¹, Amr S. Helmy¹; ¹Univ. of Toronto, Canada. The simultaneous generation of both co-polarized and cross-polarized polarization entangled photons from a monolithic semiconductor chip is demonstrated. High quality entanglement is achieved with no use of any off-chip compensation, interferometry or filtering.

JW2A.3
Avoiding Entanglement Sudden Death Using Quantum Measurement Reversal on Single-qubit, Hyang-Tag Lim¹, Jong-Chan Lee¹, Kang-Hee Hong¹, Yoon-Ho Kim¹; ¹Pohang Univ of Sci & Tech (POSTECH), USA. Decoherence on two-qubit systems degrades entanglement, and sometimes even causes entanglement sudden death (ESD). We show quantum measurement reversal on only one subsystem can avert ESD, providing methods for practical entanglement distribution under decoherence.

JW2A.4
Measurement of Energy Correlations of Photon Pairs Generated in Silicon Ring Resonators, Davide Grassani¹, Angelica Simbula¹, Matteo Galli¹, Stefano Pirodda¹, Tom Baher-Jones², Michael Hochberg², Nicholas Harris³, Christophe Galland⁴, John E. Sipe⁵, Daniele Bajoni⁶, Marco Liscidini¹; ¹Physics, Università degli Studi di Pavia, Italy; ²East West Photonics Pte Ltd, Singapore; ³Electrical Engineering and Computer Science, MIT, USA; ⁴Stuttgart Univ., Germany; ⁵Physics, Univ. of Toronto, Canada; ⁶Ingegneria Industriale e dell'Informazione, Università degli Studi di Pavia, Italy. With unprecedented resolution we measure the joint spectral density of photon pairs that would be generated by spontaneous four-wave-mixing in a silicon ring resonator, and show how the quantum correlations can be tailored.

JW2A.5
Quantum information interface for orbital angular momentum photons, Ruikai Tang¹, Xiongjie Li¹, Wenjie Wu¹, Haifeng Pan¹, Heping Zeng¹, E Wu¹; ¹East China Normal Univ., China. We have demonstrated a quantum interface based on the frequency upconversion for photons carrying orbital angular momentum (OAM) states from telecom wavelength to visible regime by sum-frequency generation with high quantum conversion efficiency.

JW2A.6
Generation and Characterization of Continuous Variable Quantum Correlations Using a Fiber Optical Parametric Amplifier, Xueshi Guo¹, Xiaoying Li¹, Nannan Liu¹, Yuhong Liu¹; ¹College of Precision Instrument and Opto-electronics Engineering, Tianjin Univ., China. We generate the quadrature entanglement and the Gaussian discord using a fiber optical parametric amplifier, and investigate the factors influencing the values of inseparability I and discord D , respectively.

JW2A.7
Fortifying Single Photon Detectors to Quantum Hacking Attacks by Using Wavelength Upconversion, Gregory S. Kanter^{1,2}; ¹NuCrypt, USA; ²Center for Photonic Communication and Computing, Northwestern Univ., USA. Upconversion detection can isolate the temporal and wavelength window over which light can be efficiently received. Using appropriate designs the ability of an eavesdropper to damage, measure, or control QKD receiver components is significantly constricted.

JW2A.8
A Controlled-NOT (CNOT) Gate Based on Quantum Interference in Cascaded Silicon Dual-ring Resonators, Lei Zhang^{1,2}, Zhanshi Yao¹, Lin Yang², Andrew W. Poon¹; ¹Photonic Device Lab, Dept. of Electronic and Computer Engineering, The Hong Kong Univ. of Science and Technology, China; ²State Key Lab on Integrated Optoelectronics, Inst. of Semiconductors, Chinese Academy of Sciences, China. We propose a controlled-NOT (CNOT) gate based on two-photon quantum interference in cascaded silicon dual-ring resonators with Mach-Zehnder interferometer-assisted coupling. We illustrate the working principle and the design parameters of the device by theoretical modeling.

JW2A.9
Photonic Quantum Walks on Finite Graphs and with Non-Localised Initial States, Sonja Barkhofen¹, Fabian Elster¹, Thomas Nitsche¹, Jaroslav Novotný², Aurél Gábris^{2,3}, Igor Jex², Christine Silberhorn¹; ¹Applied Physics, Univ. of Paderborn, Germany; ²Dept. of Physics, Faculty of Nuclear Sciences and Physical Engineering, Czech Technical Univ. in Prague, Czech Republic; ³Dept. of Theoretical Physics, Univ. of Szeged, Hungary. We present a time-multiplexed quantum walk in a fibre loop setup and introduce a fast switching electro optic modulator. Hence we can limit the spread of the wavefunction by choice and study the evolution of non-localized initial states.

JW2A.10
Multi-party Agile QKD Network with a Fiber-based Entangled Source, Eric Y. Zhu¹, Costantino Corbari², Alexey V. Gladyshev³, Peter Kazansky², Hoi-Kwong Lo¹, Li Qian¹; ¹Univ. of Toronto, Canada; ²Univ. of Southampton, UK; ³Fiber Optics Research Center of the Russian Academy of Sciences, Russia. A multi-party quantum key distribution scheme is demonstrated by utilizing a poled fiber-based broadband polarization-entangled source and dense wavelength-division multiplexing. Entangled photon pairs are delivered over 40-km of fiber, with secure key rates of more than 20 bits/s observed.

JW2A.11
Spectral Engineering and Entanglement Generation in Poled Optical Fibers, Eric Y. Zhu¹, Costantino Corbari², Alexey V. Gladyshev³, Alexey Kosolapov³, Mikhail Yashkov⁴, Peter Kazansky², Li Qian¹; ¹Univ. of Toronto, Canada; ²Optoelectronics Research Centre, Univ. of Southampton, UK; ³Fiber Optics Research Center of the Russian Academy of Sciences, Russia; ⁴Inst. of Chemistry of High-Purity Substances of the Russian Academy of Sciences, Russia. The joint spectra of the two type-II phase-matchings that add coherently to give rise to the generation of polarization-entangled photon pairs in a poled fiber are measured. Optimal parameters are identified for the generation of high-quality entanglement.

JW2A.12
Divide-and-Conquer Integrated Photon-Counting Device, Armando P. Leija¹, Jan Sperling², Markus Graefe¹, Rene Heilmann¹, Mathias Heinrich¹, Werner Vogel², Stefan Nolte¹, Alexander Szameit¹; ¹Friedrich-Schiller-Universität Jena, Germany; ²Institut für Physik, Rostock Univ., Germany. In this work we experimentally demonstrate a fully integrated photon-counting device based on a divide-and-conquer technique using linear optics in combination with on-off detectors. Our scheme is based on click-counting statistics instead of photon-counting statistics.

JW2A.13
High-Q Microresonator as a Five-Partite Entanglement Generator via Cascaded Parametric Processes, Yutian Wen¹, Qiang Lin², Guangqiang He¹; ¹Dept. of Electronic Engineering, Shanghai Jiaotong Univ., China; ²Dept. of Electrical and Computer Engineering, Univ. of Rochester, USA. We propose to produce five-partite entanglement via cascaded four-wave mixing in a high-Q microresonator that may become a key to future one-way quantum computation on chip.

JW2A.14
Integrated-photonic generation of general EPR-states, Markus Graefe¹, René Heilmann¹, Stefan Nolte¹, Alexander Szameit¹; ¹Inst. of Applied Physics, Germany. We present a novel method to generate arbitrary path-encoded EPR- states on-chip by a single operation only. Such states can be utilized to mimic the quantum statistics of fermions, bosons, and anyons.

JW2A.15
Secure Communication App on Mobile Phone Enabled by Sharing Quantum Random Numbers, Lu-Feng Qiao^{1,2}, Long Li¹, Xiao-Feng Lin^{1,2}, Xianmin Jin^{1,2}; ¹State Key Lab of Advanced Optical Communication Systems and Networks, Dept. of Physics and Astronomy, Shanghai Jiao Tong Univ., China; ²Synergetic Innovation Center of Quantum Information and Quantum Physics, Univ. of Science and Technology of China, China. We develop a mobile phone app for secure communication in which all data including text, voice, email and any other files are all encrypted and decrypted with shared quantum random numbers.

JW2A.16
Quantum Repeater with Quantum Frequency Conversion, Xiao Li¹, Neal Solmeyer², Qudsi Quraishi²; ¹Joint Quantum Inst., USA; ²U.S. Army Research Lab, USA. We report the progress of a quantum repeater with quantum frequency conversion to telecom wavelengths, which allows for quantum communication over long distances.

JW2A.17
Quantum State Engineering in Integrated Couplers, Ryan P. Marchildon¹, Amr S. Helmy¹; ¹Univ. of Toronto, Canada. The utilization of integrated couplers beyond their function as 50:50 splitters is examined. Their dispersive properties offer novel possibilities for state engineering, interference visibility behaviour, and entanglement sensitivity. Implications for photon pair separation are explored.

JW2A.18
Compressive Imaging of Broadband Single-Photon Sources With Superconducting Detectors, Jason Schaake¹; ¹Univ. of Tennessee at Knoxville, USA. We experimentally characterize the spatio-spectral properties of photon pairs generated by spontaneous parametric down-conversion in a Type-0 PPKTP waveguide using compressive imaging techniques combined with superconducting single photon detectors and dispersive fiber spectrometer.

JW2A.19
Simulation Study of the Stability of Polarization Structure in Disordered Photonic Crystal Waveguides, Ben Lang¹, Ruth Oulton¹, Daryl Beggs¹, John Rarity¹, Andrew Young¹; ¹Univ. of Bristol, UK. The effects of short range disorder on the polarization characteristics of light in W1 photonic crystal waveguides were simulated. It was found that points of local circular polarization were robust in both quantity and location.

JW2A.20
Two-photon evolution equation for multiphoton optical systems, Armando P. Leija¹, Markus Graefe¹, Rene Heilmann¹, Maxime N. Lebugle¹, Stefan Nolte¹, Hector Moya-Cessa², Demetrios N. Christodoulides³, Alexander Szameit¹; ¹Friedrich-Schiller-Universität Jena, Germany; ²Optics Dept., INAOE, Mexico; ³CREOL, Univ. of Central Florida, USA. In this work we demonstrate, theoretically and experimentally, that two-photon probability amplitudes describing propagation of light in any two-photon state are governed by an evolution equation identical to a 2D tight-binding equation.

JW2A.21

Optical and Microwave Properties of Focused Ion Beam Implanted Erbium Ions in Y_2SiO_5 Crystals, Nadezhda Kukharchyk¹, Sebastian Probst², Shovon Pal¹, Kangwei Xia³, Roman Kolesov³, Arne Ludwig¹, Alexey V. Ustinov², Pavel Bushev⁴, Andreas D. Wieck¹; ¹Angewandte Festkörperphysik, Ruhr-Universität Bochum, Germany; ²Physikalisches Institut, Karlsruhe Inst. of Technology, Germany; ³Physikalisches Institut, Universität Stuttgart, Germany; ⁴Experimentalphysik, Universität des Saarlandes, Germany. We present focused ion beam implantation as a prospective tool for realizing a patterned rare-earth spin-ensemble in a solid-state substrate. We demonstrate a successful implantation with 20% of luminescent ion activation for Erbium ions in Y_2SiO_5 crystals.

JW2A.22

Efficient Collisional Blockade Single Atom Loading in Tight Optical Microtraps, Yin Hsien Fung¹, Mikkel Andersen¹; *Jack Dodd Centre for Quantum Technology, Univ. of Otago, New Zealand*. Collisional blockade loading of single atom in tight FORT has about 50% efficiency in previous works. We experimentally observe an enhancement to about 80% by inducing controlled inelastic collisions during loading, which is supported by an analytical theory.

JW2A.23

Preservation of Transverse Spatial Coherence of an Optical Pulse in Atomic Vapor Quantum Memory, Jong-Chan Lee¹, Kwang-Kyoon Park¹, Young-Wook Cho¹, Yoon-Ho Kim¹; ¹Physics, Pohang Univ. of Science and Technology, Korea. We report preservation of transverse spatial coherence of an optical pulse stored in atomic vapor quantum memory. Using Young-type spatial interference, it is clearly demonstrated that the atomic vapor quantum memory preserves transverse spatial coherence.

JW2A.24

Withdrawn

JW2A.25

Coulomb Interaction and Delocalized States in Self-assembled InGaAs Lateral Quantum Dot Molecules, Xinran Zhou¹, Miquel Royo², Weiwen O. Liu¹, Jihoon Lee^{3,4}, Gregory Salamo⁴, Juan Clemente², Matthew Doty¹; ¹Univ. of Delaware, USA; ²Departament de Química Física i Analítica, Universitat Jaume I, Spain; ³School of Electronics and Information, Kwangju Univ., Korea; ⁴Inst. of Nanoscale Science and Engineering, Univ. of Arkansas, USA. We study self-assembled lateral quantum dot molecules (LQDMs) under varying electric and magnetic fields and deduce the electronic structure, charge configurations and delocalized states that lead to the observed photoluminescence spectra.

JW2A.26

Resonance Fluorescence Spectrum from a Quantum Dot Driven by a Periodically-Pulsed Laser, kumarasiri konthasinghe¹, Manoj Peiris¹, Ben Petrak¹, Yingyu², Zhichuan Niu², Andreas muller¹; ¹Physics, Univ. of South Florida, USA; ²Chinese Academy of Sciences, China. We report the measurement of the resonance fluorescence spectrum from a quantum dot under periodically-pulsed excitation. The evolution of the multiple sidebands and Rabi oscillations for coherently and incoherently scattered light were observed.

JW2A.27

Withdrawn

JW2A.28

Deterministic Generation of a Triexciton in a Quantum Dot, Emma Schmidgall¹, Ido Schwartz¹, Liron Gantz¹, Dan Cogan¹, David Gershoni¹; ¹Technion, Israel. We demonstrate deterministic generation of a quantum dot-confined triexciton in a well-defined coherent state using a sequence of three laser pulses.

JW2A.29

Bright phonon-tuned single-photon source, Simone L. Portalupi¹, Gaston Hornecker², Valérian Giesz¹, Thomas Grange², Aristide Lemaître¹, Justin Demory¹, Isabelle Sagnes¹, Norberto D. Lanzillotti-Kimura¹, Loïc Lanco^{1,3}, Alexia Auffèves², Pascale Senellart^{1,4}; ¹CNRS-LPN Laboratoire de Photonique et de Nanostructures, France; ²CEA/CNRS/UJF joint team "Nanophysics and Semiconductors", Institut Néel-CNRS, France; ³Département de physique, Université Paris Diderot, France; ⁴Département de physique, Ecole Polytechnique, France. We studied experimentally and theoretically a single-photon source consisting of a quantum dot coupled to a micropillar cavity. The influence of the LA-phonon bath on the brightness of the source and the indistinguishability of the emitted photons will be discussed.

JW2A.30

Interactions of Space Variant Polarization Beams with Zeeman-shifted Rubidium Vapor, Anat Szapiro¹, Liron Stern¹, Uriel Levy¹; ¹Hebrew Univ. of Jerusalem, Israel. We experimentally demonstrate the interaction between space variant polarization beams with a Zeeman shifted rubidium vapor operating as a controlled circular birefringence and dichroism media. Full Stokes parameters measurements allows for mapping the polarization distribution.

JW2A.31

A Subluminal Laser with Extreme Insensitivity to Cavity Length Change, Zifan Zhou¹, Joshua Yablon¹, Ye Wang¹, Jacob Scheuer², Selim M. Shahriar¹; ¹Northwestern Univ., USA; ²School of Electrical Engineering, Tel Aviv Univ., Israel. With a narrow peak on top of a broad-band gain profile in a laser, the group-velocity of light becomes significantly subluminal. The lasing frequency becomes extremely insensitive to cavity length change in such a laser.

JW2A.32

Simple and Efficient Filter for Single Photons from a Cold Atom Quantum Memory, Daniel T. Stack¹, Qudsiya Quraishi¹; ¹US Army Research Lab, USA. Filtering unwanted light signals is critical to the operation of neutral atom quantum memories. The addition of a novel frequency filter increases the non-classical correlations and readout efficiency of our quantum memory by $\approx 35\%$.

JW2A.33

Optimized scalable circular grating with efficient photon extraction for Nitrogen Vacancy centers in a bulk diamond, Jiabao Zheng^{1,2}, Edward Chen², Luozhou Li², Florian Dolde², Dirk R. Englund²; ¹Dept. of Electrical Engineering, Columbia Univ., USA; ²Dept. of Electrical Engineering and Computer Science, MIT, USA. We numerically demonstrate an optimized circular grating for Nitrogen-Vacancy centers with collection efficiency of 35.8% for Zero-Phonon emission into NA within 0.5, which is improved to 63.9% by adding a conductive layer. The optimal structure is fabricated using transferred hard mask lithography.

JW2A.34

Withdrawn

JW2A.35

A New Algorithm for Attosecond Pulse Characterization, Phillip D. Keathley¹, Sidharth Bhardwaj¹, Jeffrey Moses¹, Guillaume Laurent¹, Franz X. Kaertner^{1,2}; ¹Electrical Engineering and Computer Science and Research Lab of Electronics, MIT, USA; ²Center for Free-Electron Laser Science and Dept. of Physics, DESY and Univ. of Hamburg, Germany. An algorithm for characterizing attosecond EUV pulses which is not bandwidth-limited, requires no interpolation of the experimental data, and makes no approximations beyond SFA while fully retrieving both the IR and EUV pulses is introduced.

JW2A.36

Versatile Simulation Package for Ultrafast Pulse Propagation and High Harmonic Generation, Gregory J. Stein¹, Chien-Jen Lai¹, Phillip D. Keathley¹, Peter R. Kroger¹, Houkun Liang¹, Chun-Lin L. Chang¹, Kyung-Han Hong¹, Guillaume Laurent¹, Franz X. Kaertner^{1,2}; ¹MIT, USA; ²CFEL, Germany. A simulation package for 3D pulse propagation and HHG is reported. Our package is capable of emulating pulse propagation for a host of geometries and nonlinear effects, and has been employed to reproduce experimental HHG spectra.

JW2A.37

Towards Observing Dynamical Localization within the Quantum Linear Rotor, andrei kamalov^{1,2}, Doug Broege^{1,2}, Philip H. Bucksbaum^{2,1}; ¹Stanford Univ., USA; ²PULSE Inst., SLAC National Accelerator Lab, USA. We discuss novel approaches towards observation of dynamical localization, a phenomenon believed to occur in the periodically δ -kicked quantum linear rotor and is related to one-dimensional Anderson localization.

JW2A.38

Ultrafast Rotational Spectroscopy Based on a Free-space Nitrogen Ion Laser, Hongqiang Xie¹, Bin Zeng¹, Haisu Zhang¹, Guihua Li¹, Wei Chu¹, Jinping Yao¹, Chenrui Jing¹, Jielei Ni¹, Ya Cheng¹; ¹Shanghai Inst. of Optics and Fine Mechanics, China. We demonstrated that ultrafast rotational spectroscopy can be performed with a cavityless nitrogen ion laser with both high temporal and spectral resolutions. Quantum beating between the molecular rotational wave packets have been observed.

JW2A.39

Highly Efficient High-order Harmonics with Large Cutoff from Carbon Molecules using Various Laser Wavelengths, Muhammad Ashiq Fareed¹, Nicolas Thiré¹, Sudipta Mondal¹, yoann pertot¹, Maxime Boudreau¹, Bruno E. Schmidt¹, François Légaré¹, Tsuneyuki Ozaki¹; ¹INRS-EMT, Canada. Carbon molecules are used to generate intense high-order harmonics using driving lasers with 0.8 μm - 1.71 μm wavelengths. By driving plasma of reduced size ($\sim 200\mu\text{m}$) with 1.71 μm laser, we could extend the cutoff to $\sim 70\text{eV}$, while reducing the peak intensity by only $\sim 31\%$.

JW2A.40

Interaction of Metal Oxide Nanoparticles, Generated via Microparticle Ablation, with Intense XUV Pulses, Sandra Bruce^{1,2}, Ahmed M. Helal^{1,2}, Thanh Ha^{1,2}, Hernan J. Quevedo^{1,2}, Aaron C. Bernstein^{1,2}, John Keto^{1,2}, Todd Ditmire^{1,2}; ¹Center for High Energy Density Science, USA; ²Physics, The Univ. of Texas at Austin, USA. We have designed and assembled an experiment to evaluate the role of continuum lowering in XUV nanoduster ionization. Metal oxide nanoparticles, generated via laser ablation of microparticles, will be irradiated by intense coherent XUV pulses.

JW2A.41

Electron Heating by Ultra-Fast, Ultra-Intense Laser Irradiation of Wavelength-Scale Wires, Kristina Serratto¹, Franki Aymond¹, Brandon Simon¹, Aaron C. Bernstein¹, Todd Ditmire¹; ¹The Univ. of Texas at Austin, USA. Wavelength-scale platinum wires were irradiated by a 1-micron wavelength laser at relativistic intensities, accelerating electrons in the laser-matter interaction. Wire diameters and angles relative to laser polarization were varied, and emitted electron distributions were measured.

JW2A.42

Generation of High-Density, Thin Gas Targets for Intense Laser Interaction at 1 kHz Repetition Rates, Yan Tay¹, Donghoon Kuk¹, Luke Hahn¹, Howard Milchberg¹, Ki-Yong Kim¹; ¹Univ. of Maryland at College Park, USA. We report the production of high-density, thin gas targets (90 \sim 500 microns) with cryogenic cooling in continuous gas flow. Multiple nozzles are also demonstrated to produce corrugated plasma waveguides at 1 kHz repetition rates.

10:00–12:00
JW2A • Poster Session II

JW2A.43

Density-chopped Far-infrared Transmission Spectroscopy to Probe Subband-Landau Splittings and Tune Intersubband Transitions, Shovon Pal^{1,2}, Hanond Nong², Sascha R. Valentin¹, Nadezhda Kukharchyk¹, Arne Ludwig¹, Nathan Jukam², Andreas D. Wieck¹; ¹Lehrstuhl für Angewandte Festkörperphysik, Ruhr-Universität Bochum, Germany; ²AG Terahertz Spektroskopie und Technologie, Ruhr-Universität Bochum, Germany. We study the half-field subband-Landau resonant splitting of a two-dimensional electron gas and demonstrate the possibility to tune the intersubband spacings via density-chopped far-infrared transmission spectroscopy in the absence of external magnetic field.

JW2A.44

Withdrawn

JW2A.45

Optical Generation of High Spin Polarization in GaSe Nanoslabs, Yanhao Tang¹, Wei Xie¹, Krishna C. Mandal², John A. McGuire¹, Chih-Wei Lai¹; ¹Michigan State Univ., USA; ²Univ. of South Carolina, USA. We report nearly complete preservation of "spin memory" between optical absorption and photoluminescence under excitation >0.2 eV above the band gap in nanometer GaSe slabs.

JW2A.46

Control of Energy Relaxation Pathways in Graphene: Carrier-Carrier Scattering vs Phonon Emission, Zoltan Mics¹, Soren Jensen¹, Ivan Ivanov¹, Samet Varol¹, Dmitry Turchinovich¹, Frank Koppens², Mischa Bonn¹, Klaas-Jan Tielrooij²; ¹Max Planck Inst. f. Polymer Research, Germany; ²ICFO The Inst. of Photonic Sciences, Spain. We investigate the relaxation pathways of photoexcited carriers in graphene. These carriers relax their energy through either carrier-carrier scattering or phonon emission, depending on photoexcitation conditions and the Fermi level.

JW2A.47

Withdrawn

JW2A.48

Exciton States in InGaN Nano-disks in GaN Nanowires Revealed Using Nonlinear Laser Spectroscopy, Cameron Nelson¹, Albert Liu¹, Sanjya Deshpande¹, Shafat Jahangir¹, Pallab K. Bhattacharya¹, Duncan G. Steel¹; ¹Univ. of Michigan, USA. Linear and coherent non-linear resonant high resolution laser spectroscopy was used to characterize In_{0.54}Ga_{0.46}N disks in nanowires. Nonlinear optical spectroscopy and PLE reveal narrow excitonic resonances and evidence of coupling between separate excited states.

JW2A.49

Many-Body Interactions Between Excitons in GaAs Quantum Wells Quantified Using Two-Dimensional Coherent Spectroscopy, Rohan Singh¹, Travis Austry¹, Galan Moody², Gael Nardin¹, Bo Sun¹, Takeshi Suzuki¹, Steven Cundiff¹; ¹JILA, Univ. of Colorado/NIST, USA; ²NIST, USA. We have quantified excitonic many-body interaction energies in GaAs quantum wells using two-dimensional coherent spectroscopy. The anharmonic oscillator model for excitons is used to extract the inter- and intra-mode interaction energies from 2D spectra.

JW2A.50

Optical Pump - Multi-THz Probe Spectroscopy of a Single Crystal Organic Hybrid Lead Halide Perovskite, David A. Valverde-Chavez¹, Carlito Ponceca², Constantinos Stoumpos³, Arkady Yartsev², Mercurio Kanatzidis³, Villy Sundström², David G. Cooke¹; ¹Physics, McGill Univ., Canada; ²Chemical Physics, Lund Univ., Sweden; ³Chemistry, Northwestern Univ., USA. We analyzed ultrafast photocarrier generation in single crystal CH₃NH₃PbI₃ perovskite through time-resolved terahertz spectroscopy. We find a Drude-Lorentz type conductivity spectra with a carrier mobility of 35 cm²/Vs and a Lorentzian component at 45 meV possibly due to intra-excitonic transitions.

JW2A.51

THz transient non-perturbative detection of spin reorientation transition in NdFeO₃ single crystal, Guo-Hong Ma¹; ¹Shanghai Univ., China. Magnetic field-induced spin switching of NdFeO₃ crystal was demonstrated with TDS spectroscopy. The critical magnetic field to achieve the magnetic phase transition is modulated by temperature. A useful one-way spin switching has been found in NdFeO₃ crystal.

JW2A.52

Ultrafast Laser-Induced Field Emission from a Single Carbon Nanotube Based Nanotip, Mina Bionta¹, Benoit Chalopin¹, Marc Delmas², Florent Houdellier², Aurelien Masseboeuf², Julien Mauchain¹, Beatrice Chatel¹; ¹LCAR-IRSAMC Université Paul Sabatier, France; ²CEMES, France. We present the first demonstration of ultrafast laser-induced field emission from a carbon nanotube based nanotip, and measurement of the energy distribution of the electrons.

JW2A.53

Laser Assisted Electron Emission from Free Standing Carbon Nanotube Paper, Ryan Hendrix¹, Jason A. Deibel¹, Steven B. Fairchild², Benji Maruyama², Augustine Urbas², Mark Walker², Dean Brown³; ¹Wright State Univ., USA; ²Materials and Manufacturing Directorate, Air Force Research Lab, USA; ³UES, Air Force Research Lab, USA. Laser assisted electron emission from a free standing, non-aligned carbon nanotube film is observed with low power (<100 mW) continuous wave (785 nm) laser excitation. An increase in emission current by 330 times is realized.

JW2A.54

Two Dimensional Coherent Spectroscopy of CdSe/ZnS Colloidal Quantum Dots at Cryogenic Temperatures, Bo Sun¹, Diogo B. Almeida¹, Rohan Singh^{1,2}, Geoffrey M. Diederich³, Mark E. Siemens³, Lazaro A. Padilha⁴, Wan K. Bae⁵, Jeffrey Pietryga⁶, Victor Klimov⁶, Steven Cundiff^{1,2}; ¹JILA, National Inst. of Standards and the Univ. of Colorado, USA; ²Physics, Univ. of Colorado, USA; ³Dept. of Physics and Astronomy, Univ. of Denver, USA; ⁴Instituto de Física, Universidade Estadual de Campinas, Brazil; ⁵Photo-Electronic Hybrid Research Center, Korea Inst. of Science and Technology, Korea; ⁶Chemistry Division, Los Alamos National Lab, USA. We demonstrate 2D coherent spectroscopy of CdSe/ZnS nanocrystals and measure the exciton homogeneous linewidth as a function of temperature from 10K to 300K. The spectra reveal contributions to the linewidth from discrete acoustic phonon modes.

JW2A.55

Hybrid Metal Wire-Dielectric THz Fibers: Design and Perspectives, Andrey Markov¹, Hichem Guerboukha¹, Maksim Skorobogatiy¹; ¹Ecole Polytechnique de Montreal, Canada. We investigate the optical characteristics of terahertz two-wire plasmonic waveguides, porous, and foam-based dielectric waveguides. Our group demonstrates a low-loss and low-dispersion hybrid metal wire-dielectric fiber resulting from fusion of the aforementioned types of waveguides.

JW2A.56

Graded Index Porous Optical Fibers - Dispersion Management in Terahertz Range, Andrey Markov¹, Tian Ma^{1,2}, Maksim Skorobogatiy¹; ¹Ecole Polytechnique de Montreal, Canada; ²Xi'an Inst. of Optics and Precision Mechanics of CAS, China. Graded index porous fiber incorporating an air-hole array featuring variable air-hole diameters and inter-hole separations is proposed. We experimentally demonstrate smaller pulse distortion, larger bandwidth and higher excitation efficiency compared to fibers with uniform porosity.

JW2A.57

Efficiency Scaling of Narrowband Terahertz Wave Generation in PPLN by Optimizing the Pump-Pulse Format, Jan Schulte^{1,2}, Sergio Carbajo^{1,2}, Koustuban Ravi³, Damian N. Schimpf¹, Franz Kaerter^{1,3}; ¹Center for Free-Electron Laser Science, Deutsches Elektronen-Synchrotron (DESY), Germany; ²Dept. of Physics, Univ. of Hamburg, Germany; ³Dept. of Electrical Engineering and Computer Science, MIT, USA. We demonstrate a 1.5×10⁻⁴ room temperature conversion efficiency and 0.29 μJ pulse energy for narrowband terahertz generation in PPLN pumped with ultrafast pulses at 800nm by experimentally and numerically optimizing the pump-pulse format.

JW2A.58

Ultra High Dynamic Range Electro Optic Sampling for Terahertz Detection Using Fiber Based Spectral Domain Interferometry, Akram Ibrahim¹, Denis Férachou¹, Gargi Sharma², Kanwarpal (KP) Singh³, Tsuneyuki Ozaki¹; ¹INRS-EMT, Advanced Laser Light Source, Université du Québec, 1650 boul. Lionel-Boulet, J3X 1S2, Canada; ²Univ. of Massachusetts Lowell, 1 Univ. Avenue, 01854, USA; ³Harvard Medical School, Massachusetts General Hospital, 40 Blossom Street, 02114, USA. We demonstrate a novel fiber-based spectral-domain interferometry (SDI) technique for terahertz electric field measurement. Signal-to-noise ratio is enhanced by more than four folds while the scanning window is extended to >30 picoseconds compared to conventional SDI techniques.

JW2A.59

Freestanding Terahertz Metamaterials Fabricated by Laser Beam Machining, Norman Born¹, Jan C. Balzer¹, Ralf Gente¹, Ibraheem Al-Naib², Martin Koch¹; ¹Philipps Universität Marburg, Germany; ²Dept. of Physics, Queen's Univ., Canada. We demonstrate freestanding terahertz metamaterials, fabricated by laser-beam machining of commercial Aluminum-foil. This method allows for cost-efficient and rapid prototyping. Low insertion losses and outstanding transmission characteristics render the samples as high performance filters.

JW2A.60

Nano-holes vs Nano-cracks in Thin Gold Films: What Causes Anomalous THz Transmission?, Dmitry Turchinovich¹, Keno Krewer¹, Ke Jiang¹, Zoltan Mics¹, Zuanming Jin¹, Karina Bley¹, Hans-Joachim Elmers¹, Katharina Landfester¹, Mischa Bonn¹; ¹Max Planck Inst. for Polymer Research, Germany. Nano-structuring materials can change their properties extraordinarily, but so can defects caused by manufacturing. We study the effect of capacitive defects on terahertz transmission in golden nanomeshes, and find their influence crucial.

JW2A.61

Evaluation of trace amounts of liquid using THz waves, Kazunori Serita¹, Eiki Matsuda¹, Iwao Kawayama¹, Hironaru Murakami¹, Masayoshi Tonouchi¹; ¹Osaka Univ., Japan. We demonstrated terahertz near-field measurements of trace amounts of liquid. The obtained data show that the information of the solute less than nanogram in the trace amounts of liquid can be sensitively detected.

JW2A.62

Measurement of Terahertz Spectrum Using Heterodyne Technique with LO signal Generated by an MZM-Based Flat Comb Source, Isao Morohashi¹, Yoshihisa Irimajiri¹, Motohiro Kumagai¹, Akira Kawakami¹, Takahide Sakamoto¹, Norihiko Sekine¹, Tetsuya Kawanishi¹, Akifumi Kasamatsu¹, Iwao Hosako¹; ¹NICT, Japan. We demonstrated rapid measurement of spectra of terahertz (THz) radiation from a quantum cascade lasers. THz waves generated by photonic down-conversion using Mach-Zehnder-modulator-based flat comb generator were used for local oscillator signals.

JW2A.63

Effects of Photoexcitation on Intense Terahertz Field-induced Nonlinearity in Monolayer Epitaxial Graphene, Hassan Kafez Eid¹; ¹INRS-EMT, Canada. Terahertz field-induced transmission enhancement in monolayer epitaxial graphene is observed with increasing terahertz field. Photoexcitation leads to further transmission enhancement that is found to be less for the higher terahertz field amplitudes.

JW2A.64

Synthesis and all-optical self-referenced measurement of vectorial optical arbitrary waveform, Chi-Cheng Chen¹, Shang-Da Yang¹; ¹Inst. of Photonics Technologies, National Tsing Hua Univ., Taiwan. We demonstrated an integrated system that can manipulate and measure vectorial field spanning up to the entire repetition period without ambiguity, iteration, and reference.

JW2A.65

Large Time-Bandwidth Product Integrated Microwave Photonic Hilbert Transformer, Bolan Liu¹, Chaotan Sima^{1,2}, WEI YANG¹, Deming Liu¹, YU YU², JAMES C. GATES³, Christopher Holmes³, Michalis Zervas³, Peter Smith³; ¹Next Generation Internet Access National Engineering Lab (NGIA), Huazhong Univ of Science and Technology, China; ²Wuhan National Lab for Optoelectronics, China; ³Optoelectronics Research Centre, Univ. of Southampton, UK. We demonstrate an integrated largest time-bandwidth product (TBP) microwave photonic Hilbert transformer, using synthesized Bragg grating design and fabrication techniques. Devices operate from 50 GHz to 2.5 THz, with the TBP approaching 50.

JW2A.66

Two-dimensional Nanomaterial Tungsten Disulfide (WS₂) As Saturable Absorber for Mode-locked Laser Near 1550 nm, Kan Wu¹, Xiaoyan Zhang², Jung Wang², Xing Li¹, Jianping Chen¹; ¹Shanghai Jiao Tong Univ., China; ²Shanghai Inst. of Optics and Fine Mechanics, CAS, China. Saturable absorption has been discovered in two-dimensional nanomaterial tungsten disulfide (WS₂) near 1550nm. The mode-locked laser based on WS₂ saturable absorber have been demonstrated, which indicates the potential of WS₂ for ultrafast photonic applications.

JW2A.67

Improved Multiple Pulse Reconstruction from SHG FROG Spectrograms, Alexander Hause¹, Fedor Mitschke¹; ¹Univ. of Rostock, Germany. A modified algorithm is presented which significantly reduces the rate of false reconstructions of SHG FROG spectrograms. A procedure to obtain error bars is given; they allow to gauge the quality of the reconstruction.

JW2A.68

Twisted-Nematic Liquid Crystal Polarization Rotators for Broadband Laser Applications, Peter Fiala¹, Christophe Dorrer¹, Kenneth Marshall¹; ¹Univ. of Rochester, USA. Liquid crystal twisted-nematic polarization rotators in the Mauguin condition are shown to be more achromatic, less prone to high-frequency modulations caused by internal reflections than compound wave plates, and can be fabricated cost effectively at multi-inch apertures.

JW2A.69

Incoherent-light implementation of the photonic time stretch concept, Bo Li^{1,2}, Shuqin Lou², José Azaña¹; ¹INRS - Energie, Canada; ²School of Electronic and Information Engineering, Beijing Jiaotong Univ., China. We propose and experimentally demonstrate photonic time stretch of radio-frequency signals by using a time-gated (pulsed) incoherent light source, with time-stretch factors of 0.83 and 8.66, and a time-bandwidth product of > 340.

JW2A.70

Nonstoichiometric Si_{1-x}Ge_x Based Tunable Saturable Absorber for Mode-Locked Erbium-doped Fiber Laser, Chi-Cheng Yang¹, Yung-Hsiang Lin¹, Gong-Ru Lin¹; ¹National Taiwan Univ., Taiwan. Free-standing thin-film flexible Si_{1-x}Ge_x saturable absorber with Si/Ge composition-ratio dependent saturable absorbance is demonstrated to passively mode-lock the erbium-doped fiber laser for delivering a pulsewidth of 330 fs at a modulation depth of 16%.

JW2A.71

16 W All-Normal-Dispersion Mode-Locked Yb-Doped Fiber Laser With Large Core Diameter, Zhiguo Lv¹, Hao Teng², Lina Wang², Zhiyi Wei²; ¹School of Physics and Optoelectronic Engineering, Xidian Univ., China; ²Beijing National Lab for Condensed Matter Physics, Inst. of Physics, Chinese Academy of Sciences, Beijing 100190, China, Beijing National Lab for Condensed Matter Physics, Inst. of Physics, Chinese Academy of Sciences, Beijing 100190, China, China. A mode-locked all-normal-dispersion rod-fiber laser with large core diameter was demonstrated. Output power of 16 W with 270 fs pulse duration is generated. To best knowledge this is the first laser operation with 85 mm core fiber.

JW2A.72

Time Resolved Measurements of Relativistic Laser Hole Boring Using Broadband Relay Imaged GRENOUILLE, Craig Wagner¹, Aaron C. Bernstein¹, Gilliss M. Dyer¹, Todd Ditmire¹; ¹Center for High Energy Density Science, Univ. of Texas at Austin, USA. To measure relativistic laser hole boring velocities up to 0.18c, an ultra-broadband diagnostic capable of retrieving the full time resolved pulse phase is required. The design of such a device based on GRENOUILLE is presented.

JW2A.73

Single-Shot Measurement of High-Harmonic Generation Intensity Waveforms by Spatially Encoded Transmission Switching, Hsu-hsin Chu¹, Chi-Hsiang Yang¹, Shih-Cheng Liu¹, Jyhpyng Wang^{1,2}; ¹National Central Univ., Taiwan; ²Inst. of Atomic and Molecular Sciences, Academia Sinica, Taiwan. Single-shot measurement of high-harmonic generation intensity waveforms is demonstrated by utilizing tunneling ionization of H₂ gas for transmission switching. This method can be applied to different kinds of ultrashort coherent extreme-UV sources.

JW2A.74

Passively Mode-locked Fiber Laser based on CVD WS₂, Reza Khazaeinezhad¹, Saha Hosseinzadeh Kassani¹, Hwanseong Jeong², Dong-Il Yeom², Kyunghwan Oh¹; ¹Yonsei Univ., USA; ²Ajou Univ., Korea. We investigated nonlinear characteristics and applications of WS₂ for mode-locked fiber laser. The saturable absorber was prepared by transferring the synthesized CVD WS₂ onto a fabricated side-polished fiber. WS₂ showed promising potential for ultrafast-pulse generation.

JW2A.75

Real-time and Ultrafast Phase Retrieval in Optical Time-stretch Using a Modified Gerchberg-Saxton Algorithm, Yiqing Xu¹, Zhibo Ren¹, Kenneth K. Y. Wong¹, Kevin K. Tsia¹; ¹The Univ. of Hong Kong, USA. We report a new and practical scheme of using optical time-stretch with Gerchberg Saxton (GS)-like algorithm for ultrafast real-time phase retrieval, with the phase error significantly suppressed even at a wide signal bandwidth.

JW2A.76

χ⁽²⁾-Lens Mode-Locking of a Nd:YVO₄ Laser with High Average Power and Repetition Rate up to 600 MHz, Veselin S. Aleksandrov¹, Hristo Iliev², Ivan Buchvarov¹; ¹Sofia Univ. St. Kliment Ohridski, Bulgaria; ²Binovation Ltd., Bulgaria. We demonstrate χ⁽²⁾-lens mode-locking of a diode pumped Nd:YVO₄ laser. The output power is 6 W, the pulse duration is 6 ps for repetition rates from 110 MHz up to 600 MHz.

JW2A.77

Deviations from Theory by Femtosecond Lasers due to Noise, Gennady Rasskazov¹, Vadim Lozovoy¹, Marcos Dantus¹; ¹Michigan State Univ., USA. We compare deviations from theory in the yield of second harmonic generation in order to characterize high-repetition rate femtosecond laser sources where the amplitude and phase differs from pulse to pulse. Experimental results are presented for cases with phase noise and a post-pulse.

JW2A.78

Vertically Stacked AllPolymer Whispering-Gallery Mode Lasers for Biosensing Applications, Sentayehu Fetene Wondimu¹, Tobias Siegle², Uwe Bog^{1,4}, Sarah Kraemmer³, Heinz Kalt³, Timo Mappes^{1,2}, Sebastian Koeber^{1,5}, Tobias Wienhold¹, Christian Koos^{1,5}; ¹Inst. of Microstructure Technology (IMT), Karlsruhe Inst. of Technology, Germany; ²Corporate Research and Technology, Carl Zeiss AG, Germany; ³Inst. of Applied Physics (APH), Karlsruhe Inst. of Technology, Germany; ⁴Inst. of Nanotechnology (INT), Karlsruhe Inst. of Technology, Germany; ⁵Inst. of Photonics and Quantum Electronics (IPO), Karlsruhe Inst. of Technology, Germany. We report on the fabrication of polymeric whispering-gallery mode (WGM) lasers. Our approach enables high packing density by vertical stacking and multiplexed readout of resonators and lends itself to signal referencing or multi-target sensing.

JW2A.79

Fiber Optical Tweezers for Simultaneous Force Exertion and Measurements in a 3D Hydrogel Compartment, Chaoyang Ti¹, Gawain M. Thomas², Qi Wen², Yuxiang Liu¹; ¹Mechanical Engineering Dept., Worcester Polytechnic Inst., USA; ²Physics Dept., Worcester Polytechnic Inst., USA. We developed an inclined dual fiber optical tweezers (DFOTs) for simultaneous force application and measurements in a 3D hydrogel matrix. The inclined DFOTs provide a potential solution for cell mechanics study in a three-dimensional matrix.

JW2A.80

Implementation of optical multiplicative spike-timing-dependent plasticity with adaptive current feedback of semiconductor optical amplifiers, Yaolin Zhang¹, Quansheng Ren¹, Jy Zhao¹; ¹Peking Univ., China. We present the optical multiplicative spike-timing-dependent-plasticity (STDP) by adaptive control of current injection to the semiconductor optical amplifiers. As a result, we can mimic the behavior of biological STDP synapses more realistically.

JW2A.81

Resonantly-Enhanced Sensing Using Surface Plasmon Polaritons in a Sagnac Interferometer, Brian Hake¹, Herbert Grotewohl¹, Miriam Deutsch¹; ¹Univ. of Oregon, USA. We present analysis of a resonantly enhanced Sagnac interferometer. While one output port is highly sensitive to nonreciprocal phenomena and robust to reciprocal fluctuations, the complementary output can be used to simultaneously monitor reciprocal drifts.

JW2A.82

60-MHz wavelength-encoded tomography (WET), Bowen Li¹, Chi Zhang², Sisi Tan¹, Xiaoming Wei¹, Yiqing Xu¹, Kevin K. Tsia¹, Kenneth K. Y. Wong¹; ¹The Univ. of Hong Kong, Hong Kong; ²Huazhong Univ. of Science and Technology, China. Wavelength-encoded tomography (WET) is upgraded to a triple-time-lens system to perform ultrafast cross-sectional imaging through 68.4x-temporal magnification. 60-MHz A-scan rate is demonstrated by imaging a glass sample with 180-μm axial resolution.

JW2A.83

Manipulation of Nanoparticles using Quadrangular Microlens, Yuzhi Shi^{1,2}, Lip Ket Chin², Jihui Wu¹, Tianing Chen¹, Ai-Qun Liu²; ¹School of Mechanical Engineering, Xi'an Jiaotong Univ., China; ²School of Electric and Electronic Engineering, Nanyang Technological Univ., Singapore. We present an optical element, quadrangular microlens, for the generation of Bessel beam, bottle beams, slowly divergent self-healing beam and the discrete interference pattern. Thus, it can be used for the transporting, trapping, cooling, sorting and patterning of nanoparticles.

JW2A.84

Hologram Acquisition by Using Time Resolved Heterodyne Method in Optical Scanning Holography, Munseob Lee¹, Gi-hyeon Min¹, Nacwoo Kim¹, Byung-Tak Lee¹; ¹ETRI, Korea. We propose the new hologram acquisition method based on the time resolved heterodyne analysis in optical scanning holography. By applying the FFT or four phase picking algorithm method, we obtain complex hologram without reference signal.

JW2A.85

Hybrid Mid-IR OCT System for Imaging and Spectroscopy Using New High Power Low-Coherence Quantum Cascade Superluminescent Emitters, Deborah Varnell¹, Mei Chai Zheng¹, Nyan L. Aung¹, Ahmed Musse¹, Samantha Lee¹, Claire F. Gmachl¹; ¹Princeton Univ., USA. We have successfully constructed and tested a new mid-infrared optical coherence tomography imaging system capable of simultaneous imaging and spatial spectroscopy using new quantum cascade superluminescent emitters.

10:00–12:00
JW2A • Poster Session II

JW2A.86

Ellipsometry-based opto-fluidic platform for characterizing 10,000 biomolecular reactions on solid supports in real time and for identifying inhibitors against specific protein-receptor interactions, Xiangdong Zhu¹; ¹Univ. of California at Davis, USA. We developed an optical detection platform based on nulling ellipsometry for simultaneously characterizing 10,000 biomolecular reactions on solid supports and for highly efficient identification of inhibitory molecules against specific protein-protein interactions from large compound libraries.

JW2A.87

Optical Measurement on Cell Membrane Roughness Influenced by Paclitaxel and Gold Nanoparticles, Chau-Hwang Lee^{1,2}, Lan-Lin Jang¹, Huei-Jyuan Pan¹; ¹Research Center for Applied Sciences, Academia Sinica, Taiwan; ²Inst. of Biophotonics, National Yang-Ming Univ., Taiwan. We measured the membrane roughness of neuroblastoma cells under the treatments of gold nanoparticles and paclitaxel. The stabilization of microtubules by paclitaxel reduced the membrane roughness. The positive charges on nanoparticles led to similar results.

JW2A.88

Improvement in In-Plane Localization Precision of Nanoparticles Using Interference Analysis, Amihai Meiri¹, Carl Ebeling¹, Jason Martineau¹, Zeev Zalevsky², Jordan Gerton¹, Rajesh Menon¹; ¹Univ. of Utah, USA; ²Bar Ilan Univ., Israel. We present a method to improve the localization precision of nanoparticles over Gaussian fitting by imposing an interference pattern on the Point-Spread-Function. Localization precision of 0.1 nm for a single emitter was obtained.

JW2A.89

Optofluidic Detection for Virus Infection Monitoring using Effective Refractive Index, Patricia Yang Liu^{1,2}, Lip Ket Chin², Wee Ser², Teck Choon Aiy³, Eric Peng Huat Yap³, Tarik Bourouina¹, Yamin Leprince-Wang¹; ¹Université Paris-Est, France; ²Nanyang Technological Univ., Singapore; ³DSO National Labs, Singapore. This paper presents an optofluidic imaging system to detect influenza virus infection via the change of refractive index based on scattering signature. This method allows for a direct monitor of the influenza flu virus.

JW2A.90

Virtual Acousto-optic Beam Paths for Steerable Deep-tissue Optical Stimulation and Imaging, Maysamreza Chamanzar¹, Minyoung Huh¹, NINH DO¹, M. Reza Alam¹, Michel Maharbiz¹; ¹Univ. of California Berkeley, USA. Here we present the first non-invasive methodology for optical delivery and steering deep inside the brain through creating reconfigurable light paths by ultrasonic waves via modulating the refractive and diffractive properties of the medium.

JW2A.91

Ce-doped Fibers with High Axial Resolution for Optical Coherence Tomography Applications, Liu Chun-Nien¹, Yi-Chung Huang², Pi-Ling Huang¹, Sheng-Lung Huang³, Wood-Hi Cheng¹; ¹Dept. of Photonics, National Sun Yat-Sen Univ., Taiwan; ²CEO office, Brogent Technologies Inc., Taiwan; ³Graduate Inst. of Photonics and Optoelectronics, National Taiwan Univ., Taiwan. The fabrication of CeDFs with drawing-tower is demonstrated. The CeDFs exhibited a 160-nm broadband emission with 1.47- μ m axial resolution. This CeDF may be functioned as a high-resolution light source for OCT applications.

JW2A.92

Noninvasive flow cytometry by heterodyne self-mixing interferometry, Olivier Hugon¹, Mehdi Inglebert¹, Olivier Jacquin¹, Hugues Guillet de Chatellus¹, Eric Lacot¹, Chaouqi Misbah¹, Boudewijn Van Der Sanden²; ¹LIPhy, France; ²Clinatec, France. We present a device for characterizing red blood cells flows in capillaries (speed, hematocrit, aggregation, ...) . We've used the LOFI technique on a microfluidic system that mimics the human skin and subcutaneous tissues.

JW2A.93

All-Fiber Tunable Ring Laser Based on an Acousto-Optic Tunable Coupler, Ligang Huang¹, Wending Zhang², Dong Mao², Feng Gao¹, Weihua Peng¹, Fang Bo¹, Guoquan Zhang¹, Jingjun Xu¹; ¹Nankai Univ., China; ²Northwestern Polytechnical Univ., China. An all-fiber tunable ring laser consisted of an acousto-optic tunable notch filter and a tapered fiber was demonstrated with a tunable wavelength range from 1532.1 nm to 1570.4 nm and a linewidth of 0.2 nm.

JW2A.94

Supercontinuum Generated by Noise-like Pulses for Spectral-domain Optical Coherence Tomography, Yi-Jing You¹, Chengming Wang², Ping Xue², Alexey Zaytsev³, Ci-Ling Pan^{1,3}; ¹Inst. of Photonics Technologies, National Tsing Hua Univ., Taiwan; ²State Key Lab of Low-dimensional Quantum Physics, Dept. of Physics, Tsinghua Univ., China; ³Dept. of Physics, National Tsing Hua Univ., Taiwan. A supercontinuum with over 420-nm of spectral bandwidth is generated in a single-mode-fiber pumped by noise-like-pulses from an Yb-doped fiber laser. The supercontinuum source is successfully employed in a spectral-domain optical coherence tomography imaging system.

JW2A.95

Annular Cladding Erbium-Doped Multi-Core Fiber for SDM Amplification, Cang Jin^{1,2}, Bora Ung³, Younès Messaddeq^{4,2}, Sophie LaRoche^{1,2}; ¹Département de Génie Électrique et de Génie Informatique, Université Laval, Canada; ²Centre D'optique, Photonique et Laser, Canada; ³Département de Génie Électrique, École De Technologie Supérieure, Canada; ⁴Département de Physique, De Génie Physique et D'optique, Université Laval, Canada. An annular cladding ED-MCF is proposed to enhance pump power efficiency. Simulations suggest single core amplification with over 29 dB gain and less than 7.5 dB at 1550 nm using a single Watt-level pump.

JW2A.96

Transition Profile Control for Broadband Visible Supercontinuum Generation in Tapered PCF, Tongxiao Jiang¹, Aimin wang¹, Fuzeng Niu¹, Wei Zhang¹, Yawei Chang¹, Zhigang Zhang¹; ¹Peking Univ., China. Tapered photonic crystal fibers with different transition profiles were designed and fabricated to control the visible dispersive wave generation process, and broadband visible supercontinuum (350-700 nm) was achieved.

JW2A.97

Design of Supermode Fiber for Orbital Angular Momentum (OAM) Multiplexing, Shuhui Li¹, Jian Wang¹; ¹Wuhan National Lab for Optoelectronics, China. We present a supermode fiber to support orbital angular momentum (OAM) multiplexing. The designed supermode fiber can guide multiple OAM modes with favorable performance of low mode coupling, low nonlinearity, and low modal dependent loss.

JW2A.98

Widely tunable Raman laser in a tellurite fiber ring cavity, Dinghuan Deng¹, Lai Liu¹, Tonglei Cheng¹, Xiaojie Xue¹, Lei Zhang¹, Makoto Yamada², Takenobu Suzuki¹, Yasutake Ohishi¹; ¹Toyota Technological Inst., Japan; ²Osaka Prefecture Univ., Japan. A widely tunable Raman laser covering a 170-nm bandwidth was demonstrated using a single-mode tellurite fiber embedded in a ring cavity.

JW2A.99

Small signal gain for Nd/Cr:YAG ceramics at high temperature, Yoshiyuki Honda¹, Shinji Motokoshi², Takahisa Jitsuno¹, Noriaki Miyanaga¹, Kana Fujioka¹, Masahiro Nakatsuka², Minoru Yoshida³; ¹Osaka Univ., Japan; ²Inst. for Laser Technology, Japan; ³Kinki Univ., Japan. The gain coefficient of the Nd/Cr:YAG ceramics excited by the absorption line of Cr³⁺ increased with increasing temperature up to 400 K.

JW2A.100

Simulated Tempering Markov Chain Monte Carlo for Full Waveform Analysis, Weiji He¹, Wenye Yin¹, Feng Shi², Guohua Gu¹, Qian Chen¹; ¹Nanjing Univ of Science and Technology, China; ²Science & Technology on Low-light-level Night Vision Lab, China. A new approach of Simulated Tempering Markov Chain Monte Carlo (STMCMC) for full waveform LIDAR signal analysis was proposed and demonstrated. We present the theory, algorithm as well as the practical examples.

JW2A.101

Withdrawn

JW2A.102

Hybrid White Light-emitting Diodes by Organic-Inorganic materials, Kuo-Ju Chen¹, Yi-Chun Lai¹, Bin-Cheng Lin¹, Chien-Chung Lin¹, Sheng-Huan Chiu¹, Zong-Yi Tu¹, Min-Hsiung Shih², Peichen Yu¹, Po-Tsung Lee¹, Xiuling Li³, Hsin-Fei Meng¹, Gou-chung Chi¹, Teng-Ming Chen¹, Hao-Chung Kuo¹; ¹National Chiao Tung Univ., Taiwan; ²Research Center for Applied Sciences, Taiwan; ³Dept. of Electrical and Computer Engineering, Univ. of Illinois at Urbana-Champaign Urbana, USA. This study demonstrated the high uniformity hybrid white light-emitting diodes with polyfluorene (PFO) polymer and quantum dot (QD) with different CCT range from 3000K to 9000K.

JW2A.103

Flat-Plate Photovoltaics with Solar-Tracking Origami Micro-Concentrator Arrays, Chih-Wei Chien¹, Kyusang Lee¹, Matthew Shlian², Stephen Forrest¹, Max Shtein³, Pei-Cheng Ku¹; ¹Dept. of Electrical Engineering and Computer Science, Univ. of Michigan, USA; ²School of Art and Design, Univ. of Michigan, USA; ³Dept. of Materials Science and Engineering, Univ. of Michigan, USA. A new PV architecture combining the advantages of concentration and flat-plate PVs is shown. Using origami techniques, fabrication and solar tracking of micro-concentrators were achieved with minimally added complexity to the existing flat-plate PVs.

JW2A.104

Application of Fractional Fourier Transform for Interferometry, Ming-Feng Lu¹, Feng Zhang¹, Ran Tao¹, Guo-Qiang Ni¹, Ting-Zhu Bai¹; ¹Beijing Inst. of Technology, China. The Fractional Fourier transform can be understood as a chirp-based decomposition. Accordingly it can be used to process fringe patterns with quadratic phase, including denoising, quantization error reduction, sampling and reconstruction, and phase derivative estimation.

10:30–12:30 **Market Focus: Precision Manufacturing Using Ultrafast Lasers, Exhibit Hall Theater**

12:00–13:00 **Lunch and Unopposed Exhibit Only Time, Exhibit Halls 1 & 2 (concessions available)**

12:30–13:30 **VIP Industry Leaders Networking Event, Exhibit Hall 3 (lunch provided, registration required)**

12:30–15:30 **OSA Members, Family and Friends Event (Visit the OSA booth to register, as registration is required)**

CLEO: QELS-Fundamental Science

13:00–15:00

FW3A • Symposium on Cavity Quantum Electrodynamics II*Presider: Pascale Senellart; CNRS-Laboratoire de Photonique et Nanost, France*FW3A.1 • 13:00 **Invited**

Cavity-QED with a Trapped Ion in an Optical Fiber Cavity, Michael Köhl¹; ¹Universität Bonn, Germany. We report on cavity-QED experiments with trapped ions in fiber-based high-finesse optical cavities. We observe single photon emission and absorption and, in particular, demonstrate coupling to a semiconductor quantum dot by exchange of a single photon between the atomic and solid state quantum emitters.

FW3A.2 • 13:30

Fiber-Based Cavities for Ion-Trap Quantum Networks, Tracy Northup¹, Klemens Schüpfer¹, Florian Ong¹, Bernardo Casabone¹, Konstantin Friebe¹, Moonjoo Lee¹, Jakob Reichel², Rainer Blatt^{1,3}; ¹Univ. of Innsbruck, Austria; ²ENS/UPMC-Paris 6/CNRS, France; ³Inst. for Quantum Optics and Quantum Information, Austria. Fiber-based cavities offer a promising route toward the strong-coupling regime of cavity QED. I will discuss the development of a fiber-cavity experiment for single trapped calcium ions, focusing on mirror characterization and quantum-network prospects.

FW3A.3 • 13:45

Nanophotonic Quantum Memory Based on Rare-Earth-Ions Coupled to an Optical Resonator, Tian Zhong¹, Jonathan Kindem¹, Evan Miyazono¹, Andrei Faraon¹; ¹California Inst. of Technology, USA. We demonstrate optical photon storage in a Nd:YSO nano-resonator using multi-mode stimulated photon echo and atomic frequency comb protocols. Current results indicate strong prospects for on-chip nanophotonic quantum memories using rare-earth-ions.

13:00–15:00

FW3B • Novel Approach for Studying Condensed Matter*Presider: Giacomo Coslovich; Lawrence Berkeley National Lab, USA*FW3B.1 • 13:00 **Invited**

Attosecond Sources for Time-Bandwidth Balanced Spectroscopy, Alberto Simoncig¹, Sebastian Schulz¹, Ivanka Grguras³, Sasa Bajt², Adrian L. Cavalieri^{1,3}; ¹MPI-Structure and Dynamics of Matter, Germany; ²DESY, Germany; ³Univ. of Hamburg, Germany. Spectral bandwidth in attosecond pulses can span multiple energy levels simultaneously, complicating time-resolved photoemission applications. We seek to adapt attosecond sources to study condensed-matter dynamics with sub-eV resolution, unfolding on the corresponding femtosecond timescale.

FW3B.2 • 13:30

Experimental Distinction between Femtosecond Transient Demagnetization and Spin Current Dynamics in Metals, Zuanming Jin¹, Jacek Arabski², Guy Schmerber², Eric Beaupaire², Mischa Bonn¹, Dmitry Turchinovich¹; ¹MPI for Polymer Research, Germany; ²Institut de Physique et Chimie des Matériaux de Strasbourg (IPCMS), UMR 7504 CNRS - Université de Strasbourg, France. Using terahertz emission spectroscopy we probe the elementary spin dynamics in ferromagnetic metal on a femtosecond timescale, and distinguish between the two major contributions - transient demagnetization and spin current by hot electrons.

FW3B.3 • 13:45

Ultrafast Pump-probe Spectroscopy in Gallium Arsenide at 25 Tesla, Jeremy Curtis¹, Takahisa Tokumoto¹, Nicholas Nolan¹, Luke McClintock¹, Judy Cheria², Stephen McGill², David J. Hilton¹; ¹Univ. of Alabama at Birmingham, USA; ²National High Magnetic Field Lab, USA. We have conducted pump-probe spectroscopy of bulk GaAs in the Split Florida-Helix at 15 K and 25 T. We observe an electronic rise followed by a slower decay with a superimposed oscillatory response.

13:00–15:00

FW3C • Optics of Complex Media II*Presider: Hui Cao; Yale Univ., USA*FW3C.1 • 13:00 **Invited**

Spatial Coherence of Random Raman Lasing Emission, Brett H. Hokr^{1,2}, Morgan Schmidt³, Joel Bixler^{1,3}, Phillip Dyer², Gary Noojin³, Brandon Redding⁴, Robert Thomas³, Benjamin Rockwell³, Hui Cao⁴, Vladislav Yakovlev¹, Marlan Scully^{1,5}; ¹Texas A&M Univ., USA; ²TASC Inc., USA; ³Bioeffects Division, Optical Radiation Branch, 711th Human Performance Wing, Human Effectiveness Directorate, USA; ⁴Yale Univ., USA; ⁵Baylor Univ., USA. Random Raman laser emission is demonstrated to be an excellent source of narrow-band, high intensity, short duration light for speckle-free imaging. Spatial coherence measurement and strobe photography of cavitation bubbles are presented.

FW3C.2 • 13:30

Critical States Embedded in the Continuum, Milan Koirala¹, Alexey G. Yamilov¹, Ali Basiri³, Yaron Bromberg², Hui Cao², Tsampikos Kottos³; ¹Physics, Missouri Univ. of Science and Technology, USA; ²Applied Physics, Yale Univ., USA; ³Physics, Wesleyan Univ., USA. We introduce a class of critical states which are embedded in the continuum (CSC) of one-dimensional optical waveguide array with a non-Hermitian defect.

FW3C.3 • 13:45

Quantitative test of the ab initio intrinsic laser linewidth theory, Alexander Cerjan¹, Adi Pick², Yidong Chong³, Alejandro Rodriguez⁴, Steven Johnson⁵, A. Douglas Stone¹; ¹Yale Univ., USA; ²Physics, Harvard Univ., USA; ³Division of Physics and Applied Physics, Nanyang Technological Univ., Singapore; ⁴Applied Physics, Princeton, USA; ⁵Applied Math, MIT, USA. Direct FDTD simulations of the Maxwell-Bloch equations coupled to Langevin noise equations are shown to quantitatively agree with a recent analytic linewidth formula and predicted scaling relations.

13:00–15:00

FW3D • New Effects in Nanostructures and Semiconductors*Presider: Dragomir Neshev; Australian National Univ., Australia*FW3D.1 • 13:00 **Invited**

Nonlinear Effects Driven by Optically-induced Magnetic Response, Yuri S. Kivshar¹; ¹Australian National Univ., Australia. We discuss novel nonlinear effects in nanostructured metasurfaces driven by optically-induced electric and magnetic responses associated with Mie-type resonances of their metallic and dielectric structural elements including the generation of multipole harmonics and substantial power enhancement.

FW3D.2 • 13:30

Studying the Interplay of Electric and Magnetic Resonance-Enhanced Second Harmonic Generation: Theory and Experiments, Rohit Chandrasekar¹, Naresh K. Emani¹, Alexei Lagutchev¹, Vladimir M. Shalaev¹, Cristian Ciraci^{2,3}, David R. Smith², Alexander V. Kildishev¹; ¹Electrical and Computer Engineering, Purdue Univ., USA; ²Electrical and Computer Engineering, Duke Univ., USA; ³Center for Biomolecular Nanotechnologies, Istituto Italiano di Tecnologia, Italy. We present an experimental study of a metasurface, which exhibits electric and magnetic resonances, in order to understand their independent contributions to second-harmonic generation. A hydrodynamic model framework is used to match experimental results.

FW3D.3 • 13:45

Semiconductor-Superconductor Two-Photon Amplifier, Raja Marjeh¹, Evyatar Sabag¹, Alex Hayat¹; ¹Technion, Israel. We study a new effect of Cooper-pair-based two-photon gain in semiconductor-superconductor structures, showing broadband enhancement of singly- and fully-stimulated ultrafast two-photon gain. These effects can have important implications in optoelectronics and in coherent-control applications.

**CLEO: QELS-
Fundamental Science**

13:00–15:00

FW3E • Active Plasmonics and Nanolasers

President: Jie Yao; Berkeley Univ., USA

FW3E.1 • 13:00

Quantum-Coherently Assisted Deep-UV Localization of Photonic States in Active Stopped-Light Plasmonic Heterostructures, Kosmas Tsakmakidis¹, Pankaj K. Jha¹, Yuan Wang¹, Xiang Zhang¹; ¹UC Berkeley, USA. We introduce a new method to localize light-waves. We show how the interaction of a gain medium with a planar deep-UV plasmonic heterostructure, at its zero- v_g point, strongly localizes light. A quantum-coherent drive provides a means to control the localization and dramatically improve the dynamics.

FW3E.2 • 13:15

Optical Switching of Mid-Infrared Plasmonic Nanoantennas Based on Germanium, Marco Patrick Fischer¹, Christian Schmidt¹, Johannes Stock¹, Emilie Sakat², Antonio Samarelli³, Jacopo Frigerio⁴, Paolo Biagioni², Douglas J. Paul³, Giovanni Isella⁴, Alfred Leitensorfer¹, Daniele Brida¹; ¹Dept. of Physics and Center for Applied Photonics, Universität Konstanz, Germany; ²Dipartimento di Fisica, Politecnico di Milano, Italy; ³School of Engineering, Univ. of Glasgow, UK; ⁴L-NESS, Dipartimento di Fisica, Politecnico di Milano, Italy. Germanium nanoantennas are activated by triggering a mid-infrared plasma response via ultrafast interband excitation. Femtosecond control of the intrinsic semiconductor allows complete activation of the plasmonic resonance for hundreds of picoseconds.

FW3E.3 • 13:30

Enhanced Near- and Far-Field Faraday Rotation with a Monolayer Array of Core-Shell Nanoparticles, Arthur Davoyan¹, Nader Engheta¹; ¹Univ. of Pennsylvania, USA. We study Faraday rotation by magnetized core-shell nanoparticles. We theoretically show enhanced polarization rotation in the near-zone and several-fold increase of the Faraday effect in the far-zone for a periodic array of nanoparticles.

FW3E.4 • 13:45

Plasmon-mediated emission in the strong coupling regime, Thejaswi Tumkur¹, Guohua Zhu¹, Devon Courtwright¹, Mikhail A. Noginov¹; ¹Norfolk State Univ., USA. We demonstrate the strong coupling of SPPs and localized plasmons to dye molecules, characterized by splitting of the dispersion curve. We further observe an anomalous behavior in the emission of molecules strongly coupled to plasmons.

CLEO: Science & Innovations

13:00–15:00

SW3F • III-V Lasers on Silicon

President: John Bowers; Univ. of California Santa Barbara, USA

SW3F.1 • 13:00

Electrically Pumped 1.3- μ m InAs/GaAs Quantum Dot Laser Monolithically Grown on Si Substrate Lasing up to 111°C, Siming chen¹, Mingchu Tang¹, Qi Jiang¹, Jiang Wu¹, Vitaliy Dorogan², Mourad Benamara², Yuriy Mazur², Gregory Salamo², Alwyn Seeds¹, Huiyun Liu¹; ¹Univ. College London, UK; ²Univ. of Arkansas, USA. A silicon-based InAs/GaAs quantum dot laser that lases up to 111°C, with a threshold current density of 200 A/cm² and an output power exceeding 100 mW at room temperature, has been achieved.

SW3F.2 • 13:15

Hybrid III-V/SOI single-mode vertical-cavity laser with in-plane emission into a silicon waveguide, Gyeong C. Park¹, Weiqi Xue¹, Elizaveta Semenova¹, Jesper Mork¹, Il-Sug Chung¹; ¹Technical Univ. of Denmark, Denmark. We report a III-V-on-SOI vertical-cavity laser emitting into an in-plane Si waveguide fabricated by using CMOS-compatible processes. The fabricated laser operates at 1.54 μ m with a SMSR of 33 dB and a low threshold.

SW3F.3 • 13:30

Ultra-compact Wavelength Tunable Quantum Dot Laser with Silicon Photonic External Cavity, Tomohiro Kita¹, Naokatsu Yamamoto², Tetsuya Kawanishi², Hirohito Yamada¹; ¹Tohoku Univ., USA; ²National Inst. of Information and Communications Technology, Japan. Ultra-compact wavelength tunable laser diode with wide tunability was successfully developed with combining quantum dot optical amplifier and silicon micro-ring filters. The single mode laser oscillation was demonstrated with 25 nm wavelength tuning range.

SW3F.4 • 13:45

1.3- μ m InAs/GaAs Quantum Dot Lasers on Silicon-on-Insulator Substrates by Metal-Stripe Bonding, Yuan-Hsuan Jhang¹, Katsuki Tanabe², Satoshi Iwamoto^{1,2}, Yasuhiko Arakawa^{1,2}; ¹Inst. of Industrial Science, Univ. of Tokyo, Japan; ²Inst. for Nano Quantum Information Electronics, Univ. of Tokyo, Japan. We demonstrate InAs/GaAs quantum dot lasers on silicon-on-insulator substrates by metal-stripe wafer bonding technology. Our III-V-on-Si bonded laser exhibits room-temperature lasing at 1.3 μ m with current injection through the bonding metal stripe.

13:00–15:00

SW3G • Precision Spectroscopy

President: R. Jason Jones; Univ. of Arizona, USA

SW3G.1 • 13:00

Dual-Comb Femtosecond Enhancement Cavity for Precision Measurements of Plasma Dynamics and Spectroscopy in the XUV, David R. Carlson¹, Tsung-Han Wu¹, R. Jason Jones¹; ¹Univ. of Arizona, USA. We show two high power 100 fs frequency combs can be coupled to the same enhancement cavity for performing time-resolved measurements of optical nonlinearities and for simplifying dual-comb spectroscopy in the XUV.

SW3G.2 • 13:15

Broadband Dual-comb Spectroscopy with Cascaded-electro-optic-modulator-based Frequency Combs, Tadashi Nishikawa¹, Atushi Ishizawa², Ming Yan^{1,3}, Hldeki Gotoh², Theodor Hänsch^{1,3}, Nathalie Picqué^{1,3}; ¹Max-Planck-Institut für Quantenoptik, Germany; ²NTT Basic Research Labs, Japan; ³Ludwig-Maximilians-Universität München, Germany. Dual-comb spectroscopy without mode-locked lasers is demonstrated in the telecommunication region. As a proof-of-principle, we measure Doppler-limited rovibrational spectra of the 2 ν_3 band of H¹³C¹⁴N spanning more than 4 THz with resolved comb lines.

SW3G.3 • 13:30

Ramsey-comb Spectroscopy: Power and Precision Combined, Robert K. Altmann¹, Laura S. Dreissen¹, Sandrine A. Galtier¹, Kjeld S. Eikema¹; ¹LaserLab, VU Univ. (FEW), Netherlands. Ramsey-comb spectroscopy enables ultra-high precision spectroscopy with amplified pairs of high-power frequency comb laser pulses, and we extended it to the deep-UV for precision spectroscopy in krypton and molecular hydrogen.

**CLEO: Applications
& Technology**

13:00–15:00

AW3H • A&T Topical Review on Advances in Molecular Imaging I

President: Melissa Skala; Vanderbilt Univ., USA

AW3H.1 • 13:00 **Invited**

Label-Free Optical Molecular Imaging for Clinical Tissue Diagnostics, Mary-Ann Mycek¹; ¹Univ. of Michigan, USA. Label-free nonlinear optical molecular imaging methods could enable the rapid, reliable, and non-invasive assessment of living tissue-engineered constructs, potentially addressing a critical regulatory requirement in tissue engineering and regenerative medicine.

AW3H.2 • 13:30 **Invited**

Wide-Field Lifetime-Based Förster Resonance Energy Transfer in Live Animals, Xavier Intes¹; ¹Biomedical Engineering, Rensselaer Polytechnic Inst., USA. A new whole-body Fluorescence Molecular Tomography approach based on wide-field time-resolved structured illumination will be presented. Current instrumental, theoretical and experimental efforts will be summarized as well as its application to image FRET *in vivo*.

Meeting Room
211 B/D

CLEO: Science & Innovations

13:00–15:00

SW31 • Metamaterials & Metasurfaces

Presider: Ilya Goykhman; Hebrew University of Jerusalem, Israel

SW31.1 • 13:00 **Tutorial**

Nanophotonics based on Metasurfaces, Federico Capasso¹; ¹School of Engineering and Applied Sciences, Harvard Univ., USA. Metasurfaces enable new phenomena that are distinctly different from those observed in 3D metamaterials, providing us with unique capabilities to fully control wavefront and surface wave propagation with planar elements and thus realize “flat photonics”.



Federico Capasso is Professor of Applied Physics at Harvard, following 27 years at Bell Labs. His contributions include bandstructure engineering and the quantum cascade laser; the first measurement of the repulsive Casimir force; the generalized Snell laws for metasurfaces and their applications to flat photonics. He is a member of NAE, NAS and received the King Faisal Prize, the APS Schawlow Prize and the IEEE Edison Medal.

Meeting Room
212 A/C

CLEO: Applications & Technology

13:00–15:00

AW3J • Symposium on Photonics in Surgery I

Presider: Nicusor Iftimia; Physical Sciences Inc., USA

AW3J.1 • 13:00 **Invited**

Molecular Guided Surgery - Quantitative Immunologic Guidance with Optical Imaging, Brian W. Pogue^{2,1}; ¹Wellman Center for Photomedicine, Massachusetts General Hospital, USA; ²Thayer School of Engineering, Dartmouth College, USA. Molecular guided surgery is just now reaching substantial clinical trials stage, with multiple imaging systems, and a groundswell of GMP fluorescent molecular probes. Quantifying receptor expression is one potential way to guide cancer surgery.

AW3J.2 • 13:30 **Invited**

Clinical Potential of Light-Activated Tissue Crosslinking, Robert Redmond^{2,1}, Irene E. Kochevar^{2,1}, Michael C. McCormack^{3,1}, William G. Austen^{3,1}; ¹Harvard Medical School, USA; ²Wellman Center for Photomedicine, Massachusetts General Hospital, USA; ³Surgery, Massachusetts General Hospital, USA. Photocrosslinking can alter biomechanical and biological properties of tissue and close surgical wounds. This contribution focuses on potential clinical applications in vascular surgery and plastic surgery.

Meeting Room
212 B/D

CLEO: Applications & Technology

13:00–15:00

AW3K • A&T Topical Review on Optofluidics Microsystems I

Presider: Ai-Qun Liu; Nanyang Technological Univ., Singapore

AW3K.1 • 13:00 **Invited**

Fluid Coupled Optomechanical Oscillators, Hong Tang¹; ¹Yale Univ., USA. We demonstrate an optomechanical resonator operating in transparency window of water with optical Q beyond 1.5 million, which allows the detection of mechanical motion at 15am/rHz resolution with attogram mass sensitivity in liquid environment.

AW3K.2 • 13:30

Surface Sensitive Microfluidic Optomechanical Ring Resonator Sensors, Kyu Hyun Kim¹, Xudong Fan¹; ¹Univ. of Michigan, USA. Sensitivity of the optomechanical resonator to the surface mass change is demonstrated to be 1.2 Hz per pg/mm² by gradually removing SiO₂ molecules from the resonator surface. A detection limit of 83 pg/mm² is achieved.

AW3K.3 • 13:45

Single Molecule Detection with an Optomechanical Nanosensor, Wenyan Yu¹, Wei Jiang³, Qiang Lin^{3,2}, Tao Lu¹; ¹Univ. of Victoria, Canada; ²Electrical and Computer Engineering, Univ. of Rochester, USA; ³Inst. of Optics, Univ. of Rochester, USA. We report 50-milli-Hertz-linewidth optomechanical oscillation of a silica microsphere immersed in a buffer solution. Using the microsphere as a nanosensor, single 10-nm-radius silica beads and Bovine serum albumin (BSA) protein molecules were detected.

Marriott
Salon I & II

CLEO: Science & Innovations

13:00–15:00

SW3L • Nonlinear Effects in Waveguides

Presider: Peter Dragic; Univ. of Illinois at Urbana-Champaign, USA

SW3L.1 • 13:00 **Tutorial**

New Directions for Chip-based Nonlinear Optics, Benjamin J. Eggleton¹; ¹Univ. of Sydney, Australia. I review recent progress in chip-based nonlinear optics with a focus on emerging applications in quantum information processing, microwave photonics and midinfrared photonics.



Benjamin Eggleton is an ARC Laureate Fellow and Professor of Physics at the Univ. of Sydney and Director of the ARC Centre for Ultrahigh bandwidth Devices for Optical Systems (CUDOS). He obtained his Ph.D. degree in Physics from the Univ. of Sydney. Eggleton joined Bell Laboratories, Lucent Technologies as a Postdoctoral Member of Staff after graduation and was promoted to Research Director within the Specialty Fiber Business Division of Bell Laboratories. Eggleton has published more than 390 journal publications and over 150 invited presentations. He is a Fellow of the OSA and IEEE. He was President of the Australian Optical Society and is currently Editor-in-Chief for Optics Communications.

CLEO: Science & Innovations

13:00–15:00

**SW3M • Space-Division
Multiplexing***Presider: Nicolas Fontaine;
Alcatel-Lucent Bell Labs, USA*

SW3M.1 • 13:00

Microwave Photonics Mixer based on Polarization Rotation in Semiconductor Optical Amplifier, Qi Zhou¹, Mable P. Fok¹; ¹Univ. of Georgia, USA. A wideband microwave photonics mixer is experimentally demonstrated based on the use of phase coherent orthogonal carriers, generated from single sideband modulation in dual drive Mach-Zehnder modulator and polarization-rotation in semiconductor optical amplifier.

SW3M.2 • 13:15

Photonically-Enabled Phase Shift Keying of 50 GHz Bandwidth Radio-Frequency Arbitrary Waveforms, Amir Rashidinejad¹, Daniel E. Leaird¹, Andrew M. Weiner¹; ¹Purdue Univ., USA. We experimentally realize phase shift keying of ultrabroadband radio-frequency arbitrary waveforms. BPSK, QPSK and 16-PSK modulation are demonstrated for 50-GHz-bandwidth spread spectrum RF waveforms.

SW3M.3 • 13:30

Dispersion Compensation Scheme for Ultra-Wideband Coherent Matched Detection, Takahide Sakamoto¹; ¹National Inst. of Information and Communications Technology, Japan. We propose and investigate a digital processing technique for dispersion compensation in coherent matched detectors, by which ultra-wideband multi-carrier signals beyond electrical bandwidth are orthogonally demultiplexed and demodulated, fully electrically dispersion compensated.

SW3M.4 • 13:45

Widely Tunable Optoelectronic Oscillator Utilizing an Optical Notch Filter Based on the Deamplification of Stimulated Brillouin Scattering, Huanfa Peng¹, Yongchi Xu¹, Cheng Zhang¹, Peng Guo¹, Lixin Zhu¹, Weiwei Hu¹, Zhangyuan Chen¹; ¹Peking Univ., China. A novel tunable optoelectronic oscillator utilizing an optical notch filter based on stimulated Brillouin scattering is demonstrated. Tunable 3.36 to 31.4 GHz signals with phase noise of -120 dBc/Hz at 10 kHz offset are obtained.

13:00–15:00

**SW3N • Integrated Optical
Modulators***Presider: Mark Foster; Johns
Hopkins Univ., USA*

SW3N.1 • 13:00

High-speed Energy-efficient Silicon-polymer Hybrid Integrated Slot Photonic Crystal Waveguide Modulator, Xingyu Zhang¹, Amir Hosseini², Harish subbaraman², Jingdong Luo³, Alex K. Jen³, Chi-jui Chung¹, Robert Nelson⁴, Ray T. Chen¹; ¹Univ. of Texas at Austin, USA; ²Omega Optics, Inc., USA; ³Univ. of Washington, USA; ⁴Air Force Research Lab at Wright Patterson, USA. We present a high-performance silicon-polymer hybrid integrated slot photonic crystal waveguide modulator. A record-high effective in-device r_{33} of 1230pm/V, $V_{\pi} \times L$ of 0.282V \times mm, 3-dB bandwidth of 15GHz, and energy consumption of 94.4fJ/bit are experimentally demonstrated.

SW3N.2 • 13:15

WDM Transmitter Using Si Photonic Crystal Optical Modulators, Hiroyuki Ito¹, Yosuke Terada¹, Norihiro Ishikura¹, Toshihiko Baba¹; ¹Yokohama National Univ., Japan. We fabricated a WDM transmitter consisting of Si photonic crystal MZ modulators, triangular-shaped coupled-microring multiplexers and optical switches. 25 Gbps/ch operation and hitless switching of channel wavelength were successfully obtained.

SW3N.3 • 13:30

A 41 GHz Slow-Wave Series Push-Pull Silicon Photonic Modulator, David Patel¹, Venkat Veerasubramanian¹, Alireza Samani¹, Samir Ghosh¹, Mathieu Chagnon¹, Mohamed Osman¹, David Plant¹; ¹McGill Univ., Canada. We present a silicon modulator with a measured E-O bandwidth of 41 GHz at -4 V bias. Open eye diagrams are visible up to 60 Gbps. With DSP, 112 Gbps PAM-4 transmission below FEC threshold is demonstrated.

SW3N.4 • 13:45

OOK and QPSK Operation with Wide Working Spectrum in 200-300 μ m Si Photonic Crystal Slow Light Modulators, Yosuke Terada¹, Yosuke Hinakura¹, Keiko Hojo¹, Naoya Yazawa¹, Tomohiko Watanabe¹, Toshihiko Baba¹; ¹Yokohama National Univ., Japan. 25 Gbps error-free operation and 16-nm working spectrum were obtained in 200- μ m photonic crystal slow light MZ OOK modulators. QPSK modulation was also obtained in a 300- μ m device (1.0 \times 0.5 mm² footprint).

13:00–15:00

**SW3O • Parametric Sources
for Coherent Infrared Light
Generation***Presider: Shekhar Guha; US Air
Force Research Lab., USA*

SW3O.1 • 13:00

First OPO Based on Orientation-Patterned Gallium Phosphide (OP-GaP), Peter G. Schunemann¹, Leonard A. Pomeranz¹, Daniel J. Magarrell¹; ¹BAE Systems Inc, USA. Optical parametric oscillation was achieved for the first time in OP-GaP. Tm-fiber-pumped Ho:YAG (2090nm, 20W, 20kHz, 12ns) generated 350 mW signal (3.54-microns) plus idler (5.1-microns) from a 92.7-micron grating period crystal in a linear DRO.

SW3O.2 • 13:15

Multi-Milliwatt, Continuous-Wave, Mid-Infrared Source for the 6.4-7.5 μ m Spectral Range Based on Orientation-Patterned GaAs, Kavita Devi¹, Peter G. Schunemann², Majid Ebrahim-Zadeh^{1,3}; ¹ICFO -The Inst. of Photonic Sciences, Spain; ²BAE Systems, USA; ³Institutio Catalana de Recerca i Estudis Avancats (ICREA), Spain. We report a cw mid-infrared source based on OP-GaAs, tunable across 6460-7517nm, providing 51.1mW at 6790nm, with passive power stability of ~2.3% rms (>1 hour) and frequency stability of 1.8GHz (>1 minute), in high-beam quality.

SW3O.3 • 13:30

Invited High Power and High Energy Infrared Parametric Sources, Espen Lippert¹; ¹Forsvarets Forskningsinstitut, Norway. We report on ZnGeP₂-based parametric sources pumped by holmium lasers which are resonantly pumped by thulium fiber lasers. Using this scheme, we have built one source with up to 22 W average power and another with more than 0.2 J pulse energy in the mid-infrared region.

CLEO: QELS-Fundamental Science

FW3A • Symposium on Cavity
Quantum Electrodynamics II—
Continued

FW3A.4 • 14:00

A Solid-State Spin-Photon Transistor, Shuo Sun¹, Hyochul Kim¹, Glenn S. Solomon^{2,3}, Edo Waks^{1,3}, ¹Inst. for Research in Electronics and Applied Physics, Univ. of Maryland, USA; ²NIST, USA; ³Joint Quantum Inst., Univ. of Maryland, USA. We experimentally realize a solid-state spin-photon transistor using a quantum dot strongly coupled to a photonic crystal cavity. We are able to control the light polarization through manipulation of the quantum dot spin states.

FW3A.5 • 14:15

Nanoscale Optical Positioning of Single Quantum Dots for Efficient Quantum Photonic Devices, Luca Sapienza^{1,2}, Marcelo I. Davanco¹, Antonio Badolato², Kartik Srinivasan¹; ¹Center for Nanoscale Science and Technology, National Inst. of Standards and Technology, USA; ²Dept. of Physics and Astronomy, Univ. of Rochester, USA; ³School of Physics and Astronomy, Univ. of Southampton, UK. We locate single quantum dots with nanoscale accuracy through photoluminescence imaging. This enables nanophotonic device fabrication with engineered light-matter coupling, enabling bright (48±5% extraction efficiency), Purcell-enhanced (≈3), on-demand single-photon emission with >99% purity.

FW3A.6 • 14:30 **Invited**

Exploring Cavity QED with Superconducting Circuits, Andreas Wallraff¹; ¹ETH Zurich, Switzerland. Using modern micro and nanofabrication techniques we realize superconducting quantum electronic circuits based on which we probe fundamental quantum effects of microwave radiation and develop components for applications in quantum technology.

FW3B • Novel Approach for
Studying Condensed Matter—
Continued

FW3B.4 • 14:00

Dynamical Driving and Probing of Quantum Phase Transitions on the Nanoscale, Sven Doenges¹, Brian T. O'Callahan¹, Joanna M. Atkin¹, Omar Khatib¹, Markus B. Raschke¹; ¹Univ. of Colorado Boulder, USA. We extended the characterization of photoinduced quantum phase transitions into the nanoscale. We demonstrate this for VO₂ by accessing spatial inhomogeneities in the insulator-to-metal transition due to local strain and defects.

FW3B.5 • 14:15

Ultrafast Dynamics of the Skyrmion and Conical Phases in Cu₂OSeO₃, Matt Langner¹, Sujoy Roy¹, S. Mishra¹, J.C.T. Lee¹, X. W. Shi¹, M. A. Hossain¹, Y.-D. Chuang¹, S. Seki^{2,3}, Y. Tokura^{4,3}, S. D. Kevan¹, R. W. Schoenlein¹; ¹Lawrence Berkeley National Lab, USA; ²Center for Emergent Matter Science, RIKEN, Japan; ³PRESTO, Japan Science and Technology Agency, Japan; ⁴Univ. of Tokyo, Japan. We study the skyrmion structure in Cu₂OSeO₃ using resonant x-ray spectroscopy. The skyrmion structure shows long range fluctuations of ferrimagnetic ordering, and above-gap optical excitation reduces the magnetic ordering on a 40 picosecond timescale.

FW3B.6 • 14:30

Ultrafast terahertz spectroscopy of the inverse giant piezoresistance effect in silicon nanomembranes, Jaeseok Kim¹, Houk Jang¹, Min-Seok Kim¹, Jeong Ho Cho^{2,3}, Jong-Hyun Ahn¹, Hyunyoung Choi¹; ¹Yonsei Univ., Korea; ²School of Chemical Engineering, Sungkyunkwan Univ., Korea; ³SKKU Advanced Inst. of Nanotechnology (SAINT), Sungkyunkwan Univ., Korea; ⁴Center for Mass Related Quantities, Korea Research Inst. of Standards and Science, Korea. We observe the clear inverse piezoresistance effect in the silicon nanomembranes. Thickness-dependent optical-pump terahertz spectroscopy strongly corroborate that the effect originates from the carrier-concentration changes via charge carrier trapping into strain-induced defect states.

FW3B.7 • 14:45

Tailored Light-Matter Interaction through Epsilon-Near-Zero Modes, Salvatore Campione^{2,1}, Sheng Liu^{2,1}, Alexander Benz^{2,1}, John F. Klem¹, Michael B. Sinclair¹, Igal Brener^{2,1}; ¹Sandia National Labs, USA; ²Center for Integrated Nanotechnologies, Sandia National Labs, USA. We use epsilon-near-zero modes in semiconductor nanolayers to design a system whose spectral properties are controlled by their interaction with multi-dipole resonances. This design flexibility renders our platform attractive for efficient nonlinear composite materials.

FW3C • Optics of Complex
Media II—Continued

FW3C.4 • 14:00

Opportunities for Imaging in Heavily Scattering Random Media with Spatial Intensity Correlations, Kevin J. Webb¹, Jason A. Newman¹; ¹Purdue Univ., USA. We describe a method that allows imaging of objects moving within heavily scattering random media. This should prove valuable in biological imaging and other applications.

FW3C.5 • 14:15

Optical Detection and Imaging in Complex Media: How the Memory Effect Can Help Overcome Multiple Scattering, Amaury Baddon¹, Dayan Li¹, Geoffrey Lerosey¹, Claude Boccara¹, Mathias Fink¹, Alexandre Aubry¹; ¹Institut Langevin, France. We report on optical imaging through turbid media. Our approach is based on the measurement of a reflection matrix and a separation of the single scattering and multiple scattering contributions based on the memory effect.

FW3C.6 • 14:30

Device design using the steady-state ab initio laser theory, Alexander Cerjan¹, Brandon Redding¹, Hui Cao¹, A. Douglas Stone¹; ¹Yale Univ., USA. We present a method for designing highly multimode lasers for use as effectively incoherent light sources in optical imaging techniques.

FW3C.7 • 14:45

Correlation effects in Anderson localization and light transport in a 2D photonic disorder, Julien Armijo¹, Martin Boguslawski², Raphael Allio^{1,4}, Laurent Sanchez-Palencia³, Cornelia Denz²; ¹Universidad de Chile, Chile; ²Univ. of Muenster, Germany; ³Laboratoire Charles Fabry, Institut d'Optique, France; ⁴Univ. of Rennes I, France. We study the propagation of tailored wave packets in a computer controlled photo-induced disorder. Disorder correlations cause in real space a ballistic front of exponential Anderson Localization, and novel effects are observed in Fourier space.

FW3D • New Effects
in Nanostructures and
Semiconductors—Continued

FW3D.4 • 14:00

Four-fold Enhancement of Transverse Optical Magnetism in Unstructured Solids, Ayan Chakrabarty¹, Alexander Fisher¹, Elizabeth F. Dreyer¹, Stephen C. Rand¹; ¹Univ. of Michigan, USA. Scattering experiments on second-order induced magnetization in transparent Gadolinium Gallium Garnet (GGG) crystals show four times the maximum magnetic response measured previously in liquids.

FW3D.5 • 14:15

Ultrafast Magneto-Photocurrents in GaAs: Separation of Surface and Bulk Contributions, Christian B. Schmidt¹, Shekhar Priyadarshi¹, Mark Bieler¹; ¹Physikalisch-Technische Bundesanstalt, Germany. We generate ultrafast magneto-photocurrents in bulk GaAs and non-invasively separate surface and bulk contributions to the overall current. This method enables the investigation of processes such as anisotropic-distribution relaxation and the inverse Spin Hall effect.

FW3D.6 • 14:30

Analysis of soliton fission induced by free-carriers, Chad A. Husko¹, Simon Lefrancois¹, Matthias Wulf², Sylvain Combrie³, Alfredo De Rossi³, Lorenz Kobus Kuipers², Benjamin J. Eggleton¹; ¹Univ. of Sydney, Australia; ²FOM Inst. AMOLF, Netherlands; ³Thales Research and Technology, France. Previously we presented measurements of soliton fission induced by free-carriers. Here we report the derivation of a normalized free-carrier perturbation parameter to describe both those experiments and to extract more general properties of this mechanism.

FW3D.7 • 14:45

Beam Deflection Measurements of Non-degenerate Nonlinear Refractive Indices in Direct-gap Semiconductors, Peng Zhao¹, Matthew Reichert¹, Trenton Enslley¹, David J. Hagan¹, Eric W. Van Stryland¹; ¹CREOL Univ. of Central Florida, USA. We use the beam-deflection method to measure non-degenerate nonlinear refractive indices of ZnO and ZnSe and show, in agreement with theory, extremely nondegenerate nonlinear refraction is significantly larger than in the degenerate or near-degenerate case.

15:00–15:30 Coffee Break and Unopposed Exhibit Only Time, Exhibit Hall

15:00–17:00 Market Focus: Optics and Photonics Market Overview Panel, Exhibit Hall Theater

Executive Ballroom
210E

CLEO: QELS-
Fundamental Science

FW3E • Active Plasmonics and
Nanolasers—Continued

FW3E.5 • 14:00

Time-Domain Model of 4-Level Gain System Fitted to Nanohole Array Lasing Experiment, Jieran Fang¹, Jingjing Liu¹, Zhuoxian Wang¹, Xiangeng Meng¹, Ludmila Prokopenko¹, Vladimir M. Shalaev¹, Alexander V. Kildishev¹; ¹Birck Nanotechnology Center, School of Electrical and Computer Engineering, Purdue Univ., USA. We developed an accurate three dimensional time domain model of a 4-level gain system fitted to lasing experiment with a silver nanohole array. The simulated emission intensity showed clear lasing effects confirmed by optical experiments.

FW3E.6 • 14:15

Room Temperature Continuous Wave Blue Lasing in High Quality Factor III-Nitride Nanobeam Cavity on Silicon, Noelia Vico Triviño¹, Raphael Butte¹, Jean-François Carlini¹, Nicolas Grandjean¹; ¹Ecole Polytechnique Federale de Lausanne, Switzerland. Lasing is demonstrated in III-nitride photonic crystal nanobeam cavities grown on silicon. Laser characteristics are well accounted for by the large spontaneous emission coupling factor inherent to nanobeams and the InGaN quantum well material gain.

FW3E.7 • 14:30

Plasmonic Random Lasing in Strongly Scattering Regime with Slanted Silver Nanorod Array, Zhuoxian Wang¹, Xiangeng Meng¹, Seung Ho Choi², Young L. Kim², Vladimir M. Shalaev¹, Alexandra Boltasseva¹; ¹School of Electrical & Computer Engineering and Birck Nanotechnology Center, Purdue Univ., USA; ²Weldon School of Biomedical Engineering, Purdue Univ., USA. We present a plasmonic approach employing a slanted silver nanorod array for achieving controllable random lasing in a strongly scattering regime. Such random lasers can serve as a bright optical source for speckle-free imaging.

FW3E.8 • 14:45

Blackbody metamaterial lasers, Changxu Liu¹, Jianfeng Huang², Silvia Masala³, Erkki Alarousu³, Yu Han², Andrea Fratallocchi¹; ¹PRIMALIGHT, KAUST, Saudi Arabia; ²Advanced Membranes and Porous Materials Center, Division of Physical Sciences and Engineering, KAUST, Saudi Arabia; ³Solar and Photovoltaics Engineering Research Center, Division of Physical Sciences and Engineering, KAUST, Saudi Arabia. We investigate both theoretically and experimentally a new type of laser, which exploits a broadband light “condensation” process sustained by the stimulated amplification of an optical blackbody metamaterial.

Executive Ballroom
210F

CLEO: Science & Innovations

SW3F • III-V Lasers on Silicon—
Continued

SW3F.5 • 14:00

High Temperature Hybrid Silicon Micro-ring Lasers with Thermal Shunts, Chong Zhang^{2,1}, Di Liang², Geza Kurczveil², John Bowers¹, Raymond Beausoleil²; ¹UCSB, USA; ²HP Labs, USA. We demonstrate a hybrid silicon micro-ring laser design with novel thermal shunts. With this technique the hybrid silicon ring lasers with a 50 mm diameter operate continuous wave up to 105 °C.

SW3F.6 • 14:15

High-Q Silicon Resonators For High-Coherence Hybrid Si/III-V Semiconductor Lasers, Christos Santis¹, Amnon Yariv¹; ¹California Inst. of Technology, USA. We report on the design and experimental demonstration of high-Q Si resonators with Q ~ 10⁶, a fundamental figure of merit of the phase coherence of hybrid Si/III-V semiconductor lasers.

SW3F.7 • 14:30

Si-SOA Hybrid Wavelength Tunable Laser with a Tunable Coupler for High-Power Operation, Yuriko Kawamura¹, Hiroshi Yamazaki¹, Yuta Ueda², Shin Kamei², Toshikazu Hashimoto³; ¹NTT Device Technology Labs, Japan; ²NTT Device Innovation Center, Japan. We devised an output configuration for the Si-SOA hybrid laser which is suitable for high-power operation in terms of slope efficiency and suppression of nonlinear effects. These advantages were theoretically evaluated. A proof-of-concept experiment demonstrated.

SW3F.8 • 14:45

Passively Mode-locked III-V/Silicon Lasers with Low Time Jitter Using CW Optical Injection, Yuanbing Cheng¹, Xianshu Luo², Junfeng Song², Tsung-Yang Liow², Guo-Qiang Lo², Yulian Cao¹, Xiaonan Hu¹, Peng Hwei Lim³, Qijie Wang¹; ¹Nanyang Technological Univ., Singapore; ²Inst. of microelectronics, a*star, Singapore; ³DSO National Lab, Singapore, Singapore. We demonstrate 30 GHz mode-locked quantum well lasers on silicon platform using continuous-wave optical injection, which emit at the L-band wavelength with integrated root-mean-square time jitter of 1.0 ps and radio-frequency-linewidth of 150 kHz.

Executive Ballroom
210G

SW3G • Precision
Spectroscopy—Continued

SW3G.4 • 14:00

Measuring Part-per-Billion Line Shifts and Frequencies with Direct-Frequency-Comb Vernier Spectroscopy, Pablo Cancio Pastor¹, Mario Siciliani de Cumis¹, Roberto Eramo¹, Paolo De Natale¹, Nicola Coluccelli², Marco Cassinero², Gianluca Galzerano², Paolo Laporta²; ¹INO-CNR, Italy; ²Politecnico di Milano, Italy. Accurate frequency measurements of CO₂ transitions around 2 μm are performed by direct frequency-comb Vernier spectroscopy. Measurements of pressure line shifts at the ppb. accuracy level demonstrates the application of comb sources in precision molecular spectroscopy.

SW3G.5 • 14:15

Dual-Comb Modelocked Lasers, Sandro M. Link¹, Alexander Klenner¹, Mario Mangold¹, Matthias Golling¹, Bauke W. Tilma¹, Ursula Keller¹; ¹Inst. for Quantum Electronics, ETH Zurich, Switzerland. We present the first semiconductor disk laser simultaneously emitting two gigahertz modelocked pulse trains. This simply allows to establish a link from the optical domain to a microwave frequency comb. The relative carrier-envelope-offset frequency can be accessed directly.

SW3G.6 • 14:30

Discrete Fourier Transform Infrared Spectroscopy Using Precisely Periodic Pulse, Yi-DA HSIEH^{1,2}, Sho Okubo^{2,3}, Hajime Inaba^{2,3}, Mamoru Hashimoto⁴, Takeshi Yasui^{1,2}; ¹Tokushima Univ., Japan; ²ERATO Intelligent Optical Synthesizer Project, Japan; ³National Inst. of Advanced Industrial Science and Technology, Japan; ⁴Osaka Univ., Japan. A stabilized Fabry-Perot cavity with a 2.2 MHz-linewidth resonance-mode and a 566MHz FSR was fully characterized over the spectral range from 186 to 200 THz by discrete Fourier transform infrared spectroscopy using precisely periodic pulse.

SW3G.7 • 14:45

A compact iodine-stabilized diode laser at 531 nm, Takumi Kobayashi¹, Daisuke Akamatsu¹, Kazumoto Hosaka¹, Hajime Inaba¹, Sho Okubo¹, Takehiko Tanabe¹, Masami Yasuda¹, Atsushi Onae¹, Feng-Lei Hong¹; ¹NMIJ, Japan. A compact iodine-stabilized laser at 531 nm is developed with a frequency stability at the 10⁻¹² level using a coin-sized diode laser module. This laser will be used for applications including interferometric measurements.

Executive Ballroom
210H

CLEO: Applications
& Technology

AW3H • A&T Topical Review on
Advances in Molecular
Imaging I—Continued

AW3H.3 • 14:00 **Invited**

Molecular Imaging with Sum-frequency Generation Microscopy, Yang Han¹, Julie Hsu¹, Nien-Hui Ge¹, Eric O. Potma¹; ¹Chemistry, Univ. of California, Irvine, USA. We present an overview of the recent developments and biological imaging applications of sum-frequency generation (SFG) microscopy.

AW3H.4 • 14:30 **Invited**

Fluorescence lifetime imaging of cellular heterogeneity in cancer drug response, Melissa Skala¹; ¹Vanderbilt Univ., USA. Cancer is a heterogeneous disease, and sub-populations of cells can drive drug resistance. Fluorescence lifetime imaging of metabolic co-factors is used to monitor drug response on a cellular level, to optimize treatment strategies for patients.

15:00–15:30 Coffee Break and Unopposed Exhibit Only Time, Exhibit Hall

15:00–17:00 Market Focus: Optics and Photonics Market Overview Panel, Exhibit Hall Theater

Meeting Room
211 B/D

CLEO: Science &
Innovations

SW3I • Metamaterials &
Metasurfaces—Continued

SW3I.2 • 14:00

Simultaneous and Complete Control of Light Polarization and Phase using High Contrast Transmitarrays, Amir Arbabi¹, Yu Horie¹, Mahmood Bagheri², Andrei Faraon¹; ¹T. J. Watson Lab of Applied Physics, California Inst. of Technology, USA; ²Jet Propulsion Lab, California Inst. of Technology, USA. We report an efficient dielectric metasurface platform for complete control over polarization and phase of light with subwavelength spatial resolution. Using this platform, we experimentally demonstrate polarization switchable phase holograms and vector beam generators.

SW3I.3 • 14:15

Liquid Crystal Tunable Plasmonic Color, Daniel Franklin¹, Debashis Chanda¹; ¹Univ. of Central Florida, USA. We demonstrate a liquid crystal-tunable reflective surface where the color of the metasurface is changed as a function of applied voltage. Reflection spectra are compared with finite-difference time-domain numeric simulations.

SW3I.4 • 14:30 **Invited**

Nanophotonic Metastructures: Functionality at the Extreme, Nader Engheta¹; ¹Univ. of Pennsylvania, USA. We have been exploring the light-matter interaction in metastructures with scenarios that include extreme dimensionality, processing at nanoscales, extreme parameter values, unusual topology, and extreme near zones. We give an overview of our ongoing study.

Meeting Room
212 A/C

CLEO: Applications
& Technology

AW3J • Symposium on
Photonics in Surgery I—
Continued

AW3J.3 • 14:00 **Invited**

Optical Surgical Navigation for Medulloblastoma, Christopher Contag¹; ¹Stanford Univ., USA. We have developed miniaturized confocal microscope designs coupled with wide-field fluorescence microendoscopes scopes for the detection of molecular probes to improve resection of medulloblastoma of children.

AW3J.4 • 14:30 **Invited**

Recent Advance in Visible Spectrum Surgical Navigation, Victor Yang¹; ¹Sunnybrook Health Sciences Centre, Canada. Technological over-kill may not be the most efficient path towards medical device adoption. In this talk, we distill the work flow requirement of surgical navigation and examine the recent advances in 3D visible spectrum imaging with applications in neurosurgery.

Meeting Room
212 B/D

AW3K • A&T Topical Review on
Optofluidics Microsystems I—
Continued

AW3K.4 • 14:00 **Invited**

Real-time Size/Mass Spectrometry in Solution using Whispering Gallery Micro-Global Positioning, Stephen Arnold¹, David Keng¹; ¹NYU Polytechnic School of Engineering, USA. The goal of real-time nano-particle size/mass spectrometry by a microcavity in solution has been illusive for lack of binding position metrology. We demonstrate through Reactive Sensing theory and experiment that this limitation has been overcome.

AW3K.5 • 14:30

Plasmon-Assisted Optoelectrofluidics, Justus C. Ndukaife^{1,2}, Alexander V. Kildishev¹, A. G. Agwu Nnanna², Steven T. Wereley¹, Vladimir M. Shalaev¹, Alexandra Boltasseva¹; ¹Purdue Univ., USA; ²Purdue Calumet Water Inst., USA. By harnessing the photo-induced heating of a single plasmonic nanostructure and AC E-field in our research at the interface between plasmonics and optofluidics we demonstrate *on-demand* fluid flow control with unparalleled micron per second-scale velocities.

AW3K.6 • 14:45

Spontaneous Light-driven Heat Cycles in Metallic Nanofluids with Nanobubbles, J. Luis Dominguez¹, Matthew Moocarme^{1,2}, Luat Vuong^{1,2}; ¹Physics, Queens College of CUNY, USA; ²Physics, Graduate Center of CUNY, USA. We present the first experiments of spontaneous oscillatory behavior in binary-solvent nanofluids, which occurs when collimated light grazes menisci. The robust heat cycles identify nanobubbles, new mechanisms for probing nanoparticle-solvent chemistry, and novel thermo-mechanical dynamics.

Marriott
Salon I & II

CLEO: Science &
Innovations

SW3L • Nonlinear Effects in
Waveguides—Continued

SW3L.2 • 14:00

Phase-insensitive fiber parametric amplifier system with clamped output phase, Kyo Inoue¹; ¹Osaka Univ., Japan. This paper proposes a phase-insensitive fiber parametric amplifier system that outputs a phase-clamped signal. It consists of an orthogonally pumped fiber with polarization-aligned signal and a fiber loop with a polarization beam splitter.

SW3L.3 • 14:15

Spectral Narrowing of CW Light in Optical Fibers with Normal Dispersion, Serguei Papernyi¹, Anastasia Bednyakova², Sergei Tyritsyn³; ¹Lasers, MPB Communications Inc, Canada; ²Novosibirsk State Univ., Russia; ³Aston Inst. of Photonic Technologies, UK. Spectrum narrowing of CW light was observed experimentally in optical transmission fibers with normal dispersion. The effect's theoretical interpretation as an effective self-pumping parametric amplification of the spectrum's central part is confirmed by numerical modeling.

SW3L.4 • 14:30

Dual-peaked Laser Spectral Compression Generated in a Dispersion-increasing Fiber, Yu-Hsiang Lin¹, Chen-Bin Huang¹; ¹National Tsing Hua Univ., Taiwan. Adiabatic pulse propagation in a dispersion-increasing fiber is used to generate dual spectrally compressed peaks with tunable amplitudes. Our experimental results are in excellent agreements as compared to numerical calculations.

SW3L.5 • 14:45

Raman-Enhanced Phase-Sensitive Fiber Optical Parametric Amplifier, Xuelei Fu¹, Xiaojie Guo¹, Chester Shu¹; ¹Chinese Univ. of Hong Kong, Hong Kong. Backward Raman amplification is applied to enhance the performance of phase-sensitive fiber optical parametric amplification. The gain extinction ratio and the maximum signal gain are increased by 9.2 and 18.7 dB, respectively.

15:00–15:30 Coffee Break and Unopposed Exhibit Only Time, Exhibit Hall

15:00–17:00 Market Focus: Optics and Photonics Market Overview Panel, Exhibit Hall Theater

CLEO: Science & Innovations

SW3M • Space-Division
Multiplexing—Continued

SW3M.5 • 14:00 **Invited**
Experimental Demonstration of Optical Switching of Tbit/s Data Packets for High Capacity Short-Range Networks, Ashenafi Kiros Medhin¹, Valerija Kamchevska¹, Hao Hu¹, Michael Galili¹, Leif K. Oxenløwe¹; ¹*Technical Univ. of Denmark, Denmark*. Record-high 1.28-Tbit/s optical data packets are experimentally switched in the optical domain using a LiNbO₃ switch. An in-band notch-filter labeling scheme scalable to 65,536 labels is employed and a 3-km transmission distance is demonstrated.

SW3M.6 • 14:30
High speed and high resolution demodulation system for hybrid WDM/FDM based fiber microstructure sensor network by using Fabry-Perot filter, Qizhen Sun¹, Jianwei Cheng¹, Fan Ai¹; ¹*Huazhong Univ of Science and Technology, China*. Hybrid WDM/TDM enabled microstructure based optical fiber sensor network with large capacity is proposed. Assisted by Fabry-Perot filter, the demodulation system with high speed of 500Hz and high wavelength resolution less than 4.91pm is realized.

SW3M.7 • 14:45
Simple and Efficient Detection Scheme for Continuous Variable Quantum Key Distribution with m-ary Phase-Shift-Keying, Sebastian Kleis¹, Reinhold Herschel¹, Christian G. Schäffer¹; ¹*Helmut-Schmidt-Univ., USA*. A detection scheme for discriminating coherent states in quantum key distribution systems employing PSK is proposed. It is simple and uses only standard components. Its applicability at extremely low power levels of as low as 0.045 photons per symbol is experimentally verified.

SW3N • Integrated Optical
Modulators—Continued

SW3N.5 • 14:00
Linear silicon PN junction phase modulator, Yoon Ho Daniel Lee¹, Jaime Cardenas¹, Michal Lipson¹; ¹*Cornell Univ., USA*. We propose a method for linearizing the response of depletion-mode silicon waveguide modulator based on the engineering of modal overlap with the depletion region. Simulations show suppression of nonlinearities in index-voltage transfer function, enabling SFDR of 116 dB/Hz^{2/3} in MZM configuration.

SW3N.6 • 14:15
Linearity Measurement of a Silicon Single-Drive Push-Pull Mach-Zehnder Modulator, Yanyang Zhou¹, Linjie Zhou¹, Feiran Su¹, Jingya Xie¹, Haikuo Zhu¹, Xinwan Li¹, Jianping Chen¹; ¹*Shanghai Jiao Tong Univ., USA*. We investigate the linearity of a silicon Mach-Zehnder modulator with single-drive push-pull configuration. The spurious free dynamic range for second harmonic distortion (SFDR_{SH2}) is 86 dB-Hz^{1/2} with 4 dB improvement over previous best result.

SW3N.7 • 14:30
64 Gb/s silicon QPSK modulator with single-drive push-pull traveling wave electrodes, haikuo zhu¹, Linjie Zhou¹, Tao Wang², Lei Liu², Chiyuan Wong², Yanyang Zhou¹, jinting wang¹, qianqian wu¹, anbang xie¹, Rui Yang¹, zuxiang li¹, Xinwan Li¹, Jianping Chen¹; ¹*shanghai jiao tong Univ., USA*; ²*Huawei, China*. We demonstrate a silicon QPSK modulator consisting of two nested Mach-Zehnder interferometers with 3.5 mm long traveling-wave electrodes. 64 Gb/s QPSK modulation is achieved with an EVM of 24.4% and power consumption of 7.1 pJ/bit.

SW3N.8 • 14:45
Monolithically Integrated Quantum Dot Optical Modulator with Semiconductor Optical Amplifier for High-speed Optical Data Generation, Naokatsu Yamamoto¹, Kouichi Akahane¹, Toshimasa Umezawa¹, Tetsuya Kawanishi¹; ¹*National Inst Information & Comm Tech, Japan*. High-speed optical data signal generation of >6.8 Gb/s with an error-free operation was successfully demonstrated using newly developed monolithically integrated quantum dot optical modulator and semiconductor optical amplifier operated in an ultra-broad optical frequency bandwidth.

SW3O • Parametric Sources
for Coherent Infrared Light
Generation—Continued

SW3O.4 • 14:00
1064-nm-Pumped Mid-Infrared Optical Parametric Oscillator Based on Orientation-Patterned Gallium Phosphide (OP-GaP), Leonard A. Pomeranz¹, Peter G. Schunemann¹, Daniel J. Magarrell¹, John C. McCarthy¹, Kevin Zawilski¹, David E. Zelmon²; ¹*BAE Systems Inc, USA*; ²*AFRL/RXAP, US Air Force Research Lab, USA*. The first 1064-nm-pumped OP-GaP OPO was successfully demonstrated. A Q-switched Nd:YVO₄ laser (~1W, 3.3ns, 10kHz) pumped OP-GaP (16.5-mm-long, 20.8-micron grating period) yielded temperature-tunable signal and idler output wavelengths of 1385-1361 nm and 4591-4876 nm respectively.

SW3O.5 • 14:15
Long-Wave Infrared Single-Frequency OP-GaAs OPO Pumped by a Pulsed Tm:YAP Microlaser, Quentin Clement¹, Jean-Michel Melkonian¹, Jean-Baptiste Dherbecourt¹, Myriam Raybaut¹, Antoine Godard¹, Arnaud Grisard², Eric Lallier², Bertrand Gerard³, Basile Faure⁴, Grégoire Souhaité⁴; ¹*ONERA The French Aerospace Lab, France*; ²*Thales Research & Technology, France*; ³*Alcatel-Thales III-V Lab, France*; ⁴*Teem Photonics, France*. We report on a single-frequency nested cavity OPO based on OP-GaAs, pumped by a pulsed Tm:YAP microlaser. A threshold energy of 10 μJ has been measured and temperature tuning enables to cover the 10.3-10.9 μm range.

SW3O.6 • 14:30
Electro-Optically Spectrum Tailorable, Aperiodically Poled Lithium Niobate Optical Parametric Oscillators, Yen-Hung Chen¹, Hung-Ping Chung¹, Wei-Kun Chang¹, Chien-Hao Tseng¹; ¹*National Central Univ., Taiwan*. An electro-optically spectrum tailorable intracavity optical parametric oscillator (IOPO) was built based on a novel integrated aperiodically poled lithium niobate. Spectral narrowing and manipulation of the IOPO signal was demonstrated simply by electro-optic control.

SW3O.7 • 14:45
Widely tunable 1 μm optical vortex laser, Aizitiaili Abulikemu¹, Taximaiti Yusufu¹, Katsuhiko Miyamoto¹, Takashige Omatsu^{1,2}; ¹*Chiba Univ., Japan*; ²*JST, CREST, Japan*. We developed a widely tunable 1-μm optical vortex laser formed of a 0.5-μm vortex pumped optical parametric oscillator by employing non-critical phase-matching LiB₃O₅ crystals. Tunable vortex output was obtained in the wavelength range of 880-1345nm.

15:00–15:30 Coffee Break and Unopposed Exhibit Only Time, Exhibit Hall

15:00–17:00 Market Focus: Optics and Photonics Market Overview Panel, Exhibit Hall Theater

CLEO: QELS-Fundamental Science

15:30–17:30

FW4A • Quantum Computing

President: James Franson; Univ. of Maryland Baltimore County, USA

FW4A.1 • 15:30

Implementation of the Classical and Quantum Fourier Transform in Photonic Lattices, Steffen Weimann¹, Armando Perez-Leija¹, Maxime Lebugle¹, Alexander Szameit¹; ¹Institut für angewandte Physik, Germany. We report on the experimental realization of an optical version of the fractional and standard Fourier transform using discrete photonic lattices. Our approach is fully integrated and free of bulk optical components. We investigate the transformation of classical and quantum light.

FW4A.2 • 15:45

Programmable Nanophotonic Processor for Arbitrary High Fidelity Optical Transformations, Gregory Steinbrecher¹, Nicholas C. Harris¹, Jacob Mower¹, Mihika Prabhu¹, Dirk R. Englund¹; ¹Research Lab of Electronics, MIT, USA. We present an architecture for programmable nanophotonic processors capable of arbitrary discrete transformations for quantum and classical applications. A method to combat fabrication imperfections with high fidelity is discussed along with initial experimental results.

FW4A.3 • 16:00 **Invited**

A Fermionic Quantum Computer with Ultracold Atoms, Julio T. Barreiro¹; ¹Univ. of California, San Diego, USA. I will discuss how state-of-the-art experiments with ultracold atoms in optical lattices can be extended to realize fermionic quantum computations for chemistry, achieved by engineering arbitrary hopping and specific many-body interactions of fermions.

15:30–17:30

FW4B • Integrated Structures for Quantum Optics

President: Glenn Solomon; Joint Quantum Inst., USA

FW4B.1 • 15:30

Enhanced Multi-Photon Emission from Single NV Center Coupled to Graphene by Laser-Shaping, Jing Liu^{1,2}, Yaowu Hu³, Prashant Kumar³, Mikhail Y. Shalaginov^{2,4}, Alexei Lagutchev^{2,4}, Vladimir M. Shalaev^{2,4}, Gary Cheng³, Joseph M. Irudayaraj^{1,2}; ¹Dept. of Agricultural and Biological Engineering, Purdue Univ., USA; ²Birck Nanotechnology Center, Purdue Univ., USA; ³School of Industrial Engineering, Purdue Univ., USA; ⁴School of Electrical and Computer Engineering, Purdue Univ., USA. We experimentally demonstrated the enhanced multi-photon emission from single NV center coupled to 2D and 3D graphene by a nanoscale laser-shaping technique. Our results provide new non-classical light source for quantum optics and light harvesting.

FW4B.2 • 15:45 **Invited**

Fully-tunable, Purcell-enhanced On-chip Quantum Emitters, Maurangelo Petruzzella¹, Tian Xia¹, Francesco Pagliano¹, Simone Birindelli¹, Leonardo Midolo¹, Zarko Zobenica¹, Li Lianhe², Edmund Linfield², Andrea Fiore¹; ¹Eindhoven Univ. of Technology, Netherlands; ²Univ. of Leeds, UK. We report the all-electrical control over cavity-emitter systems, consisting in Stark-tunable quantum dots embedded in mechanically reconfigurable photonic crystal membranes. Purcell-effect from a single dot is demonstrated at distinct wavelengths.

15:30–17:30

FW4C • Novel Optics

President: Sebastian Knitter; Yale Univ., USA

FW4C.1 • 15:30

Control of Coherent Backscattering in a Multimode Fiber Using Nonreciprocal Phase Modulation, Yaron Bromberg¹, Brandon Redding¹, Hui Cao¹; ¹Dept. of Applied Physics, Yale Univ., USA. We used a magneto-optical effect to control coherent backscattering in a multimode fiber. A continuous transition from a backscattered peak to a dip was realized by manipulating the relative phase between reciprocal paths.

FW4C.2 • 15:45

Casimir forces in inhomogeneous media: towards a workable regularization, Ulf Leonhardt¹, Itay Griniasty¹; ¹Weizmann Inst. of Science, Israel. The most sophisticated theory of Casimir forces in realistic materials, Lifshitz theory, diverges in inhomogeneous media. Inspired by transformation optics, we have constructed a regularization procedure that appears to converge in planar materials.

FW4C.3 • 16:00

All-Solid-State Invisibility Cloak for Diffuse Light, Robert Schittny¹, Andreas Niemeyer¹, Muamer Kadic¹, Tiemo Bückmann¹, Andreas Naber¹, Martin Wegener¹; ¹Karlsruhe Inst. of Technology, Germany. We realize an all-solid-state version of a macroscopic broadband omnidirectional invisibility cloak for diffuse visible light based on polydimethylsiloxane doped with titania nanoparticles. This cloak is portable, easy to handle, and suitable for school demonstrations.

15:30–17:30

FW4D • Nonlinear Fiber Effects

President: Mark Foster; Johns Hopkins Univ., USA

FW4D.1 • 15:30

Spatiotemporal Dynamics of Multimode Optical Solitons, Logan Wright¹, William H. Renninger¹, Demetrios N. Christodoulides², Frank W. Wise¹; ¹Cornell Univ., USA; ²College of Optics and Photonics, CREOL, Univ. of Central Florida, USA. We study multimode optical solitons with up to roughly 10 spatial modes. This work provides the first evidence for solitons involving more than a few modes, and for spatiotemporal multimode soliton fission and Raman shifting.

FW4D.2 • 15:45

Dynamics of Rogue Wave and Soliton Emergence in Spontaneous Modulation Instability, Shanti Toenger¹, Thomas Godin¹, Cyril Billet¹, Frédéric Dias², Miro Erkintalo³, Göery Genty⁴, John Dudley⁴; ¹Institut FEMTO-ST, Université de Franche-Comté, France; ²School of Mathematical Sciences, Univ. College Dublin, Ireland; ³Physics Dept., Univ. of Auckland, New Zealand; ⁴Tampere Univ. of Technology, Optics Lab, Finland. Numerical simulations of spontaneous modulation instability show that localized structures in the chaotic instability field are well-described by analytic elementary and higher order soliton on finite background solutions of the nonlinear Schrödinger equation.

FW4D.3 • 16:00

Multiple Raman Soliton Generation in a Birefringence Tellurite Microstructured Optical Fiber, Lei Zhang¹, Tonglei Cheng¹, Dinghuan Deng¹, Daisuke Segal¹, Lai Liu¹, Takenobu Suzuki¹, Yasutake Ohishi¹; ¹Toyota Technological Inst., Japan. Based on a birefringence tellurite microstructured optical fiber, multiple solitons are generated by tuning the pump power and the polarization orientation. The central wavelength of the first soliton can be tuned over about 680 nm.



Executive Ballroom
210E

CLEO: QELS-
Fundamental Science

15:30–17:30

FW4E • Plasmonic Metasurfaces
and Metamaterials

President: Nanfang Yu; Columbia
Univ., USA

FW4E.1 • 15:30 **Invited**

Photon Spin Induced Collective Electron Motion on a Metasurface, Xingjie Ni¹, Jun Xiao¹, Sui Yang^{1,2}, Yuan Wang¹, Xiang Zhang^{1,2}; ¹Univ. of California, Berkeley, USA; ²Lawrence Berkeley National Lab, USA. Strong spin-orbit interaction can be induced by light-bending metasurfaces. We show that the photon spin momentum can be directly transferred to collective motion of electrons on a conductive metasurface with this interaction.

FW4E.2 • 16:00

Active Epsilon-Near-Zero Infrared Metamaterials, Nihal Arju¹, Tzuhsuan Ma¹, Simeon Trendafilov¹, JONGWON LEE¹, Mikhail A. Belkin¹, Gennady Shvets¹; ¹Univ. of Texas at Austin, USA. Metal-insulator-metal based epsilon-near-zero (ENZ) metamaterials are shown to support optical modes localized in the vicinity of a polarizable defect. ENZ-based infrared absorbers are fabricated using SiC and electrically controlled quantum wells structures.

Executive Ballroom
210F

CLEO: Science & Innovations

15:30–17:30

SW4F • Micro and Nano Lasers

President: Kent Choquette; Univ.
of Illinois, USA

SW4F.1 • 15:30

Opening up spectrum with InPAs quantum dot lasers, Ivan Karomi^{1,3}, Sam Shutts¹, Peter M. Smowton¹, Andrey Krysa²; ¹Cardiff Univ., UK; ²Sheffield Univ., UK; ³Univ. of Mosul, Iraq. Electrically injected MOVPE grown InPAs quantum dot lasers emitting at wavelengths longer than 770nm are demonstrated with 300K threshold current density of 260Acm⁻² for 2mm long uncoated facet devices and operation up to 370K.

SW4F.2 • 15:45

Quantum Cascade Laser-based Kerr Frequency Comb Generation, Caroline Lecaplain¹, Clément Javerzac-Galy¹, Erwan Lucas¹, John D. Jost¹, tobias kippenberg¹; ¹EPFL, Switzerland. We report mid-infrared Kerr comb generation based on a quantum cascade laser pumping a crystalline micro-resonator. For the first time QCL light is coupled into a microresonator via a tapered chalcogenide fiber allowing mid-IR Kerr comb generation.

SW4F.3 • 16:00 **Invited**

Very Small Lasers and Resonators, Yong-Hee Lee¹, Hoon Jang¹; ¹Physics, Korea Advanced Inst of Science & Tech, Korea. Evolution of small resonant lasers/cavities, from 1D vertical cavity surface emitting lasers to 2D photonic crystal lasers and back to 1D nanobeam lasers, will be discussed. Emphases will be placed on ultra-low threshold nanobeam lasers.

Executive Ballroom
210G

15:30–17:30

SW4G • Comb Technology

President: Brian Washburn; Kansas
State Univ., USA

SW4G.1 • 15:30

Octave Spanning Frequency Comb Generation in a Dispersion-Controlled Short Silicon-Wire Waveguide with a Fiber Laser Oscillator, Takahiro Goto^{1,2}, Atushi Ishizawa², Rai Kou^{3,4}, Tai Tsuchizawa^{3,4}, Nobuyuki Matsuda^{2,3}, Kenichi Hitachi², Tadashi Nishikawa¹, Koji Yamada^{3,4}, Tetsuomi Sogawa², Hildeki Gotoh²; ¹Tokyo Denki Univ., Japan; ²NTT Basic Research Labs, NTT Corporation, Japan; ³NTT Nanophotonics Center, NTT Corporation, Japan; ⁴NTT Device Technology Labs, NTT Corporation, Japan. We demonstrate on-chip frequency comb generation spanning from 900 to 2300 nm, the widest bandwidth with a laser oscillator (only 50-pJ pulse energy), by controlling dispersion and propagation distance of silicon-wire waveguides.

SW4G.2 • 15:45

A Hybrid III-V-Graphene Device for Modelocking and Noise Suppression in a Frequency Comb, Chien-Chung Lee¹, Kevin Silverman², Ari Feldman², Todd Harvey², Richard P. Mirin², Thomas R. Schibli^{1,3}; ¹Physics, Univ. of Colorado at Boulder, USA; ²National Inst. of Standards and Technology, USA; ³JILA, National Inst. of Standards and Technology and Univ. of Colorado, USA. We demonstrate a device that integrates a III-V semiconductor saturable absorber mirror with a graphene electro-optic modulator, which provides a monolithic solution to modelocking and noise suppression in a frequency comb.

SW4G.3 • 16:00

A Robust 2f-to-3f Collinear Interferometer with a Dual-Pitch Periodically Poled Lithium Niobate Ridge Waveguide, Kenichi Hitachi¹, Atsushi Ishizawa¹, Osamu Tadanaga², Hiroki Mashiko¹, Tadashi Nishikawa³, Tetsuomi Sogawa¹, Hildeki Gotoh¹; ¹NTT Basic Research Labs, Japan; ²NTT Device Technology Labs, Japan; ³Tokyo Denki Univ., Japan. We demonstrated that a 2f-to-3f collinear interferometer is robust against environmental noise. The out-of-loop Allan deviation of the collinear interferometer is 7x10⁻¹⁵ at gate time of 1 s, irrespective of environmental perturbation.

Executive Ballroom
210H

CLEO: Applications
& Technology

15:30–17:30

AW4H • A&T Topical Review
on Advances in Molecular
Imaging II

President: Brian Applegate; Texas
A&M Univ., USA

AW4H.1 • 15:30 **Invited**

Molecular Contrast in Interferometric Imaging, Adam Wax¹; ¹Bioomedical Engineering, Duke Univ., USA. Interferometric imaging offers many advantages for biomedical applications such as optical sectioning/depth resolution. Inclusion of molecular contrast information improves utility but requires additional efforts to either isolate spectroscopic information or detect contrast agents.

AW4H.2 • 16:00 **Invited**

Multi-Scale Optical Molecular Imaging, Yu Chen¹; ¹Univ. of Maryland at College Park, USA. An array of fluorescence molecular imaging technologies for multi-scale imaging will be presented, including planar fluorescence for macroscopic samples, fluorescence laminar optical tomography for mesoscopic samples, and two-photon fluorescence microscopy for intravital imaging.

Meeting Room
211 B/D

CLEO: Science & Innovations

15:30–17:30
SW4I • Novel Materials for On-chip Photonics
Presider: Federico Capasso; Harvard Univ., USA

SW4I.1 • 15:30
Microdisk Cavity-Coupled MoS₂ with Tunable Narrowband Emission, Jason C. Reed¹, Alexander Y. Zhu¹, Hai Zhu¹, Ertugrul Cubukcu¹; ¹Univ. of Pennsylvania, USA. We incorporate monolayer MoS₂ into a microdisk optical resonator cavity to produce narrowband emission with quality-factors of 900. The integrated photonic device has high spatial and temporal coherence and is wavelength tunable.

SW4I.2 • 15:45
Fabrication of 1D Photonic Crystal on a Single Erbium Chloride Silicate Nanowire and Microcavity Laser Design, Zhicheng Liu¹, Hao Sun², Yongzhuo Li², Jianxing Zhang², Cun-Zheng Ning^{1,2}; ¹School of Electrical, Computer, and Energy Engineering, Arizona State Univ., USA; ²Dept. of Electronic Engineering, Tsinghua Univ., China. We report on fabrication and characterization of 1D photonic crystal on a single erbium chloride silicate nanowire. Design and simulation show that a microcavity laser with Q-factor over 10000 is feasible from a single nanowire.

SW4I.3 • 16:00 **Invited**
Two-Dimensional Material Nanophotonics, Fengnian Xia¹; ¹Yale Univ., USA. We discuss optical properties of two-dimensional materials ranging from insulating hexagonal boron nitride, semiconducting transition metal dichalcogenides such as molybdenum disulfide and black phosphorus, to semi-metallic graphene. We also cover their potential applications in photonics.

Meeting Room
212 A/C

CLEO: Applications & Technology

15:30–17:30
AW4J • Symposium on Photonics in Surgery II
Presider: Jin Kang; Johns Hopkins Univ., USA

AW4J.1 • 15:30 **Invited**
Photosurgery for the skin: Younger, Healthier and Easier, Boncheol L. Goo^{1,2}; ¹Lutronic Corporation, Korea; ²Clinique L Dermatologie, Korea. Surgeons use sophisticated but imperfect clinical algorithms to analyze visible skin conditions for precise decision making. Algorithmic approaches, current limitations and future ideas will be discussed.

AW4J.2 • 16:00
Delineation of Basal Cell Carcinoma Margins with Combined RCM/OCT Imaging, Nicusor Iftimia¹; ¹Physical Sciences Inc., USA. We demonstrate a novel approach for delineation of basal cell carcinoma (BCC) margins based on combined Reflectance Confocal Microscopy (RCM)/ Optical Coherence Tomography (OCT) imaging. BCC margins delineation is very important for both disease staging and therapy guidance.

Meeting Room
212 B/D

CLEO: Applications & Technology

15:30–17:30
AW4K • A&T Topical Review on Optofluidics Microsystems II
Presider: Xudong Fan; Univ. of Michigan, USA

AW4K.1 • 15:30 **Invited**
Photonic Crystal Enhanced Microscopy, Brian T. Cunningham^{1,2}, weili chen¹, kenneth D. long², Yue Zhuo², Ji S. Choi³, Brendan A. Harley³; ¹Electrical and Computer Engineering, Univ. of Illinois at Urbana-Champaign, USA; ²Dept. of Bioengineering, Univ. of Illinois at Urbana-Champaign, USA. By modifying a microscope to perform hyperspectral imaging of reflectance from a photonic crystal, we describe a new microscopy approach that enables quantitative, spatially resolved imaging of the interaction of cells and nanoparticles with surfaces.

AW4K.2 • 16:00 **Invited**
Microfluidic Isolation and Fluorescence Microscopy in a Fully Automated Digital Diagnostic Instrument (SIMOA HD-1), William McGuigan¹, David C. Duffy¹; ¹STRATEC Biomedical USA, Inc., USA. Quanterix and Stratec Biomedical have developed an automated analyzer that enables the measurement of subfemtomolar concentrations of proteins. The development of this technology focusing on the custom optical module and microfluidic disc is outlined below.

Marriott
Salon I & II

CLEO: Science & Innovations

15:30–17:30
SW4L • Nonlinear Fiber Optics
Presider: Sze Yun Set; Alnair Labs Corporation, Japan

SW4L.1 • 15:30 **Invited**
Towards Nonlinear Optics with Cold Rydberg Atoms Inside a Hollow Core Fiber, Maria Langbecker¹, Mohammad Noaman¹, Patrick Windpassinger¹; ¹Johannes Gutenberg Universitat Mainz, Germany. We present an experimental setup for studying strongly nonlinear light-matter interactions using cold atoms inside a hollow core fiber. A Rydberg EIT process can potentially be used to generate strong and tunable effective photon-photon interactions.

SW4L.2 • 16:00
SBS Suppression in Nanosecond Fiber Amplifier with Controlled Frequency Chirp, Pavel Ionov¹, Fabio Di Teodoro¹, Todd Rose¹; ¹The Aerospace Corporation, USA. We observe a nearly 9-fold increase in the SBS threshold for a pulsed Yb fiber amplifier by applying a linear frequency-chirp to the input seed pulse. The chirp is achieved by pulse driving a phase modulator. SBS threshold data and transient SBS gain for various degrees of chirp are reported.

Technical Digest and Postdeadline Papers Available Online

- Visit www.cleoconference.org
- Select Access Digest Paper link
- Use your registration email address and password

Access is provided only to full technical attendees.

CLEO: Science & Innovations

15:30–17:15

SW4M • SDM, OAM & Free-Space Communications*Presider: Christian Malouin; Juniper Networks Inc., USA*SW4M.1 • 15:30 **Invited**

Dense Space Division Multiplexed Transmission Technology, Takayuki Mizuno¹, Hidehiko Takara¹, Akihide Sano¹, Yutaka Miyamoto¹; ¹NTT Network Innovation Labs, Japan. We review recent progress in ultra-high capacity transmission based on dense space division multiplexing (DSDM) for future scalable optical transport networks, and present the latest multi-core multi-mode fiber, spatial multi/demultiplexers, and MIMO signal processing technique.

SW4M.2 • 16:00

Experimental Demonstration of N-Dimensional 1-to-1100 Multicasting (25 Wavelengths x 22 Orbital Angular Momentum Modes x 2 Polarizations) of OFDM-mQAM Signal, Jian Wang¹, Shuhui Li¹, Jun Liu¹, Chao Li¹, Long Zhu¹, Jing Du¹, Ming Luo², Qi Yang², Shaohua Yu²; ¹Wuhan National Lab for Optoelectronics, School of Optical and Electronic Information, Huazhong Univ. of Science and Technology, China; ²State Key Lab of Optical Comm. Technologies and Networks, China. We present N-dimensional multicasting exploiting wavelength, orbital angular momentum (OAM) and polarization dimensions. 1-to-1100 multicasting (25 wavelengths x 22 OAM modes x 2 polarizations) of OFDM-16/32QAM signal is demonstrated. All 1100-fold channels achieve BER <2e-3.

15:30–17:30

SW4N • Novel Devices for Communications and Signal Processing*Presider: Takahide Sakamoto; NICT, Japan*

SW4N.1 • 15:30

Scaling Zero-Change Photonics: An Active Photonics Platform in a 32 nm Microelectronics SOI CMOS Process, Mark T. Wade¹, Fabio Pavanello¹, Jason Orcutt², Rajesh Kumar¹, Jeffrey Shainline¹, Vladimir Stojanovic³, Rajeev Ram², Milos Popovic¹; ¹Univ. of Colorado at Boulder, USA; ²MIT, USA; ³Univ. of California, USA. We demonstrate photonics monolithically integrated in a 32nm SOI microelectronics process, including grating couplers, tunable filters, and modulators, the first migration of zero-change CMOS photonics moving down the microelectronics technology-node ladder, from the 45nm node.

SW4N.2 • 15:45

III-V Nanopillar Phototransistor Directly Grown on Silicon, Indrasen Bhattacharya¹, Wai Son Ko¹, Fanglu Lu¹, Stephen Gerke¹, Connie J. Chang-Hansnain¹; ¹Univ. of California Berkeley, USA. We demonstrate InP nanopillar bipolar junction phototransistors monolithically integrated on a Silicon substrate. With a responsivity of 4 A/W and bandwidth of 7.5 GHz, these receivers indicate a route towards efficient on-chip optical interconnects.

SW4N.3 • 16:00

Performance Evaluation of GaN/InGaN Heterojunction Phototransistors, Tsung-Ting Kao¹, Jeomoh Kim¹, Yi-Che Lee¹, Mi-Hee Ji¹, A. Saniul Haq¹, Theeradetch Detchprohm¹, Russell D. Dupuis¹, Shyh-Chiang Shen¹; ¹Georgia Inst. of Technology, USA. We present a high-performance InGaN/GaN heterojunction phototransistor with the responsivity (R_r) > 8 (A/W), low noise-equivalent-power (NEP) < 1.1×10^{-17} (W-Hz^{-0.5}) and high detectivity (D^*) > 1.2×10^{14} (cm-Hz^{0.5}-W⁻¹).

15:30–17:30

SW4O • Broadband and Ultrafast Parametric Sources*Presider: Jeffrey Moses; Cornell Univ., USA*

SW4O.1 • 15:30

High-average-power, Mid-infrared Femtosecond Optical Parametric Oscillator at 7 μ m Based on CdSiP₂, Suddapalli Chaitanya Kumar¹, Joachim Krauth², K. T. Zawilski³, Peter G. Schunemann³, Harald W. Giessen², Majid Ebrahim-Zadeh^{1,4}; ¹ICFO - The Inst. of Photonic Sciences, Spain; ²4th Physics Inst. and Research Center SCOPE, Univ. of Stuttgart, Germany; ³BAE Systems, USA; ⁴Institució Catalana de Recerca i Estudis Avançats (ICREA), Spain. We report a mid-infrared femtosecond OPO based on CdSiP₂ tunable across 6786-7069 nm, generating record power of 110-mW at 7 μ m, with passive power and wavelength stability below 3% rms (1-hour) and 0.1% rms (15-min), respectively.

SW4O.2 • 15:45

Cr:ZnS Laser-pumped Subharmonic GaAs OPO with an Instantaneous Bandwidth 3.6-5.6 μ m, Viktor O. Smolski¹, Sergey Vasilyev², Peter G. Schunemann³, Sergey B. Mirov^{2,4}, Konstantin Vodopyanov¹; ¹CREOL, Univ. of Central Florida, USA; ²Mid-IR Lasers, IPG Photonics, USA; ³BAE Systems, USA; ⁴Dept. of Physics, Univ. of Alabama at Birmingham, USA. High-power (110mW) mid-IR output suitable for ultra-broadband frequency comb generation was produced in a low-threshold (20mW) subharmonic GaAs optical parametric oscillator that was synchronously pumped (175MHz) by a compact 0.5-W femtosecond Cr:ZnS (2.38 μ m) oscillator.

SW4O.3 • 16:00

Mid-Infrared Femtosecond Optical Parametric Oscillator Synchronously-Pumped Directly by a Ti:sapphire laser, Majid Ebrahim-Zadeh^{1,2}; ¹Nonlinear Optics, ICFO-Inst. of Photonic Sciences, Spain; ²ICREA-Catalan Inst. of Research and Advanced Studies, Spain. We report a deep-mid-IR femtosecond OPO based on CdSiP₂ using direct synchronous pumping by a Ti:sapphire laser, providing continuous wavelength coverage across 6-8 μ m under rapid static cavity delay tuning with high output stability.



Join the conversation. Use #CLEO15.
Follow us @cleoconf on Twitter.

CLEO: QELS-Fundamental Science

FW4A • Quantum Computing—
Continued

FW4A.4 • 16:30

Topological Protection of Path Entanglement in Photonic Quantum Walks, Mikael Rechtsman¹, Yaakov Lumer², Yonatan Plotnik², Armando Perez-Leija², Alexander Szameit², Mordechai Segev², ¹Physics Dept., The Pennsylvania State Univ., USA; ²Physics Dept., Technion Israel Inst. of Technology, Israel; ³Inst. of Applied Physics, Friedrich-Schiller-Universität Jena, Germany. We show that entangled photons propagating along the edge of a photonic topological insulator preserve their entanglement despite edge defects of any kind. This represents a novel methodology for the transport of quantum information.

FW4A.5 • 16:45

Quantum Random Walks in a Programmable Nanophotonic Processor, Nicholas C. Harris¹, Greg Steinbrecher¹, Jacob Mower¹, Yoav Lahini¹, Dirk R. Englund¹, ¹MIT, USA. We present our recent theoretical and preliminary experimental results on the role of disorder and decoherence in quantum random walks implemented in a large-scale, programmable nanophotonic processor.

FW4B • Integrated Structures
for Quantum Optics—
Continued

FW4B.3 • 16:15

Single NV Zero-Phonon Line Emission into Waveguide-Coupled GaP-on-Diamond Disk Resonators, Michael Gould¹, Nicole K. Thomas¹, Yuncheng Song², Minjoo Larry Lee², Kai-Mei Fu³, ¹Electrical Engineering, Univ. of Washington, USA; ²Electrical Engineering, Yale Univ., USA; ³Physics, Univ. of Washington, USA. We present results from waveguide-coupled GaP-on-diamond disk resonators coupled to single nitrogen-vacancy centers in diamond. We estimate zero-phonon line emission rates into one direction of a bus waveguide as high as $1.2 \times 10^4 \text{ s}^{-1}$.

FW4B.4 • 16:30

Tunable Squeezing Using Coupled Ring Resonators on a Silicon Nitride Chip, Avik Dutt¹, Steven Miller¹, Kevin Luke¹, Alexander L. Gaeta¹, Paulo Nussenzweig², Michal Lipson¹, ¹Cornell Univ., USA; ²Universidade de São Paulo, Brazil. We demonstrate continuous tuning of the degree of squeezing from 0.5 to 2 dB (0.9 to 4 dB inferred on chip) by externally controlling the coupling condition of a Si₃N₄ double ring OPO using integrated microheaters.

FW4B.5 • 16:45

Effect of Pure Dephasing and Phonon Scattering on the Coupling of Semiconductor Quantum Dots to Optical Cavities, Clément Jarlov¹, Etienne Wodey¹, Alexey Lyasota¹, Milan Calic¹, Pascal Gallo¹, Benjamin Dwir¹, Alok Rudra¹, Elyahou Kapon¹, ¹Ecole Polytechnique Fédérale de Lausanne, Switzerland. We investigate the effect of decoherence mechanisms in semiconductor quantum dot-cavity systems by performing photoluminescence measurements of InGaAs/GaAs site-controlled quantum dots coupled to photonic crystal cavities and comparing the results to a theoretical model.

FW4C • Novel Optics—
Continued

FW4C.4 • 16:15

Metasurface Optical Antireflection Coatings, Hou-Tong Chen¹, Boyang Zhang², Junpeng Guo², Joshua Hendrickson³, Nima Nader³, ¹Los Alamos National Lab, USA; ²Univ. of Alabama in Huntsville, USA; ³Air Force Research Lab, USA. We demonstrate a new strategy of optical antireflection coatings employing metasurfaces with designer surface properties in the mid-wave infrared. It has very little requirement on the choice of materials and is scalable to other wavelengths.

FW4C.5 • 16:30

Analytic Modeling of Metmaterial Absorbers, Patrick Bowen¹, Alexandre Baron¹, David R. Smith¹, ¹Duke Univ., USA. We present a fully analytical model that describes ideal absorbing metasurfaces composed of film-coupled optical nanoantennas. The model predicts the spectrum and the angular dependence of the absorption and is compared to full-wave numerical simulations.

FW4C.6 • 16:45

Highly Efficient Modulation of THz Metamaterials Using Graphene Surface Plasmons, Isaac J. Luxmoore¹, Peter Q. Liu², Sergey A. Mikhailov³, Nadja A. Savostyanova³, Federico Valmorra², Jerome Faist², Geoffrey R. Nash¹, ¹Univ. of Exeter, USA; ²ETH Zurich, Switzerland; ³Univ. of Augsburg, Germany. We introduce hybrid metamaterials consisting of split ring resonators and a graphene nanoribbon array. Electrostatic control of the graphene plasmon resonance provides dynamic control of the transmission of THz radiation with modulation depth of ~50%.

FW4D • Nonlinear Fiber
Effects—Continued

FW4D.4 • 16:15

Polarization dynamics of dissipative solitons in an erbium doped fiber laser passively mode locked by carbon nanotube polymer composite, Chengbo Mou¹, Sergey Sergeev¹, Stanislav Kolpakov¹, Raz Arif¹, Alex Rozhin¹, Maria Chernysheva¹, Sergei Turitsyn¹, ¹Aston Inst. of Photonic Technologies, UK. Here we present first investigation of polarization dynamics from a carbon nanotube mode locked erbium doped fiber laser. Both vector and polarization switching dissipative soliton have been observed.

FW4D.5 • 16:30

How Optical Spectrum of Random Fiber Laser is Formed, Dmitry V. Churkin^{1,3}, Igor Kolokolov^{4,5}, Evgeniy V. Podivilov^{2,3}, Ilya Vatik^{2,3}, Maxim Nikulin², Sergey Vergeles⁴, Ivan Terekhov^{3,6}, Vladimir Lebedev^{4,5}, Gregory Falkovich^{7,8}, Sergey A. Babin^{2,3}, Sergei Turitsyn^{1,3}, ¹Aston Inst. of Photonic Technologies, UK; ²Inst. of Automation and Electrometry, Russia; ³Novosibirsk State Univ., Russia; ⁴Landau Inst. for Theoretical Physics, Russia; ⁵Moscow Inst. of Physics and Technology, Russia; ⁶The Budker Inst. of Nuclear Physics, Russia; ⁷Weizmann Inst. of Science, Israel; ⁸Inst. for Information Transmission Problems, Russia. We experimentally and theoretically describe formation of random fiber laser's optical spectrum. We propose a new concept of active cyclod wave kinetics from which we derive first ever nonlinear kinetic theory describing laser spectrum.

FW4D.6 • 16:45

Graphene Coated Microfiber For Cascaded Four-Wave-Mixing Generating, Baicheng Yao¹, Yu Wu¹, Qiuyan Feng¹, Zegao Wang^{1,2}, Yunjiang Rao¹, Yuanfu Chen¹, Kin S. Chiang^{1,3}, ¹UESTC, China; ²Aarhus Univ., Denmark; ³City University of Hong Kong, Hong Kong. Cascaded four-wave-mixing was effectively demonstrated in a graphene-coated-microfiber, by using a pulsed pump at 1550 nm, which may be useful for realization of graphene based fiber-optic nonlinear devices, e.g. lasers, filters, modulators and regenerators.

CLEO: QELS-
Fundamental ScienceFW4E • Plasmonic Metasurfaces
and Metamaterials—Continued

FW4E.3 • 16:15

Negative refraction due to discrete plasmon diffraction, Arian Kriesch^{1,2}, Ho Wai H. Lee², Daniel Ploss¹, Stanley P. Burgos², Hannes Pfeifer^{3,1}, Jakob Naeger¹, Harry Atwater², Ulf Peschel¹; ¹*Inst. of Opt., Information and Photonics (IOIP), Cluster of Excellence Engineering of Adv. Opt. Mat. (EAM) and Graduate School in Adv. Opt. Tech. (SAOT) and MPL, Friedrich Alexander Univ. Erlangen-Nuremberg, Germany*; ²*Applied Physics and Material Sciences, California Inst. of Technology, USA*; ³*Max-Planck-Inst Physik des Lichts, Germany*. We experimentally demonstrate spectrally broad ($\lambda_0=1200-1800$ nm) in-plane negative diffraction of SPPs in an array of gap-plasmonic waveguides with negative mutual coupling resulting in negative refraction on the array's interface and refocusing in an adjacent metal layer.

FW4E.4 • 16:30

Controlled steering of Cherenkov surface plasmon wakes with a one-dimensional metamaterial, Patrice Genevet¹, Daniel Wintz¹, Antonio Ambrosio¹, Alan She¹, Romain Blanchard¹, Federico Capasso²; ¹*Harvard Univ., USA*. We show that by creating a running wave of polarization along a 1D metallic nanostructure consisting of subwavelength spaced rotated apertures that propagates faster than the surface plasmon phase velocity, we can generate surface plasmon wakes, which are the 2D analogue of Cherenkov radiation.

FW4E.5 • 16:45

Three-Dimensional Metasurface Carpet Cloak, Xingjie Ni¹, Zi Jing Wong¹, Yuan Wang¹, Xiang Zhang^{1,2}; ¹*Univ. of California, Berkeley, USA*; ²*Lawrence Berkeley National Lab, USA*. We experimentally demonstrate a three-dimensional ultra-thin metasurface carpet cloak can cover on an arbitrary-shaped object and make it undetectable by the visible light owing to the phase control capability of the metasurface.

CLEO: Science & Innovations

SW4F • SW4F • Micro and Nano
Lasers—Continued

SW4F.4 • 16:30

Waveguide-integrated Unidirectional-Emission Microspiral Lasers for Optical Interconnects, Yu Zhang¹, Andrew W. Poon¹; ¹*Photonics Device Lab, Dept. of Electronic and Computer Engineering, The Hong Kong Univ. of Science and Technology, China*. We demonstrate a room-temperature continuous-wave electrically injected unidirectional-emission AlGaInAs/InP multiple-quantum-well microspiral disk laser with a 44mA threshold current. Above 130 mA, the laser shows a unidirectional emission from the waveguide butt-coupled to the microspiral notch.

SW4F.5 • 16:45

Room Temperature UV-C Lasers with Nitride Microdisks on Silicon, Philippe Boucaud¹, Julien Sellés², Christelle Brimont², Thierry Guillet², Guillaume Cassabois², Bruno Gayral³, Meletios Maxis⁴, Fabrice Semond⁴, Iannis Roland¹, Yijia Zeng¹, Xavier Checoury¹; ¹*IEF-CNRS-Univ Paris Sud, France*; ²*L2C-Univ. Montpellier 2, France*; ³*Univ. Grenoble Alpes, INAC-SP2M, CEA-CNRS, France*; ⁴*CRHEA-CNRS, France*. We demonstrate room temperature lasing in the UV-C spectral range (~275 nm) with nitride microdisks. The nitride materials are directly grown on a silicon substrate. The active region consists of ultra-thin GaN/AlN quantum wells.

SW4G • Comb Technology—
Continued

SW4G.4 • 16:15

Ultra low noise all polarization-maintaining fiber-based Er optical frequency combs, Naoya Kuse¹, Chien-Chung Lee², Jie Jiang¹, C. Mohr¹, Thomas R. Schibli², M. E. Fermann¹; ¹*IMRA America Inc, USA*; ²*Dept. of Physics, Univ. of Colorado, USA*. We demonstrated all polarization-maintaining (PM) Er fiber frequency combs with record-low noise by using two fast actuators, a graphene-based EOM and a bulk EOM.

SW4G.5 • 16:30

Thin-Disk Lasers for Multi-100-W Average Power Frequency Combs: Challenges and Analysis, Andreas Diebold¹, Florian Emaury¹, Alexander Klenner¹, Clara J. Saraceno^{1,2}, Stephane Schilt², Thomas Sudmeyer², Ursula Keller¹; ¹*Dept. of Physics, ETH Zurich, Switzerland*; ²*Laboratoire Temps-Frequence, Universite de Neuchatel, Switzerland*. We compare the noise characteristics and cavity dynamics of a CEOstabilized 80fs Yb:CALGO SESAM-modelocked thin-disk-laser (TDL) and a 140W SESAMmodelocked Yb:YAG TDL with CEO detection. Guidelines towards tight CEOlocking in the >100-W regime are presented.

SW4G.6 • 16:45

Highly Efficient Self-Referencing of a 1-GHz Diode-Pumped Solid-State Laser Using a Silicon Nitride Chip, Aline Sophie Mayer¹, Alexander Klenner¹, Adrea R. Johnson², Kevin Luke², Michael R. Lamont², Yoshitomo Okawachi², Michal Lipson², Alexander L. Gaeta², Ursula Keller¹; ¹*ETH Zurich, Switzerland*; ²*Cornell Univ., USA*. We present the first carrier-envelope-offset (CEO) frequency detection based on multi-octave-spanning supercontinuum generation in a CMOS-compatible Si₃N₄ waveguide. Strong CEO-beat-signals (>30 dB) of a gigahertz-Yb:CALGO-laser were obtained with only 36 pJ of coupled pulse energy.

CLEO: Applications
& TechnologyAW4H • A&T Topical Review
on Advances in Molecular
Imaging II—Continued

AW4H.3 • 16:30

Invited

Fiber-optic Endomicroscopy for Label-free Optical Histology, Xingde Li¹; ¹*Johns Hopkins Univ., USA*. We report on recently developed high-resolution, fiber-optic scanning endomicroscopy technology and its capability of performing label-free optical histologic imaging *in vivo* and *in situ*. Technological advances and examples of biological tissue imaging will be presented.

Meeting Room
211 B/D

CLEO: Science &
Innovations

SW4I • Novel Materials for
On-chip Photonics—Continued

SW4I.4 • 16:30

30 GHz Zeno-based Graphene Electro-optic Modulator, Christopher T. Phare¹, Yoon Ho Daniel Lee¹, Jaime Cardenas¹, Michal Lipson¹; ¹Cornell Univ., USA. We experimentally demonstrate the first ultrafast graphene modulator by exploiting Zeno coupling effects in a graphene-on-silicon-nitride ring resonator.

SW4I.5 • 16:45

Small Footprint Barium Titanate Photonic Crystal Modulators for Photonic Integrated Circuits, Peter Girouard², Pice Chen², Yongming Tu¹, Young Kyu Jeong², Zhifu Liu², Seng Tiong Ho¹, Bruce W. Wessels²; ¹Electrical Engineering and Computer Science, Northwestern Univ., USA; ²Materials Science and Engineering, Northwestern Univ., USA. We report on the design, fabrication, and characterization of photonic crystal phase modulators on epitaxial barium titanate thin films. Modeling indicates that >50 GHz bandwidth and 0.25 V-cm voltage-length product are achievable in sub-millimeter long devices.

Meeting Room
212 A/C

CLEO: Applications
& Technology

AW4J • Symposium on
Photonics in Surgery II—
Continued

AW4J.3 • 16:15

Simple optical configuration for continuous curvilinear capsulorhexis, Heechul Lee¹, Jong Woon Choi¹, Yong Pyung Kim²; ¹Lutronic Center, Korea; ²Kyunghee Univ., Korea. A simple optical system using a wedge prism instead of a scanner for continuous curvilinear capsulorhexis [CCC] was studied.

AW4J.4 • 16:30 **Invited**

Clinical Embodiments of Laser Speckle Imaging for Real-Time Blood-Flow Monitoring, Bernard Choi^{1,2}; ¹Surgery and Biomedical Engineering, Univ. of California, Irvine, USA; ²Beckman Laser Inst. and Medical Clinic, USA. Laser Speckle Imaging (LSI) is used widely in preclinical studies of blood flow, especially in neurobiology. However, clinical application of LSI remains underexplored. Here, I describe our experiences in developing clinic-friendly embodiments of LSI.

Meeting Room
212 B/D

AW4K • A&T Topical Review on
Optofluidics Microsystems II—
Continued

AW4K.3 • 16:30

Optofluidic Microreactors for Visible-Light Photocatalysis, Xuming Zhang¹; ¹Hong Kong Polytechnic Univ., Hong Kong. Photocatalysis and optofluidics have an intrinsic synergy as both deal with the same objects - light, fluids and solvents. This study presents different designs of optofluidic microreactors to solve some major problems of current photocatalytic technology.

AW4K.4 • 16:45

Electrowetting-Based Variable Tuning Prism, Soraya Terrab¹, Alexander Watson¹, Kevin Dease¹, Juliet Gopinath¹, Victor Bright¹; ¹Univ. of Colorado Boulder, USA. We demonstrate an electrowetting-based variable prism with dual prism-lens operation. A prism apex angle change of 19° at 35 V and curvature change to infinite focal length at 18.9 V are demonstrated.

Marriott
Salon I & II

CLEO: Science &
Innovations

SW4L • Nonlinear Fiber
Optics—Continued

SW4L.3 • 16:15

Stimulated Forward Brillouin Scattering in Hollow-core Photonic Crystal Fiber, William H. Renninger¹, Heedeuk Shin¹, Ryan O. Behunin¹, Prashanta Kharel¹, Eric Kittlaus¹, Peter T. Rakich¹; ¹Yale Univ., USA. Stimulated forward Brillouin scattering is observed in hollow-core photonic bandgap fiber. Multiple acoustic closely-spaced resonances exist below 100 MHz. A quality factor enhancement is observed when air is evacuated from the fiber.

SW4L.4 • 16:30

Long-distance Superluminal Propagation Using a Single-longitudinal-mode Long-cavity Brillouin Fiber Laser, Liang Zhang¹, Li Zhan¹, Minglei Qin¹, Jinmei Liu^{1,2}; ¹Shanghai Jiao Tong Univ., China; ²East China Normal Univ., China. We propose and experimentally validate superluminal propagation using a single-longitudinal-mode long-cavity Brillouin fiber laser with a saturable absorber. The transmission distance of Brillouin-induced superluminal propagation is stretched to 100m in optical fibers.

SW4L.5 • 16:45

Crosstalk Reduction by Backward Raman Pumping in Multi-Wavelength Fiber Optical Parametric Amplification, Xiaojie Guo¹, Chester Shu¹; ¹Chinese Univ. of Hong Kong, Hong Kong. Reduction of four-wave-mixing crosstalk in multi-wavelength amplification is achieved using a backward Raman pump in a fiber optical parametric amplifier. The receiver sensitivity is improved by 1.6 dB in the amplification of three data channels.

CLEO Mobile App

Use the conference app to plan your schedule; view program updates; receive special events reminders and access Technical Papers (*separate log-in required*).

- Go to www.cleoconference.org/app.
- Select the Apple App Store or Google Play link.
- Download the app.
- Log in to use app features such as contacting fellow conference attendees—using your registration I.D. and email address.

CLEO: Science & Innovations

SW4M • SDM, OAM & Free-Space Communications—Continued

SW4M.3 • 16:15

Q-plates for Switchable Excitation of Fiber OAM Modes, Patrick Gregg¹, Mohammad Mirhosseini², Andrea Rubano³, Lorenzo Marucci³, Ebrahim Karimi⁴, Robert W. Boyd^{4,2}, Siddharth Ramachandran¹; ¹Boston Univ., USA; ²Univ. of Rochester, USA; ³Universita di Napoli Federico II, Italy; ⁴Univ. of Ottawa, Canada. We demonstrate that a $|q|=1/2$ plate plus polarization optics can tunably excite all linear combinations of $|L|=1$ fiber OAM modes with up to ~30 dB purity, enabling switch fabrics in fiber-OAM networks and disentangling of degenerate mode mixing effects in long fibers.

SW4M.4 • 16:30 **Invited**

160 Gbaud Single Nyquist Channel Transmission through Emulated 4 km Free-space Turbulence Link, Deming Kong¹, Jian Wu¹, Tong Xu¹, Yan Li¹, Miao Yu¹, Donghao Zheng¹, Yong Zuo¹, Yue Lei¹, Wei Li¹, Hongxiang Guo¹, Jintong Lin¹; ¹State Key Lab of Information Photonics and Optical Communications, Beijing Univ. of Posts and Telecommunications, China. A single 160 Gbaud Nyquist channel transmission based on coherent matched sampling under 4 km lab-emulated free-space turbulence link is demonstrated. Turbulence induced power fluctuation is found to be main reason of performance deterioration.

SW4N • Novel Devices for Communications and Signal Processing—Continued

SW4N.4 • 16:15

Photocurrent gain in graphene-silicon p-i-n junction, Tingyi Gu^{1,2}, Nick Petrone¹, Arend van der Zande¹, Yilei Li¹, Tony Heinz¹, Philip Kim^{3,1}, James Hone¹, Chee Wei Wong¹, Charles M. Santori², Raymond Beausoleil²; ¹Columbia Univ., USA; ²Hewlett-Packard Lab, USA; ³Physics, Harvard Univ., USA. We demonstrate single atomic cladding layer of graphene enhance the photocurrent profile of the monolithic silicon p-i-n junction, by spatially- and spectrally- resolved photocurrent measurement.

SW4N.5 • 16:30

First Demonstration of an Integrated Photonic Phase-Sensitive Amplifier, Wangzhe Li¹, Mingzhi Lu³, Leif Johansson², Milan Mashanovitch², Danilo Dacic¹, Shamsul Arifin¹, Larry Coldren¹; ¹ECE, Univ. of California, Santa Barbara, USA; ²freedomphotonics, USA; ³infinera, USA. For the first time, an integrated photonic phase-sensitive amplifier is reported. Approximately 6.3 dB extinction of on-chip phase-sensitive gain based on a signal-degenerate dual pump four-wave mixing architecture has been achieved.

SW4N.6 • 16:45

Polarization Transparency for Silicon Photonics, Jan Niklas Caspers^{1,2}, Jonathan St-Yves³, Lukas Chrostowski⁴, Wei Shi³, Mo Mojahedi¹; ¹Univ. of Toronto, Germany; ²Robert Bosch GmbH, Germany; ³Dept. of Electrical and Computer Engineering and the Center for Optics, Photonics, and Lasers (COPL), Université Laval, Canada; ⁴Dept. of Electrical and Computer Engineering, Univ. of British Columbia, Canada. We experimentally demonstrate the ability to couple any polarization state from a fiber to the TE-mode of a single waveguide in an integrated silicon photonics circuit. We obtain less than ± 0.6 dB standard deviation across all input polarization states at a wavelength of 1.55 μm .

SW4O • Broadband and Ultrafast Parametric Sources—Continued

SW4O.4 • 16:15

Sub-100fs Fiber Feedback Synchronously Pumped Degenerate Optical Parametric Oscillator, Kirk A. Ingold¹, Alireza Marandi¹, Michel J. Digonnet¹, Robert L. Byer¹; ¹Stanford Univ., USA. We report on a synchronously pumped degenerate OPO operated at 250 MHz that generates 280 mW of transform-limited sub-100fs pulses at 2.09 μm using a compact dispersion-compensated fiber feedback cavity.

SW4O.5 • 16:30

Broadband 7 μm OPCPA pumped by a 2 μm picosecond Ho:YLF CPA system, Daniel Sanchez¹, Michael Hemmer¹, Matthias Baudisch¹, Seth L. Cousin¹, Kevin Zawilski², Peter G. Schunemann², Vadim Smirnov³, Heinar Hoogland^{4,5}, Ronald Holzwarth⁴, Olivier Chalus⁶, Christophe Simon-Boisson⁶, Jens Biegert^{1,7}; ¹ICFO-Institut de Ciències Fotòniques, Spain; ²BAE Systems, USA; ³OptiGrate Corp., USA; ⁴Menlo Systems GmbH, Germany; ⁵Dept. of Physics, Friedrich-Alexander Univ. Erlangen, Germany; ⁶THALES Optronique S.A.S., Laser Solutions Unit, France; ⁷Institució Catalana de Recerca i Estudis Avançats (ICREA), Spain. We generate 260 μJ energy optical pulses at 7 μm with an OPCPA pumped by an optically synchronized 2 μm picosecond CPA system. The mid-IR pulses exhibit a bandwidth supporting sub-4 optical cycle duration.

SW4O.6 • 16:45

High Power, Phase-Coherent Multi-Color Source from UV to Mid-IR for Femtosecond-Resolved Pump-Probe Experiments, Matthias Baudisch¹, Michael Hemmer¹, Jens Biegert^{1,2}; ¹ICFO - Institut de Ciències Fotòniques, Spain; ²ICREA - Institució Catalana de Recerca i Estudis Avançats, Spain. We present a parametric source operating at 160 kHz repetition rate providing simultaneously phase-coherent, femtosecond pulses at 3100, 1620, 810, 405 and 270 nm wavelengths with energies suitable for strong-field pump-probe experiments.



CLEO: QELS-Fundamental Science

FW4A • Quantum Computing—
Continued

FW4A.6 • 17:00

Discorrelated Quantum States, Tim J. Bartley^{1,2}, Evan Meyer-Scott³, Lynden Shalm¹; ¹National Institute of Standards and Technology, USA; ²Applied Physics, Univ. of Paderborn, Germany; ³Inst. for Quantum Computing and Dept. of Physics & Astronomy, Univ. of Waterloo, Canada. Using the building blocks of quantum optics - single photons, coherent states, beam splitters and projective measurement - we construct a two-mode quantum state for which coincident photon number terms in each mode are removed.

FW4A.7 • 17:15

Hybridization: When two wrongs make a right, William Munro¹, Yuichiro Matsuzaki¹, Hiraku Toida¹, Kosuke Kakuyanagi¹, Norikazu Mizuochi³, Kae Nemoto², Kouichi Semba², Hiroshi Yamaguchi¹, Shiro Saito¹; ¹NTT Basic Research Labs, Japan; ²National Inst. of Informatics, Japan; ³Univ. of Osaka, Japan. We show in this presentation how the coherence properties of single electron spins (or ensembles) can be dramatically increased just by it coupling with the superconducting qubit, that is two systems with limited coherence properties can form a combined system with a much longer coherence time.

FW4B • Integrated Structures
for Quantum Optics—
Continued

FW4B.6 • 17:00

Proposed Method of Optical Spin Read-out in a Quantum Dot using the AC Stark Effect, Edward Flagg¹; ¹Dept. of Physics and Astronomy, West Virginia Univ., USA. We propose a method to read-out the spin-state of an electron in a quantum dot in a Voigt geometry magnetic field via cycling transitions induced by the AC Stark effect.

FW4B.7 • 17:15

Measurement of Nonlinear Polariton Dispersion Curves Reveals the Tavis-Cummings Quantum Ladder, Travis Autry^{1,2}, Gael Nardin¹, Daniele Bajoni³, Aristide Lemaître⁴, Sophie Bouchoule⁴, Jacqueline Bloch⁴, Steven Cundiff^{1,2}; ¹JILA, USA; ²Physics, Univ. of Colorado, USA; ³Dipartimento di Ingegneria Industriale e dell'Informazione, Università di Pavia, Italy; ⁴Laboratoire de Photonique et Nanostructures, NRS, France. The nonlinear dispersion curves of the Tavis-Cummings quantum ladder are measured for exciton-polaritons. This quantum ladder remixes the exciton-cavity system in a manner analogous to a quantum beam splitter, realizing a light-matter $n=2$ nOOn state.

FW4C • Novel Optics—
Continued

FW4C.7 • 17:00

Dielectric Metasurface Analogue of Electromagnetically Induced Transparency, Yuanmu Yang¹, Ivan I. Kravchenko², Dayrl Briggs², Jason Valentine¹; ¹Vanderbilt Univ., USA; ²Center for Nanophase Materials Sciences, Oak Ridge National Lab, USA. We present an experimental demonstration of a metasurface analogue of electromagnetically induced transparency based on silicon instead of lossy plasmonic metal, therefore achieved a record-high quality factor of 483 and a sensing figure-of-merit of 103.

FW4C.8 • 17:15

Plasmonic Metasurface for Efficient Laser-Driven Particle Acceleration, Doron Bar-Lev¹, Jacob Scheuer¹; ¹Dept. of Physical Electronics, School of Electrical Engineering, Tel Aviv Univ., Israel. A laser-driven particle accelerator based on plasmonic metasurfaces is proposed and analyzed. The concept utilizes a unique slot-patch nanoantennas combination and is shown to support ultra-short laser pulses while providing high acceleration gradients reaching 11.6GV/m.

FW4D • Nonlinear Fiber
Effects—ContinuedFW4D.7 • 17:00 **Invited**

Temporal cloaking enhancements for optical communication, Joseph M. Lukens¹, Andrew J. Metcalf¹, Daniel E. Leaird¹, Andrew M. Weiner¹; ¹Purdue Univ., USA. We demonstrate a temporal cloak with the capability to simultaneously hide and transmit optical data, as well as prevent corruption by an interfering event. Our results significantly expand the potential of time cloaking in telecommunications.

16:30–18:30 Exhibit Happy Hour and International Year of Light Celebration, *Exhibit Hall*

18:30–20:30 JW5A • Plenary Session III: International Year of Light Celebration and Awards Ceremony, *Grand Ballroom*



INTERNATIONAL
YEAR OF LIGHT
2015

Executive Ballroom
210E

CLEO: QELS-
Fundamental Science

FW4E • Plasmonic Metasurfaces
and Metamaterials—Continued

FW4E.6 • 17:00

Metasurface Engaged with a Plasmonic Spiral Achieve Super Functional Lensing, Grisha Spektor¹, Asaf David¹, Guy Bartal¹, Meir Orenstein¹; ¹*Technion, Israel Inst. of Technology, Israel*. We realized metasurface spiral plasmonic lenses, mitigating efficiency and functionality issues of conventional plasmonic lenses. The lens enhances the efficiency of linear-polarization-invariant focusing and enhances even further the efficiency of high contrast, circular dichroic detection.

FW4E.7 • 17:15

Creating Surface Plasmon Orbital Angular Momentum in a Gold Metasurface, Ching-Fu Chen¹, Chen-Ta Ku¹, Ming-Yang Pan², Pei-Kuen Wei², Chen-Bin Huang¹; ¹*Inst. of Photonics Technologies, National Tsing Hua Univ., Taiwan*; ²*Research Center for Applied Sciences, Academia Sinica, Taiwan*. Nanocavities inscribed in a gold thin film is optimized and arranged to form a metasurface. We demonstrate both numerically and experimentally that surface plasmon vortex carrying orbital angular momentum can be generated under linearly-polarized optical excitation.

Executive Ballroom
210F

CLEO: Science & Innovations

SW4F • SW4F • Micro and Nano
Lasers—Continued

SW4F.6 • 17:00

Wide and reversible tuning of an individual nanowire laser using hydrostatic pressure, Sheng Liu^{1,2}, Changyi Li³, Jeffrey Figiel¹, Igal Brener^{1,2}, Steven Brueck³, George Wang¹; ¹*Sandia National Labs, USA*; ²*The Center for Integrated Nanotechnologies, USA*; ³*Center for High Technology Materials, USA*. We report wide, continuous, and reversible tunable lasing between 367-337nm from single GaN nanowires by applying hydrostatic pressure up to ~7GPa. The pressure coefficients observed are 40% larger compared with bulk GaN or GaN microstructures.

SW4F.7 • 17:15

Room Temperature Continuous Operation of Sub-μW Threshold Nanobeam Laser, Hoon Jang¹, Indra Karnadi¹, Putu Pramudita¹, Yong-Hee Lee¹; ¹*Physics, KAIST, Korea*. Nanobeam laser with threshold 230 nW is demonstrated in continuous-wave operation at room-temperature. This is achieved by reducing the size of active medium to 1.5×0.3×0.02 μm³ via selective wet-etching of a single quantum well layer.

Executive Ballroom
210G

SW4G • Comb Technology—
Continued

SW4G.7 • 17:00

Spectrally Flattened, Broadband Astronomical Frequency Combs, Rafael Probst¹, Yuanjie Wu¹, Tilo Steinmetz², Sebastian Stark², Theodor Hänsch¹, Thomas Udem¹, Ronald Holzwarth^{1,2}; ¹*Max-Planck-Institut für Quantenoptik, Germany*; ²*Menlo Systems GmbH, Germany*. We demonstrate the generation of broadband, visible astronomical frequency combs with flattened spectral envelopes. The flat-top region of the spectrum ranges from about 450 to 730 nm, at mode spacings of 18 and 25 GHz.

SW4G.8 • 17:15

A low-dispersion Fabry-Perot cavity for generation of a 30 GHz astrocomb spanning 140 nm, Daniel Hackett^{1,2}, Gabriel Ycas^{1,2}, Scott Diddams^{2,1}; ¹*Univ. of Colorado Boulder, USA*; ²*National Inst. of Standards and Technology, Boulder, USA*. For broadband filtering of a frequency comb, ultra-low dispersion mirrors with reflectivity 99.2 - 99.6% are fabricated and characterized. A Fabry-Perot cavity is constructed, and used to filter 140 nm of optical bandwidth to 30 GHz.

Executive Ballroom
210H

CLEO: Applications
& Technology

AW4H • A&T Topical Review
on Advances in Molecular
Imaging II—Continued

AW4H.4 • 17:00

Invited

Ultra High-Resolution Photoacoustic Microscopy Using a Novel Transient Absorption Technique, Brian E. Applegate¹; ¹*Texas A&M Univ., USA*. We have recently harnessed transient absorption for ultrahigh resolution photoacoustic microscopy, achieving nearly an order of magnitude improvement in axial resolution. We will discuss recent progress in system development and time resolved measurements for hemoglobin oxygen saturation.

16:30–18:30 Exhibit Happy Hour and International Year of Light Celebration, *Exhibit Hall*

18:30–20:30 JW5A • Plenary Session III: International Year of Light Celebration and Awards Ceremony, *Grand Ballroom*



For Conference News & Insights
Visit blog.cleoconference.org

Wednesday, 13 May

Meeting Room
211 B/D

CLEO: Science & Innovations

SW4I • Novel Materials for On-chip Photonics—Continued

SW4I.6 • 17:00

Electrically Controllable Extraordinary Optical Transmission in Metallic Surface Gratings on VO₂, Junho Jeong¹, Arash Joushaghani¹, Suzanne Paradis², David Alain², Joyce K. Poon¹; ¹Univ. of Toronto, USA; ²Defence Research and Development Canada, Canada. We present metallic gratings on a VO₂ film with electrical control of the transmission spectrum. The extraordinary optical transmission was tunable by up to a factor of 2.75X to achieve an extinction ratio of 26 dB/μm.

SW4I.7 • 17:15

Lithium Niobate on Insulator (LNOI) Grating Couplers, Mohamed Mahmoud¹, Sidhartha Ghosh¹, Gianluca Piazza¹; ¹Carnegie Mellon Univ., USA. One-dimensional grating couplers and waveguides are fabricated in 500 nm X-cut Lithium Niobate thin film making use of the Lithium Niobate on Insulator (LNOI) platform. Single coupler exhibit -12 dB peak insertion loss.

Meeting Room
212 A/C

CLEO: Applications & Technology

AW4J • Symposium on Photonics in Surgery II—Continued

AW4J.5 • 17:00

Towards Endoscopic Image-Guided Laser Coagulation Using a Double-Clad Fiber Coupler, Kathy Beaudette^{1,2}, Jian Ren², Martin Villiger², Mathias Strupler¹, Wendy-Julie Madore¹, Milen Shishkov², Nicolas Godbout¹, Brett Bouma^{2,3}, Caroline Boudoux¹; ¹Ecole Polytechnique de Montreal, Canada; ²Wellman Center for Photomedicine, Harvard Medical School and Massachusetts General Hospital, USA; ³Division of Health Sciences and Technology, Harvard-MIT, USA. We demonstrate a double-clad fiber (DCF) based system using a novel DCF coupler to simultaneously combine optical coherence tomography and laser coagulation. Such a system allows monitoring of dynamic thermal processes during laser irradiation, thus enabling image-guided laser marking and therapy.

AW4J.6 • 17:15

Wide-field Imaging of Pathology Slides using Lensfree On-chip Microscopy, Yibo Zhang¹, Alon Greenbaum¹, Alborz Feizi¹, Ping-Luen Chung¹, Wei Luo¹, Shivani R. Kandukuri¹, Aydogan Ozcan¹; ¹UCLA, USA. Three-dimensional lensfree imaging of pathology slides over a large field-of-view is achieved using multi-height phase recovery that incorporates transport-of-intensity equation and rotational field transformations to overcome stagnation in iterative image reconstruction.

Meeting Room
212 B/D

AW4K • A&T Topical Review on Optofluidics Microsystems II—Continued

AW4K.5 • 17:00 **Invited**

What Is the Microfluidics Doing in Electrowetting Displays?, Tao He¹, mingliang Xu¹, xia chen¹, guofu zhou¹, Lingling Shui¹; ¹Inst. of Electronic Paper Displays, South China Academy of Advanced Optoelectronics, South China Normal Univ., China. Electrowetting display (EWD) is realized by electrically driven fluidic flow in micro-pixels. The fluidic properties including interfacial tension, viscosity and conductivity have been investigated to understand the dual-phase microfluidic behavior in micro-pixels of EWDs.

Marriott
Salon I & II

CLEO: Science & Innovations

SW4L • Nonlinear Fiber Optics—Continued

SW4L.6 • 17:00

Addressing a cavity with patterns at ultra-wideband detune, Xiaoming Wei¹, Yiqing Xu¹, Sisi Tan¹, Shanhui Xu², Zhongmin Yang², Kevin K. Tsia¹, Kenneth K. Y. Wong¹; ¹Dept. of Electrical and Electronic Engineering, The Univ. of Hong Kong, Hong Kong; ²Inst. of Optical Communication Materials and State Key Lab of Luminescent Materials and Devices, South China Univ. of Technology, China. We demonstrate an amplified fiber ring cavity at telecommunication window addressed by optical pattern at 1.0 μm. A storage time longer than 38 μs and an ultra-wideband wavelength conversion of ~500 nm have been obtained.

SW4L.7 • 17:15

Critical Review of the Gain Factor of 16 for Calculation of the Raman Threshold in Fibers, Rainer Engelbrecht¹; ¹Inst. of Micro-waves and Photonics, Friedrich-Alexander-Univ. Erlangen-Nuremberg (FAU), Germany. Analytic approximations yielding the well-known gain factor of 16 in formulas for SRS threshold in fibers are compared to rigorous simulations. This factor is shown to be larger for short and modern fibers, as used for high-power lasers.

16:30–18:30 Exhibit Happy Hour and International Year of Light Celebration, Exhibit Hall

18:30–20:30 JW5A • Plenary Session III: International Year of Light Celebration and Awards Ceremony, Grand Ballroom



INTERNATIONAL
YEAR OF LIGHT
2015

CLEO: Science & Innovations

SW4M • SDM, OAM & Free-Space Communications—Continued**SW4M.5 • 17:00**

Experimental Demonstration of a 400-Gbit/s Free Space Optical Link Using Multiple Orbital-Angular-Momentum Beams with Higher Order Radial Indices, Long Li¹, Guodong Xie¹, Yan Yan¹, Yongxiong Ren¹, peicheng liao¹, Nisar Ahmed¹, Zhe Zhao¹, Changjing Bao¹, Zhe Wang¹, Nima Ashrafi^{2,3}, Solyman Ashrafi², moshe tur⁴, alan willner¹; ¹Univ. of Southern California, USA; ²NxGen Partners, USA; ³Univ. of Texas at Dallas, USA; ⁴Tel Aviv Univ., Israel. We report a transmission of 400 Gbit/s signal over a four-channel, 1-meter mode-division-multiplexed free space optical communication link using multiple orbital-angular-momentum beams with non-zero radial indices, achieving a power penalty less than 6 dB.

SW4N • Novel Devices for Communications and Signal Processing—Continued**SW4N.7 • 17:00**

Thermal-tuned optical pulse shaper for arbitrary waveform generation with integrated waveguides, Shasha Liao¹, Yunhong Ding², Ting Yang¹, Hailong Zhou¹, Xiaolin Chen¹, Jianji Dong¹, Xinliang Zhang¹; ¹Wuhan National Lab for Optoelectronics, China; ²Technical Univ. of Denmark, Denmark. We demonstrate an on-chip thermal-tuned optical pulse shaper based on the four-path finite impulse response (FIR). Four typical waveform are demonstrated by tuning the phase and amplitude of each path.

SW4N.8 • 17:15

All-Optical Flip-Flop Memory Based on V-cavity Laser, Yingchen Wu¹, Yu Zhu¹, Xiaolu Liao¹, Jian-Jun He¹; ¹Zhejiang Univ., China. We experimentally demonstrate an all-optical flip-flop memory based on the bistability of tunable V-cavity laser with short storing and erasing response time of about 150ps and 159ps, respectively.

SW4O • Broadband and Ultrafast Parametric Sources—Continued**SW4O.7 • 17:00**

Front-End of Yb-based High-Energy Optical Waveform Synthesizer, Huseyin Cankaya^{1,2}, Anne-Laure Calendron^{1,2}, Giovanni Cirmi^{1,2}, Franz Kaertner^{1,3}; ¹Center for Free-Electron Laser Science (CFEL), Deutsches Elektronen Synchrotron (DESY), Germany; ²Centre for Ultrafast Imaging and Dept. of Physics, Universitaet Hamburg, Germany; ³Dept. of Electrical Engineering and Computer Science and Research Lab of Electronics, MIT, USA. We demonstrate a front-end of an Yb-based passively CEP-stable, two-octave wide, two-channel optical parametric synthesizer driven by slightly sub-picosecond pump pulses from a multi-mJ regenerative amplifier at 1 kHz.

SW4O.8 • 17:15

Quarter-harmonic generation of femtosecond pulses at 4.18 μm from a mode-locked Yb: fiber laser, Alireza Marandi¹, Kirk Ingold¹, Robert L. Byer¹; ¹Stanford Univ., USA. We report generation of 104 mW of 110-fs pulses at 4.18 μm using two cascaded sub-harmonic PPLN-based optical parametric oscillators pumped by a 950-mW Yb: fiber mode-locked laser at 250 MHz with expected intrinsic phase-locking.

16:30–18:30 Exhibit Happy Hour and International Year of Light Celebration, *Exhibit Hall*

18:30–20:30 JW5A • Plenary Session III: International Year of Light Celebration and Awards Ceremony, *Grand Ballroom*

**Executive Ballroom
210A**

**Executive Ballroom
210B**

**Executive Ballroom
210C**

**Executive Ballroom
210D**

CLEO: QELS-Fundamental Science

08:00–10:00

FTh1A • Quantum Entanglement III

Presider: Antonio Acin; ICFO - Inst. of Photonic Sciences, Spain

FTh1A.1 • 08:00

Noise Figure Improvement and Quantum Information Tapping in a Fiber Optical Parametric Amplifier with Correlated Quantum Fields, Xiaoying Li¹, Xueshi Guo¹, Nannan Liu¹, Yuhong Liu¹, Z. Y. Ou²; ¹Tianjin Univ., China; ²Indiana Univ.-Purdue Univ., USA. We demonstrate a low noise fiber-optical parametric amplifier (FOPA), with noise figure 0.7dB lower than a regular FOPA having vacuum at the unused input port. The scheme can be used as a quantum information tap.

FTh1A.2 • 08:15

Propagation of Two-qubit States using Interference in a Distributed Phase Sensitive Amplifier, Anjali Agarwal¹, James M. Dailey¹, Paul Toliver¹, Nicholas A. Peters¹; ¹Applied Communication Sciences, USA. We experimentally demonstrate transmission of non-orthogonal two-qubit states in a $\chi^{(3)}$ -based optical phase-sensitive amplifier (OPSA). State analysis shows that the OPSA improves the transmission probability of both non-orthogonal states without measurable degradation in two-photon visibility.

FTh1A.3 • 08:30

Effects of Distributed Amplifiers on Quantum Coherence, James D. Franson¹, Brian T. Kirby¹; ¹Univ. of Maryland Baltimore County, USA. The propagation of coherent states using a network of distributed amplifiers is analyzed. This technique can be used to calculate the coherence of other quantum states such as Schrodinger cats.

08:00–10:00

FTh1B • Quantum Control and Precision Measurements

Presider: Tessa Champion, Univ. of Oxford, UK

FTh1B.1 • 08:00

Quantum Zeno Dynamics with Rydberg Atoms, Adrien FACON¹; ¹Lab. Kastler Brossel, Collège de France, CNRS, ENS-PSL Research Univ., UPMC-Sorbonne, France. The back-action of a quantum measurement with a degenerate eigenvalue confines the evolution of the system inside the corresponding eigenspace. Using the Stark sublevels of a Rydberg atom, we report the first observation of such quantum Zeno dynamics in a non-trivial 51-dimension Hilbert space.

FTh1B.2 • 08:15

Feedback Cooling of a Nanomechanical Oscillator to Near its Quantum Ground State, dalziel wilson¹, tobias kippenberg¹, Vivishek Sudhir¹, Nicolas Piro¹, Ryan Schilling¹; ¹epfl, Switzerland. Cavity-enhanced interferometry is used to resolve the displacement of a 4.3 MHz nanobeam oscillator with an imprecision 40 dB below that at the standard quantum limit. Employing this measurement as an error signal, radiation pressure is used to feedback cool the oscillator to 5.3 mechanical quanta.

FTh1B.3 • 08:30

Search For a Permanent Electric Dipole Moment (EDM) of ²²⁵Ra Atom, Mukut Kalita^{1,3}, Michael Bishop¹, Kevin Bailey¹, matthew Dietrich⁵, John Greene¹, Roy Holt¹, Wolfgang Korsch³, Zheng-Tian Lu^{1,2}, Nathan Lemke¹, Peter Mueller¹, Thomas O'Connor¹, Richard Parker^{1,2}, Jaideep Taggart Singh⁴; ¹Argonne National Lab, USA; ²Univ. of Chicago, USA; ³Univ. of Kentucky, USA; ⁴Michigan State Univ., USA; ⁵Northwestern Univ., USA. We are searching for a permanent EDM of the ²²⁵Ra atom. Recently we have observed spin precession of ²²⁵Ra atoms in parallel electric and magnetic fields.

08:00–10:00

FTh1C • High-field and XFEL Physics

Presider: Todd Ditmire; Univ. of Texas Austin, USA

FTh1C.1 • 08:00 Invited

Getting Beyond Unity Fusion Fuel Gain in an Inertially Confined Fusion Implosion, Omar Hurricane¹; ¹Lawrence Livermore National Lab, USA. In this talk, we will discuss the progress towards ignition on the National Ignition Facility (NIF) at Lawrence Livermore National Lab (LLNL) in Northern California. We will cover the some of the setbacks encountered during the progress of the research at NIF, but also cover the great advances that have been made including the achievements of greater than unity fusion 'fuel gain' and alpha-heating dominated fusion plasmas. The research strategy for the future will also be discussed.

FTh1C.2 • 08:30

Laser Generation of Scaled Astrophysical Blast Waves in a Dynamically-Significant Magnetic Field, Nathan Riley¹, Matt Wisner^{1,2}, Sean Lewis^{1,2}, Craig Wagner¹, Vincent Minello¹, Roger Bengtson¹, Todd Ditmire¹; ¹Univ. of Texas at Austin, USA; ²Sandia National Labs, USA. We report preliminary results on the stability of a magnetized laser-launched blast wave scaled to simulate a supernova remnant. Magnetic fields appear to suppress the Vishniac overstability at high mode numbers, possibly facilitating gravitational star formation.

08:00–10:00

FTh1D • Nonlinear Resonators and Optical Frequency Combs

Presider: Marco Peccianti; Univ. of Sussex, UK

FTh1D.1 • 08:00 Invited

Temporal Cavity Solitons: From Fiber Resonators to Microresonators, Stephane Coen¹, Jae K. Jang¹, Stuart G. Murdoch¹, Miro Erkintalo¹; ¹Univ. of Auckland, New Zealand. We will present our latest experiments with temporal cavity solitons, including writing/erasing, temporal tweezing, merging, annihilation, and spontaneous excitation. We will also highlight their relevance in the context of microresonator Kerr frequency combs.

FTh1D.2 • 08:30

Monolithic microresonator for simultaneous lasing feedback and intracavity hyperparametric oscillation, Zhenda Xie^{2,1}, wei liang³, Anatoliy A. Savchenkov³, James Mcmillan¹, jan Burkhart¹, Vladimir S. Ilchenko³, Andrey B. Matsko³, Lute Maleki³, Chee Wei Wong^{2,1}; ¹Columbia Univ., USA; ²Univ. of California, Los Angeles, USA; ³OEWaves Inc., USA. We demonstrate simultaneous lasing and parametric oscillation with high-Q (> 10¹⁰) MgF₂ monolithic microresonators. Stable lasing around 698nm is achieved with sub-25kHz linewidth and 8.8nm tuning range. Multi-pair hyperparametric oscillation is observed over 137.2THz span.

Executive Ballroom
210ECLEO: QELS-
Fundamental Science

08:00–10:00

FTh1E • Electron and
Ultrafast Probing of Plasmonic
Nanostructures

Presider: Christoph Lienau; Carl V. Ossietzky Univ. Oldenburg, Germany

FTh1E.1 • 08:00

Interferometric Plasmon Propagation and Lensing with Nanohole Arrays in Gold Films: Visualization by Nonlinear Photoemission Electron Microscopy, Wayne Hess¹; ¹Pacific Northwest National Lab, USA. Non-linear photoemission electron microscopy, of nanohole arrays litho-graphically etched in gold films, is used to map propagating surface plasmon polaritons (SPPs). The recorded photoemission patterns are attributed to interferences between SPPs launched from the individual nanoholes.

FTh1E.2 • 08:15

Advanced Disc-Ring Optical Nanoantennas Investigated by Photoelectron Emission Microscopy (PEEM), Thomas Kaiser^{1,2}, Matthias Falkner^{1,2}, Jing Qi^{3,2}, Michael Steinert^{1,2}, Christoph Menzel^{1,2}, Carsten Rockstuhl^{4,5}, Thomas Pertsch^{1,2}; ¹Inst. of Applied Physics, Friedrich-Schiller-Universität, Germany; ²Abbe Center of Photonics, Friedrich-Schiller-Universität, Germany; ³Inst. of Condensed Matter Theory and Solid State Optics, Friedrich-Schiller-Universität, Germany; ⁴Inst. of Theoretical Solid State Physics, Karlsruhe Inst. of Technology, Germany; ⁵Inst. of Nanotechnology, Karlsruhe Inst. of Technology, Germany. We theoretically and experimentally investigate circular plasmonic disc nanoantennas enhanced in their performance by a surrounding Bragg grating ring structure. PEEM investigations are demonstrated to provide unprecedented insights into the field localization and enhancement.

FTh1E.3 • 08:30

Invited

Electron-Light Interaction in Optical Near-Fields studied by Ultrafast Transmission Electron Microscopy, Armin Feist¹, Katharina E. Echternkamp¹, Jakob Schauss¹, Sergey V. Yalunin¹, Sascha Schäfer¹, Claus Ropers¹; ¹IV. Physical Inst., Univ. of Göttingen, Germany. Photon-induced scattering of swift electrons with confined light is studied by ultrafast transmission electron microscopy (UTEM) and employed to locally map optical near-fields. Fluence-dependent kinetic energy spectra reveal quantum coherent scattering features.

Executive Ballroom
210F

CLEO: Science & Innovations

08:00–10:00

STh1F • Mode Division
Multiplexing

Presider: Takahide Sakamoto; NICT, Japan

STh1F.1 • 08:00

Efficient silicon PIC mode multiplexer using grating coupler array with aluminum mirror for few-mode fiber, Yunhong Ding¹, Kresten Yvind¹; ¹DTU Fotonik, Dept. of Photonics Engineering, Technical Univ. of Denmark, Denmark. We demonstrate a silicon PIC mode multiplexer using grating couplers. An aluminum mirror is introduced for coupling efficiency improvement. A highest coupling efficiency of -10.6dB with 3.7dB mode dependent coupling loss is achieved.

STh1F.2 • 08:15

Integrated Switch for Mode-Division Multiplexing (MDM) and Wavelength-Division Multiplexing (WDM), Brian Stern¹, Xiaoliang Zhu², Christine Chen², Lawrence Tzuang¹, Jaime Cardenas¹, Keren Bergman², Michal Lipson^{1,3}; ¹Cornell Univ., USA; ²Columbia Univ., USA; ³Kavli Inst. at Cornell for Nanoscale Science, USA. We demonstrate the first integrated switch for mode-division multiplexing (MDM) and wavelength-division multiplexing (WDM). We show on-chip routing of four 10 Gb/s channels with <20 dB crosstalk and 0.5-1.4 dB power penalty.

STh1F.3 • 08:30

Mode division multiplexing using chip-scale silicon coupled vertical gratings, George F. Chen¹, Ting Wang¹, Kelvin J. Ooi¹, Arthur K. Chee², Lay Kee Ang¹, D. T. H. Tan¹; ¹Singapore Univ of Technology and Design, Singapore; ²Massachusetts Institute of Technology, USA. Mode division multiplexing of modes in a silicon waveguide supporting three optical modes is demonstrated in the silicon on insulator platform. The extinction ratio is also observed to increase from 5 dB to 15dB and >25dB as mode order increases, implying an increasing cross coupling coefficient.

Executive Ballroom
210G

08:00–10:00

STh1G • Glass and Rare Earth
Doped Materials

Presider: Thomas Murphy; Univ. of Maryland at College Park, USA

STh1G.1 • 08:00

Properties of Gallium Lanthanum Sulphide Glass, Paul Bastock¹, Chris Craig¹, Khoulou Khan¹, Ed Weatherby¹, Jin Yao¹, Daniel W. Hewak¹; ¹Univ. of Southampton, UK. A series of gallium lanthanum sulphide (GLS) glasses has been studied in order to ascertain properties across the entire glass forming region. This is the first comprehensive study of GLS glass over a wide compositional range.

STh1G.2 • 08:15

Fluorescence in Erbium Doped Gallium Lanthanum Sulphide: Potential for mid-IR Waveguide Laser, Giorgos Demetriou¹, Fiona Thorburn¹, Adam Lancaster¹, Chris Craig², Ed Weatherby², Daniel W. Hewak², Ajoy Kar¹; ¹Inst. of Photonics and Quantum Sciences, Heriot Watt Univ., UK; ²Optoelectronics Research Centre, Univ. of Southampton, UK. Fluorescence is reported in waveguides fabricated via the ultrafast laser inscription technique in Erbium doped Gallium Lanthanum Sulphide (Er³⁺:GLS) for mid-infrared laser applications. The pump wavelength was 980nm leading to mid-infrared transition at 2.75 μ m.

STh1G.3 • 08:30

Photo-Induced Tuning of Chalcogenide-on-Silicon Photonic Integrated Circuits, Ran Califa¹, Hadar Genish¹, Dvir Munk¹, Yuri Kaganovskii¹, Idan Bakish¹, Michael Rosenbluh¹, Avi Zadok¹; ¹Bar-Ilan Univ., Israel. Silicon photonic devices are tuned by selective photo removal of upper chalcogenide glass layers. Phase delays in cascaded interferometer filters and couplers of ring resonators are arbitrarily adjusted. Responses remain stable following trimming.

Executive Ballroom
210H

08:00–10:00

STh1H • Nonlinear Optics for
Advanced Measurements and
Characterization

Presider: Derryck Reid; Heriot-Watt Univ., UK

STh1H.1 • 08:00

Direct Measurement of Plasma Mirror Expansion for Controlled Laser Driven Electron and Harmonic Beams, Maimouna Bocoum¹, Frederick Bohle¹, Benoit beaurepaire¹, Aline Vernier¹, Aurelie Jullien¹, Jérôme Faure¹, Rodrigo B. Lopez-Martens¹; ¹91762, Laboratoire d'Optique Appliquée, France. We present a new method of visualizing plasma expansion at the surface of a plasma mirror over a few fractions of laser wavelength and validate it by selectively generating high-order harmonics or fast electrons.

STh1H.2 • 08:15

Ultrabroadband Mid-Infrared Pump-Probe Spectroscopy using Chirped-Pulse Upconversion, Hideto Shirai¹, Tien Tien Yeh², Yutaka Nomura¹, Chih Wei Luo², Takao Fujii¹; ¹Inst. for Molecular Science, Japan; ²Dept. of Electrophysics, National Chiao Tung Univ., Taiwan. We demonstrated ultrabroadband mid-infrared pump-probe spectroscopy combined with chirped-pulse upconversion in a gas. Ultrafast reflectivity-change signal of an intrinsic germanium was observed in the region from 200 to 5000 cm^{-1} .

STh1H.3 • 08:30

Relaxation dynamics of the OH stretching overtones in isolated HDO molecules observed by IR pump-repump-probe spectroscopy, Daniel Hutzler¹, Jasper Werhahn¹, Rupert Heider¹, Maximilian Bradler², Reinhard Kienberger¹, Eberhard Riedle², Hristo Iglev¹; ¹Technische Universität München, Germany; ²Ludwig-Maximilians-Universität München, Germany. We report on a novel, purely vibrational pump-repump-probe spectroscopy technique to access the overtones of the OH stretching in isolated HDO molecules. Approaching higher-lying states, a continuous decrease of the energy separation and a reduction of the respective lifetimes is observed.

**Meeting Room
211 B/D**

CLEO: Science & Innovations

08:00–10:00
STh1I • Photodetectors
Presider: To be Determined

STh1I.1 • 08:00
Tandem Photodetectors Containing Silicon Nanowires with Selective Spectral Absorption, Hyunsung Park¹, Kenneth B. Crozier^{1,2}; ¹*School of Engineering and Applied Sciences, Harvard Univ., USA*; ²*Dept. of Electrical and Electronic Engineering, Univ. of Melbourne, Australia*. We fabricate a vertically stacked photodetector device containing silicon nanowire photodetectors formed above a silicon substrate that also contains a photodetector. The substrate photodetector converts light not absorbed by the nanowires to photocurrent.

STh1I.2 • 08:15
Waveguide-Coupled Superconducting Nanowire Single-Photon Detectors, Andrew Beyer¹, Ryan Briggs¹, Francesco Marsili¹, Justin D. Cohen², Sean M. Meenehan², Oskar J. Painter², Matthew Shaw¹; ¹*Jet Propulsion Lab, USA*; ²*California Inst. of Technology, USA*. We have demonstrated WSi-based superconducting nanowire single-photon detectors coupled to SiN_x waveguides with integrated ring resonators. This photonics platform enables the implementation of robust and efficient photon-counting detectors with fine spectral resolution near 1550 nm.

STh1I.3 • 08:30
Series-Nanowire Photon Number Resolving Detector Counting up to 24 Photons, Francesco Mattioli¹, Zili Zhou², Alessandro Gaggero¹, Rosalinda Gaudio², Roberto Leoni¹, Andrea Fiore²; ¹*Ist di Fotonica e Nanotecnologie-IFN CNR, Italy*; ²*Univ. of Technology, COBRA Research Inst., Netherlands*. A 24-pixel photon-number-resolving-detector (PNRD) based on superconducting nanowires in a series configuration is demonstrated. Distinct output levels corresponding to the detection of 0-25 photons are observed, due to the high signal-to-noise ratio.

**Meeting Room
212 A/C**

CLEO: Applications & Technology

08:00–09:45
Ath1J • Biomedical Imaging and Sensing II
Presider: Audrey Ellerbee; Stanford Univ., USA

Ath1J.1 • 08:00
Label-free imaging of biological tissues with nonlinear photothermal microscopy, JinPing He^{1,2}, Jun Miyazaki^{1,2}, Nan Wang^{1,2}, Takayoshi Kobayashi^{1,2}; ¹*Univ. of Electro-Communications, Japan*; ²*JST,CREST, Japan*. Nonlinear photothermal microscopy has been applied in imaging of mouse melanoma and spinal cord without any staining. The resolution is higher compared with linear mechanism.

Ath1J.2 • 08:15
Transmittance of Ex vivo Bovine Lens Capsule from 800 cm⁻¹ to 40000 cm⁻¹, Hanh N. Le¹, Do-Hyun Kim², Moinuddin Hassan², William Calhoun², Yong Huang¹, Ilko Ilev², Jin U. Kang¹; ¹*Johns Hopkins Univ., USA*; ²*Food and Drug Administration, Center for Devices and Radiological Health, USA*. Here we present detailed transmission measurements of ex-vivo lens capsules from 40,000 cm⁻¹ to 800 cm⁻¹. Time-dependent measurements were also performed to eliminate water absorption.

Ath1J.3 • 08:30
MEMS-Based Shadowless-illuminated variable-angle TIRF (SIVA-TIRF), Xiaoshuai Huang¹; ¹*Inst of Molecular Medicine, Peking Univ, USA*. We demonstrate a new MEMS-Based Shadowless-illuminated variable-angle TIRF (SIVA-TIRF), which can realize two-plane, two-color TIRF imaging at the speed of 25Hz.

**Meeting Room
212 B/D**

CLEO: Applications & Technology

08:00–09:45
Ath1K • Spectroscopy and Metrology
Presider: To be Determined

Ath1K.1 • 08:00 **Invited**
Monolithic Quantum Cascade Laser Arrays for Broadband Portable Infrared Spectroscopy, Mark F. Witinski^{2,1}, Christian Pflügl²; ¹*Harvard Univ., USA*; ²*Eos Photonics, USA*. Eos manufactures arrays of DFB QCLs, with each element at a different wavelength than its neighbor. In spectroscopy systems, such as standoff and in situ analyzers, this increases sensitivity, allowing for fast all-electronic wavelength tuning.

Ath1K.2 • 08:30
Enhancement of Signal to Noise in Mid-IR Photothermal Spectroscopy by Optimization of Fiber Probe Lasers, Atcha Totachawattana¹, Hui Liu¹, Shyamsunder Erramilli¹, Michelle Y. Sander¹; ¹*Boston Univ., USA*. Continuous-wave and mode-locked fiber lasers are incorporated into label-free mid-IR photothermal spectroscopy. Optimization of probe laser parameters leads to significant enhancement in the signal to noise ratio and the peak-to-baseline contrast.

**Marriott
Salon I & II**

CLEO: Science & Innovations

08:00–10:00
STh1L • Mode-Locked Fiber Lasers
Presider: Andy Chong; University of Dayton, USA; Deutsched Elektronen Synchrotron (DESY); Germany

STh1L.1 • 08:00 **Invited**
Ultralow-Jitter Mode-Locked Fiber Lasers and Their Applications, Jungwon Kim¹; ¹*Korea Advanced Inst of Science & Tech, Korea*. We present the most recent progress in the design and implementation of sub-femtosecond timing jitter mode-locked fiber lasers and their applications in ultralow-noise microwave signal generation, synchronization and remote transfer.

STh1L.2 • 08:30
High power synchronously pumped femto-second Raman fiber laser, Dmitriy Churin¹, Joshua Olson¹, Robert Norwood¹, Nasser Peyghambarian¹, Khanh Kieu¹; ¹*Univ. of Arizona, USA*. We report a synchronously pumped femtosecond Raman fiber laser operating in normal dispersion regime. The laser produces chirped pulses with up to 18nJ energy, 0.76W average power, 88% efficiency, and pulse duration ~133fs after external compression.



CLEO: Science & Innovations

08:00–10:00

STh1M • Beam Shaping for Optimized Laser-matter Interaction*Presider: Ya Cheng; Shanghai Inst. of Optics and Fine Mech., China*STh1M.1 • 08:00 **Invited**

Materials Processing based on Unconventional Femtosecond Laser Beams, Cyril Hnatovsky¹, Vladlen Shvedov¹, Wieslaw Krollikowski^{1,2}; ¹Australian National Univ., Australia; ²Texas A & M Univ. at Qatar, Qatar. We demonstrate the generation of femtosecond vector beams using a combination of a uniaxial and a biaxial crystal. The proposed beam synthesizer is achromatic and can withstand high light intensities.

STh1M.2 • 08:30

Tuning into Tyndall Windows, Benedikt Groever¹, Barmark Heshmat¹, Ramesh Raskar¹; ¹MIT, USA. We report certain liquid mixtures that exhibit exotic Tyndall effects due to large contrast in refractive index modulation of their components. A sharp minimum in scattering enables these mixtures to notably modulate their optical diffusion. This can be applied in imaging, sensing, and displays.

08:00–10:00

STh1N • Frequency Conversion of Combs*Presider: Axel Ruehl; Deutsches Elektronen Synchrotron, Germany*

STh1N.1 • 08:00

A Passively Phase-Locked Er:Fiber Frequency Comb: Free-Running Performance and Active Linewidth Narrowing, David Fehrenbacher¹, Philipp Sulzer¹, Denis Seletskiy¹, Alfred Leitenstorfer¹; ¹Dept. of Physics and Center for Applied Photonics, Univ. of Konstanz, Germany. An offset-free frequency comb generated by difference frequency mixing is established and characterized. mHz-level direct locking of the repetition rate to ⁸⁵Rb and reference-limited linewidth narrowing via an extra-cavity electro-optic modulator are demonstrated.

STh1N.2 • 08:15

Offset-free supercontinuum frequency comb for optical clocks, Takuma Nakamura¹, Isao Ito^{1,2}, Alissa Silva^{1,2}, Shuntaro Tani¹, Yohei Kobayashi^{1,2}; ¹The Inst. for Solid State Physics, Japan; ²Exploratory Research for Advanced Technology, Japan. Difference-frequency mixing two portions of a broadened Yb: fiber laser spectrum leads to an offset-free supercontinuum. To demonstrate full phase stabilization of the comb, a single comb mode was locked to an optical reference.

STh1N.3 • 08:30

Visible to Mid-Infrared Frequency Comb Generation Using a Waveguide PPLN, Kana Iwakuni^{1,2}, Sho Okubo², Osamu Tadanaga³, Hajime Inaba², Atsushi Onae², Feng-Lei Hong^{2,4}, Hiroyuki Sasada¹; ¹Keio Univ., Japan; ²National Metrology Inst. of Japan (NMIJ), National Inst. of Advanced Industrial Science and Technology (AIST), Japan; ³NTT Device Technology Labs, Japan; ⁴Dept. of Physics, Yokohama National Univ., Japan. We succeeded in generating a coherent optical frequency comb covering more than 3 octaves from visible to mid-infrared with a waveguide-type PPLN. The generated comb is demonstrated to be useful for metrology and spectroscopic applications.

08:00–10:00

STh1O • All Optical Signal Processing*Presider: Masaki Asobe; Tokai Univ., Japan*

STh1O.1 • 08:00

A High Speed All-Optical NAND Logic Gate Using Four-Wave Mixing, Kangmei Li¹, Hong-Fu Ting¹, Mark A. Foster¹, Amy C. Foster¹; ¹Johns Hopkins Univ., USA. We demonstrate a high speed all-optical NAND gate based on four-wave mixing Bragg scattering in highly nonlinear fiber. A 15.2-dB depletion of the signal is obtained and time domain measurements show 10-Gb/s NAND operation.

STh1O.2 • 08:15

Kerr Nonlinear Switching in a Core-shell Microspherical Resonator Fabricated From the Silicon Fiber Platform, Fariza Hanim Suhailin^{1,2}, Noel Healy¹, Misha Sumetsky³, John Ballato⁴, Andrew Dibbs⁵, Ursula Gibson⁵, Anna C. Peacock¹; ¹Optoelectronics Research Centre, Univ. of Southampton, UK; ²School of Fundamental Science, Universiti Malaysia Terengganu, Malaysia; ³Engineering and Applied Science, Aston Univ., UK; ⁴COMSET, School of Materials Science and Engineering, Clemson Univ., USA; ⁵Dept. of Physics, Norwegian Univ. of Science and Technology, Norway. We investigate the Kerr nonlinearity in a core-shell microspherical resonator fabricated from a silicon fiber. By exploiting the ultrafast wavelength shifting, sub-picosecond modulation is demonstrated.

STh1O.3 • 08:30

High-accuracy heterodyne detection of THz radiation exploiting telecommunication technologies, Thomas Folland¹, Antonio Ramospulido¹, Owen Marshall¹, Harvey Beere², David Ritchie², Subhasish Chakraborty¹; ¹Univ. of Manchester, UK; ²Univ. of Cambridge, UK. We report the first open-loop heterodyne technique using standard telecom optical fibre components for spectral characterization of THz semiconductor lasers. This allows the measurement of continuous modal tuning with sub-GHz accuracy and 20dB dynamic range.

Executive Ballroom
210A

Executive Ballroom
210B

Executive Ballroom
210C

Executive Ballroom
210D

CLEO: QELS-Fundamental Science

FTh1A • Quantum Entanglement III—Continued

FTh1A.4 • 08:45

Enhanced Photon-Pair Detection Using Phase-Sensitive Pre-amplification, James M. Dailey¹, Anjali Agarwal¹, Paul Toliver¹, Nicholas A. Peters¹; ¹*Applied Communication Sciences, USA*. We describe an experimental demonstration of fiber-based optical phase-sensitive amplification for improved detection of correlated single-photon pairs. A measured coincidence gain of 4.5dB provides 3dB improvement in the detection system signal-to-noise ratio.

FTh1A.5 • 09:00

Engineering large-scale entanglement in the quantum optical frequency comb, Pei Wang¹, Wenjiang Fan¹, Moran Chen¹, Olivier Pfister¹; ¹*Univ. of Virginia, USA*. We report on experimental progress toward scaling our recent 60-entangled-qumode experiment [1] to thousands of qumodes in the quantum optical frequency comb. We present a model which predicts that 3,200 entangled modes can be achieved.

FTh1A.6 • 09:15

Frequency-Resolved Reconstruction of the Biphoton Polarization State via Stimulated Emission Tomography, Bin Fang¹, Marco Liscidini², John E. Sipe³, Virginia Lorenz¹; ¹*Dept. of Physics and Astronomy, Univ. of Delaware, USA*; ²*Dept. of Physics, Univ. of Pavia, Italy*; ³*Dept. of Physics and Inst. for Optical Sciences, Univ. of Toronto, Canada*. We reconstruct the polarization-entangled state of individual frequency components of the biphoton wave function by stimulated emission tomography. The frequency-resolved polarization state enables new insight into frequency-polarization correlations of the quantum process.

FTh1B • Quantum Control and Precision Measurements—Continued

FTh1B.4 • 08:45

Nonlinear optical magnetometry with accessible in situ optical squeezing, Nils Otterstrom^{1,2}, Raphael Pooser², Benjamin Lawrie²; ¹*Dept. of Physics and Astronomy, Brigham Young Univ., USA*; ²*Quantum Information Science Group, Computational Science and Engineering Division, Oak Ridge National Lab, USA*. We demonstrate compact and accessible squeezed-light magnetometry using four-wave-mixing in a single hot rubidium vapor cell. This framework enables 4.7 dB of quantum-noise-reduction while simultaneously adding nonlinear-magneto-optical-rotation(NMOR) signals from the probe and conjugate fields.

FTh1B.5 • 09:00 Tutorial

Making the World's Best Atomic Clock, Jun Ye¹; ¹*Univ. of Colorado at Boulder JILA, USA*. I will report our recent effort towards realizing the full potential of a many-particle clock with a state-of-the-art stable laser. We have achieved fractional stability of 2.2×10^{-16} at 1 s for the JILA Sr optical atomic clock. We have also reduced the total uncertainty of our clock to 2.1×10^{-18} in fractional frequency units. Both represent new records for the performance of an atomic clock.



Jun Ye is a Fellow of JILA, NIST and University of Colorado. His research focuses on the frontier of light-matter interactions and includes precision measurement, quantum physics and ultracold matter, optical frequency metrology, and ultrafast science. He has co-authored over 280 technical papers and has delivered over 400 invited talks. He is a Fellow of the American Physical Society, The Optical Society and a member of the National Academy of Sciences.

FTh1C • High-field FTh1C • High-field and XFEL Physics—Continued

FTh1C.3 • 08:45

Laser Acceleration and Deflection of 96.3keV Electrons with a Silicon Dielectric Structure, Kenneth Leedle¹, Fabian Pease¹, Robert L. Byer¹, James S. Harris¹; ¹*Stanford Univ., USA*. Dielectric laser accelerators are a compact and scalable alternative to radio frequency accelerators. We present the first demonstration of over 200 MeV/m acceleration and deflection gradients with a silicon structure at 96.3keV electron energy.

FTh1C.4 • 09:00

He Ion Acceleration in Near Critical Density Plasma, Sergei Tochitsky¹, Chao Gong¹, Jeremy Pigeon¹, Frederico Fiuza², Chan Joshi¹; ¹*Univ. of California Los Angeles, USA*; ²*Lawrence Livermore National Lab, USA*. The CO₂ laser-plasma interactions are uniquely placed for Shock Wave Acceleration of He or other light ions. We report on experimental and numerical studies of He ion acceleration in a gas jet plasma.

FTh1C.5 • 09:15

Difference-Frequency Generation of Optical Radiation from Two-Color X-Ray Pulses, Eliyahu Shwartz¹, Sharon Shwartz^{1,2}; ¹*Physics, Bar Ilan Univ., Israel*; ²*The Inst. for Nanotechnology and Advanced Materials, Bar Ilan Univ., Israel*. We describe the process of difference-frequency generation of optical radiation from X-ray pulses. We find that the efficiency is orders of magnitude higher than similar effects, and highlight its potential application to probe atomic-scale structures.

FTh1D • Nonlinear Resonators and Optical Frequency Combs—Continued

FTh1D.3 • 08:45

Silicon Carbide Microresonators with High Optical Q and Large Kerr Nonlinearity for Nonlinear Optics, Xiyuan Lu¹, Jonathan Y. Lee¹, Steven Rogers¹, Qiang Lin¹; ¹*Univ. of Rochester, USA*. We demonstrate an amorphous silicon carbide (a-SiC) microresonator with optical Q up to 1.3×10^5 . This enables us to characterize the third-order nonlinearity of a-SiC with $n^2 = (5.9 \pm 0.7) \times 10^{-15} \text{ cm}^2/\text{W}$.

FTh1D.4 • 09:00

Frequency Comb-enhanced Coupling in Silicon Nitride Microresonators, Pei-Hsun Wang¹, Yi Xuan¹, Xiaoxiao Xue¹, Yang Liu¹, Jian Wang¹, Daniel E. Leaird¹, Minghao Qi¹, Andrew M. Weiner¹; ¹*Purdue Univ., USA*. We investigate enhanced coupling of the pump laser as a result of power transfer to the frequency comb in a silicon nitride microring designed with an over-coupled bus-waveguide.

FTh1D.5 • 09:15

Tunable Frequency Combs based on Dual Microring Resonators, Steven Miller¹, Yoshitomo Okawachi², Kevin Luke¹, Alexander L. Gaeta^{2,3}, Michal Lipson^{1,3}; ¹*School of Electrical and Computer Engineering, Cornell Univ., USA*; ²*School of Applied and Engineering Physics, Cornell Univ., USA*; ³*Kavli Inst. at Cornell for Nanoscale Science, Cornell Univ., USA*. We demonstrate tunable coupling condition of a silicon nitride microresonator frequency comb. Using a dual-coupled resonator geometry and integrated microheaters, we achieve 13.3 dB of extinction tuning and observe 10-fold increase in generated power.

Executive Ballroom
210ECLEO: QELS-
Fundamental ScienceFTh1E • Electron and
Ultrafast Probing of Plasmonic
Nanostructures—Continued

FTh1E.4 • 09:00

Ultrafast pump-probe photo-induced force microscopy at nanoscale, Junghoon Jahng¹, Jordan Brocius¹, Dmitry Fishman¹, Eric O. Potma¹; ¹Univ. of California, Irvine, USA. We perform time-resolved pump-probe microscopy measurements by recording the local force between a sharp tip and the photo-excited sample as a readout mechanism for the material's nonlinear polarization.

FTh1E.5 • 09:15

Spatially-Resolved, Three-Dimensional Investigation of Surface Plasmon Resonances in Complex Nanostructures, Jordan Hachtel^{1,2}, Daniel Mayo^{3,4}, Anas Mouti², Claire Marvinney³, Richard Mu⁴, Richard F. Haglund^{1,3}, Andrew Lupini², Matthew Chisholm², Sokrates Pantelides^{1,2}; ¹Dept. of Physics and Astronomy, Vanderbilt Univ., USA; ²Materials Science and Technology Division, Oak Ridge National Lab, USA; ³Interdisciplinary Materials Science Program, Vanderbilt Univ., USA; ⁴Dept. of Physics, Fisk Univ., USA. We report a three-dimensional study of surface plasmons in random-morphology nanoparticles by combining spatially resolved electron energy loss spectroscopy, which probes optical excitations, and cathodoluminescence, which probes radiative decay, in a scanning transmission electron microscope.

Executive Ballroom
210F

CLEO: Science & Innovations

STh1F • Mode Division
Multiplexing—Continued

STh1F.4 • 08:45

Mode Multiplexer Based on Integrated Horizontal and Vertical Polymer-Waveguide Directional Couplers, Kin S. Chiang¹, Jiangli Dong¹, Wei Jin¹; ¹City Univ. of Hong Kong, Hong Kong. We propose an integrated polymer-waveguide mode (de)multiplexer based on cascaded horizontal and vertical directional couplers for combining/separating the three lowest-order modes. Our experimental device shows crosstalks lower than -15.6 dB in the C-band.

STh1F.5 • 09:00

Photonics Integrated Circuit for WDM Mode Division Multiplexing with Phase to Intensity Demodulation, Mengyuan Ye¹, Yu Yu¹, Guanyu Chen¹, Yuchan Luo¹, Lei Shi¹, Xinliang Zhang¹; ¹Wuhan National Lab for Optoelectronics, China. We demonstrate an on-chip WDM-compatible mode multiplexing system with function of phase demodulation. The proposed scheme can be useful at the interface of long-haul and on-chip communication systems, which prefer phase and intensity modulated formats respectively.

STh1F.6 • 09:15

Demonstration of Distance Emulation for an Orbital-Angular-Momentum Beam, Nisar Ahmed¹, Martin P. Lavery^{2,1}, peicheng liao¹, Guodong Xie¹, Hao Huang¹, Long Li¹, Yongxiong Ren¹, Yan Yan¹, Zhe Zhao¹, Zhe Wang¹, Nima Ashrafi^{3,4}, Solyman Ashrafi⁴, Moshe Tur⁵, alan willner¹; ¹Univ. of Southern California, USA; ²Univ. of Glasgow, UK; ³Univ. of Texas at Dallas, USA; ⁴NxGen Partners, USA; ⁵Tel Aviv Univ., Israel. We design and experimentally demonstrate a free-space distance emulator for propagating OAM beams over long distances in a lab environment. The performance of the system is assessed by measuring spot radius and radius of curvature of propagated beams.

Executive Ballroom
210GSTh1G • Glass and Rare Earth
Doped Materials—Continued

STh1G.4 • 08:45

Visible up-conversion luminescence in (ErSc)₂O₃ epitaxial thin films and its suppression by photonic band-gap, Takehiko Tawara^{1,2}, Thomas McManus^{1,3}, Yoshihiro Kawakami⁴, Hiroo Omi^{1,2}, Adel Najari¹, Reina Kaji⁴, Satoru Adachi⁴, Hldeki Gotoh¹; ¹NTT Basic Research Labs, Japan; ²NTT Nanophotonics Center, Japan; ³Univ. of Bath, UK; ⁴Hokkaido Univ., Japan. Visible up-conversion luminescence induced by 1535-nm excitation in (ErSc)₂O₃ epitaxial layers are observed. We investigate fast up-conversion rate and propose its suppression structure by photonic band-gap for realizing higher optical gain devices on Si wafers.

STh1G.5 • 09:00

Highly Yb-doped KGd(WO₄)₂ Thin-film Amplifier, Yean-Sheng Yong^{1,2}, Shanmugam Aravazhi¹, Sergio A. Vázquez-Córdova^{1,2}, Sonia M. García-Blanco^{1,2}, Markus Pollnau^{1,3}; ¹Integrated Optical MicroSystems Group, MESA+ Inst. for Nanotechnology, Univ. of Twente, Netherlands; ²Optical Sciences Group, MESA+ Inst. for Nanotechnology, Univ. of Twente, Netherlands; ³Dept. of Materials and Nano Physics, School of Information and Communication Technology, KTH—Royal Inst. of Technology, Sweden. We report record-high small-signal gain of 1050 dB/cm at 981 nm wavelength in a KGd_{0.425}Yb_{0.575}(WO₄)₂ thin film. The sensitivity of gain to the shift of beam-focus position, which is critical under non-waveguiding conditions, is investigated.

STh1G.6 • 09:15

Extremely Low-Loss Chalcogenide Photonics Devices with Chlorine-Based Plasma Etching, Jeff Chiles¹, Marcin Malinowski¹, Ashutosh Rao¹, Spencer Novak^{1,3}, Kathleen Richardson^{1,3}, Sasan Fathpour^{1,2}; ¹Univ. of Central Florida, CREOL, USA; ²Dept. of Electrical Engineering and Computer Science, Univ. of Central Florida, USA; ³School of Materials Science and Engineering, Clemson Univ., USA. Chlorine-based plasma is employed to produce extremely low propagation loss as low as 0.42 dB/cm in chalcogenide waveguides, record-high intrinsic Q-factors of 450,000 microring resonators and fiber-to-waveguide grating couplers with a coupling efficiency of 37%.

Executive Ballroom
210HSTh1H • Nonlinear Optics for
Advanced Measurements and
Characterization—Continued

STh1H.4 • 08:45

Tunable All-Optical Modulation by Period Multiplication in a Synchronously-Pumped Optical Parametric Oscillator, Tobias Steinle¹, Vikas Kumar², Andy Steinmann¹, Marco Marangoni², Giulio Cerullo², Harald W. Giessen¹; ¹4th Physics Inst., Univ. of Stuttgart, Germany; ²IFN-CNR, Dipartimento di Fisica, Politecnico di Milano, Italy. We present the first observation of period multiplication in a synchronously-pumped OPO, enabling tunable all-optical modulation for ultrafast pulses beyond 10 MHz. Elegant pump-probe spectroscopy without external modulation is demonstrated by stimulated Raman scattering.

STh1H.5 • 09:00

Two-crystal Optical Parametric Oscillator for Broadband Dual-comb Spectroscopy, Yuwei Jin¹, Simona M. Cristescu¹, Frans J. Harren¹, Julien Mandon¹; ¹Dept. of Molecular and Laser Physics, Radboud Univ. Nijmegen, Netherlands. We present a broadband two-crystal optical parametric oscillator for mid-infrared dual-comb spectroscopy. The measured absorption and dispersion spectra of methane between 2850 cm⁻¹ and 3200 cm⁻¹ are demonstrated with a 0.2 cm⁻¹ spectral resolution.

STh1H.6 • 09:15

Visualization of the Internal Structure of Orientation-Patterned III-V Semiconductors, Pawel karpinski^{1,2}, Xin Chen¹, Vladlen Shvedov¹, Cyril Hnatovsky¹, Arnaud Grisard³, Eric Lallier³, Barry Luther-Davies¹, Wieslaw Krolikowski^{1,4}, Yan S¹; ¹Laser Physics Centre, Research School of Physics and Engineering, Australian National Univ., Australia; ²Wroclaw Univ. of Technology, Poland; ³Thales Research and Technology, France; ⁴Texas A & M Univ. at Qatar, Qatar. We investigate nonlinear diffraction in orientation-patterned semiconductors and identify Čerenkov second harmonic generation in a transverse geometry of interaction. Čerenkov second harmonic allows nondestructive 3D visualization of the internal structure of orientation-patterned semiconductor.

**Meeting Room
211 B/D**

CLEO: Science & Innovations

STh1I • Photodetectors—Continued

STh1I.4 • 08:45

High Responsivity Silicon-Graphene Schottky Avalanche Photodetectors for Visible and Telecom Wavelengths, Ilya Goykhman¹, Anna Eiden¹, Domenico De Fazio¹, Ugo Sassi¹, Matteo Barbone¹, Andrea C. Ferrari¹; ¹Cambridge Graphene Centre, Univ. of Cambridge, UK. We design, optimize and demonstrate a silicon-graphene avalanche Schottky photodetector with photoresponsivities of 1A/W and 0.5A/W for visible and telecom wavelengths respectively.

STh1I.5 • 09:00

Graphene on Silicon-on-Sapphire Waveguide Photodetectors, Zhenzhou Cheng¹, Jiaqi Wang¹, Ke Xu¹, Hon Ki Tsang¹, Chester Shu¹; ¹The Chinese Univ. of Hong Kong, Hong Kong. We describe the transfer of chemical vapor deposition grown graphene onto silicon-on-sapphire waveguides to form heterostructure waveguide photodetectors which had responsivities of 0.9 mA/W and 4.5 mA/W at 1.55 μm and 2.75 μm wavelengths, respectively.

STh1I.6 • 09:15

A CMOS-Compatible Plenoptic Sensor for Smart Lighting Applications, Javad Ghasemi¹, Alexander Neumann¹, Shima Nezadbadeh¹, Xiangyu Nie¹, Payman Zarkesh-Ha¹, Steven Brueck¹; ¹CHTM (Center for High Tech Materials), Univ. of New Mexico, USA. A CMOS-compatible, visible, plenoptic (angle, polarization and wavelength) detector, based on a grating-coupled waveguide structure, is demonstrated with an angular resolution of $< 1^\circ$ and a corresponding wavelength resolution of $< 5 \text{ nm}$.

**Meeting Room
212 A/C**

CLEO: Applications & Technology

ATH1J • Biomedical Imaging and Sensing II—Continued

ATH1J.4 • 08:45

Characterization of optical resolution photoacoustic microscopy in comparison to confocal microscope, Paweena U-Thainual¹, Do-Hyun Kim¹; ¹Food and Drug Administration, USA. Lateral resolution and depth discrimination in turbid samples was measured with optical resolution photoacoustic microscopy (ORPAM) and compared to confocal microscopy (CM). ORPAM signal strength and CM resolution were relatively less affected by scattering.

ATH1J.5 • 09:00

Degenerate Volume Holographic Imaging Techniques and Instruments for Subsurface Tissue Visualization, Raymond K. Kostuk¹, Isela D. Howlett¹, Michael Gordon¹, John Brownlee¹, Erich de Leon¹, Gabriel Orsinger¹, Jennifer Watson¹, Marek Romanowski¹, Kenneth Hatch¹, Yuan Luo², George Barbastathis³, Jennifer Barton¹; ¹Univ. of Arizona, USA; ²National Taiwan Univ., Taiwan; ³MIT, USA. Degenerate Bragg matching with a volume hologram can lead to reduction in image contrast. Incorporating very high selectivity holograms, high numerical aperture objectives, and image processing can provide image information comparable with histology stained images.

ATH1J.6 • 09:15

High-throughput Imaging of Self-luminous Objects through a Single Optical Fiber, Roman Barankov¹, Jerome Mertz¹; ¹Boston Univ., USA. We demonstrate a strategy of imaging through a fiber in which the spatial information is encoded into distinct spectrum codes spanning the bandwidth of the object spectrum, enabling high-throughput 2D imaging insensitive to fiber bending.

**Meeting Room
212 B/D**

ATH1K • Spectroscopy and Metrology—Continued

ATH1K.3 • 08:45

Advanced wideband cavity enhanced spectroscopy, Toby K. Boyson¹, Charles C. Harb¹; ¹School of Engineering and Information Technology, UNSW Australia, Australia. We present new results from a variant of cavity enhanced spectroscopy that allows large spectral bandwidths to be analysed in real time, and demonstrate new methods to apply the technique to real-time monitoring of species with broad absorbances.

ATH1K.4 • 09:00

Broadband dual-comb coherent anti-Stokes Raman spectroscopy at high signal-to-noise ratio, Ming Yan^{2,1}, Simon Holzner^{2,1}, Theodor Hänsch^{2,1}, Nathalie Picqué^{2,1}; ¹Max Planck Inst. of Quantum Optics, USA; ²Physics Dept., Ludwig-Maximilians-Universität München, Germany. Coherent anti-Stokes Raman spectroscopy is achieved on micro-second time scale with two frequency combs and a heterodyne detection with a local oscillator. The vibrational transitions reach a signal-to-noise ratio of 1600 with linear concentration dependence.

ATH1K.5 • 09:15

Depolarization Sensitive Optical Inspection of Semiconductor Integrated Circuits, Abdulkadir yurt¹, Michael Grogan¹, Selim Unlu¹, Bennett Goldberg¹; ¹Boston Univ., USA. We demonstrate dark-field, through-silicon imaging of semiconductor integrated circuits by exploiting depolarization-sensitive, high aperture angle reflectivity.

**Marriott
Salon I & II**

CLEO: Science & Innovations

STh1L • Mode-Locked Fiber Lasers—Continued

STh1L.3 • 08:45

Fast Wavelength-Tunable Picosecond Pulses from Mode-Locked Er Fiber Laser using an Intracavity Filter with Repetition Rate Compensator, Yasuyuki Ozeki¹, Daigo Tashiro¹; ¹The Univ. of Tokyo, Japan. We present a polarization-maintaining, SESAM-mode-locked fiber laser with a wavelength-tuning speed of $< 5 \text{ ms}$ and a duration of $\sim 10 \text{ ps}$. Within the tunability of $> 30 \text{ nm}$, the variation in the repetition rate was $< 300 \text{ Hz}$.

STh1L.4 • 09:00

Passively Mode-locked Holmium-doped Fiber Oscillators Optimized for Ho:YLF Amplifier Seeding, Peng Li¹, Axel Ruehl¹, Colleen Bransley^{1,2}, Ingmar Hartl¹; ¹Deutsches Elektronen Synchrotron, Germany; ²Physics Dept., Univ. of Dayton, USA. We present soliton operation of holmium-doped fiber oscillators with independently tunable central wavelengths from 2040nm to 2070nm and spectral widths from 5nm to 10nm, which can be matched to the requirements of Ho:YLF amplifiers.

STh1L.5 • 09:15

Reducing Nonlinear Limitations of Ytterbium Mode-Locked Fibre Lasers with Hollow-Core Negative Curvature Fibre, Clarissa Harvey¹, Fei Yu¹, Jonathan C. Knight¹, William Wadsworth¹, Paulo Almeida²; ¹Univ. of Bath, UK; ²Fianium Ltd., UK. Ultralow non-linearity hollow-core negative curvature fibre is used in a mode-locked Ytterbium fibre laser to prevent the onset of pulse breakup at low repetition-rates. Identical pulse peak-power limit at 37MHz and 11MHz is experimentally demonstrated.

CLEO: Science & Innovations

STh1M • Beam Shaping for Optimized Laser-matter Interaction—Continued**STh1M.3 • 08:45**

Generating Optical Tractor Beams of Improved Stability with Metasurfaces, Carl Pfeiffer¹, Cheng Zhang¹, L. Jay Guo¹, Anthony Grbic¹; ¹Univ. of Michigan, USA. A tractor beam is a propagation invariant beam that pulls objects towards a light source. Here, an efficient tractor beam with improved stability is generated by illuminating a dielectric metasurface with a Gaussian beam.

STh1M.4 • 09:00

Laser Micromachining with Femtosecond Higher-order Bessel Beams, Weibo Cheng¹, Pavel G. Polynkin¹; ¹College of Optical Sciences, Univ. of Arizona, USA. We use femtosecond higher-order Bessel beams for micromachining of borosilicate glass plates. The self-focusing of the beams inside the glass results in the production of beaded ring structures on the back surfaces of the plates.

STh1M.5 • 09:15

Light Localization in Axisymmetric Nano-Structured Plasmonic Gratings, Alexander Lozano^{1,2}, Moein shayegannia¹, Arthur Montazeri¹, Yuan Fang³, Kaveh Moussakhani¹, Nazir Kherani^{1,4}; ¹Dept. of Electrical and Computer Engineering, Univ. of Toronto, Canada; ²Dept. of Physics, Univ. of Toronto, Canada; ³Dept. of Physics, Univ. of California, Berkeley, USA; ⁴Dept. of Materials Science and Engineering, Univ. of Toronto, Canada. We present a novel technique for spectral decomposition of light in a sub-wavelength plasmonic bull's eye grating structure. Controlling plasmon coupling through the variation of groove width enables spatial control over light localization in the grating.

STh1N • Frequency Conversion of Combs—Continued**STh1N.4 • 08:45**

Measured Carrier Envelope Offset and Linewidth of Degenerate Optical Parametric Oscillator, Kevin F. Lee¹, C. Mohr¹, Jie Jiang¹, Peter G. Schunemann², M. E. Fermann¹; ¹IMRA America, Inc., USA; ²BAE Systems, USA. We measure the carrier envelope offset frequency of a degenerate optical parametric oscillator. We verify that it has half the value of the pump frequency comb, and sub-Hertz level relative linewidth.

STh1N.5 • 09:00

Frequency Comb Spanning 2.5-7.5 μm from a Subharmonic GaAs OPO and its Coherence Properties, Viktor O. Smolski¹, Sergey D. Gorelov², Jian Zhao¹, Jia Xu¹, Peter G. Schunemann³, Konstantin L. Vodopyanov¹; ¹Univ. of Central Florida, CREOL, USA; ²Univ. of Nizhny Novgorod, Russia; ³BAE Systems, USA. We demonstrate a record-wide mid-IR comb using Tm-fiber-laser-pumped near-degenerate GaAs OPO. By varying intracavity dispersion, we observe a transition from a single-comb to a two-comb state, where two combs are offset by a constant value.

STh1N.6 • 09:15

1-GHz Harmonically Pumped Femtosecond Optical Parametric Oscillator Frequency Comb, Karolis Balskus¹, Stewart Leitch¹, Zhaowei Zhang¹, Richard McCracken¹, Deryck T. Reid¹; ¹Heriot Watt Univ., USA. We present the first example of a femtosecond optical parametric oscillator frequency comb by using a 333-MHz Ti:sapphire laser to achieve a stabilized comb at 1-GHz mode spacing in the 1.1-1.6- μm wavelength band.

STh1O • All Optical Signal Processing—Continued**STh1O.4 • 08:45**

Experimental Demonstration of Tunable Homodyne Detection for Two Channels Simultaneously using Nonlinear Optical Signal Processing to Automatically Lock a Single "Local" Pump Laser to Two 20-Gbaud BPSK Data Signals, Ahmed Almaiman¹, Morteza Ziyadi¹, Amirhossein Mohajerin Ariaei¹, Yinwen Cao¹, Mohammad-Reza Chitgarha¹, Peicheng Liao¹, Youichi Akasaka⁵, Jeng-Yuan Yang⁵, Motoyoshi Sekiya⁵, Joseph Touch³, Carsten Langrock², Martin M. Fejer², Moshe Tur⁴, Alan Willner¹; ¹Univ. of Southern California, USA; ²Stanford Univ., USA; ³Information Sciences Inst., USA; ⁴Tel Aviv Univ., Israel; ⁵Fujitsu Labs of America, USA. We demonstrate homodyne detection for multiple channels using nonlinear optical signal processing to automatically lock a single "local" pump laser to these data channels simultaneously and perform experimental demonstration with two 20-Gbaud BPSK channels.

STh1O.5 • 09:00

Experimental Demonstration of Tunable and Automatically-Locked Homodyne Detection for Dual-Polarization 20-32-Gbaud QPSK Channels using Nonlinear Mixing and Polarization Diversity, Morteza Ziyadi¹, Amirhossein Mohajerin Ariaei¹, Ahmed Almaiman¹, Yinwen Cao¹, Mohammad-Reza Chitgarha¹, peicheng liao¹, Youichi akasaka², Jeng-Yuan Yang², Motoyoshi Sekiya², Joseph Touch³, Moshe Tur⁴, Carsten Langrock⁵, Martin M. Fejer⁵, Alan Willner¹; ¹Univ. of Southern California, USA; ²Fujitsu Labs of America, USA; ³Information Sciences Inst., USC, USA; ⁴Tel Aviv Univ., Israel; ⁵Stanford Univ., USA. We experimentally demonstrate a tunable homodyne receiver on polarization multiplexed QPSK signals. PPLN waveguides inside the polarization diversity loops are used to frequency/phase lock the signals with the LO. Open eye diagrams with BER measurements are shown.

STh1O.6 • 09:15

Demonstration of Tunable and Automatic Frequency/Phase Locking for Multiple-Wavelength QPSK and 16-QAM Homodyne Receivers using a Single Nonlinear Element, Morteza Ziyadi¹, Amirhossein Mohajerin Ariaei¹, Mohammad-Reza Chitgarha¹, Yinwen Cao¹, Ahmed Almaiman¹, Youichi Akasaka², Jeng-Yuan Yang², Guodong Xie¹, Peicheng Liao¹, Motoyoshi Sekiya², Joseph Touch³, Moshe Tur⁴, Carsten Langrock⁵, Martin M. Fejer⁵, Alan Willner¹; ¹Univ. of Southern California, USA; ²Fujitsu Labs of America, USA; ³Information Sciences Inst., USC, USA; ⁴Tel Aviv Univ., Israel; ⁵Stanford Univ., USA. We experimentally demonstrate a tunable homodyne receiver on multiple-wavelength QPSK and 16-QAM channels at 20/30 Gbaud. A single PPLN waveguide is used to frequency/phase lock the signals with their tones. Open eye diagrams with BER measurements are shown.

Executive Ballroom
210A

Executive Ballroom
210B

Executive Ballroom
210C

Executive Ballroom
210D

CLEO: QELS-Fundamental Science

FTh1A • Quantum Entanglement III—Continued

FTh1A.7 • 09:30

High Resolution Bi-Photon Spectral Correlation Measurements from a Silicon Nanowire in the Quantum and Classical Regimes, Iman Jizan¹, Luke G. Helt², Chunle Xiong¹, Matthew J. Collins¹, Duk-Yong Choi³, Chang Joon Chae⁴, Marco Liscidini⁵, Michael J. Steel², Benjamin J. Eggleton¹, Alex Clark¹; ¹Centre for Ultrahigh bandwidth Devices for Optical Systems, School of Physics, The Univ. of Sydney, Australia; ²CUDOS and MQ Photonics Research Centre, Dept. of Physics and Astronomy, Macquarie Univ., Australia; ³Laser Physics Centre, Research School of Physics & Engineering, Australian National Univ., Australia; ⁴NICTA Victoria Laboratory, Melbourne School of Engineering, The Univ. of Melbourne, Australia; ⁵Dipartimento di Fisica, Università degli Studi di Pavia, Italy. We use classical stimulated four-wave mixing to directly characterize quantum spectral correlations generated in a silicon nanowire for two different pump durations. Signal to noise is increased and acquisition time reduced compared to coincidence detection.

FTh1A.8 • 09:45

Temporal Position Modulation of Biphoton Correlations through Pump Frequency Tuning, Ogaga D. Odele¹, Joseph M. Lukens¹, Jose A. Jaramillo-Villegas¹, Carsten Langrock², Martin M. Fejer², Daniel E. Leaird¹, Andrew M. Weiner¹; ¹Purdue Univ., USA; ²Stanford Univ., USA. We describe and demonstrate a novel approach for controlling the temporal position of the biphoton correlation by pump frequency tuning. Our method relies on precise waveguide engineering as well as the nonlocal dispersion cancellation effect.

FTh1B • Quantum Control and Precision Measurements—Continued

FTh1C • High-field FTh1C • High-field and XFEL Physics—Continued

FTh1C.6 • 09:30

Investigation of the Newly Proposed Carrier-Envelope-Phase Stable Attosecond Pulse Source, Zoltan Tibai¹, György Tóth², Zsuzsanna Nagy-Csiha¹, József Fülöp², Gábor Almási^{1,2}, János Hebling^{1,2}; ¹Univ. of Pécs, Hungary; ²MTA-PTE High Field Terahertz Research Group, Hungary. The carrier-envelope-phase and energy stability of formerly proposed accelerator-based attosecond source is investigated numerically. Carrier-envelope-phase stable pulses with tens of nJ energy and 80 as duration are predicted with 31 mrad phase stability.

FTh1C.7 • 09:45

Intense broadband THz pulse generation from relativistic laser-plasma interaction, Sudipta Mondal¹; ¹INRS-Energie Matériaux Télécommunication, Canada. We demonstrate intense broadband terahertz pulse generation from the interaction of high intensity femtosecond laser with solid density plasmas. We measure substantial enhancement of terahertz pulse energy (32 mJ/pulse) by using aligned copper nanorod targets.

FTh1D • Nonlinear Resonators and Optical Frequency Combs—Continued

FTh1D.6 • 09:30

Synchronization of multiple parametric frequency combs, Yanan H. Wen¹, Michael R. Lamont¹, Alexander L. Gaeta¹; ¹Cornell Univ., USA. We theoretically demonstrate passive synchronization of solitons in systems of two- and three-microresonator-based parametric frequency combs resulting in time-locked pulses and frequency-locked comb lines.

FTh1D.7 • 09:45

A New Route for Fabricating On-Chip Chalcogenide Microcavity Resonators, Ozan Aktas^{1,2}, Ersin Huseyinoglu^{2,3}, Mehmet Bayindir^{1,2}; ¹Bilkent Univ., Turkey; ²UNAM-National Nanotechnology Research Center, Bilkent Univ., Turkey; ³Inst. of Materials Science and Nanotechnology, Bilkent Univ., Turkey. We report a novel versatile method for the high yield production and on-chip integration of self-assembled globally oriented high-Q Whispering Gallery Mode (WGM) chalcogenide microresonators. The results of optical and material characterization of the microresonators are given.

09:30–12:30 Technology Transfer Program, Exhibit Hall Theater

10:00–15:00 Exhibits Open, Exhibit Hall

10:00–14:00 Coffee Break (10:00–10:30) and Unopposed Exhibit Only Time, Exhibit Hall

Join the Exhibitors for Pizza

Thursday, 14 May

12:30–14:00

Exhibit Hall

Executive Ballroom
210E

**CLEO: QELS-
Fundamental Science**

**FTh1E • Electron and
Ultrafast Probing of Plasmonic
Nanostructures—Continued**

FTh1E.6 • 09:30
Withdrawn

FTh1E.7 • 09:45
Coherent Control in Single Plasmonic Nanostructures, Alberto Comin¹, Richard Ciesielski¹, Alexandre Bouhelier², Achim Hartschuh¹; ¹Dept. Chemie, Ludwig-Maximilians-Universität, Germany; ²Laboratoire Interdisciplinaire Carnot de Bourgogne, Université de Bourgogne, France. Coherent control in plasmonic nanostructures is a door to space-time confinement of optical excitation and femtosecond super-resolution spectroscopy. Towards this goal, here we demonstrate femtosecond pulse-shaping of single gold nanostructure and local phase compensation.

Executive Ballroom
210F

**STh1F • Mode Division
Multiplexing—Continued**

STh1F.7 • 09:30
Detecting orbital angular momentum of light with an arc slit, Hailong Zhou¹, Jianji Dong¹, Pei Zhang², Yifeng Zhou¹, Xinliang Zhang¹; ¹Wuhan National Lab for Optoelectronics, China; ²MOE Key Lab for Nonequilibrium Synthesis and Modulation of Condensed Matter, Dept. of Applied Physics, Xi'an Jiaotong Univ., China. When the orbital angular momentum (OAM) beam is incident on a 90 degree arc slit, a focus will be generated and have a displacement which is nearly linear with the topological charge of the incoming OAM beam. It can detect the OAM beams with a very simple structure.

STh1F.8 • 09:45
2x2 Broadband Adiabatic 3-dB Couplers on SOI Strip Waveguides for TE and TM modes, Han Yun¹, Zeqin Lu¹, Yun Wang¹, Wei Shi², Lukas Chrostowski¹, Nicolas A. Jaeger¹; ¹Electrical and Computer Engineering, Univ. of British Columbia, Canada; ²Electrical and Computer Engineering, Université Laval, Canada. We demonstrated adiabatic 3-dB couplers on silicon-on-insulator strip waveguides. We obtained average splitting ratios, from 1500 nm to 1600 nm, of 44.5%/55.5% and 50.5%/49.5% for our transverse electric and transverse magnetic couplers, respectively.

Executive Ballroom
210G

CLEO: Science & Innovations

**STh1G • Glass and Rare Earth
Doped Materials—Continued**

STh1G.7 • 09:30
Characterization of Ge₂₈Sb₁₂Se₆₀ Waveguides, Molly R. Krogstad¹, Sungmo Ahn¹, Wounghang Park¹, Juliet Gopinath¹; ¹Univ. of Colorado, USA. Single-mode Ge₂₈Sb₁₂Se₆₀ waveguides, fabricated with thermal evaporation and lift-off, were characterized at 1.03 and 1.53 μm. Measured linear propagation loss agrees with theoretical predictions, and large nonlinear absorption at 1.03 μm has optical limiting applications.

STh1G.8 • 09:45
Solution processed Chalcogenide photonic crystal, Tingyi Gu^{1,2}, Chao Lu³, Tony Heinz¹, Alejandro Rodriguez³, Craig Arnold³; ¹Columbia Univ., USA; ²Hewlett-Packard Lab, USA; ³Princeton Univ., USA. We demonstrate formation of amorphous chalcogenide photonic crystal light emitter by using microtrench filling method in solution processing.

Executive Ballroom
210H

**STh1H • Nonlinear Optics for
Advanced Measurements and
Characterization—Continued**

STh1H.7 • 09:30
High-Resolution Sub-Surface Microscopy of CMOS Integrated Circuits Using Radially Polarized Light, Marius Rutkauskas¹, Carl Farrell¹, Christophe Dorrer², Kenneth Marshall², Ted Lundquist³, Praveen Vedagarbha³, Deryck T. Reid¹; ¹Heriot-Watt Univ., UK; ²Univ. of Rochester, USA; ³DCG Systems Inc., USA. Comparison of high-resolution sub-surface microscopy shows that illumination with linear polarization resolves an edge with resolutions of 95 nm and 120 nm, depending on E-field orientation, while radial polarization achieves a resolution of 98 nm.

STh1H.8 • 09:45
3-D Scanning Mid-IR Imaging of Buried Structures Using Extremely Nondegenerate Two-photon Absorption in a GaN Photodiode, Himansu S. Pattanaik¹, Matthew Reichert¹, David J. Hagan¹, Eric W. Van Stryland¹; ¹Univ. of Central Florida, CREOL, USA. We demonstrate a scanning 3-D IR imaging technique using extremely nondegenerate two-photon absorption in an uncooled GaN photodiode, and obtain ~2 μm depth resolution at a wavelength of ~5 μm in buried semiconductor structures.

09:30–12:30 **Technology Transfer Program, Exhibit Hall Theater**

10:00–15:00 **Exhibits Open, Exhibit Hall**

10:00–14:00 **Coffee Break (10:00–10:30) and Unopposed Exhibit Only Time, Exhibit Hall**

**Technical Digest and Postdeadline Papers
Available Online**

- Visit www.cleoconference.org
- Select Access Digest Paper link
- Use your registration email address and password

Access is provided only to full technical attendees.

Meeting Room
211 B/D

CLEO: Science & Innovations

STh1I • Photodetectors—Continued

STh1I.7 • 09:30

Enhanced Responsivity up to 2.85 A/W of Si-based $\text{Ge}_{0.9}\text{Sn}_{0.1}$ Photoconductors by Integration of Interdigitated Electrodes, Thach Pham¹, Benjamin Conley¹, Joe Margetis², Huong Tran¹, Seyed Amir Ghetmiri¹, Aboozar Mosleh¹, Wei Du¹, Gregory Sun³, Richard Soref³, John Tolle², Hameed Naseem¹, Baohua Li⁴, Shui-Qing Yu¹; ¹Univ. of Arkansas, USA; ²ASM, USA; ³Univ. of Massachusetts Boston, USA; ⁴Arktonics, USA. The $\text{Ge}_{0.9}\text{Sn}_{0.1}$ photoconductor was fabricated with interdigitated structures on Si using a CMOS-compatible process. Temperature-dependent responsivity and specific detectivity were measured. The peak responsivity of 2.85A/W at 77K was achieved due to enhanced photoconductive gain.

STh1I.8 • 09:45

Dual-Drifting-Layer Uni-Traveling Carrier Photodiode for Wide Bandwidth and High Power Performance, li jin¹, Xiong Bing¹, Sun Changzheng¹, Yi Luo¹; ¹Tsinghua Univ., China. Uni-traveling-carrier photodiodes with novel dual-drifting-layer structure is proposed to realize wide bandwidth and high saturation power performance. High-speed operation at high bias voltage is demonstrated by optimizing the electric field profile within the dual-drifting-layer structure.

Meeting Room
212 A/C

CLEO: Applications & Technology

ATh1J • Biomedical Imaging and Sensing II—Continued

ATh1J.7 • 09:30

Three-color two-photon three-axis digital scanned light-sheet microscopy (3C2P3S-DSLM), Weijian Zong^{1,2}, Zuosheng Liu¹, Fuzheng Niu¹, Shaowa Li¹, Jia Zhao¹, Aimin wang¹, Liangyi Chen¹; ¹Peking Univ., China; ²China Dept. of Cognitive Sciences, Inst. of Basic Medical Sciences, China. We demonstrate a new two-photon light-sheet microscopy with three-color excitation, diffraction-limited thickness and tailorable illumination area, capable of multi-color multi-scale live imaging in one setup.

Meeting Room
212 B/D

CLEO: Applications & Technology

ATH1K • Spectroscopy and Metrology—Continued

ATH1K.6 • 09:30

External Cavity Semiconductor Laser Optimized for Frequency Metrology, Wei Liang¹, Vladimir S. Ilchenko¹, Danny Eliyahu¹, Elijah Dale¹, Anatoliy A. Savchenkov¹, David Seidel¹, Andrey B. Matsko¹, Lute Maleki¹; ¹OEwaves Inc, USA. A frequency modulatable 795 nm semiconductor laser is created. The laser is characterized with residual amplitude modulation below -80 dB and frequency noise better than 300 Hz/Hz^{1/2} at offset frequencies ranging from 100 Hz to 10 MHz.

Marriott
Salon I & II

CLEO: Science & Innovations

STh1L • Mode-Locked Fiber Lasers—Continued

STh1L.6 • 09:30

Timing Jitter of Normal-Dispersion Mode-Locked Er- and Yb-Fiber Lasers, Junho Shin¹, Peng Qin², Kwangyun Jung¹, Youjian Song², Ming-lie Hu², Chingyue Wang², Jungwon Kim¹; ¹Korea Advanced Inst of Science & Tech, Korea; ²Tianjin Univ, China. We experimentally identify that narrow bandpass-filtering can significantly reduce the timing jitter in normal-dispersion fiber lasers. Both the split-step method-based jitter simulation and the modified Namiki-Haus analytic model agree well with the measured jitter spectrum.

STh1L.7 • 09:45

Generation of 10 W, 100 fs, 10 GHz pulse train using high power EDFA-MOPA system with cascaded Raman pumping, Akira Fujisaki^{1,2}, Masato Yoshida¹, Toshihiko Hirooka¹, Masataka Nakazawa¹; ¹Tohoku Univ., Japan; ²Furukawa Electric, Japan. We demonstrate a record high output power 10 W, 100 fs 10 GHz pulse train using an all-fiber MOPA system at 1562 nm with a high-power EDFA and 1480 nm cascaded Raman laser pumping.

09:30–12:30 Technology Transfer Program, Exhibit Hall Theater

10:00–15:00 Exhibits Open, Exhibit Hall

10:00–14:00 Coffee Break (10:00–10:30) and Unopposed Exhibit Only Time, Exhibit Hall



For Conference News & Insights
Visit blog.cleoconference.org

CLEO: Science & Innovations

STh1M • Beam Shaping for Optimized Laser-matter Interaction—Continued**STh1M.6 • 09:30**

Ultra-broadband Tunable Polarization Converter for Micro-fluidic-meta-surfaces, Pin Chieh Wu², Libin Yan², Qinghua Song², Weiming Zhu², Zhang Wu², Din Ping Tsai^{1,3}, Federico Capasso⁴, Ai-Qun Liu²; ¹National Taiwan Univ., Taiwan; ²Nanyang Technological Univ., Singapore; ³Academia Sinica, Taiwan; ⁴Harvard Univ., USA. We present a widely tunable polarization converter with ultra-broad working frequency for microfluidic metasurface. By adjusting the configuration of L-shaped antenna, both cross and circular polarization conversion can be achieved under a linear-polarized illumination.

STh1M.7 • 09:45

Unraveling the Effects of Radiation Forces in Water, Nelson G. Astrath^{1,2}, Luis Malacarne¹, Mauro Baesso¹, Gustavo Lukasiewicz¹, Stephen Bialkowski²; ¹Universidade Estadual de Maringá, Brazil; ²Utah State Univ., USA. We measure the surface deformation at the air-water interface induced by laser excitation and match this to rigorous theory of radiation forces. The experimental results are quantitatively described by the numerical calculations of radiation forces.

STh1N • Frequency Conversion of Combs—Continued**STh1N.7 • 09:30**

Mid-Infrared 333-MHz Frequency Comb Continuously Tunable from 1.95 μm to 4.0 μm , Karolis Balskus¹, Zhaowei Zhang¹, Richard A. McCracken¹, Derryck T. Reid¹; ¹Heriot Watt Univ., USA. Idler pulses from a 333-MHz femtosecond optical parametric oscillator were carrier-envelope-offset stabilized using a versatile locking technique which allowed the resulting comb to be tuned continuously over a range from 1.95 μm to 4.0 μm .

STh1N.8 • 09:45

Adaptive Sampling Dual Comb Spectroscopy in Terahertz Region Using Unstabilized Dual Femtosecond Lasers, Ryuichi Ichikawa¹, Yi-Da Hsieh^{1,2}, Kenta Hayashi¹, Kaoru Minoshima^{3,2}, Hajime Inaba^{4,2}, Takeshi Yasui^{1,2}; ¹Tokushima Univ., Japan; ²ERATO Intelligent Optical Synthesizer Project, JST, Japan; ³The Univ. of Electro-Communications, Japan; ⁴National Inst. of Advanced Industrial Science and Technology, Japan. The adaptive sampling clock was extracted by dual THz-comb-referenced spectrum analyzers and used for THz dual comb spectroscopy (THz-DCS) with unstabilized dual lasers. The demonstrated results implied better spectroscopic performance than THz-DCS with stabilized lasers.

STh1O • All Optical Signal Processing—Continued**STh1O.7 • 09:30**

All-Optical Ultrafast Wavelength and Mode Converter Based on Inter-Modal Nonlinear Wave Mixing in Few-Mode Fibers, Yi Weng¹, Xuan He¹, Junyi Wang², Zhongqi Pan¹; ¹Dept. of Electrical & Computer Engineering, Univ. of Louisiana at Lafayette, USA; ²Qualcomm Technologies Inc., USA. An ultrafast all-optical simultaneous wavelength and mode conversion scheme is proposed based on intermodal nonlinear wave mixing, with the capability of switching state of polarization and mode degeneracy orientation in few-mode fibers with high efficiency.

STh1O.8 • 09:45

Record Phase Sensitive Extinction Ratio in a Silicon Germanium Waveguide, Mohamed A. Ettabib¹, Francesca Parmigiani¹, Alexandros Kapsalis², Adonis Bogris², Mickael Brun³, Pierre Labeye³, Sergio Nicoletti³, Kamal Hammani⁴, Dimitris Syvridis², David Richardson¹, P. Petropoulos¹; ¹Univ. of Southampton, UK; ²Dept. of Informatics and Telecommunications, National and Kapodistrian Univ. of Athens, Greece; ³CEA-Leti, France; ⁴Laboratoire Interdisciplinaire Carnot de Bourgogne, France. A binary step-like phase response and phase-sensitive extinction ratio in excess of 28dB under CW pump operation was demonstrated in a 20mm-long low birefringence SiGe waveguide, using a polarization-assisted phase sensitive amplifier scheme.

09:30–12:30 Technology Transfer Program, Exhibit Hall Theater

10:00–15:00 Exhibits Open, Exhibit Hall

10:00–14:00 Coffee Break (10:00–10:30) and Unopposed Exhibit Only Time, Exhibit Hall

11:30–13:00
JTh2A • Poster Session III

JTh2A.1

Generation of Broadband Chaos Signal by Self-injection Monolithic Integrated Mode-beating Amplified Feedback Laser, Biwei Pan¹, Dan Lu¹, Liqiang Yu¹, Limeng Zhang¹, Lingjuan Zhao¹; ¹*Inst. of Semiconductors, Chinese Academy of Sciences, China*. A broadband chaos generation scheme using monolithic integrated mode-beating amplified feedback laser under self-injection is presented. A robust chaotic spectrum that extends over 50 GHz with a flatness of ± 5 dB is experimentally achieved.

JTh2A.2

Lithographic VCSEL Reliability Under Extreme Operating Conditions, Xu Yang¹, Guowei Zhao², Mingxin Li¹, Dennis Deppe^{1,2}; ¹*CREOL, Univ. of Central Florida, USA*; ²*sd-Photonics, LLC, USA*. Data are presented showing lithographic VCSELs has higher reliability than oxide VCSELs in a stress test with a severe condition. The increased reliability is consistent with its lower junction temperature and reduced internal stress.

JTh2A.3

Improved Performance of Tunable Single Mode Laser Array Based on Non Uniformly Spaced Slots, Azat Abdullaev¹, Qiao Y. Lu¹, Wei H. Guo², Michael Wallace¹, Marta Nawrocka¹, James O. Callaghan³, John Donegan¹; ¹*Trinity College Dublin, USA*; ²*School of Electrical and Electronic Engineering, Wuhan Univ., China*; ³*Tyndall National Inst., Ireland*. We present a 12-channel wavelength-tunable single-mode laser array based on non-uniformly spaced slots. A quasi-continuous tuning range of >36 nm is obtained over 35°C (from 10°C–45°C) temperature range with side mode suppression ratio >50 dB.

JTh2A.4

Arrayed Waveguide Grating Based Monolithic Multi-wavelength Mode-locked Semiconductor Laser, Songtao Liu¹, Qing Ke¹, Mengdie Sun¹, Dan Lu¹, Ruikang Zhang¹, Chen Ji¹; ¹*Inst. of Semiconductors, CAS, China*. We report a novel monolithic multi-wavelength mode-locked semiconductor laser design based on arrayed waveguide grating (AWG) for the first time. 19.6 ps pulses at a repetition rate of 2.9 GHz are obtained.

JTh2A.5

Fiber Pump-Delivery System for Spectral Narrowing and Wavelength Stabilization of Broad-Area Lasers, Jordan P. Leidner¹, John R. Marcianti¹; ¹*The Inst. of Optics, USA*. Off-axis far-field coupling of a broad-area laser to a single-mode fiber containing a fiber Bragg grating is used for spatio-spectral filtering. This results in a $\sim 10\times$ narrower spectral width and potential spatial brightness improvements.

JTh2A.6

Withdrawn

JTh2A.7

High performance 2150nm InAs/InGaAs/InP quantum well lasers grown by metal-organic vapor phase epitaxy, Luo Shuai¹, Ji Haiming¹, Feng Gao¹, Xiaoguang Yang¹, Tao Yang¹; ¹*Key Lab of Semiconductor Materials Science, Inst. of Semiconductors, CAS, China*. We demonstrate high performance 2150 nm InAs/InGaAs/InP quantum well (QW) lasers grown by metalorganic vapor phase epitaxy (MOVPE).

JTh2A.8

GaSb-based Mid Infrared Photonic Crystal Surface Emitting Laser, Chien Hung Pan¹, Chien Hung Lin², Tien Yuan Chang³, Tien-Chang Lu³, Chien Ping Lee²; ¹*CNST, National Chiao Tung Univ., Taiwan*; ²*Dept. of Electronics Engineering, National Chiao Tung Univ., Taiwan*; ³*Dept. of Photonics, National Chiao Tung Univ., Taiwan*. We demonstrate an optically pumped GaSb-based mid-Infrared photonic crystal surface emitting laser (PCSEL) at 2.3 μ m with line width of 0.3nm. The PCSEL was operated with temperature up to 350K, showing a shift rate of 0.21 nm/K.

JTh2A.9

Modulation-Frequency Dependence of the Phase-Amplitude Coupling in Quantum Dot Lasers, Cheng Wang^{1,2}, Marek A. Osinski^{1,3}, Kevin Schires¹, Jacky Even², Frederic Grillot¹; ¹*Telecom-Paristech, France*; ²*Institut National des Sciences Appliquées, France*; ³*The Univ. of New-Mexico, USA*. The phase-amplitude coupling of quantum dot lasers is studied by taking into account carrier dynamics and the contribution of off-resonant states to the refractive index change. Calculations reveal a strong dependence on the modulation frequency.

JTh2A.10

Volume Holographic Grating Stabilized 780 nm Ridge Waveguide Laser With an Output Power of 380 mW, Simon Rauch¹, Joachim Sacher¹; ¹*Sacher Lasertechnik GmbH, Germany*. A ridge waveguide laser stabilized by a compact holographic grating-cavity with an output power of 380 mW, a linewidth of 18 kHz and a nearly diffraction-limited beam for saturation spectroscopy of rubidium is presented.

JTh2A.11

Broadband quantum cascade laser at wavelength $\lambda \sim 10$ mm based on continuum-to-continuum design, Bo Meng¹, Yuan Quan Zeng¹, Etienne Rodriguez¹, Qijie Wang¹; ¹*Nanyang Technological Univ., Singapore*. Broadband mid-infrared quantum cascade lasers (QCLs) at ~ 10 mm based on the continuum-to-continuum design are presented. The prototypes show broadband lasing spectra (978 cm^{-1} –1055 cm^{-1}), 580 mW peak powers and 0.5 W/A slope efficiencies.

JTh2A.12

Timing Jitter Reduction of a Passively Mode-Locked External-Cavity Semiconductor Laser Via Repetition Rate Transitions and Optical Feedback, Simon Rauch^{2,1}, Lukas Drzewietzki², Andreas Klehr³, Joachim Sacher¹, Wolfgang Elsässer², Stefan Breuer²; ¹*Sacher Lasertechnik GmbH, Germany*; ²*Inst. of Applied Physics, Technische Universität Darmstadt, Germany*; ³*Ferdinand-Braun-Institut, Leibniz-Institut für Höchstfrequenztechnik, Germany*. We investigate experimentally the influence of harmonic mode-locking and optical feedback on the timing-jitter of a passively mode-locked external-cavity diode laser yielding a jitter reduction of up to a factor of 10 and we compare the results with numerical simulations.

JTh2A.13

A Modulated Segmented Contact Method for the Measurement of Internal Optical Mode Loss, Peter Rees¹, Robert Pascoe¹, Peter M. Smowton¹, Peter Blood¹; ¹*Cardiff Univ., UK*. An order of magnitude improvement in the precision of measurements of internal optical mode losses to better than 0.1 cm^{-1} is demonstrated using a modulated segmented contact method.

JTh2A.14

The Effect on Dot Gain Behaviour of Confining Layer Composition in InP/(Al)GaInP Quantum Dot Lasers, Martyn Smith¹, Stella Elliott¹, Makarimi Kasim¹, Peter M. Smowton¹, Andrey Krysa²; ¹*Cardiff Univ., UK*; ²*Sheffield Univ., UK*. Reductions in non-radiative recombination and α , with increasing Ga composition of the upper-confining-layer in InP self-assembled quantum-dot lasers reduce threshold-current-density and temperature dependence. Carrier population of 2-D layers limits further improvement at higher Ga compositions.

JTh2A.15

External Cavity Quantum Cascade Laser Based on Fabry-Perot Reflector, Deivis Vaitiekus¹, Michael Hemingway¹, Andrey Krysa¹, John Cockburn¹, Dmitry G. Revin¹; ¹*The Univ. of Sheffield, UK*. External cavity quantum cascade laser based on Fabry-Pérot etalon design is demonstrated for the first time. Fabry-Pérot reflector was adjusted to produce single mode emission across the whole gain region.

JTh2A.16

Femtosecond Laser Repairing of the effects in Glass Materials Induced by Ion Implantation, Qiang Cao¹, Jiajun Zhang¹; ¹*Beijing Inst. of Technology, China*. Metal ion implantation in glass causes lots of defects in lattice during its fabricating process. We found that the femtosecond laser irradiation have a great efficiency to repair these defects with high spatial selectivity.

JTh2A.17

Frequency Degenerate Two Beam Coupling in Organic Media Using a Single Nanosecond Pump, Jonathan Slagle^{2,1}, Joseph Haus³, Shekhar Guha², Daniel McLean^{2,1}, Douglas Krein^{2,4}; ¹*Leidos, Inc., USA*; ²*Materials and Manufacturing Directorate, Air Force Research Lab, USA*; ³*Electro-Optics Program, Univ. of Dayton, USA*; ⁴*General Dynamic Information Technology, USA*. We present degenerate two-beam coupling in organic dye solutions using a single nanosecond beam where the probe originates from a Fresnel reflection and the phase and frequency shifts are the result of transient self-phase modulation.

JTh2A.18

Stabilization of Premixed High Flow Speed Methane/air Flames Using a Nanosecond Laser Induced Plasma, Xiaohui Li^{1,2}, Xin Yu^{1,2}, Yang Yu^{1,2}, Rongwei Fan^{1,2}, Deying Chen^{1,2}, Rui Sun³; ¹*National Key Lab of Science and Technology on Tunable Laser, Harbin Inst. of Technology, China*; ²*Inst. of Opto-electronics, Harbin Inst. of Technology, China*; ³*Inst. of Combustion Engineering, Harbin Inst. of Technology, China*. Stabilization of premixed methane/air flames with a flow speed up to 20 m/s was realized using a 50 Hz nanosecond Nd:YAG laser induced plasma. The stability of the flames in terms of blow off limit and the temporal evolution of the flame kernel generated by the laser plasmas were investigated.

JTh2A.19

Photon-stimulated desorption surface spectroscopy by VUV emissions from a laser-produced plasma, Masanori Kaku¹, Daichi Kai¹, Masahito Katto¹, Atsushi Yokotani¹, Wataru Sasaki², Shoichi Kubodera¹; ¹*Univ. of Miyazaki, Japan*; ²*NTP inc., Japan*. We have developed photon-stimulated desorption surface spectroscopy system using broadband VUV emissions from a laser-produced plasma. Observed desorbed atoms or molecules from material surfaces depended on bond energy or molecular structure.

JTh2A.20

Optical Scattering of Airy Beam and Gaussian Beam Through Turbid Medium, Romanus Hutchins¹, Miao Zhang¹, Lixin Ma¹, Ping Yu¹; ¹*Univ. of Missouri-Columbia, USA*. We compared optical scattering of Airy and Gaussian beams, generated simultaneously using a LCD panel, through a turbid medium. The Airy beam had a smaller speckle size due to its self-healing property.

JTh2A.21

Generalizing and extending Kubelka-Munk theory, Chris Sandoval¹, Arnold D. Kim¹; ¹*Applied Mathematics, Univ. of California, Merced, USA*. Kubelka-Munk theory is an intuitive theory that approximates the flow of power through a plane parallel slab of a scattering medium. We derive it from the radiative transport equation, accounting for general boundary sources and non-homogeneous terms, and then generalize it to three dimensions.

JTh2A.22

Fano Resonance Structural Color in Patterned Dielectric Surfaces, Emma Regan¹, Yichen Shen², Marin Soljacic²; ¹Physics, Wellesley College, USA; ²Physics, MIT, USA. Fano resonance is used to generate structural color in microscopically structured dielectric materials that can be tuned through the visible spectrum.

JTh2A.23

Sm³⁺ Ions Doped Phosphate Glasses for Multiband Visible Laser Applications, Nitin Jha¹, K Linganna², C K Jayasankar², Ajoy Kar¹; ¹Heriot-Watt University, UK; ²Physics, Sri Venkateswara Univ., India. Sm³⁺ ions doped phosphate glasses have been fabricated. Their absorption and emission properties have been studied. Significant amplification in emission with side pumping is being reported indicating its potential application for visible lasers.

JTh2A.24

GaN-based Ridge Waveguides with Very Smooth and Vertical Sidewalls by ICP Dry Etching and Chemical Etching, Wanyong Li¹, Yi Luo¹, Bing Xiong¹, Sun Changzheng¹, Wang Lai¹, Jian Wang¹, Han Yanjun¹, Ji-anchang Yan², Tongbo Wei², Hongxi Lu²; ¹Tsinghua Univ., China; ²Chinese Academy of Sciences, China. GaN-based ridge waveguides with very smooth and vertical sidewalls are fabricated with combined inductively coupled plasma (ICP) etching and chemical etching. Reduction in scattering loss is estimated to be 2 dB/mm at 1.55 μm.

JTh2A.25

Inband-Pumped Ho:KLu(WO₃)₂ Microchip Laser Q-switched with a PbS-Quantum-Dot-Doped Glass, Xavier Mateos¹, Pavel Loiko^{2,1}, Josep Maria Serres¹, Konstantin Yumashev², Alexander Malyarevich², Alexei Onushchenko³, Valentin Petrov⁴, Uwe Griebner⁴, Magdalena Aguilo¹, Francesc Diaz¹; ¹Universitat Rovira i Virgili, Spain; ²Center for Optical Materials and Technologies, Belarusian National Technical Univ., Belarus; ³Vavilov State Optical Inst., Russia; ⁴Max Born Inst., Germany. Maximum average output power of 84 mW, slope efficiency of 42%, and pulse duration of 55 ns are achieved at 2.06 μm with a passively Q-switched Ho:KLu(WO₃)₂ microchip laser inband-pumped by a Tm:KLu(WO₃)₂ microchip laser.

JTh2A.26

A new type of Yb³⁺ doped fiber with an octagonal-shaped core, Wang Yibo¹, Nan zhao¹, Lei Liao¹, Nengli Dai¹, Jinggang Peng¹, Haiqing Li¹, Jinyan Li¹; ¹Wuhan National Lab of Electroptics, China. A new type of Yb³⁺ doped fiber with an octagonal-shaped core is fabricated. This fiber has the potential to be applied into the laser system to optimize the beam quality when this type of fiber core is introduced into the CCC fiber, an easier coupling of the HOM to the side cores can be observed.

JTh2A.27

Structural optimization for modulation efficiency enhancement in a top-gated graphene optical modulator, Kaori Warabi¹, Rai Kou^{2,3}, Hidetaka Nishizaki^{2,3}, Shinichi Tanabe³, Yuzuki Kobayashi¹, Tsuyoshi Yamamoto³, Koji Yamada^{2,3}, Hirochika Nakajima¹; ¹Waseda Univ., USA; ²NTT Nanophotonics Center, Japan; ³NTT Device Technology Labs., Japan. We investigated a top-gated graphene optical modulator on a CMOS compatible silicon photonic platform. The structural optimization results revealed that the modulation efficiency is able to reach to 0.05 dB/μm with very low insertion loss.

JTh2A.28

Growth and Electroluminescent Property of Multi-Facet InGaN/GaN Multiple Quantum Well Light Emitting Device, Yun-Jing Li², Shih-Pang Chang³, Yuh-Jen Cheng¹, Hao-Chung Kuo³, Chun-Yen Chang²; ¹Academia Sinica, Taiwan; ²Dept. of Electronics Engineering and Inst. of Electronics, National Chiao Tung Univ., Taiwan; ³Dept. of Photonics and Inst. of Electro-Optical Engineering, National Chiao Tung Univ., Taiwan. We report the study of InGaN/GaN multiple quantum wells (MQWs) grown on multi-facet micro-rods. The multi-facet MQWs have broad emission spectrum. Electrical injection was demonstrated with emission color ranged from red to blue.

JTh2A.29

Silicate Spin-on-Glass as an Overcoat Layer for SiO₂ Ridge Waveguides, Matthew Stott¹, Thomas Wall¹, Damla Ozcelik², Josh Parks², Gopikrishnan G. Meena², Erik Hamilton¹, Roger Chu¹, Holger Schmidt², Aaron Hawkins¹; ¹Electrical and Computer Engineering, Brigham Young Univ., USA; ²Univ. of California, Santa Cruz, USA. Silicate spin-on-glass is used to coat PECVD SiO₂ waveguides in order to smooth out surface topology and act as a moisture barrier. The measured optical throughput improved compared to uncoated waveguides.

JTh2A.30

Fabrication and Characterization of Fiber Waveguides from Single-Crystal Er³⁺-Doped YAG, Elizabeth F. Dreyer¹, Logan Stagg¹, Stephen Trembath-Reichert², Christopher Hoefl², Craig D. Nie³, James A. Harrington³, Stephen C. Rand^{1,2}; ¹Electrical Engineering and Computer Science, Univ. of Michigan, USA; ²Physics, Univ. of Michigan, USA; ³Material Science, Rutgers Univ., USA. Rod-in-tube preforms and laser heated pedestal growth were used successfully to fabricate graded-index Erbium doped YAG fibers suitable for low-loss waveguides in laser gain or power delivery applications.

JTh2A.31

Strain Relaxation in InGaN/GaN Multiple-Quantum Wells by Nano-Patterned Sapphire Substrates with Smaller Period, Po-Hsun Chen^{4,1}, Vin-Cent Su⁴, Ming-Lun Lee⁴, Yao-Hong You^{4,1}, Yen-Pu Chen⁴, Zheng-Hung Hung⁵, Ta-Cheng Hsu², Yu-Yao Lin², Ray-Ming Lin³, Chieh-Hsiung Kuan⁴; ¹Kingwave Corporation, Taiwan; ²Epistar Corporation, Taiwan; ³Graduate Inst. of Electronic Engineering and Green Technology Research Center, Chang Gung Univ., Taiwan; ⁴Graduate Inst. of Electronics Engineering, Dept. of Electrical Engineering, National Taiwan Univ., Taiwan; ⁵Graduate Inst. of Photonics and Optoelectronics, Dept. of Electrical Engineering, National Taiwan Univ., Taiwan. The growth of InGaN-based light-emitting diodes (LEDs) on dry-etched patterned sapphire substrates (DPSs) with nano-sized periods can relax the residual compressive strain in InGaN/GaN multiple-quantum wells (MQWs), given that the stronger the light emitted.

JTh2A.32

Extraordinary Optical Properties of Atomic-Layer Doped Transparent Conductive Oxide Superlattice, Do-Joong Lee¹, Jiyeon Kim², Gustavo E. Fernandes¹, Jin Ho Kim¹, Carlos Bledt¹, Ki-Bum Kim², Jimmy Xu¹; ¹Brown Univ., USA; ²Seoul National Univ., Korea. Atomic-layer doped transparent conductive oxide superlattices are prepared by ALD. Extraordinary optical properties, such as enhanced optical transparency, bandgap widening, and improved crystallinity with atomic-layers doping, that counter expectations based on conventional models, are observed.

JTh2A.33

Numerical Study of a 10 GHz Optical Flip-Flop Based on a Short Asymmetric DFB Laser, Amin Abbasi¹, Gunther Roelkens¹, Geert Morthier¹; ¹Dept. of Information Technology, Univ. of Ghent-IMEC, Belgium. We report on a numerical optimization of an all-optical flip-flop based on an asymmetric DFB laser. For the optimized design the repetition rate can increase up to 10 GHz and the switching time can reduce to 5 ps.

JTh2A.34

Dispersion Engineering Employing Curved Space Mapping and Chromo-Modal Excitation, Haeri Park¹, Mohammad Asghari¹, Bahram Jalali¹; ¹UCLA, USA. We report a new optical design capable of providing large group delay dispersion with tunable nonlinear dispersion profile.

JTh2A.35

Integrated Photonic Reservoir Computing based on Hierarchical Time-multiplexing Structure, Hong Zhang¹, Xue Feng¹, Boxun Li¹, Yu Wang¹, Kaiyu Cui¹, Fang Liu¹, Weibei Dou¹, Yidong Huang¹; ¹Tsinghua Univ., China. An integrated photonic reservoir computing based on hierarchical time-multiplexing structure is proposed by numerical simulations. Error rates of 2.2~6.5% for chaotic time series prediction are achieved with the sample rate of 1.3~0.4Gbps and bandwidth of 40~10GHz.

JTh2A.36

Stable, Tuneable, All-optical Pulse Generation with 1 Hz Phase Noise, Amr S. Helmy¹, Fangxin Li¹; ¹Univ. of Toronto, Canada. Feedback-free, RF-free, long-term stable, all optical, short pulse generation utilizing gain-induced FWM is demonstrated. The approach utilizes passive mode-locked (10 MHz) laser for injection locking to provide pulses with a phase noise of 1 Hz.

JTh2A.37

Metamaterial Electric-LC Resonators on Electro-Optic Modulator for Wireless THz-Lightwave Signal Conversion, Yusuf Nur Wijayanto¹, Atsushi Kanno¹, Tetsuya Kawanishi¹; ¹NICT, Japan. Metamaterial electric-LC resonators on an electro-optic modulators are proposed for wireless THz-lightwave signal conversion. Strong electric field can be induced on the resonators by wireless THz irradiation and converted to lightwave signals through electro-optic modulation.

JTh2A.38

Robust Large-Port-Count Hybrid Switches with Relaxed Control Tolerances, Qixiang Cheng¹, Adrian Wonfor¹, Richard V. Pentyl¹, Ian H. White¹; ¹Univ. of Cambridge, UK. The control tolerances of large-port-count optical switches with up to 128×128 ports using the MZI-SOA hybrid design are investigated. The first quantitative analysis is presented showing tolerant control requirements of the hybrid switch design.

JTh2A.39

A Multi-frequency Optoelectronic Oscillator based on a Single Phase-Modulator, Pei Zhou¹, Fangzheng Zhang¹, Shilong Pan¹; ¹Nanjing Univ Aeronautics & Astronautics, China. A multi-frequency optoelectronic oscillator is proposed based on a single phase modulator. Simultaneous generation of 10 and 40 GHz signals is demonstrated and the phase noise is -100.62 dBc/Hz and -84.64 dBc/Hz@10kHz offset, respectively.

JTh2A.40

Pure Single-Sideband Modulation Using High Extinction-Ratio Parallel Mach-Zehnder Modulator with Third-Order Harmonics Superposition Technique, Yuya Yamaguchi¹, Atsushi Kanno², Tetsuya Kawanishi², Masayuki Izutsu^{1,3}, Hirochika Nakajima¹; ¹Waseda Univ., Japan; ²National Inst. of Information and Communications Technology, Japan; ³Japan Society for the Promotion of Science, San Francisco, USA. We demonstrate high spurious suppression ratio single-sideband modulation by a high extinction-ratio parallel Mach-Zehnder modulator. An electrical third-order nonlinearity suppression technique can enhance the suppression ratio as high as 47 dB.

JTh2A.41

High-Speed Data Transmission Through Silicon Contra-Directional Grating Coupler Optical Add-Drop Multiplexers, Michael Caverley¹, Robert Boeck¹, Lukas Chrostowski¹, Nicolas A. Jaeger¹; ¹Univ. of British Columbia, Canada. We demonstrate 12.5 Gbit/s data transmission through a silicon contra-directional grating coupler optical add-drop multiplexer while signals are being simultaneously added and dropped at the same wavelength.

11:30–13:00 JTh2A • Poster Session III

JTh2A.42

Suppressed XMD in Multi-carrier, RF-amplified RF Photonic Link by Cascaded MZMs, Xiaodong Liang¹, Feifei Yin¹, Yitang Dai¹, Jianqiang Li¹, Kun Xu¹; ¹Beijing Univ. of Posts and Telecoms, China. We experimentally demonstrate the elimination of cross-modulation distortion (XMD) in multicarrier, intensity-modulation direct-detection (IMDD) analog photonic links by cascaded Mach-Zehnder modulators (MZMs). XMD, from both the MZMs and electrical amplifiers, is suppressed by 33 dB.

JTh2A.43

Optical Leaky Wave Antenna Experiment Demonstration and Electronic Modulation Investigation, Qiancheng Zhao¹, Yuewang Huang¹, Caner Guclu¹, Filippo Capolino¹, Ozdal Boyraz¹; ¹Univ. of California, Irvine, USA. Fabrication and characterization of optical leaky wave antennas with dielectric waveguides and semiconductor perturbations is presented. Directive radiation at 1550nm is measured. Detailed study on electrical modulation capability with bandwidth exceeding 75GHz is presented.

JTh2A.44

A Time-to-frequency Converter Utilizing a Modified Time Lens, Dong Wang¹, Li Huo¹, Yanfei Xing¹, Caiyun Lou¹; ¹Tsinghua Univ., USA. A time-to-frequency converter based on a modified time lens is proposed and demonstrated experimentally. Return-to-zero pulse with a duty cycle of 33 % and 67 % are both accurately mapped into the spectral domain.

JTh2A.45

Wide-spectrum-range Power-efficient Compact Thermo-optic Switch Based on Coupled Photonic Crystal Microcavities, Xingyu Zhang¹, Swapnajat Chakravarty², Chijui Chung¹, Zeyu Pan¹, Ray T. Chen^{1,2}; ¹Univ. of Texas at Austin, USA; ²Omega Optics, Inc., USA. We demonstrate a thermo-optic switch comprising a 3.78 μ m-long coupled photonic crystal resonators coupled to a photonic crystal waveguide. The device has 6nm optical bandwidth, 20dB optical extinction ratio, 18.2mW switching power, and 14.8 μ sec rise time.

JTh2A.46

Permanent Trimming of Silicon Ring Resonator Filters by Thermal Modification, Steven Spector¹, Jeffrey M. Knecht¹, Paul W. Juodawlkis¹; ¹Massachusetts Inst of Tech Lincoln Lab, USA. Reported here is a method for trimming the resonant frequency of microring resonators by permanent thermal modification of a waveguide cladding. This method would use in-situ heaters, avoiding the need for highly specialized equipment.

JTh2A.47

High-speed Directly Modulated Laterally-coupled Twin Stripe Lasers for Optical Interconnects, Hiroki Taniguchi¹, Hamed Dalir¹, Fumio Koyama¹; ¹Tokyo Inst. of Technology, Japan. We present the modeling of a laterally coupled twin-stripe laser for boosting the modulation bandwidth far beyond relaxation frequencies. The 3dB-modulation bandwidth is increased to be doubled thanks to optical feedback in laterally coupled cavities.

JTh2A.48

Photonically-Enabled Microwave Function Generation Via Tailored Distortion, Amit Bhatia¹, Hong-Fu Ting¹, Mark A. Foster¹; ¹Johns Hopkins Univ., USA. We demonstrate a microwave function generator based on precisely engineering the distortion in a microwave photonic link. By distorting a 5-GHz sinusoid we are able to generate a 5-GHz triangle wave and square pulse train.

JTh2A.49

Fiber Nonlinearity Tolerance of Traceback Equalization for Non-Uniformly Distorted QAM Signals, Takahide Sakamoto¹, Guo-Wei Lu¹, Tetsuya Kawanishi¹; ¹NICT, Japan. We investigate fiber nonlinearity tolerance of traceback equalization (TBE) for mitigating non-uniform distortion caused by unbalance of modulation electrodes in QAM transmitters. TBE outperforms conventional FIR-based adaptive equalizers in an adequately linear transmission regime.

JTh2A.50

Real-time heterodyne-based measurements of fiber laser spectral dynamics, Srikanth Sugavanam¹, Simon Fabbri¹, Thai L. Son¹, Ivan Lobach², Sergey I. Kablukov², Serge Khorev³, Dmitry V. Churkin^{1,4}; ¹Aston Inst. of Photonic Technologies, UK; ²Inst. of Automation and Electrometry, Russia; ³Zecotek Photonics, Canada; ⁴Novosibirsk State Univ., Russia. We present a method to measure in real-time the instantaneous generation spectrum of fiber lasers over consecutive cavity round-trips.

JTh2A.51

Analytical Step-Size Selection Rule for Simulation of Signal Propagation in Vector Optical Fiber Channel, Qun Zhang¹, Liudong Xing³, Hyekyung Min¹, M.I. Hayee²; ¹Minnesota State Univ. Mankato, USA; ²Univ. of Minnesota Duluth, USA; ³Univ. of Massachusetts Dartmouth, USA. An analytical step-size selection rule is proposed for the simulation of polarization multiplexed signal propagation through the single mode optical fiber. The method leads to approximately constant one step simulation error and high computational efficiency.

JTh2A.52

Novel Unipolar Sign Encoded OFDM for Next Generation PONs, Mohammed Mohammed¹, Ziad A. El-Sahn¹; ¹Photonics Group, Electrical Engineering Dept., Alexandria Univ., Egypt. We propose a novel unipolar encoding technique for orthogonal frequency-division multiplexing (OFDM) that increases the bandwidth efficiency by 33% and reduces computational complexity by 50% compared to conventional intensity modulation/direct detection (IM/DD) OFDM systems.

JTh2A.53

Evaluation of Nonlinear Interference in Few-Mode Fiber Using the Gaussian Noise Model, Abdulaziz E. El-Fiqi², Abdallah Ismail², Ziad A. El-Sahn³, Hossam M. Shalaby^{2,3}, Rameash K. Pokharel¹; ¹E-JUST Center, Kyushu Univ., Japan; ²Elect. and Comm. Dept., Egypt-Japan Univ. of Science and Technology (E-JUST), Egypt; ³Photonics Group, Electrical Engineering Dept., Alexandria Univ., Egypt. The nonlinear propagation in few-mode fibers (FMFs) is modeled using a Gaussian approach, where a closed-form formula for the nonlinear interference is derived. The impacts of different nonlinearity penalties are investigated using this model.

JTh2A.54

Fiber-Optic Distribution of Arbitrary Radio-Frequency Waveforms with Stabilized Group Delay, Assaf Ben Amram¹, Yonatan Stern¹, Avi Zadok¹; ¹Bar-Ilan Univ., Israel. Arbitrary RF waveforms are distributed over long fiber with stable group delay, using chromatic dispersion. Input and control waveforms modulate separate tunable lasers. Tracking of the control wave phase is used to adjust both wavelengths.

JTh2A.55

Symbol Rate Identification Using Asynchronous Delayed Sampling, Jin Shang^{1,2}, Sheng Cui^{1,2}, Changjian Ke^{1,2}, Zijie Xia^{1,2}, Songnian Fu^{1,2}, Deming Liu^{1,2}; ¹School of OEI, Huazhong Uni. of Sci.&Technology, China; ²NGIA, China. A symbol rate identification method is proposed for optical signals with commonly used modulation formats. Numerical simulation and experimental results show it is accurate and robust to different link impairments.

JTh2A.56

Frequency Transfer and Time Synchronization Via Urban Fiber, Nan Cheng¹, Wei Chen¹, Qin Liu², Dan Xu¹, Fei Yang¹, Youzhen Gui², Haiwen Cai¹; ¹Shanghai Key Lab of All Solid-State Laser and Applied Techniques, Shanghai Inst. of Optics and Fine Mechanics, Chinese Academy of Sciences, China; ²Key Lab for Quantum Optics, CAS, Shanghai Inst. of Optics and Fine Mechanics, Chinese Academy of Sciences, China. The frequency transfer and time synchronization system over 110km urban fiber link is described. The precise frequency transfer and accurate time synchronization are verified experimentally and demonstrated in the paper.

JTh2A.57

Tunable, narrow line-width silicon microring laser source for coherent optical communications, Ying Qiu¹; ¹WRI, China. We demonstrate a tunable laser source based on a silicon microring. 1.1 kHz line-width, >8 mW output power and wide tuning range are achieved. 4-QAM and 16-QAM coherent transmissions using this laser are also demonstrated.

JTh2A.58

Frequency Chirp Reducing of a Colorless Laser Diode for 40-Gbit/s 256-QAM OFDM Transmission, Cheng-Ting Tsai¹, Yu-Chieh Chi¹, Gong-Ru Lin¹; ¹National Taiwan Univ., Taiwan. A wavelength controlled and frequency chirp reduced colorless laser diode is directly modulated by 256-QAM-OFDM data to achieve a high spectral efficiency of 8 bit/sec/Hz at 40 Gbit/s with an optimized BER of 3.7 \times 10⁻³.

JTh2A.59

LDPC-Coded 16-Dimensional Modulation Based on the Nordstrom-Robinson Nonlinear Block Code, Toshiaki Koike-Akino¹, David S. Millar¹, Keisuke Kojima¹, Kieran Parsons¹, Kenya Sugihara², Yoshikuni Miyata², Tsuyoshi Yoshida²; ¹Mitsubishi Electric Research Labs, USA; ²Information Technology R&D Center, Mitsubishi Electric Corporation, Japan. We propose a new high-dimensional modulation (HDM) format, based on the Nordstrom-Robinson code, which is the best-known nonlinear block code in 16 dimensions. With EXIT chart, we optimize LDPC codes for various HDM formats, and show their benefits.

JTh2A.60

Routing Algorithm to Optimize Loss and IPDR for Rearrangeably Non-Blocking Integrated Optical Switches, Minsheng Ding¹, Qixiang Cheng¹, Adrian Wonfor¹, Richard V. Pentyl¹, Ian H. White¹; ¹Dept. of Engineering, Univ. of Cambridge, UK. A practical path-selection algorithm is proposed to optimize the worst-case path loss and IPDR for large-scale integrated switches. The modeling of an 8 \times 8 Clos-tree switch shows an improvement of up to 2.7dB/1.9dB in loss/IPDR.

JTh2A.61

SNR Equalized Optical Direct-Detected OFDM Transmission with CAZAC Equalization, Zhenhua Feng¹, Ming Tang¹, Rui Lin^{1,2}, Ruoxu Wang¹, Qiong Wu¹, Liangjun Zhang¹, Liang Xu¹, Xiaolong Wang¹, Cong Zhou¹, Jiadi Wu¹, Shiwei Zhou¹, Lei Deng¹, Songnian Fu¹, Deming Liu¹, Ping Shum³; ¹Huazhong Univ. of Science & Technology, China; ²School of Information and Communication Technology, The Royal Inst. of Technology (KTH), Sweden; ³Nanyang Technological Univ., Singapore. 50Km SSMF optical direct-detected OFDM transmission with Constant Amplitude Zero Auto Correlation Sequence (CAZAC) equalization is experimentally demonstrated with over 15dB power budget. 2.5dB enhancement in sensitivity has been achieved simultaneously with 3dB PAPR suppression.

JTh2A.62

Performance Metrics for a Free-space Communication Link Based on Multiplexing of Multiple Orbital Angular Momentum Beams with Higher Order Radial Index, Guodong Xie¹, Long Li¹, Yan Yan¹, Yongxiong Ren¹, Zhe Zhao¹, peicheng liao¹, Nisar Ahmed¹, Zhe Wang¹, Nima Ashrafi^{2,3}, Solyman Ashrafi², moshe tur⁴, alan willner¹; ¹U. of Southern California, USA; ²NxGen Partners, USA; ³Univ. of Texas at Dallas, USA; ⁴Tel Aviv Univ., USA. We analyze and measure the performance metrics for a free-space communication link using OAM beams with non-zero radial index p . The received power of OAM beams with $p=1$ is ~ 6 dB higher than $p=0$.

JTh2A.63

Experimental Demonstration of Using Multi-Layer-Overlay Technique for Increasing Spectral Efficiency to 1.18 bits/s/Hz in a 3 Gbit/s Signal over 4-km Multimode Fiber, Guodong Xie¹, Changjing Bao¹, Yongxiong Ren¹, Yan Yan¹, ahmed almainan¹, Long Li¹, peicheng liao¹, Zhe Zhao¹, Nisar Ahmed¹, Zhe Wang¹, yinwen cao¹, Hao Huang¹, Nima Ashrafi^{2,3}, Solyman Ashrafi², moshe tur⁴, alan willner¹; ¹U. of Southern California, USA; ²NxGen Partners, USA; ³Univ. of Texas at Dallas, USA; ⁴Tel Aviv Univ., Israel. We report a transmission of 3 Gbit/s signal over a 4-km grade-index multimode fiber within a bandwidth of 2.54 GHz using multiple-layer-overlay (MLO) modulation format, achieving a spectral efficiency of 1.18 symbols/s/Hz.

JTh2A.64

Low-Cost In-Band OSNR Monitoring based on Coherent Hybrid in CO-OFDM System, liangjun zhang¹, Zhenhua Feng¹, Ruoxu Wang¹, Rui Lin^{1,2}, Liang Xu¹, Xiaolong Wang¹, Cong Zhou¹, Jiadi Wu¹, Shiwei Zhou¹, Lei Deng¹, Songnian Fu¹, Ming Tang¹, Deming Liu¹; ¹Next Generation Internet Access National, China; ²The Royal Inst. of Technology, Sweden. We proposed and demonstrated a cost-effective in-band optical signal to noise ratio (OSNR) monitoring technique based on coherent hybrid in 20Gb/s CO-OFDM system. Less than 0.5dB monitoring error is achieved with 400MHz balanced photo-detector (PD).

JTh2A.65

Sub-Harmonic Injection-Locking of Quantum Dash Laser Through Spectral Enrichment for All-Optical Clock Recovery, Manas Srivastava¹, Prince M. Anandarahaj², Balaji Srinivasan¹, Sean O Duill², Deepa Venkitesh¹, Pascal Landais²; ¹Indian Inst. of Technology, Madras, India; ²School of Electronics Engineering, Dublin City Univ., Ireland. We perform injection-locking of a passively mode-locked Fabry-Perot quantum dash laser at 40 GHz using 10 Gbps PRBS data in NRZ-OOK format after spectral enrichment and thus demonstrate all-optical clock recovery through sub-harmonic injection-locking.

JTh2A.66

56 Gb/s WDM transmitter module based on silicon microrings using comb lasers, Heiko Fuser¹, Anna Lena Giesecke¹, Andreas Prinzen¹, Stephan Suckow², Caroline Porschatis¹, Daniel Schall¹, Holger Lerch¹, Mohsin M. Tarar², Jens Bolten¹, Thorsten Wahlbrink¹, Heinrich Kurz¹; ¹AMO GmbH, Germany; ²Institut für Halbleitertechnik, RWTH Aachen Univ., Germany. We demonstrate the performance and the reliable fabrication process of a 56 Gb/s wavelength-division multiplexing transmitter module with integrated feedback structures. The device is based on microring silicon depletion modulators, optimized for O-band comb-laser operation.

JTh2A.67

Experimental Demonstration of Free-Space Optical Communications Using Orbital Angular Momentum (OAM) Array Encoding/Decoding, Shuhui Li¹, Zhidan Xu¹, Jun Liu¹, Nan Zhou¹, Yifan Zhao¹, Long Zhu¹, Fei Xia¹, Jian Wang¹; ¹Wuhan National Lab for Optoelectronics, China. We present a novel free-space communication link using orbital angular momentum (OAM) array encoding/decoding.

JTh2A.68

Arrays of WSi Superconducting Nanowire Single Photon Detectors for Deep Space Optical Communications, Matthew Shaw¹, Francesco Marsili¹, Andrew Beyer¹, Jeffrey Stern¹, Giovanni Resta¹, Prasana Ravindran², Su Wei Chang², Joseph Bardin², Ferze Patawaran¹, Varun Verma³, Richard P. Mirin³, Sae Woo Nam³, William Farr¹; ¹Jet Propulsion Lab, USA; ²Electrical Engineering, Univ. of Massachusetts, USA; ³National Inst. of Standards and Technology, USA. We have developed 64 pixel free space coupled arrays of WSi SNSPDs as a pathfinder for the ground detector in a deep space optical communication system. Our receiver prototype was used to close a real time deep space optical communication link at 47 Mbps.

JTh2A.69

A Colorless ONU Scheme for WDM-OFDM-PON with Symmetric Bitrate and Low-cost Direct-detection Receivers, Cheng Lei¹, Minghua Chen¹, Hongwei Chen¹, Sigang Yang¹, Shizhong Xie¹; ¹Tsinghua Univ., China. By suppressing one of the conjugated sidebands, the phase-modulated downstream OFDM signal can be directly detected and remodulated for upstream transmission simultaneously. Thus, colorless ONU can be realized with symmetric bitrate and low-cost direct-detection receiver.

JTh2A.70

Experimental Demonstration of Bandwidth Reduction using Nyquist Shaped PSK for Flexible udWDM, Jose A. Altabas¹, Jose A. Lazaro², Felix Sotelo¹, Ignacio Garcés¹; ¹Univ. of Zaragoza, Spain; ²Universitat Politècnica de Catalunya, Spain. Nyquist shaped PSK for flexible udWDM is proposed. 1.25Gb/s (2.5Gb/s) Nyquist-PSK with a 1200 homodyne coherent receiver reduces the used optical bandwidth to 3.75GHz (5GHz) with receiver sensitivity of -48.5dBm at BER=10⁻³.

JTh2A.71

Dynamic Adaptation of Bandwidth Granularity for Multipath Routing in Elastic Optical OFDM Networks, Luae Altarawneh¹, Sareh Taebi¹; ¹Electrical and Computer Engineering, Southern Illinois Univ., USA. We introduce the concept of bandwidth granularity dynamic adaptation for spectrum allocation using multipath provisioning in elastic optical OFDM networks. Results show that dynamic bandwidth adaptation significantly improves the performance in terms of throughput and blocking probability.

JTh2A.72

Study of Methane Saturated Dispersion Resonances Amplitude near 2.36 μm over the Temperature Range 77-300 K, Vladimir A. Lazarev¹, Mikhail K. Tarabrin¹, Valeriy E. Karasik¹, Alexey N. Kireev², Alexander S. Shelkovnikov², Yuri P. Podmarkov^{2,4}, Yuri V. Korostelin², Mikhail P. Frolov^{2,4}, Vladimir I. Kozlovsky², Mikhail A. Gubin^{2,3}; ¹Science and Education Center Photonics and IR-Techniques, Bauman Moscow State Technical Univ., Russia; ²P. N. Lebedev Physical Inst. of the Russian Academy of Sciences, Russia; ³National Research Nuclear Univ. MEPhI, Russia; ⁴Moscow Inst. of Physics and Technology, Russia. Saturated dispersion resonances of the methane E(2)-line ν₁+ν₂-band over the temperature range 77-300 K were observed with two-mode Cr²⁺:ZnSe laser with intracavity absorption cell. The resonances amplitudes were measured and compared with calculations.

JTh2A.73

Phase Noise Measurement of Microwave Signal Sources based on Microwave Photonic Technologies, Fangzheng Zhang¹, Dengjian Zhu¹, Shilong Pan¹; ¹Nanjing Univ Aeronautics & Astronautics, China. Phase noise measurement of microwave signal sources using microwave photonic technologies is demonstrated. Accurate measurement is achieved in an operation bandwidth from 5 to 40 GHz, and the sensitivity is below -130 dBc/Hz@10 kHz offset.

JTh2A.74

Proposal and Experimental Verification of Brillouin Optical Correlation Domain Reflectometry with Lock-in Detection Scheme, Yuguo Yao¹, Masato Kishi¹, Kazuo Hotate¹; ¹The Univ. of Tokyo, Japan. We have newly proposed a Brillouin optical correlation domain reflectometry with lock-in detection scheme. The scheme is verified by experiments using intensity and phase modulation. The phase modulation suppresses the background noise effectively.

JTh2A.75

Composite 1-GHz Optical Parametric Oscillator Frequency Comb from 400 - 1900 nm, Richard A. McCracken¹, Karolis Balskus¹, Zhaowei Zhang¹, Deryck T. Reid¹; ¹Heriot-Watt Univ., UK. We report a fully-stabilized synchronously-pumped optical parametric oscillator frequency comb at 1-GHz repetition frequency, comprising pump, signal and idler combs as well as combs at their sum-frequency and second-harmonic frequencies.

JTh2A.76

Laser Noise Improvement Through Pulse Nonlinear Propagation in a Dispersion-Increasing Fiber, Ming-Hsien Lin¹, Chen-Bin Huang¹; ¹National Tsing Hua Univ., Taiwan. We demonstrate experimentally that laser amplitude and timing jitters can be improved when the laser pulse undergoes adiabatic spectral compression in a dispersion-increasing fiber.

JTh2A.77

Doppler-free spectroscopy of ²³P→³D and spin-forbidden ²³P→³D transitions at 588 nm, Pei-Ling Luo¹, Jinneng Hu², Yan Feng², Li-Bang Wang¹, Jow-Tsong Shy^{1,3}; ¹Dept. of Physics, National Tsing Hua Univ., Taiwan; ²Shanghai Key Lab of Solid State Laser and Application and Shanghai Inst. of Optics and Fine Mechanics, Chinese Academy of Sciences, China; ³Inst. of Photonics Technologies, National Tsing Hua Univ., Taiwan. We demonstrated the Doppler-free intermodulated fluorescence spectroscopy of the ⁴He ²³P→³D transitions using a one-watt compact laser system at 588 nm. The power-dependent spectra of the ²³P→³D transitions were studied and the Doppler-free spectrum of the ²³P→³D transitions was first achieved.

JTh2A.78

Semiconductor Optical Amplifier with Holding Beam Injection for Single Path Accurate Time Transmission, Josef Vojtech¹, Jan Radil¹, Vladimir Smotlacha¹; ¹CESNET, Czech Republic. We experimentally demonstrated an accurate time transfer over 200 km single fiber path using semiconductor optical amplifiers in bidirectional operation with holding beam injection. Experiments show significant reductions of spontaneous lase of the fiber path.

JTh2A.79

Ultra-Narrow Linewidth, Micro-Integrated Semiconductor External Cavity Diode Laser Module for Quantum Optical Sensors in Space, Christoph Pyrllic¹, Wojciech Lewoczko-Adamczyk^{1,2}, Sven Schwertfeger¹, Johannes Häger¹, Andreas Wicht^{1,2}, Achim Peters^{1,2}, Götz Erbert¹, Günther Tränkle¹; ¹Ferdinand Braun Inst., Germany; ²Humboldt Universität zu Berlin, Germany. We present an external-cavity-diode-laser for quantum sensor applications based on distributed feedback diode laser with resonant feedback from an external cavity. The intrinsic linewidth is 31 Hz. Design, micro-integration concept and experimental results are shown.

JTh2A.80

Frequency-Control Characteristics of an Erbium-Based Mode-Locked Fiber Laser with an Optically Pumped Ytterbium Fiber, Hajime Inaba¹, Sho Okubo¹, Malte Schramm¹, Kenta Gunji¹, Feng-Lei Hong², Kazumoto Hosaka¹, Atsushi Onae¹; ¹National Metrology Inst. of Japan (NMIJ), Japan. Frequency-control characteristics of a mode-locked erbium-fiber laser with an intracavity optically pumped ytterbium-fiber were investigated. The fixed frequency of the comb when the pump power to the ytterbium-fiber is changed varies with the power.

JTh2A.81

Photonic Generation of Linearly-Chirped Microwave Waveform With Tunable Center Frequency and Time-Bandwidth Product, Hao Zhang¹, Weiwen Zou¹, Jianping Chen¹; ¹State Key Lab of Advanced Optical Communication Systems and Networks, Dept. of Electronic Engineering, Shanghai Jiao Tong Univ., China. A novel approach is presented to generate linearly-chirped microwave waveforms with tunable center frequency and expandable time-bandwidth product (TBWP). Different types of waveforms are demonstrated and the maximum measured TBWP is up to ~166.4.

11:30–13:00 JTh2A • Poster Session III

JTh2A.82

Investigation of Trace Gas Sensor Based on QEPAS Method Using Different QTFs, Yufei Ma¹, Guang Yu¹, Jingbo Zhang¹, Xin Yu¹, Hao Luo¹, Deying Chen¹, Rui Sun¹, Frank K. Tittel²; ¹Harbin Inst. of Technology, China; ²Dept. of Electrical and Computer Engineering, Rice Univ., USA. A trace gas sensor platform based on quartz-enhanced photoacoustic spectroscopy using quartz tuning forks (QTFs) with resonant frequency of 38 kHz and 40 kHz were experimentally investigated and theoretically analyzed for the first time.

JTh2A.83

Optical Heterodyne Micro-Vibration Measurement Based on All-Fiber Acousto-Optic Frequency Shifter, Ligang Huang¹, Weihua Peng¹, Wending Zhang², Feng Gao¹, Fang Bo¹, Guoquan Zhang¹, Jingjun Xu¹; ¹TEDA Applied Physics Inst. and School of Physics, Nankai Univ., China; ²Northwestern Polytechnical Univ., China. We provide an optical heterodyne detection configuration based on an all-fiber acousto-optic structure, which acts as both frequency shifter and coupler simultaneously, with a resolution of 0.01 nm from 10 kHz to 90 kHz.

JTh2A.84

Dual-parameters sensing based on multi-mode microfiber with Fresnel reflection, Qizhen Sun^{1,2}, Haipeng Luo¹, Zhilin Xu¹, Deming Liu¹, Lin Zhang², Xiaohui Sun¹; ¹Huazhong Univ of Science and Technology, China; ²Aston Inst. of Photonic Technologies, Aston Univ., UK. A compact and low cost fiber sensor based on microfiber with Fresnel reflection is proposed and demonstrated for simultaneous measurement of refractive index (RI) and temperature with high sensitivities.

JTh2A.85

Analysis of signal amplitude in Chirped Laser Dispersion Spectroscopy, Jacek Wodecki¹, Michal P. Nikodem¹; ¹Wrocław Research Centre EIT+, Poland. Signals measured with Chirped Laser Dispersion Spectroscopy setup implemented with intensity modulator are analyzed experimentally. Potential strategies for signal retrieval and amplitude enhancement possibilities are described.

JTh2A.86

Cylindrical multipass reflection cells for optical trace gas sensing, Markus Mangold^{1,2}, Lukas Emmenegger¹, Béla Tuzson¹, Herbert Looser²; ¹Empa, USA; ²IRsweep, Switzerland; ³FHNW, Switzerland. Single-piece cylindrical multipass cells effectively fold a long optical path in a small detection volume. We present a systematic survey of various cell configurations and the respective mirror shapes for enhanced path-to-volume ratios.

JTh2A.87

Doppler-Based Flow Rate Sensing in Microfluidic Channels, Avraham Bakal¹, Liron Stern¹, Mor Tzur¹, Maya Veinguer¹, Noa Mazurski¹, Nadav Cohen², Uriel Levy¹; ¹The Hebrew Univ. of Jerusalem, Israel; ²Tel Aviv Univ., Israel. We design, fabricate and experimentally demonstrate a novel generic method to detect flow rates velocity in microfluidic devices. The method is appealing for variety of applications where a simple and accurate speed measurement is needed.

JTh2A.88

Stand-off Detection of Liquid Thin Films using Active Mid-Infrared Hyperspectral Imaging, Luke Maidment^{1,2}, Zhaowei Zhang¹, Christopher R. Howle², Stephen T. Lee³, Allan Christie³, Deryck T. Reid¹; ¹Scottish Universities Physics Alliance (SUPA), Inst. of Photonics and Quantum Sciences, School of Engineering and Physical Sciences, Heriot-Watt Univ., UK; ²Defence Science and Technology Lab, UK; ³Thales Optronics, UK. The idler output of an ultrafast optical parametric oscillator is used with a mid-infrared camera to distinguish between water and deuterium oxide, demonstrating the potential for standoff detection of a wide range of liquids.

JTh2A.89

Filaments for Raman Spectroscopy, Chengyong Feng¹, James Hendrie¹, Jean-Claude Diels¹, Ladan Arissian¹; ¹CHTM, Univ. of New Mexico, USA. Impulsive rotational/vibrational Raman scattering of molecules excited by IR filaments and thereafter probed by a narrow line-width UV beam is proposed. We show results of rotational Raman scattering of air molecules for preliminary demonstration.

JTh2A.90

Experimental and Numerical Analysis of Commercial and Homemade Tuning Forks for QEPAS, Guillaume Aoust¹, Raphaël Levy¹, Myriam Raybaut¹, Béatrice Bourgeteau¹, Jean-Baptiste Dherbecourt¹, Jean-Michel Melkonian¹, Antoine Godard¹, Michel Lefebvre¹; ¹ONERA, the french aerospace lab, France. Characteristics of two commercial quartz tuning forks and a homemade tuning fork are compared for standard QEPAS experiments. An analytical model is also derived to compare theory and experiment with a reasonable agreement.

JTh2A.91

Electronics-assisted ultra-narrow optical filtering and its application in low phase noise lasing, Yitang Dai¹, Ziping Zhang¹, Feifei Yin¹, Yue Zhou¹, Jianqiang Li¹, Kun Xu¹; ¹Beijing Univ of Posts & Telecom, China. A MHz-level optical filtering is achieved by frequency conversion pair between optical and radio carriers as well as electronic filtering. Narrow linewidth lasing is then obtained with 20-kHz 20-dB linewidth and 65-dB side-mode suppression ratio.

JTh2A.92

A New Method of Longitudinal Mode Selection in Q-switched Lasers, Efim A. Khazanov^{1,2}, Andrey Shaykin¹, Konstantin Burdonov¹; ¹Inst. of Applied Physics of the Russian Academy of Science, Russia; ²National Univ. of Science and Technology "MISIS", Russia. The effect of post-pulse (the second giant pulse at the neighboring longitudinal mode) generation in a Q-switched laser was revealed in experiment. Based on this effect, a new method of longitudinal mode selection was implemented.

JTh2A.93

Laser Eigenvalue, Coherence Time, Q-factor, and Linewidth, Markus Pollnau¹, Marc Eichhorn²; ¹Dept. of Materials and Nano Physics, KTH-Royal Inst. of Technology, Sweden; ²French-German Research Inst. of Saint-Louis ISL, France. We generalize the theory of continuous-wave lasers by considering spontaneous emission in the photon rate equation. We relate the laser coherence time, Q-factor, and linewidth to the passive-resonator parameters, thereby unifying resonator and laser theory.

JTh2A.94

Nonlinear Polarization Switching and Preservation Effects in 55 μm Core Polygonal-CCC Fibers, Ning Hu¹, Cheng Zhu¹, Michael Haines¹, Timothy McComb², Geoff Fanning², Roger Farrow², Almantas Galvanauskas¹; ¹Univ. of Michigan, USA; ²Light, USA. Study of nonlinear, intensity-dependent polarization evolution in 55μm core polygonal-CCC fibers reveals that both nonlinear polarization switching as well as robust and intensity-independent polarization maintenance can be achieved depending on input signal polarization.

JTh2A.95

Novel Design of Simple and Compact Tunable Fiber Laser, Yasushi Fujimoto¹, Osamu Ishii², Masaaki Yamazaki³; ¹Osaka Univ., Japan; ²Production Engineering Section, Optical Glass Production Dept., Sumita Optical Glass, Inc., Japan; ³Glass Research Division, R&D Dept., Sumita Optical Glass, Inc., Japan. We propose and demonstrate a novel design of simple and compact tunable fiber laser skillfully using chromatic aberration of a lens relay and a slit-like effect of optical fiber core.

JTh2A.96

Spatially-resolved Pulse-front-tilt and Pulse-width Distributions of Q-switched Pulses from an Unstable Nd:YAG Resonator, Chengyong Feng¹, Xiaozhen Xu¹, Jean-Claude Diels¹; ¹CHTM, Univ. of New Mexico, USA. Pulse-front-tilt and negligible pulse-width spread across the laser beam are reported, both experimentally and numerically, for pulses from a Q-switched unstable resonator with a variable-reflectivity-mirror under different operation conditions.

JTh2A.97

Single Frequency 310ps, 1.67J Laser Pulses Generation with Nonfocusing-pumped Stimulated Brillouin Scattering, Xuehua Zhu¹, Zhiwei Lu¹, Yulei Wang¹, Hengkang Zhang¹; ¹Harbin Inst. of Technology, China. We obtained single frequency laser pulses with energy of 1.67-J and duration of 310-ps based on the nonfocusing-pumped stimulated Brillouin scattering. A high-power Nd:glass laser system delivers 3-ns super-Gaussian-shaped pulses is used as the light-source.

JTh2A.98

Widely-tunable high-power narrow-line-width thulium-doped all-fiber superfluorescent source, Jiang Liu¹, Hongxing Shi¹, Chen Liu¹, Pu Wang¹; ¹Beijing Univ. of Technology, China. Power scaling of narrow-linewidth thulium-doped fiber superfluorescent source with wavelength tunable from 1940–2010nm is reported. The all-fiber superfluorescent source yielded 364W of output power at central wavelength of 1980nm with 3dB spectral bandwidth of 1.9nm.

JTh2A.99

UV Laser Beam Stabilization System for the European XFEL Electron Injector Laser Beamline, Florian Kaiser¹, Sebastian Köhler¹, Falko Peters¹, Lutz Winkelmann¹, Ingmar Hartl¹; ¹DESY, Germany. We present a beam drift stabilization system for the 22 m UV-laser beam delivery to the electron gun of the European XFEL. The camera-based system is robust to dynamic variations in power, beam size and shape.

JTh2A.100

Spectroscopic characterization of Pr³⁺:ZnSe crystals fabricated via post growth thermal diffusion, Alan Martinez¹, Ozarfar Gafarov¹, Dmitry Martyshev¹, Vladimir V. Fedorov¹, Sergey B. Mirov¹; ¹Univ. of Alabama at Birmingham, USA. We demonstrate post-growth thermal diffusion rates of praseodymium ions into ZnSe. Near and middle infrared luminescence spectra and kinetics of Pr:ZnSe crystals were studied at RT.

JTh2A.101

Withdrawn

JTh2A.102

Power Scaling of Femtosecond Ti:sapphire Laser Double-Side-Pumped by High-Power Green InGaN Diode Lasers, Ryota Sawada¹, Hiroki Tanaka¹, Ryosuke Kariyama¹, Kenichi Hirotsawa¹, Fumihiko Kannari¹; ¹Dept. of Electronics and Electrical Engineering, Keio Univ., Japan. We demonstrate a mode-locked Ti:sapphire laser pumped by high-power green InGaN diode lasers from both sides of the crystal and achieved a highest laser power of 50 mW.

JTh2A.103

Developed objective system for measuring the visibility of the display with metal mesh as a capacitive touch sensor, Kim T. Young^{1,2}; ¹SAMSUNG, Korea; ²Center of Information Storage Devices, Yonsei Univ., Korea. In this paper, we introduce a new method to measure the visibility of a metal-mesh ITO-replacement touch panels. The reason why we have developed this system is to clear up the ambiguity of the visibility estimation or readability property of the metal mesh electrodes in touch sensors.

JTh2A.104

Fabrication of Gratings with Low Spacing Error by the Dual-Beam Exposure System with Spherical Lenses, Shiwei Wang¹, Lijiang Zeng¹; ¹Tsinghua Univ., USA. We propose a feedback method of adjusting the dual-beam exposure system with spherical collimation lenses based on deducing the spacing error from diffraction wavefront. The grating of 0.03 λ in 70×70 mm² can be achieved.

12:30–14:00 Pizza Lunch with Exhibitors, *Exhibit Hall*

13:00–14:30 Market Focus: U.S. Export Control - Review of Government Rules and Open Discussion of Possible Changes,
Exhibit Hall Theater

NOTES

Executive Ballroom
210A

CLEO: Applications
& Technology

14:00–16:00
ATH3A • Symposium on Science and Technology of Laser Three Dimensional Printing I
Presider: Timo Mappes; Carl Zeiss AG, Germany

ATH3A.1 • 14:00 **Invited**
Dynamic Optics for Three-Dimensional Laser Material Processing, Martin J. Booth¹; ¹Univ. of Oxford, UK. Dynamic optical elements, including spatial light modulators and deformable mirrors, improve the capabilities of laser fabrication systems. Advantages include aberration correction, parallelization and spatial control over the temporal intensity profile of ultrashort pulses.

ATH3A.2 • 14:30 **Invited**
Laser Written 3D Lightwave Circuits and Applications, Simon Gross¹, Nicolas Riesen², John Love³, Michael J. Withford¹; ¹Macquarie Univ., Australia; ²The Univ. of Adelaide, Australia; ³The Australian National Univ., Australia. Three dimensional lightwave circuits, fabricated using femtosecond laser direct-write techniques, are enabling new applications in quantum optics, astronomy and telecommunications. We review those and highlight our recent work on 3D compact, passive mode selective couplers.

Executive Ballroom
210B

CLEO: QELS-Fundamental Science

14:00–16:00
FTh3B • NV – Centers for Metrology and Photonics
Presider: Dirk Englund; MIT, USA

FTh3B.1 • 14:00
Deterministic High-yield Creation of Nitrogen Vacancy Centers in Diamond Photonic Crystal Cavities and Photonic Elements, Tim Schroder¹, Luozhou Li¹, Edward Chen¹, Michael Walsh¹, Matthew E. Trusheim¹, Igal Bayn¹, Jiabao Zheng¹, Sara Mouradian¹, Hassaram Bakhr², Ophir Gaathon¹, Dirk R. Englund¹; ¹MIT, USA; ²Univ. at Albany, USA. We demonstrate the high-yield creation of nitrogen-vacancy centers in the mode-maxima of a variety of functional photonic elements with less than 30nm precision. We create 1.1 NVs per photonic-crystal-cavity and show strong Purcell enhancement.

FTh3B.2 • 14:15
Direct laser writing aligned with nano-diamonds containing NV-centers as single-photon emitters, Qiang Shi¹, Joachim Fischer¹, Patrik Rath¹, Bernd Sontheimer², Andreas Schell², Wolfram Pernice¹, Oliver Benson², Andreas Naber¹, Martin Wegener¹; ¹Karlsruhe Inst. of Technology, Germany; ²Humboldt-Universität zu Berlin, Germany. We present and apply an instrument allowing for localizing NV-centers in nano-diamonds in a photoresist, measuring the $g^2(\tau)$ correlation function without exposing the photoresist, and performing three-dimensional direct laser writing aligned with the single-photon emitters.

FTh3B.3 • 14:30
Efficient collection from a nitrogen-vacancy qubit in a circular grating, Luozhou Li¹, Edward Chen¹, Jiabao Zheng², Sara Mouradian¹, Florian Dolde¹, Tim Schroder¹, Sinan Karaveli¹, Matthew Markham³, Daniel Twitchen³, Dirk R. Englund¹; ¹MIT, USA; ²Columbia Univ., USA; ³Element Six, USA. We demonstrate a circular 'bullseye' diamond grating enabling efficient collection of single photons from a single nitrogen-vacancy center with a spin coherence time of 1.7 ms. Back-focal-plane studies indicate efficient redistribution into low-NA modes.

Executive Ballroom
210C

14:00–16:00
FTh3C • Attosecond Spectroscopy
Presider: Martin Schultze; Max Planck Institut fuer Quantenoptik, USA

FTh3C.1 • 14:00 **Tutorial**
Attosecond Ionization Dynamics and Time Delays, Ursula Keller¹; ¹ETH Zurich, Switzerland. Although time is not a quantum-mechanical operator, novel attosecond techniques can measure very fundamental time delays. Using the tunneling time as an example, this tutorial should give a better insight on current issues and hot topics.



Ursula Keller has been a tenured professor of physics at ETH Zurich since 1993 and currently serves as director of the NCCR MUST program in ultrafast science. She received a Masters at ETH 1984, a Ph.D. at Stanford Univ. 1989, and was a Member of Technical Staff at Bell Labs from 1989 to 1993.

Executive Ballroom
210D

14:00–16:00
FTh3D • Synthetic Lattices & Topological Phenomena
Presider: Alexander Szameit; Friedrich-Schiller-Universität Jena, Germany

FTh3D.1 • 14:00
Anderson Localization in Synthetic Photonic Lattices, Ilya Vatanik^{1,2}, Alexey M. Tikan², Dmitry V. Churkin^{3,2}, Andrey A. Sukhorukov⁴; ¹Inst. of Automation and Electrometry SB RAS, Russia; ²Novosibirsk State Univ., Russia; ³Aston Inst. of Photonic Technologies, UK; ⁴The Australian National Univ., Australia. We experimentally demonstrate Anderson localization for optical pulses in time domain, using a photonic mesh lattice implemented with coupled optical fiber loops. We also discuss interplay of photonic band-gaps and disorder in such lattices.

FTh3D.2 • 14:15
Experimental realization of a topological Anderson insulator, Simon Stützer¹, Mikael Rechtsman², Paraj Titum³, Yonatan Plotnik², Yaakov Lumer², Julia M. Zeuner¹, Stefan Nolte¹, Gil Refael³, Netanel Lindner², Mordechai Segev², Alexander Szameit¹; ¹Inst. of Applied Physics, Friedrich-Schiller-Universität, Germany; ²Dept. of Physics, Israel Inst. of Technology, Israel; ³Dept. of Physics, Inst. of Quantum Information and Matter, USA. We experimentally demonstrate that disorder can induce a topologically non-trivial phase. We implement this „Topological Anderson Insulator“ in arrays of evanescently coupled waveguides and demonstrate its unique features.

FTh3D.3 • 14:30
Topological Insulators in PT-Symmetric Lattices, Gal Harari¹, Yonatan Plotnik¹, Miguel A. Bandres¹, Yaakov Lumer¹, Mikael Rechtsman¹, Mordechai Segev¹; ¹Physics Dept., Technion Israel Inst. of Technology, Israel. We present the first PT-symmetric topological insulator system: topologically-protected transport of edge states in PT-symmetric photonic honeycomb lattices.

Executive Ballroom
210E

CLEO: QELS-
Fundamental Science

14:00–16:00
FTH3E • Light Harvesting and
Electroplasmionics
Presider: Dirk Englund; MIT, USA

FTH3E.1 • 14:00 **Invited**
**Ultrafast Coherent Charge Transfer in
Solar Cells and Artificial Light Harvesting
Systems: Toward Movies of Electronic Motion**,
Christoph Lienau¹; ¹Inst. of Physics, Carl
von Ossietzky Univ. Oldenburg, Germany. We
have recently established a new approach,
combining high-time resolution optical
spectroscopy and time-dependent density
functional theory to probe the most elementary
processes of light-to-current conversion
in nanostructures. I will present an overview
and discuss most recent findings.

FTH3E.2 • 14:30
**Atomically-thin van der Waals Hetero-
structure Solar Cells**, Thomas Mueller¹,
Marco Furchi¹, Armin Zechmeister¹, Simone
Schuler¹, Andreas Pospischil¹; ¹Vienna Univ. of
Technology, Austria. We present atomically-
thin photovoltaic solar cells based on van der
Waals heterostructures of transition metal
dichalcogenides and other two-dimensional
semiconductors.

Executive Ballroom
210F

14:00–16:00
Sth3F • Microwave Photonic
Devices
Presider: Mark Foster; Johns
Hopkins Univ., USA

Sth3F.1 • 14:00
**Linearized Intensity-Modulation Link
by a Direct-Detection Intermodulation-
Compensation Receiver**, Dan Tu¹, Feifei
Yin¹, Xiaodong Liang¹, Yitang Dai¹, Jian-
qiang Li¹, Kun Xu¹; ¹Beijing Univ. of Posts
and Telecommunications, China. By the
bias-voltage-dependent responsivity, a
direct-detection photo detector is proposed
to eliminate the third-order intermodulation
for the intensity-modulation analog photonic
link. Spurious-free dynamic range of 123.4
dB within 1-Hz bandwidth is achieved with
18.1-dB improvement.

Sth3F.2 • 14:15
**Frequency Band Selectable Microwave
Photonic Multiband Bandpass Filter based
on Lyot filter**, Jia Ge¹, Mable P. Fok¹; ¹Univ.
of Georgia, USA. We present a microwave
photonic multiband bandpass filter with
four selectable operating states, which can
either work as an all-block, single-pass or
multi-pass bandpass filter with up to 46 dB
sidelobe suppression.

Sth3F.3 • 14:30 **Invited**
**Silicon-photonics-based Signal Processing
for Microwave Photonic Frontends**, Ming-
hua Chen¹, Hongchen Yu¹, Jingjing Wang¹,
Hongwei Chen¹, Sigang Yang¹, Shizhong
Xie¹; ¹Tsinghua Univ., China. Integrated signal
processors offer potential high resolution,
tunability and programmable microwave
photonic signal processing. The high per-
formance integrated FIR/IIR signal proces-
sors have been presented, accompanying
an application for the full-band microwave
photonic frontends.

Executive Ballroom
210G

CLEO: Science & Innovations

14:00–16:00
Sth3G • Fabrication
Techniques I
Presider: Amy Foster; Johns
Hopkins Univ., USA

Sth3G.1 • 14:00 **Tutorial**
**Heterogeneous 2D and 3D Photonic
Integration for Future Chip-Scale Micro-
systems**, S. J. Ben Yoo¹; ¹Univ. of California
Davis, USA. This tutorial reviews state-of-
the-art heterogeneous 2D/3D photonic
integration technologies involving various
novel fabrication techniques leading to
realization of chip-scale microsystems with
photonic-electronic-integrated-circuits.
Future prospects and challenges in comput-
ing and networking applications will also
be discussed.



S. J. Ben Yoo is a Professor of Electrical
Engineering at University of California at
Davis (UC Davis). His research at UC Davis
includes photonic integration for future
computing, communication, imaging, and
navigation systems. Prior to joining UC Davis
in 1999, he was a Senior Research Scientist
at Bellcore, leading technical efforts in
integrated photonics, optical networking,
and systems integration. He received BS'84,
MS'86, PhD'91 from Stanford University.
Prof. Yoo is Fellow of IEEE, OSA, NIAC and
a recipient of the DARPA Award for Sustained
Excellence (1997), the Bellcore CEO Award
(1998), the Mid-Career Research Faculty
Award (2004), and the Senior Research Fac-
ulty Award (2011).

Executive Ballroom
210H

14:00–16:00
Sth3H • Materials and Devices
for Nonlinear Frequency
Upconversion
Presider: Antoine Godard;
ONERA - French Aerospace Lab,
France

Sth3H.1 • 14:00 **Invited**
**Nonlinear Optical Processes and DUV
Generation in Random Domain Structures
of SBO**, Aleksandr S. Aleksandrovsky^{1,2};
¹L.V.Kirensky Institute of Physics, Russia;
²Photonics and Laser Technologies Deoart-
ment, Siberian Federal Univ., Russia. Random
domain structures in strontium tetraborate
enhance nonlinear optical conversion for vari-
ety of processes within transparency window
(121 nm). Properties of material, frequency
doubling, autocorrelation measurements
and conversion of supercontinuum to UV
are described.

Sth3H.2 • 14:30
**Generation of Coherent Vacuum UV Ra-
diation in Randomly Quasi-Phase-Matched
Strontium Tetraborate**, Peter Trabs¹, Frank
Noack¹, Aleksandr S. Aleksandrovsky^{2,3},
Alexandre Zaitsev^{2,3}, Valentin Petrov¹; ¹Max
Born Inst., Germany; ²L. V. Kirensky Inst. of
Physics, Russia; ³Siberian Federal Univ., Rus-
sia. Tunable coherent radiation is generated
in the VUV down to 121 nm using random
quasi-phase-matching in strontium tetrabo-
rate, the shortest wavelength ever produced
with a second-order nonlinear optical process
in a solid-state material.



**Meeting Room
211 B/D**

CLEO: Science & Innovations

14:00–16:00

STh3I • Optomechanics I

Presider: Philip Russell; Max-Planck-Inst Physik des Lichts, Germany

STh3I.1 • 14:00

Diamond Electro-optomechanical Devices with Resonance Frequencies above 100 MHz, Patrik Rath¹, Sandeep Ummethala¹, Silvia Diewald², Georgia Lewes-Malandrakis³, Dietmar Brink³, Nicola Heidrich³, Christoph Nebel³, Wolfram Pernice¹; ¹Inst. of Nanotechnology, Karlsruhe Inst. of Technology, Germany; ²Center for Functional Nanostructures, Karlsruhe Inst. of Technology, Germany; ³Fraunhofer Inst. for Applied Solid State Physics, Germany. We realize diamond electro-optomechanical resonators operated at frequencies above 100 MHz. The nano-mechanical motion is read-out via on-chip diamond photonic circuits showing Q-factors above 1300.

STh3I.2 • 14:15

GaAs nanobeam piezo-optomechanical crystals, Krishna C. Balram^{1,2}, Marcelo I. Davanco¹, Ju Young Lim³, Jin Dong Song³, Kartik Srinivasan¹; ¹Center for Nanoscale Science and Technology, National Inst. of Standards and Technology, USA; ²Maryland Nanocenter, Univ. of Maryland, USA; ³Center for Opto-Electronic Convergence Systems, Korea Inst. of Science and Technology, Korea. We demonstrate GaAs optomechanical crystals with large coupling rates ($g_0/2\pi \approx 1.1$ MHz) through the photoelastic effect. We show a significant orientation ($\approx 30\%$) dependence of g_0 , observe 2.5 GHz regenerative oscillations, and explore excitation via piezoelectrically-driven surface-acoustic-waves.

STh3I.3 • 14:30

Diamond Nanobeam Waveguide Optomechanics, Behzad Khanaliloo^{1,2}, Harishankar Jayakumar¹, David Lake¹, Paul E. Barclay^{1,2}; ¹Univ. of Calgary, Canada; ²National Inst. for Nanotechnology, Canada. Single crystal diamond (SCD) waveguide nanomechanical resonators with mechanical quality factors exceeding 5×10^5 in cryogenic conditions are demonstrated. Mechanical self-oscillations are observed with amplitudes of 200 nm.

**Meeting Room
212 A/C**

CLEO: Applications & Technology

14:00–16:00

ATH3J • Clinical Technologies and Systems I

Presider: Jin Kang; Johns Hopkins Univ., USA

ATH3J.1 • 14:00 Invited

Finding Bugs in your Ear: Clinical Imaging of Middle-Ear Infections and Biofilms using OCT, Stephen A. Boppart¹; ¹Univ of Illinois at Urbana-Champaign, USA. Handheld OCT scanners have been developed for screening and characterizing middle-ear infections that are highly prevalent in the pediatric population. OCT enables non-invasive identification of bacterial biofilms that will impact clinical treatment of this disease.

ATH3J.2 • 14:30 Invited

Integrative Advances for OCT-Guided Ophthalmic Surgery and Intraoperative OCT, Yuankai K. Tao¹, Mohamed El-Haddad¹, Sunil Srivastava¹, Daniel Feiler¹, Amanda Noonan², Andrew Rollins², Justis Ehlers¹; ¹Cole Eye Inst. Cleveland Clinic, USA; ²Biomedical Engineering, Case Western Reserve Univ., USA. Microscope-integrated intraoperative OCT (iOCT) allows live cross-sectional imaging concurrent with ophthalmic surgery and dynamic visualization of tissue-instrument interactions. We present a microscope-integrated iOCT system with heads-up display (HUD) and novel semi-transparent ophthalmic surgical instruments.

**Meeting Room
212 B/D**

CLEO: Science & Innovations

14:00–16:00

STh3K • Novel Microscopy Techniques and OCT

Presider: Chulmin Joo; Yonsei Univ., Korea

STh3K.1 • 14:00 Invited

Brillouin Microscopy For Tissue And Cell Biomechanics, Giuliano Scarcelli^{2,1}; ¹Harvard Medical School, USA; ²Bioengineering, Univ. of Maryland, USA. We have developed an all-optical approach to measure material mechanical properties using Brillouin light scattering. Brillouin imaging uses the elastic modulus as contrast mechanism. We demonstrate its application in vivo for tissue and cellular biomechanics.

STh3K.2 • 14:30

Enhanced Detection of Longitudinal Field of a Radially Polarized Beam in Confocal Laser Microscopy, Yuichi Kozawa¹, Shunichi Sato¹; ¹Inst. of Multidisciplinary Research for Advanced Materials, Tohoku Univ., Japan. The wave scattered by the longitudinal component of a tightly focused radially polarized beam is clearly detected in a confocal system, which may lead to the enhancement of the spatial resolution in confocal microscopy.

**Marriott
Salon I & II**

14:00–16:00

STh3L • Ultrafast Fiber Lasers

Presider: Peter Fendel; Thorlabs Inc., USA

STh3L.1 • 14:00

All-fiber bidirectional optical parametric oscillator for precision rotation sensing, Roopa Gowda¹, Nam Nguyen¹, Jean-Claude diels², Robert Norwood¹, Nasser Peyghambarian¹, Khanh Q. Kieu¹; ¹Univ. of Arizona, USA; ²Physics, Univ. of New Mexico, USA. We demonstrate the first all-fiber bidirectional OPO which generates two highly coherent frequency combs in opposite directions. The OPO may find important applications in precision measurements including rotation sensing with ultra-large sensing area and sensitivity.

STh3L.2 • 14:15

Pulse-to-pulse spectral evolution of breathing bound solitons in a mode-locked fiber laser, Srikanth Sugavanam¹, Chengbo Mou^{1,2}, Junsong Peng¹, Dmitry V. Churkin^{1,2}; ¹Aston Inst. of Photonic Technologies, UK; ²Novosibirsk State Univ., Russia. We make first direct observation of breathing bound solitons in mode-locked laser. We measure pulse-to-pulse spectrum evolution and reveal internal interactions between bound solitons in real-time.

STh3L.3 • 14:30

Dissipative soliton thulium fiber laser with pulse energy above 10 nJ, Yuxing Tang¹, Frank W. Wise¹; ¹Cornell Univ., USA. Dissipative-soliton operation of a Tm fiber laser yields 11 nJ pulses, which is several times the energy of prior femtosecond Tm fiber lasers. The pulses can be dechirped to 200 fs duration.

CLEO: Science & Innovations

14:00–16:00

STh3M • Fundamental Light-material Interaction I*Presider: Emmanuel Haro-Poniatowski; UAM-Iztapalapa, Mexico***STh3M.1 • 14:00****Rapid and highly-sensitive detection using Fano resonances in ultrathin plasmonic nanogratings**, Beibei Zeng¹; ¹Lehigh Univ., USA. We developed a nanoplasmonic sensor employing extraordinary optical properties of 30nm-thick ultrathin Ag nanogratings. An order-of-magnitude improvement in the temporal and spatial resolutions was achieved relative to state-of-the-art nanoplasmonic sensors, for comparable detection resolutions.**STh3M.2 • 14:15****Far-field Scattering Measurement of a Single Gold Nanorod Using Total-Internal-Reflection Illumination**, Donghyeong Kim¹, Kwang-Yong Jeong², Ho-Seok Ee¹, Hong-Gyu Park², Min-Kyo Seo¹; ¹Physics, Korea Advanced Inst. of Science and Technology(KAIST), Korea; ²Physics, Korea Univ., Korea. We demonstrate a novel method for measuring far-field scattering of a single nanostructure with a high signal-to-background ratio using total-internal-reflection illumination. Direct far-field scanning overcomes the numerical aperture limit of the typical back-focal plane imaging.**STh3M.3 • 14:30****Fabrication of high-Q lithium niobate microresonators using femtosecond laser micromachining for second harmonic generation**, Jintian Lin¹, Yingxin Xu², Zhiwei Fang¹, Min Wang¹, Jiangxin Song¹, Nengwen Wang¹, Lingling Qiao¹, Wei Fang², Ya Cheng¹; ¹Shanghai Inst of Optics and Fine Mech, USA; ²Dept. of Optical Engineering, Zhejiang Univ., State Key Lab of Modern Optical Instrumentation, China. We report on fabrication of high-Q (i.e., a quarter million) lithium niobate whispering-gallery-mode microresonators using femtosecond laser micromachining. Second harmonic generation with a normalized conversion efficiency of $1.35 \times 10^{-5}/\text{mW}$ has been experimentally demonstrated.

14:00–16:00

STh3N • Time and Frequency Transfer*Presider: Jungwon Kim; KAIST, USA***STh3N.1 • 14:00****Ultra-low Jitter Timing Transfer over a Multi-km Fiber Network with 10^{21} Relative Stability**, Kemal Shafak¹, Ming Xin¹, Michael Y. Peng², Franz X. Kaertner^{1,2}; ¹Center for Free-Electron Laser Science, Deutsches Elektronen-Synchrotron, Germany; ²Dept. of Electrical Engineering and Computer Science and Research Lab of Electronics, MIT, USA. Long-term stable timing transfer over a multi-km fiber network is reported. Output of two independently timing-stabilized fiber links shows only 0.73 femtoseconds RMS total jitter over 35 hours corresponding to 10^{21} relative link stability.**STh3N.2 • 14:15****Simultaneous Time and Frequency Transfer over a 158-km-Long Fiber Network Using a Mode-Locked Laser**, Maurice Lessing^{1,2}, Helen S. Margolis¹, C. Tom A. Brown², Giuseppe Marra¹; ¹National Physical Lab, UK; ²School of Physics and Astronomy, Univ. of St Andrews, UK. We present a technique for simultaneous optical and microwave frequency transfer as well as time transfer using a mode-locked laser. We demonstrate a time deviation of 300 fs at 10 s averaging time on an installed 158 km fiber link.**STh3N.3 • 14:30****Ultrastable Frequency Dissemination Based on Feed-forward Digital Phase Compensation Technology**, Xing Chen¹, Jian Zhang¹, Jinlong Lu¹, Yifan Cui¹, Xing Lu¹, Zhiqiang Lv¹, Xusheng Tian², Cheng Ci², Bo Liu², Hong Wu², Tingsong Tang³, Kebin Shi¹, Zhigang Zhang¹; ¹Peking Univ., China; ²Nankai Univ., China; ³Beijing Satellite Navigation Center, China. We demonstrate a feed-forward digital compensation scheme in an optical frequency comb based microwave frequency dissemination system over 120-km telecommunication fiber link. The dissemination fractional frequency instability (Λ -counter) was measured at $5.28 \times 10^{-16}/\text{s}$.

14:00–16:00

STh3O • Remote and Standoff Optical Detection*Presider: Michael Wojcik; Space Dynamics Lab, USA***STh3O.1 • 14:00****Monostatic All-Fiber Rangefinder System**, Jeffrey Leach¹, Stephen R. Chinn², Lew Goldberg¹; ¹NVESD, USA; ²Fulcrum Company, USA. An all-fiber monostatic laser rangefinder, using a double cladding fiber to transmit and receive light through a single lens is described. Ranging to >50 m with 12 uJ, 8 ns, 1540 nm pulses is shown. The all-fiber system is compact and needs no precise receiver/transmitter beam alignment.**STh3O.2 • 14:15****Continuous-Wave Laser Range Finder Based on Incoherent Compression of Periodic Sequences**, Nadav Arbel¹, Lior Hirschbrand¹, Shai Weiss¹, Nadav Levanon², Avi Zadok¹; ¹Bar-Ilan Univ., Israel; ²Tel Aviv Univ., Israel. Continuous and incoherent laser range finder is presented, based on repeating transmission of Legendre amplitude codes and post detection compression. The cyclic correlation sidelobes of the sequences are identically zero. The concept is demonstrated experimentally.**STh3O.3 • 14:30****Experimental Demonstration of Differential Synthetic Aperture Ladar**, Zeb W. Barber¹, Jason R. Dahl¹; ¹Montana State Univ. - Spectrum Lab, USA. Differential SAL measures phase slopes to reduce the inherent sensitivity to piston phase errors during the data collection process. The first experimental demonstrations of the technique and comparisons to image based phase compensation are presented.

Executive Ballroom
210A

CLEO: Applications
& Technology

ATH3A • Symposium on Science and Technology of Laser Three Dimensional Printing I—Continued

ATH3A.3 • 15:00 Invited
3D Printing Sets New Standards in Microfabrication, Martin Hermatschweiler¹; ¹Nanoscribe GmbH, Germany. Two-photon polymerization has emerged as highest precision additive manufacturing standard for micro- to mesoscale fabrication and superior maskless lithography technique. Design freedom, resolution and processing speed drive diverse scientific as well as industrial applications.

Executive Ballroom
210B

CLEO: QELS-Fundamental Science

FTh3B • NV – Centers for Metrology and Photonics—Continued

FTh3B.4 • 14:45
Strain coupling of diamond nitrogen vacancy centers to nanomechanical resonators, Srujan Meesala¹, Young-Ik Sohn¹, Haig A. Atikian¹, Michael J. Burek¹, Samuel Kim¹, Jennifer Choy¹, Marko Loncar¹; ¹Harvard Univ., USA. We fabricate high quality factor diamond cantilevers containing nitrogen vacancy (NV) centers. Strain-mediated coupling of the NV spin to the displacement of a mechanical mode is observed in optically detected electron spin resonance measurements.

FTh3B.5 • 15:00
Atom-Photon Coupling from Nitrogen-vacancy Centers Embedded in Tellurite Microspheres, Yinlan Ruan⁵, Brant C. Gibson¹, Des W. Lau¹, Andrew Greentree¹, Hong Ji⁵, Heike Ebendorff-Heidepriem⁵, Brett C. Johnson², Takeshi Ohshima³, Tanya Monro^{4,5}; ¹School of Applied Science, RMIT Univ., Australia; ²School of Physics, Univ. of Melbourne, Australia; ³Semiconductor Analysis & Radiation Effects Group, Japan Atomic Energy Agency, Japan; ⁴Univ. of South Australia, Australia; ⁵School of Chemistry & Physics, Univ. of Adelaide, Australia. A technique was developed for creating tellurite microspheres with embedded nanodiamonds. The whispering gallery mode modulated fluorescence of the nitrogen vacancy centers in the nanodiamonds was observed with resonance Q over 10,000.

FTh3B.6 • 15:15
Electrochemical potential control of charge state and fluorescence of nitrogen vacancy centers in nanodiamonds, Sinan Karaveli^{1,2}, Ophir Gaathon^{1,3}, Abraham Wolcott^{1,4}, Reyu Sakakibara¹, Darcy Peterka⁵, Jonathan S. Owen⁴, Rafael Yuste⁵, Dirk R. Englund¹; ¹Dept. of Electrical Engineering and Computer Science, MIT, USA; ²Dept. of Electrical Engineering, Columbia Univ., USA; ³Diamond Nanotechnologies, Inc., USA; ⁴Dept. of Chemistry, Columbia Univ., USA; ⁵Dept. of Biological Sciences, Columbia Univ., USA. We use spectro-electrochemical microscopy to demonstrate that the equilibrium charge state and fluorescence of nitrogen vacancy centers in nanodiamonds can be dynamically controlled by externally applied potentials.

Executive Ballroom
210C

FTh3C • Attosecond Spectroscopy—Continued

FTh3C.2 • 15:00
Fano Resonances in the Time Domain, Andreas Kaldun¹, Christian Ott¹, Alexander Blättermann¹, Thomas Ding¹, Andreas Fischer¹, Philipp Raith¹, Kristina Meyer¹, Martin Laux¹, Jörg Evers¹, Christoph H. Keitel¹, Thomas Pfeifer¹, Chris H. Greene²; ¹Max-Planck-Institut für Kernphysik, Germany; ²Dept. of Physics, Purdue Univ., USA. The Fano phase formalism enables measurement and control of phase and amplitude of an emitting dipole. Here, we use this formalism to measure and understand the dynamics of bound states in strong laser fields.

FTh3C.3 • 15:15
Quantum Beats in Attosecond Transient Absorption of Krypton Autoionizing States, Yan Cheng¹, Michael Chini¹, Xiao-Min Tong², Andrew Chew¹, Julius Biedermann^{1,3}, Yi Wu¹, Eric Cunningham¹, Zenghu Chang¹; ¹Univ. of Central Florida, USA; ²Univ. of Tsukuba, Japan; ³Friedrich-Schiller Universität, Germany. Quantum beats with periods of 5-10 fs are observed in various near-threshold autoionizing states of krypton atoms in an attosecond transient absorption experiment, such measurement allows reconstruction of the valence state wave packets.

Executive Ballroom
210D

FTh3D • Synthetic Lattices & Topological Phenomena—Continued

FTh3D.4 • 14:45
Topological Transport in Photonic Quasicrystals, Miguel A. Bandres¹, Mikael Rechtsman¹, Mordechai Segev¹; ¹Physics, Technion, Israel. We show that it is possible to have topological transport in photonic quasicrystals, and therefore this lattices have one-way extended edge states that are topologically protected against backscattering as they pass through defects or around corners.

FTh3D.5 • 15:00
Supersymmetric Laser Arrays, Ramy El-Ganainy¹, Mercedeh Khajavikhan², Demetrios N. Christodoulides², Li Ge³; ¹Physics, Michigan Technological Univ., USA; ²CREOL, College of Optics and Photonics, Univ. of Central Florida, USA; ³Dept. of Engineering Science and Physics, College of Staten Island, CUNY, USA. We present a new strategy for regulating light emission dynamics in high power laser arrays. Our approach is based on engineering the properties of non-Hermitian supersymmetric optical arrays and offers several advantages over previous investigations.

FTh3D.6 • 15:15
Asymmetric conical diffraction and generation of non-integer phase singularities in photonic graphene, Daohong Song¹, Sheng Liu^{2,3}, Vassilis Paltoglou⁴, Daniel Galdardo³, Liqin Tang¹, Jingjun Xu¹, Nikolaos K. Efremidis⁴, Zhigang Chen^{3,1}; ¹Nankai Univ., China; ²Northwestern Polytechnical Univ., China; ³San Francisco State Univ., USA; ⁴Univ. of Crete, Greece. We demonstrate asymmetric conical diffraction accompanied by pseudospin-mediated non-integer phase singularities when two sublattices of photonic graphene are equally excited near the Dirac points. Experimental and numerical results agree with analysis of the Dirac equation.

Executive Ballroom
210ECLEO: QELS-
Fundamental ScienceFTh3E • Light Harvesting and
Electroplasmionics—Continued

FTh3E.3 • 14:45

Plasmonic Internal Photoemission Detectors with Responsivities above 0.12 A/W, Sascha Muehlbrandt¹, A. Melikyan¹, K. Köhnle¹, T. Harter, A. Muslija¹, P. Vincze¹, S. Wolf¹, P. Jakobs¹, W. Freude¹, C. Koos¹, M. Kohl¹, Y. Fedoryshyn², J. Leuthold²; ¹Karlsruhe Inst. of Technology, Germany; ²ETH-Zurich, Switzerland. We demonstrate first plasmonic photodetectors based on internal photoemission featuring responsivities exceeding 0.12 A/W at 1550 nm. The devices consist of ultra-compact plasmonic waveguides with electrode spacing below 100 nm receiving on-off-keying signals at 40 Gbit s⁻¹.

FTh3E.4 • 15:00

Hot Electron Schottky Detection Based on Internal Photoemission in Silicon Structures, Boris Desiatov, Noa Mazurski, Joseph Shapir, Jacob Khurgin², Uriel Levy¹; ¹Hebrew Univ. of Jerusalem, Israel; ²Electrical and Computer Engineering, Johns Hopkins Univ., USA. We demonstrate the design, fabrication and characterization of plasmonic enhanced silicon photo-detector for infrared light. Theoretical model, experimental results and comparison between different geometric configurations will be presented and discussed.

FTh3E.5 • 15:15

Hot-Electron Plasmonics: Quantum Transport Limitations, Ahmet A. Yanik¹, Imran Hossain¹; ¹Univ. of California, Santa Cruz, USA. Hot-electron plasmonics has created much excitement for solar-energy harvesting. However, experimental quantum efficiencies are too low for practical applications. Here, we develop a bottom-up quantum-transport model and introduce design parameters to achieve high efficiency solar-cells.

Executive Ballroom
210FSTh3F • Microwave Photonic
Devices—Continued

STh3F.4 • 15:00

Tunable Microwave Photonic Phase Shifter Using On-Chip Stimulated Brillouin Scattering, Mattia Pagani¹, David Marpaung¹, Duk-Yong Choi², Stephen Madden², Barry Luther-Davies², Benjamin J. Eggleton¹; ¹School of Physics, Univ. of Sydney, Australia; ²Australian National Univ., Australia. We present the first microwave photonic phase shifter using on-chip stimulated Brillouin scattering. We show that shorter integrated platforms can potentially achieve lower insertion loss than fiber implementations, due to their higher pump depletion threshold.

STh3F.5 • 15:15

Photonic Generation of High-Power Pulsed Microwave Signals with Peak Powers up to 14.2 Watt, Xiaojun Xie¹, Kejia Li¹, Qinglong Li¹, Andreas Beling¹, Joe C. Campbell¹; ¹Dept. of Electrical and Computer Engineering, University of Virginia, USA. We demonstrate photonic generation of pulsed 1 GHz and 10 GHz microwave signals with peak power levels as high as 41.5 dBm (14.2 W) and 40 dBm (10 W), respectively, using a modified uni-traveling carrier (MUTC) photodiode.

Executive Ballroom
210G

CLEO: Science & Innovations

STh3G • Fabrication
Techniques I—Continued

STh3G.2 • 15:00

Fabrication of Gray-Scale Semiconductor Structures with Dynamic Digital Projection Photochemical Etching, Kaiyuan Wang¹, Chris Edwards¹, Shailendra N. Srivastava¹, Lynford L. Goddard¹; ¹Univ. of Illinois at Urbana-Champaign, USA. Digital projection photochemical etching is a novel single-step process for fabricating customized gray-scale semiconductor structures. Several features including a variable height pyramid array are fabricated, demonstrating the resolution, range, accuracy, and dynamics of the technique.

STh3G.3 • 15:15

Ultra-High Q Silicon Resonators in Planarized LOCOS, Alex Naiman¹, Boris Desiatov¹, Liron Stern¹, Noa Mazurski¹, Joseph Shapir¹, Uriel Levy¹; ¹The Hebrew Univ. of Jerusalem, Israel. We describe a modified local oxidation of silicon process as a platform for the fabrication of waveguides and ultra-high Quality factor (5.3 million) silicon resonators, with nearly fully planar interface for multilayer silicon integration

Executive Ballroom
210HSTh3H • Materials and Devices
for Nonlinear Frequency
Upconversion—Continued

STh3H.3 • 14:45

Frequency Conversion in Periodically Oriented Gallium Nitride, Steven R. Bowman¹, Christopher G. Brown², Jennifer Hite¹, Francis J. Kub¹, Charles Eddy¹, Igor Vurgaftman¹, Jerry R. Meyer¹, Jacob H. Leach³, Kevin Udaway³; ¹US Naval Research Lab, USA; ²Univ. Research Foundation, USA; ³Kyba Technologies, USA. Broadband transparency, high thermal conductivity, and strong nonlinearity make gallium nitride a promising material for high power frequency conversion. We have fabricated and tested periodically oriented gallium nitride (PO-GaN) devices for quasi-phase matched (QPM) frequency conversion.

STh3H.4 • 15:00

Violet second harmonic generation in adhered slab waveguide based on periodically poled lithium tantalate, Hwanhong Lim¹, Sunao Kurimura¹, Kazufumi Fujii¹, Masayuki Okano², Shigeki Takeuchi^{2,3}; ¹National Inst. for Materials Science, Japan; ²Kyoto Univ., Japan; ³Hokkaido Univ., Japan. We demonstrated CW SHG at 400 nm in a first-order QPM adhered slab waveguide with a periodically-poled Mg-doped stoichiometric lithium tantalate core. The measured SHG normalized conversion efficiency was 34.7%/W for a 20 mm length.

STh3H.5 • 15:15

PP-LBGO device with 2nd-order QPM structure for 266nm generation, Junji Hirohashi¹, Tetsuo Taniuchi², Koichi Imai¹, Yasunori Furukawa¹; ¹Oxide Corporation, Japan; ²FRIS, Tohoku Univ., Japan. Second harmonic 266nm generation was demonstrated by periodically-poled LaBGeO5 (PP-LBGO) with 2nd-order QPM structure. More than 15mW of 266nm was obtained from nano-second-pulsed 532nm laser. Circular beam at 266nm without walk-off was obtained.

**Meeting Room
211 B/D**

CLEO: Science & Innovations

STh3I • Optomechanics I—Continued

STh3I.4 • 14:45

Enhanced Coupling in Si₃N₄ Slot-Mode Optomechanical Crystals via Stress Tuning, Karen Grutter¹, Marcelo I. Davanco¹, Kartik Srinivasan¹; ¹NIST, USA. We demonstrate Si₃N₄ slot-mode optomechanical crystals with optical Qs up to 1.65 × 10⁵ and mechanical frequencies around 3.4 GHz. Tensile stress tunes gap widths down to 24 nm, enhancing coupling and enabling radiation-pressure-driven self-oscillation.

STh3I.5 • 15:00

Subharmonics radio-frequency division in chip-scale optomechanical oscillators, Jiagui Wu^{1,2}, Yongjun Huang^{1,3}, Mingbin Yu⁴, Dim-Lee Kwong¹, Chee Wei Wong¹; ¹Dept. Of Electrical Engineering, Univ. of California, Los Angeles, ²Mesoscopic Optics and Quantum Electronic, USA; ³Southwest Univ., School of Physics, China; ⁴School of Communication and Information Engineering, Univ. of Electronic Science and Technology of China, Centre for RFIC and System Technology, China; ⁵The Inst. of Microelectronics, Singapore. Subharmonics radio-frequency division and generation are experimentally demonstrated in nano-optomechanical cavity. The dual-coupled intracavity nonlinear optomechanical and Drude plasma oscillators demonstrate new dynamics regimes, with free-running high amplitude low-phase-noise clocking.

STh3I.6 • 15:15

Synchronization and Phase Noise Reduction in Arrays of Optomechanical Oscillators, Mian Zhang¹, Michal Lipson¹; ¹Cornell Univ., USA. We demonstrate the reduction of phase noise 10 dB below the thermomechanical noise limit of individual oscillators in arrays up to seven synchronized self-sustaining optomechanical oscillators.

**Meeting Room
212 A/C**

CLEO: Applications & Technology

ATH3J • Clinical Technologies and Systems I—Continued

ATH3J.3 • 15:00

Deuterated Cholesterol Uptake Revealed With Stimulated Raman Microscopy, Alba Alfonso Garcia¹, Simon Pfisterer², Howard Riezman³, Elina Ikonen², Eric O. Potma¹; ¹Univ. of California Irvine, USA; ²Inst. of Biomedicine, Univ. of Helsinki, Finland; ³Dept. of Biochemistry, Université de Genève, Switzerland. Cholesterol is involved in multiple vital processes, thus in multiple diseases. Synergies between coherent Raman microscopy and deuterated compounds provide the ultimate tool towards live visualization of cholesterol pathways.

ATH3J.4 • 15:15

Dynamic vocal fold imaging by integrating optical coherence tomography with laryngeal high-speed video endoscopy, Gopi Maguluri¹, Ernest Chang¹, Nicusor Iftimia¹; ¹Physical Sciences Inc., USA. We demonstrate three-dimensional vocal fold imaging during phonation by integrating optical coherence tomography with high-speed videoendoscopy. Results from ex vivo larynx experiments yield reconstructed vocal fold surface contours for ten phases of periodic motion.

**Meeting Room
212 B/D**

CLEO: Science & Innovations

STh3K • Novel Microscopy Techniques and OCT—Continued

STh3K.3 • 14:45

Towards Automated Detection of Basal Cell Carcinoma from Polarization Sensitive Optical Coherence Tomography Images of Human Skin, Tahereh Marvdashti¹, Lian Duan¹, Katherine Ransohoff¹, Sumaira Aasi¹, Jean Tang¹, Audrey Ellerbee¹; ¹Stanford Univ., USA. We report on the initial results of the first automated classifier to distinguish basal cell carcinomas and healthy skin using polarization sensitive optical coherence tomography (PS-OCT) with a sensitivity and specificity of 84.2% and 85.8%

STh3K.4 • 15:00

Phase-inverted sidelobe-annihilated optical coherence tomography to break through the temporal diffraction limit, Chi Zhang^{2,1}, Kenneth K. Y. Wong¹; ¹Univ. of Hong Kong, Hong Kong; ²Wuhan National Lab for Optoelectronics, Huazhong Univ. of Science and Technology, China. Understand the tomography system as a temporal microscopy by space-time duality, a simple adjustment was performed on a conventional swept-source optical coherence tomography (SS-OCT), and achieved sharper resolution (~4 μm) for the single layer measurement.

STh3K.5 • 15:15

Ultrafast spectral-domain optical coherence tomography realized by parametric spectro-temporal analyzer, Chi Zhang^{2,1}, Xiaoming Wei¹, Yiqing Xu¹, Jianbing Xu¹, Luoqin Yu¹, Bowen Li¹, Sisi Tan¹, Andy K. S. Lau¹, Xie Wang¹, Xing Xu¹, Kevin K. Tsia¹, Kenneth K. Y. Wong¹; ¹Univ. of Hong Kong, Hong Kong; ²Wuhan National Lab for Optoelectronics, Huazhong Univ. of Science and Technology, China. Performance of the spectral-domain optical coherence tomography is limited by its A-scan rate, namely the frame rate of spectrometer. In this paper, 60-MHz A-scan rate is achieved by adopting a recently demonstrated parametric spectro-temporal analyzer.

**Marriott
Salon I & II**

STh3L • Ultrafast Fiber Lasers—Continued

STh3L.4 • 14:45

Observing the spectral dynamics of a mode-locked laser with ultrafast parametric spectro-temporal analyzer, Xiaoming Wei¹, Chi Zhang¹, Bowen Li¹, Kenneth K. Y. Wong¹; ¹Wuhan National Lab for Optoelectronics & School of Optical and Electronic Information, Huazhong Univ. of Science and Technology, China. We experimentally observe the spectral dynamics of a passively mode-locked fiber laser by using a parametric spectro-temporal analyzer (PASTA) with a frame rate up to 100 MHz, and different non-repeating transient dynamics has been observed.

STh3L.5 • 15:00

Tutorial

Nonlinearity Engineering of Ultrafast Lasers and Laser-Material Interactions, F. Ömer Ilday^{1,2}; ¹Dept. of Electrical and Electronics Engineering, Bilkent Univ., Turkey; ²Dept. of Physics, Bilkent Univ., Turkey. From novel mode-locking regimes to laser-induced self-assembly of nanostructures, it is not only possible, but highly rewarding to exploit the underlying nonlinear dynamics of photonic systems towards achieving superior technical functionality. These different dissipative systems manifest similar phenomena, such as nonlinear gain, feedback, and modulation instability.



F. Ömer Ilday received his PhD from Cornell Univ. in 2003 and served as a postdoc at MIT until 2006. In 2006, he joined Bilkent Univ.. He has co-authored >200 journal and conference publications and has given >100 invited talks. In 2014, he was awarded an ERC Consolidator Grant.

Technical Digest and Postdeadline Papers Available Online

- Visit www.cleoconference.org
- Select Access Digest Paper link
- Use your registration email address and password

Access is provided only to full technical attendees.

CLEO: Science & Innovations

**STh3M • Fundamental
Light-material Interaction I—
Continued****STh3M.4 • 14:45**

Cavity-Enhanced Mid-IR Optical Frequency Comb Spectroscopy: Enhanced Time and Spectral Resolution, Oliver H. Heckl¹, Ben Spaun¹, Peter B. Changala¹, Bryce Bjork¹, Dave Patterson², John M. Doyle², Jun Ye¹; ¹JILA, CU Boulder, USA; ²Dept. of Physics, Harvard Univ., USA. CE-DFCS has been applied to buffer gas cooled acetylene achieving a Doppler-limited spectral resolution of 90 MHz. Additionally TRFCS allows for the detection of *trans*-DOCOC in photolysis reaction kinetics with a molecular sensitivity of 10^{10} cm⁻³

STh3M.5 • 15:00

3D Laser Ablation of Biocompatible Silk Fibroin Hydrogels for Biomedical Applications, Matthew Applegate¹, Benjamin P. Partlow¹, Jeannine Coburn¹, Jodie Moreau¹, Benedetto Marelli¹, David Kaplan¹, Fiorenzo Omenetto^{1,2}; ¹Biomedical Engineering, Tufts Univ., USA; ²Physics, Tufts Univ., USA. Voids were created inside biocompatible, optically transparent silk fibroin hydrogels via multiphoton ablation in arbitrary 3D patterns at a maximum depth of nearly 1 cm without exogenous photoinitiators.

STh3M.6 • 15:15

Super-resolution Optical Nanolithography: Beyond the far-field diffraction limit, Apratim Majumder¹, Farhana Masid¹, Benjamin Pollock², Trisha Andrew², Rajesh Menon¹; ¹Univ. of Utah, USA; ²Univ. of Wisconsin-Madison, USA. We report on overcoming the far-field diffraction limit using an approach that we call Absorbance Modulation Optical Lithography (AMOL).

**STh3N • Time and Frequency
Transfer—Continued****STh3N.4 • 14:45**

Phase Stabilized Radio Frequency Signal Transmission via Optical Fiber Link, Anxu Zhang¹, Feifei Yin¹, Yitang Dai¹, Jianqiang Li¹, Kun Xu¹; ¹Beijing Univ. of Posts and Telecommunications, China. A phase-stabilized RF transmission scheme is demonstrated with suppressed noise. A 2.48GHz signal has been transferred through a 60km optical fiber link, with stability of 8.1×10^{-14} at 1s and 1.1×10^{-16} at 2000s averaging time, respectively.

STh3N.5 • 15:00 Tutorial

Frequency and Timing Distribution using Optical Methods, Nathan R. Newbury¹; ¹NIST, USA. With the ever-increasing performance of optical clocks, it is important to develop parallel methods for optically-based frequency/timing distribution. I will review frequency combs, established methods for distribution over fiber-optics, and recent demonstrations over free-space links.



Nathan Newbury leads a group in NIST's Quantum Electronics and Photonic Division that focuses on the development and application of fiber-based frequency combs. He has received the Bronze medal, Silver medal, and Fleming award from the Department of Commerce. He is a fellow of The Optical Society.

**STh3O • Remote and Standoff
Optical Detection—Continued****STh3O.4 • 14:45**

Rapid Swept-Wavelength External Cavity Quantum Cascade Laser for Open Path Sensing, Brian Brumfield¹, Mark C. Phillips¹; ¹Pacific Northwest National Lab, USA. A rapidly tunable external cavity quantum cascade laser system is used for open path sensing. The system permits acquisition of transient absorption spectra over a 125 cm⁻¹ tuning range in less than 0.01 s.

STh3O.5 • 15:00

Low Power Integrated Path Differential Absorption Lidar Detection of CO₂, CH₄, and H₂O over a 5.5 km Path using a Waveform Driven EO Sideband Spectrometer, David F. Plusquellic¹, Gerd Wagner¹, Stephen Maxwell¹, Kevin Douglass¹, David Long¹, Joseph T. Hodges¹, Adam J. Fleisher¹; ¹NIST, USA. A rapid-scan remote-sensing spectrometer based on an arbitrary waveform driven electro-optic phase modulator for spectral scans over 37 GHz and a telescope/photon counting system for detection was used to measure long term ambient level concentrations of greenhouse gases from natural targets.

STh3O.6 • 15:15

Progress toward a high-resolution single-photon camera based on superconducting single photon detector arrays and compressive sensing, Thomas Gerrits¹, Shane Allman¹, Daniel Lum², Varun Verma¹, John Howell², Richard P. Mirin¹, Sae Woo Nam¹; ¹NIST, USA; ²Dept. of Physics and Astronomy, Univ. of Rochester, USA. We present our results on utilizing an SNSPD array and compressive imaging techniques to perform single photon imaging and present our progress toward a high-resolution single-photon camera for the mid-IR.

**Executive Ballroom
210A**

**CLEO: Applications
& Technology**

ATH3A • Symposium on Science and Technology of Laser and Three Dimensional Printing I—Continued

ATH3A.4 • 15:30

Achromatic polarization rotator imprinted in glass by ultrafast laser nanostructuring, Rudy Desmarchelier¹, Matthieu Lancry¹, Mindaugas Gecevicius², Martynas Beresna², Peter Kazansky², Bertrand Poumellec¹; ¹Universite de Paris Sud, France; ²ORC, UK. We demonstrate an achromatic polarization rotator imprinted by femtosecond laser nanostructuring in silica glass. The broadband 600-1500nm operation is achieved by replicating the structure of twisted nematic liquid crystal.

ATH3A.5 • 15:45

Characterization of melt-flow dynamics in selective laser melting (SLM) processes, Manyalibo J. Matthews¹, Sasha Rubenchik¹, Gabe Guss¹, Nielsen Norman¹; ¹Lawrence Livermore National Lab, USA. High speed microscopic imaging and thermography of stainless steel microsphere assemblies exposed to high power laser light is analyzed to understand the melt-flow dynamics associated with selective laser melting processes.

**Executive Ballroom
210B**

CLEO: QELS-Fundamental Science

FTh3B • NV – Centers for Metrology and Photonics—Continued

FTh3B.7 • 15:30 Invited

Nanoscale Magnetic Imaging using Quantum Defects in Diamond, Ronald Walsworth¹; ¹Physics, Harvard Univ., USA. I describe recent progress in nanoscale magnetic imaging using Nitrogen-Vacancy (NV) quantum defects in diamond, which provide an unparalleled combination of magnetic field sensitivity and spatial resolution in a room-temperature solid, with wide-ranging applications.

**Executive Ballroom
210C**

FTh3C • Attosecond Spectroscopy—Continued

FTh3C.4 • 15:30

Excitation Energy Dependent Attosecond Photoemission Timing in Tungsten, Michael Jobst^{1,3}, Stefan Neppel², Johann Riemensberger^{1,3}, Marcus Ossiander^{1,3}, Martin Schäffer^{1,3}, Elisabeth Bothschafter⁴, Michael Gerl^{1,3}, Andreas Kim^{3,1}, Johannes Barth³, Ferenc Krausz^{1,5}, Peter Feulner³, Reinhard Kienberger^{3,1}; ¹Max Planck Inst. for Quantum Optics, Germany; ²Ultrafast X-Ray Science Lab, Lawrence Berkeley National Lab, USA; ³Technical Univ. Munich, Germany; ⁴Paul Scherrer Institut, Switzerland; ⁵Ludwig Maximilians Univ., Germany. A multitude of physical effects have been proposed to determine the photoemission delay between core and valence electrons in tungsten. We present selected streaking experiments that clarify its origins.

FTh3C.5 • 15:45

Attosecond Transient Absorption Explores Coupling Mechanisms of Autoionizing States, Birgitta Bernhardt^{1,2}, Xuan Li¹, Annelise Beck^{1,2}, Erika R. Warrick^{1,2}, Daniel J. Haxton¹, C W. McCurdy^{1,3}, Daniel M. Neumark^{1,2}, Stephen R. Leone^{1,2}; ¹Lawrence Berkeley National Lab, USA; ²Dept. of Chemistry, UC Berkeley, USA; ³Dept. of Chemistry, UC Davis, USA. High spectral resolution attosecond transient absorption spectroscopy in xenon is used to validate quantum dynamical multi-level simulations of the on and off resonant absorption behavior of highly excited states and their strong-field induced coupling mechanisms.

**Executive Ballroom
210D**

FTh3D • Synthetic Lattices & Topological Phenomena—Continued

FTh3D.7 • 15:30

Generalized three-dimensional Dirac points and Z_2 gapless surface states in a topological photonic crystal, Ling Lu¹, Chen Fang¹, Timothy H. Hsieh¹, Liang Fu¹, Steven Johnson¹, John D. Joannopoulos¹, Marin Soljacic¹; ¹MIT, USA. We discover robust three-dimensional generalized Dirac points - linear four-fold point degeneracies - in a non-symmorphic photonic crystal readily realizable at near-infrared wavelengths. The surface states exhibit gapless line-nodes characterized by a Z_2 topological invariant.

FTh3D.8 • 15:45

Supersymmetry and transformation optics on the line, Mohammad-Ali Miri¹, Matthias Heinrich^{2,1}, Demetrios N. Christodoulides¹; ¹Univ. of Central Florida, USA; ²Inst. of Applied Physics, Abbe Center of Photonics, Friedrich-Schiller-Univ., Germany. We investigate scattering properties of supersymmetric partner structures. We show that SUSY transformations can be used as a new type of transformation optics to address inverse scattering problems in one-dimensional optical settings.

16:00–16:30 Coffee Break, Concourse Level



Join the conversation. Use #CLEO15.
Follow us @cleoconf on Twitter.

Executive Ballroom
210E

CLEO: QELS-
Fundamental Science

FTh3E • Light Harvesting and
Electroplasmonics—Continued

FTh3E.6 • 15:30

Integrated On-Chip Silicon Plasmonic Four Quadrant Detector in the Near Infrared, Meir Y. Grajower¹, Noa Mazurski¹, Boris Desiatov¹, Uriel Levy¹; ¹Hebrew Univ. of Jerusalem, Israel. We demonstrate an integrated four quadrant detector in silicon for infrared light, based on integration of plasmonic splitting, focusing an plasmonic enhanced internal photoemission detection on a single silicon plasmonic chip.

FTh3E.7 • 15:45

Controlling Plasmon Drag with Illumination and Surface Geometry, Natalia Noginova, V. Rono, A. Jackson², M. Durach³; ¹Norfolk State Univ., USA; ²Purdue Univ., USA; ³Georgia Southern Univ., USA. We study electric signals associated with surface plasmon propagation in rough and smooth silver films. The polarity of the signal can be controlled with light illumination conditions and system geometry.

Executive Ballroom
210F

STh3F • Microwave Photonic
Devices—Continued

STh3F.6 • 15:30

Impact of the Coulomb Interaction on the Franz-Keldysh Effect in a High-Current Photodetector, Yue Hu¹, Curtis R. Menyuk¹, Meredith Hutchinson², Vincent J. Urick², Keith J. Williams²; ¹Univ. of Maryland Baltimore County, USA; ²Naval Research Lab, USA. The Franz-Keldysh effect causes semiconductor absorption to oscillate as a function of wavelength. We include this effect in calculating the nonlinear response of a high-current photodetector and obtain excellent agreement with experiments.

STh3F.7 • 15:45

Improved Carrier-to-Sideband Ratio for Free Space Millimeter Wave-Coupled Electro-Optic Polymer High Speed Phase Modulators, Dong Hun Park^{1,2}, Vincent R. Pagan^{1,2}, Thomas E. Murphy², Jingdong Luo³, Alex K. Jen³, Warren N. Herman¹; ¹Lab for Physical Sciences, USA; ²Electrical and Computer Engineering, Univ. of Maryland, USA; ³Materials Science and Engineering, Univ. of Washington, USA. The carrier-to-sideband ratio was improved more than 20 dB by using a SiO₂ protection layer in antenna-coupled electro-optic phase modulators operating at 37 GHz based on an in-plane polymeric waveguide using the nonlinear polymer. We also demonstrate detection of 3-GHz modulation of the RF carrier.

Executive Ballroom
210G

CLEO: Science & Innovations

STh3G • Fabrication
Techniques I—Continued

STh3G.4 • 15:30

Improvement of Silicon Dioxide Ridge Waveguides Using Low Temperature Thermal Annealing, Josh Parks¹, Hong Cai¹, Thomas Wall², Matthew Stott², Roger Chu², Erik Hamilton², Aaron Hawkins², Holger Schmidt¹; ¹Univ. of California Santa Cruz, USA; ²Brigham Young Univ., USA. Penetration of liquids into SiO₂ ridge waveguides during standard processing steps is shown to cause poor mode confinement and increased loss. Thermal annealing repeatedly restores a core with uniform index and low-loss mode confinement.

STh3G.5 • 15:45

Photonic Damascene Process for high-Q SiN Microresonator Fabrication for Nonlinear Photonics, Martin Pfeiffer¹, Arne Kordts¹, Victor Brasch¹, Caroline Lecaplain¹, John D. Jost¹, Michael Geiselmann¹, Tobias Kippenberg¹; ¹Ecole Polytechnique Federale de Lausanne, Switzerland. Integrated microresonators based on SiN waveguides are an attractive platform for nonlinear optics. Here we present a new photonic Damascene fabrication process that solves common problems in SiN waveguide fabrication and demonstrate frequency comb formation.

Executive Ballroom
210H

STh3H • Materials and Devices
for Nonlinear Frequency
Upconversion—Continued

STh3H.6 • 15:30

Tunable Second Harmonic Generation of a Continuous-wave Carbon Dioxide Laser Using 3 mm Thick Orientation Patterned GaAs Crystals in Fan-out and Single-grating-period Configurations, Shekhar Guha¹, Jacob Barnes³, Leonel P. Gonzalez¹, Peter G. Schunemann²; ¹US Air Force Research Lab, USA; ²BAE Corporation, USA; ³UES, Inc., USA. We report room temperature frequency doubling of a continuous-wave carbon dioxide laser tuned from 9.26 to 10.65 micrometers using large-aperture OPGaAs crystals (>3 mm thick by >7.5 mm wide) in fan-out and single grating configurations.

STh3H.7 • 15:45

Third harmonic generation in ultrathin epsilon-near-zero media, Ting S. Willie Luk^{4,6}, Domenico de Ceglia², Gordon Keeler⁴, Rohit P. Prasankumar^{1,3}, Maria A. Vincenti², Sheng Liu^{4,6}, Michael Scalora⁵, Michael B. Sinclair⁴, Salvatore Campione^{4,6}; ¹Los Alamos National Lab, USA; ²National Research Council-AMRDEC, USA; ³Center for Integrated Nanotechnologies-Los Alamos National Labs, USA; ⁴Sandia National Labs, USA; ⁵Charles M. Bowden Research Lab AMRDEC, USA; ⁶Center for Integrated Nanotechnologies - Sandia National Labs, USA. We demonstrate efficient third harmonic generation from a 21.6nm indium tin oxide film on glass substrate for a pump fundamental wavelength of 1350nm using the field enhancement properties of optical modes supported by epsilon-near-zero media.

16:00–16:30 Coffee Break, Concourse Level

Meeting Room
211 B/D

CLEO: Science & Innovations

STh3I • Optomechanics I—Continued

STh3I.7 • 15:30

Frequency instability and phase noise characterization of an integrated chip-scale optomechanical oscillator, Yongjun Huang^{1,3}, Jiagui Wu^{1,2}, Xingsheng Luan², Shu-Wei Huang^{1,2}, Mingbin Yu⁴, Guo-Qiang Lo⁵, Dim-Lee Kwong⁴, Guangjun Wen⁵, Chee Wei Wong^{1,2}; ¹Electrical Engineering Dept., Univ. of California at Los Angeles, USA; ²Mechanical Dept., Columbia Univ., USA; ³Univ of Electronic Sci & Tech of China, China; ⁴The Inst. of Microelectronics, Singapore. We characterize the frequency instability and single-sideband phase noise of chip-scale optomechanically-driven oscillators, with integrated Ge photoreceivers. At 400- μ W, an open-loop frequency instability at 10^{-8} is observed, with -125 dBc/Hz phase noise at 10-kHz offset.

STh3I.8 • 15:45

Multi-stable Synchronization of Delay-Coupled Optomechanical Oscillators, Shreyas Y. Shah¹, Mian Zhang¹, Michal Lipson^{1,2}; ¹School of Electrical and Computer Engineering, Cornell Univ., USA; ²Kavli Inst. at Cornell, Cornell Univ., USA. We demonstrate synchronization between two independent optomechanical oscillators coupled through an optical delay of 138.76ns. By varying the coupling strengths, we observe multiple stable synchronised states with different frequencies, enabling applications in reconfigurable RF networks.

Meeting Room
212 A/C

CLEO: Applications & Technology

ATh3J • Clinical Technologies and Systems I—Continued

ATh3J.5 • 15:30

Imaging Patient Derived Breast Cancer Xenografts in an Orthotopic Mammary Window Chamber Model, Hui M. Leung^{1,2}, Rachel Schafer^{1,4}, Arthur F. Gmitro^{1,3}; ¹Univ. of Arizona (OSC), USA; ²College of Optical Sciences, USA; ³Dept. of Medical Imaging, Univ. of Arizona, USA; ⁴Dept. of Biomedical Engineering, Univ. of Arizona, USA. We demonstrate for the first time optical and magnetic resonance imaging of breast cancer patient derived xenografts in an orthotopic mammary window chamber model. *In vivo* imaging of oxygen saturation, apparent diffusion coefficient and blood perfusion were performed.

ATh3J.6 • 15:45

Highly Selective VOC Breath Analysis Using a 3.3 μ m Broadly-Tunable VECSEL, Jana Jággerská¹, Herbert Looser², Béla Tuzson¹, Ferdinand Felder³, Luc Tappy⁴, Lukas Emmenegger¹; ¹EMPA, Switzerland; ²FHNW, Switzerland; ³Camlin Technologies AG, Switzerland; ⁴Université de Lausanne, Switzerland. Mid-infrared VECSEL tunable over 50 cm^{-1} is employed to measure trace gas concentrations of acetone in human breath. A detection limit of 25 ppb is demonstrated without any sample preparation.

Meeting Room
212 B/D

CLEO: Science & Innovations

STh3K • Novel Microscopy Techniques and OCT—Continued

STh3K.6 • 15:30

Photothermal detection of single nanoparticle by using single element interferometer, Yuki Nagata¹, Yasuhiro Mizutani¹, Tetsuo Iwata¹, Yukitoshi Otani²; ¹The Univ. of Tokushima, Japan; ²Utsunomiya Univ., Japan. A photothermal imaging microscope for single metal nanoparticles using single element interferometer has been developed. In this report, 20-nm gold nanoparticles in scattering environment was detected selectively with SNR ~20.

STh3K.7 • 15:45

Dynamic Label-free Imaging of Live-cell Adhesion Using Photonic Crystal Enhanced Microscopy (PCEM), Yue Zhuo^{1,2}, Ji S. Choi^{3,4}, Hojeong Yu^{5,2}, Brendan A. Harley^{3,4}, Brian T. Cunningham^{1,2}; ¹Dept. of Bioengineering, Univ. of Illinois at Urbana-Champaign, USA; ²Micro and Nanotechnology Lab, Univ. of Illinois at Urbana-Champaign, USA; ³Dept. of Chemical and Biomolecular Engineering, Univ. of Illinois at Urbana-Champaign, USA; ⁴Inst. for Genomic Biology, Univ. of Illinois at Urbana-Champaign, USA; ⁵Dept. of Electrical and Computer Engineering, Univ. of Illinois at Urbana-Champaign, USA. We demonstrate label-free imaging of cell attachment upon a photonic-crystal biosensor surface. Newly-implemented image-analysis software is used to dynamically visualize individual live-cell movement and demonstrate the spatiotemporal-distribution of cellular material during adhesion and motion.

Marriott
Salon I & II

STh3L • Ultrafast Fiber Lasers—Continued

16:00–16:30 Coffee Break, Concourse Level

Technical Digest and Postdeadline Papers Available Online

- Visit www.cleoconference.org
- Select Access Digest Paper link
- Use your registration email address and password

Access is provided only to full technical attendees.

CLEO: Science & Innovations

**STh3M • Fundamental
Light-material Interaction I—
Continued****STh3M.7 • 15:30**

The optical absorption in zincblende and wurtzite GaP nanowire polytypes, Mahtab Aghaeipour¹, Nicklas Anttu¹, Gustav Nylund¹, Lars Samuelson¹, Sebastian Lehmann¹, Mats-Erik Pistol¹; ¹*Solid State Physics, Lund Univ., Sweden*. Diameter-dependent absorption resonances in semiconductor nanowires are promising for tunable detectors. Here, we show that the optical resonances for both wurtzite and zincblende GaP nanowires can be tuned down to $\lambda \approx 330$ nm by decreasing the diameter of the nanowires to 35 nm.

STh3M.8 • 15:45

Strong exciton-photon coupling in monolayer heterostructures in tunable microcavities, Stefan Schwarz¹, Scott Dufferwiel¹, Freddie Withers², Aurelien Trichet³, Feng Li¹, Caspar Clark⁴, Konstantin Novoselov², Jason M. Smith³, Maurice S. Skolnick¹, Dimitrii N. Krizhanovskii¹, Alexander Tartakovskii¹; ¹*Univ. of Sheffield, UK*; ²*Univ. of Manchester, UK*; ³*Univ. of Oxford, UK*; ⁴*Helia Photonics, UK*. Strong light-matter interaction in two-dimensional molybdenum diselenide (MoSe₂) is observed using a tunable optical microcavity. Polariton states with a Rabi splitting of 20 and 29 meV are observed for a monolayer MoSe₂ and a 'double-well' MoSe₂/hBN/MoSe₂, respectively.

**STh3N • Time and Frequency
Transfer—Continued****STh3O • Remote and Standoff
Optical Detection—Continued****STh3O.7 • 15:30**

Computational Optical Density-Density Correlation Sensing, Milad Akhlaghi Bouzan¹, Aristide Dogariu¹; ¹*CREOL, Univ. of Central Florida, USA*. Numerical and experimental results demonstrate a stochastic sensing technique based on enhancing intensity fluctuations. Statistical moments of reflectivity can be recovered, which characterize scattering from static and dynamic targets placed in random environments.

STh3O.8 • 15:45

Standoff Detection of Buried Landmines Using Genetically Engineered Fluorescent Bacterial Sensors, Yossi Kabessa¹, Ori Eyal¹, Ofer Bar-On¹, Sharon Yagur-Kroll¹, Shimshon Belkin¹, Aharon J. Agranat¹; ¹*HUJI, Israel*. A Standoff detection scheme for buried landmines and concealed explosive charges based on genetically engineered bacterial biosensors is presented. Concentrations of 4 mg/L of 2,4-DNT on soil were detected from a distance of 50 meters.

16:00–16:30 Coffee Break, Concourse Level

Executive Ballroom
210A

**CLEO: Applications
& Technology**

16:30–18:00

ATH4A • Symposium on Science and Technology of Laser Three Dimensional Printing II

President: Yves Bellouard; Ecole Polytechnique Federale de Lausanne, Switzerland

ATH4A.1 • 16:30 **Invited**

Strategies for Nanofabrication based on Optothermal Manipulation of Plasmonic Nanoparticles, Theobald Lohmüller¹; ¹Physics, LMU Munich, Germany. Optothermal manipulation of individual gold nanoparticles renders it possible to control polymerization reactions and thermal curing of polymers at the nanoscale. This can be used to synthesize polymer nanoparticles and -wires with sub-diffraction limited resolution.

ATH4A.2 • 17:00 **Invited**

Multiphoton Processing Technologies for Applications in Biology and Tissue Engineering, Jan Torgersen¹, Aleksandr Ovsianikov², Robert Liska³, Juergen Stampfl²; ¹Nanoscale Prototyping Lab, Stanford Univ., USA; ²Inst. of Materials Science and Technology, Vienna Univ. of Technology, Austria; ³Inst. of Applied Synthetic Chemistry, Vienna Univ. of Technology, Austria. Versatile micro-fabrication technologies are presented utilizing photochemistry induced by multiphoton absorption of ultra-short laser pulses. Processing novel biophotopolymers, we show how customized cell microenvironments can be fabricated mimicking the complexity of the natural extra-cellular matrix.

Executive Ballroom
210B

CLEO: QELS-Fundamental Science

16:30–18:30

FTh4B • Quantum Memories

President: Irina Novikova; College of William & Mary, USA

FTh4B.1 • 16:30

Bad Cavities for Good Memories: Storing Broadband Photons with Low Noise, Joshua Nunn¹, Tessa F. Champion¹, Joseph Munns^{1,2}, Cheng Qiu^{1,3}, Dylan Saunders¹, Ian A. Walmsley¹; ¹Univ. of Oxford, UK; ²Physics, Imperial College, UK; ³Physics, East China Normal Univ., China. Quantum memories are vital for synchronising photonic operations. Broadband, room-temperature storage in Raman memories is hampered by four-wave mixing noise. Here we show how to eliminate the noise with a low-finesse cavity.

FTh4B.2 • 16:45

Complete Control of Frequency-Time Correlation of Narrow-Band Biphotons from Cold Atoms, Young-Wook Cho^{1,2}, Kwang-Kyoon Park¹, Jong-Chan Lee¹, Yoon-Ho Kim¹; ¹Pohang Univ. of Science and Technology (POSTECH), Korea; ²Quantum Science, Centre for Quantum Computation and Communication Technology, Australia. The nonclassical photon pair is naturally endowed with a specific form of frequency-time quantum correlations. Here, we report complete control of time quantum correlations of narrowband biphotons generated in a cold atomic ensemble.

FTh4B.3 • 17:00

Optical Nanofibers as Light-Matter Interfaces for Quantum Networks, Baptiste Gouraud¹, Dominik Maxein¹, Adrien Nicolas¹, Olivier Morin^{1,2}, Julien Laurat¹; ¹Laboratoire Kastler Brossel, UPMC-Sorbonne Universités, CNRS, ENS-PSL Research Univ., Collège de France, France; ²Max-Planck-Institut für Quantenoptik, Germany. We report the single-photon-level storage of light tightly guided in an optical nanofiber. Our setup is based on electromagnetically induced transparency for atoms interacting with the evanescent field surrounding the nanofiber.

Executive Ballroom
210C

16:30–18:30

FTh4C • Attosecond Dynamics and Strong-field Interactions

President: François Légaré; INRS-Energie Mat & Tele Site Varennes, Canada

FTh4C.1 • 16:30

Attosecond Spectroscopy of Band-gap Dynamics, Martin Schultze¹, Krupa Ramasasha², Annkatrin Sommer¹, Das Pemmaraju³, Shunsuke Sato⁴, Desiré Whitmore², Andrey Gandman², James S. Prell², Lauren J. Borja², David Prendergast³, Daniel M. Neumark², Stephen R. Leone², Ferenc Krausz¹, Elisabeth Bothschafter¹, Kazuhiro Yabana⁴; ¹Max Planck Institut fuer Quantenoptik, Germany; ²Chemistry, UC Berkeley, USA; ³The Molecular Foundry, USA; ⁴Graduate School of Pure and Applied Sciences, Univ. of Tsukuba, Japan. Attosecond solid state spectroscopy tracks electronic excitation mechanisms in solids. Here the technique is used to show that few-cycle laser pulses can create a transient metallization in dielectrics or permanent population transfer in semiconductors both with sub-femtosecond response time.

FTh4C.2 • 16:45

Using Attosecond Transient Absorption to Study Non-Adiabatic Molecular Dynamics, Chen-Ting Liao¹, Xuan Li², Daniel J. Haxton², C W. McCurdy^{3,2}, Arvinder Sandhu^{4,1}; ¹College of Optical Sciences, Univ. of Arizona, USA; ²Chemical Sciences Division, Lawrence Berkeley National Lab, USA; ³Dept. of Chemistry, Univ. of California, USA; ⁴Dept. of Physics, Univ. of Arizona, USA. We investigate superexcited Oxygen using attosecond transient absorption. Spectral lineshape evolution is used to resolve the autoionization dynamics and strong-field control is explored. We find that the symmetry of electronic states plays an important role.

FTh4C.3 • 17:00

Photoionization Time Delay Dynamics in Noble Gase, Sebastian Heuser¹, Mazyar Sabbar¹, Robert Boge¹, Matteo Lucchini¹, Lukas Gallmann², Claudio Cirelli¹, Ursula Keller¹; ¹Physics Dept., ETH Zurich, Switzerland; ²Inst. of Applied Physics, Univ. of Bern, Switzerland. For the first time, we implemented both RABBITT and attosecond energy streaking using an AttoCOLTRIMS apparatus and exploit its advantages to determine energy- and angle-resolved single-photon ionization time delays for different noble gases.

Executive Ballroom
210D

16:30–18:30

FTh4D • Quantum and Fundamental Phenomena

President: Zhigang Chen; San Francisco State Univ., USA

FTh4D.1 • 16:30 **Tutorial**

Probing and Controlling Quantum Matter in Crystals of Light, Immanuel Bloch^{1,2}; ¹Max-Planck-Institut für Quantenoptik, Germany; ²Fakultät für Physik, Ludwig Maximilians Univ., Germany. The tutorial will focus on the remarkable opportunities offered by ultracold quantum gases trapped in optical lattices to address fundamental physics questions ranging from condensed matter physics over statistical physics to high energy physics with table-top experiment.



Immanuel Bloch is scientific director at the Max-Planck-Inst. of Quantum Optics, Garching and professor for experimental physics at the Ludwig-Maximilians Univ. in Munich. Bloch received several international prizes for his work, among them the Senior Prize for Fundamental Aspects of Quantum Electronics and Optics and the Körber European Science Prize.

Executive Ballroom
210ECLEO: QELS-
Fundamental Science

16:30–18:30

FTh4E • Nanophotonics
for Thermal Transfer and
Wavguiding

Presider: Dordaneh Etezadi;
EPFL, Switzerland

FTh4E.1 • 16:30 **Invited**

Near-Field Radiative Heat Transfer between Integrated Nanostructures using Silicon Carbide, Raphael St-Gelais¹, Linxiao Zhu², Biswajeet Guha¹, Shanhui Fan², Michal Lipson¹; ¹Cornell Univ., USA; ²Stanford Univ., USA. We present the first experimental demonstration near-field radiative heat transfer using silicon carbide. We achieve a 110× near-field enhancement, relative to the far-field limit, of the radiative heat transfer between integrated nanostructures.

FTh4E.2 • 17:00

The analog of superradiant emission in quantum emitters leads to the well-known superradiant, Ming Zhou¹, Soongyu Yi¹, Ting S. Willie Luk², Qiaoqiang Gan³, Zongfu Yu¹; ¹Electrical and Computer Engineering, Univ. of Wisconsin at Madison, USA; ²Sandia National Labs, USA; ³Electrical and Computer Engineering, State Univ. of New York at Buffalo, USA. The superradiant spontaneous emission is caused by the collective interaction of quantum emitters. Such collective interaction also exists in nanoscale resonant thermal emitters, resulting in the analog of superradiance in thermal emission.

Executive Ballroom
210F

CLEO: Science & Innovations

16:30–18:30

STh4F • Photonic, Microwave
Signal Processing

Presider: Takahide Sakamoto;
NICT, Japan

STh4F.1 • 16:30

DPSK Demodulation Using Coherent Perfect Absorption, Richard R. Grote^{2,1}, Jacob M. Rothenberg², Jeffrey B. Driscoll², Richard M. Osgood²; ¹Univ. of Pennsylvania ESE Dept., USA; ²Microelectronics Sciences Labs, Columbia Univ., USA. We propose a scheme for on-chip DPSK demodulation with balanced detection by using coherent perfect absorption (CPA) in a microring resonator. Device operation is demonstrated with finite-difference time-domain simulations.

STh4F.2 • 16:45

Continuous 119.2-GSample/s Photonic Compressed Sensing of Sparse Microwave Signals, Jasper Stroud¹, Bryan Bosworth¹, Dung Tran¹, Timothy McKenna², Thomas Clark², Trac Tran¹, Sang Chin¹, Mark A. Foster¹; ¹Johns Hopkins Univ., USA; ²Johns Hopkins Applied Physics Lab, USA. We demonstrate 119.2-GSample/s compressive microwave frequency detection using spectrally-encoded ultrafast laser pulses. We sense sparse tones over > 35-GHz instantaneous bandwidth with 2-MHz accuracy using < 300 consecutive compressive measurements acquired at a 400-MHz rate.

STh4F.3 • 17:00

Experimental Demonstration of Arbitrary Waveform Generation Using Anamorphic Stretch Transform, Gao hongbiao^{1,2}, Mohammad Asghari², Bahram Jalali²; ¹Tsinghua Univ., China; ²Univ. of California, Los Angeles, USA. We experimentally demonstrate, for the first time, that using anamorphic stretch transform, the time-bandwidth product of photonic-assisted time-stretch arbitrary waveform generation can be greatly increased above the fundamental limit set by the spectral encoding.

Executive Ballroom
210G

16:30–18:30

STh4G • Fabrication
Techniques II

Presider: Zhaowei Liu; Univ. of
California, San Diego, USA

STh4G.1 • 16:30

Metamaterials Assembled by Light, Sui Yang^{1,2}, Xingjie Ni¹, Xiaobo Yin¹, Boubacar Kante¹, Yuan Wang¹, Xiang Zhang^{1,2}; ¹NSF Nano-scale Science and Engineering Center (NSEC), Univ. of California Berkeley, USA; ²Materials Sciences Division, Lawrence Berkeley National Lab, USA. Metamaterials are designed to achieve unprecedented light-matter interactions. Here we demonstrate a novel viable and scalable assembly route to optical metamaterials with structures dictated by their own light-matter interactions.

STh4G.2 • 16:45

Self-assembled Micro-reflectors for Signal Enhancement in Fluorescence Microscopy, Zoltán Göröcs¹, Euan McLeod¹, Shiv Acharya¹, Aydogan Ozcan^{1,2}; ¹Electrical Engineering, UCLA, USA; ²Bioengineering, UCLA, USA. Three-fold enhancement of fluorescent light collection in low numerical aperture optical systems is demonstrated using self-assembled micro-reflectors around individual micro-particles.

STh4G.3 • 17:00

Electrospun dye-doped fiber networks: Lasing emission from randomly distributed cavities, Sarah Kraemmer¹, Christoph Vanhame², Cameron L. Smith², Tobias Grossmann¹, Michael Jenne¹, Stefan Schierle¹, Lars Jørgensen³, Minh Tran¹, Anders Kristensen², Ioannis Chronakis³, Heinz Kalt¹; ¹Inst. of Applied Physics, Karlsruhe Inst. of Technology, Germany; ²Dept. of Micro- and Nanotechnology, Technical Univ. of Denmark, Denmark; ³DTU Food, Technical Univ. of Denmark, Denmark. Dye-doped polymer fiber networks fabricated with electrospinning exhibit comb-like laser emission. We identify randomly distributed ring resonators being responsible for lasing emission by making use of spatially resolved spectroscopy. Numerical simulations confirm this result quantitatively.

Executive Ballroom
210H

16:30–18:30

STh4H • Novel Applications and
Phenomena of Nonlinear Optics

Presider: Valentin Petrov; Max
Born Institute, Germany

STh4H.1 • 16:30

Highly Efficient Backward Stimulated Polariton Scattering in Periodically Poled KTiOPO₄, Hoon Jang¹, Andrius Zukauskas¹, Carlota Canalias¹, Valdas Pasiskevicius¹; ¹Royal Inst. of Technology (KTH), Sweden. X(2)-nonlinearity enhanced by crystal lattice contribution in the THz-region is behind backward stimulated polariton scattering with efficiencies exceeding 50% in PPKTP where forward scattering process is suppressed. 10-times compression of counter-propagating signal is observed.

STh4H.2 • 16:45

Laser Induced Damage Thresholds of KTiOPO₄ and Rb:KTiOPO₄ at 1 μm and 2 μm, Riaan Stuart Coetzee¹, Nicky Thilmann¹, Andrius Zukauskas¹, Carlota Canalias¹, Valdas Pasiskevicius¹; ¹Royal Inst. of Technology (KTH), Sweden. Optimum design of high-energy parametric down-conversion schemes mandate investigation of nanosecond laser-induced damage threshold in KTiOPO₄ and Rb:KTiOPO₄ at 1.064 μm and 2 μm. A surface damage threshold of 10 J/cm² at 2 μm was determined for both materials.

STh4H.3 • 17:00

Enhanced Spontaneous Raman Signal Collected Evanescently by Silicon Nitride Slot Waveguides, Ashim Dhakal¹, Frederic Peyskens¹, Ananth Subramanian¹, Nicolas Le Thomas¹, Roel Baets¹; ¹INTEC, Univ. of Ghent, Belgium. We investigate the effect of waveguide geometry on the conversion efficiency of Raman signals collected by integrated photonic waveguides. Compared to strip-type photonic wires, we report a six-fold increase in conversion efficiency for silicon-nitride slot-waveguides.

**Meeting Room
211 B/D**

CLEO: Science & Innovations

16:30–18:30
STh4I • Optomechanics II
Presider: Peter Rakich; Yale Univ., USA

STh4I.1 • 16:30
Chip-based Silica Microspheres for Cavity Optomechanics, Xue-Feng Jiang¹, Mark Kuzyk¹, Thein Oo¹, Hailin Wang¹; ¹Univ. of Oregon, USA. We realized on-chip silica microspheres, featuring excellent thermal coupling to the silicon-wafer. These chip-based microspheres can overcome the problem of thermal bistability and are especially suitable for optomechanical studies in vacuum or at low temperature.

STh4I.2 • 16:45
An Optomechanical Induced Short Pulse Raman Laser, Wenyan Yu¹, Wei Jiang², Qiang Lin^{2,3}, Tao Lu¹; ¹Univ. of Victoria, Canada; ²Inst. of Optics, Univ. of Rochester, USA; ³Electrical and Computer Engineering, Univ. of Rochester, USA. We observed pulsations of Raman lasing on an optomechanically oscillating silica microsphere. The harmonic tones from the oscillation regeneratively produce 223.5-ns-width Raman laser pulses above a pump threshold of 186 μ W.

STh4I.3 • 17:00
Strong Mechanical Nonlinearity of Optomechanically Driven Suspended Photonic Crystal Membrane, Pui-Chuen Hui^{1,2}, Alejandro Rodriguez³, David Woolf⁴, Eiji Iwase⁵, Mughees Khan⁶, Federico Capasso¹, Marko Loncar¹; ¹School of Engineering and Applied Sciences, Harvard Univ., USA; ²Wellman Center for Photomedicine, Massachusetts General Hospital, USA; ³Dept. of Electrical Engineering, Princeton Univ., USA; ⁴Physical Sciences Inc, USA; ⁵Dept. of Applied Mechanics and Aerospace Engineering, Waseda Univ., Japan; ⁶Wyss Inst. for Biologically Inspired Engineering, Harvard Univ., USA. We demonstrated the nonlinear mechanics of an optomechanically driven silicon membrane suspended 100nm over a nearby substrate. The estimated optical force-induced Duffing nonlinearity is 10^{28} Hz²/m², significantly larger than that afforded by the nonlinear Casimir potential.

**Meeting Room
212 A/C**

CLEO: Applications & Technology

16:30–18:30
ATH4J • Clinical Technologies and Systems II
Presider: Yuankai Tao; Cole Eye Inst. Cleveland Clinic, USA

ATH4J.1 • 16:30 Invited
Blood Coagulation Sensing at the Point of Care, Seemantini K. Nadkarni^{1,2}; ¹Harvard Medical School, USA; ²Wellman Center for Photomedicine, Massachusetts General Hospital, USA. We describe a new approach that measures a patient's coagulation status at the bedside from laser speckle fluctuations. This technology addresses the critical unmet need to manage patients at risk of life-threatening hemorrhage.

ATH4J.2 • 17:00 Invited
Multi-spectral Imaging for Determining End-point of Photo-thermal Damage on Tissue, Do-Hyun Kim¹; ¹Food and Drug Administration, USA. Multi-spectral imaging (MSI) and its analysis methods were investigated to determine end-point of photothermal damage of tissue. MSI revealed denatured porcine tissue after irradiation of laser with irradiance lower than photothermal damage threshold.

**Meeting Room
212 B/D**

CLEO: Science & Innovations

16:30–18:30
STh4K • Super-resolution Imaging
Presider: Dmitry Dylov; GE Global Research, USA

STh4K.1 • 16:30 Tutorial
Accelerating Localisation Microscopy, Susan Cox¹; ¹King's College London, UK. Fluorescence localisation microscopy is a powerful tool for imaging cell structures at a lengthscale of tens of nm, but its utility for live cell imaging is limited, as it takes a long time to acquire the data needed for a super-resolution image. However, the data acquisition time can be cut by more than two orders of magnitude by using advanced algorithms which can analyse dense data. Different algorithms offer tradeoffs between acquisition and processing time, and quality of the fitted data.



Susan Cox leads a research group at King's College London developing new high speed super-resolution microscopy techniques, and applying them to imaging cytoskeletal dynamics. Following a PhD at Cambridge and postdoctoral fellowships at Los Alamos and King's, she was awarded a Royal Society Univ. Research Fellowship in 2011.

**Marriott
Salon I & II**

16:30–18:30
STh4L • Fiber Lasers
Presider: Ming-lie Hu; Tianjin Univ., China

STh4L.1 • 16:30
Cladding-pumped Yb-doped Fiber Laser with Vortex Output Beam, Din Lin¹, W.A. Clarkson¹; ¹Univ. of Southampton, UK. A simple technique for selectively generating a donut-shaped LP11 mode with vortex phase front in a cladding-pumped ytterbium-doped fiber laser is reported. The laser yielded 36W of output with a slope efficiency of 74%.

STh4L.2 • 16:45
All-fiber passively Q-switched fiber laser based on the multimode interference effect, Quan Sheng¹, Xiushan Zhu², Wei Shi^{1,3}, Jianquan Yao^{1,3}, Robert Norwood², Nasser Peyghambarian²; ¹College of Precision Instrument and Optoelectronics Engineering, Tianjin Univ., China; ²College of Optical Sciences, Univ. of Arizona, USA; ³Tianjin Inst. of Modern Laser & Optics Technology, China. An all-fiber passively Q-switched Er-Yb co-doped fiber laser (EYDFL) using a single mode-multimode-single mode (SMS) fiber structure based on the multimode interference (MMI) effect was proposed and experimentally demonstrated for the first time.

STh4L.3 • 17:00
Enhancement of OCT Imaging Depth by Pulse-modulated Dispersion-tuned Swept Fiber Laser, Yuya Takubo¹, Shinji Yamashita¹; ¹Meguro-ku, Japan. The linewidth of dispersion-tuned fiber laser was improved by pulse modulation. The laser was applied to swept-source optical coherence tomography system and images with deeper imaging range were obtained.

CLEO: Science & Innovations

16:30–18:30

STh4M • Fundamental Light-material Interaction II*Presider: Tsing-Hua Her; Univ of North Carolina at Charlotte, USA*

STh4M.1 • 16:30

First-principles calculations for ultrafast laser-induced damage in dielectrics, Shunsuke Sato¹, Kazuhiro Yabana¹, Yasushi Shinohara², Tomohito Otobe³, Kyung-Min Lee³, George F. Bertsch⁴, ¹Univ. of Tsukuba, Japan; ²Max Planck Inst., Germany; ³Inst. for Basic Science, Korea; ⁴Univ. of Washington, USA; ⁵Japan Atomic Energy Agency, Japan. Irradiation of intense and ultrashort laser pulses on dielectric surface is calculated using a first-principles theory. It is found that calculated energy distribution transferred from light to matter explains measured laser damage threshold.

STh4M.2 • 16:45

Doping-controlled Coherent Electron-Phonon Coupling in Vanadium Dioxide, Kannatassen Appavoo^{2,1}; ¹Vanderbilt Univ., USA; ²Center for Functional Nanomaterials, Brookhaven National Lab, USA. Broadband femtosecond transient spectroscopy and density functional calculations reveal that substitutional tungsten doping of a phase-change thin-film of vanadium dioxide modifies the coherent phonon response compared to the undoped film due to altered electronic and structural dynamics.

STh4M.3 • 17:00

Unusual Conductivity Increase Related to UV-light Assisted Domain Inversion in Mg-doped Lithium Niobate Crystals, Xiaojie Wang¹, Fang Bo¹, Shaolin Chen¹, Jing Chen¹, Yongfa Kong¹, Jingjun Xu¹, Guoquan Zhang¹; ¹Nankai Univ., China. We observed an unusual conductivity increase during and after the ultraviolet-light assisted domain inversion in Mg-doped lithium niobate crystals, which may be related to the dislocation of Nb ions during the domain inversion process.

16:30–18:30

STh4N • Micro and GHz Combs*Presider: Franklyn Quinlan; NIST, USA*STh4N.1 • 16:30 **Invited**

Photonic Chip Based Optical Frequency Comb Using Soliton Induced Cherenkov Radiation, Victor Brasch¹, Michael Geiselmann¹, Tobias Herr², Grigoriy Lihachev², Martin Pfeiffer¹, Michael Gorodetsky², tobias kippenberg¹; ¹EPFL, Switzerland; ²Moscow State Univ., Russia; ³CSEM, Switzerland. We show for the first time a fully coherent frequency comb generated in a SiN photonic chip which spans 2/3 of an octave using solitons and soliton induced Cherenkov radiation. Additionally we stabilize the spectrum.

STh4N.2 • 17:00

Parametric soliton formation in narrow-band laser-gain driven microresonators, Yanan H. Wen¹, Michael Lamont¹, Alexander L. Gaeta¹; ¹Cornell Univ., USA. We investigate comb formation in laser-gain driven microresonators for various gain bandwidths and show that broadband cavity solitons exist for gain as narrow as one cavity mode, in close correspondence to parametric frequency combs.

16:30–18:30

STh4O • Optical Sensing Techniques for Combustion and Energy Research*Presider: Gerard Wysocki; Princeton Univ., USA*STh4O.1 • 16:30 **Tutorial**

Advances in Tunable Diode Laser Absorption Spectroscopy (TDLAS) for Measurements of Gas Properties in Combustion Systems, Ronald K. Hanson¹; ¹Stanford Univ., USA. Laser absorption is ideal for monitoring reactive systems with applications ranging from fundamental studies of combustion chemistry to control of power plant emissions. Sensor design, new schemes for sensitivity in harsh environments, and successful applications are reviewed.



Ronald Hanson, the Woodard Professor of mechanical engineering at Stanford Univ., has advised over 95 PhD students in the fields of laser diagnostics and laser-based sensors, shock wave physics and combustion chemistry. He is a Fellow of AIAA, ASME and The Optical Society, a member of NAE, and a gold medal award winner of the Combustion Inst.



Executive Ballroom
210A

CLEO: Applications
& Technology

ATH4A • Symposium on Science and Technology of Laser Three Dimensional Printing II—Continued

ATH4A.3 • 17:30 Invited
Hybrid Subtractive and Additive Micro-manufacturing using Femtosecond Laser for Fabrication of True 3D Biochips, Koji Sugioka¹, Dong Wu¹, Jian Xu¹, Felix Sima¹, Katsumi Midorikawa¹; ¹RIKEN Center for Advanced Photonics, Japan. We propose conjugation of subtractive and additive 3D manufacturing using femtosecond laser for fabrication of functional biochips. Specifically, femtosecond laser 3D glass micromachining followed by two-photon polymerization are performed to realize true 3D biochips.

Executive Ballroom
210B

CLEO: QELS-Fundamental Science

FTh4B • Quantum Memories—Continued

FTh4B.4 • 17:15
THz-bandwidth molecular memories for light, Philip J. Bustard¹, Jennifer Erskine¹, Duncan England¹, Rune Lausten¹, Benjamin Sussman¹; ¹National Research Council Canada, Canada. We use the vibrational levels of hydrogen molecules as a memory for light to store 100-fs pulses. We also demonstrate non-classical correlations in an emissive quantum memory using rotational levels of hydrogen molecules.

FTh4B.5 • 17:30
Storage and retrieval of ultrafast single photons using a room-temperature diamond quantum memory, Kent Fisher¹, Duncan England², Jean-Philippe Maclean¹, Phillip Bustard², Rune Lausten², Kevin J. Resch¹, Benjamin Sussman²; ¹Univ. of Waterloo, Canada; ²National Research Council of Canada, Canada. We experimentally demonstrated the storage and retrieval of THz-bandwidth single photons in a room-temperature diamond quantum memory. We have shown that the non-classical nature of retrieved light is preserved by the memory process.

FTh4B.6 • 17:45
Scalable Integration of Solid State Quantum Memories into a Photonic Network, Sara L. Mouradian¹, Tim Schroder¹, Carl B. Poitras², Luozhou Li¹, Jordan Goldstein¹, Edward Chen¹, Jiabao Zheng³, Igal Bayn³, Jacob Mower¹, Nicholas C. Harris¹, Andrew Dane¹, Karl K. Berggren¹, Michal Lipson², Dirk R. Englund¹; ¹MIT, USA; ²EECS, Cornell Univ., USA; ³Columbia Univ., USA. Single nitrogen vacancy centers in nanostructured diamond form high quality nodes integrated into low-loss photonic circuitry, enabling on-chip detection and signal manipulation. Pre-selection provides near-unity yield. Long coherence times are demonstrated in integrated nodes.

Executive Ballroom
210C

FTh4C • Attosecond Dynamics and Strong-field Interactions—Continued

FTh4C.4 • 17:15
Structure Tomography of Argon Trimer with Laser-Driven Coulomb Explosion Imaging, Chengyin Wu¹, Xiguo Xie¹, Qihuang Gong¹; ¹Peking Univ., China. The structure distribution of argon trimer was experimentally reconstructed with laser-driven Coulomb explosion imaging technique and compared with our finite-temperature ab initio calculations.

FTh4C.5 • 17:30
Explosion Dynamics of Methane Clusters Irradiated by 38 nm XUV Laser Pulses, Ahmed M. Helal^{2,1}, Sandra Bruce^{2,1}, Hernan J. Quevedo^{2,1}, Aaron C. Bernstein^{2,1}, John Keto^{2,1}, Todd Ditmire^{2,1}; ¹Univ. of Texas at Austin, USA; ²Center for High Energy Density Science, USA. Explosions of methane clusters using 38 nm XUV laser pulses were studied. Ion fragmentation dynamics depends upon cluster size. Coulomb explosion of protons followed by recombination of methane fragments has been observed.

FTh4C.6 • 17:45
Direct Observation of Rescattering from Strong Field Ionization by Two-Color Circularly Polarized Laser Fields, Christopher A. Mancuso^{1,2}, Daniel Hickstein^{1,2}, Patrik Grychtol^{1,2}, Ronny Knut^{1,2}, Ofer Kfir³, Xiao-Min Tong⁴, Franklin Dollar^{1,2}, Dmitry Zusin^{1,2}, Maitreyi Gopalakrishnan^{1,2}, Christian Gentry^{1,2}, Emrah Turgut^{1,2}, Jennifer Ellis^{1,2}, Ming-Chang Chen⁵, Avner Fleischer^{3,6}, Oren Cohen³, Henry C. Kapteyn^{1,2}, Margaret M. Murnane^{1,2}; ¹Univ. of Colorado at Boulder, USA; ²JILA, USA; ³Physics, Solid State Inst., Israel; ⁴Division of Material Science, Univ. of Tsukuba, Japan; ⁵Inst. for Photonics Technologies, National Tsing Hua Univ., Taiwan; ⁶Physics and Optical Engineering, Ort Braude College, Israel. The photoelectron distribution from strong field ionization by a two-color counter-rotating circularly polarized laser field uniquely exhibits distinct low-energy features. These can be attributed to electron-ion Coulomb rescattering, providing a new window into this process.

Executive Ballroom
210D

FTh4D • Quantum and Fundamental Phenomena—Continued

FTh4D.2 • 17:30
Bloch Oscillations of Einstein-Podolsky-Rosen States, Maxime Lebugle¹, Markus Gräfe¹, René Heilmann¹, Armando Perez-Leija¹, Stefan Nolte¹, Alexander Szameit¹; ¹Inst. of Applied Physics, Abbe School of Photonics, Friedrich-Schiller Universität Jena, Germany. We report on the first experimental observation of Bloch Oscillations of nonlocal quantum states. Our integrated photonic circuit could serve as a platform for quantum simulation of the dynamics of bosonic, anyonic and fermionic particles.

FTh4D.3 • 17:45
Optically tunable entangled photon state generation in a nonlinear directional coupler, Frank Setzpfandt^{1,2}, Alexander S. Solntsev¹, James Titchener¹, Che W. Wu¹, Chunle Xiong³, Thomas Pertsch², Roland Schiek⁴, Dragomir N. Neshev¹, Andrey A. Sukhorukov¹; ¹Centre for Ultrahigh Bandwidth Devices for Optical Systems (CUDOS) and Nonlinear Physics Centre, Research School of Physics and Engineering, Australian National Univ., Australia; ²Inst. of Applied Physics, Abbe Center of Photonics, Friedrich-Schiller-Universität Jena, Germany; ³CUDOS, the Inst. of Photonics and Optical Science (IPOS), School of Physics, Univ. of Sydney, Australia; ⁴Univ. of Applied Sciences Regensburg, Germany. We propose and experimentally demonstrate an all-optically tunable biphoton quantum light source using a nonlinear directional coupler. The source can generate high-fidelity NOON states, completely split states, and states with variable degrees of entanglement.



For Conference News & Insights
 Visit blog.cleoconference.org

Executive Ballroom
210ECLEO: QELS-
Fundamental ScienceFTh4E • Nanophotonics
for Thermal Transfer and
Waveguiding—Continued

FTh4E.3 • 17:15

Near complete violation of detailed balance in thermal radiation, Linxiao Zhu¹, Shanhui Fan¹; ¹Stanford Univ., USA. We introduce general principles for maximally violating detailed balance in thermal radiation. We validate these principles by direct calculations, based on fluctuational electrodynamics, on thermal emitters constructed from magneto-optical photonic crystals.

FTh4E.4 • 17:30

Controlling Guided Waves In Telecom Waveguides Using One Dimensional Phased Antenna Arrays, Zhaoyi Li¹, Myoung Hwan Kim¹, Nanfang Yu¹; ¹Columbia Univ., USA. We theoretically demonstrate a few novel small-footprint and broadband integrated photonic devices based on optical waveguides patterned with phased antenna arrays. These devices include waveguide mode converters, polarization rotators, perfect absorbers, and optical power diodes.

FTh4E.5 • 17:45

Epsilon-near zero wave diffraction in the optical domain, Daniel Ploss¹, Arian Kriesch^{1,2}, Jakob Naeger¹, Ulf Peschel¹; ¹Inst. of Opt., Information and Photonics (IOIP), Cluster of Excellence Engineering of Adv. Opt. Mat. (EAM) and Graduate School in Adv. Opt. Technology (SAOT) and MPL, Friedrich Alexander Univ. Erlangen-Nuremberg, Germany; ²Applied Physics and Material Sciences, California Inst. of Technology, USA. We experimentally demonstrate wave propagation in 2D nanophotonic epsilon-near-zero (ENZ) waveguides. We show an ENZ double-slit experiment, investigate ENZ diffraction and observe the disappearance of wavelength-scale obstacles close to the cut-off of the waveguide mode.

Executive Ballroom
210FSTh4F • Photonic, Microwave
Signal Processing—Continued

STh4F.4 • 17:15

Novel Photonic Radio-frequency Arbitrary Waveform Generation based on Photonic Digital-to-Analog Conversion with Pulse Carving, Jinxin Liao¹, Boyu Chen¹, Shangyuan Li¹, Xiao Yang¹, Xiaoping Zheng¹, Hanyi Zhang¹, Bingkun Zhou¹; ¹Tsinghua Univ., China. We firstly propose a photonic radio-frequency arbitrary waveform generator based on photonic digital-to-analog conversion with pulse carving, and demonstrate 10GS/s 4-bit resolution arbitrary waveform generations with 15GHz and 30GHz up-converting.

STh4F.5 • 17:30

All-Optical Optomechanical Modulation Enabling Real-Time Signal Tracking, Jianguo Huang^{1,2}, Bin Dong², Hong Cai³, Jiuhui Wu¹, Tianning Chen¹, Yuandong Gu³, Ai-Qun Liu²; ¹Xian Jiaotong Univ., China; ²Nanyang Technological University, Singapore; ³Inst. of Microelectronics, A*STAR, Singapore. We present a novel all-optical light tracker by taking advantage of the nonlinear optomechanical signal amplification and modulation, which can transfer the information carried by a signal light to tracking light without electro-optical converting.

STh4F.6 • 17:45

Towards Highly Linear Intensity Modulator for High Resolution Photonic ADCs Using a Three-Section Mode-Locked Laser, Edris Sarailou¹, Peter J. Delfyett¹; ¹College of Optics and Photonics, CREOL, Univ. of Central Florida, USA. A novel highly linear intensity modulator is proposed using an injection-locked three-section mode-locked laser. Modulating the passive section of the mode-locked laser reduces V_{π} to 1.1 mV and should greatly increase SFDR.

Executive Ballroom
210GSTh4G • Fabrication
Techniques II—Continued

STh4G.4 • 17:15

Withdrawn

STh4G.5 • 17:30

Light-induced Material Displacement in Polymer Films: A New Tool for Optical Materials Structuring, Emanuele Orabona¹, Pasqualino Maddalena¹, Antonio Ambrosio^{1,2}; ¹CNR-SPIN, Italy; ²School of Engineering and Applied Sciences, Harvard Univ., USA. Isomerization cycles of light-activated molecular switches in a polymeric matrix can result into the polymer surface structuring with nanometric resolution. This still debated phenomenon allows designing and realizing complex architectures in plasmonic and photonic devices.

STh4G.6 • 17:45

Etch-Free Patterning of PEDOT:PSS for Optoelectronics, Steven A. Rutledge¹, Amr S. Helmy¹; ¹Univ. of Toronto, Canada. A process was developed to enable polymer-based optoelectronics without need for any etch steps. The process root causes were established using optical spectroscopy. It was then used to fabricate OLED arrays and touch sensor matrices.

Executive Ballroom
210HSTh4H • Novel Applications
and Phenomena of Nonlinear
Optics—Continued

STh4H.4 • 17:15

Inhibiting Stimulated Brillouin Scattering in a Highly Nonlinear Waveguide, Moritz Merklein¹, Irina Kabakova¹, Thomas Buettner¹, Duk-Yong Choi², Stephen Madden², Barry Luther-Davies², Benjamin J. Eggleton¹; ¹CUDOS/IPOS, Univ. of Sydney, Australia; ²CUDOS, Laser Physics Centre, Australian National Univ., Australia. We demonstrate the inhibition of stimulated Brillouin scattering using a Bragg grating in a highly nonlinear chalcogenide rib waveguide on a chip.

STh4H.5 • 17:30

Broadband Fourier-transform Stimulated Raman Scattering, Julien Rehault¹, Francesco Crisafi¹, Vikas Kumar¹, Marco Marangoni¹, Giulio Cerullo¹, Dario Polli¹; ¹Politecnico di Milano, Italy. We demonstrate a new approach to broadband stimulated Raman scattering based on time-domain-Fourier-transform detection of the stimulated Raman gain. Our method blends the sensitivity of single-channel lock-in detection with the spectral resolution of Fourier-transform spectroscopy.

STh4H.6 • 17:45

Handedness Control of Mid-infrared (9-12 μ m) Vortex Laser, Michael-Tomoki Horikawa¹, Azusa Ogawa¹, Kenji Furuki¹, Katsuhiko Miyamoto¹, Takashige Omatsu^{1,2}; ¹Chiba Univ., Japan; ²JST, CREST, Japan. Handedness control of the mid-infrared vortex output from a ZnGeP₂ difference frequency generator pumped by a 1- μ m vortex pumped KTiOPO₄ optical parametric oscillator was demonstrated over a frequency range of 9-12 μ m.

Meeting Room
211 B/D

CLEO: Science & Innovations

STh4I • Optomechanics II—Continued

STh4I.4 • 17:15

Unifying Brillouin scattering and cavity optomechanics in silicon photonic wires, Raphaël Van Laer¹, Bart Kuyken¹, Roel Baets¹, Dries Van Thourhout¹; ¹*Ghent Univ. - imec, Belgium*. We prove a connection between the Brillouin gain and the zero-point optomechanical coupling rate. Moreover, we report on observations of Brillouin scattering in silicon photonic nanowires—showing efficient coupling between near-infrared light and gigahertz sound.

STh4I.5 • 17:30 **Invited**

Optomechanical Nonlinearities in Micro-structured Optical Fibers, Philip S. Russell¹, Anna Butsch¹, Johannes Koehler¹, Roman E. Noskov¹, Meng Pang¹; ¹*Max-Planck-Inst Physik des Lichts, Germany*. Light-driven mechanical motion or vibration in micro-structured glass fibers can result in very large Raman-like optomechanical nonlinearities that may be used, e.g., to mode-lock fibre ring lasers at a high harmonic of their round-trip frequency.

Meeting Room
212 A/C

CLEO: Applications & Technology

ATH4J • Clinical Technologies and Systems II—Continued

ATH4J.3 • 17:30

Design and Implementation of a Volume Holographic Imaging Endoscope, Isela D. Howlett¹, Michael Gordon¹, Gabriel Orsinger¹, John Brownlee¹, Marek Romanowski¹, Jennifer Barton¹, Raymond K. Kostuk¹; ¹*Univ. of Arizona, USA*. The design and packaging of a volume holographic imaging endoscope suitable for clinical studies is presented. The system is capable of simultaneous image projection from multiple tissue depths. Preliminary results show resolution to 4 μm .

ATH4J.4 • 17:45

In vivo longitudinal cellular imaging of small intestine by side-view confocal endomicroscopy, Jinhyo Ahn¹, Kibaek Choe¹, Taejun Wang², Yoonha Hwang¹, Ki Hean Kim², Pilhan Kim¹; ¹*Korea Advanced Inst of Science & Tech, USA*; ²*Pohang Univ. of Science and Technology, Korea*. In vivo longitudinal repetitive observation of microvasculature and fluorescent cells in a small intestinal tract of single mouse in minimally invasive manner was demonstrated by using GRIN lens based side-view confocal endomicroscopy.

Meeting Room
212 B/D

CLEO: Science & Innovations

STh4K • Super-resolution Imaging—Continued

STh4K.2 • 17:30

An Azimuthal Polarizer Assures Localization Accuracy in Single-Molecule Super-Resolution Fluorescence Microscopy, Matthew D. Lew^{1,2}, W. E. Moerner¹; ¹*Dept. of Chemistry, Stanford Univ., USA*; ²*Dept. of Electrical Engineering, Stanford Univ., USA*. Imaging only azimuthally-polarized light from single fluorescent molecules avoids emission from the z component of their transition dipole moments, resulting in accurate measurement of location regardless of emitter orientation and degree of objective lens misfocus.

STh4K.3 • 17:45

Maximally Informative Point Spread Functions for 3D Super-Resolution Imaging, Yoav Shechtman¹, Steffen J. Sahl^{1,2}, Adam S. Backer¹, W. E. Moerner¹; ¹*Stanford Univ., USA*; ²*Max Planck Inst. for Biophysical Chemistry, Germany*. We generate optimal point spread functions (PSFs) for 3D super-resolution imaging, and demonstrate their application in biological conditions. These PSFs exhibit significantly improved precision and depth of field over the current state of the art.

Marriott
Salon I & II

STh4L • Fiber Lasers—Continued

STh4L.4 • 17:15

Pulse Coherence in Self-sweeping Fiber Laser, Ivan A. Lobach¹, Sergey I. Kablukov¹, Evgeniy V. Podivilov^{1,2}, Andrei A. Fotiadi^{3,4}, Sergey A. Babin^{1,2}; ¹*Inst. of Automation and Electrometry, Russia*; ²*Novosibirsk State Univ., Novosibirsk, Russia*; ³*Faculté Polytechnique de Mons, Service d'Electromagnétisme et de Télécommunications, Belgium*; ⁴*Ulyanovsk State Univ., Russia*. Investigation of a self-sweeping fiber laser with regular dynamics shows that the phases of modes generated with different pulses are not random. A superposition of 18 consequent laser pulses inside an external ring fiber cavity highlights their coherent combining into a train of nanosecond pulses.

STh4L.5 • 17:30

Rogue Waves in a Normal-Dispersion Fiber Laser, Zhanwei Liu¹, Shumin Zhang², Frank W. Wise¹; ¹*Cornell Univ., USA*; ²*Hebei Normal Univ., China*. The first observations of rogue-wave formation in a normal-dispersion fiber laser are reported. With an interference filter in the cavity, non-Gaussian distributions with pulses as large as 6 times the significant wave height are observed.

STh4L.6 • 17:45

High Peak Power Single-Frequency Efficient Erbium-Ytterbium Doped LMA Fiber, William Renard¹, Thierry Robin², Benoît Cadier², Julien Le Gouët¹, Laurent Lombard¹, Anne Durécu¹, Pierre Bourdon¹, Guillaume Canat¹; ¹*DOTA, ONERA, France*; ²*IXfiber, France*. We report on single-frequency all-fiber amplifiers based on Er-Yb doped P2O5-Al2O3-SiO2 fibers. Peak power up to 1120 W at 1545 nm for 108 ns pulse duration has been obtained with 18 % slope-efficiency. Continuous-wave operation generated up to 14 W.



CLEO: Science & Innovations

STh4M • Fundamental Light-material Interaction II—Continued**STh4M.4 • 17:15**

Non-thermal ablation and deposition of graphite induced by ultrashort pulsed laser radiation. Christian Kalupka¹; ¹RWTH Aachen, Germany. We study the non-thermal ablation threshold of graphite in dependence on the applied ultrashort pulse duration. Our results indicate lattice motions to play a relevant role in the non-thermal ablation process.

STh4M.5 • 17:30

Single photon sources using diamond colour centres in novel open access microcavities. Philip Dolan¹, Sam Johnson¹, Aurelien Trichet¹, Lucas Flatten¹, Laiyi Weng¹, Jason M. Smith¹; ¹Univ. of Oxford, UK. Finite difference time domain results support the design of microcavities which can be produced with unparalleled fidelity to the modelled surface with a focused ion beam. Coupling of NV centres at low temperature is also shown.

STh4M.6 • 17:45

Electrical Valley Excitation by Spin Injection in Monolayer TMDC. Yu Ye¹, Xiaobo Yin^{1,2}, Hailong Wang³, Ziliang Ye¹, Hanyu Zhu¹, Yuan Wang¹, Jianhua Zhao³, Xiang Zhang^{1,4}; ¹UC Berkeley, USA; ²Univ. of Colorado Boulder, USA; ³Chinese Academy of Sciences, Inst. of Semiconductors, China; ⁴Lawrence Berkeley National Laboratory, Materials Sciences Division, USA. We show experimentally the new valley indices of carriers can be electrically generated by spin injection, unifying the spintronics and emerging valleytronics.

STh4N • Micro and GHz Combs—Continued**STh4N.3 • 17:15**

Spectral broadening of Kerr Frequency Combs Generated from a Normal Dispersion Silicon Nitride Microresonator. Yang Liu¹, Andrew J. Metcalf¹, Yi Xuan¹, Xiaoxiao Xue¹, Pei-Hsun Wang¹, Minghao Qi¹, Andrew M. Weiner¹; ¹Purdue Univ., USA. We demonstrate a scheme to broaden the bandwidth of the Kerr frequency comb generated through mode interaction in a normal dispersion SiN microresonator. The broadened comb has a bandwidth of over 5 THz and can be compressed to the bandwidth limited time profile via dispersive fiber propagation.

STh4N.4 • 17:30

Microwave to Optical Link Using an Optical Microresonator. John D. Jost¹, Tobias Herr^{1,2}, Caroline Lecaplain¹, Erwan Lucas¹, Victor Brasch¹, Martin Pfeiffer¹, Tobias Kippenberg¹; ¹EPFL, Switzerland; ²CSEM, Switzerland. Microresonator based optical frequency combs have the potential to greatly extend optical frequency measurements. Here we demonstrate the first self-referenced microresonator based optical comb suitable for optical frequency metrology applications.

STh4N.5 • 17:45

Self-referencing a 10 GHz Electro-optic Comb. Daniel C. Cole¹, Katja Beha¹, Frederick N. Baynes¹, Pascal Del'Haye¹, Antoine Rolland¹, Tara M. Fortier¹, Franklyn Quinlan¹, Scott Diddams¹, Scott B. Papp¹; ¹NIST Boulder, USA. An octave-spanning frequency comb is generated using electro-optic modulation of a 1550 nm laser and nonlinear broadening. With this comb we demonstrate offset frequency detection, precise metrology, and ultrastable synthesis of 10 GHz microwaves.

STh4O • Optical Sensing Techniques for Combustion and Energy Research—Continued**STh4O.2 • 17:30**

Cavity-Enhanced Optical Frequency Comb Spectroscopy of High-Temperature Water in a Flame. Amir Khodabakhsh¹, Zhechao Qu², Chadi Abd Alrahman¹, Alexandra C. Johansson¹, Lucile Rutkowski¹, Florian M. Schmidt², Aleksandra Foltynowicz-Matyba¹; ¹Dept. of Physics, Umeå Univ., Sweden; ²Thermochemical Energy Conversion Lab, Dept. of Applied Physics and Electronics, Umeå Univ., Sweden. We demonstrate detection of broadband high-temperature water spectra in a laminar, premixed methane/air flat flame using high-resolution near-infrared cavity-enhanced optical frequency comb spectroscopy incorporating a fast-scanning Fourier transform spectrometer.

STh4O.3 • 17:45

Fiber Optical Chemical Sensors Rated for 800°C Operation. Aidong Yan¹, Rongzhang Chen¹, Zsolt L. Poole¹, Paul R. Ohodnicki³, Tino Elsmann², Tobias Habisreuther², Manfred Rothhardt², Hartmut Bartelt², Kevin P. Chen¹; ¹Univ. of Pittsburgh, USA; ²Leibniz Inst. of Photonic Technology, Germany; ³National Energy Technology Lab, USA. A high-temperature fiber optical hydrogen sensor is demonstrated. The sensor is based on single-crystal sapphire fiber coated with nanostructured Pd-doped TiO₂ thin film. The sensitivity of the sensor was evaluated for hydrogen concentrations varying from 0.02 % to 3% at temperature up to 800°C.

Executive Ballroom
210A

Executive Ballroom
210B

Executive Ballroom
210C

Executive Ballroom
210D

**CLEO: Applications
& Technology**

CLEO: QELS-Fundamental Science

**FTh4B • Quantum Memories—
Continued**

FTh4B.7 • 18:00

Towards Detection of Single Rare-Earth-Ions in a Nanophotonic Resonator, Tian Zhong¹, Jonathan Kindem¹, Evan Miyazono¹, Andrei Faraon¹; ¹California Inst. of Technology, USA. We report a scheme for detecting single rare-earth-ions coupled to an Yttrium Orthosilicate (YSO) nanophotonic resonator, which could enable precise optical addressing of individual ions as single qubits for quantum information applications.

FTh4B.8 • 18:15

Coupling an erbium spin ensemble to a 3D superconducting cavity at zero magnetic field, Yu-Hui Chen¹, Xavier Fernandez-Gonzalvo¹, Jevon Longdell¹; ¹Univ. of Otago, New Zealand. We report zero-magnetic-field electron-paramagnetic-resonance experiments of an ¹⁶⁷Er:Y₂SiO₅ crystal coupled to a tunable 3D superconducting cavity of a 10⁵ Q-factor.

**FTh4C • Attosecond Dynamics
and Strong-field Interactions—
Continued**

FTh4C.7 • 18:00

Sub-Ångström Scale Imaging of Aligned Acetylene, Benjamin Wolter¹, Michael G. Pullen¹, Anh-Thu Le², Matthias Baudisch¹, Michele Sciafani¹, Hugo Pires¹, Michael Hemmer¹, Arne Senftleben³, Claus Dieter Schröter¹, Joachim Ullrich^{4,5}, Robert Moshhammer⁴, Chii-Dong Lin², Jens Biegert^{1,6}; ¹ICFO -The Inst. of Photonic Sciences, Spain; ²J. R. Macdonald Lab, Physics Dept., Kansas State Univ., USA; ³Inst. of Physics, Center for Interdisciplinary Nanostructure Science and Technology (CINSaT), Univ. of Kassel, Germany; ⁴Max-Planck-Institut für Kernphysik, Germany; ⁵Physikalisch-Technische Bundesanstalt (PTB), Germany; ⁶ICREA - Institutio Catalana de Recerca i Estudis Avancats, Spain. We present the simultaneous measurement of the C-C and C-H bond lengths of aligned acetylene. Our approach combines an ultrafast 160 kHz mid-IR source with 3D electron-ion coincidence detection towards imaging of molecular dynamics.

FTh4C.8 • 18:15

Observation of High-Lying Rydberg States Survived from Strong Field Interaction, Seyedreza Larimian¹, Sonia Erattupuzha¹, Raffael Maurer¹, Christoph Lemell², Stefan Nagele², Shuhei Yoshida², Joachim Burgdörfer², Andrius Baltuska¹, Markus Kitzler¹, Xinhua Xie¹; ¹Photonics Inst., Vienna Univ. of Technology, Austria; ²Inst. for Theoretical Physics, Vienna Univ. of Technology, Austria. We observed high-lying (n>238) Rydberg states which survived from strong field interaction of atoms and molecules with electron and ion coincidence detection. The high-lying Rydberg states are measured through field ionization with weak DC fields.

**FTh4D • Quantum and
Fundamental Phenomena—
Continued**

FTh4D.4 • 18:00

Nondegenerate Two-Photon Gain in GaAs, Matthew Reichert¹, David J. Hagan¹, Eric W. Van Stryland¹; ¹Univ. of Central Florida, CREOL, USA. We present data indicating two-photon gain using extremely nondegenerate (END) photons in optically excited GaAs. These results are consistent with our demonstration of END two-photon absorption enhancement and points a possible way to two-photon lasing.

FTh4D.5 • 18:15

Optical Bistability in Electrically Driven Polariton Condensates, Matthias Amthor¹, Timothy C. H. Liew², Christian Metzger¹, Sebastian Brodbeck¹, Lukas Worschech¹, Martin Kamp¹, Ivan A. Shelykh², Alexey V. Kavokin^{3,4}, Christian Schneider¹, Sven Höfling¹; ¹Technische Physik, Univ. of Wuerzburg, Germany; ²Division of Physics and Applied Physics, Nanyang Technological Univ., Singapore; ³Spin Optics Lab, St-Petersburg State Univ., Russia; ⁴Physics and Astronomy School, Univ. of Southampton, UK. We observe a bistability in an electrically driven polariton condensate, which is manifested by a memory dependent threshold characteristic. The bistability is explained by a dependence of the electron-hole tunneling lifetime on the carrier density.

18:30–20:00 **Dinner Break** (on your own)

20:00–22:00 **Postdeadline Paper Sessions**
Locations announced in the postdeadline paper digest.

**Technical Digest and Postdeadline Papers
Available Online**

- Visit www.cleoconference.org
- Select Access Digest Paper link
- Use your registration email address and password

Access is provided only to full technical attendees.

Executive Ballroom
210E

**CLEO: QELS-
Fundamental Science**

**FTh4E • Nanophotonics
for Thermal Transfer and
Waveguiding—Continued**

FTh4E.6 • 18:00

Coupling Control Based on Adiabatic Elimination in Densely Integrated Nano-Photonics, Michael Mrejen¹, Haim Suchowski¹, Taiki Hatakeyama¹, Chihhui Wu¹, Liang Feng¹, Kevin O'Brien¹, Yuan Wang¹, Xiang Zhang¹; ¹Univ. of California Berkeley, USA. We experimentally demonstrate a novel approach based on adiabatic elimination scheme to control the coupling between densely packed waveguides. At the nano-scale, cancellation of the coupling between the waveguides can be achieved.

FTh4E.7 • 18:15

Plasmonic Waveguide Array: Simulating Topological Photonic States and Massless Dirac Fermion, Q.Q. Cheng^{1,2}, Tao Li^{1,2}; ¹College of Engineering and Applied Sciences, Nanjing Univ., China; ²National Lab of Solid State Microstructures, Nanjing Univ., China. In the binary plasmonic waveguide array (PWA), we experimentally demonstrated a topologically protected optical mode with immunity against structural disorders, and theoretically proposed an optical analogue of massless Dirac Fermion by alternating positive and negative couplings.

Executive Ballroom
210F

**STh4F • Photonic, Microwave
Signal Processing—Continued**

STh4F.7 • 18:00

On-Chip Instantaneous Microwave Frequency Measurement System based on a Waveguide Bragg Grating on Silicon, Maurizio Burla¹, Xu Wang², Ming Li³, Lukas Chrostowski², José Azaña¹; ¹Institut National de la Recherche Scientifique, Canada; ²Univ. of British Columbia, Canada; ³Inst. of Semiconductors, Chinese Academy of Sciences, China. We experimentally demonstrate an instantaneous frequency measurement system based on a 65 μm-long integrated Bragg grating filter. An amplitude comparison function based on its transmission and reflection responses allows identification of unknown RF frequencies above 30 GHz.

STh4F.8 • 18:15

Large frequency range photonic-assisted software-defined radio transceiver, Jingjing Wang¹, Hongchen Yu¹, Minghua Chen¹, Hongwei Chen¹, Sigang Yang¹, Shizhong Xie¹; ¹Tsinghua Univ., China. We present a novel software-defined radio transceiver, which takes advantages of RF photonic techniques to realize the state-of-the-art performance in the aspect of the frequency range to cover from C band to Ka band.

Executive Ballroom
210G

CLEO: Science & Innovations

**STh4G • Fabrication
Techniques II—Continued**

STh4G.7 • 18:00

Microfluidic Reconfigurable Metasurface: A Demonstration of Tunable Focusing from Near Field to Far Field, Weiming Zhu¹; ¹Nanyang Technological Univ., USA. We present a reconfigurable transmission metasurface based on microfluidic system. As a proof of concept, the focal length of the metasurface is tuned from near-field region (1 λ) to far-field region (18 λ).

STh4G.8 • 18:15

On-Demand Fabrication of Micro-Wired Rods and Nano-Coupling Control for 3D Polymeric Optical System, Hiroaki Yoshioka¹, Noboru Hirakawa¹, Mitsuhiro Nakano¹, Yuji Oki¹; ¹Dept. of Electronics, Kyushu Univ., Japan. Fully polymeric 3D microcavity system was proposed and demonstrated in which integrates whisper-gallery-mode microrod lasers and output coupling waveguide. As on-site additive-manufacturing technique, microdispensing wired 7.3 μmφ polymer-microrods. Their repositioning accuracy <100 nm was attained.

Executive Ballroom
210H

**STh4H • Novel Applications
and Phenomena of Nonlinear
Optics—Continued**

STh4H.7 • 18:00

Electrically Controllable Saturable Absorption in Hybrid Graphene-Silicon Waveguides, Koen Alexander^{1,2}, Yingtao Hu^{1,2}, Marianna Pantouvaki³, Steven Brems³, Inge Asselberghs³, Simon-Pierre Gorza⁴, Cedric Huyghebaert³, Joris Van Campenhout³, Bart Kuyken^{1,2}, Dries Van Thourhout^{1,2}; ¹Photonics Research Group, Depart. of Information Technology, Ghent Univ.-IMEC, Belgium; ²Center for Nano- and Biophotonics (NB-Photonics), Ghent Univ., Belgium; ³IMEC, Belgium; ⁴Service OPERA-photonique, Université libre de Bruxelles (U.L.B.), Belgium. Electrical tunability of saturable absorption is demonstrated in a graphene/SOI hybrid waveguide. The saturation modulation depth is tunable between 0 and 2.2 dB (~0-40% decrease of absorption at saturation), with saturation powers between ~1.25-2.5 W.

STh4H.8 • 18:15

Ultra-low power passive mode-locking using an integrated nonlinear microring resonator, Christian Reimer¹, Michael Kues¹, Benjamin Wetzel¹, Piotr Roztock¹, Brent E. Little², Sai T. Chu³, David Moss^{1,4}, Roberto Morandotti¹; ¹INRS-EMT, Canada; ²Xi'an Inst. of Optics and Precision Mechanics of CAS, China; ³Depart. of Physics and Material Science, City Univ. of Hong Kong, China; ⁴School of Electrical and Computer Engineering, RMIT Univ., Australia. Using high nonlinear enhancement in a CMOS compatible microring resonator incorporated in a SOA based nonlinear loop-mirror laser architecture, we observe passive mode-locking at extremely-low power levels generating 570ps pulses at a 14.8MHz repetition rate.

18:30–20:00 **Dinner Break** (on your own)

20:00–22:00 **Postdeadline Paper Sessions**
Locations announced in the postdeadline paper digest.

Meeting Room
211 B/D

CLEO: Science & Innovations

STh4I • Optomechanics II—Continued

STh4I.6 • 18:00
Microwave Frequency Traveling Surface Acoustic Wave Induced Transparency, Huan Li¹, Semere A. Tadesse^{1,2}, Qiyu Liu¹, Mo Li¹; ¹Dept. of Electrical and Computer Engineering, Univ. of Minnesota, USA; ²School of Physics and Astronomy, Univ. of Minnesota, USA. Inter-digital transducers and photonic crystal cavities are integrated on a piezoelectric aluminum nitride film sputtered on an oxidized silicon wafer, which leads to the first demonstration of microwave frequency traveling surface acoustic wave induced transparency.

STh4I.7 • 18:15
Surface Acoustic Wave Modulation of Optical Cavities on a Suspended Membrane, Semere Tadesse¹, Huan Li¹, Qiyu Liu¹, Mo Li¹; ¹Univ. of Minnesota, USA. Optical race-track resonators and one-dimensional photonic crystal cavities are integrated with surface acoustic wave devices on a suspended piezoelectric aluminum nitride film to realize strong, ultrafast sound-light interaction.

Meeting Room
212 A/C

CLEO: Applications & Technology

ATH4J • Clinical Technologies and Systems II—Continued

ATH4J.5 • 18:00
In Vivo Real-time Observation of ICG Pharmacokinetics by NIR Laser-scanning Confocal Microscopy, Yoonha Hwang¹, Hwanjun Yoon¹, Kibaek Choe¹, Ji Ho Park¹, Pilhan Kim¹; ¹Korea Advanced Inst of Science & Technology, Korea. By utilizing custom-design video-rate near-infrared laser-scanning confocal microscope, we imaged the pharmacokinetic dynamics of intravenously injected ICG at the skin and liver of mouse in sub-cellular scale *in vivo*.

ATH4J.6 • 18:15
Field-Portable Smartphone Microscopy Platform for Wide-field Imaging and Sizing of Single DNA molecules, Qingshan Wei¹, Wei Luo¹, Samuel Chiang¹, Tara Kappel¹, Crystal Mejia¹, Derek Tseng¹, Raymond Yan Lok Chan¹, Eddie Yan¹, Hangfei Qi¹, Faizan Shabbir¹, Haydar Ozkan¹, Steve Feng¹, Aydogan Ozcan¹; ¹Univ. of California Los Angeles, USA. We demonstrate a field-portable smartphone-based fluorescence microscopy platform for imaging and sizing of single DNA molecules across ~2 mm² field-of-view with <1 kbp length accuracy.

Meeting Room
212 B/D

CLEO: Science & Innovations

STh4K • Super-resolution Imaging—Continued

STh4K.4 • 18:00
Adaptive optics for single molecule switching nanoscopy, Martin J. Booth¹; ¹Univ. of Oxford, UK. Specimen-induced aberrations frequently affect image quality in high-resolution microscopes. Aberration effects can be even more problematic in super-resolution methods. We show adaptive aberration correction in STORM microscopy of deep cell and tissue specimens.

STh4K.5 • 18:15
Single-Shot Sparsity-based Sub-wavelength Fluorescence Imaging of Biological Structures Using Dictionary Learning, Maor Mutzafi¹, Yoav Shechtman^{2,1}, Yonina C. Eldar¹, Mordechai Segev¹; ¹Technion Israel Inst. of Technology, Israel; ²Chemistry, Stanford Univ., USA. We present a novel technique to algorithmically enhance the resolution in optical microscopy. To do that, we exploit the characteristic features of biological images to construct a dictionary which enables sparsity-based reconstruction of sub-wavelength features.

Marriott
Salon I & II

STh4L • Fiber Lasers—Continued

STh4L.7 • 18:00
2.6 mJ Energy and 81 GW Peak Power Femtosecond Laser-Pulse Delivery and Spectral Broadening in Inhibited Coupling Kagome Fiber, Benoît Debord¹, Frédéric Gérôme¹, Pierre-Mary Paul², Anton Husakou³, Fetah Benabid¹; ¹Xlim Research Inst., Université de Limoges, France; ²Amplitudes Technologies, France; ³Max Born Inst., Germany. We report on 800nm laser-pulse delivery record by using inhibited coupling Kagome fiber. Strong spectral broadening and projected pulse compression down to ~10fs were achieved with input 2.6mJ energy and 81GW peak power.

STh4L.8 • 18:15
High-power, high-efficiency random fiber lasing with a low reflectivity mirror, Zinan Wang¹, Han Wu¹, Mengqiu Fan¹, Li Zhang¹, Weili Zhang¹, Yunjiang Rao¹; ¹Univ. Electronic Sci. & Tech. of China, China. We theoretically investigate the role of point reflector's reflectivity in the performance of forward-pumped high power random fiber lasing, and demonstrate that the maximum 1st-order random lasing output power can even increase when the reflectivity decreases from 0.9 to 0.01.

18:30–20:00 Dinner Break (on your own)

20:00–22:00 Postdeadline Paper Sessions
Locations announced in the postdeadline paper digest.

NOTES

CLEO: QELS-Fundamental Science

CLEO: Science & Innovations

08:00–10:00

FF1A • Quantum Key Distribution

Presider: Ping Lam; Australian National Univ., Australia

FF1A.1 • 08:00 **Invited**

Device-Independent Quantum Key Distribution, Antonio Acin^{1,2}; ¹ICFO -The Inst. of Photonic Sciences, Spain; ²ICREA-Institutio Catalana de Recerca i Estudis Avançats, Spain. Device-independent quantum key distribution protocols allow distributing a secret key whose security does not rely on any assumption on the inner working of the devices in the implementation. We discuss recent progress on the problem.

FF1A.2 • 08:30

Practical High-Dimensional Quantum Key Distribution with Decoy States, Darius Bunandar¹, Zheshen Zhang¹, Jeffrey Shapiro¹, Dirk R. Englund¹; ¹MIT, USA. We propose a high-dimensional quantum key distribution protocol secure against photon-number splitting attack by employing only one or two decoy states. Decoy states dramatically increase the protocol's secure distance.

08:00–09:30

FF1B • Quantum Optics with Quantum Dots

Presider: Sergey Polyakov; NIST, USA

FF1B.1 • 08:00

Highly indistinguishable photons from a QD-microcavity with a large Purcell-factor, Sebastian Unsleber¹, Dara McCutcheon², Michael Dambach¹, Matthias Lerner¹, Niels Gregersen², Sven Höfling^{1,3}, Jesper Mork², Christian Schneider¹, Martin Kamp¹; ¹Technische Physik, Univ. of Wuerzburg, Germany; ²Dept. of Photonics Engineering, Technical Univ. of Denmark, Denmark; ³Univ. of St Andrews, SUPA, School of Physics and Astronomy, UK. We demonstrate the emission of highly indistinguishable photons from a quasi-resonantly pumped coupled quantum dot-microcavity system operating in the weak coupling regime. Furthermore we model the degree of indistinguishability with our novel microscopic theory.

FF1B.2 • 08:15

Screening Nuclear Field Fluctuations in Quantum Dots for Indistinguishable Photon Generation, Ralph Malein¹, Ted Santana¹, Joanna Zajac¹, Pierre Petroff², Brian Gerardot¹; ¹Inst. of Photonics and Quantum Sciences, Heriot-Watt Univ., UK; ²Materials Dept., Univ. of California, USA. We probe the effect of nuclear spin interaction with a resident electron spin in a quantum dot using resonance fluorescence spectroscopy and two-photon interference experiments. Screening of the nuclear field fluctuations is demonstrated to successfully generate indistinguishable single photons.

FF1B.3 • 08:30

Phonon-Assisted Population Inversion of a Single Quantum Dot, Alistair Brash¹, John H. Quilter¹, Feng Liu¹, Martin Glässl², Andreas Barth², Vollrath M. Axt², Andrew Ramsay³, Maurice S. Skolnick¹, A. Mark Fox¹; ¹Univ. of Sheffield, UK; ²Institut für Theoretische Physik III, Universität Bayreuth, Germany; ³Hitachi Cambridge Lab, Univ. of Cambridge, UK. We demonstrate a new method to produce a population inversion in an InGaAs quantum dot by quasi-resonant, incoherent excitation within the LA phonon sideband. A maximum exciton population of 0.67 is measured; applications include single photon sources and single QD lasers.

08:00–10:00

FF1C • Nanophotonics and Photonic Crystals

Presider: To be Determined

FF1C.1 • 08:00 **Tutorial**

Nanophotonics in material-systems of Large Sizes, Marin Soljačić¹; ¹MIT, USA. Recent nano-fabrication developments enabled implementation of many nanophotonic techniques to macroscopic scales, which is crucial for many applications of interest (e.g. energy conversion, displays, lighting). Some exciting new opportunities in this area will be presented.



Marin Soljačić is a Professor of Physics at MIT. He is the recipient of the Adolph Lomb medal from The Optical Society (2005), the TR35 award of the Technology Review magazine (2006), MacArthur fellowship "genius" grant (2008), and Blavatnik National Award (2014).

08:00–10:00

SF1D • Nonlinear Optics Frequency Conversion with Integrated Optical Devices

Presider: Michal Lipson; Cornell Univ., USA

SF1D.1 • 08:00 **Invited**

AlGaAs Guided-Wave Optical Parametric Oscillator: Results and Perspectives, Giuseppe Leo¹, Sara Ducci¹, Ivan Favero¹, Cécile Ozanam¹, Xavier Lafosse²; ¹Université Paris-Diderot Paris VII, France; ²Laboratoire de Photonique et Nanostructures, CNRS, France. We demonstrate the first near-infrared optical parametric oscillator in a semiconductor waveguide. With an AlGaAs/AlOx heterostructure placed in a 2 μm-centered doubly-resonant monolithic cavity, we reach the threshold at 210 mW in the CW regime.

SF1D.2 • 08:30

Exact Solutions and Scaling Laws for Kerr Frequency Combs, William H. Renninger¹, Peter T. Rakich¹; ¹Yale Univ., USA. An exact, closed-form solution is analyzed for Kerr frequency combs. The model reproduces the behavior of both soliton and wavetrain regimes. Simple scaling laws validate the results and predict new regimes of performance.

Thank you for
attending CLEO:2015.

Look for your
conference survey via
email and let us know
your thoughts.

Executive Ballroom
210E

CLEO: Applications
& Technology

08:00–10:00

AF1E • A&T Topical Review on
High Performance Optics I

Presider: Vladimir Pervak; Ludwig-Maximilians-Universität München, Germany

AF1E.1 • 08:00 **Invited**

Multilayer Optics for Ultrafast Applications, Michael K. Trubetskov^{1,2}; ¹Lab for Attosecond Physics, Max Planck Inst. of Quantum Optics, Germany; ²Research Computing Center, Moscow State Univ., Russia. Design and production of multilayer optical coatings is considered as multi-stage integral problem. The combination of state-of-the-art design methods and modern deposition techniques advances coating performance to theoretical limits.

AF1E.2 • 08:30 **Invited**

Dispersive Mirror Compressors for Few-Cycle Laser Pulses, Fabian Lücking¹, Tuan Le¹, Catalin Neacsu¹, Gabriel Tempea¹; ¹Femtolasers Produktions GmbH, Austria. The implementation of multilayer optics for the compression and delivery of few-cycle femtosecond pulses will be discussed in the case of several cutting-edge applications.

Executive Ballroom
210F

CLEO: Science & Innovations

08:00–10:00

SF1F • Solid State Lasers

Presider: Shawn Redmond; Massachusetts Inst of Tech Lincoln Lab, USA

SF1F.1 • 08:00

Mid-IR and Near-IR Photoluminescence of Fe²⁺ and Cr²⁺ Ions in ZnSe Excited via Ionization Transitions, Jeremy Peppers¹, Vladimir V. Fedorov¹, Sergey B. Mirov¹; ¹Univ. of Alabama at Birmingham, USA. Spectroscopic characterization of Iron and Chromium doped ZnSe under visible excitation into the charge transfer bands of Transition Metal ions is reported. Energy transfer rates to the upper laser level are sufficient for population inversion.

SF1F.2 • 08:15

High Average Power (35 W) Pulsed Fe:ZnSe laser tunable over 3.8-4.2 μm, Dmitry V. Martyshkin¹, Vladimir V. Fedorov¹, Mike Mirov¹, Igor Moskalev¹, Sergey Vasilyev¹, Sergey B. Mirov¹; ¹IPG Photonics Mid-IR Lasers, USA. We report to the best of our knowledge the highest output average power of 35W (0.35J per pulse) of Fe:ZnSe laser operating at 100 Hz repetition rate in nonselective cavity, and 23 W (0.23J per pulse) in dispersive cavity. The lasing wavelength was tuned over 3.88-4.17 μm at 77K.

SF1F.3 • 08:30

High Energy and Low Noise Ho:YLF Regenerative Amplifiers: A Noise and Stability Analysis, Peter Kroetz^{1,2}, Axel Ruehl³, Krishna murari^{2,3}, Huseyin Cankaya^{2,3}, Anne-Laure Calendron^{2,3}, Franz Kaertner^{2,3}, Ingmar Hartl³, R.J. Dwayne Miller^{1,2}; ¹The Atomically Resolved Dynamics Division, Max-Planck Inst. for the Structure and Dynamics of Matter (MPSD), Germany; ²Center for Free-Electron Laser Science, Germany; ³Deutsches Elektronen-Synchrotron (DESY), Germany. The dynamics and stability of Ho:YLF regenerative amplifiers is studied experimentally and numerically, whereas operating conditions are analyzed with respect to energy fluctuations. We propose a low-noise laser design operating at a second stability point.

Executive Ballroom
210G

08:00–10:00

SF1G • Novel Devices

Presider: Real Vallee; Universite Laval, China

SF1G.1 • 08:00 **Invited**

All-carbon photodetectors, Frank Wang¹, Yuanda Liu¹, X Wang², E Flahaut^{3,4}, Y Li¹, x wang⁵, X. R. Wang¹, Y Xu¹, Y Shi¹, R Zhang¹; ¹School of Electronic Science and Engineering, Nanjing Univ., China; ²Dept. of Electrical Engineering, Yale Univ., USA; ³UPS, INP; Institut Carnot Cirimat, Université de Toulouse, France; ⁴CNRS; Institut Carnot Cirimat, France; ⁵School of Chemistry and Chemical Engineering, Nanjing Univ., China. We demonstrate a graphene/nanotube hybrid phototransistor, in which photogating provided by the nanotube layer leads to a dramatically enhanced photoresponsivity (>100A/W) in the visible range, corresponding to ~10⁴ enhancement with respect to a graphene-only device.

SF1G.2 • 08:30

Highly Efficient Hybrid Quantum Dot Light Emitting Diodes with Prolonged Lifetime, Shun-Chieh Hsu¹, Yin-Han Chen², Zong-Yi Tu³, Hau-Vei Han³, Shih-Li Lin², Teng-Ming Chen⁴, Hao-Chung Kuo³, Chien-Chung Lin¹; ¹Inst. of Photonic System, Natl Chiao Tung Univ, Taiwan; ²Inst. of Lighting and Energy Photonics, College of Photonics, National Chiao-Tung Univ., Taiwan; ³Inst. of Electro-Optical Engineering, National Chiao-Tung Univ., Taiwan; ⁴Dept. of Applied Chemistry, National Chiao-Tung Univ., Taiwan. A highly efficient LED is demonstrated by incorporating the colloidal quantum dots and sodium chloride. Further lifetest shows great stability up to 104 hours under 194 mW/cm² of UV pump power.

CLEO: Science & Innovations

CLEO: Applications
& Technology

08:00–10:00
SF1H • Microcavities
Presider: To be Determined

08:00–10:00
SF1I • Lasers for Optical
Communications
Presider: To be Determined

08:00–10:00
AF1J • Measurement of Process
Parameters
Presider: Robert Hickernell; NIST,
USA

SF1H.1 • 08:00
Visible Photoluminescence in Cubic (3C) Silicon Carbide Coupled to High Quality Microdisk Resonators, Marina Radulaski¹, Thomas M. Babinec¹, Kai Muller¹, Konstantinos G. Lagoudakis¹, Jingyuan L. Zhang¹, Sonia M. Buckley¹, Kassem Alassaad², Gabriel Ferro², Jelena Vuckovic¹; ¹Stanford Univ., USA; ²Universite de Lyon, France. We present the design, fabrication and characterization of cubic (3C) silicon carbide microdisk resonators with high quality factor modes at visible and near infrared wavelengths which couple to the intrinsic luminescence in silicon carbide.

SF1H.2 • 08:15
Silicon Carbide Nanobeam Cavities with High Q/V, Jonathan Yiho Lee¹, Xiyuan Lu¹, Qiang Lin¹; ¹Univ. of Rochester, USA. We demonstrate photonic-crystal nanobeam cavities in amorphous SiC. The fundamental mode exhibits intrinsic-Q of 7.69×10^4 with mode volume of $\sim 0.60(\lambda/n)^3$. This is, to the best of our knowledge, the highest Q/V value in SiC cavities.

SF1H.3 • 08:30
Monolithic Single Crystal Diamond High-Q Optical Microcavities, Matthew Mitchell^{1,2}, Behzad Khanaliloo^{1,2}, Aaron Hryciw^{2,3}, Paul E. Barclay^{1,2}; ¹Inst. for Quantum Science & Technology, Canada; ²NRC-National Inst. for Nanotechnology, Canada; ³nanoFAB, Univ. of Alberta, Canada. Monolithic whispering gallery mode (WGM) optical microcavities are fabricated from bulk single crystal diamond (SCD) via a scalable process. Optical quality factors of $Q \sim 1.15 \times 10^5$ at 1.5 μm are demonstrated.

SF1I.1 • 08:00
Tunable Parity-Time-Symmetric Microring Lasers, Hossein Hodaei¹, William Hayenga¹, Mohammad-Ali Miri¹, Absar Ulhassan¹, Demetrios N. Christodoulides¹, Mercedeh Khajavikhan¹; ¹Univ. of Central Florida, CREOL, USA. Wavelength tuning in a single mode parity-time (PT) symmetric semiconductor microring laser is demonstrated. Stable continuous tuning over a spectral range of 4 nm has been obtained at telecom wavelengths by adjusting the ambient temperature.

SF1I.2 • 08:15
Widely-tunable narrow-linewidth lasers with monolithically integrated external cavity, Tin Komljenovic¹, Sudharsanan Srinivasan¹, Michael Davenport¹, Erik Norberg², Greg Fish², John Bowers¹; ¹UCSB, USA; ²Aurion Inc, USA. We demonstrate preliminary results from a monolithically integrated tunable laser with narrow-linewidth. We show tuning in excess of 54 nm in the O-band as well as significant reduction in linewidth due to the external cavity. The measured linewidth, limited by measurement setup, is around 150 kHz.

SF1I.3 • 08:30
Continuously Tunable Laser Based on Multiple-Section DFB Laser Technology for 1.25 Gbps WDM-PON Applications, Dion McIntosh-Dorsey¹, Rajesh Bikky¹, Huanlin Zhang¹, K. Alex Anselm¹, Justin Lii¹, Hsiu-Che Wang¹, Hao-Hsiang Liao¹, I Lung Ho¹, Hang Xie¹, Lingjun Bo¹, Patrick Lorenzo¹, Yi Wang¹, Jun Zheng¹; ¹Applied Optoelectronics Inc, USA. A low-cost continuously tunable laser based on multiple in-line DFB sections and thermal tuning is demonstrated. It is capable of 16 channel tuning and 1.25 Gbps operation. Transceiver performance will also be shown.

AF1J.1 • 08:00 **Invited**
Diode Laser Spectroscopy based Monitoring of Pharmaceutical Freeze Drying: Linking Measurements to Critical Process Parameters, William J. Kessler¹; ¹Physical Sciences Inc., USA. Freeze drying is used to produce dry solid from a solution to improve product stabilization. We have applied absorption spectroscopy to monitor water sublimation rates and determine product temperature during drying, a critical process parameter.

AF1J.2 • 08:30
Real-time Full Characterization of Colloidal Dynamics, Jose R. Guzman-Sepulveda¹, Aristide Dogariu¹; ¹CREOL, College of Optics and Photonics, Univ. of Central Florida, USA. We present an optical technique capable of measuring simultaneously hydrodynamic size and mass density of colloidal suspensions. The technique is fiber optic-based, non-invasive, and permits continuous online measurements over a broad range of colloidal parameters.



CLEO: Science & Innovations

08:00–09:15
SF1K • Flexgrid Networking
*Presider: David Geisler; MIT
Lincoln Lab, USA*

SF1K.1 • 08:00 **Invited**
High Speed and Flexible Optical Transport Network, Tiejun J. Xia¹, Glenn A. Wellbrock¹; ¹Verizon Communications Inc, USA. Optical network operators have been focused on increasing channel speeds and fiber capacities to meet high data traffic demand growth in past decades. Network efficiency improvement with flexible optics will be network operators' next focus.

SF1K.2 • 08:30 **Invited**
Experimental Demonstration of 3D Elastic Optical Networking in Space, Time and Frequency, Chuan Qin¹, Binbin Guan¹, Ryan P. Scott¹, Roberto Proietti¹, Nicolas K. Fontaine², S.J.B. Yoo¹; ¹Univ. of California Davis, USA; ²Bell Labs, USA. We demonstrate elasticity in time, frequency and space domains for an optical link at 960-Gb/s with 6.4-b/s/Hz spectral efficiency. Modulation format and number of spatial modes are selected based on Shannon's Law and crosstalk-dependent impairments.

08:00–10:00
SF1L • Frequency Standards and Timing
Presider: Kristan Corwin; Kansas State Univ., USA

SF1L.1 • 08:00 **Invited**
Frequency comparisons of Sr, Yb, and Hg based optical lattice clocks and their applications, Hidetoshi Katori^{1,2}; ¹Univ. of Tokyo, Japan; ²Quantum Metrology Lab, RIKEN, Japan. We report recent progress of optical lattice clocks with strontium, ytterbium and mercury atoms with an emphasis on their synchronous frequency comparison inside a Lab and inter-Labs connected by a phase-stabilized fiber link.

SF1L.2 • 08:30
Broadband Phase Noise Limit in the Direct Detection of Ultralow Jitter Optical Pulses, Franklyn Quinlan¹, Wenlu Sun², Tara M. Fortier¹, Jean-Daniel Deschenes¹, Yang Fu², Joe C. Campbell², Scott Diddams¹; ¹NIST, USA; ²Dept. of Electrical and Computer Engineering, Univ. of Virginia, USA. The lowest measured phase noise floors of photonically generated microwave signals are orders-of-magnitude above the quantum limit. We show this discrepancy is likely due to photocarrier scattering in high speed, high linearity photodetectors.

08:00–10:00
SF1M • Symposium on OPA/OPCPA – Next Generation of Ultra-Short Pulse Laser Technology I
Presider: Albert Stolow; National Research Council Canada, Canada

SF1M.1 • 08:00 **Invited**
High Energy and Power Optical Waveform Synthesizers, Franz X. Kaertner^{2,1}; ¹MIT, USA; ²Center for Free-Electron Laser Science, Deutsches Elektronen Synchrotron, Germany. We report on recent progress in high-energy optical waveform synthesis with optical parametric amplifiers pumped by high-energy Ti:Sapphire and Yb-based lasers delivering more than 2-octave spanning sub-cycle waveforms with multi-mJ energy.

SF1M.2 • 08:30 **Invited**
Third-generation femtosecond technology, Hanieh Fattahi¹, Nicholas E. Karpowicz¹, Thomas Metzger², zsuzsanna Major¹, Ferenc Krausz¹; ¹Max-Planck-Institut für Quantenoptik, Germany; ²TRUMPF Scientific Lasers, Germany. The design of a 3-channel OPCPA system, generating ultrashort pulses with terawatt peak and sub-kilowatt average powers is presented. Coherent synthesis of the channels is predicted to produce intense, sub-cycle transients, presenting a route toward keV attosecond pulses.

CLEO: QELS-Fundamental Science

CLEO: Science & Innovations

FF1A • Quantum Key Distribution—Continued

FF1A.3 • 08:45

Multi-Photon Quantum Key Distribution Based on Double-Lock Encryption, Kam Wai C. Chan¹, Mayssaa El Rifai¹, Pramode Verma¹, Subhash Kak², Yuhua Chen³; ¹School of Electrical and Computer Engineering, Univ. of Oklahoma-Tulsa, USA; ²School of Electrical and Computer Engineering, Oklahoma State Univ., USA; ³Dept. of Electrical and Computer Engineering, Univ. of Houston, USA. We present a quantum key distribution protocol based on the double-lock cryptography. It exploits the asymmetry in the detection strategies between the legitimate users and the eavesdropper. With coherent states, the mean photon number can be as large as 10.

FF1A.4 • 09:00

Quantum Teleportation over 100 km of Fiber using MoSi Superconducting Nanowire Single-Photon Detectors, Hiroki Takesue¹, Shellee D. Dyer², Martin J. Stevens², Varun Verma², Richard P. Mirin², Sae Woo Nam²; ¹NTT Basic Research Labs, Japan; ²National Inst. of Standards and Technology, USA. Using high-efficiency superconducting nanowire single-photon detectors based on MoSi, we successfully achieved quantum teleportation of weak coherent states over 100 km of fiber with an average fidelity of 82.9% for six distinct input states.

FF1A.5 • 09:15

Polarization Insensitive 100 MHz Clock Subcarrier Quantum Key Distribution over a 45 dB Loss Optical Fiber Channel, Artur V. Gleim¹, Vladimir Egorov¹, Yuri V. Nazarov¹, Semen V. Smirnov¹, Vladimir V. Chistyakov¹, Oleg I. Bannik¹, Andrey A. Anisimov¹, Sergei M. Kynev¹, Robert J. Collins², Sergei A. Kozlov¹, Gerald S. Buller²; ¹Dept. of Photonics and Optical Information Technology, ITMO Univ., Russia; ²Inst. of Photonics and Quantum Sciences, Heriot-Watt Univ., UK. We experimentally demonstrate quantum key distribution at 28 bit/s rate in a telecommunications fiber channel with 45 dB loss using a subcarrier wave approach. This approach offers polarization independency, high bitrates and wide multiplexing capabilities.

FF1B • Quantum Optics with Quantum Dots—Continued

FF1B.4 • 08:45

Coherent Writing of the Dark Exciton State Using One Picosecond Long Optical Pulse, Ido Schwartz¹, Dan Cogan¹, Emma R. Schmidgall¹, Liron Gantz¹, Yaroslav Don¹, David Gershoni¹; ¹Physics, Technion, Israel. We demonstrate a one to one correspondence between the polarization of a picosecond optical pulse and the coherent spin state of the long lived dark exciton that it deterministically photogenerates in a single quantum dot.

FF1B.5 • 09:00

Single Emitter Vacuum Rabi Splitting Measured Through Direct Free Space Spontaneous Emission, Yasutomo Ota¹, Ryuichi Ohta², Naoto Kumagai¹, Satoshi Iwamoto^{1,2}, Yasuhiko Arakawa^{1,2}; ¹Nanoquine, Univ. of Tokyo, Japan; ²IIS, The Univ. of Tokyo, Japan. We measured the vacuum Rabi splitting of a single quantum emitter through direct free space spontaneous emission. This lays the groundwork for accessing diverse cavity quantum electrodynamics phenomena manifesting themselves only in the spontaneous emission.

FF1B.6 • 09:15

Two-Photon Spectrum of the Light Scattered by a Quantum Dot, Manoj Peiris¹, Ben Petrak¹, kumarasiri konthasinghe¹, Ying yu², Zhichuan Niu², Andreas muller¹; ¹Univ. of South Florida, USA; ²Chinese Academy of Sciences, China. We report the measurement of the two-photon spectrum of the light scattered by a single InAs quantum dot interacting with a strong near-resonant monochromatic laser.

FF1C • Nanophotonics and Photonic Crystals—Continued

FF1C.2 • 09:00

Circularly Polarized Light Emission of Quantum Dots at the Band Edge of Three-Dimensional Chiral Photonic Crystals, Shun Takahashi¹, Takeyoshi Tajiri¹, Yasutomo Ota¹, Jun Tatebayashi¹, Satoshi Iwamoto¹, Yasuhiko Arakawa¹; ¹Univ. of Tokyo, Japan. We demonstrate highly circularly polarized emission from quantum dots in semiconductor chiral photonic crystals. The emission is influenced by the difference in density of states between the orthogonal circular polarizations at the polarization band edge.

FF1C.3 • 09:15

Enhanced Transverse Photo-Induced Voltage by Slow Light, Nicholas Proscia^{1,2}, Ilona Ketzschmar², Ronald Koder², Vinod M. Menon², Luat T. Vuong¹; ¹Queens College-CUNY, USA; ²Physics, City College of New York-CUNY, USA. We demonstrate the presence of spin-polarized transverse voltage in a metal-dielectric two-dimensional photonic crystal in the visible regime and determine that the presence of slow light at the photonic band edge leads to voltage enhancement.

SF1D • Nonlinear Optics Frequency Conversion with Integrated Optical Devices—Continued

SF1D.3 • 08:45

Generation of Mid-IR Radiation by Four-Wave Mixing in Metal Coated Waveguides, Tobias Flöry¹, Pavel Malevich¹, Audrius Pugzlys¹, Aleksander Voronin², Aleksei Zhel'tikov^{2,3}, Andrius Baltuska¹; ¹Photonics Inst., TU Vienna, Austria; ²Physics Dept., International Laser Center, M.V. Lomonosov Moscow State Univ., Russia; ³Dept. of Physics and Astronomy, Texas A&M Univ., USA. 2.7- μ m microjoule femtosecond pulses are generated in a metal coated hollow fiber thru four-wave-mixing parametric amplification. Numerical simulations predict generation of few-cycle optical pulses with the central wavelength extending beyond 10 μ m.

SF1D.4 • 09:00

Signal Gain from Four-Wave Mixing in Anomalous AlGaAs nanowaveguides, Pisek Kultavewuti¹, Vincenzo Pusino², Marc Sorel², J. Stewart Aitchison¹; ¹Dept. of Electrical and Computer Engineering, Univ. of Toronto, Canada; ²School of Engineering, Univ. of Glasgow, UK. We experimentally demonstrate efficient four-wave mixing with a net signal gain of 4.1 dB and a conversion efficiency of 5.3 dB in low-loss AlGaAs nanowaveguides in an anomalous dispersion regime.

SF1D.5 • 09:15

Low-Noise Silicon Mid-Infrared Frequency Comb, Austin G. Griffith¹, Yoshitomo Okawachi¹, Jaime Cardenas¹, Alexander L. Gaeta¹, Michal Lipson¹; ¹Cornell Univ., USA. We demonstrate low-noise mid-infrared frequency comb generation using a silicon microresonator. Using an integrated PIN-diode detector, we show a transition to a low RF-amplitude-noise state consistent with demonstrations of phase-locking in other microresonator platforms.

Technical Digest and Postdeadline Papers Available Online

- Visit www.cleoconference.org
- Select Access Digest Paper link
- Use your registration email address and password

Access is provided only to full technical attendees.

CLEO: Applications
& TechnologyAF1E • A&T Topical Review
- High Performance Optics I—
Continued

AF1E.3 • 09:00

Ultra-broadband Spectral Beam Combiner, Eric Stanton¹, Martijn J. Heck¹, Jock Bovington¹, Alexander Spott¹, John Bowers¹; ¹*Univ. of California Santa Barbara, USA*. A novel ultra-broadband spectral beam combiner is designed and demonstrated spanning greater than four octaves from ultraviolet to mid-wave infrared bands with low M squared output.

AF1E.4 • 09:15

Mobility Enhancement of Graphene Nanoribbon by ALD HfO₂ and Its Optoelectronic Properties, Xuechao Yu¹, Qi Jie Wang^{1,2}; ¹*OPTIMUS, Photonics Centre of Excellence, School of Electrical and Electronic Engineering, Nanyang Tech Univ, Singapore*; ²*Centre for Disruptive Photonic Technologies, Nanyang Technological Univ., Singapore*. We demonstrated that depositing HfO₂ film on graphene nanoribbons greatly enhance the mobility through weakening the Coulombic interactions. As a result, the graphene nanoribbon photodetectors with HfO₂ layer exhibits high responsivity of ~2A/W at room temperature.

CLEO: Science & Innovations

SF1F • Solid State Lasers—
Continued

SF1F.4 • 08:45

Design and Development of a High-Power LED-Pumped Ce:Nd:YAG Laser, Brenden Villars¹, E. S. Hill¹, Charles G. Durfee¹; ¹*Colorado School of Mines, USA*. Our quasi-continuous wave Ce:Nd:YAG solid-state laser was directly pumped by LED arrays, yielding a maximum of 8mJ/pulse. Comparison of pumping at 460nm and 810nm allows analysis of the performance and potential of this laser system.

SF1F.5 • 09:00

Compact, Passively Q-Switched 523-nm Laser, Bhabana Pati¹, Eric D. Park¹, Ken Stebbins¹; ¹*Q-Peak, Inc., USA*. We have developed a compact, passively Q-switched, intra-cavity frequency doubled Nd:YLF laser that produces 1-mJ of energy in a 10-ns pulse at a 1-20 Hz repetition rate.

SF1F.6 • 09:15

Microchip Tm:KYW Laser with 2.5 W of Output Power, Maxim S. Gaponenko¹, Nikolai Kuleshov², Thomas Sudmeyer¹; ¹*Université de Neuchâtel, Switzerland*; ²*BNTU, Belarus*. Diode-pumped 1.9-um Tm:KYW microchip laser with 1.6 W TEM₀₀ cw output power operates with 72% slope eff. to absorbed pump power. Output power of 2.5 W is achieved with generation of a "doughnut" mode. Q-switched operation with pulse duration of 2.2 ns at 1.5 MHz repetition rate is demonstrated.

SF1G • Novel Devices—
Continued

SF1G.3 • 08:45

Inhibited Coupling Kagome Fibers with Ultra-large Hollow-core Size for High Energy Ultrafast Laser Applications, Benoît Debord¹, Abhilash Amsanpally¹, Meshaal Alharbi¹, Luca Vincetti², Jean-Marc Blondy¹, Frédéric Gérôme^{1,3}, Fetah Benabid^{1,3}; ¹*GPPMM group, Xlim Research Inst., UMR CNRS 7252, Univ. of Limoges, France, France*; ²*Dept. of Engineering "Enzo Ferrari", Univ. of Modena and Reggio Emilia, I-41125 Modena Italy, Italy*; ³*GLPhotonics S.A.S, France*. We report on enlarged hollow-core diameter inhibited coupling Kagome fibers with record loss of 100 dB/km and ppm power overlap with silica surround, suitable for high energy ultrafast laser handling.

SF1G.4 • 09:00

Electro-optic effect in silicon nitride, Steven Miller¹, Yoon Ho Daniel Lee¹, Jaime Cardenas¹, Alexander L. Gaeta^{2,3}, Michal Lipson^{1,3}; ¹*School of Electrical and Computer Engineering, Cornell Univ., USA*; ²*School of Applied and Engineering Physics, Cornell Univ., USA*; ³*Kavli Inst. at Cornell for Nanoscale Science, Cornell Univ., USA*. We present the first demonstration of the electro-optic effect in Si₃N₄ by using a multi-slot waveguide structure. We measure the maximum EO coefficient of 8.31±5.6fm/V, and demonstrate EO modulation at 1GHz.

SF1G.5 • 09:15

Suppression of Optical Damage in Electro-Optical Modulator Using Potassium Lithium Tantalate Niobate, Yossi Kabessa¹, Aharon J. Agranat¹; ¹*HUJI, Israel*. Suppression of optical damage in a KLTN based electrooptical modulator operated with 30 W/cm² light beam at λ=445 nm is demonstrated. The modulator is driven by bipolar voltage which prevents the induced space-charge from accumulating.

CLEO: Science & Innovations

CLEO: Applications
& TechnologySF1H • Microcavities—
Continued

SF1H.4 • 08:45

Optical Microresonators as Single-Molecule Spectrometers, Kevin H. Heylman¹, Kasandra Knapper¹, Erik H. Horak¹, Randall H. Goldsmith¹; ¹Univ. of Wisconsin Madison, USA. A new approach is described for sensing and spectroscopy of single non-luminescent nano-objects which combines the spatial and spectral selectivity of laser microscopy with the tremendous sensitivity of ultrahigh-quality factor optical microresonators.

SF1H.5 • 09:00

Photocurrent-induced Peak-dragging in a Nanobeam Photonic Crystal Cavity, Majid Sodagar¹, Mehdi Miri¹, Ali Eftekhar¹, Ali Adibi¹; ¹Georgia Inst. of Technology, USA. We demonstrate here the peak-dragging phenomenon in a nanobeam photonic crystal cavity with low optical power thresholds. In our device, Joule-heating mechanism enhances the absorption-induced heat by collecting the generated photocarriers in a reverse-biased pn-junction.

SF1H.6 • 09:15

Free-Space Read-Out of WGM Lasers Using Circular Micromirrors, Tobias Wienhold¹, Sarah Kraemmer³, Andreas Bacher¹, Heinz Kalt³, Christian Koos^{1,4}, Sebastian Koeber^{1,4}, Timo Mappes^{1,2}; ¹Inst. of Microstructure Technology (IMT), Karlsruhe Inst. of Technology (KIT), Germany; ²Corporate Research and Technology, Carl Zeiss AG, Germany; ³Inst. of Applied Physics (APH), Karlsruhe Inst. of Technology (KIT), Germany; ⁴Inst. of Photonics and Quantum Electronics (IPQ), Karlsruhe Inst. of Technology (KIT), Germany. We report on efficient free-space read-out of whispering-gallery mode microlasers using circular micromirrors. A ten-fold improvement in detection efficiency can be achieved by directing emission from all azimuthal angles of the cavity to the detector.

SF1I • Lasers for Optical
Communications—Continued

SF1I.4 • 08:45

All-Optical Carrier Recovery Using a Single Injection Locked Semiconductor Laser Stabilized by an Incoherent Optical-Feedback, Aaron Albores-Mejia¹, Toshimitsu Kaneko², Eiichi Banno², Katsumi Uesaka², Hajime Shoji², Haruhiho Kuwatsuka¹; ¹National Inst. of AIST, USA; ²Sumitomo Electric Industries, Ltd, Japan. Novel all-optical-hardware-efficient carrier recovery unit for carrier-suppressed BPSK signals is demonstrated. For the first time, carrier recovery with an optically stabilised injection-locked semiconductor laser enabled successful homodyne detection of 32-Gbit/s carrier-suppressed BPSK signals.

SF1I.5 • 09:00

Double Half-Wave-Coupled Rectangular Ring-FP Semiconductor Laser with 19-nm Quasi-Continuous Tuning Range, Mengtian Sun¹, Lin Wu¹, Xiaohai Xiong¹, Xiaolu Liao¹, Jian-Jun He¹; ¹Dept. of Optical Engineering, Zhejiang Univ., China. We present our latest experimental results of the double half-wave-coupled rectangular ring-FP laser in a XMD TOSA package. A 19-nm quasi-continuous tuning range with over 30dB side mode suppression ratio is obtained.

SF1I.6 • 09:15

Effect of microcavity size to the RIN and 40 Gb/s data transmission performance of high speed VCSELS, Fei Tan¹, Mong-Kai Wu¹, Curtis Wang¹, Michael Liu¹, Milton Feng¹, Nick Holonyak¹; ¹Dept. of Electrical and Computer Engineering, Univ. of Illinois at Urbana-Champaign, USA. We demonstrated that larger aperture VCSELS have better performance in 40Gb/s error free data transmission, and smaller aperture VCSELS have lower laser RIN. Medium aperture VCSELS may excel in high fidelity and high speed applications.

AF1J • Measurement of Process
Parameters—Continued

AF1J.3 • 08:45

Indentation hardness and scratch tests for thin layers manufactured by sol-gel process, Hervé Piombini¹, Christel Ambard¹, François Compoin¹, Karine Valle¹, Philippe Belleville¹, Clément Sanchez²; ¹CEA Le Ripault, France; ²Collège de France, France. We introduce our first tests to characterize the mechanical properties of elastic layer manufactured by sol-gel process obtained with an indenter designed from a microscope. They are performed with a microscope and a diamond tip

AF1J.4 • 09:00

Fiber-optic SERS detection enabled by light-induced gold nano-particle aggregation, Haitao Liu¹, Jiansheng Liu¹, Luoyang Chen¹, Hongwen Zhou¹, Zheng Zheng^{1,2}; ¹School of Electronic and Information Engineering, Beihang Univ., China; ²Collaborative Innovation Center of Geospatial Technology, China. We demonstrated a SERS detection scheme where fiber-optic light-induced aggregation of gold nano-particles enhances the Raman signal by 30-fold over the non-aggregation case, even by exciting and collecting light through low-cost, standard silica fibers.

AF1J.5 • 09:15

Picometer-Scale Surface Roughness Measurements Inside Hollow Glass Fibres, Xavier Buet^{1,2}, Coralie Brun^{1,3}, Bruno Bresson¹, Matteo Ciccotti¹, Marco Petrovitch⁴, Francesco Poletti⁴, David Richardson⁴, Damien Vandembroucq¹, Gilles Tessier¹; ¹ESPCI, USA; ²Neurophotonics Lab, France; ³Institut Langevin, France; ⁴orc, UK. A differential optical profilometry technique with picometre-range sensitivity is adapted to the non invasive measurement of the roughness inside hollow glass fibres by use of immersion objectives and index-matching liquid.

CLEO: Science & Innovations

SF1K • Flexgrid Networking—
Continued

SF1K.3 • 09:00

Wavelength Conflict Resolution by Spectral Overlap of Two Nyquist-WDM Signals, Lingchen Huang¹, Shuang Gao², Chun-Kit Chan²; ¹Center for Optical and Electromagnetic Research, Zhejiang Univ., China; ²Dept. of Information Engineering, The Chinese Univ. of Hong Kong, China. Two Nyquist-WDM signals are spectrally overlapped to resolve the possible wavelength conflict in network routing. Recovery of individual signals is realized by digital signal processing techniques and has been experimentally demonstrated and characterized.

SF1L • Frequency Standards
and Timing—Continued

SF1L.3 • 08:45

Electro-optical frequency division and stable microwave synthesis, Xu Yi¹, Jiang Li¹, Hansuek Lee¹, Scott Diddams^{1,2}, Kerry Vahala¹; ¹California Inst. of Technology, USA; ²National Inst. of Standard and Technology, USA. Optical frequency division and stable microwave generation is demonstrated using an electro-optical-based frequency comb created through phase modulation of two stable optical signals. The technique is simple, tunable and scalable to higher division ratios.

SF1L.4 • 09:00

Attosecond-Resolution Timing Jitter Spectrum Measurement of Free-Running Mode-Locked Lasers Over 10 Decades of Fourier Frequency, Kwangyun Jung¹, Jungwon Kim¹; ¹Korea Advanced Inst of Science & Tech, Korea. We show timing jitter spectrum measurement of free-running mode-locked lasers from 1-mHz to 40-MHz Fourier frequency. The demonstrated method can resolve different noise mechanisms that cause specific jitter characteristics from <100-ns to >1000-s time scales.

SF1L.5 • 09:15

Attosecond Timing Jitter Characterization of Mode-locked Lasers Using Optical Heterodyne Techniques, Dong Hou¹, Chien-Chung Lee¹, Zhengyin Yang¹, Kevin Silverman², Ari Feldman², Todd Harvey², Richard P. Mirin², Thomas R. Schibli¹; ¹Univ. of Colorado Boulder, USA; ²National Inst. of Standards and Technology, USA. We demonstrate timing jitter characterization of mode-locked lasers with attosecond-resolution using optical heterodyne techniques. The measured integrated jitter for a free-running mode-locked Er:Yb:glass laser was found below 20 as from 10 kHz to 5 MHz.

SF1M • Symposium - OPA/
OPCPA - Next Generation
of Ultra-Short Pulse Laser
Technology I—Continued

SF1M.3 • 09:00

Sub-Two-Cycle Millijoule Optical Pulses at 1600 nm from a BiB₃O₆ Optical Parametric Chirped-Pulse Amplifier, Nobuhisa Ishii¹, Keisuke Kaneshima¹, Teruto Kanaï¹, Shuntaro Watanabe², Jiro Itatani¹; ¹Inst. for Solid State Physics, Japan; ²Tokyo Univ. of Science, Japan. We report on the generation of 10.1-fs, 1.5-mJ pulses at 1 kHz from a BiB₃O₆ OPCA with passive CEP stabilization. This light source is promising for the generation of high-flux isolated soft x-ray pulses.

SF1M.4 • 09:15

High-Energy Infrared Femtosecond Pulses by Dual-Chirped Optical Parametric Amplification, Yuxi FU¹, Eiji J. Takahashi¹, Katsumi Midorikawa¹; ¹Attosecond Science Research Team, RIKEN Center for Advanced Photonics, RIKEN, Japan. A total output energy exceeding 30 mJ has been achieved in the infrared region by dual-chirped optical parametric amplifier for generating soft x-ray harmonic pulses. Obtained spectrum supports a pulse duration shorter than 40 fs.

CLEO: QELS-Fundamental Science

CLEO: Science & Innovations

FF1A • Quantum Key Distribution—Continued

FF1A.6 • 09:30

Integrated Photonic Devices for Quantum Key Distribution, Philip Sibson¹, Mark Godfrey¹, Chris Erven¹, Shigehito Miki², Taro Yamashita², Mikio Fujiwara², Masahide Sasaki², Hirotsuka Terai², Michael G. Tanner³, Chandra M. Natarajan³, Robert H. Hadfield³, Jeremy O'Brien¹, Mark G. Thompson¹; ¹Univ. of Bristol, UK; ²National Inst. of Information and Communications Technology, Japan; ³Univ. of Glasgow, UK. We demonstrate a fully integrated photonic transmitter for time-bin based multi-protocol quantum key distribution. This GHz rate Indium Phosphide device prepares states for Coherent One Way (COW), Differential Phase Shift (DPS), and BB84 protocols.

FF1A.7 • 09:45

Quantum hacking of continuous-variable quantum key distribution systems: real-time Trojan-horse attacks, Birgit Stiller^{1,2}, Imran Khan^{1,2}, Nitin Jain^{1,2}, Paul Jouguet³, Sebastien Kunz-Jacques³, Eleni Diamanti⁴, Christoph Marquardt^{1,2}, Gerd Leuchs^{1,2}; ¹Max-Planck-Institut for the Science of Light, Germany; ²Inst. for Optics, Information and Photonics, Germany; ³SeQureNet, France; ⁴LTCL, CNRS - Telecom ParisTech, France. We experimentally demonstrate successful Trojan-horse attacks on Lab and commercial continuous-variable quantum key distribution systems with binary and Gaussian modulation. Furthermore, we analyze appropriate countermeasures regarding their spectral performance.

FF1B • Quantum Optics with Quantum Dots—Continued

FF1B.7 • 09:30

Withdrawn

FF1B.8 • 09:45

Withdrawn

FF1C • Nanophotonics and Photonic Crystals—Continued

FF1C.4 • 09:30

Region Specific Enhancement of Quantum Dot Emission Using Interleaved Two-dimensional Photonic Crystals, Gloria G. See¹, Lu Xu¹, Matt Naughton¹, Tiantian Tang¹, Yolanda Bonita¹, Jake Joo², Peter Trefonas², Kishori Deshpande³, Paul Kenis¹, Ralph G. Nuzzo¹, Brian T. Cunningham¹; ¹Univ of Illinois at Urbana-Champaign, USA; ²Dow Electronic Materials Company, USA; ³The Dow Chemical Company, USA. A photonic crystal (PC) incorporating two interleaved regions, each with distinct periods in orthogonal directions, enables simultaneous resonant coupling of ultraviolet excitation photons to quantum dots and visible emission for up to 5.8X enhancement of photon extraction for multiple types of QDs.

FF1C.5 • 09:45

GaN L3 Photonic Crystal Cavities With an Average Quality Factor in Excess of 16000 in the Near Infrared, Noelia Vico Triviño¹, Momchil Minkov¹, Giulia Urbinati², Matteo Galli², Jean-François Carlin¹, Raphael Butte¹, Vincenzo Savona¹, Nicolas Grandjean¹; ¹Ecole Polytechnique Federale de Lausanne, Switzerland; ²Universita di Pavia, Italy. GaN L3 photonic crystal cavities were fabricated based on a genetic algorithm optimization. Optical characterization of several replicas led to an average unloaded quality factor of 16900, which is well accounted for by first-principles simulations.

SF1D • Nonlinear Optics Frequency Conversion with Integrated Optical Devices—Continued

SF1D.6 • 09:30

Mode-Locked and Repetition-Rate-Tunable Comb Generation Using Dual Coupled Microrings, Xiaoxiao Xue¹, Yi Xuan^{1,2}, Pei-Hsun Wang¹, Yang Liu¹, Daniel E. Leaird¹, Minghao Qi^{1,2}, Andrew M. Weiner^{1,2}; ¹School of Electrical and Computer Engineering, Purdue Univ., USA; ²Birk Nanotechnology Center, Purdue Univ., USA. A method incorporating controllable mode interaction is proposed for Kerr frequency comb generation in normal-dispersion microresonators. Repetition-rate-tunable combs and broadband mode-locking transitions are demonstrated by using dual silicon nitride microrings.

SF1D.7 • 09:45

Parametric Frequency Conversion in Silicon Carbide Waveguides, Jaime Cardenas¹, Steven Miller¹, Yoshitomo Okawachi¹, Sven Ramelow¹, Austin G. Griffith¹, Alessandro Farsi¹, Alexander L. Gaeta^{1,2}, Michal Lipson^{1,2}; ¹Cornell Univ., USA; ²Kavli Inst. at Cornell for Nanoscale Science, USA. We show the first demonstration of frequency conversion via four wave mixing in a silicon carbide channel waveguide with a conversion efficiency as high as -19.5 dB over a 180 nm wavelength range.

10:00–10:30 Coffee Break, Concourse Level



For Conference News & Insights
Visit blog.cleoconference.org

Executive Ballroom
210E

CLEO: Applications
& Technology

AF1E • A&T Topical Review on
High Performance Optics I—
Continued

AF1E.5 • 09:30

Selective Lasing and Nonlinear Relaxation of Confined Exciton-Polaritons, Gabriele Grosso^{1,2}, Stéphane Trebaol^{1,3}, Michiel Wouters⁴, François Morier-Genoud¹, Marcia Portella Oberli¹, Benoît Deveaud¹; ¹ICMP, Ecole Polytechnique Fédérale de Lausanne (EPFL), Switzerland; ²EECS, MIT, USA; ³UMR Foton, Université de Rennes, France; ⁴TQC, Univ. of Antwerp, Belgium. We detail an innovative laser device based on a new relaxation mechanism for confined exciton-polaritons which preserves nonlinearity. We demonstrate the selective activation of polariton lasers at different wavelengths allowing to perform all-optical logic operations with fully coherent output.

AF1E.6 • 09:45

All-Optical Tunable Multilevel Amplitude Regeneration Based on Coherent Polarization Mixing, Zahra Bakhtiari¹, Alexander Sawchuk¹; ¹USC, USA. We propose an all-optical phase-preserving scheme for multilevel amplitude regeneration based on coherent polarization mixing for optical star-8QAM/star-16QAM signals with a power ratio of 1:5. A regeneration factor of 5.3 for star 8-QAM is achieved.

Executive Ballroom
210F

CLEO: Science & Innovations

SF1F • Solid State Lasers—
Continued

SF1F.7 • 09:30

Synchronously Pumped Mid-IR Hollow Core Fiber Gas Laser, Muhammad Rosdi Abu Hassan¹, Fei Yu¹, Zefeng Wang^{1,2}, Walter Belardi¹, William Wadsworth¹, Jonathan Knight¹; ¹Dept. of Physics, Centre for Photonics and Photonic Materials, Univ. of Bath, UK; ²College of Optoelectronic Science and Engineering, National Univ. of Defense Technology, China. We report a synchronously pumped 3.16 μm acetylene fiber laser based entirely on low-loss silica hollow-core fiber. Our system oscillates at 2.568 MHz repetition rate, when pumped with a modulated amplified 1.53 μm diode laser.

SF1F.8 • 09:45

Single-frequency crystalline Raman amplifier at 1178 nm, Zhaojun Liu¹, Zhenhua Cong¹, Sasa Zhang¹, Shaojie Men¹, Yang Liu¹, Jinbao Xia¹, Wenyong Cheng¹, Yongfu Li¹, Chaoyang Tu², Xingyu Zhang¹; ¹Shandong Univ., China; ²Fujian Inst. of Research on the Structure of Matter, Chinese Academy of Sciences, China. Single-frequency crystalline Raman amplifier at 1178 nm was demonstrated. After three stages of amplifications, the output pulse energy was 26.7 mJ and the pulse width was 2.9 ns. The linewidth was less than 500 MHz.

Executive Ballroom
210G

SF1G • Novel Devices—
Continued

SF1G.6 • 09:30

Graphene-Based Saturable Absorber for Passive Q-switching of Tm:KLu(WO₄)₂ Microchip Laser, Xavier Mateos¹, Josep Maria Serres¹, Pavel Loiko^{2,1}, Konstantin Yumashev², Valentin Petrov³, Uwe Griebner³, Magdalena Aguilo¹, Francesc Diaz¹; ¹Universitat Rovira i Virgili, Spain; ²Center for Optical Materials and Technologies, Belarusian National Technical Univ., Belarus; ³Max Born Inst., Germany. A diode-pumped Q-switched Tm:KLu(WO₄)₂ microchip laser generated a maximum average output power of 310 mW with $M^2 < 1.2$ at 1947 nm. The shortest pulse duration was 285 ns at a pulse repetition rate of 190 kHz.

SF1G.7 • 09:45

A ZnO/InN/GaN Heterojunction Photodetector with Extended Infrared Response, Lung-Hsing Hsu¹, Shun-Chieh Hsu², Hsin-Ying Lee³, Yu-Lin Tsai⁴, Da-Wei Lin⁴, Hao-Chung Kuo⁴, Yi-Chia Hwang², Yin-Han Chen², Jr-Hau He⁵, Yuh-Jen Cheng⁶, Shih-Yen Lin⁶, Chien-Chung Lin²; ¹Inst. of Lighting and Energy Photonics, National Chiao Tung Univ., Taiwan; ²Inst. of Photonic System, National Chiao Tung Univ., Taiwan; ³Dept. of Photonics, National Cheng Kung Univ., Taiwan; ⁴Inst. of Electro-Optical Engineering, National Chiao Tung Univ., Taiwan; ⁵Inst. of Photonics and Optoelectronics, National Taiwan Univ., Taiwan; ⁶Research Center for Applied Sciences, Academia Sinica, Taiwan. An extended infrared photoresponse is observed in a ZnO/InN/GaN heterojunction diode with InN grown by MOCVD. The external quantum efficiency is measured between 1200 and 1800 nm and can be as high as 3.55%.

10:00–10:30 Coffee Break, Concourse Level

CLEO: Science & Innovations

CLEO: Applications
& Technology

SF1H • Microcavities—
Continued

SF1I • Lasers for Optical
Communications—Continued

AF1J • Measurement of Process
Parameters—Continued

SF1H.7 • 09:30

Yb³⁺-doped Silica WGM Milled Microrod laser, Shahab Bakhtiari Gorajooobi¹, Ganapathy Senthil Murugan¹, Michalis Zervas¹; ¹Optoelectronics Research Centre, Univ. of Southampton, UK. A fast and versatile fabrication method for high Q milled microrod resonators, directly on rare-earth doped fibers, is demonstrated using a pulsed CO₂ laser. Evanescently pumped WGM microlaser with ~9μW output power has been achieved.

SF1I.7 • 09:30

Millimeter-wave Modulation of 850 nm VCSELS for Radio over Fiber Applications, Hamed Dalir¹, Fumio Koyama²; ¹Electronics and Applied Physics, Tokyo Inst. of Technology, Japan. A slow-light modulator-integrated with 850nm-VCSEL is presented, exhibiting small signal response of over 55dB enhancement at frequencies beyond 35GHz. Also, the direct modulation bandwidth is expanded beyond 20GHz thanks to optical-feedback in the integrated device.

AF1J.6 • 09:30 **Invited**

Metrology for Quantum Communications, Christopher Chunnillall¹; ¹NPL, UK. Industrial technologies based on single photons are emerging. We report on work to develop traceable metrology for the quantum optical devices used in quantum key distribution (QKD), one of the most commercially-advanced quantum technologies.

SF1H.8 • 09:45

Demonstration of the first monolithically integrated self-rolled-up tube based vertical photonic coupler, Xin Yu¹, Ehsan Arbabi^{1,2}, Xiuling Li¹, Lynford L. Goddard¹, Xiaogang Chen¹; ¹Univ of Illinois at Urbana-Champaign, USA; ²California Inst. of Technology, USA. We demonstrated the first monolithically integrated self-rolled-up SiN_x tube based vertical photonic coupler on top of a planar ridge waveguide. The coupling efficiency between the elements is >10 times higher than similar non-integrated device.

SF1I.8 • 09:45

Microwave Signal Generation Using a 1550 nm VCSEL Subject to Dual-Beam Orthogonal Optical Injection, Pablo Pérez^{1,2}, Ana Quirce³, Angel Valle¹, Luis Pesquera¹, Antonio Consoli⁴, Ignacio Esquivias⁵; ¹Instituto de Física de Cantabria (CSIC-UC), Spain; ²Departamento de Física Moderna, Universidad de Cantabria, Spain; ³Faculty of Engineering Sciences, Brussels Photonics Team, Vrije Universiteit Brussel, Belgium; ⁴Instituto de Ciencia de Materiales de Madrid, CSIC, Spain; ⁵Departamento de Tecnología Fotónica, Universidad Politécnica de Madrid, Spain. We experimentally and theoretically investigate microwave signal generation using a 1550nm VCSEL subject to two-frequency orthogonal optical injection. It is found that microwave linewidth is given by the sum of the linewidths of the two master lasers.

10:00–10:30 Coffee Break, Concourse Level

NOTES

Blank lined area for notes.

CLEO: Science & Innovations

SF1L • Frequency Standards
and Timing—Continued

SF1L.6 • 09:30

Fiber-based portable optical frequency standard for telecommunication, Marco Triches^{1,2}, Anders Bruschi¹, Jan Hald¹, Jesper Lægsgaard², Ole Bang²; ¹DFM A/S - Danish Fundamental Metrology Inst., Denmark; ²Dept. of Photonics Engineering, Technical University of Denmark, Denmark. Gas-filled hollow-core fiber-based portable optical frequency standard is developed for laser stabilization to the ¹³C₂H₂ transition at 1.5 μm using saturated absorption. The system, assembled in an easy-to-use configuration, has an Allan deviation 8×10^{-11} ($1 < \tau < 1000$ s) with 60 kHz locking accuracy.

SF1L.7 • 09:45

Compact and robust laser system for precision atom interferometry based on a frequency doubled telecom fiber bench, Fabien Theron¹, Nassim Zahzam¹, Yannick Bidet¹, Malo Cadoret¹, Alexandre Bresson¹; ¹ONERA, France. We present a compact and robust narrow linewidth laser system for onboard Rubidium atom interferometry using only one laser source based on a frequency doubled telecom fiber bench.

SF1M • Symposium on OPA/
OPCPA – Next Generation
of Ultra-Short Pulse Laser
Technology I—Continued

SF1M.5 • 09:30

Improved Characteristics of High Repetition Rate Non-Collinear Optical Parametric Amplifiers for Electron-Ion Coincidence Spectroscopy, Federico J. Furch¹, Alexandria Anderson¹, Sascha Birkner¹, Yicheng Wang¹, Achut Giree^{1,2}, Claus Peter Schulz¹, Marc Vrakking¹; ¹Max Born Inst., Germany; ²Amplitude Technologies, France. A non-collinear optical parametric amplifier (NOPA) for applications in attosecond science is presented. The amplifier delivers carrier-envelope phase (CEP) stable few-cycle pulses at an average power of 5 W at 400 and 800 kHz.

SF1M.6 • 09:45

High-Power 300-kHz OPCPA System Generating CEP-Stable Few-Cycle Pulses, Marcel Schultze¹, Stephan Prinzl^{1,2}, Matthias Haefner¹, Catherine Y. Teisset¹, Robert Bessing¹, Knut Michel¹, Thomas Metzger¹; ¹TRUMPF Scientific Lasers, Germany; ²Dept. of Physics, Technische Universität München, Germany. An OPCPA system with 15 W of average power at 300 kHz repetition rate generating CEP-stable few-cycle pulses is presented. The system exhibits pulse durations below 6 fs, a peak power of 4.5 GW and an excellent long-term performance over hours of operation with power fluctuations of less than 1.5%.

10:00–10:30 Coffee Break, Concourse Level

NOTES

Blank lined area for notes.

CLEO: QELS-Fundamental Science

CLEO: Science & Innovations

10:30–12:30

FF2A • Single Photon Detectors
Presider: Jevon Longdell; Univ. of Otago, New Zealand

FF2A.1 • 10:30

Low-jitter single-photon detector arrays integrated with silicon and aluminum nitride photonic chips, Faraz Najafi¹, Jacob Mower¹, Nicholas C. Harris¹, Francesco Bellei¹, Andrew Dane¹, Catherine Lee¹, Xiaolong Hu¹, Sara Mouradian¹, Tim Schroder¹, Prashanta Kharel², Francesco Marsili³, Solomon Assefa⁴, Karl K. Berggren¹, Dirk R. Englund¹; ¹MIT, USA; ²Columbia Univ., USA; ³Jet Propulsion Lab, USA; ⁴IBM TJ Watson Research Center, USA. We present progress on a scalable scheme for integration of single-photon detectors with silicon and aluminum nitride photonic circuits. We assemble arrays of low-jitter waveguide-integrated single-photon detectors and show up to 24% system detection efficiency.

FF2A.2 • 10:45

Probing Number-Correlated States of up to 50 Photons, Georg Harder¹, Tim J. Bartley^{2,1}, Adriana Lita², Sae Woo Nam², Thomas Gerrits², Christine Silberhorn¹; ¹Applied Physics, Univ. of Paderborn, Germany; ²National Inst. for Standard and Technology, USA. Using spontaneous parametric down-conversion in ppKTP waveguides, we probe photon-number correlated states of up to 50 photons with a Klyshko efficiency of >60%, in a single mode characterised by an unheralded marginal $g^{(2)}(0)=1.87\pm 0.05$.

FF2A.3 • 11:00

Saturated Photon Detection Efficiency in NbN Superconducting Photon Detectors, Ryan Murphy¹, Matthew Grein¹, Theodore Gudmundsen¹, Adam McCaughan², Faraz Najafi², Karl K. Berggren², Francesco Marsili³, Eric Dauler¹; ¹MIT Lincoln Lab, USA; ²Research Lab of Electronics, MIT, USA; ³Jet Propulsion Lab, USA. In this work, we demonstrate saturated photon detection efficiency with narrow NbN nanowires and SNAPs to boost the signal-to-noise ratio, and we demonstrate a stabilizing choke inductance that is part of the optically-active area.

10:30–12:30

FF2B • Quantum Nonlinear Optics
*Presider: Michal Bajcsy; Univ. of Waterloo, Canada*FF2B.1 • 10:30 **Invited****Giant Polarization Rotation Induced by a Single Spin: a Cavity-Based Spin-Photon Interface**, Justin Demory¹, Christophe Arnold¹, Vivien Loo¹, Aristide Lemaître¹, Isabelle Sagnes¹, Mikhail Glazov², Olivier Krebs¹, Paul Voisin¹, Pascale Senellart¹, Loic Lanco^{1,2}; ¹LPN-CNRS, France; ²Université Paris Diderot Paris 7, France; ³Ioffe Physical-Technical Inst., Russia. We report the amplification by three orders of magnitude of the spin-photon interaction, using a single hole spin in a quantum dot-pillar cavity system: a macroscopic and spin-dependant polarization rotation is induced on incident photons by a single spin, initialized either in the up or down state.

FF2B.2 • 11:00

Macroscopic Kerr Rotation from a Bright Negatively Charged Quantum Dot in a Low-Q Micropillar Cavity, Petros Androvitsaneas¹, Andrew Young¹, Christian Schneider², Sven Höfling^{2,3}, Martin Kamp², Edmund Harbord¹, John Rarity¹, Ruth Oulton¹; ¹Univ. of Bristol, UK; ²Universität Würzburg, Germany; ³Univ. of St. Andrews, UK. We report the measurement of macroscopic phase shifts of several degrees for reflected incident light resonant with a bright negatively charged quantum dot (QD) in a micropillar structure of Q-factor less than 200.

10:30–12:30

FF2C • Near-field Imaging, Spectroscopy and Optomechanics
Presider: To be Determined

FF2C.1 • 10:30

High-Contrast Nanoparticle Sensing using a Hyperbolic Metamaterial, Wenqi Zhu¹, Ting Xu¹, Amit Agrawal¹, Henri J. Lezec¹; ¹NIST, USA, USA. Using planar hyperbolic metamaterials composed of alternating layers of metal (Ag) and dielectric (SiO₂), we demonstrate a transmission device for nanoparticle sensing that exhibits extremely high optical contrast.

FF2C.2 • 10:45

Gap Mode Formation in Metallic, Nanofocusing SNOM Tapers for High Spatial Resolution Broadband Spectroscopy, Martin Esmann¹, Simon Becker¹, Kyung Wan Yoo^{1,2}, Heiko Kollmann¹, Petra Gross^{1,3}, Ralf Vogelgesang¹, Nam Kyoo Park², Christoph Lienau¹; ¹Carl V. Ossietzky Universität, Germany; ²Seoul National Univ., Korea; ³Universität Osnabrück, Germany. Nanofocusing of surface plasmon polaritons enables broadband elastic scattering spectroscopy on individual nanoantennas without any signal demodulation. Clear experimental signatures of tip-sample gap mode formation hint at a potential increase in lateral resolution to single nanometers.

FF2C.3 • 11:00

Holographic 3D Superlocalization of Brownian Scattering Particles for Stochastic Optical Mapping, Ariadna Martinez-Marrades¹, Jean-François Rupprecht³, Michel Gross⁴, Gilles Tessier^{2,1}; ¹Institut Langevin, ESPCI, CNRS UMR 7587, France; ²Neuro-photonics lab, Université Paris Descartes, France; ³Laboratoire de Physique Théorique de la Matière Condensée, UPMC, UMR CNRS 7600, France; ⁴Laboratoire Charles Coulomb, UMR CNRS 5221, Université Montpellier 2, France. We present a wide field microscopy technique for the 3D mapping of optical intensity using Brownian gold nanoparticles as local probes. Localization by off-axis holography allows stochastic subwavelength optical characterization in water-based systems.

10:30–12:30

SF2D • Supercontinuum Generation: Fundamentals Issues and New Technologies
Presider: Jaime Cardenas; Cornell Univ., USA

SF2D.1 • 10:30

Coherent Supercontinuum from a Silicon Nitride Waveguide, Adrea R. Johnson¹, Aline Sophie Mayer², Alexander Klenner², Kevin Luke³, Erin S. Stranford¹, Michael Lamont^{1,3}, Yoshitomo Okawachi¹, Frank W. Wise¹, Michal Lipson^{3,4}, Ursula Keller², Alexander L. Gaeta^{1,4}; ¹School of Applied and Engineering Physics, Cornell Univ., USA; ²Dept. of Physics, Inst. of Quantum Electronics, ETH Zurich, Switzerland; ³School of Electrical and Computer Engineering, Cornell Univ., USA; ⁴Kavli Inst. at Cornell for Nanoscale Science, Cornell Univ., USA. We show experimentally and theoretically that the coherence of a two-octave-spanning supercontinuum generated in a silicon nitride waveguide via 1- μ m-pumping with ~100-fs pulses is fully coherent over most of its bandwidth.

SF2D.2 • 10:45

Blue-enhanced supercontinuum generation pumped by a giant-chirped SESAM mode-locked fiber laser, Shoufei Gao¹, Ruoyu Sun¹, Dongchen Jin¹, Pu Wang¹; ¹Inst. of Laser Engineering, Beijing Univ. of Technology, China. We report a blue-enhanced supercontinuum generation pumped by a giant-chirped SESAM mode-locked ytterbium-doped fiber laser. An extremely wide optical spectrum spanning from 380 nm to 2400 nm with total power of 3 W is obtained.

SF2D.3 • 11:00

Silicon-on-Sapphire Nanowire for Mid-IR Supercontinuum Generation, Neetesh Singh¹, Darren Hudson¹, Yi Yu², Christian Grillet³, Andrew Read⁴, Petar Atanackovic⁴, Steven Duval⁴, Stephen Madden², David Moss⁵, Barry Luther-Davies², Benjamin J. Eggleton¹; ¹Univ. of Sydney, Australia; ²Australian National Univ., Australia; ³Univ. of Lyon, France; ⁴Silanna Semiconductor, Australia; ⁵RMIT, Australia. We demonstrate an octave spanning, 1.9-6.2 μ m supercontinuum generation in a low loss silicon on a sapphire (SOS) nanowire. This establishes SOS as a promising new platform for integrated nonlinear photonics in the mid-IR.

Executive Ballroom
210E

CLEO: Applications
& Technology

10:30–12:30

AF2E • A&T Topical Review on
High Performance Optics II

Presider: Michael Trubetskov;
Max Planck Inst. of Quantum
Optics, Germany

AF2E.1 • 10:30 **Invited**

Laser-Induced Ionization and Damage of High-Performance Optics by Ultrashort Pulses, Vitaly Gruzdev¹; ¹Univ. of Missouri-Columbia, USA. Damage of high-performance optics by ultrashort laser pulses is attributed to the laser-induced ionization and electron excitation. New theoretical models and current state of knowledge in the field are overviewed and critically analyzed based on the recent developments and results.

AF2E.2 • 11:00 **Invited**

Laser-induced damage of nodular defects in dielectric multilayer coatings, Zhanshan Wang¹, Xinbin Cheng¹, Jinlong Zhang¹, Tao Ding¹, Hongfei Jiao¹, Bin Ma¹; ¹Tongji Univ., China. This paper reviews our recent studies on the laser-induced damage of nodules in dielectric multilayer coatings, where the influence of the electric-field enhancement and the mechanical stability on the thermo-mechanical damage of nodules is discussed.

Executive Ballroom
210F

CLEO: Science & Innovations

10:30–12:15

SF2F • Novel Approaches

Presider: Efim Khazanov; Inst. of
Applied Physics, Russia

SF2F.1 • 10:30

Novel Diode Pumped Sulfur Oxide Laser: DPSOL, William F. Krupke¹; ¹WFK Lasers, USA. The concept of a diode pumped molecular gas laser is introduced, with energy storing sulfur monoxide (SO) as the active molecule. Key spectroscopic and kinetic characteristics are presented, along with a kW laser point design.

SF2F.2 • 10:45

Diode Pumped Sodium Molecular Laser, Walter Luhs¹, B. Wellegehausen²; ¹Photonic Engineering Office, Germany; ²Institut für Quantenoptik, Universität Hannover, Germany. First continuous laser oscillation around 554 nm on B¹Π_g → X¹Σ_g⁺ transitions of Na₂ has been obtained, optically pumped with a common cw blue emitting InGaN diode laser at 461 nm. Spectroscopic investigations and laser experiments are reported.

SF2F.3 • 11:00

Doubly-Resonant Fabry-Perot Cavity for Power Enhancement of Burst-Mode Picosecond Ultraviolet Pulses, Abdurahim Rakhman^{1,2}; ¹Oak Ridge National Lab, USA; ²Dept. of Physics and Astronomy, Univ. of Tennessee, USA. We report on a first experimental demonstration of locking a doubly-resonant Fabry-Perot cavity to burst-mode 402.5MHz/50ps ultraviolet (UV) pulses with a MW level peak power by using a temperature controlled dispersion compensation method at the Spallation Neutron Source.

Executive Ballroom
210G

10:30–12:00

SF2G • III/V Photonics

Presider: To be Determined

SF2G.1 • 10:30

Realization of A SOI-Like III-V Platform Based On the Integration of GaAs With Silicon, Rajat Sharma¹, Hung-Hsi Lin¹, Matthew W. Puckett¹, Yeshiahu Fainman¹; ¹Univ. of California, San Diego, USA. We demonstrate the integration of gallium arsenide with silicon to create a SOI-like platform capable of exploiting the optical properties of III-V materials. We fabricate nanoscale waveguides and design Bragg gratings on this new platform.

SF2G.2 • 10:45

Recovery Time Control in a Nanophotonic Nonlinear Gate Using Atomic Layer Deposition, Gregory Moille¹, Sylvain Combré¹, Gaëlle Lehoucq¹, Laurence Morgenroth², François Neuilly², Didier Decoster², Alfredo De Rossi¹; ¹Thales Research & Technology, France; ²Institut d'Electronique de Micro-electronique et de Nanotechnologie, France. Atomic Layer Deposition is used to control the surface recombination of carriers in GaAs photonic crystal cavities. All-optical wavelength conversion at a GHz repetition rate is demonstrated with recovery time below 10 ps.

SF2G.3 • 11:00

1.5µm High Density Quantum Dots Waveguide Photodetector with Avalanche Effect, Toshimasa Umezawa¹, Kouichi Akahane¹, Naokatsu Yamamoto¹, Atsushi Kanno¹, Tetsuya Kawanishi¹; ¹National Inst of Information & Comm Tech, Japan. We have fabricated a waveguide photodetector using a 1.55-µm high-density InAs quantum dot absorption layer. A high responsivity (0.4 A/W) without using fiber coupling designs, and a large avalanche multiplication factor of over 10 could be successfully achieved.

CLEO: Science & Innovations

CLEO: Applications
& Technology

10:30–12:30
SF2H • Photonic Crystals
President: Paul Barclay; Univ. of
Calgary, Canada

10:30–12:30
SF2I • Laser Surface Nano-
structuring
President: Emmanuel Haro-
Poniatowski; UAM-Iztapalapa,
Mexico

10:30–12:30
AF2J • Chemical and Gas
Sensing
President: Ekaterina Golovchenko;
TE Connectivity, USA

SF2H.1 • 10:30
Over-1mm-long Wideband on-Chip Slow-
light Waveguides Realized by 1,000
Coupled L3 Nanocavities, Eiichi Kuramochi¹,
Nobuyuki Matsuda¹, Kengo Nozaki¹, Hiroki
Takesue¹, Masaya Notomi¹; ¹NTT Corpora-
tion, Japan. Enhanced coupling in slanted
L3 nanocavity array expanded bandwidth to
4 THz at telecom wavelength. High-Q tuned
L3 nanocavity realized 1,000 coupled cavities
with acceptable propagation loss and delay-
bandwidth product over 100.

SF2I.1 • 10:30 **Tutorial**
Nano-Ablation by Femtosecond Laser-
Matter Interactions, Shuji Sakabe^{1,2}, Ma-
saki Hashida^{1,2}; ¹Inst. for Chemical Research,
Kyoto Univ., Japan; ²Graduate School of
Science, Kyoto Univ., Japan. Distinguishing
ablation characteristic, nanometer phe-
nomena such as surface morphology and
ion emission, resulting from femtosecond
laser-matter interactions for metals, and some
their applications are reviewed, comparing
with conventional nanosecond laser-matter
interactions and ablation.

AF2J.1 • 10:30
Silicon on Sapphire Chip Based Pho-
tonic Crystal Waveguides for Detection of
Chemical Warfare Simulants And Volatile
Organic Compound, Yi Zou¹, Parker Wray¹,
Swapnajt Chakravarty², Ray T. Chen^{1,2}; ¹Univ.
of Texas at Austin, USA; ²Omega Optics Inc.,
USA. We experimentally demonstrate the
first holey and slotted photonic crystal wave-
guides in silicon-on-sapphire at mid-infrared
wavelength of 3.43 μ m. Chemical warfare
simulant triethylphosphate was detected in
gas phase at 10ppm concentration via optical
absorbance signature.

SF2H.2 • 10:45
Systematic tuning of ultrahigh-Q no-miss-
ing-hole (H0) nanocavity, Eiichi Kuramochi¹,
Hadrien Duprez¹, Hideaki Taniyama¹, Hisashi
Sumikura¹, Kengo Nozaki¹, Akihiko Shinya¹,
Masaya Notomi¹; ¹NTT Corporation, Japan.
Systematic multi-hole tuning of H0 nanocav-
ity with theoretical Q of $\sim 10^7$ is reported that
outperforms L3 and other a-few-missing-hole
nanocavities over a wide slab-thickness
range. Experimental Q of $\sim 10^6$ is achieved.



Shuji Sakabe acquired a master's degree in
1980 and a doctoral degree of engineering
in 1984 from Osaka Univ. He was an Assistant
Professor at the Institute of Laser Engineer-
ing, Osaka Univ. during the 1980's and also
served as Associate Professor, Faculty of
Engineering from 1998 to 2002. Between
his terms at Osaka Univ. he was a researcher
at the Max-Planck Institute for Quantum
Optics. Associate Professor, Currently he is
a full Professor at the Institute for Chemical
Research at Kyoto University.

He has been studying laser plasma phys-
ics, laser nuclear fusion, and laser isotope
separation (1977-2002), and contributed
to the construction of laser facility GEKKO
XII (1983-84). Currently he is involved in
the research for the physics of intense laser
matter interaction and its applications. He
serves on the board of directors for Laser
Society of Japan.

AF2J.2 • 10:45
Highly Sensitive Chemical Gas Sensor
Based on Graphene Deposited D-shaped-
fiber, Yu Wu¹, Baicheng Yao¹, Xuli Cao¹,
Zegao Wang^{1,2}, Yunjiang Rao¹, Yuanfu Chen¹,
Kin S. Chiang^{1,3}; ¹UESTC, China; ²Aarhus
Univ., Denmark; ³City University of Hong
Kong, Hong Kong. A graphene coated
D-shaped fiber chemical-gas sensor demon-
strated, with maximum sensitivity ~ 0.04 ppm
and ~ 0.1 ppm for NH₃ and H₂O gas detec-
tions, respectively. This work may pave a
way to explore graphene based lab-on-fiber
devices.

SF2H.3 • 11:00
Bending Behavior of Flexible Crystalline
Silicon Nanomembrane Photonic Crystal
Microcavities, Xiaochuan Xu^{2,1}, Harish
subbaraman², Swapnajt Chakravarty², Ray
T. Chen^{1,2}; ¹Univ. of Texas at Austin, USA;
²Omega Optics, Inc., USA. We demonstrated
a flexible crystalline silicon nanomembrane
photonic crystal microcavity with a quality
factor of 22,000 and experimentally studied
its bending behavior.

AF2J.3 • 11:00
Mid-infrared detection of atmospheric
CH₄, N₂O and H₂O based on a single
continuous wave quantum cascade laser,
Yingchun Cao¹, Nancy P. Sanchez¹, Robert
Griffin¹, Frank K. Tittel¹; ¹Rice Univ., USA.
A continuous wave, distributed feedback
quantum cascade laser based absorption
system was developed and demonstrated
for simultaneous atmospheric CH₄, N₂O and
H₂O detection, with minimum detection
limits below 2% of their typical atmospheric
concentrations.



Join the conversation. Use #CLEO15.
Follow us @cleoconf on Twitter.

CLEO: Science & Innovations

10:30–11:45

SF2K • Short Reach & PON Communication

Presider: Neda Cvijetic; NEC Labs America, USA

SF2K.1 • 10:30

100Gb/s WDM-SSB-DD-OFDM using a Gain Switched Monolithically Integrated Passive Feedback Comb Source, Prince M. Anandarajah¹, Tong Shao¹, Rui Zhou¹, Deseada Gutierrez Pascual^{1,2}, Liam P. Barry¹; ¹Dublin City Univ., Ireland; ²Pilot Photonics, Ireland. We demonstrate a 100Gb/s short reach system using a multi-carrier transmitter based on a gain switched monolithically integrated laser. 25km SSMF transmission of a 5x20Gb/s WDM-SSB-DD-OFDM channels with a SE of 1.6b/s/Hz is reported.

SF2K.2 • 10:45

Up to 16 Gb/s CAP16 Modulation over 100 km IM/DD Dispersion Uncompensated Transmission using Dual-EML, Mohamed Essghair Chaibi¹, Christophe Kazmierski², Didier Erasme¹; ¹Institut MINES-TELECOM, TELECOM ParisTech, France; ²III-V Lab-Common Lab of "Alcatel-Lucent Bell Labs France", "Thales Research and Technology" and "CEA Leti", France. Transmissions at 16 Gb/s of 16-QAM CAP signals over 100 km IM/DD dispersive channel are reported. They are performed in an optical SSB context generated with an integrated Dual-EML.

SF2K.3 • 11:00

Design of 100G PDM-QPSK Unrepeated Transmission Systems with EDFA Only Amplification, Xuan He^{1,2}, Bo Zhang², Dan Pudvay², Rob Lofland², Massimiliano Salsi², Qiang Wang², Jason O'neil², Yang Yue², Jon Anderson², Zhongqi Pan¹; ¹Univ. of Louisiana at Lafayette, USA; ²Juniper Networks, USA. We investigate three EDFA only amplification architectures for 100G unrepeated transmission. With > 4 dBQ margin, pre-amplifier only, booster only and both booster and pre-amplifier amplifications can achieve 130, 150 and 220 km reach respectively.

10:30–12:30

SF2L • Ranging and Metrology

Presider: Mark Notcutt; Stable Laser Systems, USA

SF2L.1 • 10:30

Fiber-based optical frequency comb interferometer with nm-stability and meters-wide scanning range, Yoshiaki Nakajima^{2,1}, Kaoru Minoshima^{2,1}; ¹JST, ERATO, Japan; ²The Univ. of Electro-Communications, Japan. A 167-m fiber-based optical frequency comb interferometer was stabilized to nm-level with extremely wide scanning of 2.8 m by frequency scanning. Fiber noise cancellation with direct use of a frequency comb was also demonstrated.

SF2L.2 • 10:45

Attosecond-Resolution Time-of-Flight Stabilization of Optical Pulse Train in 76-m Indoor Atmospheric Link, Jinho Kang¹, Junho Shin¹, Chur Kim¹, Kwangyun Jung¹, Jungwon Kim¹; ¹Korea Advanced Inst of Science & Tech, Korea. We demonstrate sub-100-attosecond-resolution time-of-flight stabilization method for optical pulse trains in atmospheric links. The rms excess fluctuation in timing for 76.2-m-long indoor free-space transfer is suppressed from >230 fs to 2.6 fs over 130-hour.

SF2L.3 • 11:00

Dual-comb absolute ranging using balanced optical cross-correlator as time-of-flight detector, Haosen Shi¹, Youjian Song¹, Fei Liang¹, Liming Xu¹, Ming-lie Hu¹, Chingyue Wang¹; ¹Tianjin Univ., China. We demonstrate dual-comb absolute ranging using balanced optical cross correlator as high resolution pulse time-of-flight detector. Actual test performed at ~3 meters target distance proves a 200 nm ranging precision at 50 ms acquisition time.

10:30–12:30

SF2M • Symposium on OPA/OPCPA – Next Generation of Ultra-Short Pulse Laser Technology II

Presider: Dong Eon Kim; Max Planck Center for Attosecond Science, Germany

SF2M.1 • 10:30 **Invited**

Tunable Few-optical-Cycle Pulses by Group-velocity-matched OPAs, Giulio Cerullo¹, Cristian Manzoni¹, Daniele Brida²; ¹Politecnico di Milano, Italy; ²Univ. of Konstanz, Germany. We review our work on the development of ultra-broadband OPAs. By group-velocity matching between signal and idler waves, we generate pulses with duration of few optical cycles and tunability from the visible to the infrared.

SF2M.2 • 11:00 **Invited**

Few-Cycle and Phase Stable OPCPA Systems with High Repetition Rate, Uwe Morgner^{1,2}, Jan Ahrens^{1,3}, Tino Lang^{1,2}, Marcel Schultze⁴, Thomas Binhammer³, Oliver Prochnow³, Anne Harth⁵, Piotr Rudawski⁵, Cord L. Arnold⁵, Anne L'Huilier⁵; ¹Inst. of Quantum Optics, Leibniz Universität Hannover, Germany; ²QUEST, Leibniz Universität Hannover, Germany; ³VENTEON Laser Technologies GmbH, Germany; ⁴TRUMPF Scientific Lasers GmbH & Co. KG, Germany; ⁵Dept. of Physics, Lund Univ., Sweden. We present different approaches for high repetition rate, few-cycle pulse generation with μ J-level energy from compact OPCPA systems. The sources are based on octave spanning Ti:Sa oscillators with all-optical synchronization to state-of-the-art Ytterbium based amplifiers.

CLEO: QELS-Fundamental Science

CLEO: Science & Innovations

FF2A • Single Photon Detectors—Continued

FF2A.4 • 11:15

Polarization-Insensitive Superconducting Nanowire Single-Photon Detectors, Shellee D. Dyer¹, Hiroki Takesue², Varun Verma¹, Robert Horansky¹, Richard P. Mirin¹, Sae Woo Nam¹; ¹NIST, USA; ²NTT Basic Research Labs, NTT, Japan. We report MoSi superconducting nanowire single-photon detectors (SNPDs) with low polarization sensitivity over a 120 nm wavelength range, covering the standard fiber telecom wavelengths. Our models indicate that this low polarization sensitivity is consistent with the design geometry.

FF2A.5 • 11:30

Superconducting Nanowire Detectors Based on MgB₂, Francesco Marsili¹, Daniel P. Cunnane¹, Ryan Briggs¹, Matthew D. Shaw¹, Boris S. Karasik¹, Matthaeus Wolak², Narendra Acharya², Xiaoxing Xi²; ¹Jet Propulsion Lab, USA; ²Temple Univ., USA. We fabricated and characterized the optical response of MgB₂ nanowires with critical temperature $T_c = 33$ K. The devices showed optical response at 4 K and subnanosecond relaxation time. The detectors responded to the simultaneous absorption of three photons, but not to single photons.

FF2A.6 • 11:45

A Robust Optical Coupler for Alignment of Superconducting Nanowire Detector Array, R. H. Shepard¹, Andrew Guzman¹, Matthew Grein¹, Eric Dauler¹, Danna Rosenberg¹, Theodore Gudmundsen¹, Ryan Murphy¹; ¹Massachusetts Inst of Tech Lincoln Lab, USA. We present an athermalized design and performance analysis of a robust imaging system used to couple light from an input fiber to a superconducting nanowire single photon detector.

FF2B • Quantum Nonlinear Optics—Continued

FF2B.3 • 11:15

Optical Pumping of Individual Spins in Self-Assembled and Site-Controlled Quantum Dots, Konstantinos Lagoudakis¹, Peter L. McMahon¹, Kevin Fischer¹, Kai Muller¹, Tomas Sarmiento¹, Shruti Puri¹, Dan Dalacu², Philip Poole², Michael Reimer³, Val Zwiller³, Yoshihisa Yamamoto⁴, Jelena Vuckovic¹; ¹Stanford Univ., USA; ²National Research Council of Canada, Canada; ³T U Delft, Netherlands; ⁴National Inst. of Informatics, Japan. We investigate optical spin pumping of self-assembled p-type δ -doped InAs quantum dots as well as site-controlled InP nanowire quantum dots and find that they are both promising for scalable quantum information processing platforms.

FF2B.4 • 11:30

Nonlinear Optics with Single Molecules, Benjamin Gmeiner^{1,2}, Andreas Maser^{1,2}, Tobias Utikal^{1,2}, Stephan Götzinger^{1,2}, Vahid Sandoghdar^{1,2}; ¹Max Planck Inst., Germany; ²Friedrich Alexander Univ., Germany. We report on four-wave mixing in a single organic molecule placed at the tight focus of two near resonant laser beams. By directly monitoring the intensity of a weak probe beam after the interaction with the molecule, we observe a rich set of resonance profiles in excellent agreement with theory.

FF2B.5 • 11:45

Xenon-based Nonlinear Fabry-Perot Interferometer for Quantum Information Applications, Garrett Hickman¹, Todd B. Pittman¹, James D. Franson¹; ¹Univ. of Maryland, Baltimore County, USA. We describe a nonlinear Fabry-Perot interferometer useful for optical quantum information applications. We observe self-phase modulation and other nonlinear effects with ultra-low input powers using metastable xenon in a high-finesse cavity.

FF2C • Near-field Imaging, Spectroscopy and Optomechanics—Continued

FF2C.4 • 11:15

FRET-based Scanning Probe Microscopy with a Donor Dye Coated AFM Tip, Basanth Kalanoor¹; ¹Bar Ilan Univ., Israel. A FRET-based method of near-field fluorescence lifetime imaging is developed. Lumogen dye attached to the apex of an AFM tip acts as a nanometric light source for exciting the sample via non-radiative energy transfer.

FF2C.5 • 11:30

Optical Trapping of a Colloidal Quantum Dot, I-Chun Huang¹, Russel Jensen², Ou Chen², Jennifer Choy¹, Thomas Bischof², Mounji Bawendi², Marko Loncar¹; ¹Harvard Univ., USA; ²MIT, USA. Bowtie apertures fabricated by lift-off were used to optically trap a 30-nm silica coated quantum dot (scQD) with 1.56-MW/cm² intensity at 1064-nm wavelength. The trapped scQD emitted fluorescence by two photon excitation from the trapping laser.

FF2C.6 • 11:45

Nonreciprocal Optical Interaction of Dissimilar Particles, Sergey Sukhov¹, Alexander Shalin², David Haefner¹, Aristide Dogariu¹; ¹Univ. of Central Florida, CREOL, USA; ²National Research Univ. of Information Technologies, Mechanics and Optics, Russia. We show that optical interaction of dissimilar particles results in apparent violation of *actio et reactio* principle. Interaction asymmetry in an optically-bound dimer can lead to unexpected movement transversal to the direction of light propagation.

SF2D • Supercontinuum Generation: Fundamentals Issues and New Technologies—Continued

SF2D.4 • 11:15

Relative Timing Jitter of Raman Solitons and its Effect on Nonlinear Wavelength Conversion, Gengji Zhou^{1,2}, Ming Xin¹, Franz Kaerter^{1,2}, Guoqing Chang^{1,3}; ¹CFEL, DESY, Germany; ²Univ. of Hamburg, Germany; ³MIT, USA. We demonstrate that shorter fiber length and the excitation pulse with shorter duration and higher energy can reduce a Raman soliton's relative timing jitter and leads to reduced noise in nonlinear wavelength conversion.

SF2D.5 • 11:30

Enhanced Supercontinuum Generation by Polarization Control of Filamentation in Molecular Gases, Shermineh Rostami¹, Michael Chini², Khan Lim², Magali Durand², Matthieu Baudalet², Martin Richardson², Jean-Claude Diels¹, Ladan Arissian¹; ¹Univ. of New Mexico, USA; ²Univ. of Central Florida, USA. Supercontinuum generation by filamentation in molecular gases is optimized by studying the ellipticity of the pulse polarization during the interaction with the species of the gas medium via strong field ionization and molecular alignment effects.

SF2D.6 • 11:45

Visible-to-near-Infrared Octave Spanning Supercontinuum Generation in a Partially Underetched Silicon Nitride Waveguide, Haolan Zhao^{1,2}, Bart Kuyken^{1,2}, Francois Leo^{1,2}, Stephane Clemmen^{1,2}, Edouard Brainis^{2,3}, Gunther Roelkens^{1,2}, Roel Baets^{1,2}; ¹Photonics Research Group, Dept. of Information Technology, Ghent Univ.-imec, Belgium; ²Center for Nano- and Biophotonics (NB-Photonics), Ghent Univ., Belgium; ³Physics and Chemistry Nanostructures Group, Dept. of Electronics and Information Systems, Ghent Univ., Belgium. The generation of an octave spanning supercontinuum covering most of the visible spectrum is demonstrated for the first time in a silicon nitride waveguide. This result is achieved by dispersion engineering through partially underetching a waveguide.

CLEO: Applications
& TechnologyAF2E • A&T Topical Review on
High Performance Optics II—
Continued

AF2E.3 • 11:30

Generating Structural Colors from Dielectric Surface Resonances, Yichen Shen¹, Veronika Rinnerbauer¹, Marin Soljacic¹, John D. Joannopoulos¹, imbert wang¹; ¹MIT, USA. We propose a new structural color generation mechanism that produces colors by the Fano resonance effect. We experimentally realize the proposed idea by fabricating the samples that show resonance-induced colors with weak angular dependence.

AF2E.4 • 11:45

Laser Damage of Interference Coatings at = 1.6 μm with an Optical Parametric Chirped Pulse Amplifier, Drew Schiltz¹, Dinesh Patel¹, Cory Baumgarten¹, Brendan Reagan¹, Jorge J. Rocca¹, Carmen S. Menoni¹; ¹Electrical and Computer Engineering, Colorado State Univ., USA. Laser damage of interference coatings is investigated with 1.6 μm wavelength, 2 picosecond pulses from an optical parametric chirped pulse amplification system. 7 J/cm² damage thresholds are achieved and deviation from conventional damage models is reported.

CLEO: Science & Innovations

SF2F • Novel Approaches—
Continued

SF2F.4 • 11:15

Double Pass Gain in Helium-Xenon Discharges in Hollow Optical Fibres at 3.5 μm , Adrian Love¹, Sam Bateman¹, Walter Belardi¹, Colin Webb², William Wadsworth¹; ¹Univ. of Bath, UK; ²Dept. of Physics, Univ. of Oxford, UK. Gain is observed in a double pass of a Helium-Xenon gas DC discharge in a 90cm long flexible hollow core fibre. Output at 3.5 μm increases with discharge current up to the maximum of 0.55mA.

SF2F.5 • 11:30

The Physical Origin of Kramers-Kronig Self-Phasing in Coherent Laser Beam Combination, James R. Leger¹, Hung-Sheng Chiang¹, John Hanson¹; ¹Univ. of Minnesota Twin Cities, USA. The Kramers-Kronig self-phasing observed in coherently coupled fiber laser arrays is experimentally shown to originate from a change in the supermode intensity distribution. The conditions that lead to accurate self-phasing are modeled and experimentally confirmed.

SF2F.6 • 11:45

Phase Locking of Many Lasers by Combined Talbot Cavity and Fourier Filtering, Chene Tradonsky¹, Vishwa Pal¹, Ronen Chriki¹, Asher A. Friesem¹, Nir Davidson¹; ¹Weizmann Inst. of Science, Israel. Efficient in-phase coupling of hundreds of lasers by means of combined Talbot cavity and intra-cavity spatial Fourier filtering is developed. Simulated and experimental results for square, triangular and honeycomb laser arrays are presented.

SF2G • III/V Photonics—
Continued

SF2G.4 • 11:15

Monolithically Integrated Multi-Color (Blue and Green) Light-Emitting Diode Chips, Chu-Hsiang Teng¹, Lei Zhang¹, Yu-Lin Tsai², Chien-Chung Lin², Hao-Chung Kuo², Hui Deng¹, Pei-Cheng Ku¹; ¹Univ. of Michigan, USA; ²National Chiao Tung Univ., Taiwan. An LED chip with monolithically integrated, individually addressable multi-color pixels was demonstrated with a color tuning range from blue to green on a single epitaxial wafer.

SF2G.5 • 11:30

GaNAs/InP MQW light-emitting diode fabricated on wafer bonded InP/Quartz substrate, Keiichi Matsumoto¹, Makoto Takasu¹, Yoshinori Kanaya¹, Junya Kishikawa¹, Kazuhiko Shimomura¹; ¹Sophia Univ., Japan. GaInAs/InP multi quantum wells light-emitting diode, emitting at 1.3- μm , was fabricated by metal organic vapor phase epitaxy on wafer bonded InP/Quartz substrate. The device has been operated under continuous wave operation at room temperature.

SF2G.6 • 11:45

Phosphor-free Monolithic High-Efficiency White Light-Emitting-Diodes on Ternary InGaN Substrates, Yu Kee Ooi¹, Jing Zhang¹; ¹Dept. of Electrical and Microelectronics Engineering, Rochester Inst. of Technology, USA. Phosphor-free monolithic high-efficiency tunable white LEDs are realized on ternary InGaN substrates. This proof-of-concept study demonstrates that high quantum efficiency and stable white color emission are achieved by using ternary substrates and correctly-engineered device structures.

CLEO: Science & Innovations

CLEO: Applications
& Technology

SF2H • Photonic Crystals—
Continued

SF2I • Laser Surface Nano-
structuring—Continued

AF2J • Chemical and Gas
Sensing—Continued

SF2H.4 • 11:15

Femtojoule Optical Switching in Hydrogenated Amorphous Silicon Photonic Crystal Nanocavities, Jason Pelc¹, Ranojoy Bose¹, Charles Santori¹, Tho Tran¹, Raymond Beausoleil¹; ¹Hewlett Packard Labs, USA. We demonstrated 1.5- μm -band optical switching using the Kerr effect in hydrogenated amorphous silicon (a-Si:H) photonic crystal nanocavities. Switching with pulse energies down to 18 fJ using a degenerate pump-probe technique was observed in cavities with Q-factors up to 30,000.

SF2H.5 • 11:30

Experimental demonstration of non-reciprocal transmission in a nonlinear photonic-crystal Fano structure, Yi Yu¹, Yaohui Chen¹, Hao Hu¹, Weiqi Xue¹, Kresten Yvind¹, Jesper Mork¹; ¹Danmarks Tekniske Universitet, Denmark. We demonstrate a photonic-crystal structure with >30 dB difference between forward and backward transmission levels. The non-reciprocity relies on the combination of ultrafast carrier nonlinearities and spatial symmetry breaking in a Fano structure employing a single nanocavity.

SF2H.6 • 11:45

Low-loss Mode Converter for Silicon-Polymer Hybrid Slot Photonic Crystal Waveguide, Xingyu Zhang¹, Harish subbaraman², Zeyu Pan¹, Chi-jiu Chung¹, Amir Hosseini², Ray T. Chen^{1,2}; ¹Univ. of Texas at Austin, USA; ²Omega Optics, Inc., USA. We demonstrate an efficient adiabatic mode converter for coupling light into a silicon slot photonic crystal waveguide with slot width as large as 320nm. The loss of the mode converter is measured to be 0.08dB.

SF2I.2 • 11:30

Deep and Near Sub wavelength Ripples on Natural MoS₂ Induced by Femtosecond Laser with Threshold Dependence, Yusong Pan¹, Yumei Li¹, Jianghong Yao¹, Qiang Wu¹, Jingjun Xu¹; ¹Nankai Univ., China. We generate deep and near sub-wavelength ripples on MoS₂ by femtosecond laser irradiation with incident fluence dependence and pulse number insensitivity. Raman analysis demonstrates that no amorphous or oxidative exhibition remains after laser processing.

SF2I.3 • 11:45

Laser fluence dependence of periodic structures on metals produced by femtosecond double pulse laser, Masaki Hashida¹, Laura Gemini², Takaya Nishii¹, Yasuhiro Miyasaka¹, Hitoshi Sakagami³, Shunsuke Inoue¹, Jiri Limpouch², Tomas Mocek⁴, Shuji Sakabe¹; ¹Kyoto Univ., Japan; ²FNSPE, Czech Technical Univ., Czech Republic; ³National Inst. for Fusion Scienc, Japan; ⁴Inst. of Physics, HiLASE Project, Czech Republic. The formation mechanism of LIPSS has been investigated for titanium irradiated by double pulse. We found that variation of the surface plasma density characterized by first pulse led to a variation of the grating interspaces.

AF2J.4 • 11:15 **Tutorial**

Miniature and Handheld Spectroscopic Instruments for Chemical Sensing and Security Applications: Enabled by Photonics, Richard A. Crocombe¹; ¹Thermo Fisher Scientific Inc, USA. Consumer electronics gave us powerful mobile platforms, compact batteries, displays, user interfaces, while telecomm photonics has revolutionized miniature optics, sources and detectors. Handheld spectrometers are now routinely used for chemical sensing and security applications.



Richard Crocombe graduated from Oxford Univ. and Southampton Univ. in the UK in chemistry and spectroscopy. He has spent his career developing analytical instruments, in the last dozen years focussing on portable and handheld instrumentation. Crocombe is co-chair of SPIE's 'Next-Generation Spectroscopic Technologies' conference.



CLEO: Science & Innovations

SF2K • Short Reach & PON
Communication—Continued

SF2K.4 • 11:15

Software-Defined Intra-PON Optical Flow Transmission via a Quasi-Passive Reconfigurable (QPAR) Node, Shuang Yin¹, Thomas Shun Rong Shen¹, Yingying Bi¹, Jing Jin¹, Leonid Kazovsky¹; ¹Stanford Univ., USA. This paper demonstrates Intra-PON optical Flow transmission via a QPAR node. Simulations show 2 to 20x traffic waiting time reduction comparing to no or fixed Intra-PON designs. Experiments show error-free Intra- and Inter-traffic with/without QPAR reconfiguration.

SF2K.5 • 11:30

8-User PAM-ECDMA PON with 25.6 Gb/s Aggregate Data Rate, Xuhan Guo¹, Xin Li¹, Adrian Wonfor¹, Lei Zhou², Liming Fang², Richard V. Penty¹, Ian H. White¹; ¹Univ. of Cambridge, UK; ²Huawei Technologies, China. We report a PAM-ECDMA PON system with 2.5-fold performance improvement over the prior NRZ-ECDMA system. Error-free transmission of two channels in an 8-user 25.6 Gb/s aggregate-data-rate PON is achieved in a proof-of-principle demonstration.

SF2L • Ranging and
Metrology—Continued

SF2L.4 • 11:15

Dual-comb Reciprocal Temporal Scanning for Absolute Distance Measurement, Hongyuan Zhang¹, Xuejian Wu¹, Haoyun Wei¹, Yan Li¹; ¹Tsinghua Univ., China. Pulse trains from dual combs with different repetition rates are coupled and directed onto a target for simultaneous absolute distance measurement. Non-ambiguity range extension is immune to drift and accuracy is about 100 nm.

SF2L.5 • 11:30

Stabilization of Squeezed Vacuum States Using Weak Pump Depletion, Timo Denker¹, Dirk Schütte¹, Maximilian H. Wimmer¹, Trevor Wheatley³, Eleanor H. Huntington², Michele Heurs¹; ¹Max-Planck-Institut für Gravitationsphysik (Albert-Einstein-Institut), and Institut für Gravitationsphysik, Leibniz Universität Hannover, Germany; ²College of Engineering and Computer Science, Australian National Univ., Australia; ³School of Engineering and Information Technology, Univ. of New South Wales, Australia. We present a new phase-locking technique based on weak pump depletion. It allows for the first experimental realization of a pump-phase lock of an optical parametric oscillator by reading out the pre-existing phase information in the pump field. No degradation of the detected squeezed states occurs.

SF2L.6 • 11:45

Factor of 18 Enhancement in the Sensitivity-Bandwidth Product of the aLIGO Gravitational Wave Detector Using a White Light Cavity, Minchuan Zhou¹, Zifan Zhou¹, Selim M. Shahriar¹; ¹Northwestern Univ., USA. We show that the sensitivity-bandwidth product of the aLIGO gravitational wave detector can be enhanced by a factor of 18, while remaining below the standard quantum limit, by employing a white light cavity configuration.

SF2M • Symposium on OPA/
OPCPA – Next Generation
of Ultra-Short Pulse Laser
Technology II—Continued

SF2M.3 • 11:30

Broadband 2D-QPM Frequency Domain OPA, Christopher R. Phillips¹, Benedikt Mayer¹, Lukas Gallmann^{1,2}, Ursula Keller¹; ¹ETH Zurich, Switzerland; ²Univ. of Bern, Switzerland. We demonstrate broadband mid-IR frequency-domain OPA (FOPA) in the Fourier-plane of a 4f pulse shaper via two-dimensional (2D) quasi-phasesmatching (QPM) device adapted to the pump intensity profile and spatial chirp of the mid-infrared beam.

SF2M.4 • 11:45

500 kHz OPCPA-Based UV-XUV Light Source For Time-Resolved Photoemission Spectroscopy, Michele Puppin¹, Yunpei Deng¹, Chris Nicholson¹, Claude Monney^{1,3}, Marcel Krenz¹, Oliver Prochnow², Jan Ahrens^{2,4}, Thomas Binhammer², Uwe Morgner⁴, Martin Wolf¹, Ralph Ernstorfer¹; ¹Fritz-Haber Institut, Germany; ²VENTEON Laser Technologies, Germany; ³Dept. of Physics, Zurich Univ., Switzerland; ⁴Inst. of Quantum Optics, Leibniz Universität Hannover, Germany. A 15 W, sub-20 fs OPCPA based on an Yb laser is used to demonstrate 6.3 eV fourth harmonic-based UV photoelectron spectroscopy with sub-60 fs time resolution and XUV high harmonic generation at 500 kHz.

CLEO: QELS-Fundamental Science

CLEO: Science & Innovations

FF2A • Single Photon Detectors—Continued

FF2A.7 • 12:00

Using Double Compressive Sensing in Simultaneous Imaging of Spatial Entanglement, Samuel H. Knarr^{1,2}, Gregory Howland³, James Schneeloch^{1,2}, Daniel Lum^{1,2}, John Howell^{1,2}; ¹Univ. of Rochester, USA; ²Center for Coherence and Quantum Optics, Univ. of Rochester, USA; ³Air Force Research Lab, USA. We use compressive sensing in the image and Fourier planes of a spontaneous parametric down conversion source to simultaneously gather the joint position and momentum distributions. We witness entanglement by violating a continuous variable steering inequality.

FF2A.8 • 12:15

Classical Imaging with Undetected Photons, Jeffrey H. Shapiro¹, Dheera Venkatraman¹, Franco N. Wong¹; ¹MIT, USA. We describe a classical-state system capable of mimicking the essential features of Barreto Lemos et al.'s quantum imaging with undetected photons [Nature, **512**, 409-412 (2014)], but with a much higher signal-to-noise ratio.

FF2B • Quantum Nonlinear Optics—Continued

FF2B.6 • 12:00

Experimental Generation of Quadruple Quantum Correlated Beams from Cascaded Four-Wave Mixing Processes in Hot Rubidium Vapors, Jietai Jing¹; ¹East China Normal Univ., China. We report on our recent experimental results of generating quadruple quantum correlated beams by using cascaded four-wave mixing processes in hot rubidium vapor. The intensity-difference squeezing of the four beams is about 8.0 dB.

FF2B.7 • 12:15

Continuous Generation of Rubidium Vapor in a Hollow Core Photonic Band-Gap Fiber, Prathamesh Donvalkar¹, Sven Ramelow¹, Stephane Clemmen¹, Alexander L. Gaeta¹; ¹Cornell Univ., USA. We demonstrate high optical depths of > 50 lasting over 100 minutes in a Rubidium filled PBGF using an off-resonant CW laser beam, which enables straightforward measurement of cross-phase modulation at the single photon level.

FF2C • Near-field Imaging, Spectroscopy and Optomechanics—Continued

FF2C.7 • 12:00

Optical manipulation of Janus nanoparticles, Ognjen Ilic¹, Ido Kaminer¹, Yoav Lahini¹, Hrvoje Buljan², Marin Soljacic¹; ¹MIT, USA; ²Dept. of Physics, Univ. of Zagreb, Croatia. We explore optical forces and torques acting on Janus nanoparticles in a plane electromagnetic wave. We find rotationally stable points and propose a scheme for all-optical manipulation of orientation and position of Janus nanoparticles.

FF2C.8 • 12:15

Simultaneous Transport of Multiple Nanoparticles Across a Patterned Plasmonic Substrate, Jason Ryan¹, Yuxin Zheng¹, Paul Hansen¹, Tiffany Huang¹, Lambertus Hesselink¹; ¹Stanford Univ., USA. We demonstrate the controlled transport of simultaneous nano-scale particles across a patterned gold film. Nanopillars patterned onto the gold surface load particles onto nearby plasmonic conveyor belts formed from C-shaped engravings.

SF2D • Supercontinuum Generation: Fundamentals Issues and New Technologies—Continued

SF2D.7 • 12:00 **Invited**

Mid-Infrared Supercontinuum Generation Spanning More Than 11 μm in a Chalcogenide Step-Index Fiber, Christian R. Petersen¹, Uffe Møller¹, Irnis Kubat¹, Binbin Zhou¹, Sune Dupont², Jacob Ramsay², Trevor Benson³, Slawomir Sujecki³, Nabil Abdel-Moneim³, Zhuoqi Tang³, David Furniss³, Angela Seddon³, Ole Bang^{1,4}; ¹DTU Fotonik, Dept. of Photonics Engineering, Danmarks Tekniske Universitet, Denmark; ²Dept. of Chemistry, Aarhus Univ., Denmark; ³George Green Inst. for Electromagnetics Research, Univ. of Nottingham, UK; ⁴NKT Photonics A/S, Denmark. Supercontinuum generation covering an ultra-broad spectrum from 1.5-11.7 μm and 1.4-13.3 μm is experimentally demonstrated by pumping an 85mm chalcogenide step-index fiber with 100fs pulses at a wavelength of 4.5 μm and 6.3 μm , respectively.

NOTES

CLEO: Science & Innovations

CLEO: Applications
& Technology

SF2H • Photonic Crystals—
Continued

SF2H.7 • 12:00

Flat-top Drop Filter based on a Single Topology Optimized Photonic Crystal Cavity, Lars H. Frandsen¹, Yuriy Elesin², Xiaowei Guan¹, Ole Sigmund³, Kresten Yvind¹; ¹DTU Fotonik, Dep. Photonics Engineering, Denmark; ²Haldor Topsoe, Denmark; ³Dept. of Mechanics Engineering, DTU Mekanik, Denmark. A flat-top drop filter has been realized in silicon-on-insulator material by applying 3D topology optimization to a single L3 photonic crystal cavity. Measurements reveal that the pass-band of the drop channel is flat within 0.44 dB over a wavelength range of 9.7 nm with an insertion loss <0.85 dB.

SF2H.8 • 12:15

Photonic Surfaces for Designable Nonlinear Power Shaping, Roshni Biswas¹, Michelle Povinelli¹; ¹Univ. of Southern California, USA. We introduce a mechanism for nonlinear optical power transmission using partially absorptive resonances in photonic crystal slabs. We experimentally demonstrate increasing, decreasing, and nonmonotonic transmission as a function of optical power.

SF2I • Laser Surface Nano-
structuring—Continued

SF2I.4 • 12:00

Polarization Sensitive Printing by Ultrafast Laser Nanostructuring in Amorphous Silicon, Rokas Drevinskas¹, Martynas Beresna¹, Mindaugas Gecevičius¹, mark khenkin², andrey G. kazanskii², oleg I. konkov³, Peter Kazansky¹; ¹Univ. of Southampton, UK; ²Physics Dept., M.V. Lomonosov Moscow State Univ., Russia; ³Russian Academy of Sciences, A.F. Ioffe Physicotechnical Inst., Russia. We demonstrate femto- and picosecond laser assisted nanostructuring of hydrogenated amorphous silicon (a-Si:H). The laser-induced periodic sub-wavelength structures exhibit the dichroism and giant form birefringence giving extra dimensions to the polarization sensitive image recording.

SF2I.5 • 12:15

Influence of Self-scattering on the Fabrication of Surface Nanostructures in Zinc Phosphate Glass Using Fs-laser Pulses, Jasper Clarijs², Javier Hernandez Rueda¹, Marcel Scholten², Hao Zhang², Denise M. Krol^{1,2}, Dries van Oosten²; ¹Univ. of California Davis, USA; ²Utrecht Univ., Netherlands. Zinc-phosphate glass surface ablation was investigated using tightly focused fs-laser pulses. Evidences of self-scattering effects due to the interaction between the laser light and a transient plasma generated during surface ablation have been investigated.

AF2J • Chemical and Gas
Sensing—Continued

AF2J.5 • 12:15

An Interband Cascade Laser based Sulfur Dioxide Sensor for Emission Monitoring Applications, Peter Geiser¹, Ove Bjorøy¹, Peter Kaspersen¹, Lars Nähle², Julian Scheuermann², Michael von Edlinger², Johannes Koeth²; ¹Norsk Elektro Optikk A/S, Norway; ²nanoplus Nanosystems and Technologies GmbH, Germany. A mid-infrared sensor for sulfur dioxide in emission monitoring applications using a monomode DFB ICL at 4 μm and second harmonic detection has been developed. The detection limit of the sensor is below 3 ppm·m.

NOTES

Lined area for taking notes.

CLEO: Science & Innovations

SF2L • Ranging and
Metrology—Continued

SF2L.7 • 12:00

Nested Fabry-Perot in mode-locked lasers to monitor minute changes of index, James Hendrie¹, Ladan Arissian¹, Koji Masuda¹, Adam Hecht¹, Jean-Claude Diels¹; ¹*Univ. of New Mexico, USA*. An uncoated glass etalon inserted in a mode-locked laser results generating two nested frequency combs. The ratio of their frequencies, insensitive to external parameters, is an accurate measure of the optical path in the etalon.

SF2L.8 • 12:15

Ultrahigh Resolution Frequency-to-Time Mapping Based on Frequency Shifting Recirculating Lasers, Hugues Guillet de Chatellus¹, José Azaña²; ¹*LIPhy, France*; ²*EMT-INRS, Canada*. We demonstrate a novel implementation of frequency-to-time mapping based on a frequency shifting recirculating laser, achieving a 10 kHz-frequency resolution and a time-bandwidth product greater than 1000.

SF2M • Symposium on OPA/
OPCPA – Next Generation
of Ultra-Short Pulse Laser
Technology II—Continued

SF2M.5 • 12:00

Multi-mJ, kHz, intense picosecond deep-ultraviolet source, Chun-Lin L. Chang¹, Peter R. Kroger¹, Houkun Liang¹, Gregory J. Stein¹, Jeffrey Moses¹, Chien-Jen Lai¹, Jonathas P. Siqueira¹, Luis E. Zapata¹, Franz X. Kaertner^{1,2}, Kyung-Han Hong¹; ¹*Dept. of Electrical Engineering and Computer Science and Research Lab of Electronics, MIT, USA*; ²*Dept. of Physics, Univ. of Hamburg, Center for Free-Electron Laser Science, DESY, Germany*. We demonstrate a 2.74 mJ, 1 kHz, ~4.2 ps DUV laser at ~257.7 nm with M²~2.54 from a frequency-quadrupled hybrid Yb-doped chirped-pulse amplifier. An infrared-to-DUV conversion efficiency of ~10% is achieved.

SF2M.6 • 12:15

Deviation From [Pump=Signal + Idler] Photon Energy Conservation in an Ultrafast Optical Parametric Amplifier, Oleksandr Isaenko¹, Victor Klimov¹; ¹*Los Alamos National Lab, USA*. We report on considerable photon energy losses of [signal+idler] pair (~60 meV) in KTiOPO₄ optical parametric amplifier pumped by <40-fs 800-nm pulses and explains it by optical rectification enhanced by coupling to large third-order nonlinearity.

NOTES

Friday, 15 May